Alessandro Tarantino · Enrique Romero
Yu-Jun Cui (Eds.)

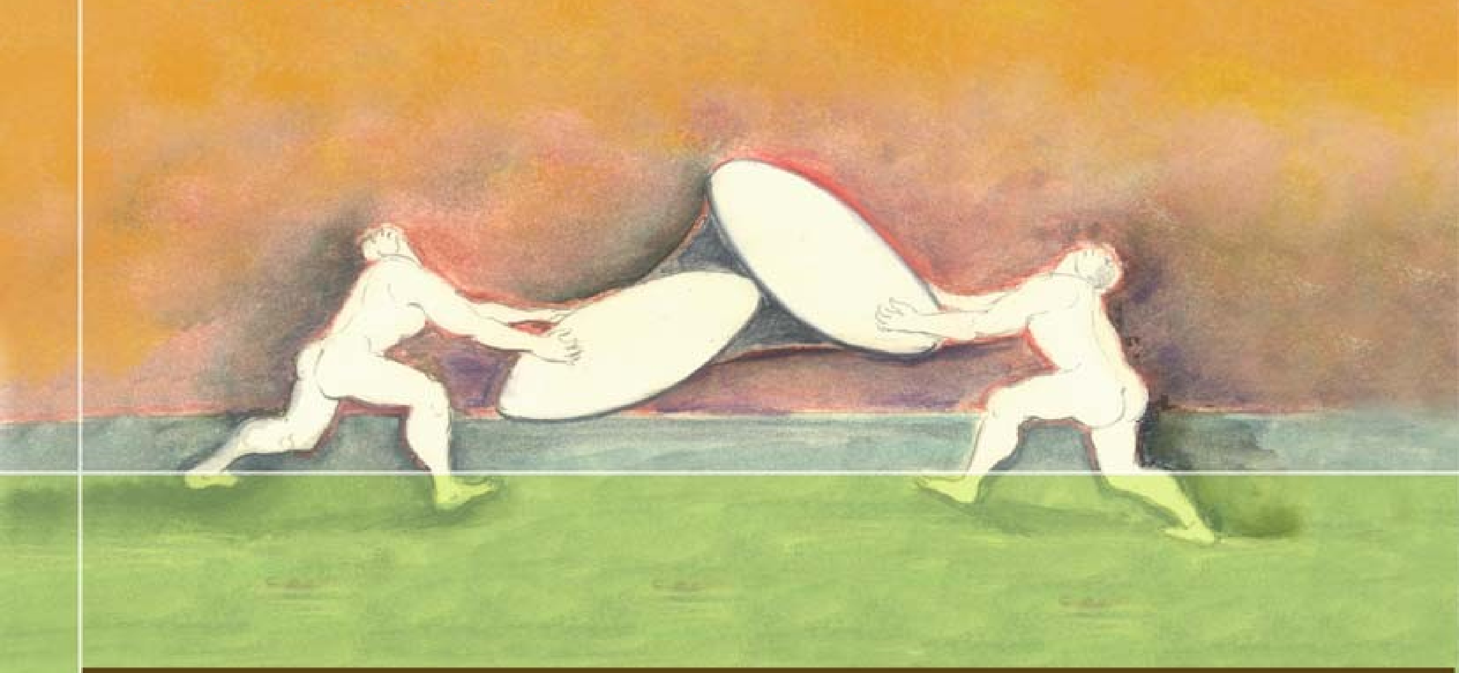

Laboratory and Field Testing of Unsaturated Soils

Springer

Laboratory and Field Testing of Unsaturated Soils

A. Tarantino · E. Romero · Y.-J. Cui
Editors

Laboratory and Field Testing of Unsaturated Soils

Foreword by Alessandro Tarantino, Enrique Romero and Yu-Jun Cui

Reprinted from *Geotechnical and Geological Engineering*, Volume 26, No. 6, 2008

Springer

Editors

Alessandro Tarantino
Università degli Studi
di Trento
38050 Trento
Italy
alessandro.tarantino@ing.unitn.it

Enrique Romero
Universitat Politècnica
de Catalunya
08034 Barcelona
Spain
enrique.romero-morales@upc.edu

Yu-Jun Cui
Ecole Nationale
des Ponts et Chaussées
77455 Marne la Vallee
France
cui@cermes.enpc.fr

Cover illustration: Painting reproduced courtesy of Ms. Maria Mantegna.

ISBN: 978-1-4020-8818-6 eISBN: 978-1-4020-8819-3

Library of Congress Control Number: 2008942097

Printed on acid-free paper.

springer.com

Contents

Preface: Special Issue on Laboratory and Field Testing of Unsaturated Soils

A. Tarantino · E. Romero · Y. J. Cui

Originally published in the journal *Geotechnical and Geological Engineering*, Volume 26, No. 6, 613–614.
DOI: 10.1007/s10706-008-9194-3

The scope of this special issue focuses on recent advances in laboratory and field testing of unsaturated soils. Leading researchers from fourteen countries to represent global research in the area of experimental unsaturated soil mechanics have been invited to contribute to this issue. Twelve reports are presented dealing with measurement and control of suction and water content, mechanical, hydraulic, and geo-environmental testing, microstructure investigation, and applications of unsaturated soil monitoring to engineering behaviour of geo-structures.

The main motivation behind this issue is the rapid growth of experimental unsaturated soil mechanics over the last couple of decades. Several innovative laboratory and field techniques have been introduced in mechanical, hydraulic, and geo-environmental testing. However, this information is widely dispersed in journals and conference proceedings and researchers and engineers beginning to work in the field of unsaturated soil mechanics may find it difficult to identify suitable equipment and instrumentation for research or professional purposes. This volume aims at providing scientists and practitioners with a comprehensive overview of experimental techniques in unsaturated soil mechanics.

The first group of papers focuses on measurement and control of matric and total suction.

MARINHO, TAKE & TARANTINO report on the high-capacity tensiometer and the axis translation technique, which share the measurement of a pressure differential across a high air entry porous ceramic. The paper examines the underlying physical concepts of capillarity, water surface tension and phase change and discusses challenges to be faced in both experimental techniques.

BULUT & LEONG present working principles, calibration, procedures, and application areas of indirect methods of suction measurement. These include thermocouple, transistor, and chilled-mirror psychrometer (primary methods), filter paper (secondary methods), and thermal and electrical conductivity sensors (tertiary methods). Capabilities, limitations, and pitfalls of these methods are discussed.

VANAPALLI, NICOTERA & SHARMA focus on negative water column and axis translation techniques for matric suction control. They discuss in detail the limitations of these techniques with respect to air diffusion, water volume change and evaporation.

A. Tarantino (✉)
Dipartimento di Ingegneria Meccanica e Strutturale,
Università degli Studi di Trento, via Mesiano 77,
38050 Trento, Italy
e-mail: alessandro.tarantino@ing.unitn.it

E. Romero
Universitat Politècnica de Catalunya,
Barcelona, Spain
e-mail: Enrique.romero-morales@upc.edu

Y. J. Cui
Ecole Nationale des Ponts et Chaussées,
Paris, France
e-mail: cui@cermes.enpc.fr

DOI: 10.1007/978-1-4020-8819-3_1

BLATZ, CUI & OLDECOP examine the vapour equilibrium and osmotic techniques for controlling matric and total suction in oedometer, direct shear and triaxial tests. They provide a summary of some recent developments and knowledge regarding the use of these techniques highlighting limitations and drawbacks of these methods.

The second group of papers focuses on mechanical, hydraulic, and geo-environmental testing where techniques for suction measurement and control are implemented for investigating unsaturated soil behaviour.

HOYOS, LALOUI & VASSALLO report on recent advances in laboratory testing of unsaturated soils giving emphasis on volume change measurements in triaxial systems and true triaxial devices, and methods for measuring small-strain stiffness using the resonant column and bender elements.

MASROURI, BICALHO & KAWAI examine the experimental methods for determining the water hydraulic constitutive functions. They address two problems that are important area of current research, the hydraulic testing of quasi-saturated soils (soils with entrapped air) and deformable soils (swelling/shrinking soils).

DELAGE & ROMERO present recent developments in experimental techniques for investigating retention and transfer properties of aqueous liquids, non-aqueous liquids (hydrocarbons), and gases, accounting for thermal and chemical interactions. These techniques find important applications in soil contamination and waste disposal.

In recent years, microstructure investigation has become a common method to complement hydraulic and mechanical testing. *ROMERO & SIMMS* focus on the evaluation of the current state of use and the development of mercury intrusion porosimetry and environmental scanning electron microscopy. They show the use of these techniques to explore fundamental properties of water retention characteristics, water permeability, and micro and macrostructural interactions.

Finally, the last group of paper deals with field applications.

TARANTINO, RIDLEY & TOLL discuss advantages and limitations of instruments for direct (tensiometer) and indirect (porous block sensors, filter paper and psychrometer) measurement of suction. Techniques for water content measurement based on dielectric methods are also reviewed.

CUI & ZORNBERG present methods for measuring evapotranspiration based on meteorological information. Case histories involving direct and indirect measurements of evapotranspiration are then presented. These include approaches based on energy balance and water balance.

NG, SPRINGMAN & ALONSO report a range of recent field studies of the mechanisms of rainfall infiltration into unsaturated weathered and expansive soil slopes and unsaturated well-graded alpine moraines slopes. In addition, they report some physical simulations of unsaturated soil slopes subjected to rainfall, groundwater table rising as well as moisture changes in centrifuge model tests.

ALONSO, SPRINGMAN & NG document two large scale "in situ" demonstration experiments. The first test involves the hydration of a compacted bentonite barrier whereas the second test involves the progressive de-saturation of Opalinus clay induced by maintained ventilation of an unlined tunnel. The paper analyses the performance of different sensors and a comparison of field behaviour with modelling results.

We hope this volume will provide guidance to researchers and engineers in their laboratory and field experiments.

Measurement of Matric Suction Using Tensiometric and Axis Translation Techniques

F. A. M. Marinho · W. A. Take · A. Tarantino

Originally published in the journal *Geotechnical and Geological Engineering*, Volume 26, No. 6, 615–631.
DOI: 10.1007/s10706-008-9201-8

Abstract Experimental equipment for the measurement of matric suction in unsaturated soils using hydraulic tensiometers and the axis translation technique share a common working principle; that is, the measurement of a pressure differential across a high air entry porous ceramic. In this paper, the current state of the art in these two suction measurement techniques is presented and discussed together with the underlying physics thereby giving the reader the necessary basis to use and interpret the results obtained from those two techniques.

Keywords Tensiometer · Cavitation · Suction · Axis translation technique · Unsaturated soil · Water retention curve

1 Introduction

Measurement of negative pore-water pressure is of primary importance in the analysis and prediction of unsaturated soil behaviour. Conventional tensiometers (Stannard 1992) can measure negative water pressures only in the range from 0 to 80 kPa and their application is therefore quite limited. In the early 1990's, Ridley and Burland (1993, 1995) first developed high-capacity tensiometers capable of measuring negative water pressures down to −1,500 kPa. Since then, a number of instruments have been developed and successfully used in laboratory and field experiments (Ridley et al. 1997; Take and Bolton 2003; Cunnigham et al. 2003; Oliveira and Marinho 2003; Tarantino and Tombolato 2005). Nonetheless, the spread of this type of instrument is still fairly limited. Development of 'homemade' and commercial high-capacity tensiometers is hampered by a lack of knowledge of basic principles, suitable design and experimental techniques. Although state-of-the-art reports on tensiometric measurement have already been presented in the literature (Ridley and Wray 1996; Tarantino 2004), many points are worthy to be addressed in the light of the most recent findings.

Tensiometric technique shares with axis translation technique a common working principle; that is, the measurement of a pressure differential across a high air entry porous ceramic. For this reason, these two suction measurement techniques are presented and discussed together to underline their similarities (saturation procedures, the need for intimate contact, air diffusion, air entry, etc) and their differences (absolute positive and negative pressures, cavitation, etc.) thereby giving to the reader the necessary basis

F. A. M. Marinho (✉)
Universidade de Sao Paulo, Prédio da Engenharia Civil – PEF, Av. Prof. Almeida Prado 271, CEP 05508-900 São Paulo, Brasil
e-mail: fmarinho@usp.br

W. A. Take
Queen's University, Kingston, ON, Canada

A. Tarantino
Università degli Studi di Trento, Trento, Italy

to use and interpret the results obtained from those two techniques. The axis-translation technique as a system to control suction in unsaturated soil testing is discussed in detail elsewhere in this issue (Vanapalli et al. 2008, this issue)

2 Basic Concepts

2.1 Gauge vs. Absolute Pressure

In most Geotechnical Engineering applications, fluid pressures are typically thought of and reported in terms of gauge pressure, i.e. relative to atmospheric pressure. Thus, pressure reduced to a value below atmospheric, is referred to as negative if the fluid is water or a vacuum if the fluid is air. However this definition of pressure, although useful in engineering practice, is of limited value in the quantification of phase relationships as these are defined in terms of absolute pressure. When referring to pressure in absolute terms, the zero pressure origin is defined as a total vacuum, the atmospheric pressure at sea-level is approximately 101.6 kPa, positive water pressures imply compression, and negative water pressures imply that the water is being held in tension (i.e. it is being stretched).

2.2 Surface Tension, Contact Angle, and Hysteresis

The physics of the contact angle hysteresis is useful to illustrate, at least in a qualitative way, the mechanisms likely to control cavitation in high suction tensiometer. It also provides a conceptual justification for the axis-translation technique.

The *surface tension*, T, of a liquid is the force per unit length acting in the plane of the surface of a liquid in contact with its own vapour resulting from the unsymmetrical force field at a liquid surface. Consider a liquid in equilibrium with its own vapour and a solid surface as shown in Fig. 1a. The angle between the solid surface and the gas-liquid interface at the three-phase line of contact is defined as the *contact angle*, θ (measured through the liquid). The contact angle is the result of a balance between the cohesive forces in the liquid and the adhesive forces between solid and liquid. A liquid with a contact angle less than 90° (e.g. water) is said to wet a surface

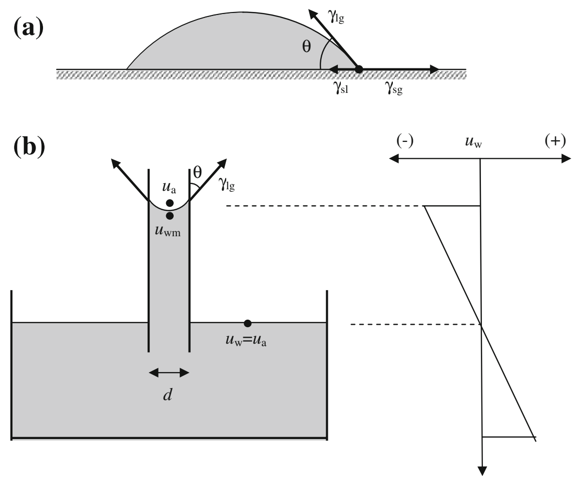

Fig. 1 (**a**) Contact angle for an ideal smooth, homogenous and non-deformable surface (γ = surface tension, *sl* = solid-liquid, *sg* = solid-gas, *lg* = liquid-gas). (**b**) Capillary rise of wetting fluid

as a drop of the liquid tends to spread when placed on a solid surface.

The phenomena of capillarity occurs in fluid-surface systems of contact angles less than 90°. In these cases, the contact angle of the system causes the liquid to rise in small diameter pores such as the idealised circular pore of Fig. 1b. The water pressure, u_{wm}, at the back of the meniscus can be calculated by considering the vertical force equilibrium at the air–water interface:

$$u_{wm} = u_a - \frac{4T\cos\theta}{d} \tag{1}$$

where d is the diameter of the capillary and u_a is the air pressure. Since $\cos\theta > 0$, water pressure at the back of the meniscus, $u_{\rm wm}$, is less than air pressure. As a result, the meniscus will rise in the capillary until hydrostatic conditions are established. Let us assume that air pressure is atmospheric (i.e. 101.6 kPa absolute pressure), $T = 0.072$ N/m (air–water surface tension at 20°C) and $\theta = 0$. Equation 1 indicates that the absolute water pressure is zero when d = 2.8 μm and becomes more and more negative as the radius of the pore decreases. As will be seen in the next section, the magnitude of this negative pressure is limited by the phase relationships of the pore fluid and the phenomenon of cavitation.

Gibbs (1948) showed that one and only one stable contact angle exists for a given system for the case of smooth, homogenous and nondeformable solids. In practice, however, this is rarely, if ever, the situation. If these assumptions are removed, it can be shown within the framework of classical thermodynamics that many different stable angles exist for a given system, i.e. the contact angle exhibits hysteresis (Johnson and Dettre 1969). The concept of contact angle hysteresis can perhaps be best explained by considering the following example. As shown in Fig. 2a, a drop of liquid can be placed on surface and is progressively tilted until the drop rolls off the plate. At a small inclination, the contact angles at the leading and trailing edge of the drop will increase and decrease respectively and prevent the drop periphery from moving. This will continue until a limit condition is attained when these angles become the advancing and receding angles, θ_a and θ_r respectively, at which point the drop will roll off the plate. Thus, a number of macroscopic stable contact angles exist for a given system in the range from θ_r to θ_a.

The hysteresis of the contact angle can be produced by surface roughness. Consider once again a drop on a tilting plate, this time with a rough surface (Fig. 2b). Even though the leading and trailing edges of the drop both meet the solid with the same intrinsic angle, θ_0, the macroscopic angles measured with respect to the tilt plane are different at the front and back of the drop.

Surface heterogeneity can also cause contact angle hysteresis. If, in our example the tilting plate is heterogeneous (Fig. 2c), the leading edge of the drop will tend to stop at the boundaries of the high-contact-angle regions. The advancing angles may then be associated with the intrinsic angle of the high-contact-angle regions, whereas the receding angles are controlled by the low-contact-angle regions (Johnson and Dettre 1969).

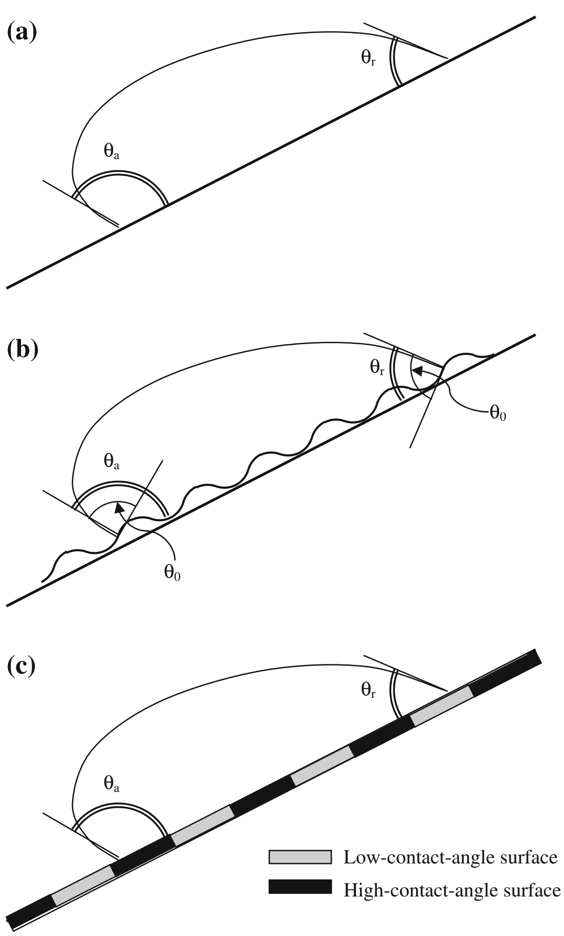

Fig. 2 Hysteresis of contact angle for real surfaces (after Johnson and Dettre 1969). (**a**) Water drop on a tilted surface. (**b**) Effect of roughness on hysteresis. (**c**) Effect of heterogeneity on hysteresis

2.3 Stable and Metastable States of Water

The phase diagram for water (Fig. 3) is reported in undergraduate textbooks as the diagram defining whether water will take the form of a solid (ice), liquid, or gas (vapour) at a given temperature and

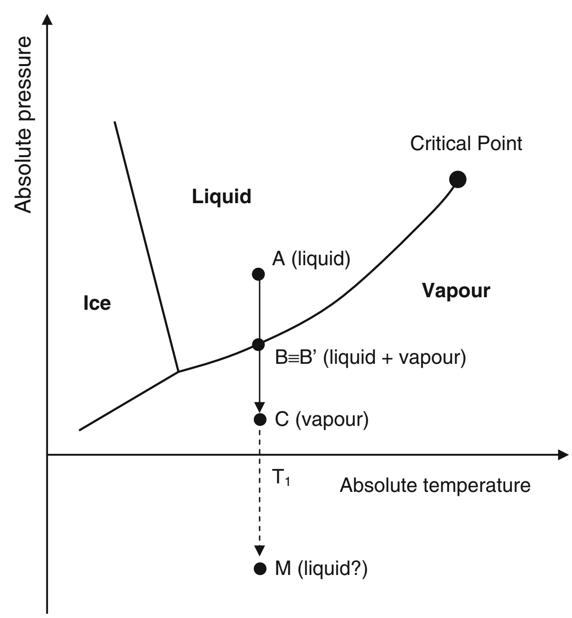

Fig. 3 Phase diagram for water

pressure. To explore the phase diagram, consider a closed system containing liquid water at the temperature and pressure of point A. If pressure is reduced isothermally, the liquid-gas equilibrium line is eventually reached at point B, where bubbles normally form in the liquid. In order for the pressure to be further reduced to Point C, only vapour must be present in the system.

Since absolute vapour pressure can not be negative, the phase diagram shown in Fig. 3 seems to suggest that also the minimum absolute liquid pressure (point B) can not be negative. This has led to the common misassumption that liquids can not withstand absolute negative pressures. The phase diagram for water shown in Fig. 3 only represents the *stable* states for water. However, other states are possible (including water under negative pressure) which do not violate the principles of classic thermodynamics. To elucidate this point, it is useful to represent the phase diagram of water in the pressure-molar volume plane (Fig. 4a). If liquid water at point A is subjected to isothermal expansion, pressure will decrease according to the equation of state of the fluid. At point B, liquid water will transform into vapour water at constant pressure (and temperature). As point B' is reached, liquid water will no longer be present in the system and further expansion will bring water vapour to point C according to the equation of state of water vapour.

A question that might be asked is whether liquid water in D may exist in (meta)stable state if no gas is present in the system. To answer this question it may be useful to consider the equation of state of fluids proposed by van der Waals:

$$\left(p+\frac{a}{v^2}\right)(v-b)=RT \tag{2}$$

where p = pressure, v = molar volume, R = universal gas constant, T = absolute temperature, a and b the van der Waals' constants depending on the type of fluid. This equation, though quantitatively inaccurate, provides a simple picture of vapour–liquid equilibrium (De Benedetti 1996). With respect to the equation of ideal gas law, van der Waals' equation accounts for the intermolecular repulsive and attractive forces and describe the continuity between gaseous and liquid states (Rowlinson 1988). If the temperature is high enough that the average kinetic energy of a molecule greatly exceeds the molecular attraction the fluid behaves as a gas. If

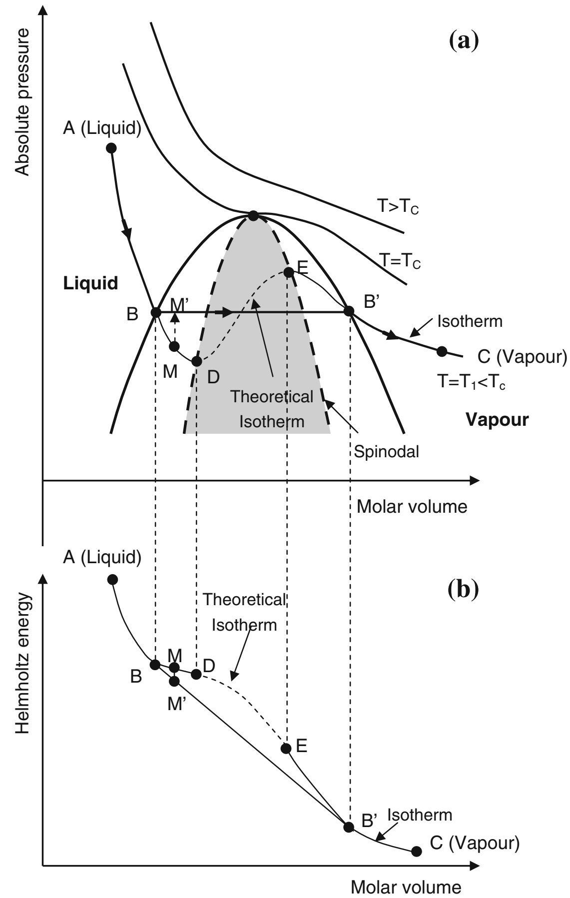

Fig. 4 Isotherms in the pressure–partial volume plane and Helmoltz energy of vapour and liquid water at constant temperature (T_c = critical temperature)

temperature is low enough, attractive forces prevail and the fluid behaves as a liquid. Van der Waals' isotherms are plotted in Fig. 5 for liquid water at five different temperatures.

Using Gibbs' general criteria of equilibrium, it can be shown that the fluid along the isotherm is stable when the fluid isotropic compressibility, K_T, is positive (De Benedetti 1996). More thermodynamics is required to explain this stability criterion which has, however, a clear intuitive meaning. Equilibrium is stable if pressure increases when the substance is compressed isothermally (K_T is positive). In this case, the increase in fluid pressure will counterbalance the external applied pressure. On the other side, the equilibrium is unstable if pressure decreases when the substance is compressed isothermally (K_T is negative), because the fluid pressure cannot counterbalance the

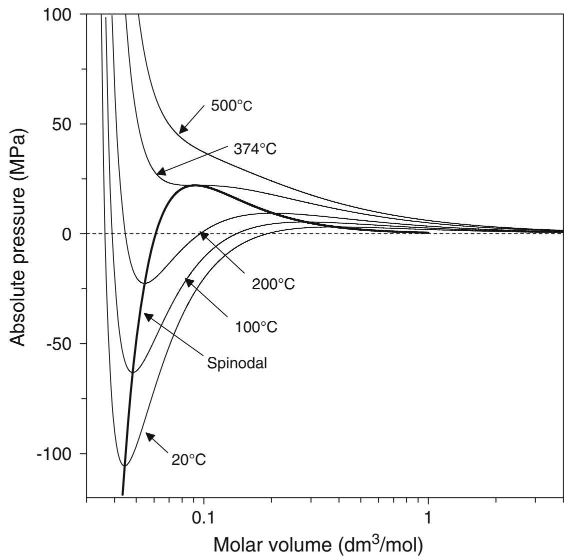

Fig. 5 Van der Waals isotherms for water in the absolute pressure–partial volume plane

external applied pressure. According to this stability criterion, the dashed part of the van der Waals' isotherms (DE) in Fig. 4a represents unstable states, i.e. impossible states for the fluid. On the other side, states along BD and EB' are stable states, as stability criteria are satisfied. These states are however called *metastable* because a gas phase will rapidly separate in the liquid if an amount of gas is present in the liquid (see Fig. 4b, path M–M').

This can be shown in Fig. 4b, where the Helmholtz energy is plotted against molar volume for isothermal paths. Calculation of Helmoltz energy variation at constant temperature can be found in De Benedetti (1996). According to Gibbs' general criteria of equilibrium, a system at constant volume, temperature, and mass will move to states of minimum Helmholtz energy (Gibbs, 1948; Berry et al. 1980). Helmholtz energy along the theoretical isotherm BD is higher than Helmholtz energy along the coexistence line BB'. If the liquid water is at point M and gas nuclei are present in the system, liquid water will partially transform into vapour water to bring the system to a lower Helmholtz energy (M'). However, if the system were ideally free of any gas, the water would remain liquid in M. The locus passing through the minimum and maximum of the isotherms in Fig. 4a that separate the region of unstable states from the one of metastable states is called the *spinodal*.

The van der Waals' isotherms for water are plotted in Fig. 5 with the constant *a and b* calculated from the critical constants (Alberty 1987). This figure shows that liquid water at 20°C can remain in a metastable state down to a pressure slightly greater than 100 MPa. This pressure would be the theoretical tensile strength of water according to the van der Waals' equation for fluid. This value seems to capture the correct order of magnitude of liquid water tensile strength although different values can be calculated using a more accurate equation of state.

2.4 Homogeneous and Heterogeneous Cavitation

Despite pure water having a high theoretical tensile strength on the order of 100 MPa, experimental studies have for years failed to approach this value. For example, prior to the 1970's experimental determinations of the maximum attainable tensile stress in water ranged approximately from 1.3 to 27 MPa (Knapp et al. 1970). However more recently, Zheng et al. (1991) were able to measure a tensile stress of 140 MPa in a single crystal of water, a value believed to be very close to the maximal tension that water can sustain. This wide variation in experimental data can be explained by imperfections that lead to instability and transition to points such as M' in Fig. 4.

Imperfections can typically occur in two forms. The thermal motions within the liquid form temporary, microscopic voids that constitute the nuclei necessary for rupture and growth to macroscopic bubbles. This is termed *homogenous nucleation*. The tension necessary to cause homogenous nucleation in pure water can be estimated by a simple calculation (Brennen 1995). Let us assume that the ephemeral vacancy caused by thermal motions has diameter equal to the intermolecular distance of water (d = 0.35 nm) and that such a vacancy rapidly saturates with water vapour, having absolute pressure equal to the vapour pressure of water (p_v = 2.3 kPa at 20°C). The absolute water pressure necessary to cause the expansion of the cavity can then be calculated using Laplace's equation (derived in a similar way as Eq. 1):

$$p_w = p_v - \frac{4T}{d} = -823 \text{ MPa} \tag{3}$$

This value, however, has never been measured in laboratory experiments. More often, major weakness occurs at the boundary between the liquid and the solid wall of the container or between the liquid and small particles suspended in the liquid. Rupture that occurs at these sites it is termed *heterogeneous nucleation*. This latter type of cavitation is of interest in tensiometer measurement.

The concept of heterogeneous cavitation will be further developed by considering the behaviour of a water reservoir bounded by a saturated ceramic filter (i.e. a tensiometer) as shown in Fig. 6. In this example, the saturation of the container system is imperfect—as shown in enlarged inset of Fig. 6a, there exists an idealised crevice on the container boundary which contains a finite quantity of air and water vapour. If the water pressure in the reservoir is dropped, the pressure within the crevice must also decrease, thereby increasing the gas volume according to its equation of state (Fig. 6b). If the water pressure in the sensor is dropped further, or if the volume of gas increases due to diffusion, a critical contact angle will eventually be reached which is the higher between the crevice opening angle and the receding contact angle (Mongiovì and Tarantino 2002). At this point, the stability of the growing air cavity cannot be maintained and it will be pulled from the crevice in a form of free cavity (Fig. 6c). An example of heterogenous cavitation triggered by air trapped in wall crevices is observed in a glass of champagne where diffusion of carbon dioxide into trapped air-filled crevices causes steady streams of bubbles to form on the sides of the glass (Balibar 2002).

The newly formed free cavity is unstable and will almost instantaneously expand to occupy a large part of the water reservoir. As the gas pressure in the cavity is initially very close to the water vapour pressure, the tensiometer will read an absolute pressure close to zero and a gauge pressure of about −100 kPa. This rapid jump to approximately −100 kPa gauge pressure is therefore a clear indication of cavitation having occurred in the system. It must be noted that heterogeneous cavitation in the tensiometer may also be triggered by gas nuclei entrapped in the porous ceramic rather than in the container wall as discussed by Tarantino and Mongiovì (2001) and Tarantino (2004).

2.5 Air-Entry

The *air-entry* value of a saturated porous solid is the gas-minus-liquid pressure differential which must be applied to the initially liquid-saturated material to initiate advective gas transport through the material. This ability results from menisci that form at the saturated-material boundary. The air-entry value can then be theoretically calculated by considering the force equilibrium at the air–water interface in a single narrow pore at the material outer surface. This leads to Equation 1 indicating that the magnitude of air–water pressure differential at break-through will be

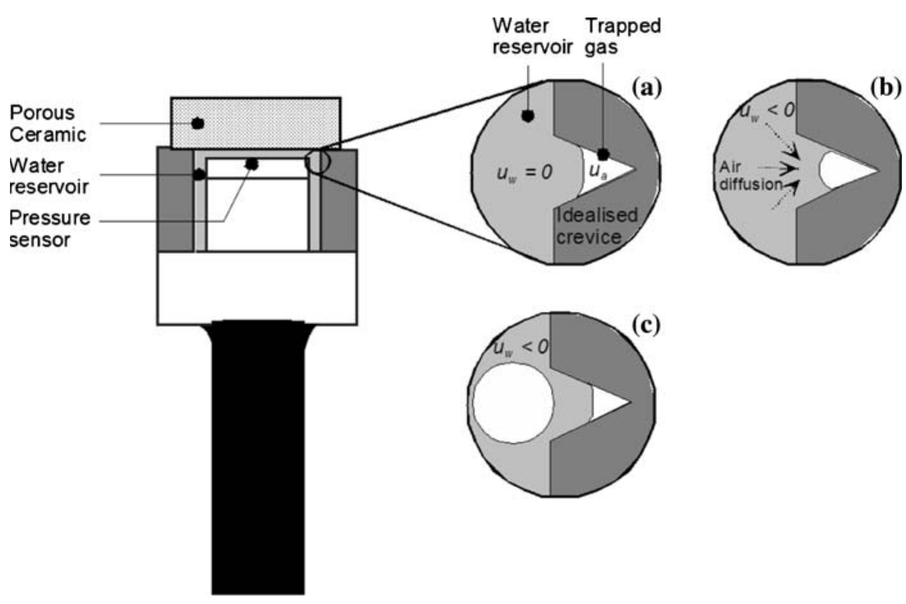

Fig. 6 The crevice model of heterogeneous nucleation

inversely proportional to the pore diameter. Therefore porous ceramics are typically used for this application as they can be made with uniform, highly controlled pore size distributions. The typical pore sizes used in tensiometers ranges from 6 µm to 0.16 µm corresponding to nominal air-entry values of 50–1,500 kPa, respectively. The actual air-entry value is typically provided by the manufacturer by measuring the air pressure applied to one side of the ceramic necessary to cause bubbling on the other side (*bubbling pressure*). Possible differences between air-entry value and bubbling pressure have been discussed by Tarantino (2004).

3 Measurement of Matric Suction Using Tensiometers

3.1 Evolution of the Tensiometer

Occasionally in the literature, users of tensiometers would record pressures below −100 kPa, but it was not until the work of Ridley (1993) was published that the geotechnical community became aware of the possibility of creating a tensiometer which can reliably measure negative water pressures down to −1,500 kPa. This work created a new class of tensiometer, known as the high capacity tensiometer (HCT), which took advantage of available higher air entry value ceramics (0.3, 0.55, 1.5 MPa) and was designed to permit the water reservoir of the device to achieve true tensile pressures.

3.2 HCT Design

The HCT design of Ridley (1993) and that of those that followed after it was designed to delay heterogeneous cavitation within the water contained within these devices. This involves minimising the volume and surface area of the internal water reservoir to reduce the absolute number of possible nucleation sites, with the aim being to be statistically less likely to suffer from unpredictable tension breakdowns (Ridley 1993). The second modification, introduced by Ridley and Burland (1995), involves the elimination from the design of the tensiometer any materials which are particularly good sources of nucleation sites, such as o-rings and elastomers. The influence of elastomers on the behaviour of HCT’s has been demonstrated by Take (2003). In an early version of the tensiometer developed at Cambridge University by Take (2003), an elastomer was used in the design to isolate the pressure sensor from externally applied effective stresses. Despite measuring tensions in excess of 100 kPa, these early prototypes illustrated a wide variation of maximum measurable suctions ranging from 270 kPa to 480 kPa. Once the elastomer was removed from the design of the sensor, nucleation occurred only at tensions greater than the nominal air entry value. This variation in maximum attainable tension was also reported in the observations of Guan and Fredlund (1997) in which an o-ring was also used in the design.

The schematics of several HCT reported in the literature are presented in Fig. 7, including the HCT developed at Imperial College (Ridley and Burland 1993, 1995), University of Saskatchewan (Guan and Fredlund 1997), University of São Paulo (Marinho and Pinto 1997), University of Trento (Tarantino and Mongiovi 2002), Massachusetts Institute of Technology (Sjoblom 2000; Toker 2002), Cambridge University (Take and Bolton 2003) and University of Durham (Lourenço et al. 2006). Also included in Fig. 7, is the Druck PDCR-81, a commonly used miniature pore pressure transducer which has sometimes been modified to act as a tensiometer. As can be seen in Fig. 7, all of these devices share a common design, with the only slight modification being in the Cambridge and the Druck devices which are intended for burial within soil, and as such, are designed to isolate the internal pressure sensing diaphragm from the effective stresses exerted on the outer case of the device. The gap between the pressure sensor and the outer shell ensures that any strains in the outer casing of the device are not transferred to the pressure sensing diaphragm, thus creating an apparent pressure change. This issue is obviously only relevant for HCT’s placed in a stress field, and not in the measurement of matric suction in soil samples.

3.3 Saturation

Although the design of HCT is an important consideration, design alone cannot ensure the measurement of tensile water pressures. Indeed, it can be argued that the most important factor determining the success or failure of tensiometer measurements relates to the saturation and preconditioning of the

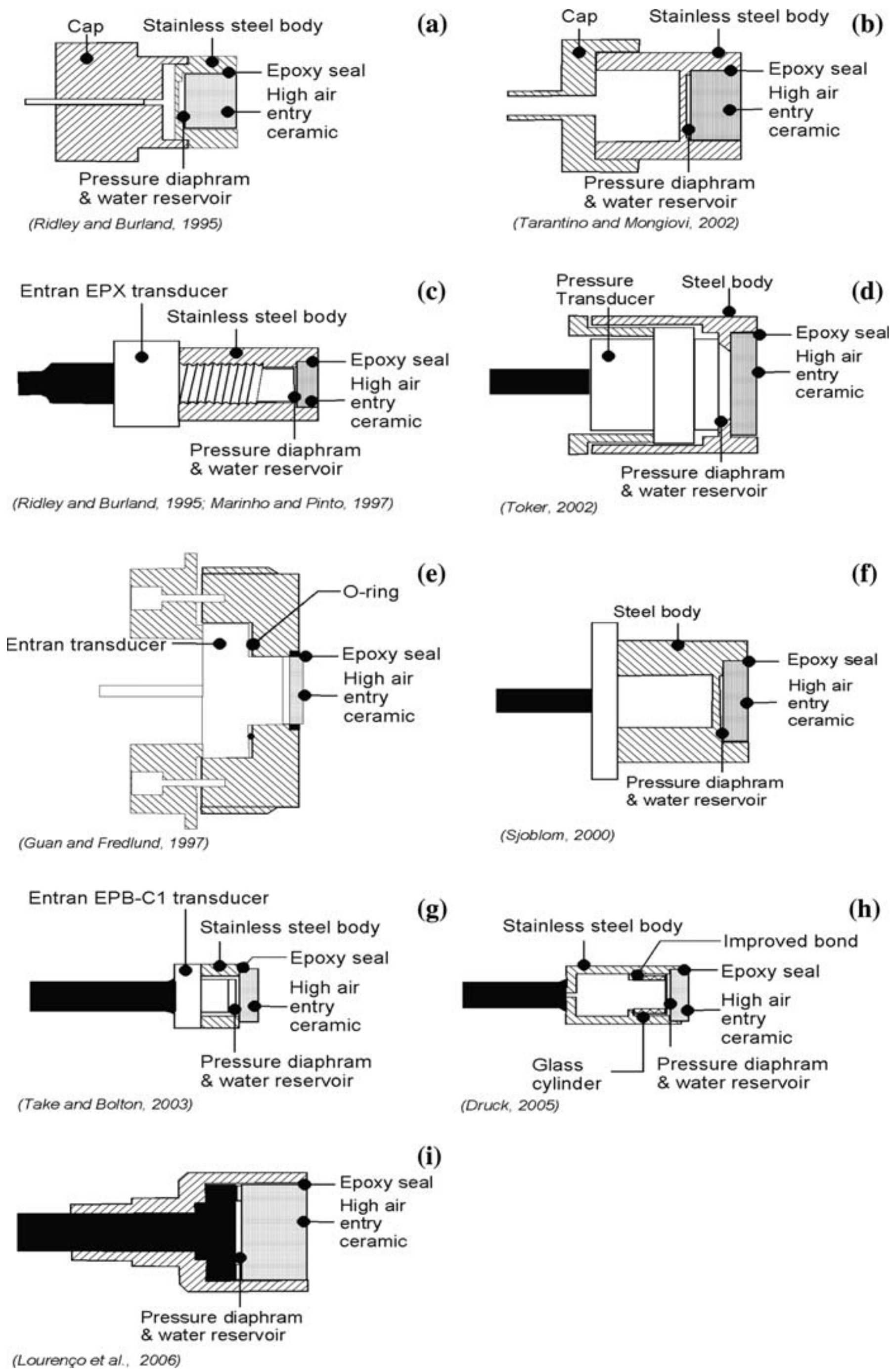

Fig. 7 High capacity tensiometers reported in the literature

water contained within the porous filter and reservoir of the device. The process of saturation of tensiometers has been examined by Take and Bolton (2003) following the work of Bishop and Eldin (1950) and Lowe and Johnson (1960). This work is based on the assumption that the air–water interface is flat and indicates that air within a porous filter of initial degree of saturation, S_i, and at an initial absolute pressure of P_i, will compress according to Boyle's law when pressure ΔP is applied, allowing water to enter pores once occupied by air if the volume of the porous ceramic is assumed constant. Henry's law dictates that the higher pressure will also result in additional air being dissolved into the pore water. The pressure change, ΔP, required to increase the degree of saturation of a porous element to its final saturation value, S, has been shown to be:

$$\Delta P = P_i \frac{(S - S_i)(1 - H)}{1 - S(1 - H)} \quad (4)$$

where, H is Henry's constant which is approximately 0.02 ml of air per ml of water at room temperature.

Since full saturation is required in the tensiometer (i.e. $S = 1$), the theoretical magnitude of applied pressure required to perform this task is a function of both the initial absolute pressure of the air in the voids and the initial degree of saturation of the porous disk. Therefore, if the initial absolute pressure is dropped close to 0 kPa absolute in a tensiometer which is as dry as possible, the pressure required for saturation can be minimized. Thus, Equation 4 provides a theoretical justification for a two-stage saturation process in which the tensiometer is first introduced to water under a high vacuum before a large positive pressure is applied. Such a process has been experimentally determined by researchers (e.g. Ridley and Burland 1999) to give the best results, with Tarantino and Mongiovì (2002) and Take and Bolton (2003) giving particular attention to the role of initial dryness of the porous filter by proposing a two chamber saturation to evacuate the tensiometer in the absence of water.

Indeed, pressure ΔP given by Eq. 4 is sufficient to dissolve most but not all the air in the ceramic and in the reservoir. This is because the air–water interface of air cavities retracting into the small pores of the ceramic and crevices on the reservoir walls is no longer flat but must become concave on the water side. The meniscus is then capable of sustaining high water pressures, thus preventing air dissolution. Figure 8a illustrates an ideal conical crevice. The depth h of the air cavity depends on the water pressure p_w, gas pressure p_g, the advancing contact angle θ_a and crevice opening φ as follows (Mongiovì and Tarantino 2002):

$$h = \frac{2T\cos(\theta_a - \varphi)}{\tan\varphi\ (p_g - p_w)} \quad (5)$$

Equation 5 suggests that the application of a positive water pressure will cause h to decrease, and hence the amount of air that is dissolved in water to increase. If, on return to atmospheric pressure, a significant quantity of the recently dissolved air does not return to the cavity, but rather, is preferentially exsolved where the water meets the free air (Ridley and Wray 1996), the amount of gas within the total system will be reduced. Thus, a higher water tension will be required to initiate nucleation at these nucleation sites than had existed previously. This is the reason why high capacity tensiometers are conditioned by the application of large positive water pressures prior to measurement (often called pre-pressurisation).

Equation 5 also suggests that depth h can reduce to zero (i.e. the air cavity completely dissolves) only if $\theta_a \leq 90 + \varphi$. The meniscus remains convex on the water side and will not be able to sustain a water pressure p_w greater than gas pressure p_g. In contrast, if $\theta_a > 90 + \varphi$, the meniscus can reverse its curvature and become concave on the water side. According to Equation 5, the air cavity will not dissolve regardless of the water pressure applied and its depth h will increase as the advancing contact angle θ_a increases. According to Harvey et al. (1944), air cavities that remain entrapped in crevices are likely to trigger cavitation when pressure is reduced and the meniscus curvature is reversed (Fig. 8b).

The cavitation nuclei that remain undissolved upon pressurization can be 'extracted' by cycles of cavitation followed by large positive pressures according to the mechanism suggested by Tarantino and Mongiovì (2001). This saturation technique is particularly important in HCT's with very high air entry value ceramic filters (e.g. 1.5 MPa), as it has been observed that one application of high positive pressures is not sufficient to dissolve sufficient trapped gas within a HCT (e.g. Tarantino and Mongiovì 2001) but cycles of cavitation followed by pressurisation can significantly improve measurement duration and maximum sustainable tension

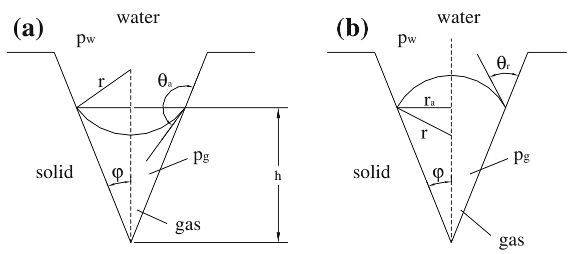

Fig. 8 Idealised conical crevice. (**a**) Gas cavity subjected to positive pressure. (**b**) cavity subjected to negative pressure

(Tarantino 2004). In lower air entry value porous filters (e.g. 0.1, 0.3 MPa), a single pressurisation event has been observed by Take and Bolton (2003) to be sufficient for accurate measurement.

The duration of application of high pre-pressurisation pressures is another factor that may affect saturation of the porous filter. Intuitively, the higher the duration of pressurisation, the higher should be the saturation of the ceramic filter and, hence, the measurement duration and maximum sustainable tension. However, Tarantino and Mongiovì (2001) report the response of one Imperial College tensiometer after 1 year saturation at 4 MPa. During this period, the tensiometer remained continuously stored in the saturation chamber since not in use. The first measurement recorded by this tensiometer, after removal from the saturation chamber showed cavitation occurred after just some seconds at a tensile stress of about 650 kPa. This poor response was unexpected as the tensiometer was assumed to be fully saturated after such a long period of pressurisation.

After a single cycle of cavitation followed by pressurisation, the tensiometer was capable of measuring a remarkable suction, even much higher than the nominal air entry value of the porous ceramic (2600 kPa). This would suggest that cycles of cavitation/pressurisation are more effective than pressurisation itself. However, more data would be needed to corroborate such an assumption.

3.4 Measurement Range

If saturated sufficiently, it has been shown by Ridley and Burland (1995) that the maximum sustainable suction of a HCT is strictly a function of the air entry value of the ceramic. This is because the highest air entry value of currently available ceramics is nominally 1,500 kPa, whilst the tensile strength of water is approximately two orders of magnitude greater. As discussed by Take and Bolton (2004), caution should be exercised when interpreting observations of suction in excess of the nominal air entry value. The observed suction in this case could either be the true value or could be an artefact of the ongoing process of air entry. Thus, the reliable measurement range of a HCT should be taken as the maximum full scale positive pressure of the pressure sensitive diaphragm to a negative value corresponding to the magnitude of the porous filter's air entry value.

3.5 Contact

If good contact is not established between the soil pore water and the porous filter of the HCT, misleading observations of matric suction will be obtained. The most drastic example is of a tensiometer with no contact. In this scenario, the device will quickly desaturate as it attempts to come into moisture equilibrium with the air in the gap between the tensiometer and the soil surface. The measured suction will therefore not be representative of that found in the soil. This issue has been overcome by placing a small amount of slurry on the tip of the tensiometer to ensure intimate contact between the porous filter and the surrounding soil. It is recommended to prepare the slurry at a water content near the liquid limit, preferably using the fines of the same material in which the tensiometer is going to be installed. It should be noted that the response time of the HCT will depend on the degree of saturation and unsaturated permeability of the soil, but also on the water content of the slurry used to improve the contact. If the slurry is prepared excessively wet of the liquid limit, the addition of this extra moisture into the system will lengthen the time required for moisture equilibrium to occur with the native soil (e.g. Boso et al. 2004; Oliveira and Marinho 2008).

3.6 Osmotic Effect of the Porous Ceramic

Marinho and Chandler (1994) suggested that the fine porous stone interface could prevent the passage of ions from the soil water into the tensiometer reservoir. As a result, an osmotic suction could develop in the tensiometer because of the concentration gradient. The tensiometer would then measure a value ranging between matric suction and total suction.

A simple test was carried out by Tarantino (2004) to verify whether porous ceramic has an osmotic effect, i.e. is capable of retaining ions dissolved in soil water. The tensiometer was immersed in 4 different NaCl solutions having osmotic suction of 216, 432, 650, and 880 kPa. The tensiometer was kept in salt water for about 15 min and then replaced in free water for other 15 min prior to testing the subsequent NaCl solution. The pressure recorded by the tensiometer did not change throughout the test, indicating that the high air entry ceramic does not have an osmotic effect, at least for this type of solute.

However, it is possible that osmotic effects could arise for different type of solutes.

3.7 Challenges

3.7.1 Interpretation

Unlike the measurement of positive pore water pressures, the measurement of negative water pressures brings with it some unique challenges—particularly in the interpretation of suction data, and in the long term measurement of soil suction. When measuring suctions using tensiometers, it is not always apparent when the tensiometer has stopped recording the true value of suction. Indeed, it has been argued that the biggest challenge associated with tensiometer measurement is how to discriminate a good measurement from a bad one (Tarantino 2004). This challenge has been rigorously demonstrated by Take and Bolton (2003) in which tensiometers were saturated to various degrees of saturation. To illustrate this problem, the behaviour of a tensiometer having been saturated to a degree of saturation of 0.77 has been reproduced as Fig. 9. The tensiometer was placed in water and then subjected to known values of negative water pressure. As shown in Fig. 9, the device initially correctly measures the suction and continues to do so until the applied pressure drops below −65 kPa (point B), at which point the device becomes completely detached from reality. This demonstration illustrates the high probability for erroneous tensiometer measurements if the device is not properly saturated or has been allowed to desaturate in-situ. Other examples of erroneous measurement occurring when ceramic disk is not adequately saturated are provided by Tarantino (2004). Strategies to overcome this issue include only relying on highly qualified personnel to saturate, install and monitor tensiometers; using two HCT's to check the internal consistency of suction observations by using two or more tensiometers simultaneously placed on the same sample (Tarantino and Mongiovì 2001); identifying indicators of adequate saturation of the ceramic disk (Tarantino 2004); or using tensiometers paired with other indirect methods of suction measurement, again to check for consistency (Whalley et al. 2006).

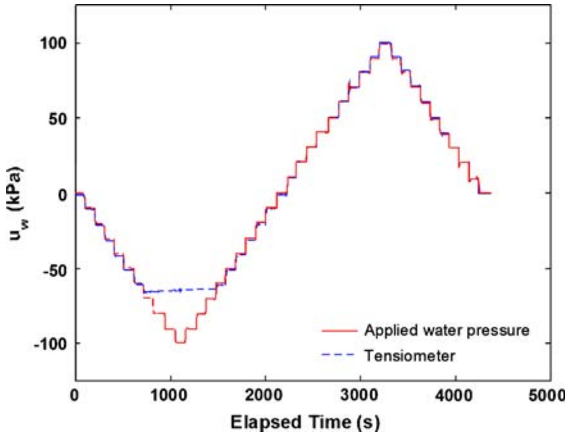

Fig. 9 Challenge of interpreting tensiometer data (Take and Bolton 2003)

3.7.2 Long Term Measurement

The second major challenge currently facing HCT's relates to their ability to obtain long term measurements. Although the conditioning process of applying high positive water pressures can reduce the amount of gas trapped in crevices, it can never completely eliminate it. It has already been noted that the process of diffusion can slowly lead to bubble growth over the long term. Thus, the stabilisation afforded by the conditioning process must be viewed as temporary—the water held in the reservoir is metastable and all tensiometers will inevitably experience nucleation. However, no experimental data currently exists to adequately predict the length of time a tensiometer can remain operational at high suctions; such is the variability in the instability of tension breakdown. This topic is a current area of research.

Measurements at relatively high suction (800–900 kPa) may last several days. Cunningham et al. (2003) report measurement of s = 850 kPa for 8 days and suction measurement in the osmotic oedometer presented by Tarantino and Mongiovì (2000) could last more than 24 days for suctions ranging from 250 to 800 kPa.

4 Measurement of Matric Suction Using the Axis Translation Technique

4.1 Principle

The historical limitation of traditional tensiometer measurements to matric suction values up to 80 kPa led to the development of an alternative laboratory technique (Richards 1941, 1947) which sidesteps this obstacle by artificially raising the atmospheric pressure experienced by a soil sample. The working principle of this technique is the familiar model of a capillary pore and is reproduced in Fig. 10a for the typical case in which the pore is subjected to atmospheric air pressure (i.e. zero gauge pressure) with the water climbing the capillary tube having pressure less than atmospheric. If in the laboratory environment, this same capillary tube was close-ended and subjected to an elevated air pressure, the system would respond as shown in Fig. 10b. In Fig. 10b, the assumption has been made that the water and solid boundaries are sufficiently incompressible that the curvature of the meniscus interface is not significantly altered (Olson and Langfelder 1965). If this is true, Eq. 2 predicts that the pressure difference $u_a - u_w$, otherwise known as the matric suction, also does not change. The end result is that the water pressures within the capillary tube have now risen to positive gauge pressures.

The significance of this elevation in water pressure is illustrated in Fig. 11 for the measurement of matric suction in unsaturated soils. In Fig. 11a, a sample of soil has a matric suction $(u_a - u_w)$ in excess of 100 kPa. As a result, if this suction is to be quantified a pore water pressure lower than −100 kPa must be recorded. However, if this same sample is subjected to a large positive air pressure, the water pressure in the soil can be raised to an easily measurable positive gauge pressure. If drainage of the pore water is prevented from the sample, the matric suction in the

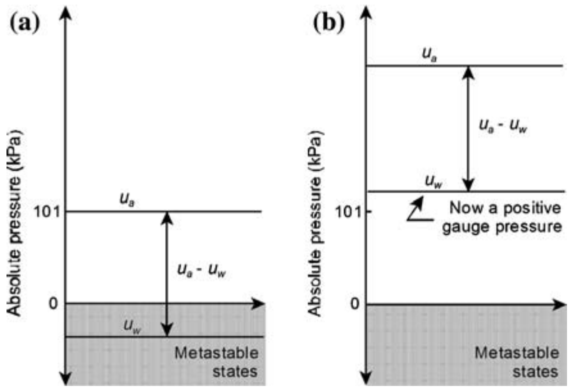

Fig. 11 Use of the axis translation technique to avoid metastable states. (**a**) Atmospheric conditions; (**b**) axis-translation

soil can now be calculated as the difference of these two known pressures. Thus, this technique is referred to as the "axis translation technique" as water pressure has been translated upwards with the air pressure origin and away from the region of metastable states. The above discussion has focussed on the use of the axis translation technique to measure suction. This technique may also be used to impose or control suction. This can be accomplished by once again elevating the ambient air pressure within the test cell, but this time controlling also the pore water pressure through a saturated porous filter in contact with the sample (and, hence, allowing water drainage from the sample until equilibrium conditions are obtained).

4.2 Design of Axis Translation Test Chambers

The axis translation technique has been used to measure or control suction in triaxial tests, oedometers, and in direct shear tests (e.g. Vanapalli et al. 2008, this issue). However, by far the most common use of the axis translation technique is in the pressure plate apparatus which is used to determine the soil water retention curve (e.g. Bocking and Fredlund 1980; Leong et al. 2004; Wang and Benson 2004, amongst others). If only suction measurement is required, only a sealed chamber which eliminates the possibility of advective air flow and a pore water pressure measurement device is required. If the axis translation technique is applied to impose suction, a highly saturated porous ceramic filter and water reservoir are also required to permit water to enter or

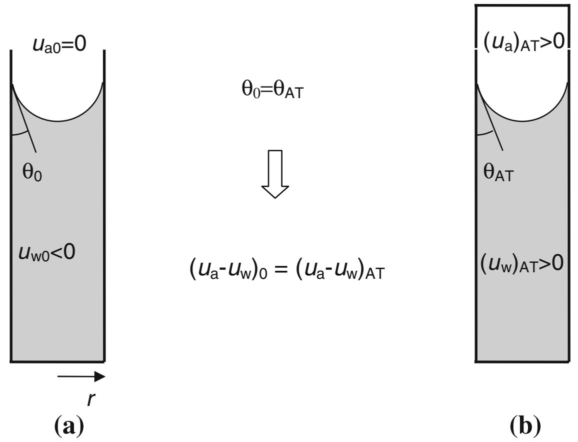

Fig. 10 Working principle of axis translation technique

leave the sample, as is a procedure to quantify these moisture changes.

4.3 Saturation

As was the case in the measurement of matric suction with HCT's, it could be argued that the most important factor determining the success or failure of the axis translation technique relates to the adequate saturation of the porous ceramic disk. For if the ceramic disk is not sufficiently saturated or if bubbles exist in the water reservoir, any measured water volume changes in response to changes in applied matric are meaningless. However, it must be stressed that unlike the HCT the porous ceramic disk and water reservoir are never subjected to negative gauge pressures. As a result, the highly controlled procedures for the conditioning of porous filter—reservoir system to suppress potential cavitation nuclei are typically not followed with the same rigour. However, saturation is typically achieved by broadly the same two stage method: the air chamber above the ceramic is typically evacuated before water is introduced into the cell, followed by pressurising the system to a high positive water pressure. The measurement of the saturated permeability is a good reference for the saturation condition of the system.

4.4 Measurement Range

The range of axis translation technique to measure or control matric suction is limited by two factors: the maximum air pressure which can be imposed on the system, and the air entry value of the ceramic filter. In practice, the maximum measurable suction using the axis translation technique is strictly a function of the air entry value of the ceramic, as the highest air entry value of currently available ceramics is nominally 1,500 kPa.

4.5 Contact

The contact between the pore water and the water of the porous filter is paramount for reliable measurements of suction using the axis translation technique. Poor contact may dramatically increase the drainage time required for equilibrium or may completely eliminate water flow through the ceramic. If there is no continuity of the water in the soil and the water in the ceramic disk, the air pressure will act around the soil sample causing a no flow condition to occur.

4.6 Challenges

4.6.1 Equilibrium Time

The axis translation technique, when used to impose matric suction, does not yield instantaneous results. Even in the absence of soil, the time required for the porous ceramic filter to come into equilibrium with a change in air pressure is on the order of a few minutes, provided the amount of free water on the top of the ceramic disk is small (e.g. Schreiner 1988). Once a soil sample has been added to the system, the time for equilibrium is extended due to the size and permeability of the soil sample. The ASTM D-6836-02 standard establishes that the equilibrium time should be monitored according to the level of suction and states that for suction less than 500 kPa it is considered equilibrated the system that does not drain any water for at least 24 h, for suction between 500 and 1,000 kPa this time should be 48 h and for suction greater than 1,000 kPa no water should be drained for at least 96 h. Many authors monitored the equilibrium time behaviour, some of them reporting that the equilibrium is not reached (e.g. Gee et al. 2002) and others reporting that the equilibrium is reached (e.g. Leong et al. 2004). A close look in the data of those papers seems to suggest that the condition established by the ASTM D-6836 is not attained. Thus, one of the challenges associated with the axis translation technique is the potentially long equilibrium time for each imposed suction.

One interesting strategy to overcome this challenge is to adopt the controlled outflow method developed by Lorentz et al. (1993). The method consist in applying air pressure allowing water to drain as in the usual procedure, but closing the water drainage before equilibration is attained. Closing the water drainage before equilibrium is reached will induce an equilibrium of pressure, related to the water content present in the sample. The air pressure applied minus the water pressure response is the suction imposed. This method claims to be quicker than the original procedure. Lorentz et al. (1993) reported that for sands each point of the soil water retention curve takes between 20 and 40 min. This method has been used by many authors with reported success (e.g. Fourie and Papageorgiou 1995; Machado and Dourado 2001; Knight and Kotha 2001).

4.6.2 Moisture Loss Through Compressed Air Lines

The most intuitive way to apply the elevated air pressure required for the axis translation technique is to use compressed air. However, this could lead to a non-obvious consequence of completely erroneous measurements at low suctions. Figure 12 presents the thermodynamic relation between suction and relative humidity. If a suction of 50 kPa is to be imposed in a soil sample the equivalent relative humidity should be 99.96%. In the case of the air coming from the compressor be at a relative humidity of 99.7% (which is high and possible) the equivalent suction should be about 400 kPa. This difference will cause instability of the system as equilibrium will never be attained. In order to minimize this effect a closed system may be adopted using nitrogen. A numerical analysis of the effect of moisture loss through compressed air lines has been carried out by Romero (2001).

4.6.3 Air Diffusion

The long equilibrium times associated with the drained axis translation technique make these tests particularly susceptible to the process of air diffusion. Fredlund and Rahardjo (1993) suggest that tests lasting more than one day (without equilibrium attained) will experience air diffusion. As mentioned earlier, if bubbles exist in the water reservoir, measured volume changes are rendered meaningless.

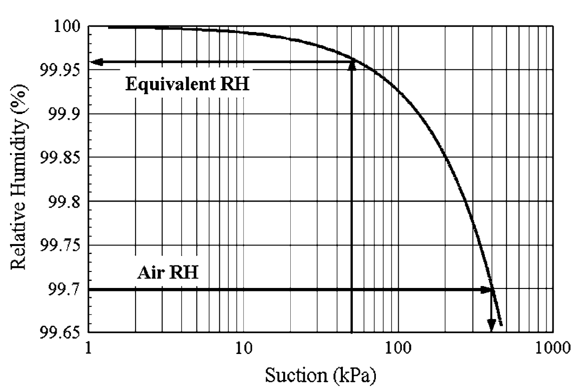

Fig. 12 Thermodynamic relation between suction and relative humidity and the eventual difference between applied suction and the equivalent suction of the air

Air diffusion through the ceramic disk can be minimised by elevating the water pressure in the reservoir. The rate of accumulation of dissolved air beneath the ceramic disc can be derived by considering the Fick's law for air diffusion combined with the ideal gas law to convert air mass to air volume and concentration differential to matric suction (Fredlund and Rahardjo 1993; Romero 1999):

$$\frac{dV_d}{dt} = \frac{nADh(u_a - u_w)}{(u_w + u_{\mathrm{atm}})\ t_c} \qquad (6)$$

where V_{d} is the volume of accumulated air, t is the time, n, A, and t_{c} are the porosity, cross-sectional area, and thickness disc of the ceramic respectively, h is the volumetric coefficient of solubility (h = 0.018 at 22°C), D is the air diffusion coefficient through the saturated ceramic disc, u_{atm} represents the absolute atmospheric pressure, u_{a} and u_{w} refer to the air and water gauge pressure, and $u_{\mathrm{a}} - u_{\mathrm{w}}$ is the applied matric suction. Equation (6) shows that the rate of accumulation of dissolved air at given matric suction $u_{\mathrm{a}} - u_{\mathrm{w}}$ can be reduced if water pressure in the reservoir u_{w} is increased, i.e. a back-water pressure is applied.

4.6.4 High Degrees of Saturation

As demonstrated in Fig. 10, the basic assumption upon which the axis translation technique has been built states that the water and solid boundaries are sufficiently incompressible to not modify the curvature of the interface upon the application of an elevated air pressure. If the curvature of the menisci remains constant, any change in air pressure is directly translated into an equal increase in pore water pressure. This is valid provided there are no isolated air bubbles in the soil mass. This assumption has been validated by Hilf (1956) and Bishop and Donald (1961), by allowing a sample to come to equilibrium under a specific matric suction ($u_a - u_w$) and then changing the air pressure and measuring the corresponding change in pore water pressure, and Tarantino et al. (2000) in the range of absolute negative pressures.

In general the air pressure is considered to be atmospheric before the axis translation technique is applied. Hilf (1956) suggested that air pressure immediately after compaction may be initially higher than atmospheric but rapidly tends to recover to the atmospheric value. Barden and Sides (1970) infer from experimental data that the occluded air bubbles do not equilibrate rapidly as usually assumed. The coefficient of diffusion of free water is 50 times higher than that occurring in saturated soils. This difference seems to be due to increase in viscosity and tortuosity. This has great implication on the use of axis translation technique.

Bocking and Fredlund (1980) performed a theoretical study evaluating the effect of occluded air during the use of the axis translation technique for measuring suction. The results suggested that the suction is over estimated if the soils have a highly compressible structure. Chahal and Yong (1965) is surprisingly one of the very few studies that has attempted to validate the use of the axis translation technique by using tensiometers in the same apparatus. The expected effect of the use of the axis translation technique is that it may inhibit the formation of nucleation inside the soil. Chahal and Yong (1965) showed that when the pressure plate apparatus is converted into a tensiometer by the reduction of the air pressure to the atmospheric conditions the pore water pressure measured is smaller than the difference between air and water pressure during the axis translation. Lourenço et al. (2006) has more recently noted a similar discrepancy.

One theory to explain this response can be generated by considering again the capillary tube conceptual model. Unlike the capillary tubes discussed earlier in the paper, the capillary tube in this

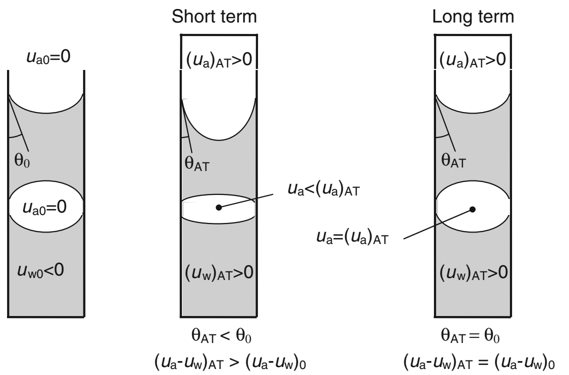

Fig. 13 Working principle of axis translation technique in presence of occluded air. (**a**) Negative water pressure. (**b**) Positive water pressure in the short term. (**c**) Positive water pressure in the long term

discussion (Fig. 13a) contains an entrapped air cavity at some elevation below the atmospheric air–water interface dictated by the contact angle θ_0. If in the laboratory environment, this same capillary tube was sealed and subjected to an elevated air pressure, the relative high compressibility of the air cavity will lead to a significant reduction in the cavity's volume, the increase in the cavity air pressure being lower than the external air pressure increase. If the gas-liquid-solid junction of the outer meniscus remains fixed, as occurs to the drop on the tilting plate in Fig. 2, the curvature of the air–water interface θ_{AT} will increase because of the compression of the entrapped air cavity as shown in Fig. 13b, causing the pressure differential between air and water pressure to increase. This is in agreement with the findings of Chahal and Yong (1965). This change in contact angle with applied air pressure is in contrast to the assumptions behind the axis translation technique.

However, if in the long term the external air at elevated pressure would diffuse through the liquid into the air cavity, an equilibrium will be restored. The outer meniscus will recover the original curvature and so will the suction (Fig. 13c). In other words, limitations of the axis-translation technique at high degrees of saturation essentially lie on the slow rate of air diffusion to the air cavities.

To avoid the meniscus deformation shown in Fig. 13b, the external air pressure can be varied slowly to allow the air to diffuse towards the cavities (Di Mariano 2000; Romero 2001). When controlling suction using the axis-translation, an alternative technique is to modify the water pressure while keeping constant the external air pressure. Such a technique is referred to as 'air-overpressure' technique in contrast to the classical 'water-subpressure' technique where air pressure is changed while keeping constant the water pressure (Romero 2001). Using the air-overpressure technique, deformation associated with the temporary suction increase shown in Fig. 13b can be avoided. This deformation can also be viewed as generated by the external air pressure which temporarily acts as total stress.

5 Final Remarks

Experimental equipment for the measurement of matric suction in unsaturated soils using tensiometers and the axis translation technique have been shown to share a common working principle; that is, the measurement of a pressure differential across a high air entry ceramic disk. In this paper, the current state of the art in these two suction measurement techniques has been presented and discussed together to underline their similarities in saturation procedures, the need for intimate contact, measurement range, and challenges and limitations associated with air diffusion and air entry. Although the advent of the HCT has now permitted direct matric suction measurements to $-1{,}500$ kPa, the ease of use of the axis translation technique will ensure that both of these techniques will be used to quantify the matric suction of soils in laboratory tests for the foreseeable future.

References

Alberty RA (1987) Physical chemistry. Wiley

Balibar S (2002) Nucleation in quantum liquids. J Low Temp Phys 129(5–6):363–421

Barden L, Sides GR (1970) Engineering behaviour and structure of compacted clay. ASCE J Soil Mech Found Div 96(SM4): 33–51

Berry RS, Rice SA, Ross J (1980) Physical chemistry. Wiley

Bishop AW, Donald IB (1961) The experimental study of partly saturated soil in the triaxial apparatus. In: Proceedings of 5th international conference on soil mechanics, vol 1. Paris, pp 13–21

Bishop AW, Eldin G (1950) Undrained triaxial tests on saturated sands and their significance in the general theory of shear strength. Géotechnique 2(1):13–32

Bocking KA, Fredlund, DG (1980) Limitation of the axis translation technique. In: 4th International conference on expansive soils, vol 1. Colorado, pp 117–135

Boso M, Tarantino A, Mongiovì L (2004) Shear strength behaviour of a reconstituted clayey silt. Advances in testing, modelling and engineering applications. In: Mancuso C, Tarantino A (eds) Proceedings of an international workshop. Anacapri, 22–24 June 2004. Balkema, Rotterdam, pp 1–14

Brennen CE (1995) Cavitation and bubble dynamics. Oxford University Press

Chahal RS, Yong RN (1965) Validity of the soil water characteristic determined with the pressurized apparatus. Soil Sci 99(2): 98–103

Cunningham MR, Ridley AM, Dineen K, Burland JB (2003) The mechanical behaviour of a reconstituted unsaturated silty clay. Géotechnique, 53:183–194

De Benedetti PG (1996) Metastable liquids. Princeton University Press

Di Mariano A (2000) Le argille a scaglie e il ruolo della suzione sulla loro deformabilità. PhD Thesis, Università di Palermo e di Catania

Fourie AB, Papageorgiou G (1995) A technique for the rapid determination of the moisture retention relationship and hydraulic conductivity of unsaturated soils. In: 1st International conference on unsaturated soils, vol 1. Paris, pp 485–490

Fredlund DG, Rahardjo H (1993) Soil mechanics for unsaturated soils. Wiley-Interscience Publications

Gee GW, Ward AL, Zhang ZF, Campbell GS, Mathison J (2002) The influence of hydraulic nonequilibrium on pressure plate data. Vadose Zone J 1:172–178

Gibbs JW (1948) The collected works of J. Willard Gibbs. Volume 1: Thermodynamics. Yale University Press

Guan Y, Fredlund DG (1997) Use of tensile strength of water for the direct measurement of high soil suction. Can Geotech J 34:604–614

Harvey EN, Barnes DK, McElroy WD, Whiteley AH, Pease DC, Cooper KW (1944) Bubble formations in animal, 1-physical factor. J Cell Comp Physiol 24(1): 1–22

Hilf JW (1956) An investigation of pore-water pressure in compacted cohesive soils. Ph.D. thesis, Technical Memorandum 654, U.S. Department of the Interior Bureau of Reclamation, Denver, Colorado

Johnson RE, Detre RH (1969) Wettability and contact angles. In: Matijevic E, Eirich FR (eds) Surface and colloid science, vol 2. Wiley, pp 85–152

Knapp RT, Daily JW, Hammit FG (1970) Cavitation. McGraw-Hill Book Company

Knight MA, Kotha SM (2001) Measurement of geotextile-water characteristic curves using a controlled outflow capillary pressure cell. Geosynth Int 8(3): 271–282

Leong EC, Tripathy S, Rahardjo H (2004) A Modified Pressure Plate Apparatus. Geotech Test J 27(3):322–331

Lorentz SA, DurnFord DS, Corey A (1993) Liquid retention measurement on porous media using a controlled outflow cell. In: Proceedings of American Society of Agronomy – Crop Science Society of America – Soil Science Society of America 1991 annual meeting. Denver, Colorado

Lourenço SDN, Gallipoli D, Toll DG, Evans FD (2006) Development of a commercial tensiometer for triaxial testing of unsaturated soils. In: Miller GA, Zapata CE, Houston SL, Fredlund DG (eds) Proceedings of 4th international conference on unsaturated soils, Phoenix, Geotechnical Special Publication 147, vol 2. ASCE, Reston, pp 1875–1886

Lowe J, Johnson TC (1960) User of back-pressure to increase degree of saturation of triaxial test specimens. ASCE research conference on shear strength of cohesive soils. Bolder, Colorado, pp 819–836

Machado SL, Dourado KA (2001) New techniques for determining the soil water characteristic curve for soils. In: 4th Brazilian symposium on unsaturated soils, vol 1. Porto Alegre, pp 325–336 (In Portuguese)

Marinho FAM, Chandler RJ (1994) Discussion: a new instrument for the measurement of soil moisture suction. Géotechnique 44(3):551–556

Marinho FAM, Pinto CS (1997) Soil suction measurement using a tensiometer. Symposium on recent development in soil and pavement mechanics, Rio de Janeiro, June, pp 249–254

Mongiovì L, Tarantino A (2002) Pore water pressure measurement in unsaturated soils. In: Proceedings of international workshop on "Clay behaviour: chemo-mechanical coupling", Maratea, Italy, June 2001. A. A. Balkema, Rotterdam, pp 233–246

Oliveira OM, Marinho FAM (2003) Unsaturated shear strength behaviour of a compacted residual soil. In: Second Asia conference on unsaturated soils, vol 1. Osaka, pp 237–242

Oliveira OM, Marinho FAM (2008) Suction equilibration time for a high capacity tensiometer. Geotech Test J 31(1):1–5 (Submitted for publication)

Olson RE, Langfelder LJ (1965) Pore water pressure in saturated soils. ASCE J Soil Mech Found Div SM4:127–150

Richards LA (1941) A pressure-membrane extraction apparatus for soil solution. Soil Sci 51(5):377–386

Richards LA (1947) Pressure-membrane apparatus – construction and use. Agric Eng 28:451–460

Ridley, AM (1993) The measurement of soil moisture suction. Ph.D. Thesis, University of London

Ridley AM, Burland JB (1993) A new instrument for the measurement of soil moisture suction. Géotechnique 43(2): 321–324

Ridley AM, Burland JB (1995) Measurement of suction in materials which swell. Appl Mech Rev 48(9):727–732

Ridley AM, Burland JB (1999) Discussion: use of tensile strength of water for the direct measurement of high soil suction. Can Geotech J 36:178–180

Ridley AM, Wray WK (1996) Suction measurement: a review of current theory and practices. In: Alonso EE, Delage P (eds) Unsaturated soils, pp 1293–1322

Ridley AM, Schnaid F, da Silva GF, Bica AVD (1997) In situ suction measurements in a residual soil of southern Brasil. In: de Campos TMP, Vargas EA Jr, Bastos F (eds) NSAT'97–3° Simpósio Brasileiro sobre Solos Não Saturados, Rio de Janeiro, Brasil, vol 2, pp 537–542

Romero E (1999) Characterisation and thermo-hydromechanical behaviour of unsaturated Boom Clay: an experimental study. PhD thesis, Universitad Politecnica de Cataluna

Romero E (2001) Controlled-suction techniques. 4° Simpósio Brasileiro de Solos Nâo Saturados Ñ SAT'2001. In: Gehling WYY, Schnaid F (eds) PortoAlegre, Brasil, pp 535–542

Rowlinson JS (1988) J.D. van der Waals: on the continuity of the gaseous and liquid states. North-Holland

Schreiner, HD (1988) Volume change of compacted highly plastic African clays. PhD thesis, Imperial College, 313 pp

Sjoblom KJ (2000) The mechanisms involved during the desaturation process of a porous matrix. PhD dissertation, Massachusetts Institute of Technology, Boston

Stannard DI (1992) Tensiometers – theory, construction, and use. Geotech Test J 15(1):48–58

Take WA (2003) The influence of seasonal moisture cycles on clay slopes. PhD dissertation, University of Cambridge, Cambridge

Take WA, Bolton MD (2003) Tensiometer saturation and the reliable measurement of matric suction. Geotechnique 53(2):159–172

Take WA, Bolton MD (2004) Discussion. Geotechnique 54(3):229–232

Tarantino A (2004) Panel lecture: direct measurement of soil water tension. In: Proceedings of 3rd international conference on unsaturated soils, vol 3. Recife, Brasil, pp 1005–1017

Tarantino A, Mongiovì L (2000) Experimental investigations on the stress variables governing unsaturated soil behaviour at medium to high degrees of saturation. In: Tarantino A, Mancuso C (eds) Experimental evidence and theoretical approaches in unsaturated soils. A.A. Balkema, Rotterdam, pp 3–19

Tarantino A, Mongiovì L (2001) Experimental procedures and cavitation mechanisms in tensiometer measurements. Geotech Geol Eng 19(3–4): 189–210

Tarantino A, Mongiovì L (2002) Design and construction of a tensiometer for direct measurement of matric suction. In: Proceedings of 3rd international conference on unsaturated soils, vol 1. Recife, pp 319–324

Tarantino A, Tombolato S (2005) Coupling of hydraulic and mechanical behaviour in unsaturated compacted clay. Géotechnique 55(4):307–317

Toker NK (2002) Improvements and reliability of MIT tensiometers and studies on soil moisture characteristic curves. MSc dissertation, Massachusetts Institute of Technology, Boston

Vanapalli SK, Sharma RS, Nicotera MV (2008) Axis-translation and negative water column techniques for suction control. Geotech Geol Eng (this issue). doi:10.1007/s10706-008-9206-3

Wang X, Benson C (2004), Measuring the soil water characteristic curve with the leak-free pressure plate extractor. ASTM Geotech Test J 27(2):1–10

Whalley WR, Clark LJ, Take WA, Bird NRA, Leech PK, Cope RE, Watts CW (2007) A porous-matrix sensor to measure the matric potential of soil water in the field. Eur J Soil Sci 58(1):18–25. doi:10.1111/j.1365-2389.2006.00790.x

Zheng Q, Durben DJ, Wolf GH, Angell CA (1991) Liquids at large negative pressures: water at the homogeneous nucleation limit. Science 254(5033):829–832

Indirect Measurement of Suction

Rifat Bulut · Eng Choon Leong

Originally published in the journal *Geotechnical and Geological Engineering*, Volume 26, No. 6, 633–644.
DOI: 10.1007/s10706-008-9197-0

Abstract This paper reports on indirect soil suction measurement methods. Indirect suction measurement techniques measure the moisture equilibrium condition of the soil instead of suction. The moisture equilibrium condition of the soil can be determined by primary means as in vapor pressure, secondary means as through another porous medium or tertiary means as in measuring other physical properties of the porous medium that indicates its moisture equilibrium condition. Indirect suction measurement techniques employing primary means include thermocouple psychrometers, transistor psychrometer and chilled-mirror psychrometer. Indirect suction measurement techniques employing secondary means includes the filter paper method and indirect suction measurement techniques employing tertiary means include thermal conductivity sensors and electrical conductivity sensors. These techniques have been widely used in engineering practice and in research laboratories. However, each of these techniques has its own limitations and capabilities, and active research into improving these techniques is ongoing in universities, research laboratories, and private sector. This paper outlines working principles, calibration, measurement, and application areas of these methods based on recent literature and practice.

Keywords Soil suction · Thermocouple · Transistor · Chilled-mirror · Psychrometer · Filter paper · Thermal conductivity · Electrical conductivity

R. Bulut (✉)
School of Civil & Environmental Engineering, Oklahoma State University, 207 Engineering South, Stillwater, OK 74078, USA
e-mail: rifat.bulut@okstate.edu

E. C. Leong
School of Civil and Environmental Engineering, Nanyang Technological University, Singapore, Singapore

1 Introduction

The understanding and wide acceptance of unsaturated soil mechanics principles has produced a gradual change in geotechnical engineering practice. There is more than ever a greater need for reliable soil suction measurement techniques as soil suction becomes an integral part of engineering practice in many situations involving unsaturated soils. Soil suction is a result of capillary action, surface energy properties of soil particles, and ionic concentration of the pore water. Total suction results when both mechanisms are active. Matric suction results when only capillary action and surface energy properties are active. Significant contributions have been made by geotechnical engineers in the measurement of soil suction. However, there is still need for research into the measurement of both matric and total suction in

DOI: 10.1007/978-1-4020-8819-3_3

the field and laboratory. Almost all suction measurement methods have shortcomings including such aspects as the range of application, cost, reliability, and practicality.

This paper reviews indirect suction measurement techniques based on the means of measuring moisture equilibrium conditions in the soil. Indirect measurement techniques employing primary means measure the vapor pressure, e.g. thermocouple psychrometer, transistor psychrometer, and chilled-mirror psychrometer. Indirect measurement techniques employing secondary means measure the moisture equilibrium condition of another porous medium, e.g. the filter paper method. Indirect measurement techniques employing tertiary means measure other physical properties of the other porous medium's moisture equilibrium condition, e.g. thermal conductivity sensors and electrical conductivity sensors. The paper summarizes basic working principle, calibration, measurement, and application areas of indirect soil suction measurement methods based on the most recent literature. A critical evaluation of the capabilities, limitations, and pitfalls of these methods is also presented.

2 Primary Methods

Total suction of a soil sample may be inferred from measurements within the vapor phase that is in equilibrium with the sample. Devices that measure relative humidity can be employed to infer total suction. Thermocouple psychrometer, transistor psychrometer, and chilled-mirror psychrometer are examples of such devices.

2.1 Thermocouple Psychrometers

There are two types of thermocouple psychrometers for determining total suction measurements in soils: the wet-loop type sensor described by Richards and Ogata (1958) and the Peltier type sensor described by Spanner (1951). The wet-loop sensor is only used with the psychrometric measurement technique, whereas the Peltier sensor can be used with both the psychrometric and hygrometric measurement methods. The primary difference between these two sensors is the manner by which water is applied to the sensing junction. The wet-loop sensor is wetted by manually placing a drop of water on a small ring that is at the sensing junction. The wet-loop type sensor technique has been improved in a new psychrometric device which is called transistor psychrometer and it is discussed in the next section.

Two important principles underlie the usefulness of Peltier type thermocouple psyhcrometers: the Seebeck effect and the Peltier effect. The Seebeck effect is the phenomenon that permits a thermocouple to be used for temperature measurement. A thermocouple is formed when two different metals are joined together (Fig. 1a). If both ends of the wire are joined to form a closed loop, electrical current will flow through the wires whenever the junctions are at different temperatures. The magnitude of the voltage produced is dependent upon the temperature difference between the junctions. The Peltier effect is the phenomenon which allows a thermocouple junction to be cooled by passing an electrical current through the junction. When current flows across the junction of two dissimilar metals, heat will be either absorbed or released at the junction. If the current flows in the

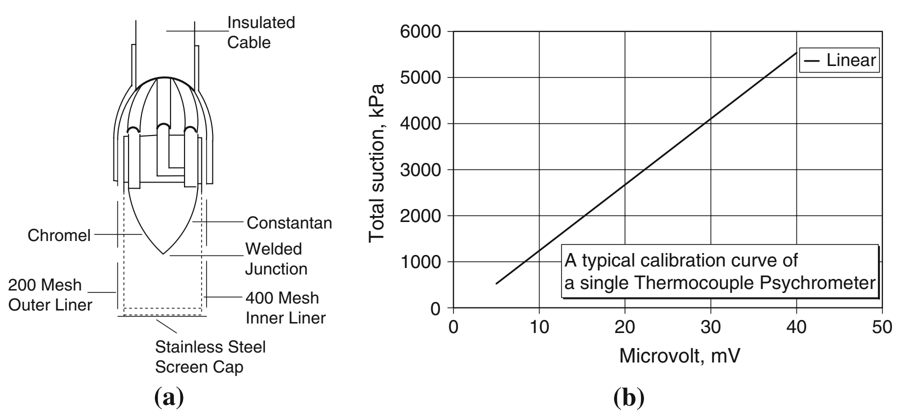

Fig. 1 (**a**) Schematic drawing of a thermocouple psychrometer and (**b**) a typical calibration curve

same direction as the current produced by the Seebeck effect at the hot junction, heat is absorbed. If the current flows in the opposite direction, heat is released.

Wescor, Inc. and Campbell Scientific, Inc. developed two thermocouple psychrometric methods for the measurement of equilibrium relative humidity from which total suction can be determined. These are the psychrometric (wet bulb) and the hygrometric (dew point) methods. Thermocouple psychrometers that are commercially available from Wescor are the PST-55 stainless steel and PCT-55 ceramic cup. The PST-55 sensor has a non-removable stainless steel shield, which has a larger pore size. The PCT-55 sensor has a removable ceramic shield. The same sensors are used for either method but the electronic control and measuring apparatus operate differently. The Wescor HR-33T is a single-channel datalogger and can be used to determine the total suction of a sample using either dew point (hygrometric) or wet bulb (psychrometric) methods. The Wescor/Campbell CR7 datalogger and the new Wescor datalogger PSYPRO use only the psychrometric method. The PSYPRO data logger has eight channels. The CR7 series data logger has several channel configurations (14, 28, 40, 70 and 140 channels). Using either method with any of the instruments, a cooling current is used to cool the thermocouple junction below the dew point of the air surrounding the sample causing water to condense on the junction. Water evaporation and condensation is equilibrated and a voltage is created. This voltage is converted to total suction using standard salt solutions in the case for calibration.

Careful cleaning and thorough drying of the psychrometers before and after calibration and measurements are essential to reliable instrument performance. Contaminants, such as salts, can affect cooling, evaporation, and microvolt output. The pore size of the protective housing on the thermocouple psychrometer prevents most of contaminants, such as soil particles, from entering the sensor cavity. The most serious contamination occurs if dissolved contaminants migrate through or accumulate on the protective housing. Psychrometers can be cleaned with distilled or deionized water. A range of sodium chloride (NaCl) and potassium chloride (KCl) solutions of known osmotic suctions is typically used to establish the relationship between total suction and microvolt output. Typical NaCl solution concentrations versus their osmotic suction values are given in Table 1. A typical calibration curve for thermocouple psychrometer is shown in Fig. 1b.

Calibration solutions are chosen to cover the anticipated range of total suction to be measured. Correct calibration of thermocouple psychrometers is extremely important because the accuracy of all subsequent measurements and interpretations will be based on these data. For routine measurements across the entire range, a minimum of four calibration solutions are typically selected to characterize each psychrometer's response to changes in total suction at a given temperature. Thermocouple psychrometers are typically calibrated by direct immersion into a small container of calibration solution or by suspension of the sensor over the solution in the container. The immersion method has often been selected because this configuration helps to control the temperature fluctuations better. The disadvantage with the immersion method is the possibility of salts getting on the sensors. Sensors should be immersed at a fairly shallow depth otherwise there will be an added

Table 1 Osmotic suction of NaCl solutions at 25°C (from Bulut et al. 2001)

Molality (m)	Osmotic coefficient (ϕ)	Osmotic suction (kPa)	Molality (m)	Osmotic coefficient (ϕ)	Osmotic suction (kPa)
0.000	1.00000	0.00	0.300	0.92123	1370.19
0.002	0.98402	9.76	0.500	0.92224	2286.15
0.005	0.97604	24.20	0.700	0.92691	3216.82
0.010	0.96804	47.99	0.900	0.93350	4165.31
0.020	0.95832	95.02	1.200	0.94567	5626.15
0.050	0.94357	233.90	1.600	0.96487	7653.84
0.100	0.93250	462.32	2.200	0.99818	10887.35
0.200	0.92387	916.08	2.600	1.02263	13182.03

pressure component that may force the solution through the mesh liner and subsequently onto the sensor. The pore size of typical screen-cage and ceramic-cup housing is sufficiently small to prevent liquid from entering the air-filled sensor cavity (Pinnock 2005, personal communication) at low pressures. A water bath is usually employed to maintain temperature stability. The microvolt output from a thermocouple psychrometer is very sensitive to ambient temperature fluctuations. Under isothermal conditions, the equilibration between thermocouple psychrometer sensor and vapor pressure from the salt solution is usually established within an hour. The resulting microvolt readings are plotted against corresponding osmotic suctions of the salt solutions to obtain a calibration curve (Fig. 1b). The practical range over which total suction measurements can be made with thermocouple psychrometers is between about 300 and 7,000 kPa. Total suction values between about 300 and 500 kPa should be evaluated very carefully since this is the range most affected by temperature fluctuation. Suction values below 300 kPa should be carefully evaluated for validity.

Application of thermocouple psychrometers to infer total suction of unsaturated soils in geotechnical engineering research and practice has greatly broadened in the recent years. In one recent application, Bulut et al. (2005) monitored the total suction change of cylindrical Shelby tube soil samples over time with thermocouple psychrometers to determine unsaturated soil moisture diffusion coefficients. In another application, Blatz and Graham (2003) embedded Wescor PST55 in triaxial specimens to measure suction during isotropic loading and shearing.

2.2 Transistor Psychrometer

Transistor psychrometer consists of a thermally insulated container that holds the psychrometer probes and a datalogger for measurement and recording of output. The instrument is very similar in operation to the thermistor psychrometer (Woodburn et al. 1993). The transistor psychrometer is an electronic wet and dry bulb thermometer in which a wet and dry transistor probe is used instead of wet and dry thermometer bulbs as in thermistor psychrometers. The sensor is used for inferring the relative humidity of the air space in equilibrium with a soil sample. The temperature depression of the wet transistor, which holds a standard-size water drop, is measured with the sensors in the probe (Fig. 2a). The wet and dry transistors are employed as heat sensors and the voltage output from the probe is used to infer total suction.

Improvements in performance have been made that allow the device to measure a much wider range of total suction, from about 100 kPa to about 10,000 kPa. Much of the improvement is due to calibration procedure and advances in micro-chip technology (Woodburn et al. 1993). The range and accuracy in measurements are also attributed to sensitivity of the transistors to changes in temperature. Soil Mechanics Instrumentation (Woodburn et al. 1993) produces two types of thermally insulated containers for the transistor probes: 12-probe unit and 8-probe unit. The 8-probe psychrometer is equipped with an insulated lid for better temperature control. Each probe can measure total suction in about 1 h. Twelve and eight soil total suction measurements can

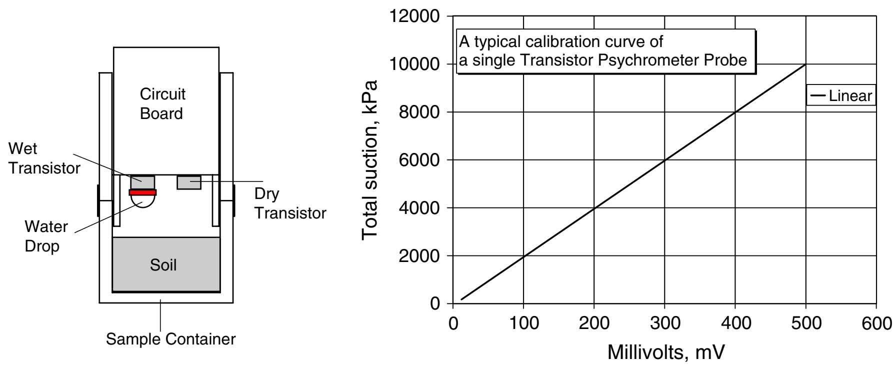

(a) **(b)**

Fig. 2 (**a**) Schematic drawing of a transistor psychrometer probe and (**b**) a typical calibration curve be made within an hour with the 12- and 8-probe units, respectively.

The calibration of the psychrometer probes, determined from the relationship between millivolt output from the transistor and a known osmotic suction value of a salt solution (Table 1), should be carried out carefully. A typical calibration curve of a transistor psychrometer probe is depicted in Fig. 2b. The calibration curve can be affected by several factors: temperature fluctuations, hysteresis, and water drop size. The transistor probes are first equilibrated for at least 4 h at zero total suction over distilled water and the output is adjusted to the initial zero reading before any calibration process or soil suction measurements. Afterwards, the different voltage outputs are recorded from the datalogger following 1 h equilibration period for each suction level. The relationship between relative humidity and total suction (e.g., Kelvin equation) is used to determine the soil total suction. The thermally insulated container provided for the probes maintains a fairly constant temperature during the period of the test. Greater accuracy and reproducibility of results is obtained in a room where temperature is controlled to about ±0.5°C (Woodburn et al. 1993). Transistor psychrometer can only do point measurements (e.g., applicable for small soil specimens of 15 mm in diameter and 13 mm in height). The limitation of soil specimen size when using the transistor psychrometer is also widely recognized.

Transistor psychrometers have been used around the world. In Australia and New Zealand this instrument has been used for unsaturated expansive soils applications (Woodburn 2005, personal communication). It has practically replaced thermocouple psychrometers in many laboratory soil suction measurements. Recent studies by Bulut et al. (2000, 2002) showed that transistor psychrometer has a better capability of measuring total suction at lower levels when compared with other psychrometric methods.

2.3 Chilled-Mirror Psychrometer

A chilled-mirror psychrometer uses the chilled mirror dew point technique to infer total suction under isothermal conditions in a sealed container (Fig. 3a). The chilled-mirror psychrometer discussed in this paper is a product of Decagon Devices, Inc. and is known as a WP4 Dew Point Potentiameter (www.decagon.com). Measurement of total suction with the WP4 is based on equilibrating the liquid phase of the water in a soil sample with the vapor phase of the water in the air space above the sample in a sealed chamber. A Peltier cooling device is used to cool the mirror until dew forms and then to heat the mirror to eliminate the dew. Temperature of the sample is measured with an infrared thermometer. An optical sensor is also employed to detect the dew formed on the mirror. A thermocouple attached to the chilled mirror measures the dew point temperature. A small fan is also employed to circulate the air in the sensing chamber and speed up vapor equilibrium. Both the dew point and soil sample temperature are then used to determine the relative humidity above the soil sample within the closed chamber.

The chilled mirror technique offers a fundamental characterization of humidity in terms of the temperature at which vapor condenses. Therefore, the calibration of the instrument with different concentrations of salt solutions is not necessary. However, the performance of the instrument should be checked

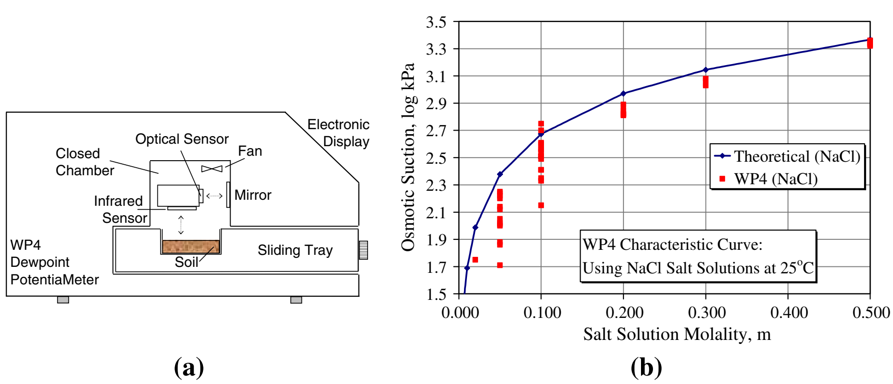

Fig. 3 (**a**) Schematic drawing of the WP4 chilled-mirror psychrometer and (**b**) the characteristic curve at low suction range (from Bulut et al. 2002)

prior to total suction measurement by measuring the total suction of a salt solution with a known osmotic potential (WP4 User Manual). When the temperature readings have stabilized, the instrument will determine the relative humidity of the enclosed space above the soil sample and will display the total suction of the sample. Temperature control is very important. The measured difference between dew point and sample temperatures must be kept small. The WP4 chilled-mirror psychrometer is a very robust instrument that is suitable for rapid total suction measurements, usually less than 10 min. It is important to avoid contamination of the instrument. The sample cup should be filled to less than full capacity to minimize the potential of contaminating the chamber. If necessary, the mirror and fan can be cleaned according to procedures outlined in the user's manual.

Bulut et al. (2002) developed a complete characteristic curve for the WP4 instrument using the relationship between osmotic suction and salt solution concentration. Figure 3b shows the characteristic curve for this instrument at low suction levels. Figure 3b shows that once osmotic suction falls below about 1,000 kPa the scatter in suction increases. Bulut et al. (2002) compared the accuracy of the chilled-mirror psychrometer with the filter paper method for total suction measurements of undisturbed soil samples. Bulut et al. (2002) found that the degree of error associated with the WP4 psychrometer is higher than with the filter paper method at low suction levels, but very good correlation between the two methods at high total suction levels.

Leong et al. (2003) evaluated the accuracy of a chilled mirror dew point device using compacted soil samples. A thorough calibration of the instrument using several standard salt solutions was performed. The equilibration time during calibration and total suction measurement was short, less than 15 min. The total suction measurements on the compacted samples were compared to the sum of matric and osmotic suctions of the same soils that were measured independently. The matric suction of the soils was measured with the null-type axis-translation apparatus and the osmotic suction of the samples was estimated from electrical conductivity measurements of the soil water solution obtained from a pore fluid squeezer device. The test results showed that total suctions obtained using the chilled mirror dew point device were always greater than the sum of the matric and osmotic suctions measured independently. In ASTM D6836-02 , the chilled-mirror hygrometer is used in Method D for determining the desorption soil water characteristic curve for suction range above 1,000 kPa as the limitation of the chilled-mirror hygrometer for low suction levels is widely recognized. Another promising psychrometer that has been used for measurement of total suction is the polymer capacitance sensor which consists of two electrodes separated by a film of thermoset polymer that absorbs or releases water as the relative density of the surrounding air changes (Albrecht et al. 2003). Siemens and Blatz (2005) introduced a Xeritron XN1018 relative humidity sensor for total suction measurements. The sensor was modified so that it could be used inside triaxial specimens.

3 Secondary Methods

Secondary methods employ a separate porous medium to achieve moisture equilibrium with the soil where suction measurement is required. Filter paper has become the de-facto material for suction measurement. The soil suction measurement procedure using filter paper is outlined in detail in ASTM D5298-94, Houston et al. (1994), and Bulut et al. (2001).

3.1 The Filter Paper Method

Among all the known suction measurement methods, the filter paper technique is the only method from which both total and matric suction can be inferred. Using the filter paper method, the soil specimen and filter paper are brought to moisture equilibrium either in contact (matric suction) or not in direct contact (total suction) in a constant temperature environment (Fig. 4). Direct contact between the filter paper and the soil allows water in the liquid phase and solutes to exchange freely, whereas separation between the filter paper and the soil by a vapor barrier limits water exchange to the vapor phase only and prevents solute movement. Matric suction measurements using the filter paper method are similar to the total suction measurements except that intimate contact must be provided between the filter paper and the soil (Fig. 4). After equilibrium is established between the filter paper and soil, the water content of the filter paper is

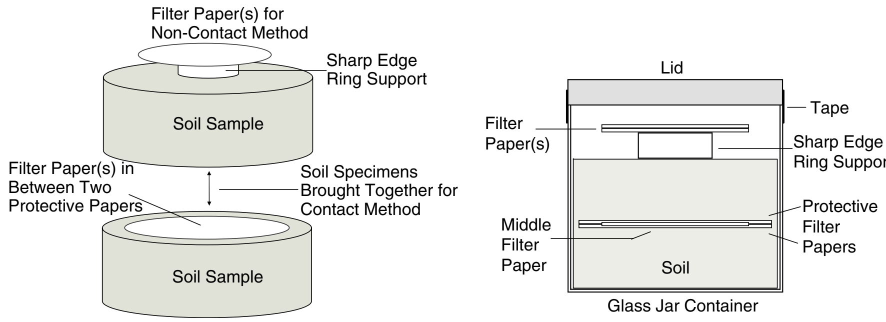

Fig. 4 Schematic drawings of soil total and matric suction measurements

measured. Then, by using the appropriate filter paper calibration curve, the suction of the soil is estimated. The calibration curves are usually obtained from the processes of wetting and drying the filter papers through vapor transfer (salt solutions) and drying and wetting the filter papers through fluid transfer (porous plates). There are still many concerns about the reliability of the filter paper method. The filter paper method is a simple technique and can be reliable if the basic principles of the method are understood and a strictly practiced laboratory protocol is carefully followed.

As accuracy of the filter paper technique is dependent on the accuracy of the filter paper water content versus suction calibration curve, the calibration technique of the filter paper method has been investigated by numerous researchers (e.g. Houston et al. 1994; Bulut et al. 2001; Leong et al. 2002). Calibration equations should be developed specifically for the specific filter paper being used. The most commonly used filter papers are Whatman No. 42 and Schleicher & Schuell No. 589-WH. The Schleicher & Schuell No. 589-WH filter paper is now called grade 989-WH in the US. The reason for this name change in the US is that in Europe the grade name 589-WH is used for a filter paper that has different specifications to the US version (Reeves 2003, personal communication). This means that prior to year 2003 the calibration curves for Schleicher & Schuell No. 589-WH filter papers were different depending if they were produced in US or Europe.

Until Houston et al. (1994) all suction measurements were based on a single calibration curve. Houston et al. (1994) developed two calibration curves for Fisher quantitative coarse (9.54 A) filter paper: one for total suction and one for matric suction and reported that the curves were different. Bulut et al. (2001) developed two calibration curves for Schleicher & Schuell No. 589-WH filter papers: one by the process of wetting from initially dry filter papers through vapor flow using NaCl solutions and one by the process of drying from initially saturated filter papers through fluid flow using pressure plates and membranes. Leong et al. (2002) developed different calibration curves for total and matric suctions for Whatman No. 42 and Schleicher & Schuell No. 589-WH filter papers from initially dry filter papers using NaCl solutions and pressure plate. The calibration curves constructed by Leong et al. (2002) and Bulut and Wray (2005) are given in Fig. 5. In a more recent study, Bulut and Wray (2005) re-evaluated the filter paper method based on a new calibration curve and the most recent published literature.

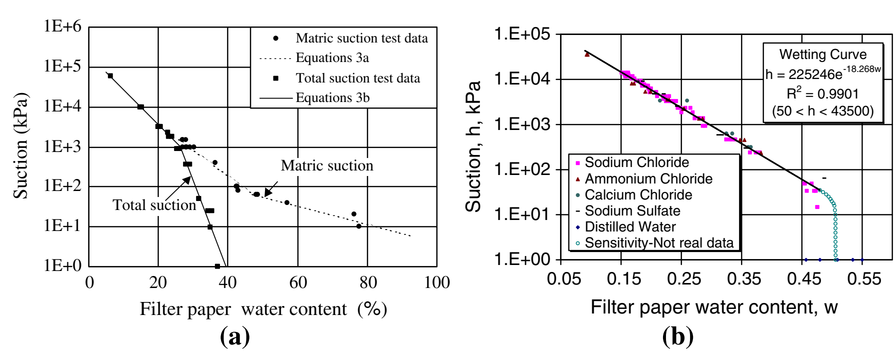

Fig. 5 Total and matric suction calibration curves for (**a**) Whatman No. 42 (Leong et al. 2002) and (**b**) Schleicher & Schuell No. 589-WH filter papers (Bulut and Wray 2005)

The differences in the filter paper calibration curves in the literature are attributed to several factors such as the suction source for the calibration, thermodynamic definitions of suction components, and equilibration time (Fredlund and Rahardjo 1993; Houston et al. 1994; Bulut et al. 2001; Leong et al. 2002; Bulut and Wray 2005; Walker et al. 2005). Walker et al. (2005) evaluated total suction measurements of a soil sample using transistor psychrometer and filter paper method. Walker et al. (2005) adopted the filter paper calibration curve in Hamblin (1981) and found that total suction measurements from the filter papers were significantly smaller than the total suction measurements from the transistor psychrometer. Walker et al. (2005) suggested that the total suction calibration curves represent a transient condition during the calibration period and that a unique, single calibration curve should be used for both total and matric suction measurements. In other words, Walker et al. (2005) suggested that if sufficient time is allowed for equilibration, the total suction calibration curve will tend towards the matric suction calibration curve. Bulut et al. (2001) and Bulut and Wray (2005) stated that a single calibration curve based on water vapor measurements is adequate for both total and matric suction measurements. Leong et al. (2002) attributed the differences between the calibration curves to the initial condition of the filter paper whether it is from the dry or wet condition. Leong et al. (2002) stated that if the calibration curves are from the initially wet filter paper condition, then it may be possible that both calibration curves are similar. However, two different calibration curves are obtained when the initially dry filter papers are adopted. Leong et al. (2002) and Bulut and Wray (2005) discussed in detail the different calibration curves of filter papers and the time required for equilibration.

It is extremely important to minimize temperature gradients during the calibration with salt solutions as well as during total suction measurement. During calibration, it is suggested that temperature fluctuations should be maintained within an accuracy of ±0.1°C or better. It would be ideal to maintain a similar accuracy during total suction measurements, but it may be difficult to obtain such accuracy in a geotechnical engineering laboratory. Therefore, this accuracy may be relaxed to some degree. Temperature fluctuations are extremely critical at high relative humidity levels. Bulut and Wray (2005) described the sensitivity of suction at high relative humidity levels and illustrated that minor changes in relative humidity result in very large changes in suction. For instance, relative humidity values of 0.999656 and 0.999063 result in osmotic suction values of 47.199 and 128.6 kPa, respectively. Filter papers should also be allowed to equilibrate for a sufficient time. Recent literature suggested that an upper limit of equilibration time of 14 days is sufficient for filter paper calibration over salt solutions and distilled water, and 1 week of equilibration period is usually considered satisfactory for most soil suction measurements.

4 Tertiary Methods

The disadvantage of the secondary methods of indirect suction measurement is the need to determine the moisture content of the porous medium in equilibrium with the soil. Tertiary methods of indirect suction measurement overcome this problem by measuring properties of the porous medium that indicate its moisture content. Examples of devices that employ the tertiary method of indirect suction measurement are thermal conductivity sensor and electrical conductivity sensors.

4.1 Thermal Conductivity Sensor

A thermal conductivity sensor employs a porous block, typically ceramic, as a medium to measure matric suction indirectly. If a matric suction gradient exists between the soil and porous block, water flux will occur until their suctions are equal. The thermal conductivity of the block consists of the thermal conductivity of the solid and the fluid (air or/and water) that fills the voids in the porous block. The thermal conductivity of water is about 25 times that of air. Therefore, as the moisture content of the porous block increases, the thermal conductivity of the block increases. The moisture content of the block is measured by heating the porous block with a heater embedded in the centre of the porous block and measuring the temperature rise during heating. The temperature rise is related to the thermal conductivity of the porous medium and the moisture content. The temperature rise can then be used as an index of matric suction in the soil. The time to equilibrate depends on the temperature gradient and the hydraulic conductivity of the porous medium and surrounding soil. Soil salinity has an insignificant effect on the thermal conductivity sensor readings. The basic design of thermal conductivity sensor essentially follows the design of Phene et al. (1971) as shown in Fig. 6a. Over the years, the performance of the thermal conductivity sensor has been improved. Thermal conductivity sensors have been used in the laboratory as well as in the field (Fredlund and Wong 1989; Oloo and Fredlund 1995; O'Kane et al. 1998; Marjerison et al. 2001; Zhang et al. 2001; Nichol et al. 2003). Currently, thermal conductivity sensors are available commercially (e.g. Campell Scientific, Inc. and GCTS). The Campbell Scientific thermal conductivity sensor CSI 229 has a matric suction measurement range from 10 to 1,500 kPa whilst the GCTS thermal conductivity sensor FTC-100 has a matric suction measurement range from 1 to 1,500 kPa. For the CSI 229, a 50 mA current is used with a 20–30 s heating time. Typically the ambient temperature and the temperature after the heating period is recorded from which the matric suction is inferred from the calibration curve. For the FTC-100, a 200 mA current is used with a 60 s heating period. The heating curve is recorded for 3 min during a measuring cycle. The diameter and length of the CSI 229 thermal conductivity sensor porous block are 15 and 25 mm, respectively, whilst those of the FTC-100 thermal conductivity sensor are 28 and 38 mm, respectively. The CSI 229 is more sensitive at matric suctions less than 300 kPa (He 1999). The resolutions of the FTC-100 suction measurements in the ranges of 1–10, 10–100, 100–1,000 kPa are 0.1, 1, and 5–10 kPa, respectively (UST 2004).

The main problem with the thermal conductivity sensor is the variable uniformity of the porous block from sensor to sensor. This means that a separate calibration curve is required for each thermal conductivity sensor. In addition, the thermal conductivity sensor shows hysteretic behavior on drying and wetting. Reece (1996) suggested that the thermal conductivity of the CSI 299 be normalized with the thermal conductivity measured after oven drying the sensor. With the normalization, Reece (1996) obtained a linear calibration curve between the inverse of the normalized thermal conductivity and the natural logarithm of matric suction up to 1,200 kPa. Above a matric suction of 1,200 kPa, a non-linear calibration curve is obtained. The hysteretic effect was not considered in the interpretation of matric suction measurement. Zhang et al. (2001) evaluated 30 CSI 229 sensors and showed that the effect of hysteresis in the CSI 229 thermal conductivity sensor should be taken into consideration when measuring matric suction. Different calibration curves were obtained for the drying and wetting of the CSI 229 as shown in Fig. 6b.

Similar hysteretic effects were also observed in the precursor of the FTC-100 sensor (Feng and Fredlund 2003). The equilibration time of the thermal conductivity sensor is dependent on the contact condition between the central element (heater and temperature sensor) and the porous block. Even the contact condition between the sensor and the soil affects the response of the CSI 229 (Zhang et al. 2001). Zhang et al. (2001) found that equilibration time of the CSI 229 thermal conductivity sensor can vary from several hours to several tens of hours irrespective of the suction level due to contact condition between the sensor and the soil. Furthermore, the porous block of the CSI 229 thermal conductivity sensor could be

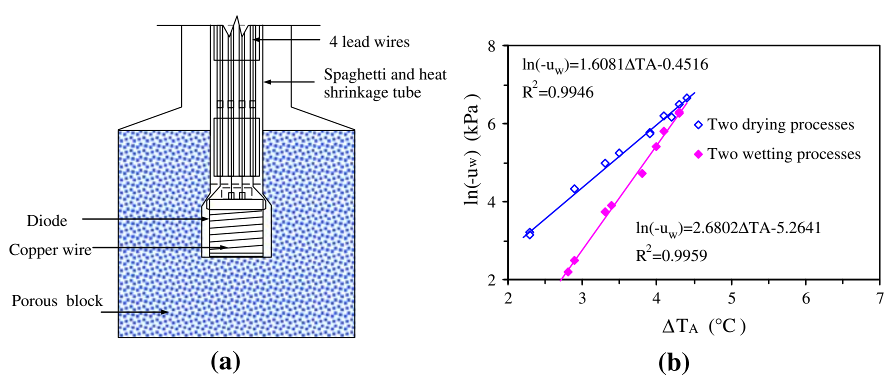

Fig. 6 (**a**) Cross-section of a thermal conductivity sensor (from Phene et al. 1971) and (**b**) calibration curves of a typical CSI 229 thermal conductivity sensor for 24 s heating time with a 50 Ma current (from Zhang et al. 2001)

easily damaged during installation. Nichol et al. (2003) installed 18 FTC-100 type of thermal conductivity sensors in the field at depths of 0.2 and 4.5 m. They found long-term drift of the thermal conductivity sensors. However O'Kane et al. (1998) and Marjerison et al. (2001) did not experience such problems in their long term monitoring of matric suction with thermal conductivity sensors.

4.2 Electrical Conductivity Sensor

The electrical conductivity sensor consists of a porous block and two concentric electrodes embedded inside the block (Fig. 7a). The porous block serves the same purpose as the porous block in the thermal conductivity sensor. However instead of thermal conductivity, the electrical conductivity sensor measures the electrical conductivity of the porous block. As the moisture content of the porous block increases, the electrical resistance of the block decreases. The electrical resistance of the porous block can be related to the matric suction of the block. Unfortunately, the electrical resistance of the porous block is also dependent on the salt concentration of the soil solution and may not be a direct indication of the moisture content of the porous block. The electrical conductivity sensor must be excited by a small AC voltage to prevent polarization. Polarization effects will cause the results to be distorted and deterioration of the electrical conductivity sensor. The AC signal must then be converted back to DC voltage for reading. The need for conversion of AC signal to DC signal means additional hardware is needed to interpret the reading. Usually the electrical conductivity sensor is read manually from a meter, limiting the number of readings when used in the field (Skinner et al. 1997).

Electrical conductivity sensors are commercially available (e.g. Soilmoisture Inc., Measurement Engineering Australia, Delmhorst Instrument Company, Irrometer Company Inc., and Environmental Sensors Inc.). Gypsum was found to be the most suitable porous block material as gypsum took the shortest time to saturate and responded fastest in matric suction measurements (Buoyoucos and Mick 1940). Gypsum also tends to buffer the soil salinity thereby decreasing the effect of soil salinity. This however has the unintended effect of degrading the electrical conductivity sensor as the gypsum eventually dissolves completely into the soil solution. Similar to the thermal conductivity sensor, the gypsum block of the electrical conductivity sensor also suffers from hysteresis. The electrical conductivity sensor has a long equilibration time (2–3 weeks) in a rapidly changing moisture environment (Aitchison and Richards 1965). These shortcomings had led to a diminished use of electrical conductivity sensor for matric suction measurement even in the agricultural industry (Skinner et al. 1997). He (1999) evaluated the performance of the Soilmoisture model 5201 gypsum electrical conductivity sensors. The gypsum block has a diameter of 32 mm and a length of 35 mm. The electrical conductivity sensor is used together with a Soilmoisture model 5910-A meter. The meter provides a 60 Hz square wave, 1-V_{pp} excitation voltage and gives a digital readout. The equilibration times of the gypsum electrical conductivity sensors were found to vary with matric suction ranging from 6 h for a matric suction of 50 kPa to 50 h for a matric suction of 1,500 kPa. The

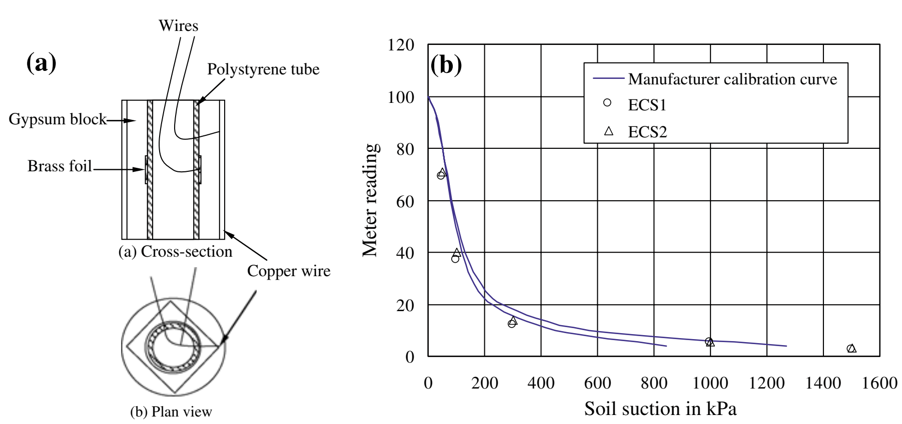

Fig. 7 (**a**) A typical electrical conductivity sensor (from Ridley 1993) and (**b**) calibration curves for the Soilmoisture model 5201 electrical conductivity sensor using Model 5910-A Soilmoisture meter (from He 1999)

calibration curves of two Soilmoisture model 5201 gypsum electrical conductivity sensors (ECS1 and ECS2) are shown in Fig. 7b. The sensitivity of the electrical conductivity sensor becomes very low when the matric suction exceeds 300 kPa. Currently, research on the electrical conductivity sensor is still ongoing to overcome its shortcomings.

5 Summary

This paper has summarized basic working principles, calibration, measurement, and application of indirect soil suction measurement methods based on the most recent literature. The indirect suction measurement methods have been grouped into primary methods which measure the vapor pressure, secondary methods which measure the moisture content of a porous medium, and tertiary methods which measure other properties of the porous medium which indicate its moisture content. Table 2 summarizes key characteristics of indirect suction measurement methods. The source/manufacturer mentioned in the paper is meant for reference and does not represent product endorsement by the authors. The list is also not meant to be exhaustive.

6 Conclusion

Accurate total suction measurement is still difficult with current technology, especially for total suction levels below about 100 kPa. Difficulties with the primary methods measurement techniques basically arise from two main sources. The first stems from the fact that relative humidity in the soil air phase changes only a small amount within the typical range of suction interest. Most measurements of interest to studies of unsaturated soils lie in the narrow relative humidity range from about 0.94 and 1.00. The second main source of difficulty arises from the fact that minor temperature fluctuations may lead to large errors in determination of total suction. Refinements to minimize the temperature sensitivity of the psychrometric techniques may be possible through careful analysis of heat and vapor flow through and around the measuring sensors. More research is needed to improve primary methods of suction measurement. The secondary methods of indirect suction measurement are prone to operator error. Unless a strictly practiced laboratory protocol is followed, the filter paper method may give questionable results. However the filter paper method is simple and is the most affordable indirect suction measurement method. The tertiary methods of indirect suction measurement (thermal conductivity sensor and electrical conductivity sensor) measure the properties of the porous medium associated with its moisture condition from which matric suction is inferred. However, the most severe limitation of the thermal conductivity sensor and the electrical conductivity sensor is hysteresis. Correct matric suction is obtained only if the appropriate calibration curve is used.

Table 2 Summary of indirect soil suction measurement methods

Category	Method	Suction	Suction range (kPa)	Equilibrium time	Source/manufacturer
Primary	TP[a]	Total	300–7000	1 h	Wescor: www.wescor.com
					Campbell Scientific: www.campbellsci.com
	TrP[a]	Total	100–10,000	1 h	Soil Mechanics Instrumentation: Australia
	CMP[a]	Total	500–30,000 (or higher)	10 min	Decagon Devices: www.decagon.com
Secondary	FPM[a]	Total/Matric	50–30,000 (or higher)	5–14 days	Whatman: www.whatman.com
					Schleicher & Schuell: www.schleicher-schuell.com
Tertiary	TCS[a]	Matric	1–1,500	Hours to days	Campbell Scientific: www.campbellsci.com
					GCTS: www.gcts.com
	ECS[a]	Matric	50–1,500	6–50 h	Soil Moisture Equipment: www.soilmoisture.com

[a] TP, thermocouple psychrometer; TrP, transistor psychrometer; CMP, chilled-mirror psychrometer; FPM, filter paper method; TCS, thermal conductivity sensor; ECS, electrical conductivity sensor

References

Aitchison GD, Richards BG (1965) A broad-scale study of moisture conditions in pavement subgrades throughout Australia. In: Moisture in soils beneath covered areas. Butterworths, Australia, pp 198–204

Albrecht BA, Benson CH, Beuermann S (2003) Polymer capacitance sensors for measuring soil gas humidity in drier soils. Geotech Test J 26(1):1–9

ASTM D5298-94 (1994) Standard test method for measurement of soil potential (suction) using filter paper. In: 1994 Annual book of ASTM standards. ASTM, Philadelphia

ASTM D6836-02 (2003) Standard test methods for determination of the soil water characteristic curve for desorption using a hanging column, pressure extractor, chilled mirror hygrometer, and/or centrifuge. In: 2003 Annual book of ASTM standards. ASTM, Philadelphia

Blatz JA, Graham J (2003) Elastic-plastic modelling of unsaturated soil using results from a new triaxial test with controlled suction. Geotechnique 53(1):113–122

Bulut R, Wray WK (2005) Free energy of water—suction—in filter papers. Geotech Test J 28(4):355–364

Bulut R, Aubeny CP, Lytton RL (2005) Unsaturated soil diffusivity measurements. In: International symposium on advanced experimental unsaturated soil mechanics, Trento, Italy, 27–29 June

Bulut R, Lytton RL, Wray WK (2001) Soil suction measurements by filter paper. In: Vipulanandan C, Addison MB, Hasen M (eds) Expansive clay soils and vegetative influence on shallow foundations, ASCE geotechnical special publication no. 115. Houston, Texas, pp 243–261

Bulut R, Hineidi SM, Bailey B (2002) Suction measurements—filter paper and chilled mirror psychrometer. In: Proceedings of the Texas Section American Society of Civil Engineers, Fall Meeting, Waco, 2–5 October

Bulut R, Park S-W, Lytton RL (2000) Comparison of total suction values from psychrometer and filter paper methods. In: Unsaturated soils for Asia. Proceedings of the Asian conference on unsaturated soils, UNSAT-ASIA 2000, Singapore, 18–19 May, pp 269–273

Bouyoucos GJ, Mick AH (1940) Comparison of absorbent materials employed in the electrical resistance method of making a continuous measurement of soil moisture under field conditions. Proc Soil Sci Soc Am 5:77–79

Feng M, Fredlund DG (2003) Calibration of thermal conductivity sensors with consideration of hysteresis. Can Geotech J 40(5):1048–1055

Fredlund DG, Rahardjo H (1993) Soil mechanics for unsaturated soils. John Wiley & Sons, Inc, New York

Fredlund DG, Wong DKH (1989) Calibration of thermal conductivity sensors for measuring soil suction. Geotech Test J 12(3):188–194

Hamblin AP (1981) Filter paper method for routine measurement of field water potential. J Hydrol 53:355–360

He L-C (1999) Evaluation of instruments for measurement of suction in unsaturated soils. MEng Thesis, School of Civil & Structural Engineering, Nanyang Technological University, Singapore

Houston SL, Houston WR, Wagner AM (1994) Laboratory filter paper measurements. Geotech Test J 17(2):185–194

Leong E-C, He L, Rahardjo H (2002) Factors affecting the filter paper method for total and matric suction measurements. Geotech Test J 25(3):322–333

Leong E-C, Tripathy S, Rahardjo H (2003) Total suction measurement of unsaturated soils with a device using the chilled-mirror dew-point technique. Geotechnique 53(2):173–182

Marjerison B, Richardson N, Widger A, Fredlund DG, Berthelot C (2001) Installation of sensors and measurement of soil suction below thin membrane of surface pavements in Sasketchewan. In: Proceedings of 54th Canadian geotechnical conference, Calgary, Alta, 16–19 September, pp 1328–1334

Nichol C, Smith L, Beckie R (2003) Long term measurement of matric suction using thermal conductivity sensors. Can Geotech J 40(3):587–597

O'Kane M, Wilson GW, Barbour SL (1998) Instrumentation and monitoring of an engineered soil cover system for mine waste rock. Can Geotech J 35:828–846

Oloo SY, Fredlund DG (1995) Matric suction measuring in an expansive soil subgrade in Kenya. In: Unsaturated soils: proceedings of 1st international conference on unsaturated soils, Paris

Phene CJ, Hoffman GJ, Rawlins SL (1971) Measuring soil matric potential in-situ by sensing heat dissipation within a porous body: I. Theory and sensor construction. Proc Soil Sci Soc Am 35:27–33

Reece CF (1996) Evaluation of a line heat dissipation sensor for measuring soil matric potential. Soil Sci Soc Am J 60(4):1022–1028

Richards LA, Ogata G (1958) A thermocouple for vapor pressure measurement in biological and soil systems at high humidity. Science 128:1089–1090

Ridley AM (1993) The measurement of soil matric suction. PhD thesis, Imperial College of Science, Technology and Medicine, University of London

Siemens GA, Blatz JA (2005) Soil suction measurement using the Xeritron Sensor in two different types of infiltration tests on a swelling soil. In: International symposium on advanced experimental unsaturated soil mechanics, Trento, 27–29 June

Skinner A, Hignett C, Dearden J (1997) Resurrecting the gypsum block for soil moisture measurement. In: Australian viticulture, October/November 1997

Spanner DC (1951) The Peltier effect and its use in the measurement of suction pressure. J Exp Bot 2:145–168

UST 2004. http://www.soilvision.com/subdomains/unsaturatedsoil.com/sensor.shtml

Walker SC, Gallipoli D, Toll DG (2005) The effect of structure on the water retension of soil tested using different methods of suction measurement. In: International symposium on advanced experimental unsaturated soil mechanics, Trento, 27–29 June

Woodburn JA, Holden JC, Peter P (1993) The transistor psychrometer: a new instrument for measuring soil suction. In: Houston SL, Wray WK (eds) Unsaturated soils. ASCE geotechnical special publication no. 39. Dallas, Texas, pp 91–102

Zhang X, Leong EC, Rahardjo H (2001) Evaluation of a thermal conductivity sensor for measurement of matric suction in residual soil slopes. In: Proceedings of 14th southeast Asian geotechnical conference, Hong Kong, pp 611–616

Axis Translation and Negative Water Column Techniques for Suction Control

Sai K. Vanapalli · M. V. Nicotera · Radhey S. Sharma

Originally published in the journal *Geotechnical and Geological Engineering*, Volume 26, No. 6, 645–660.
DOI: 10.1007/s10706-008-9206-3

Abstract Negative water column and axis translation techniques are conventionally used experimental techniques for obtaining data to interpret the engineering behavior of unsaturated soils. The negative or the hanging water column technique is used as a suction control method in the low suction range (i.e., 0–30 kPa). The axis translation technique is used in the suction range 0 to 500 kPa or higher. This technique is particularly useful for testing specimens with suction values greater than 100 kPa avoiding problems associated with cavitation. While the axis-translation technique has been commonly used, the limitations associated with this technique related to air diffusion, water volume change and evaporation are not discussed in greater detail in the literature. This paper highlights some of the key aspects related to the negative water column and axis translation technique that are of interest both to the researchers and practicing engineers.

Keywords Unsaturated soils · Negative water column technique · Single column technique · Axis translation technique · Suction measuring techniques · Limitations

S. K. Vanapalli (✉)
Civil Engineering Department, University of Ottawa, A020, 161 Louis Pasteur, Ottawa, ON, Canada K1N 6N5
e-mail: vanapall@eng.uottawa.ca

M. V. Nicotera
University of Napoli Federico II, Naples, Italy

R. S. Sharma
Louisiana State University, Baton Rouge, LA, USA

1 Introduction

Several disciplines such as soil science, hydrogeology, petroleum, agricultural, ceramics especially geotechnical and geo-environmental engineering have contributed towards our present understanding of the mechanics of unsaturated soils. Significant advancements were made particularly during the last two decades with respect to the development of the theoretical frameworks, experimental methods and numerical techniques related to geotechnical and geo-environmental engineering applications. During this period, four International Conferences on Unsaturated Soils were also held: Paris (France) in 1995, Beijing (China) in 1998, Recife (Brazil) in 2002, and Phoenix (USA) in 2006. As a result, we have a better understanding of the engineering behaviour of unsaturated soils today. Approximately 20% of the publications of recent years in geotechnical and geo-environmental journals are either directly or indirectly related to the research area of unsaturated soils. In spite of the advances of extending the mechanics of unsaturated soils into engineering practice based on experimental methods, there is still a need to better understand the conventionally used negative water column and axis translation techniques that are commonly used in the laboratory testing techniques.

DOI: 10.1007/978-1-4020-8819-3_4

2 Background

The successful implementation of Terzaghi's effective stress principle for saturated soils in the engineering practice has led many researchers to attempt to extend a stress stable variable framework to unsaturated soils. For example Bishop (1959) modified Terzaghi effective stress equation with the introduction of a soil parameter, χ (which is a function of degree of saturation) to interpret the mechanical behaviour of unsaturated soils. Several researchers during the last three decades have proposed frameworks for interpreting the engineering behavior of unsaturated soils in terms of two or more independent stress state variables over a large suction range (Fredlund and Morgenstern 1977; Toll 1990; Wheeler and Sivakumar 1995).

The research direction in recent years has been towards understanding the comprehensive behaviour of unsaturated soils by extending the critical state soil mechanics concepts (Alonso et al. 1990; Wheeler and Sivakumar 1995; Maâtouk et al. 1995; Cui and Delage 1996). More recently, Gallipoli et al. (2003), Wheeler et al. (2003), Tarantino and Tombalato (2005) and Infante Sedano et al. (2007) have proposed coupling of hydro-mechanical behaviour of unsaturated soils. The above research studies were based on experimental studies in which axis translation technique was mainly used as a tool for understanding the comprehensive hydraulic and mechanical behaviour of unsaturated soils.

In recent years several investigators have also proposed indirect methods to predict or estimate the engineering behavior of unsaturated soils. The relationship between water content and suction which, in the literature, is referred to as the soil–water characteristic curve (SWCC) or soil–water retention curve (SWRC) or soil–moisture curve (SMC) has been used as a tool to predict the flow, shear strength and volume change behaviour of unsaturated soils (Fredlund and Rahardjo 1993; Vanapalli et al. 1996; Barbour 1998; Leong and Rahardjo 1997). The negative water column technique which was originally introduced by Haines (1927) and Haines (1930) or axis translation technique proposed by Hilf (1956) are commonly used techniques to study the hydraulic and the mechanical behaviour of unsaturated soils.

In this paper, firstly the negative water column technique and its use in suction control is explained. Secondly, several details related to the axis translation technique and its applications are presented. In addition, the limitations of the axis-translation technique and the methods that can be used to alleviate some of these limitations are highlighted. Various parameters that influence the axis-translation technique such as air diffusion, water volume change, long term testing and evaporation are briefly described.

3 Hanging Water Column

Buckingham (1907) was one of the pioneering scientists who measured the relationship between capillary potential and water content (i.e., SWRC) and expressed it as a continuous function using hanging water column (i.e., negative water column) technique. This relationship has been considered as an important milestone in the history of soil physics and the mechanics of unsaturated soils (Barbour 1998; Narasimhan 2005). Buckingham measured the SWRC of different soils (Fig. 1) using 48-inches-tall soil columns packed into metal cylinders, which were allowed to come to equilibrium with a reservoir of water at a fixed elevation of about 50 mm (2 inches) from the bottom end of the columns. The upper end of the columns was closed to prevent evaporation. The gravitational potential energy within the water at any elevation above the reference reservoir elevation after attaining equilibrium conditions was referred to as the capillary potential. Richards (1928) further simplified and refined this technique and proposed an experimental procedure for determining the SWRC using thin specimens and a water reservoir connected to a vacuum

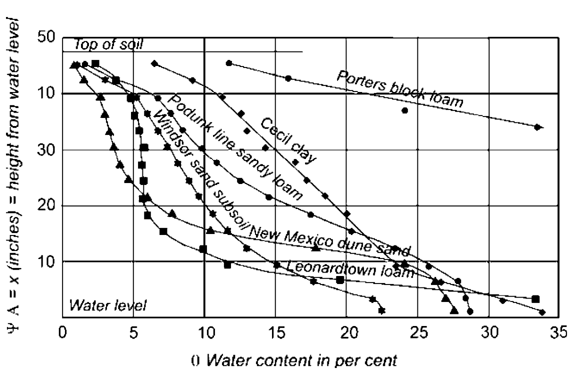

Fig. 1 Soil–water retention curves for six different soils obtained from 48-inch columns (modified after Buckingham 1907)

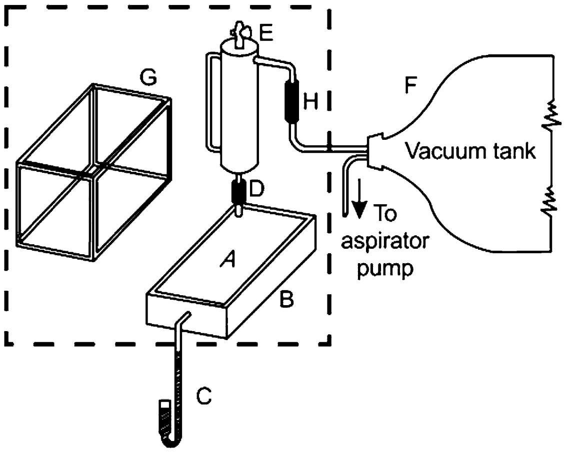

Fig. 2 Richards Apparatus (Richards 1928) (A, Porous plate; B, aluminum case; C, manometer copper tube connection to water reservoir E; F, vacuum tank; G, glass tank; and D, H, rubber connection)

tank (Fig. 2). A constant water level is maintained in this technique; however, it is not possible to monitor water volume changes. In addition, water column height should be checked and adjusted continuously to maintain a constant value of suction.

Figure 3a shows the details of Buchner-Haines funnel apparatus set up. This set up was modified after Haines (1930) who originally introduced the concept of hanging water column technique that can be used for the measurement of the SWRC of coarse-grained soils. The pressure in the water below the porous plate in this apparatus can be reduced to subatmospheric levels by increasing the difference between the elevation of the specimen and the elevation of the reservoir.

More recently, Sharma and Mohamed (2003) used the Buchner funnel apparatus (water column) to investigate contaminants migration in unsaturated/saturated sand for determining the SWRC. The layout of the apparatus is shown in Fig. 3b. Typically, in the Buchner funnel apparatus, specimens are prepared by pouring sand from a fixed height into the water-filled funnel by keeping the water level always above the sand level. The fully saturated specimens are then subjected to increasing capillary tension (i.e., matric suction) by lowering the burette to a given height, to obtain the main drying curve. Similarly, wetting and scanning curves can be obtained by extending this technique. The partial re-wetting of the drying curve by reducing suction and allowing the specimen to imbibe moisture is defined as the scanning curve.

Figure 4 (Dane and Hopmans 2002) can be used to illustrate the Haines' approach in which the matric suction can be regulated varying the level z_1. In Haines apparatus suction is controlled by means of a hanging water column technique that uses both

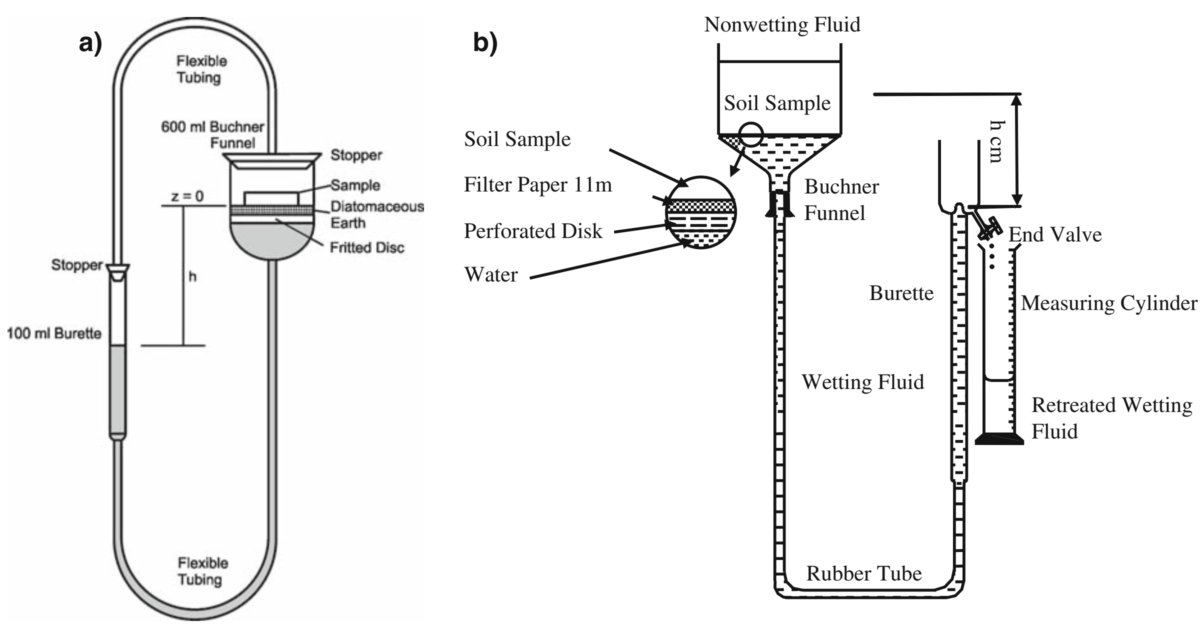

Fig. 3 (**a**) Buchner-Haines funnel apparatus (after Haines 1930); (**b**) Layout of Buchner Funnel for Obtaining SWRC (from Sharma and Mohamed 2003)

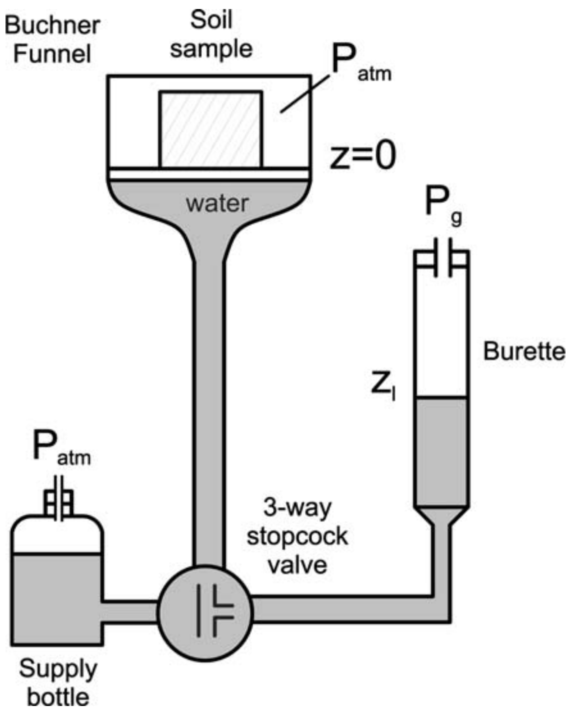

Fig. 4 Diagram of a classical hanging column apparatus (modified after Dane and Hopmans 2002)

vacuum control and hanging column. In the Richards' technique, matric suction can be regulated controlling gas pressure P_g. In the combined apparatus, suction can be regulated either varying the level z_l or by controlling gas pressure P_g.

The maximum suction that can be achieved by the hanging column techniques is typically limited to 20–30 kPa due to practical limitations of achieving higher pressures by adjusting the elevation of the soil specimen and the water level in the column. In the hanging column technique, level z_1 can be adjusted with a resolution of 1 mm and hence suction can be controlled with a resolution of 0.01 kPa. Typically, the hanging column technique is used for investigating water retention features of coarse-grained soils with little fines that drain readily at very low suction values. This technique should be useful to determine SWRCs reliably at low suction values and accurately estimate air entry suction values.

Higher suction values can be attained by "multiple columns" techniques which are described later in the paper. On the contrary, the vacuum control technique permits to directly apply matric suction values in the range from 0 to 80 kPa but requires more sophisticated devices.

One key difference between the hanging column and vacuum control method is associated to the process of air diffusion. Under vacuum control conditions, the gas pressure P_g (see Fig. 4) is maintained at subatmospheric values. However, the air pressure above the porous plate is atmospheric and hence air can diffuse through the drainage system towards the burette. The diffused air can affect the measurements of the water volume flowing in or out of the specimen. However, in the original hanging column technique, the gas pressure P_g above the water reservoir is maintained atmospheric and hence there is no problem associated with air diffusion through the porous plate in the drainage system.

In the vacuum control method, saturated soil specimens are placed in contact with water saturated porous plates or membranes. Matric suction is applied by reducing pore water pressure while maintaining pore gas pressure at atmospheric conditions. The application of matric suction causes water to flow from the specimen until the equilibrium water content corresponding to the applied matric suction is reached.

Different methods can be used to verify the equalization of suction. In the Haines' apparatus (see Fig. 5) equilibrium is established by monitoring the water level; the main shortcoming of this method is related to

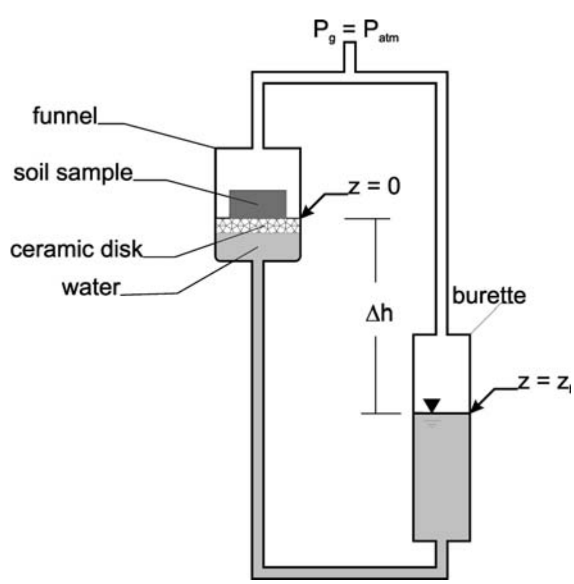

Fig. 5 Haines' apparatus

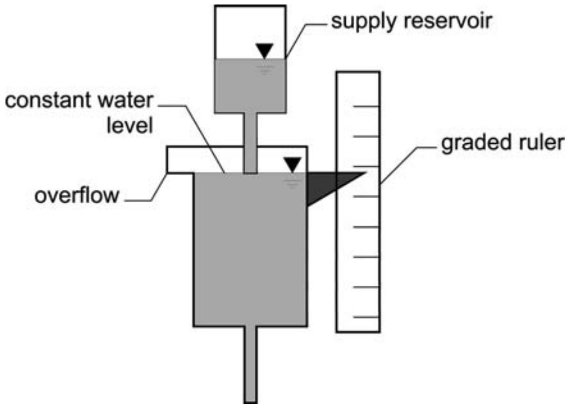

Fig. 6 Levelling device

the burette position which should be continuously adjusted in order to maintain the distance Δh constant. It should be noted that evaporation of water can occur either from the specimen and the porous stone or from the burette. An additional hanging water column should be set up without a soil specimen to measure the evaporation in the system. The information obtained from this additional hanging water column would be useful to apply corrections.

Figure 6 shows a simple levelling device that is useful to keep water flow from the reservoir level constant at the elevation of the overflow. However, equilibrium conditions cannot be assessed by measuring water outflow or inflow from the specimen. To determine suction equilibrium conditions, it is necessary to periodically remove the specimen from the apparatus and measure equilibrium water content. The calculated water content is an average value and corresponds to one matric suction value. This assumption is reasonable for fine textured soil with a gradual change in pore size. However, the same assumption cannot be extended for coarse-grained soils (Dane et al. 1992). The equilibrium matric suction varies linearly with elevation and therefore water content changes along the specimen height. These variations could be significant in the case of coarse-grained soils and hence some corrections should be introduced while measuring the SWRC in the lower suction range (Liu and Dane 1995a; Liu and Dane 1995b).

A recent ASTM standard (ASTM 2003) assumes the configuration of hanging column apparatus represented in Fig. 7. The apparatus consists of a specimen chamber, an outflow measurement tube, and a suction supply system. Water volumes flowing in or out of the specimen during the test are measured using a capillary tube connected to the outflow end of the specimen chamber. The other end of this capillary tube is connected to a vacuum control system consisting of two reservoirs. The relative elevation of these two reservoirs is adjusted to maintain subatmospheric pressures within the water inside the capillary tube. The capillary tube is disposed horizontally at the same elevation of the bottom of the soil specimen; therefore the magnitude of the suction applied can be measured with a manometer. The main advantage of this version

Fig. 7 Hanging column apparatus (ASTM 2003)

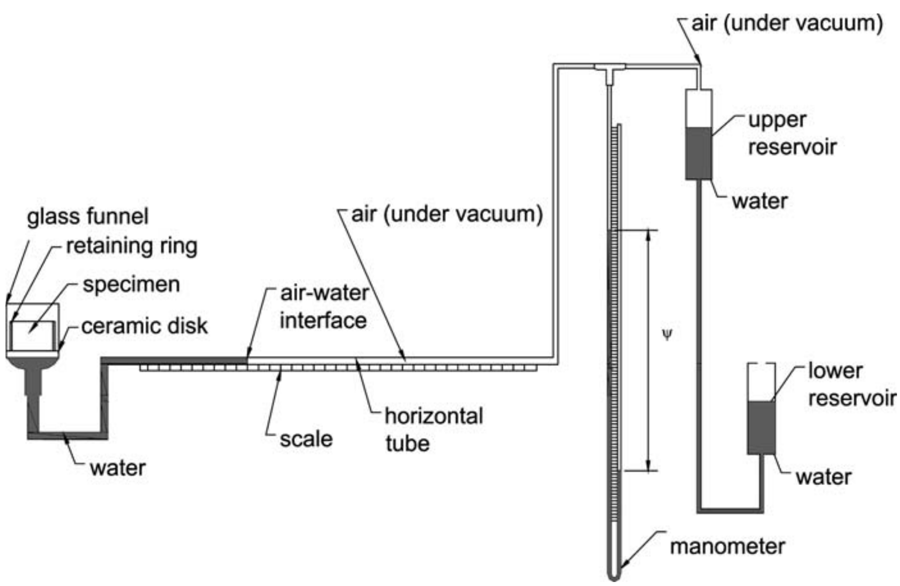

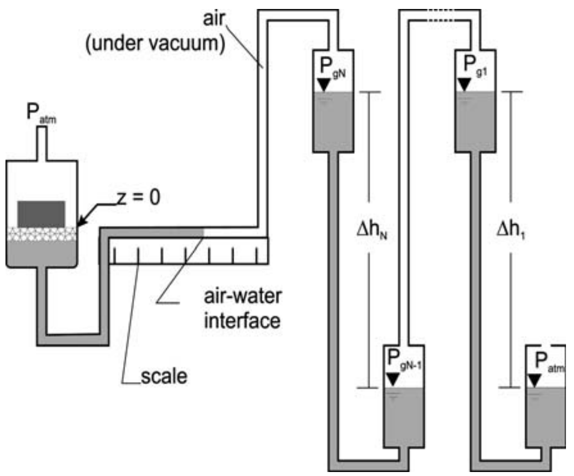

Fig. 8 Multiple hanging water column apparatus

of the hanging column apparatus consists in the fact that equilibrium is established when the water ceases to flow in or out of the specimen without the necessity of continuously adjusting the relative elevation of the reservoirs in order to maintain a constant applied suction. The air diffusion towards the capillary tube however can affect the measurements of the water volume flowing in or out of the specimen.

Multiple hanging water columns with reduced heights can be used to achieve suction values exceeding the limit of 20 to 30 kPa as shown in Fig. 8. As previously stated, higher suction values can be reached using a vacuum control system which consists of a vacuum source and a subatmospheric pressure regulator. An interesting application of the vacuum control system to a suction table is described by Romano et al. (2002). Figure 9 shows an overview of the suction table connected to the devices for controlling the applied suctions in the range from 10 kPa to about 40 kPa. A series of constant-head cylinder (CHC) are used to control the applied suction. Each constant-head cylinder consists of a Mariotte clear plastic or glass cylinders (MAT) forming a bubble tower (BBT). The cylinder has a two-hole rubber stopper at the top. A bubble tube is inserted in one hole of the rubber stopper, whereas the other hole is used to receive a shorter tube for the connection to the adjacent cylinder and, passing through a T-shaped connector, to a valve placed on a panel (PA). The last cylinder in the series is directly connected to the vacuum pump system (VPS). Air bubbles escape out of the bubble tube in the last Mariotte cylinder when the difference between air pressure in the line connected to the vacuum pump system (VPS) and the air pressure in the line of the last bubble tower exceeds the difference between the water pressure at the base of the bubble tube and the air pressure above the water in the column. To keep the release of bubbles to a minimum, it is important to maintain a constant difference between the air pressures in the two lines connected to the bubble tower. Different values of constant suctions can be achieved based on the length of the bubble tube. Applied suction can be adjusted stepwise by sequentially operating the valves on the panel (PA). However fine continuous regulation may be achieved by means of a subatmospheric regulator inserted into the line connecting the bubble towers to the vacuum pump.

More recently, Padilla et al. (2005) provided the design details of a device that can be used for

Fig. 9 Schematic diagram of a suction table connected to an high suction system based on vacuum control (after Romano et al. 2002)

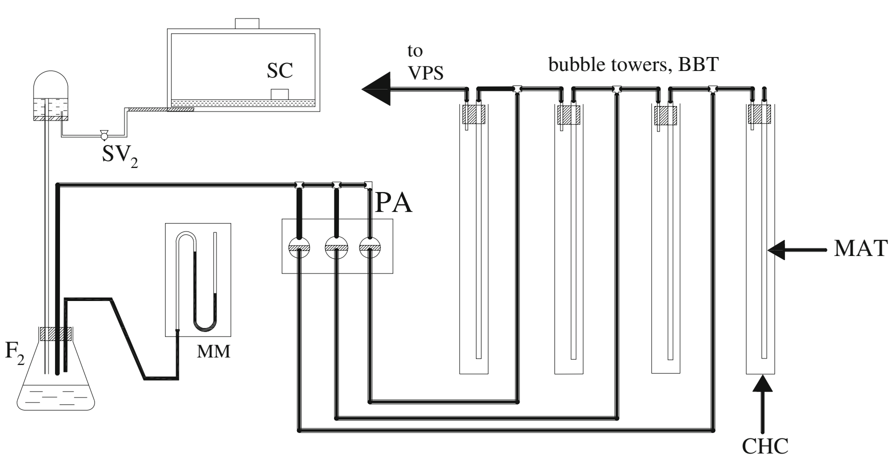

measuring SWRCs using relatively thin specimens which facilitate the correction of air diffusion.

4 Axis Translation Technique

Matric suction in an unsaturated soil specimen is defined as the difference between the pore-air pressure, u_a, and the pore-water pressure, u_w. Typically, in an unsaturated soil, pore-air pressure is atmospheric (i.e., $u_a = 0$) and pore water pressure is negative with respect to the atmospheric pressure. The axis-translation technique is conventionally used to determine or apply matric suction to soil specimens (higher than the atmospheric pressure, i.e., greater than 100 kPa) in a laboratory environment without any problems associated with cavitation (Richards 1931; Hilf 1956). This technique translates the origin of reference for the pore-water pressure from standard atmospheric conditions to the final air pressure in the chamber. Figure 10 shows the principle associated with the axis-translation technique (Marinho et al. 2008).

4.1 Equipment Details

The equipment used for measuring the matric suction of an unsaturated soil specimen using the axis translation technique is conventionally called a null pressure plate apparatus. A typical null-type pressure plate assembly is shown in Fig. 11a and the set up of null-type pressure plate device for measuring matric suction is shown in Fig. 11b.

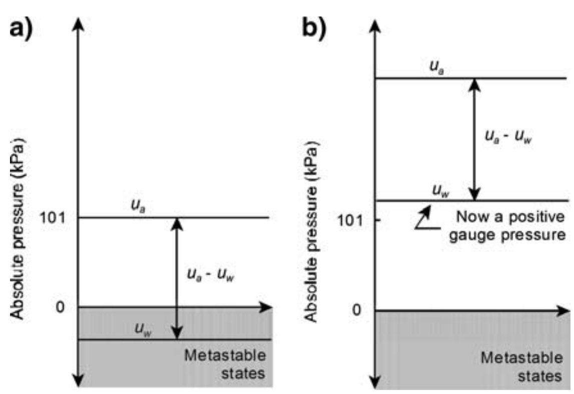

Fig. 10 Use of the axis translation technique to avoid metastable states. (**a**) atmospheric conditions. (**b**) axis-translation (Marinho et al. 2008.)

The axis-translation technique allows the pore-water pressure, u_w, in an unsaturated soil to be measured (or controlled) using a ceramic disk with fine pores (i.e., referred to as the high air-entry disk). These disks are conventionally used in unsaturated soil testing in place of porous disks used in saturated soil testing. The high air-entry disk acts as an interface that separates air and water phases. The separation of water and air phases can be achieved only up to the air-entry value of the disk. The air-entry value refers to the maximum matric suction to which the high air-entry disk can be subjected before free air passes through the disk. The maximum sustainable difference between the air pressure and water pressure is a function of the surface tension and the maximum effective pore size of the ceramic disk material (Fredlund and Rahardjo 1993; Lu and Likos 2004)

The soil specimen is placed in the stainless steel pressure chamber (Fig. 11) on top of the high-air entry disk, which is previously saturated. Several techniques are discussed with respect to the procedures that can be used for saturating the high-air entry disk (Fredlund and Rahardjo 1993; Fredlund and Vanapalli 2002). A good contact should be assured between the soil and the high-air entry disk. As soon as the soil specimen is placed on the high-air entry disk, the water in the tube (see Fig. 11b) goes into tension, which is measured using a pressure gauge (Fig. 11a). The tendency of the water to go into tension is resisted by increasing the air pressure in the chamber. A condition of equilibrium is attained when water in the specimen does not go into tension (i.e., attains “null” condition). The applied pore-air pressure, u_a, is the matric suction when the pore-water pressure, u_w, is set to zero (i.e., open to atmospheric pressure conditions). The equilibration time is dependent of the type of soil, size of specimen and air-entry value of the disk. In many cases, the equilibration occurs in 3 to 6 h in 20 mm thick compacted specimens (Vanapalli et al. 1999; Fredlund and Vanapalli 2002).

In some cases, pore water extraction tests can also be conducted using this apparatus by increasing the air pressure and allowing drainage from the specimen through the ceramic disk pores. The drainage continues until the water content of the specimen reaches equilibrium conditions with the applied matric suction, which is recorded as the difference between the water pressure on one side of the disk, which is

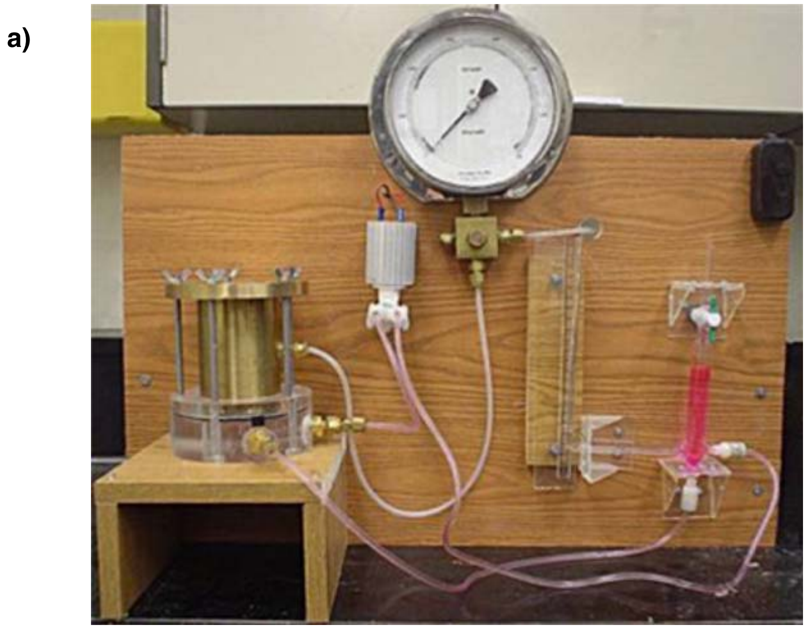

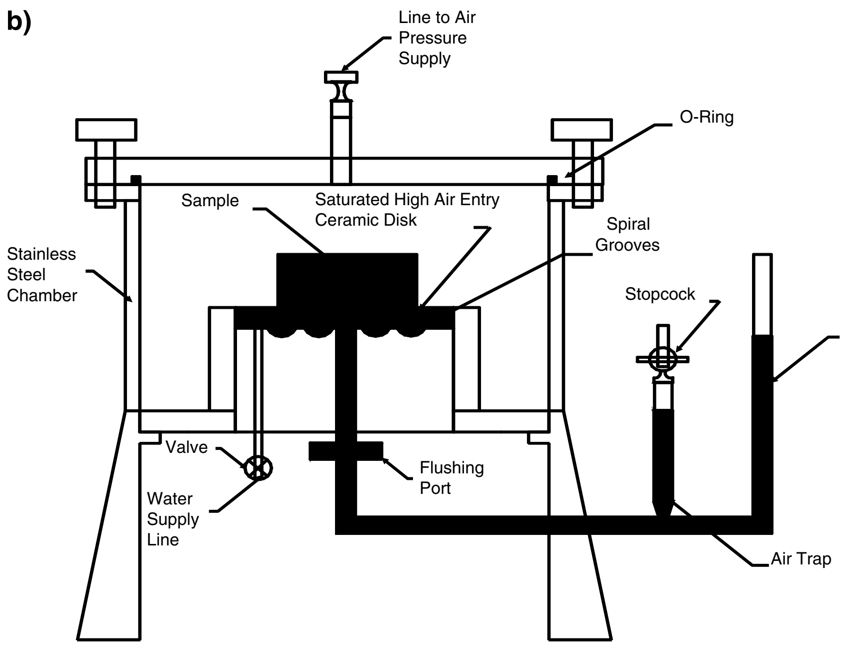

Fig. 11 Axis-translation equipment (from Power 2005)

often atmospheric, and the pore air pressure on the other side of the disk (Lu and Likos 2004).

The pore fluid pressures can be controlled independently from the ports located at the top and the bottom of the chamber (Fig. 11). As the axis-translation chamber should be pressurized with air, the thickness of chamber wall should be sufficiently thick for safety purposes. Also, the time between the unsaturated soil specimen placement and pressurization need be as short as possible. The axis-translation technique is best suited for measuring matric suction of unsaturated soil specimens in which the air phase is continuous. More details related to the limitations of the axis translation equipment are detailed in a later section.

The axis translation technique is routinely extended to different types of equipment for the determination of the mechanical properties of unsaturated soils such as the shear strength, volume change and the coefficient of permeability. Several investigators have successfully used this technique over the last 50 years which paved way for our present understanding of the mechanics of unsaturated soils (Matyas and Radhakrishna 1968; Barden et al. 1969; Fredlund and Morgenstern 1977; and many others during the last thirty years).

4.2 High-air Entry Stone Placement

Several geotechnical laboratories design special equipments that are not commercially available for studying hydraulic and mechanical properties of unsaturated soils extending axis-translation technique. One of the common problems with the design of axis-translation equipment is associated with the air-leakage. The key source of air leakage is through the boundaries of the ceramic stones where it is glued (i.e., epoxied around the edge to form a seal with the pedestal).

Figure 12 shows the recommended procedure for effectively gluing the ceramic stone in stages (i.e., typically two or three) to reduce the formation of air bubbles. Each layer needs to harden before the next layer of glue is placed. A useful guideline is to cure each layer over night under heat lamp before the next layer is placed (Power 2005). Any air bubbles formed in preceding layer should be opened up and filled with epoxy forming the next layer. Air bubbles, if any, will reduce the bonding strength between the ceramic stone and the stainless steel or brass ring leading to leakage with time.

4.3 Flushing System

There will be some air that can diffuse through the high air-entry disk when the axis translation technique is conducted over long periods of time (Fig. 13). It is essential to remove any air bubbles that form under the saturated high air-entry disk

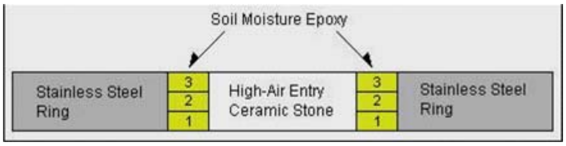

Fig. 12 Gluing high-air entry stone (from Power 2005)

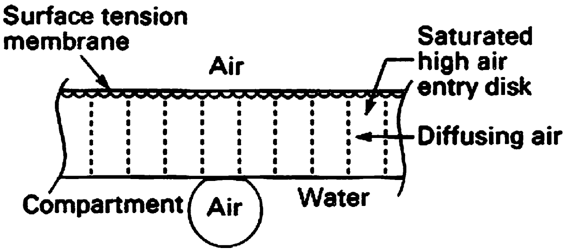

Fig. 13 Diffusion of air into the high-air entry disk (from Villar et al. 2005)

Fig. 14 Flushing diffused air from spiral groove of acrylic chamber

preferably using circular groves below the base of the ceramic stone (Fig. 14). The applied or measured matric suction value is not reliable if diffused air is not accounted for. It is therefore important to incorporate a flushing system to periodically remove any dissolved air that can appear within the null pressure plate system during testing.

The important features of the flushing system are: a pump and dimmer switch, an air trap with stopcock, and a glass tube to indicate the null position during testing (see Fig. 15). The pumps are connected to a common electrical dimmer in order to control the pumping force and eliminate any cavitation that may occur during flushing. In the event that air bubbles do form under the ceramic discs, the pump would be turned on and the air bubbles would flush into the air trap.

Air diffusion through the ceramic disk can be minimised by elevating the water pressure under the saturated air-entry disk, i.e. by applying a back-water pressure (Romero 2001; Marinho et al. 2008)

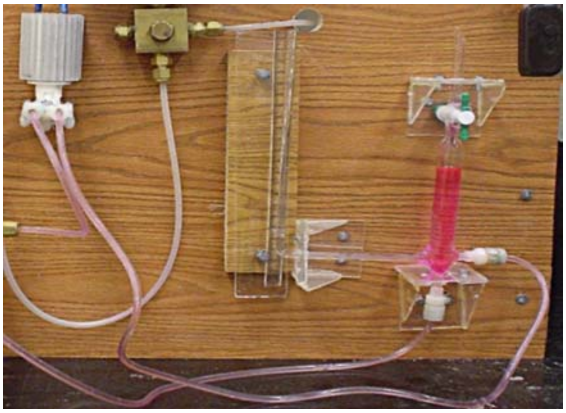

Fig. 15 The important features of the flushing system: the pump and dimmer switch, the air trap with stopcock, and the glass tube to indicate the null position during testing (from Power 2005)

4.3.1 Air-trap for the Flushing System

The air bubbles should be removed from the acrylic base of the equipment and facilitate to flow into the air trap shown in Fig. 15. It is recommended to use acrylic base for the axis translation equipment to facilitate the visualization of air bubbles, if any. Larger air-traps which allow more room for air bubbles are also recommended.

4.4 Axis Translation Technique Limitations

In the axis-translation technique, the air pressure, u_a, is higher than the atmospheric pressure and the pore water pressure, u_w, is positive. Such pressures are not representative of field conditions for unsaturated soils. Due to the applied air pressure in the axis-translation technique, air could seep or diffuse through the ceramic stone as discussed earlier into the drainage system of the apparatuses. The applied air pressure will have a significant effect on the measurements of water exchanges from in and out of the unsaturated soil specimen. For this reason, the rate of air diffusion should be measured for each axis-translation apparatus. To track changes in specimen water content throughout the test in which the axis translation technique is applied, the diffused air volume must be measured and correction to the pore water volume change must be made. This task is generally accomplished by flushing water (and diffused air) out of the ceramic disk into a burette, where the air volume causes change in the water level that can be measured.

In some cases, depending on the rate of application of the chamber air pressure and the compressibility characteristics of the soil specimen, it is possible to temporarily overshoot the actual suction value. In such a case, the peak should not be interpreted as the actual suction, nor should the subsequent down turn of the curve be interpreted as the onset of significant air diffusion. In other words, great care should be applied in the interpretation of the results so that matric suction can be reliably measured using axis translation technique.

The theory associated with the axis translation technique is only valid for soils with totally interconnected pore-air voids and for soil particles that are incompressible and only when air–water interphase is continuous, which is typically observed in specimens with degree of saturation, S, $< 90\%$) (Olson and Langfelder 1965; Bocking and Fredlund 1980). Validity of the axis-translation technique at very high degrees of saturation is discussed by Marinho et al. (2008)

Matric suction in two specimens (say specimens A and B) can be significantly different from one another in spite of having the same dry density, total volume and gravimetric water content. This could be attributed to the arrangement of the soil particles and the amount of air bubbles which may be significantly different from one specimen to the other depending upon the method of compaction. The water phase can be discontinuous due to the presence of occluded air bubbles (for example say, in Specimen A). The trapped water within the air bubbles may not be effective and hence water content of Specimen A can be likely low and hence the suction would be overestimated compared to a specimen without occluded air bubbles (say, in specimen B).

The diffusion of air through porous ceramic disks (i.e., high air-entry disks) also imposes a practical limit on the duration of the test. To alleviate problems associated with diffusion it is necessary to either eliminate diffusion in the drainage system or resort to periodic air washing of the drainage system at the bottom of the high air-entry disk.

There are three key processes that are associated with air diffusion as summarized by Romero (1999) and Farulla and Ferrari (2005):

(i) The first step is to asses the amount of air dissolution into the water in the soil pores.

Henry's law can be used as a tool to understand and calculate the amount of air dissolution.

(ii) The second step is to calculate the dissolved air diffusion through the pore-water in the ceramic disk. Fick's law can be used for calculating the air diffusion.

(iii) The third step is to asses the air coming out from the solution in the water drain lines.

In addition, matric suction in soil specimens is also influenced due to water evaporation originated by the vapour pressure gradient between the pore voids and the soil specimen. Some details on these parameters are presented in later sections on this topic in the paper. However, detailed discussions are beyond the scope of this paper. More information on related topics is available in Romero (1999, 2001) and Oliveira and Fernando (2006). All of the above details related to the null pressure plate equipment is also valid for equipment such as modified direct and triaxial shear equipments and other equipment which use axis translation technique for the determination of the unsaturated soil properties.

5 Special Devices or Equipments

Several investigators developed special devices or equipments to alleviate some of the problems associated with diffusion of air while applying axis translation technique during the measurement of unsaturated soil properties. The suction and volume changes of an unsaturated soil specimen cannot be reliably measured unless diffusion effects are accounted for. The applied or the measured suction values may not be reliable if the ceramic stone in the axis translation equipment is not in a state of fully saturated condition. There can be loss of continuity between the liquid phase in the high-air entry disk (i.e., ceramic stone) with time due to diffusion effects while measuring the unsaturated soil properties extending axis-translation technique for a long period of time (Romero 1999).

The use of bubble pump along with air traps was originally suggested by Bishop and Donald (1961) for alleviating some of the problems associated with diffusion by flushing out the bubbles collected at the bottom the ceramic disk. Fredlund (1975) suggested using Diffused air-volume indicators (DAVI) for

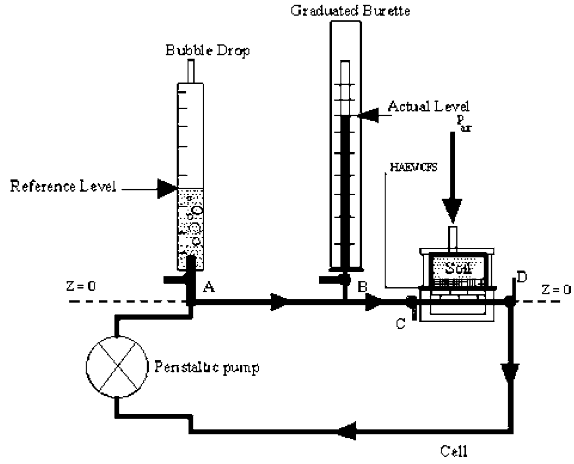

Fig. 16 Double Burette System for Measuring Diffused Air (De Gennaro et al. 2002)

measuring the diffused air volume when axis translation technique is employed. More details related to the DAVI are available in Fredlund and Rahardjo (1993). Comprehensive details related to the measurement of volume changes associated with diffusion using different types of equipment are available in Romero (1999) and Vilar et al. (2005).

In recent years several investigators used different techniques to measure both total volume and air volume changes associated with unsaturated soil testing and discussed the merits of methods they investigated (Adams et al. 1996; Macari et al. 1997; Romero et al. 1997, Ng et al. 2002; Aversa and Nicotera 2002). Also, more sophisticated equipments are available now to measure the diffused air volumes in unsaturated soil specimens when axis translation techniques are employed. For example, De Gennaro et al. (2002) suggested a technique for measuring the quantity of air diffused and then removing it using a double burette system (Fig. 16).

Lawrence et al. (2005) suggested power pulse technique for the measurement of air volume diffused from the specimen through a high air-entry disk into the measuring system. In this technique, the diffused air doesn't necessarily have to be flushed; its volume simply needs to be measured. By comparing the changes in water volume reading to the initial readings for a given pressure (through the determination of correction factor) it is possible to calculate the volume of air from Boyle's law. This is a promising technique.

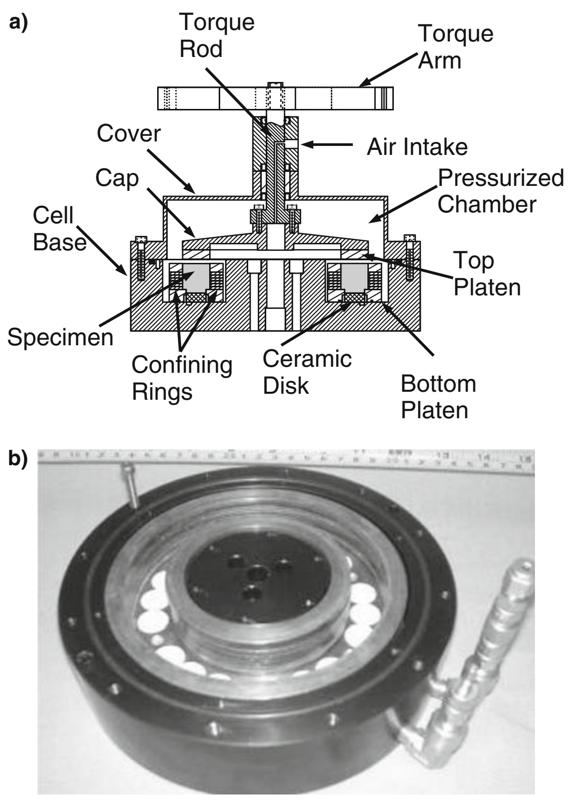

Fig. 17 (**a**) Schematic of modified ring shear cell assembly (**b**) Base of unsaturated ring shear cell with ceramic disks and inner confining ring stacks in place (from Infante Sedano 2006)

5.1 Implementing Axis-translation Technique in Mechanical Testing

A modified ring shear test equipment has been designed and reliable test data have been obtained related to the hydraulic and mechanical behavior of unsaturated soils (Vanapalli et al. 2005; Infante Sedano et al. 2007). A schematic view of this equipment is shown in Fig. 17. For the purpose of the determination of the hydraulic and mechanical behavior of an unsaturated soil specimen, the cell should be enclosed in a sealed chamber so that the specimen can be subjected to a high air pressure for the application of the axis translation technique. The key components are the ring shear cell, an air trap, and an electronic scale for the measurement of water overflow from the soil specimen (Fig. 18). A pump forces the water to circulate below the ceramic disks in the modified ring shear apparatus to flush the air bubbles that are collected below the base of ceramic disks. The flushed out air accumulates in the air trap, where a small bore syringe is used to reset the water level to a fixed reference mark after flushing. Any overflow water is collected in a small plastic container placed on an electronic balance for measuring the mass of water. This technique of flushing out the air bubbles can be used with the double burette or any other method using an air trap in conjunction. More details about the correction for air diffusion are detailed in the next section.

5.1.1 Correcting for Air Diffusion

Figure 19a illustrates a typical water mass measurement readings versus time curve obtained during a suction increase stage. Breaks in the curve are apparent at the time of flushing the air bubbles. With time, as more air bubbles form, any subsequent flushing will show other breaks in the curve. There will be drop in the water mass reading after flushing which is equal to the actual volume of air removed. The rate of air infiltration (which includes combined diffusion and air leakage) is the reduction in the water mass reading divided over the time interval between flushing operations (Fig. 19b). If the curve after each flushing break point is moved upward, as shown in Fig. 19c, a continuous curve is generated. This continuous curve corresponds to the condition where no flushing would have been performed. The curve tends towards a constant slope, which indicates that the rate of air infiltration is also constant (Fig. 19c). This constant rate of air infiltration is now plotted in Fig. 19d, and is shown as line i). By subtracting the ordinate of line i) from curve ii), and adding the magnitude of the initial reading as a constant, the corrected curve iii) is generated. Curve iii) represents the best estimate of the readings that would have been generated had there been no infiltration.

5.1.2 Correcting for Evaporation and Condensation

Even after having applied the corrections for air infiltration, it is possible that the resulting curve showing water mass readings over time will not converge to a horizontal asymptote as would be expected in an ideal system. This may be due to evaporation if humidity is lost to a relatively dry air phase in the pressurized chamber or due to condensation if a saturated air phase transmits humidity to the soil.

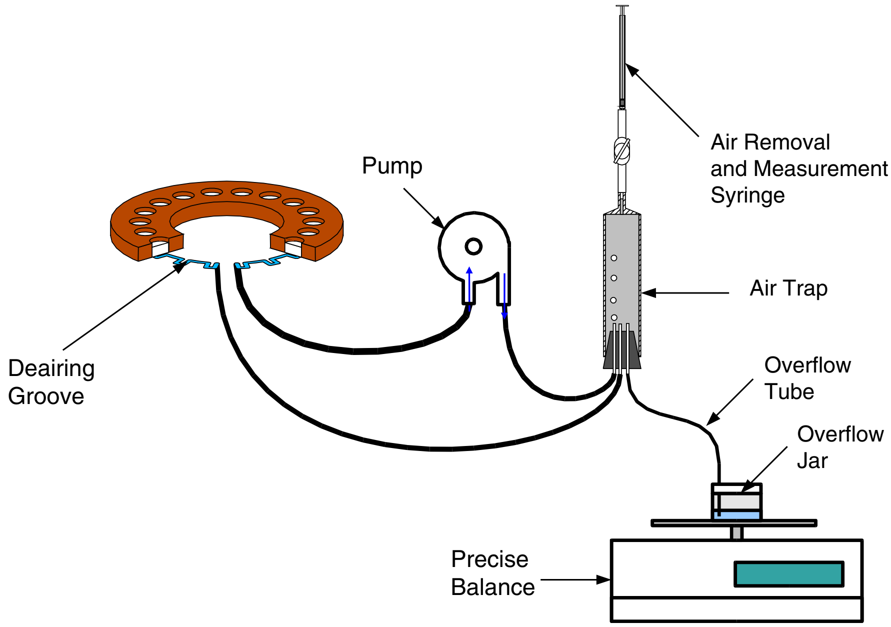

Fig. 18 Idealized schematic of the de-airing system for the modified ring shear apparatus (modified after Infante Sedano et al. 2007)

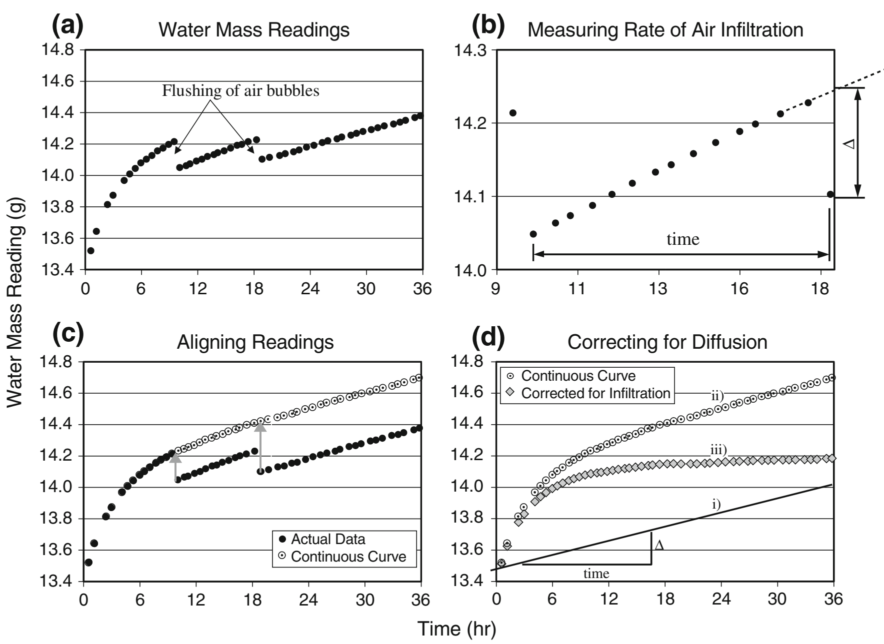

Fig. 19 Measurement of air infiltration, and its correction to the water content measurement (after Infante Sedano et al. 2007)

Although the air used to pressurize the ring shear chamber is bubbled through water, it is still possible for it to be relatively dry for a number of reasons including leakage in the cell. The dry air could cause the corrected water mass reading curve to show a downward trend, suggesting evaporation from the specimen (see curve a in Fig. 20a) Alternatively, if there is no leakage and the water phase can become saturated through contact with the bubbling chamber, then there will be a tendency to transfer moisture to the specimen, unless the degree of saturation of the air phase is in equilibrium with the matric suction of the specimen (Fig. 20b). More details related to this equipment design are discussed in Infante Sedano (2006).

In addition, details along similar lines related to soil water evaporation along a wetting path have been

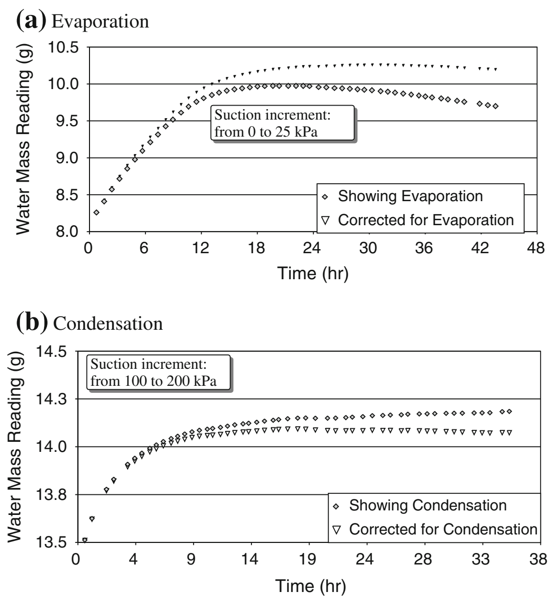

Fig. 20 Measurement of air infiltration, and its correction to the water content measurement (after Infante Sedano et al. 2007)

suggested by Romero (1999) and Vilar et al. (2005) for tests undertaken using triaxial shear apparatus. Several new equipments are now available that can be used to address challenges associated with unsaturated soils testing (Padilla et al. 2006; Hoyos et al. 2006). In years to come it is likely that we will have more reliable experimental data that can be useful for developing rigorous constitutive models for unsaturated materials.

6 Summary

Significant advancements were made during the last two decades related to our present understanding of the mechanics of unsaturated soils using experimental methods. This paper provides a summary of the two techniques which are commonly employed in the testing of the hydraulic and mechanical behavior of unsaturated soils (i.e., negative water column and axis translation techniques). All aspects related to the testing procedures and other details could not be summarized in greater detail due to space limitations. However, an attempt was made to provide several of the key references that would be useful in providing the remainder of the details.

Acknowledgements The authors would like to acknowledge the help received from Cevat Catana, Infante Sedano and Kenton Power in the preparation of slides for presenting this paper at the EXPERUS 2005 conference. Special thanks go to Dr. Alessandro Tarantino, Dr. Enrique Romero, Cevat Catana, Dr. Infante Sedano, and Dr. Marinho and for their comments and suggestions during the preparation of this paper.

References

Adams BA, Wulfsohn D, Fredlund DG (1996) Air volume change measurement in unsaturated soil testing using a digital-pressure volume controller. Geotech Testing J 19(1):12–21

Alonso EE, Gens A, Josa A (1990) A constitutive model for partially saturated soils. Géotechnique 40(4):405–430

Aversa S, Nicotera MV (2002) A triaxial and oedometer apparatus for testing unsaturated soils. Geotech Testing J 25(1):3–15

ASTM (2003) D 6836–Standard test methods for determination of the soil water chararcteristic curve for desorption using a hanging column, pressure extractor, chilled mirror hygrometer, and/or centrifuge. American Society for Testing Materials, Philadelphia

Barbour SL (1998) Nineteenth Canadian geotechnical colloquium: the soil–water characteristic curve: a historical perspective. Can Geotech J 35:873–894

Barden L, Madedor O, Sides GR (1969) Volume changes characteristics of unsaturated clay. ASCE J Soil Mech And Found Div 5(1):33–52

Bocking KA, Fredlund DG (1980) Limitations of the axis translation technique.In: Proceedings of the 4th international conference expansive soils, Denver, pp 117–135

Buckingham E (1907) Studies on the movement of soil moisture. Bull 38 USDA, Bureau of Soils, Washington DC

Bishop AW (1959) The principle of effective stress. Teknisk Ukeblad I Samarabeide Med Teknikk, Oslo, Norway 106(39):859–863

Bishop AW, Donald IB (1961) The experimental study of partly saturated soil in the triaxial apparatus. In: Proceedings 5th ICSMFE, vol 1. Paris, pp 13–21

Cui YJ, Delage P (1996) Yielding and plastic behaviour of an unsaturated compacted silt. Géotechnique 46(2):291–311

Dane JH, Oostrom M, Missildine BC (1992) An improved method for the determination of capillary pressure-saturation curves involving TCE, water and air. J Contam Hydrol 11:69–81

Dane JH, Hopmans JW (2002) Hanging water column. In: Dane JH, Topp GC (eds) Methods of soil analysis—part 4—physical methods. Soil Sci Soc of Am, Inc., Madison, Wisconsin, USA

DeGennaro V, Cui YJ, Delage P, De Laure E (2002) On the use of high air entry value prous stones for suction control and related problems. In: Juca JFT, de Campos TMT, Marinho FAM (eds) Second international conference on unsaturated soils. Swets & Zeitlinger, Lissee, pp 435–441

Farulla A, Ferrari A (2005) Controlled suction oedometric test: analysis of some experimental aspects. In: Tarantino A, Romero E, Cui YJ (eds) Advanced experimental unsaturated soil mechanics. Trento, Italy, pp 43–48

Fredlund DG (1975) A diffused air volume indicator for unsaturated soils. Can Geotech J 12:533–539

Fredlund DG, Morgenstern NR (1977) Stress state variables for unsaturated soils. J Geotech Eng Div. ASCE 103:447–466

Fredlund DG, Rahardjo H (1993) Soil mechanics for unsaturated soils. Wiley, New York

Fredlund DG, Vanapalli SK (2002) Shear strength of unsaturated soils. In: Dane JH, Topp GC (eds) Methods of soil analysis, part 4-physical methods, Soil Sci Soc of Am, Inc., Madison, pp 324–360

Gallipoli D, Gens A, Sharma RS, Vaunat J (2003) An elasto-plastic model for unsaturated soil incorporating the effect of suction and degree of saturation on mechanical behavior. Géotechnique 53(1):123–135

Haines WB (1927) A further contribution to the theory of capillary phenomenon in soils. J Agric Sci 17:264–290

Haines WB (1930) Studies in the physical properties of soil: V. The hysteresis effect in capillary properties, and the modes of moisture distribution associated therewith. J Agric Sci 20:97–116

Hilf JW (1956) An investigation of pore-water pressure in compacted cohesive soils, Ph. D. Thesis. Technical Memorandum No. 654, United State Department of the Interior Bureau of Reclamation, Design and Construction Division, Denver, Colorado, USA

Hoyos LR, Takkabutr P, Puppala AJ (2006) A modified pressure plate device for SWCC testing under anisotropic stress state. In: Miller GA, Zapata CE, Houston SL, Fredlund DG (eds) Unsaturated soils 2006, GSP No. 147, vol 2. Am Soc of Civ Eng, pp 1753–1762

Infante Sedano, JA (2006) A modified ring shear test device for determining the hydro-mechanical behavior of unsaturated soils. Ph.D. thesis. University of Ottawa

Infante Sedano JA Vanapalli SK Garga VK (2007) Modified ring shear apparatus for unsaturated soils Testing. Geotech Testing J. Am Soc Testing Mater 30(1):1–12

Lawrence CA Houston WN Houston SL (2005) Pressure pulse technique for measuring diffused air volume. In: Tarantino A, Romero E, Cui YJ (eds) Advanced experimental unsaturated soil mechanics, Trento, Italy, pp 9–13

Leong EC Rahardjo H (1997) Permeability functions for unsaturated soils. J Geotech Geoenviron Eng 123:1118–1126

Liu HH Dane JH (1995a) Improved computational procedure for retention relations of immiscible fluids using pressure cells. Soil Sci Soc Am J 59:1520–1524

Liu HH, Dane JH (1995b) Computation of the Brooks–Corey parameters at a physical point based on pressure cell data. Department of Agronomy and Soils Special Report, July 1995. Alabama Agricultural Experiment Station, Auburn University, AL

Lu N, Likos WJ (2004) Unsaturated soil mechanics. Wiley, New York

Maâtouk A, Leroueil S, La Rochelle P (1995) Yielding and critical state of a collapsible unsaturated silty soil. Géotechnique 45(3):465–477

Macari EJ, Parker JK, Costes NC (1997) Measurement of volume changes in triaxial tests using digital imaging techniques. Geotech Testing J 20(1):103–109

Marinho FAM, Take WA, Tarantino A (2008) Measurement of matric suction using tensiometric and axis translation techniques. Geotech Geol Eng. doi:10.1007/s10706-008-9201-8

Matyas EL, Radhakrishna HS (1968) Volume change characteristics of partially saturated soils. Géotechnique 18(4):432–448

Narasimhan TN (2005) Buckingham, 1907: an appreciation. Vadose Zone J 4:434–441

Ng CWW, Zhan LT, Cui YJ (2002) A new simple system measuring volume changes in unsaturated soils. Can Geotech J 39(3):757–764

Oliveria OM, Fernanado FAM (2006) Study of equilibration in the pressure plate. In: Miller GA, Zapata CE, Houston SL, Fredlund DG (eds) Unsaturated soils 2006, GSP No. 147, vol 2. Am Soc of Civ Eng, pp 1864–1874

Olson RE, Langfelder J (1965) Pore-water pressures in unsaturated soils. J Soil Mech Found Div, Proc of Am Soc of Civ Eng 91(4):127–160

Padilla JM, Perera YY, Houston WN, Fredlund DG (2005) A new soil–water characteristic curve device. In: Tarantino et al. (eds) Proceedings of the advanced experimental unsaturated soil mechanics, EXPERUS 2005. Balkema Publishers, pp 15–22

Padilla JM, Perera YY, Houston WN, Perez N, Fredlund DG (2006) Quantification of air diffusion through high air-entry cerfamic disks. In: Miller GA, Zapata CE, Houston SL, Fredlund DG (eds) Unsaturated soils 2006, GSP No. 147, vol 2. Am Soc of Civ Eng, pp. 1852–1863

Power KC (2005) Suction and compressibility characteristics of an unsaturated till. M.Sc. thesis. University of Ottawa, 229 pp

Richards LA (1928) The usefulness of capillary potential to soil moisture and plant investigators. J Agric Res 37:719–742

Richards LA (1931) Capillary conduction of liquids though porous medium. J Phys 1:318–333

Romano N, Hopmans JW, Dane JH (2002) Suction table. In: Dane JH, Topp GC (eds) Methods of soil analysis—part 4—physical methods, Soil Sci Soc of Am, Inc., Madison, Wisconsin, USA

Romero E. Facio JA, Lloret A, Gens A, Alonso EE (1997) A new suction and temperature controlled triaxial apparatus. In: Proceedings 14th international conference on soil mechanics and foundation engineering. Balkema, Hamburg, Rotterdam, pp 185–188

Romero E (1999) Characterisation and thermo-hydromechanial behavior of unsaturated Boom clay: an experimental study. Ph.D. thesis. Universitat Politecnica de Catalunya

Romero E (2001) Controlled-suction techniques. In: Gehling WYY, Schnaid F (eds) Proceedings 4º Simposio Brasilerio de Solos Nao Saturadoes, ABMS, Porto Alege, pp 533–542

Sharma RS, Mohamed MHA (2003) An experimental investigation of LNAPL migration in an unsaturated/saturated sand. J Eng Geol 70/3–4:305–313

Toll DG (1990) A framework for unsaturated soil behaviour. Géotechnique 40(1):31–44

Tarantino A, Tombalato S (2005) Coupling hydraulic and mechanical behavior in unsaturated compacted clay. Géotechnique 55(4):307–317

Vanapalli SK, Fredlund DG, Pufahl DE, Clifton AW (1996) Model for the prediction of shear strength with respect to soil suction. Can Geotech J 33(3):379–392

Vanapalli SK, Fredlund DG, Pufahl DE (1999) Influence of soil structure and stress history on the soil-water characteristics of a compacted till. Géotechnique 49(2):143–159

Vanapalli SK, Garga VK, Infante Sedano JA (2005) Determination of the shear strength of unsaturated soils using the modified ring shear apparatus. In: International symposium on advanced experimental unsaturated soil mechanics, Trento, Italy, pp 125–130

Villar MV, Romero E. Buenfil C, Lloret A, Martin PW (2005) The application of the axis translation technique to the triaxial testing of unsaturated soils. In: Proceedings of the international conference on problematic soils, 25–27 May 2005, vol 1. Eastern Mediterranean University Press, pp 87–94

Wheeler SJ, Sivakumar V (1995) An elasto-plastic critical state framework for unsaturated soil. Géotechnique 45(1):35–53

Wheeler SJ, Sharma RS, Buisson MSR (2003) Coupling of hydraulic hysterisis and stress–strain behaviour in unsaturated soils. Géotechnique 53(1):41–54

Vapour Equilibrium and Osmotic Technique for Suction Control

James A. Blatz · Yu-Jun Cui · Luciano Oldecop

Originally published in the journal *Geotechnical and Geological Engineering*, Volume 26, No. 6, 661–673.
DOI: 10.1007/s10706-008-9196-1

Abstract The vapour equilibrium method and osmotic technique have gained widespread acceptance as reliable methods for controlling relative humidity and thereby suction in soil specimens. The ability to impose suction on soil specimens allows for drying and wetting stress paths to be imposed to evaluate resulting changes in strength, deformation and flow characteristics. The two methods presented and discussed in this paper have been adapted for use with a number of traditional laboratory tests including the oedometer, direct shear and triaxial tests. This report provides a summary of some recent developments and knowledge regarding the use of these techniques highlighting the limitations and drawbacks of the methods.

Keywords Laboratory tests · Unsaturated soil · Suction · Osmotic method · Vapour equilibrium

J. A. Blatz (✉)
Civil Engineering, University of Manitoba, 368 EITC Building, R3T 5V6 Winnipeg, MB, Canada
e-mail: blatzja@cc.umanitoba.ca

Y.-J. Cui
Ecole Nationale des Ponts et Chaussées, CERMES, Paris, France

L. Oldecop
IDIA, Universidad Nacional de San Juan, San Juan, Argentina

1 Introduction

With increasing attention regarding the development of analytical and design tools for unsaturated soils the need for reliable suction control and measurement techniques has attracted significant research attention around the world. This report provides a summary of some key recent developments in the application of the vapour equilibrium method and the osmotic method for applying suctions to soil specimens in laboratory testing.

Soil suction is defined by Richards (1974) as the water potential in a soil-water system. Richards (1974) lists three components of suction in unsaturated soils, namely capillarity, adsorption of water on the surface of the clay minerals, and osmotic phenomena. Only two components of total suction are generally considered for engineering studies, the matric and osmotic components. Matric suction is generated by capillarity and the osmotic suction is generated by pore fluid chemistry and water adsorption (Fredlund and Rahardjo 1993). Matric suction is generally considered to be the dominant component of total suction in non-plastic cohesionless soils with a relatively pure pore fluid. Osmotic suction can be appreciable in high plastic clays that have high activity due to the clay mineralogy or in cases where the pore fluid activity is high due to the presence of dissolved salts. Osmotic suction is generally assumed to be insensitive to changes in water content as long as the pore fluid chemistry remains constant.

However, this is not always true. In cases with active clay minerals, the water adsorption can be strongly dependent on the distance between the clay sheets and therefore the water content. As a general approach changes in total suction in unsaturated soils can generally be attributed to changes in the matric suction component (Fredlund and Rahardjo 1993).

The total suction is then written as:

$$\psi = (u_a - u_w) + \pi \tag{1}$$

where the matric suction is given by $(u_a - u_w)$ and the osmotic suction is given by π. The total suction of a soil (ψ) is related to the relative humidity by Kelvin's law (Fredlund and Rahardjo 1993) as shown in Eq. 2

$$\psi = \frac{-R \cdot T}{M_w(1/\rho_w)} \cdot \ln(RH) \tag{2}$$

where R is the universal gas constant (8.31432 J/mol K), T is the absolute measured temperature in degrees Kelvin, M_w is the molecular weight of water (18.016 kg/kmol), ρ_w is the unit weight of water in kg/m^3 as a function of T, and RH is the measured relative humidity (partial pressure of porewater vapor in the specimen divided by the saturation pressure of water vapor over a flat surface of water at the same temperature).

2 Controlled Suction

As shown in the formulation, soil suction can be controlled by creating controlled relative humidity conditions. Two established methods of controlling suction in soil specimens are discussed in this paper. The first method is the vapour equilibrium method and the second is the osmotic technique. It is important to note that the vapour equilibrium technique controls total suction whereas the osmotic technique controls matric suction. This distinction will be discussed in further detail in a later section. Both of the methods discussed apply suctions but do not provide direct measurements of the suction applied.

2.1 Vapour Equilibrium Technique (VET)

As shown in the formulation, environments of constant suction can be created in sealed containers using the osmotic potential of chemical solutions. This technique is commonly referred to as the vapour equilibrium technique (Tessier 1984; Delage et al. 1998; Romero 1999; Delage and Cui 2000; Villar 2000; Tang and Cui 2005). Figure 1 shows an example of a glass desiccator with a porous disk over the solution which suspends soil specimens in the vapour environment above the chemical solutions. A net water exchange between the liquid and vapour phases occurs in the desiccator headspace until equilibrium between the two phases is achieved. The partial vapour pressure resulting due to the environment in the desiccator is directly a function of the concentration of the solution. Partial vapour pressures of common chemical systems can be found in Stokes and Robinson (1948) and Young (1967). Suctions are produced in soil specimens by the water exchange between the specimen and the vapour in the headspace of a desiccator.

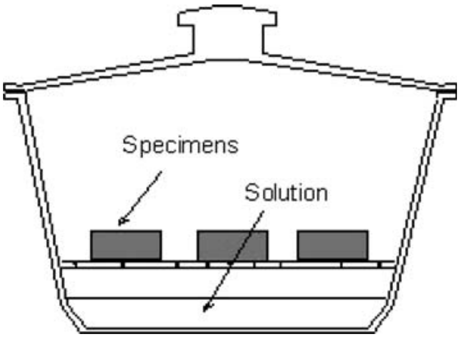

Fig. 1 Soil specimens in constant suction environment (after Tang et al. 1998)

Application of suction using sealed glass containers with soil specimens suspended over binary salt solutions is common (Kanno and Wakamatsu 1993: Delage et al. 1998; Saiyouri et al. 2000; Tang et al. 1998; Romero et al. 2001; Leong and Rahardjo 2002). The technique has also been applied to modified testing apparatus to control suction during traditional laboratory testing.

Generally there are two types of osmotic solutions that are used to generate constant suction conditions. The first type of solution is to use saturated salt solutions and the second type is to use unsaturated acid solutions. The saturated salt solutions provide the benefit that the concentration of the osmotic solution does not change as water exchange takes place between specimens and the vapour environment. The limitation of using salt solutions is that the control of suction is limited for each specific type of salt based on the properties and purity of the specific chemical component. Mixtures of sodium chloride and potassium chloride are often used to achieve desired target suction values. The salt solutions are also generally limited to a lower range of suction values (0–10 MPa range). A range of salt solutions and the relative humidity levels that can be generated using them are available in many published works (e.g. Tang and Cui 2005) and chemistry handbooks (Bruno and Svoronos 2003). The second type of solution is generated using unsaturated acid solutions. The benefit of the acid solutions is that much higher suctions can be imposed and suction set points can be established much easier by careful control of the concentration of the solution. The drawback of using this approach is that the concentration of the osmotic solution changes during the water exchange thereby altering the target suction value. This becomes even more difficult when applying higher suction values (above 150 MPa) where the relationship between acid concentration and relative humidity is highly non-linear and small changes in the concentration can have a dramatic impact on the applied suction. A correction can be applied by assuming that water loss or uptake by the soil specimen is added or removed from the osmotic solution in the constant mass environment. Once the specimen has reached equilibrium the change in concentration can be calculated and therefore the equilibrium suction can be established. Another approach that can be used to alleviate large changes in suction over the equilibration period is to ensure that the volume of osmotic solution is very large relative to the anticipated addition or loss of water from the specimens.

There are a few important considerations that are common to both types of osmotic solutions used in the vapour equilibrium method. The first consideration is that long time periods are required to achieve equilibrium conditions due to the diffusion process that controls transfer of water vapour between the specimens and the vapour in the desiccator headspace. For example, for fine-grained two inch triaxial specimens, equilibrium times are in the range of 30–50 days (Tang et al. 1998). The second important consideration for this method of suction control is the requirement for strict control of temperatures (Tang and Cui 2005). Small variations in temperature can dramatically impact the applied suction. Usually water baths are used to house the glass containers to minimize temperature variation due to advective air flow and convection cells in laboratory environments. Correction equations have also been developed to deal with temperature changes during testing (Romero 1999). One final consideration is the accuracy of relative humidity control in the low suction range. Due to the non-linearity of the relationship between suction and relative humidity, small variations in relative humidity at low suctions can lead to large errors in the actual applied suction. Typical errors that can be introduced during mixing of the solution include losses of water component due to evaporation, losses in the mixing and scale calibration errors. Agus and Schanz (2005) and Oldecop and Alonso (2004) show the error accumulation that can occur at low suctions (and therefore high relative humidity) due to small errors in measurement of constituent materials in the solution. Figure 2 taken from Agus and Schanz (2005) shows the error with an assumed 0.5% error in the relative humidity applied.

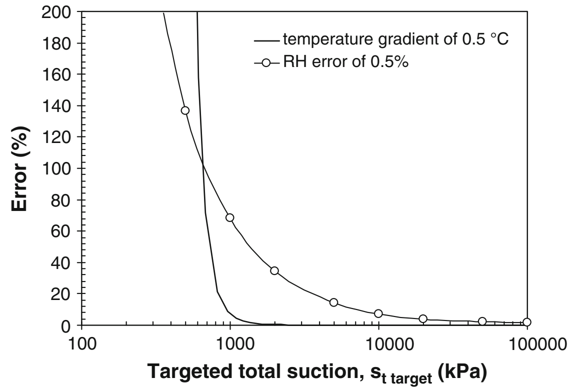

Fig. 2 Error in total suction (after Agus and Schanz 2005)

Many applications where the vapour equilibrium method is used for controlling suction use a separate independent sensor device (tensiometer, psychrometer, etc.) to verify that the target suctions are achieved within the specimen at equilibrium.

2.2 Osmotic Technique

The osmotic technique was initially developed by biologists (Lagerwerff et al. 1961) and later adopted by soil scientists (Zur 1966). It was introduced in geotechnical engineering by Kassiff and Benshalom

(1971). In this technique losses or uptakes of water are caused by the process of osmosis. The soil specimen is placed in contact with a semi-permeable membrane behind which an aqueous solution of large sized polyethyleneglycol (PEG) molecules are circulated. Since water molecules can cross the membrane whereas PEG molecules cannot, an osmotic suction that increases with the PEG concentration is applied to the soil through the semi-permeable membrane. Since water transfer takes place in the liquid phase and ions can cross the semi-permeable membrane freely, the osmotic technique controls the matric suction of a soil and not the osmotic suction.

The relationship between osmotic pressure and PEG concentration is well known for two molecular weights (PEG 6,000 and 20,000). Williams and Shaykewich (1969) found acceptable agreement between different calibrations performed by various authors either by direct pressure measurement or by controlling the relative humidity induced by PEG solutions. The suction covered ranges from 0 to 1.5 MPa. More recently, Delage et al. (1998) extended this calibration up to 10 MPa as shown in Fig. 3. It is observed that the calibration is independent of the molecular weight of the PEG: similar relationships are obtained for PEG 1,500, 4,000, 6,000 and 20,000. Obviously, higher suctions can be obtained by using smaller sized PEG molecules. However, use of small weight PEG necessarily implies use of small molecular weight cut-off with semi-permeable membranes; therefore water flow is reduced by the low permeability of the semi-permeable membrane, and the test duration is increased. Thus in practice it is important to use larger weight PEG when desired suction allow it.

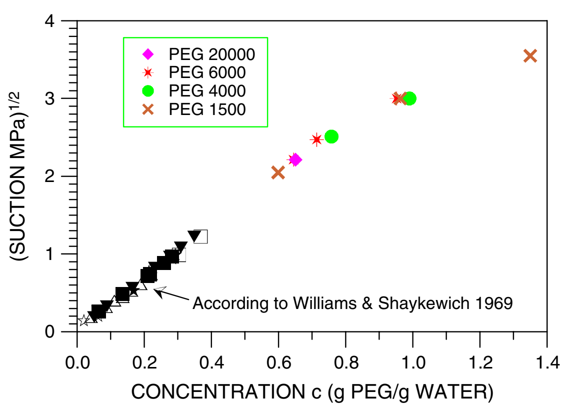

Fig. 3 PEG calibration curve for different molecular weights (after Delage et al. 1998)

Waldron and Manbeian (1970) measured the suctions generated by PEG solutions using a null type osmometer. Their results showed some difference with respect to the above calibration data. This difference was confirmed by direct suction measurement carried out by Dineen and Burland (1995). These authors suspected that a membrane effect could modify the calibration data by reducing the applied suction. This effect was further analyzed by Slatter et al. (2000).

The main advantage of the osmotic technique is its ease in reaching high suctions in a safe manner. In addition, it applies a direct water potential to liquid water as opposed to the axis translation technique, therefore it is particularly well suited to high water content samples. The main disadvantage is the weakness of the membrane and its sensitivity to microbial attack. It is necessary to add some drops of penicillin in the solution before use to prevent from bacteria.

The osmotic technique can be easily used to impose a suction value to a soil specimen under null stress. The soil sample is placed in a tube-shaped semi-permeable membrane and immersed in a PEG solution (Fig. 4) which is stirred by a magnetic stirrer to maintain its homogeneity (Cui and Delage 1996) (Figs. 5, 6).

3 Application in Traditional Laboratory Tests

The vapour equilibrium method and osmotic technique have been adapted for use in controlling suctions in traditional tests to establish the mechanical properties of unsaturated materials under various stress paths and initial conditions. There has been considerable work by independent groups that have resulted in similar systems and approaches all with their own specific benefits and limitations generally suited to the specific soil type or application being examined. The following sections give a summary of a limited selection of more recent applications where the vapour equilibrium technique and the osmotic method have been implemented in mechanical testing to apply target suctions during testing. The discussion is by no means meant to be exhaustive but is intended

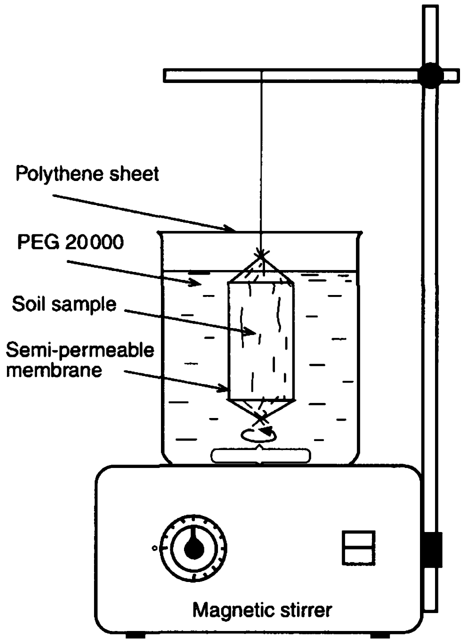

Fig. 4 Use of osmotic technique to impose a suction (after Cui and Delage 1996)

to give a report on some examples of how the method is currently being utilized.

3.1 Oedometer Test

Oedometers have been utilized by many research groups to examine the impact of suction on compressibility and the swelling properties of highly plastic unsaturated clays subjected to wetting conditions. Some of the earlier work included Jenning and Burland (1962), Matyas and Radhakrishna (1968) and Fredlund and Morgenstern (1977). In many of the original works specimens were placed in the oedometer in an unsaturated state and the behaviour of specimens following inundation with water was observed to examine the swelling characteristics. In tests where wetting was applied by liquid phase water, the suction was not directly controlled except to say that the end point was known to give zero matric suction. Early work by Escario (1969) and Escario and Sáez (1986) incorporated the pressure membrane apparatus directly in testing to control the suction level. More recently Belanteur et al. (1997), Villar (1999) and Cuisinier and Masrouri (2004) have provided further improvements to the testing methodology. However the equilibrium times were still relatively long (Tang and Cui 2005). Cui et al. (2002), Lloret et al. (2003) and Marcial (2003) improved the equilibrium times by introducing active systems to circulate the headspace vapour around specimens to accelerate equilibrium. In many cases the times were reduced from a few weeks to just under one week.

The application has generally included a closed mass circulation system where the vapour at target suction is circulated through the pedestal base porous stone and vapour exchange takes place between the specimen and the circulating air. The second

Fig. 5 Oedometer with controlled suction (after Esteban 1990)

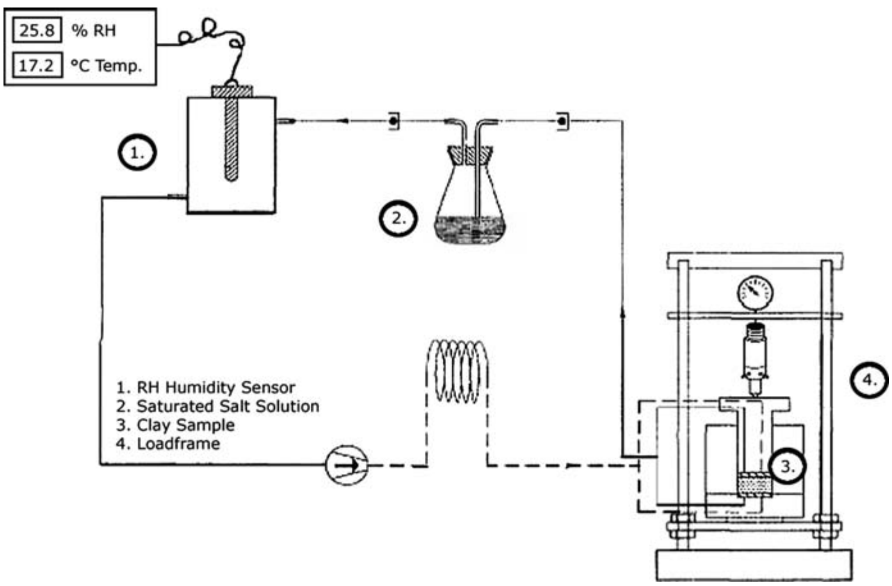

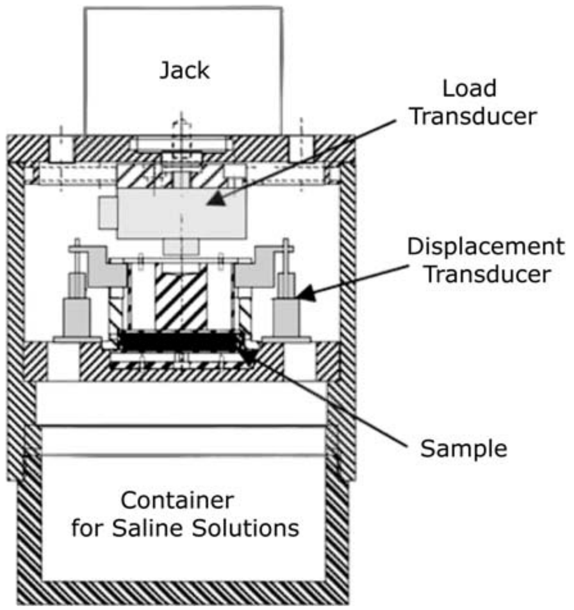

Fig. 6 Oedometer with controlled suction (after Cuisinier and Masrouri 2004)

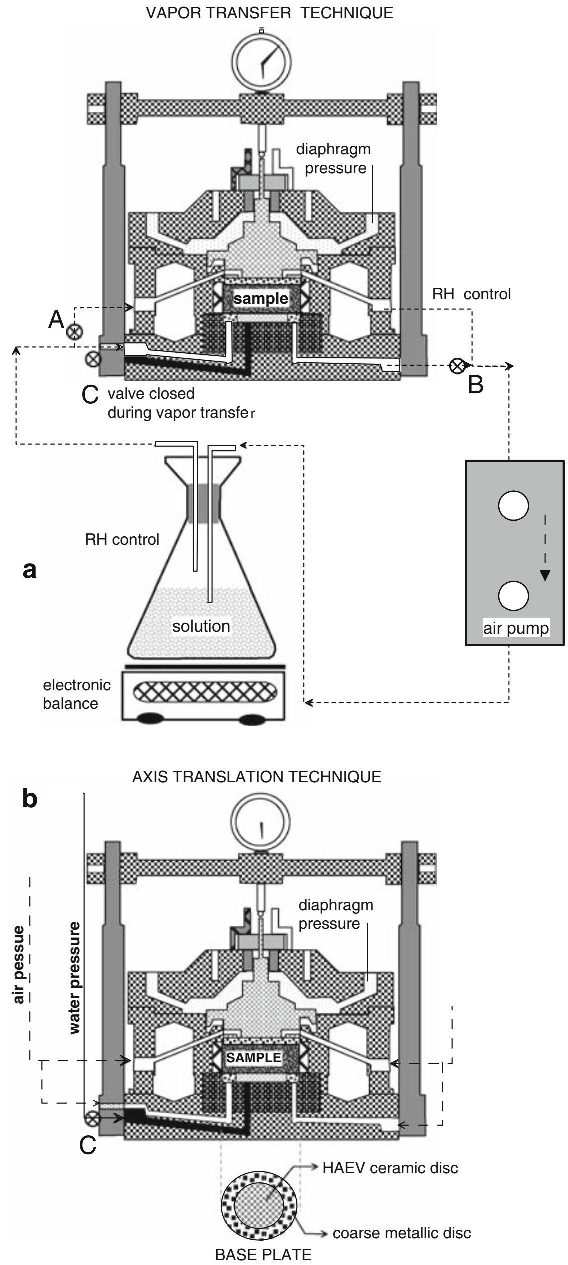

Fig. 7 UPC oedometer cell and testing set-up (after Hoffman et al. 2005)

approach is to enclose the entire oedometer apparatus (or the cell that houses the specimen) inside a chamber with relative humidity control. Both applications face the general limitations and drawbacks discussed previously.

Esteban (1990) showed an excellent example of an oedometer with suction control. The method of circulating the vapour through the porous stones provided decreased equilibration times.

Cuisinier and Masrouri (2004) showed an example of an oedometer with suction control provided by placing the oedometer cell entirely in a controlled suction environment. Cuisinier and Masrouri (2004) also provided a discussion regarding issues of uncertainty of the actual applied suction using the VET method.

More recently Hoffman et al. (2005) have combined methods of suction control to create a hybrid oedometer apparatus that has the ability to alter the applied suction method based on the desired suction range. This allows for the method of suction application to be optimized based on the specific desired suction levels for the tests. The results reported show consistent results and demonstrate the value of this unique approach. The combined oedometer apparatus is shown in Fig. 7.

The osmotic technique was adapted to oedometer tests by Kassiff and Ben Shalom (1971). Figure 8 presents the system of Kassiff and Ben Shalom (1971) improved by Delage et al. (1992). Compared to the initial adaptation, a system allowing PEG circulation inside a closed circuit was added. Concentric grooves are machined in the base pedestal and

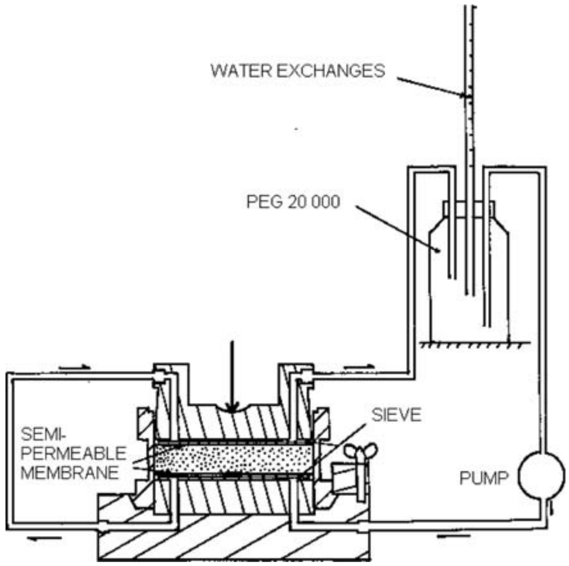

Fig. 8 Osmotic oedometer (after Kassiff and Ben Shalom 1971; Delage et al. 1992; Delage 2002)

top piston for the solution circulation. A thin sieve mesh is placed over the grooves and covered by the semi-permeable membrane, which is glued with an epoxy resin (it can be also clamped between the ring and base pedestal). A capillary tube placed in the closed bottle that contains the solution allows monitoring of water exchanges during the tests. Any liquid level elevation change would mean a water exchange with the soil sample. This system for water volume monitoring is obviously affected by temperature conditions.

It is important to carry out the test in a room with strict temperature control (Tang and Cui 2005). As a general rule, temperature fluctuations should be controlled within +/−0.1°C to minimize temperature effects. An alternative method of controlling water exchanges by placing the bottle on a balance has been proposed by Dineen and Burland (1995). In this case the temperature influence is totally avoided which is a considerable benefit to the testing methodology.

3.2 Direct Shear Test

Early efforts to control suction in the direct shear test were developed by Escario (1980) using the pressure membrane apparatus. Apart from the testing by Escario (1980) little if any evidence could be found regarding the application of the vapour equilibrium method for direct shear testing following the earlier work until recently. Several authors have used the vapour equilibrium technique (as well as air-drying which is a simplified form) to generate initial suctions that are then assumed to act on the failure plane in subsequent direct shear testing (Vanapalli and Lane 2002; Cokca et al. 2004) but few use the two methods discussed for active control.

The one exception that has been presented is a comprehensive apparatus the both controls and measures the suction independently. Boso et al. (2005) developed an osmotic shear box (Fig. 9) in which the problem related to evaporation is overcome using silicone grease. The PEG solution reservoir was composed of a 3 mm thick porous plate placed 1 mm higher than the bottom of the reservoir. A 4 mm thick steel plate was designed to clamp the membrane. Two tensiometers were installed on the loading pad for suction measurement. This apparatus shows considerable potential due to it's independent control and measurement of suction.

3.3 Triaxial Shear Strength Tests

The limitations of the oedometer test and direct shear test in terms of stress path control led to the desire to implement suction control in the triaxial apparatus. Early work focused on the use of axis translation (Fredlund and Rahardjo 1993) which was well suited to the triaxial device but was limited to a lower range of matric suction values. In cases where the examination of high plastic clays was of interest, higher suction control was required and again the vapour equilibrium technique and osmotic method were employed to achieve higher suction levels.

Recent developments incorporated closed circulation systems where vapour in a container headspace was circulated through the pedestal base (Cunningham et al. 2003; Nishimura and Fredlund 2003) and at times along the length of the specimens (Blatz and Graham 2003).

Cunningham et al. (2003) circulated air from the laboratory through the pedestal base of the triaxial cell and verified the application of suction with independent suction probes. The drying air was at ambient conditions from the lab which did not impose a set end point suction value. As such the drying process was non-uniform with maximum drying at the edge of specimens and minimum at

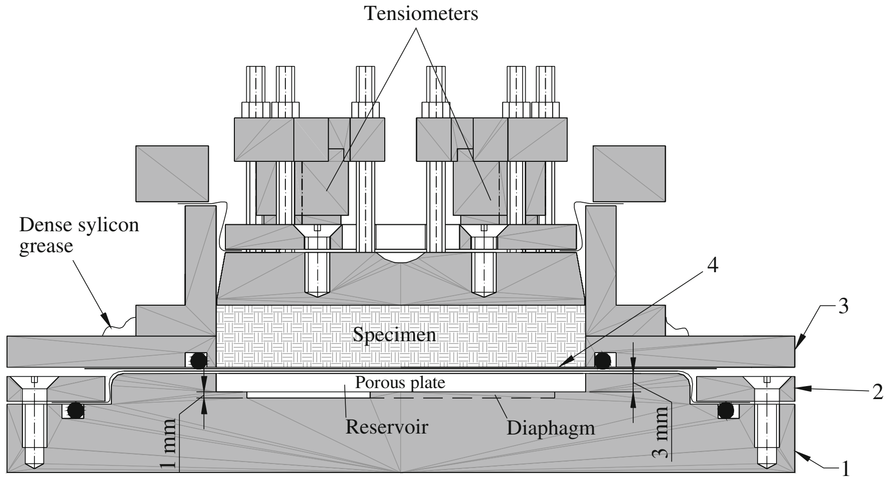

1) Base with reservoir	3) Shear box lower half
2) Plate to fix the membrane	4) Metallic sheet with sand paper

Fig. 9 Osmotic shear box (after Boso et al. 2005)

the center of specimens. When the drying air was shut off, specimens were allowed to equilibrate so some hysteresis in specimens would be expected before reaching equilibrium.

Blatz and Graham (2000) used a closed system with a target suction applied in a glass desiccator connected with a sealed circulation system. Figure 10 shows a schematic of the apparatus.

As with Cunningham et al. (2003) the suction was applied using vapour exchange and verified with an independent sensor that ensured that suction reached equilibrium within specimens. Vapour circulation was aided through the addition of non-woven geotextile strips along the length of specimens. The connection in the circulation system was the overlap of the geotextile strips with the top and bottom porous stone.

A more recent modification has been presented by Nishimura and Fredlund (2003) which utilizes the control of relative humidity using an air regulator and air bubbler system (Fig. 11). The importance of independent assessment of applied suction is achieved with a relative humidity sensor embedded in the circulation system; however there is no sensor in the soil specimen which avoids the issue of any possible influence of the sensor itself on the mechanical performance of the specimen. Figure 11 shows the triaxial apparatus developed by Nishimura and Fredlund (2003).

The osmotic system has been adapted to triaxial testing by Delage et al. (1987) and Cui and Delage (1996) (Fig. 12). As in the osmotic oedometer, the

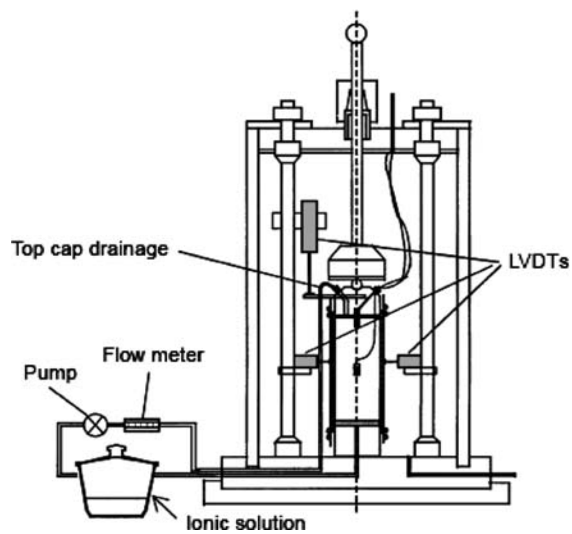

Fig. 10 Triaxial apparatus with VET suction control (after Blatz and Graham 2000)

soil specimen is put in contact on both bottom and top with the semi-permeable membrane, reducing the drainage length to half of the sample height. The PEG solution is contained in a closed circuit comprising the grooved base pedestal, the top grooved cap, a reservoir and a peristaltic pump. The reservoir is large enough (more than one liter) to ensure a relatively constant PEG concentration in spite of water exchanges between the specimen and the solution. The graduated capillary tube inserted into the reservoir is used for monitoring water exchanges. In order to ensure a constant pore air pressure equal

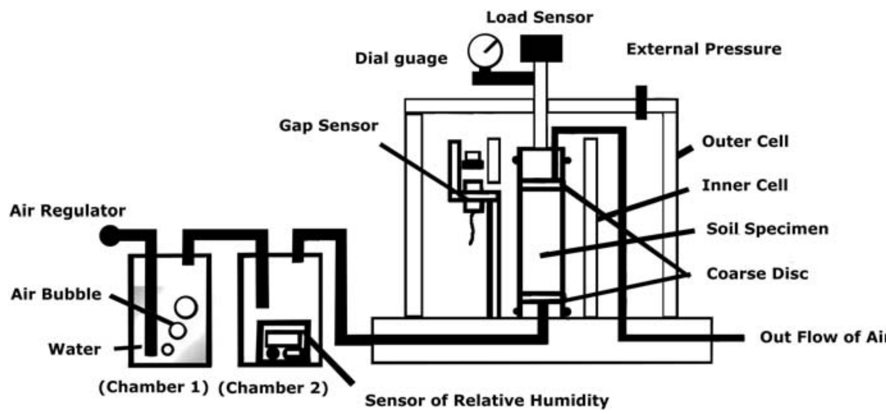

Fig. 11 Triaxial test with suction control (after Nishimura and Fredlund 2003)

to the atmospheric pressure within the sample, an air vent was machined on the base of the cell. This vent is connected with an antievaporation system to neutralize water evaporation from the sample.

In Fig. 12 PEG 20, 000 was used with Spectrapor 4 membrane which has a molecular weight cut-off of 14, 000–16, 000. Volume changes of the sample was monitored using a cathetometer. A cylindrical glass tube was mounted around the sample and filled with slightly colored water. A thin layer of silicon oil was put above the water in order to avoid any water evaporation. Volume changes were monitored by following changes of the air–oil interface level.

3.4 Other Applications

In addition to traditional tests for characterizing the behaviour of soils, there have been a number of modifications to other testing apparatus to apply controlled suction using the vapour equilibrium and osmotic techniques. A few are described to demonstrate the flexibility of the methods.

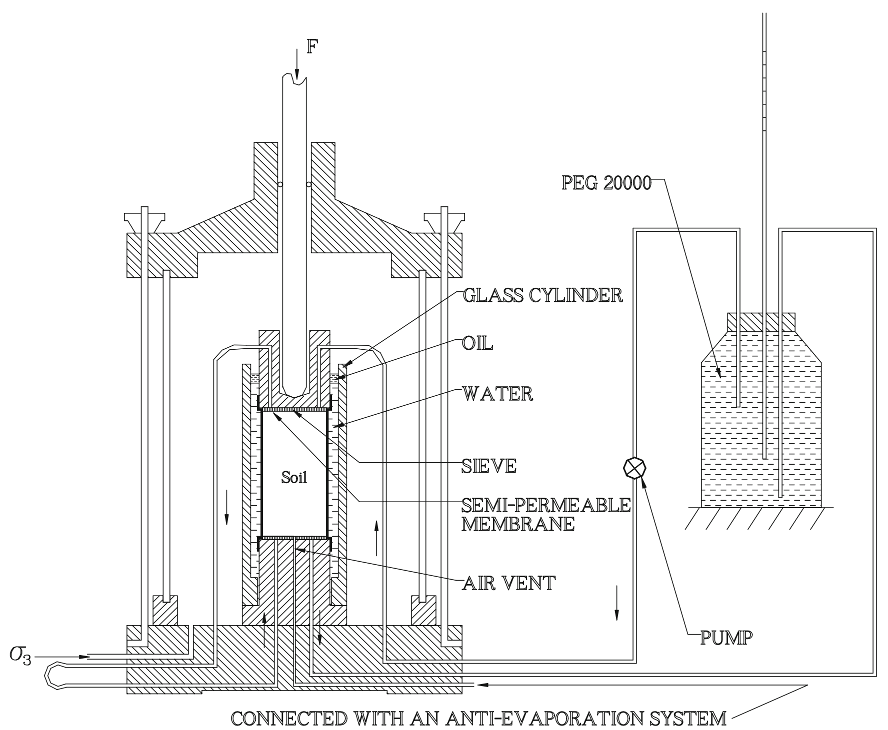

Fig. 12 Triaxial apparatus with suction control by osmotic technique (after Cui and Delage 1996)

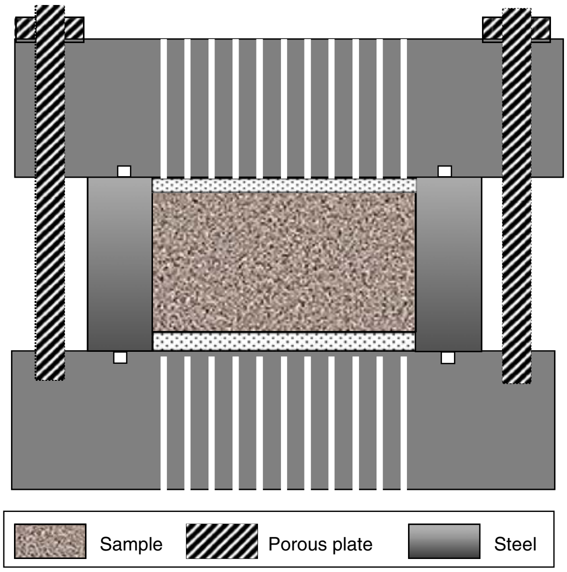

Fig. 13 Schematic layout of the non-deformable cell for the determination of the retention curve (after Villar et al. 2005)

Villar et al. (2005) have developed a constant volume cell that is placed in a controlled suction chamber (using VET) such that water retention curves for high plastic clay can be determined under constant volume conditions consistent with in-situ conditions for a proposed waste repository. Figure 13 shows a cross-section of the cell.

The schematic shows the ports drilled in the steel cell to provide a pathway for water vapour exchange between the specimen and the surrounding environment while maintaining constant suction conditions.

Oldecop and Alonso (2004) used the vapour equilibrium method to test rockfill materials where other methods of suction control could not be practially used due to their limitations. The application of the method was adapted to the large size of the rockfill materials to deal with specific issues encountered. Figure 14 shows the detailed large scale oedometer apparatus.

4 Discussion and Conclusions

The vapour equilibrium and osmotic techniques are well established methods for controlling suction. The methods apply relative humidity directly to soil specimens which is consistent with physical conditions experienced by soil in nature. The methods have been compared in a number of studies and show that application of the two methods provide reasonably consistent behaviour.

The methods have been successfully adapted for use in traditional soil testing including the oedometer, direct shear and triaxial tests by a number of research groups worldwide. There are similarities and differences amongst the many developments that are generally specific to materials being tested or stress paths being examined. The discussion of various apparatus in the preceding sections is by no means intended to be exhaustive but is intended to give some recent examples of current developments. The preceding discussion has also shown some examples of where the VET and osmotic techniques have been adapted for non-standard tests to successfully control suction. Again the discussion of application of VET and the osmotic tests has been limited due to space constraints.

The main drawbacks of the VET method are the long equilibrium time which can be reduced using circulation systems, the difficulty in applying high suctions due to the changes in concentration of the ionic solution and the need for precise control of temperature to ensure accurate assessment of the applied suction. In many cases independent sensors have been used to verify the magnitudes and equilibration of applied suctions. The difficulty of using the two methods for application at very low suctions (high relative humidity) has also been outlined. These considerations are important for assessing if the method is appropriate for any intended applications of controlled suction.

The osmotic technique is commonly applied within the suction range of approximately 0–10 MPa. It compensates well for the difficulties that occur when applying the VET method at lower suctions. It is worth noting again the difficulty that is encountered with the highly non-linear relationship between relative humidity and suction which generates difficulties with precise control of suction at low suction levels. This is not a phenomena that is restricted to issues of application of suction, it is directly dealt with in issues of inferring suction from measurement of relative humidity to verify suctions imposed using the VET method. As such, internal measurement of relative humidity as an attempt to verify suctions applied using the VET method is not a sure method to overcome the limitations of

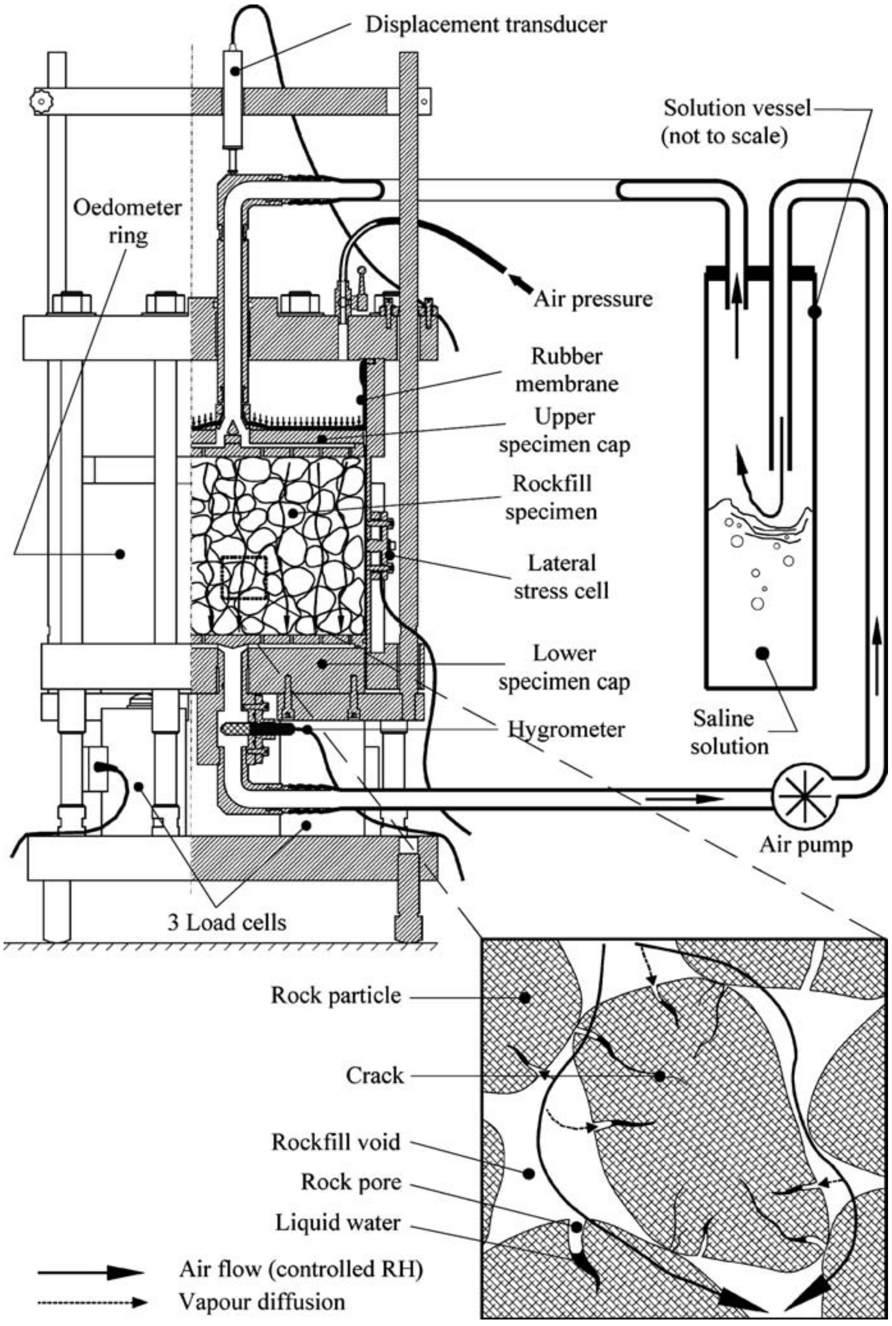

Fig. 14 300 mm large-scale oedometer with controlled suction using VET (after Oldecop and Alonso 2004)

uncertainty in preparing solutions at the low suction spectrum.

The osmotic technique allows liquid water exchanges between the soil sample and PEG solution; therefore the equilibrium time is much shorter as compared to the VET method. When applying a suction of several hundreds of kilopascals to a silty soil from slurry state, 4 days are sufficient to reach equilibrium (Vicol 1990). Very often it is the low permeability membrane that governs test duration, and it is important to properly section the PEG molecular weight and the semi-permeable membrane. The main drawback of this technique is the weakness of the semi-permeable membrane. It is strongly recommended to add penicillin in the PEG solution before use in order to avoid bacterial attack.

Experience has shown that with penicillin (under standard laboratory conditions) the semi-permeable membrane can last for up to a month. Moreover it is necessary to minimize the risk of tear by any traction on the membrane. There is obviously no risk in oedometer testing but the risk is appreciable in triaxial tests because of the shear stress applied. Note also that for the water exchange monitoring, the capillary tube system needs strong control of room temperature, and the use of a balance instead has the advantage of not being affected by temperature variations.

References

Agus SS, Schanz T (2005) An investigation into hydro-mechanical behavior of an expansive soil using axis-translation and vapor equilibrium techniques. International symposium advanced experimental unsaturated soil mechanics, Trento

Belanteur N, Tacherifet S, Pakzad M (1997) Étude des comportements mécanique, thermo-mécanique et hydromécanique des argiles gonflantes et non gonflantes fortement compactées. Rev Fr Geotech 78:31–50

Blatz JA, Graham J (2000) A system for controlled suction in triaxial tests. Géotechnique 50(4):465–478

Blatz JA, Graham J (2003) Elastic plastic modelling of unsaturated high-plastic clay using results from a new triaxial test with controlled suction. Géotechnique 53(1):113–122

Boso M, Tarantino A, Mongiovì L (2005) A direct shear box improved with the osmotic technique. Proceedings of advanced experimental unsaturated soil mechanics, Trento, pp 85–91

Bruno TJ, Svoronos PDN (2003) Handbook of basic tables for chemical analysis, 2nd edn. CRC Press, Boca Raton, FL, USA

Cokca E, Erol O, Armangil F (2004) Effects of compaction moisture content on the shear strength of an unsaturated clay. Geotech Geol Eng 22(2):285–297

Cui YJ, Delage P (1996) Yielding and plastic behaviour of an unsaturated compacted silt. Géotechnique 46(2):291–311

Cui YJ, Yahia-Aissa M, Delage P (2002) A model for the volume change behaviour of heavily compacted swelling clays. Eng Geol 64(2–3):233–250

Cuisiner O, Masrouri F (2004) Testing the hydromechanical behavior of a compacted swelling soil. Geotech Test J 27(6):598–606

Cunningham MR, Ridley AM, Dineen K, Burland JB (2003) The mechanical behaviour of a reconstituted unsaturated silty clay. Geotechnique 53(2):183–194

Delage P (2002) Experimental unsaturated soil mechanics: State-of-art-report. 3rd International conference on unsaturated soils, vol 3, Recife

Delage P, Cui YJ (2000) L'eau dans les sols non saturés. Éditions Techniques de l'ingénieur, Paris, vol C2, article C 301, Traité Construction

Delage P, Suraj De Silva GPR, et De Laure E (1987) Un nouvel appareil triaxial pour les sols non saturés, vol 1. 9e European conference on soil mechanics and foundation engineering, Dublin, pp 26–28

Delage P, Suraj De Silva GPR, Vicol T (1992) Suction controlled testing of non saturated soils with an osmotic consolidometer. 7th International conference expansive soils, Dallas, pp 206–211

Delage P, Howat M, Cui YJ (1998) The relationship between suction and swelling properties in a heavily compacted unsaturated clay. Eng Geol 50(1–2):31–48

Dineen K, Burland JB (1995) A new approach to osmotically controlled oedometer testing. Proceedings of the 1st conference on unsaturated soils Unsat'95, vol 2. Balkema, Paris, pp 459–465

Escario V (1969) Swelling of soils in contact with water at negative pressure. Proceedings of the 2nd international conference expansive clay soils, Texas A&M University, pp 207–217

Escario V (1980) Suction controlled penetration and shear tests. Proceeedings of the 4th international conference on expansive soils, vol II. Denver, American Society of Civil Engineers, pp 781–797

Escario V, Saez J (1986) The shear strength of partly saturated soils. Geotechnique 36(3):453–456. H.D. Schreiner and authors reply: Geotechnique, 37(4):523–524

Esteban F (1990). Caracterización de la expansividad de una roca evaporítica. Identificación de los mecanismos de hinchamiento. Tesis doctoral de la Universidad de Cantabria, Santander

Fredlund DG, Morgenstern NR (1977) Stress state variables for unsaturated soils. J Geotech Eng ASCE 103(5):447–461

Fredlund DG, Rahardjo H (1993) Soil mechanics for unsaturated soils. John Wiley and Sons, New York

Hoffmann C, Romero E, Alonso EE (2005) Combining different controlled-suction techniques to study expansive clays. International symposium advanced experimental unsaturated soil mechanics, Trento, June 27–29, 2005

Jennings JEB, Burland JB (1962) Limitations to the use of effective stresses in partly saturated soils. Géotechnique 12(2):125–144

Kanno T, Wakamatsu H (1993) Moisture adsorption and volume change of partially saturated bentonite buffer materials. Material research society symposia proceedings, vol 294. pp 425–430

Kassiff G, Benshalom A (1971) Experimental relationship between swell pressure and suction. Géotechnique 21: 245–255

Lagerwerff JV, Ogata G, Eagle HE (1961) Control of osmotic pressure of culture solutions with polyethylene glycol. Science 133:1486–1487

Leong EC, Rahardjo H (2002) Soil-water characteristic curves of compacted residual soils. In: Jucá JFT, de Campos TMP, Marinho FAM (eds) Unsaturated soils. Proceedings of the 3rd international conference on unsaturated soils (UNSAT 2002), Recife, Brazil, vol 1. Swets & Zeitlinger, Lisse, The Netherlands. pp 271–276, 10–13 March 2002

Lloret A, Villar MV, Sanchez M, Gens A, Pintado X, Alonso EE (2003) Mechanical behaviour of heavily compacted bentonite under high suction changes. Géotechnique 53(1):27–40

Marcial D (2003) Comportement hydromécanique et microstructural des matériaux de barrière ouvragée. Ph.D. thesis, École nationale des ponts et chaussées, Paris, France

Matyas EL, Radhakrishna HS (1968) Volume change characteristics of partially saturated soils. Geotechnique 18(4):432–448

Nishimura T, Fredlund DG (2003) A new triaxial apparatus for high total suctions using relative humidity. Proceedings of the 12th Asian regional conference on soil mechanics and geotechnical engineering, vol 1. Singapore, pp 65–68

Oldecop LA, Alonso EE (2004) Testing rockfill under relative humidity control. Geotech Test J ASTM 27(3):10. Paper ID: GTJ11847

Richards BG (1974) Behaviour of unsaturated soils. In: Lee IK (ed), Soil mechanics—new horizons. American Elsevier, New York, pp 112–157

Romero E (1999) Perturbation of the heat transfer and the friction factor of a rib roughened surface in an annular passage due to localized removal of the ribbing. Nucl Eng Des 188(1):85–96

Romero E, Gens A, Lloret A (2001) Temperature effects on the hydraulic behaviour of an unsaturated clay. Geotech Geol Eng 19(3–4):311–332

Saiyouri N, Hicher PY, Tessier D (2000) Microstructural approach and transfer water modelling in highly compacted unsaturated swelling clays. Mech Cohes Frict Mater 5:41–60

Slatter EE, Allman AA, Smith DW (2000) Suction controlled testing of unsaturated soils with an osmotic oedometer. Proceedings of the international conference on geo-engineering 2000. Melbourne, Australia

Stokes RH, Robinson RA (1948) Ionic hydration and activity in electrolyte solutions. J Am Chem Soc 70:1870–1878

Tang A-M, Cui Y-J (2005) Controlling suction by the vapour equilibrium technique at different temperatures and its application in determining the water retention properties of MX80 clay. Can Geotech J 42:287–296

Tang GX, Graham J, Wan AWL (1998) On yielding behaviour of an unsaturated sand-bentonite mixture. In Proceedings of the 2nd international conference on unsaturated soils, vol 1. Beijing, pp 149–154

Tessier D (1984) Étude expérimentale de l'organisation des matériaux argileux: hydratation, gonflement et structuration au cours de la dessiccation et de la réhumectation. Ph.D. thesis, Université de Paris VII, Paris, France

Vanapalli SK, Lane J (2002) A simple technique for determining the shear strength of unsaturated soils using the conventional direct shear apparatus. Second Canadian specialty conference on computer applications in geotechnique. Winnipeg, pp 245–253, April, 2002

Vicol T (1990) Comportement hydraulique et mécanique d'un limon non saturé. Application à la modélisation. Thèse de doctorat de l'ENPC, Paris, 257 p

Villar MV (2000) Caracterización termo-hidro-mecánica de una bentonita de Cabo de Gata. Ph.D. thesis, Universidad Complutense de Madrid, Madrid, Spain

Villar MV, Martín PL, Lloret A (2005) Determination of water retention curves of two bentonites at high temperature. International symposium advanced experimental unsaturated soil mechanics. Trento

Waldron LJ, Manbeian T (1970) Soil moisture characteristics by osmosis with polyethylene glycol: a simple system with osmotic pressure data and some results. Soil Sci 110(6):401–404

Williams J, Shaykewich CF (1969) An evaluation of polyethylene glycol PEG 6000 and PEG 20000 in the osmotic control of soil water matric potential. Can J Soil Sci 102(6):394–398

Young DF (1967) Effect of time-dependent stenosis on flow through a tube. American Society of Mechanical Engineers, 67-WA/BHF-2, 7 p

Zur B (1966) Osmotic control the matric soil water potential. Soil Sci 102:394–398

Mechanical Testing in Unsaturated Soils

Laureano R. Hoyos · Lyesse Laloui · Roberto Vassallo

Originally published in the journal *Geotechnical and Geological Engineering*, Volume 26, No. 6, 675–689.
DOI: 10.1007/s10706-008-9200-9

Abstract The state-of-the-art report presented herein is aimed at documenting, to the largest extent possible, some of the recent advances in laboratory testing of unsaturated soils for stress–strain–strength–stiffness characterization under suction-controlled isotropic, axisymmetric, and true triaxial stress states. The report is intended to be neither comprehensive nor fully inclusive, offering plenty of room for further discussion on recent refinements and techniques not yet reported in the literature. The main sections in this report are devoted to describing current methods and technologies using cylindrical triaxial systems, including advances in volume change measurements; resonant column/torsional shear systems; bender element-based systems; and suction-controlled testing under true triaxial stress states. Concluding remarks are included in the last section of the report.

L. R. Hoyos (✉)
Department of Civil and Environmental Engineering, The University of Texas at Arlington, 416 Yates Street, Suite 417, Arlington, TX 76019, USA
e-mail: lhoyos@uta.edu

L. Laloui
School of Architecture, Civil and Environmental Engineering, Ecole Polytechnique Fédérale de Lausanne, Lausanne, Switzerland

R. Vassallo
Dipartimento di Strutture, Geotecnica, Geologia Applicata all'Ingegneria, Università degli Studi della Basilicata, Potenza, Italy

Keywords Axis-translation · Matric suction · Volume change · Small-strain stiffness · True triaxial stress state

1 Introduction

The adoption of matric suction, $(u_a - u_w)$, and the excess of total stress over air pressure, that is, net normal stress, $(\sigma - u_a)$, as relevant stress state variables, has facilitated the modelling of key features of unsaturated soil behaviour via suction-controlled testing using axis-translation technique. It is the relative success of this technique that has prompted researchers in the unsaturated soil discipline to devote countless hours to fine-tuning the myriad details of the existing testing devices and keep the focus of their efforts on expanding their testing capabilities.

The present report is aimed at documenting, to the largest extent possible, recent advances in laboratory testing of unsaturated soils to model the mechanics of their response under suction-controlled isotropic, axisymmetric and true triaxial stress states. The report is intended to be neither comprehensive nor fully inclusive, offering plenty of room for further discussion on recent refinements and techniques not yet reported in the literature.

Section 2 is devoted to describing current methods using cylindrical triaxial systems, including volume change and stiffness measurements. Section 3 describes current methods for measuring small-strain stiffness using resonant column and bender element based systems. Section 4 documents recent advances in suction-controlled testing under true triaxial stress states. Concluding remarks are included in Sect. 5.

2 Cylindrical Triaxial Systems

2.1 General Considerations

2.1.1 Air-Water Pressure Control

Most triaxial apparatuses reported in the literature feature an HAE (high-air-entry) ceramic disk at the bottom pedestal and a coarse porous stone at the top cap for independent control of pore-water and pore-air pressures, respectively (Bishop and Donald 1961; Josa et al. 1987; Sivakumar 1993; Rampino et al. 1999). In recent years, however, double-drainage systems have been increasingly used for triaxial testing on low-permeability soils, involving simultaneous application of u_a and u_w at both ends of the specimen. Each end features a peripheral annular coarse porous stone and an internal HAE disk (Fig. 1; Romero 1999; Barrera 2002). Alternatively, u_w can be applied at both ends while u_a is applied only at one end (Sharma 1998). Both techniques yield a significant reduction in equalization time; however, air bubbles may be trapped in the middle of the specimen when two wetting fronts advance in opposite direction due to a suction reduction at specimen boundaries. This could be avoided by applying u_a at the middle of the sample and u_w at both ends (Maâtouk 1993); volume change, however, cannot be measured.

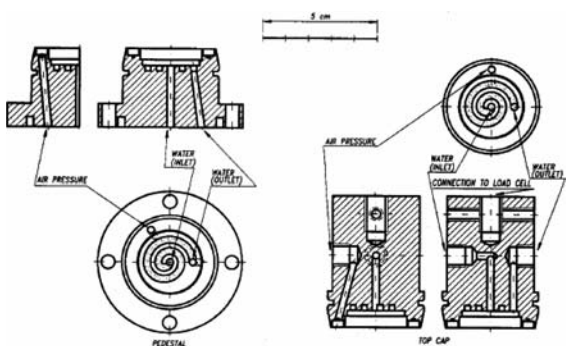

Fig. 1 Pedestal and top cap of a double-drainage system (Romero 1999)

2.1.2 Water Sub-pressure Versus Air Over-pressure

The air over-pressure technique involves inducing a desired suction by changing u_w while u_a remains constant (Barrera 2002). Higher u_w can be used when low suctions are to be applied, which is an advantage when the target state is close to saturation. Higher u_w also ensures full saturation of drainage lines. The water sub-pressure technique, on the other hand, involves a simultaneous change in σ and u_a, which may induce instantaneous soil deformation due to bedding errors. Some researchers, however, do prefer this technique (Rampino et al. 1999; Vassallo 2003). The lower the u_w, the lower the possibility of leakage in the water system. Moreover, a lower value of u_w allows investigating a larger $(\sigma - u_a)$ range under a given suction state, facilitating, for instance, a better definition of the isotropic compression curve during triaxial testing.

Differences between water sub-pressure and air over-pressure technique are also discussed by Romero (2001) and Marinho et al. (Ibid.).

2.1.3 Equalization Stage

During triaxial testing, the σ and u_a are usually increased simultaneously under undrained conditions, after which the desired u_w is applied by opening the drainage line. This procedure is best suited for continuous air pressure. When occluded air is present in pore water, the application of σ could yield an initial shrinkage of the specimen. However, as suction is maintained constant at the specimen boundaries, stabilization of deformations is eventually observed. Air diffusion allows for u_a stabilization, hence any significant difference between externally applied u_a and occluded bubble pressure can be reasonably neglected (Mancuso et al. 2002).

2.1.4 Isotropic Loading Rate

Advantages of continuous loading versus step-loading during isotropic compression have been discussed by Sivakumar (1993) and Cui and Delage (1996). According to the latter, soil compressibility is overestimated, and hence yield stresses are underestimated, by step-loading, since undesired u_w overpressure is induced by each instantaneous load increment. The only advantage of step-loading may lie in the simpler and less costly system involved (usually manual). A simple empirical way to check if the chosen stress rate is appropriate is by stopping the continuous compression and observe whether further significant changes in volume and water volume still occur (Rampino 1997; Barrera 2002).

2.1.5 Shearing Rate

Likewise, a suitable way for choosing an appropriate rate for drained shearing is by stopping the test and checking for any significant changes in volume and water volume. Sivakumar (1993) proposed extending the equation by Bishop and Henkel (1962), for evaluating the time t_f necessary for failure in saturated soils, using the coefficient of consolidation of the unsaturated material, that is, $t_f = (20h^2)/(0.75c_v)$, where h is the maximum drainage path. A shearing stage carried out all the way to failure can typically take 1–2 weeks. Suitable constant-water (undrained) shearing rates, on the other hand, are yet to be devised. When direct suction measurement is feasible, e.g. via tensiometers (Tarantino and Mongiovì 2003), it is advantageous performing undrained tests with duration significantly lower than drained tests.

2.2 Volume Change Measurements

During unsaturated soil testing, compression of air phase can result in volume changes in addition to those induced by drainage. Soil volume change cannot be computed purely on the basis of variation in water volume, nor can it be measured by using the same techniques used in conventional saturated soil testing. Several measurement techniques have been developed for unsaturated soil volume change, which can be classified in three broad categories (Laloui et al. 2006):

2.2.1 Cell Liquid Measurement

In this approach, specimen volume changes are deduced from volume changes in confining cell liquid. This requires the cell to be completely filled with water (or other fluid) and appropriate corrections for piston intrusion into the cell and for volume changes of the whole cell. Several problems are often associated with this method, such as immediate expansion of cell wall caused by a pressure increase, Plexiglas creep under constant stress and possible water leakage. Consequently, measurements must be corrected at the end for these effects. The advantage of the cell liquid measurement method is simplicity. A standard triaxial cell can be used if carefully calibrated. However, the measurement of the specimen volume remains indirect and the accuracy of the method depends on the quality of the calibration procedure, the volume capacity and the precision of the measurements.

Lade (1988) discussed the volume capacity/precision of volume change devices.

Ideally, numerous calibrations are needed, as corrections depend on time, stress path and stress level. Factors that affect the movement of water into or out of the cell and which must, hence, be taken into account in volume change measurements have been listed by Head (1986). Leong et al. (2004) mainly focused on the effects of stiffness of the pressure cell and temperature fluctuations.

As the measurement error increases with increasing confining liquid volume, Bishop and Donald (1961) proposed the addition of an inner cylinder sealed to the outer cell base (a double cell) to minimise the liquid volume. To enhance accuracy, mercury is used as the cell fluid between the inner cylinder and the specimen. The outer liquid is water, and the mercury is enclosed in an internal jacket with the cell pressure applied to both sides of the jacket. The rise or fall of the mercury vertical level in the inner cylinder is measured by a cathetometer measuring the movement of a floating stainless ball on the mercury. Overall volume changes can then be deduced. The method was widely adopted in subsequent years. Josa et al. (1987) introduced the automatic monitoring of mercury level via a metal ring floating on its surface. Use of mercury, however, was gradually abandoned for safety reasons.

Cui (1993) and Cui and Delage (1996) made some improvements by replacing mercury with water and measuring water levels via high-precision cathetometer based readings. Further improvements to the inner cylinder technique have been introduced by Rampino et al. (1999), Toyota et al. (2001), Aversa

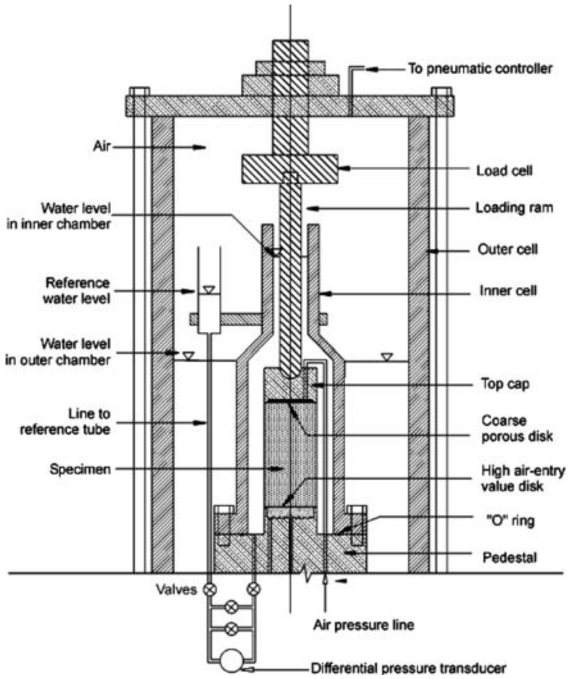

Fig. 2 Volume change measurement by inner cylinder technique (Ng et al. 2002)

and Nicotera (2002). Ng et al. (2002) no longer measure the fluid level by a cathetometer but rather record the differential pressure between the water inside the open-ended inner cell and the water inside a reference tube using a high accuracy differential pressure transducer (Fig. 2).

Some authors minimized the confining liquid by using double-walled cells (e.g., Wheeler 1988; Sivakumar 1993). Here, an inner cylinder is sealed to both the top and the base of the cell. Soil volume change is inferred from the volume leaving or entering the inner cell. Most of the possible errors discussed by Head (1986) can be reduced with this system.

2.2.2 *Direct Air-Volume and Water-Volume Measurements*

In this approach, the soil volumetric changes are deduced by simple addition of the air and water volume changes. This technique may be successful as soon as the gas phase is continuous. Both volume changes of air and water entering or leaving the pore spaces are monitored by separating draining pore-water from pore-air via porous stones and HAE ceramics, respectively, and then independently measuring each by pressure-volume controllers. The basic principle consists of an air-volume controller filled with air instead of water. However, undetectable air leakage and diffusion through tubes and connections must be estimated. Small temperature and atmospheric pressure changes also affect volume measurement and must be taken into account. Adams et al. (1996) evaluated a digital pressure-volume controller as an air-volume change indicator, including effects of temperature, confined volume, and precompression of the measurement medium. The controller was shown to perform satisfactorily as air-volume change measurement device. This technique of air-water volume measurement also permits measurement of air-volume change simultaneously with axis-translation implementation. A wide range of test paths can then be implemented as the air volume/pressure can be monitored separately.

To minimize the errors from changes in atmospheric pressure and temperature, an improved device was proposed by Geiser (1999), which is a mixed air and water controller that allows reduction of air-volume to the tubing only. Laudahn et al. (2005) proposed a method for measuring pore-air volume changes in drained tests under atmospheric conditions. Pore-air excess pressure can be generated during the test and lead to a misinterpretation of the measured volume change. To avoid this error, a U-tube was connected to a GDS volume controller for pore air. This tube is filled with ethanol and its level monitored with a photoelectric sensor: any change in the level is then reversed by an appropriate movement of the piston of the GDS controller; this way, pore air is maintained at atmospheric pressure.

2.2.3 *Direct Measurements on the Specimen*

In this category, soil volume change is computed from the direct measurements of axial and radial specimen displacements. Three direct measurement approaches can be devised. A *first approach*, one commonly used, involves local displacement sensors attached directly onto the specimen to measure axial/radial deformations during the test (e.g., Clayton et al. 1989). Several technologies have been tested, mainly miniature LVDTs (Costa-Filho 1982; Klotz and Coop 2002), and Hall effect transducers (Clayton and Khatrush 1986). Generally, radial displacements are measured at one to three discrete points and assumptions are made as to the shape of the specimens to assess the volumetric strain. Sensor placing is quite delicate: if not done correctly, it may lead to experimental errors; hence this approach is best suited for small deformation tests, requiring an initially rigid specimen. Such direct measurements become meaningless as a means of measuring soil volume change if a shear plane forms across the specimen.

A *second approach* involves non-contacting techniques such as lasers (Romero et al. 1997). Laser sweeping over the entire specimen height allows more accurate determination of the specimen volume. Radial deformations on two diametrically opposite sides of the specimen are measured via non-contact, long-range, electro-optical lasers mounted outside the chamber (Fig. 3) This also allows detection of non-uniformities and localized deformations. The technique requires costly and sophisticated installation procedures. A similar technique has been used by Hird and Hajj (1995): proximity transducers are mounted on a rigid tube around the sample, providing an output voltage proportional to the distance of a lightweight conductive target placed on the specimen. Generally, this type of transducer is not waterproof and has to be sealed in housing. As a major drawback, the target must be aligned with the sensor, which requires extreme care.

A *third approach* is an alternative direct measurement technique based on image processing (Gachet et al. 2003). It mainly consists of taking photographs through the Plexiglas cell during the test and then analysing the images to obtain specimen profile and volume. The approach is similar to that of Macari et al. (1997), except that, in this case, the method used to correct the magnification effect due to the cell shape and the different refraction indices (water, Plexiglas, air) is simpler. Rifaï et al. (2002) reported tests in which the images were taken using a digital computer controlled camera fixed at a constant distance from the cell (Fig. 4). Before testing, calibration is applied to a false rigid specimen to optimise the accuracy and correct optical distortions. The specimen is then placed into the triaxial cell and several photos are taken and analysed during the test. As with lasers, direct contact with the specimen is not required, and the soil profile is measured over its entire height.

Laloui et al. (2006) reported volume change measurements during shearing of unsaturated sandy silt at a constant suction of 100 kPa (the air-entry value of the tested soil was 80 kPa) using both mixed air/water controller and image processing techniques. Both techniques showed reasonably good agreement until the appearance of strain localization (at an axial strain of approximately 12%; Fig. 5).

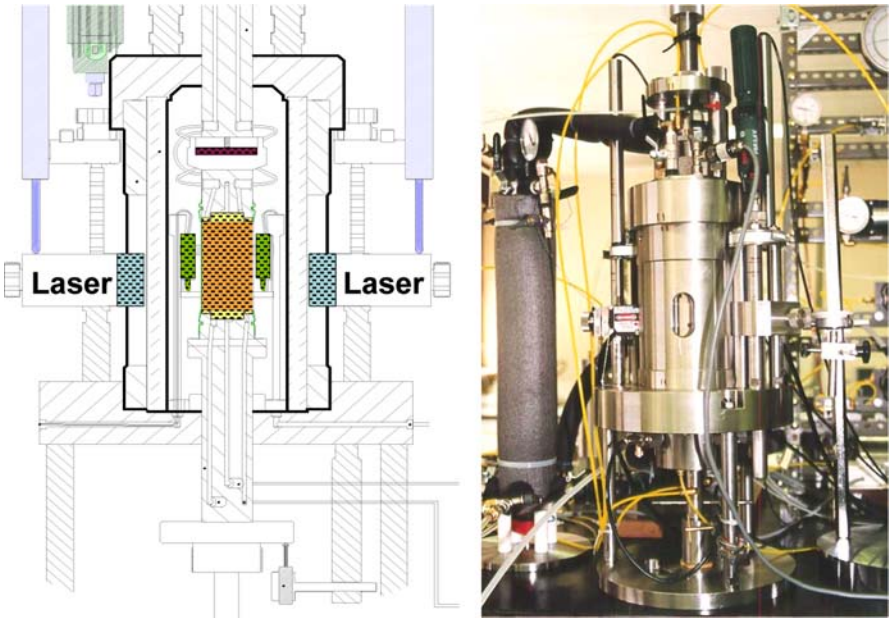

Fig. 3 Volume change measurement by electro-optical lasers (Romero et al. 1997)

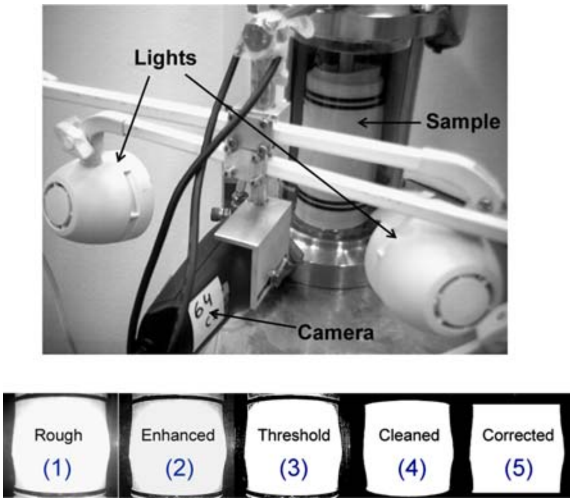

Fig. 4 Volume change measurement by image processing (Rifaï et al. 2002)

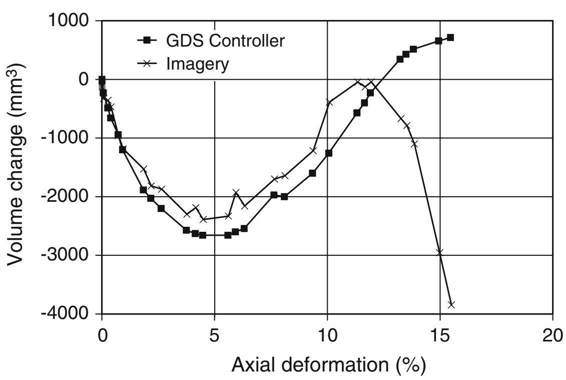

Fig. 5 Volume change measurements during constant-suction shearing using mixed air/water controller and image processing (Laloui et al. 2006)

2.2.4 Triaxial Cell Featuring a Combination of Various Techniques

The three approaches summarized above may be combined for more accurate results. Chávez et al. (2005) introduced a new triaxial cell that enables volume change measurement of partially saturated rockfill up to 250 mm diameter and 500 mm high under controlled-suction conditions (Fig. 6). An inner chamber allows for global measurements of specimen volume changes by recording the differential pressures between the water level in the inner chamber and that of a reference tube using a Differential Pressure Transducer.

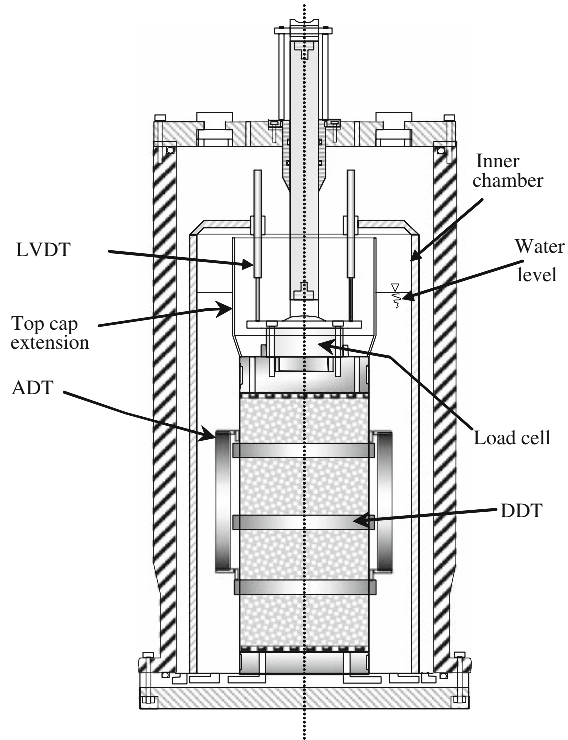

Fig. 6 Volume change measurement via inner chamber and local displacement transducers (Chavez et al. 2005)

Three internal LVDTs measure global axial displacements of an upper stainless steel loading plate in contact with the specimen. Local radial instrumentation is made up of three Diametrical Deformation Transducers. Local axial displacements are measured via two Axial Deformation Transducers resting on a special holder screwed to the external DDTs. These transducers use strain gauges, following a measuring principle similar to that of the LDTs (Goto et al. 1991), although the earlier yield linear response over a larger working range.

3 Resonant Column and Other Bender Element Based Systems

3.1 Resonant Column Systems

The resonant column device is used to determine dynamic shear modulus G and damping D of solid or hollow cylindrical specimens (ASTM 2006). The specimen's lower end is rigidly fixed to a rough-surfaced pedestal while the top end is loaded in torsion until attaining its fundamental mode of torsional vibration, measuring resonant frequency and amplitude of vibration (Isenhower 1979).

Initially, researchers simply used conventional devices for saturated soils for the testing of unsaturated soil specimens with no suction control (Au and Chae 1980; Wu et al. 1985; Quian et al. 1991). Specimens were first consolidated to a desired cell pressure before the stiffness measurements were performed. Subsequently, the specimens were retrieved and the degree of saturation indirectly inferred.

Vinale et al. (1999) and Vassallo (2003) reported a Resonant Column Torsional Shear (RCTS) system, developed at the University of Naples Federico II (Italy), to test soil specimens under controlled suction (Fig. 7). Classical interpretations of shearing stages require no torsional restraint anywhere along the specimen height but at the lower base, hence u_a and u_w are both applied through the base pedestal while ensuring a fixed-free condition. The procedure for inducing suction is similar to that typically followed in triaxial testing. For silty sand and clayey silt, an isotropic loading rate of 4 kPa/h was found to be appropriate to ensure drained (constant suction) conditions (Vassallo 2003).

Upon equalization of the pore fluids under the desired value of suction, results in the small-shear strain amplitude range (<0.0001%) can be considered drained, i.e. without affecting the constant suction state. Thus, the measured stiffness can be related to stress variables ($\sigma - u_a$) and ($u_a - u_w$) attained just before shearing. When the final point of the pre-established stress path is reached, torque can be increased up to the maximum allowed by the system in order to obtain normalized G/G_{max} or D/D_{min} versus shear strain γ curves.

In this system (Fig. 7), air bubble entrapment in the upper part of the specimen may be possible. Vassallo (2003) obtained a branch of the water-retention curve of a medium plasticity clayey silt with initial suction of about 140 kPa by using both a triaxial cell (controlling u_a on top and u_w at bottom) and the resonant column cell (controlling both u_a and u_w at bottom). Both curves were shown to be reasonably similar for the 50–400-kPa suction range. Also, water contents measured along specimen height at the end of tests showed no significant lack of homogeneity.

This apparatus also features an inner cylinder for volume change measurements, similar to that described in Sect. 2.2.1 for triaxial systems. Water content changes are measured through a system of two double-walled burettes connected to a differential pressure transducer DPT (Fig. 7). An automatic flushing system, including a peristaltic pump, is used to flush out diffused air bubbles through the spiroidal groove in contact with the HAE disk. Fig. 8 shows RC results obtained at University of Naples Federico II and reported by Vassallo et al. (2007). Data pertaining to saturated state are also reported for comparison purposes.

3.2 Bender Element Based Systems

The critical role of small-strain soil stiffness in the design of geosystems is now widely accepted. In the last decade, significant progress has been made on suction-controlled testing using triaxial systems with self-contained bender elements (BE). Bender

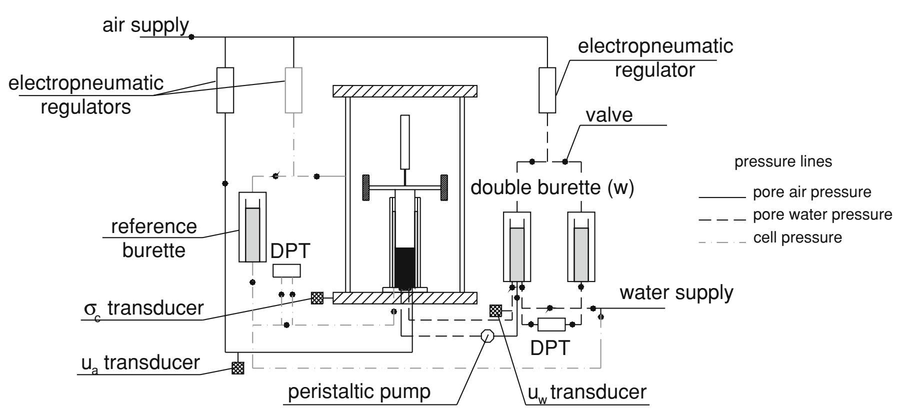

Fig. 7 Layout of the suction controlled RCTS cell (Vassallo 2003)

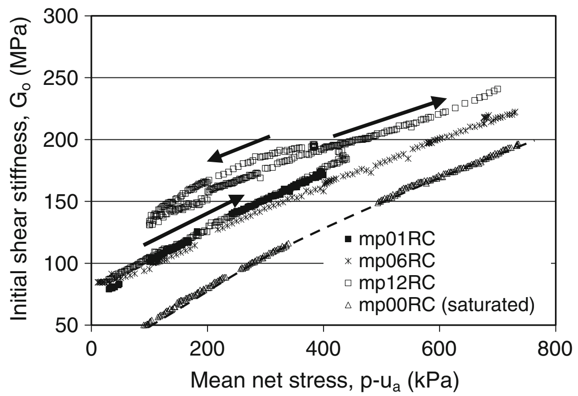

Fig. 8 Initial shear stiffness from RC tests conducted during compression at constant 100-kPa suction (Vassallo 2003)

elements are protruded into the opposite ends of a soil specimen. A voltage pulse is applied to the BE transmitter, which causes it to produce a *s*-wave. When the *s*-wave reaches the other end, distortion of the BE receiver produces another pulse. The time difference between the two voltage pulses is measured and divided by the distance between the BE tips to give *s*-wave velocity V_s. Small-strain shear modulus can then be determined as $G = \rho(V_s)^2$.

One such example was reported by Cabarkapa et al. (1998) and Cabarkapa and Cuccovillo (2006; Fig. 9). The triaxial cell features self-contained bender elements, a full set of internal LVDTs and a radial strain belt for overall volume change measurements. Results from normally consolidated quartz silt show that the unsaturated small-strain shear modulus can be readily obtained by multiplying the saturated value, corresponding to the same net confinement, by a factor that only depends on axis-translation induced suction.

Marinho et al. (1995) reported BE based measurements on statically compacted and undisturbed specimens of high plasticity soil. Specimens were gradually dried and, upon equalization, total suction was estimated via filter paper. Picornell and Nazarian (1998) performed BE measurements on coarse-grained and fine-grained reconstituted specimens. In coarse-grained soil, the bender elements were directly mounted inside the mould where specimens were compacted. A progressive drying process was imposed using a pressure plate extractor and, upon equalization,

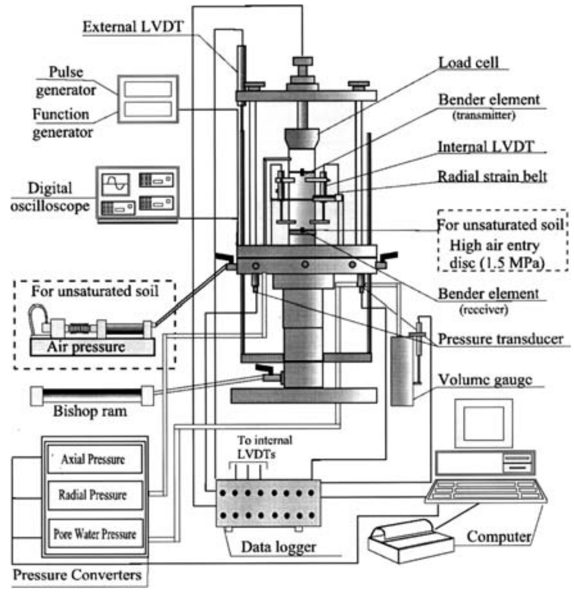

Fig. 9 Triaxial cell featuring bender elements (Cabarkapa and Cuccovillo 2006)

V_s was measured. Cho and Santamarina (2001) developed an aerometric cell in which bender elements were mounted on its top and bottom platens. The cell was used to measure stiffness changes induced by a temperature driven drying process. The lateral shell was perforated in several points and cotton threads were installed in each hole to facilitate evaporation and to facilitate a more homogeneous water content distribution. Results are reported in terms of shear-wave velocity V_s versus saturation S_r.

4 True Triaxial Systems

4.1 General Considerations

In geotechnical boundary-value problems involving partially saturated soils, the accurate prediction of the stress–strain behavior of soil-structure systems requires that the soil constitutive relations be valid for all major stress paths likely to be experienced in the field. It is in this context that a true triaxial apparatus, capable of testing specimens along multi-axial stress paths under controlled suction states, plays a fundamental role in their complete stress–strain–strength characterization.

4.2 True Triaxial with Rigid Loading Plates

Matsuoka et al. (2002) reported a true triaxial apparatus with three pairs of rigid loading plates in three orthogonal directions (Fig. 10). A silty soil specimen of 10-cm side seats between upper and lower loading plates with remaining four lateral surfaces covered by latex. Each plate houses a 70-mm HAE disk (300-kPa entry value) and two 5-mm coarse stones covered with polyfluorotetraethylene filters.

Suction in the specimen is attained by inducing negative pore-water pressures via an external vacuum based system (Fig. 11). Cubical specimens are compacted in five layers in a separate cubical frame, with each layer statically compacted 226 times using a 1.2-cm diameter plunger up to a vertical stress of 300 kPa. Ceramic disks in the upper and lower plates are carefully saturated before testing in a custom-made cylindrical cell that allows saturation of the disk while mounted in the loading plate.

After setting the specimen between loading plates, a 98-kPa isotropic pressure was applied under a constant negative u_w (suction) of 59 kPa. Principal stresses are applied by stress-controlled loading method, with the full shearing process divided into about ten steps until peak failure. A new stress increment was applied when all of the axial strain rates reached less than 10^{-5}/min, and the drained volumetric strain rate reached less than 10^{-3}/h. All plain-strain shear tests were conducted under drained conditions (constant u_w) adjusting the intermediate σ_2 and minor σ_3 principal stresses to meet the requirement of absolute intermediate strain less than 0.01% at a given σ_1. In this study, true triaxial tests were conducted along radial stress paths in the π-plane (constant Lode-angle θ). Since normal stresses on the specimen are applied by three pairs of rigid steel plates, interference between the loading plates in the σ_1 and σ_2 directions becomes notable when θ is large. Hence, only stress paths with $\theta = 0$–$30°$ were accomplished (Fig. 12a).

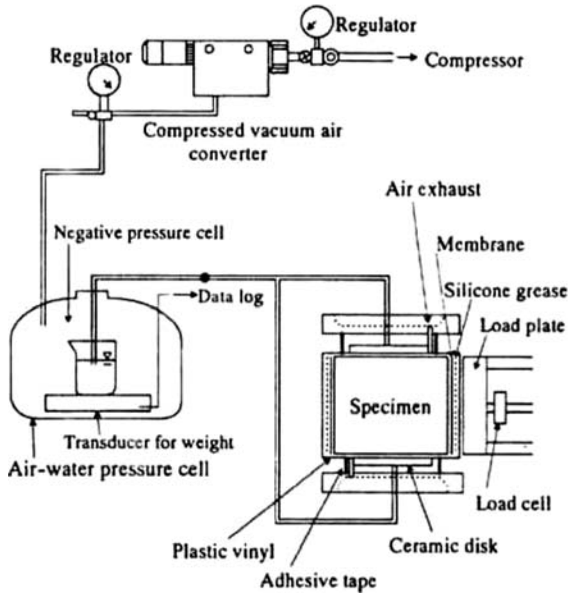

Fig. 11 System for applying negative pore-water pressure (Matsuoka et al. 2002)

In order to calibrate the true triaxial tests, Matsuoka et al. (2002) also performed a comparison of test results for conventional triaxial and true triaxial tests using same soil and stress conditions, i.e. triaxial

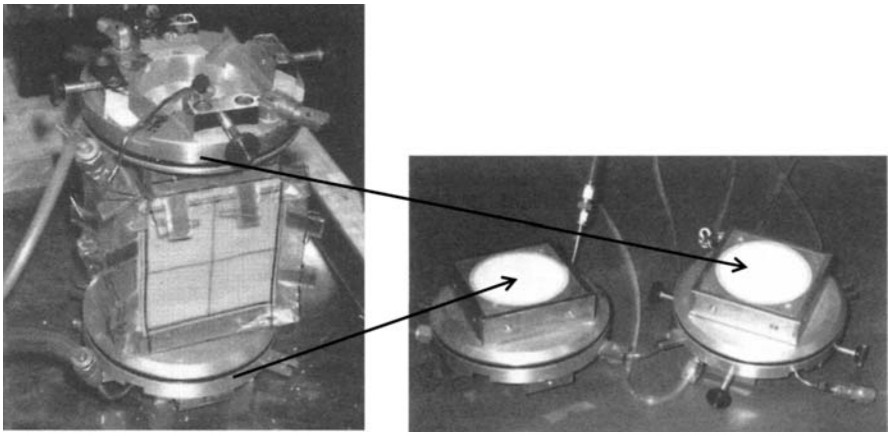

Fig. 10 True triaxial cell with rigid loading plates (Matsuoka et al. 2002)

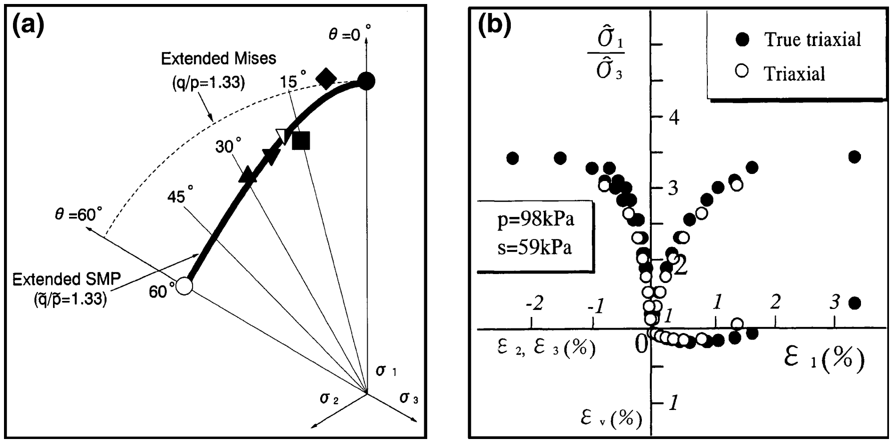

Fig. 12 True triaxial results: (**a**) stress paths in octahedral plane; (**b**) stress–strain relationships (Matsuoka et al. 2002)

compression (TC) tests, $\theta = 0°$, $p = 98$ kPa, and $s = 59$ kPa. However, the method for controlling suction in each device was different: negative u_w method ($s = -u_w$, $u_a = 0$) was used during true triaxial testing while positive u_a method ($s = u_a$, $u_w = 0$) was used during conventional triaxial testing. Stress–strain relationships measured by the two methods showed reasonably good agreement (Fig. 12b).

4.3 True Triaxial with Flexible Loading Membranes

Hoyos and Macari (2001) implemented a mixed-boundary type of true triaxial apparatus, with a 10-cm side specimen seated on top of a HAE disk and between five flexible latex/porex™ membranes on the remaining sides of the cube (Fig. 13a). The setup consists basically of a frame (1) that accommodates five (one top and four lateral) flexible latex/porex™ (2), and a cubical base piece (3) housing a 5-bar HAE disk (4). Once the specimen (5) is compacted, the remaining five walls (6) are assembled to the frame. Three LVDTs per face (7) monitor soil deformations. Hydraulic fluid is used to pressurize the specimen. External pressure is transmitted to hydraulic fluid through pressure inlet/outlet connections (8) on the walls. Pore-air pressure u_a is applied to the top and four lateral faces of the specimen via a small cooper block (9) attached to the flexible membranes with a threaded stem. External air pressure is applied via flexible nylon tubing (10). A 5-outlet manifold distributes the air pressure to the top and lateral faces simultaneously. Pore-water pressure u_w is applied at the bottom of the specimen via the HAE disk (4). Water pressure is also applied via nylon tubing (11). A flushing mechanism (12) is added to the bottom wall assembly. Tests are entirely computer-driven.

The flexible membranes were prepared using a GIT-603TE type of latex rubber possessing medium-to-high tear strength and low stiffness (Fig. 13b). The edges of the latex were doubled in thickness to reinforce its tear resistance at these critical boundaries. A 3.2-mm thick, 9.65-cm side, coarse flexible polyethylene (porex™) sheet, is placed between the latex and the specimen to uniformly distribute the air pressure, supplied from the exterior, to the pores of the soil (Hoyos 1998).

A procedure similar to that suggested by Bishop and Henkel (1962) to ensure in-place saturation of a HAE disk, was adapted to the working conditions of the HAE disk in the modified test cell. After saturation of the disk, the disk remains covered with a thin film of water until the first layer of soil is to be compacted. All cubical specimens are gently compacted in 10 layers of approximately 1-cm thickness via in-place tamping compaction. Once the specimen has been fully compacted, the temporary rigid membranes are removed and the latex/porex™, along with the assemblies containing the pore-air-pressurizing units, is set into place.

Compressibility of the latex/porex™ was found to be 0.065 cm under a 1 MPa pressure, which was deducted from total deformations of the specimen. The interface friction angle between porex and silty sand was found to be 6.2° from direct shear test. This results in a relatively low coefficient of friction (μ) of

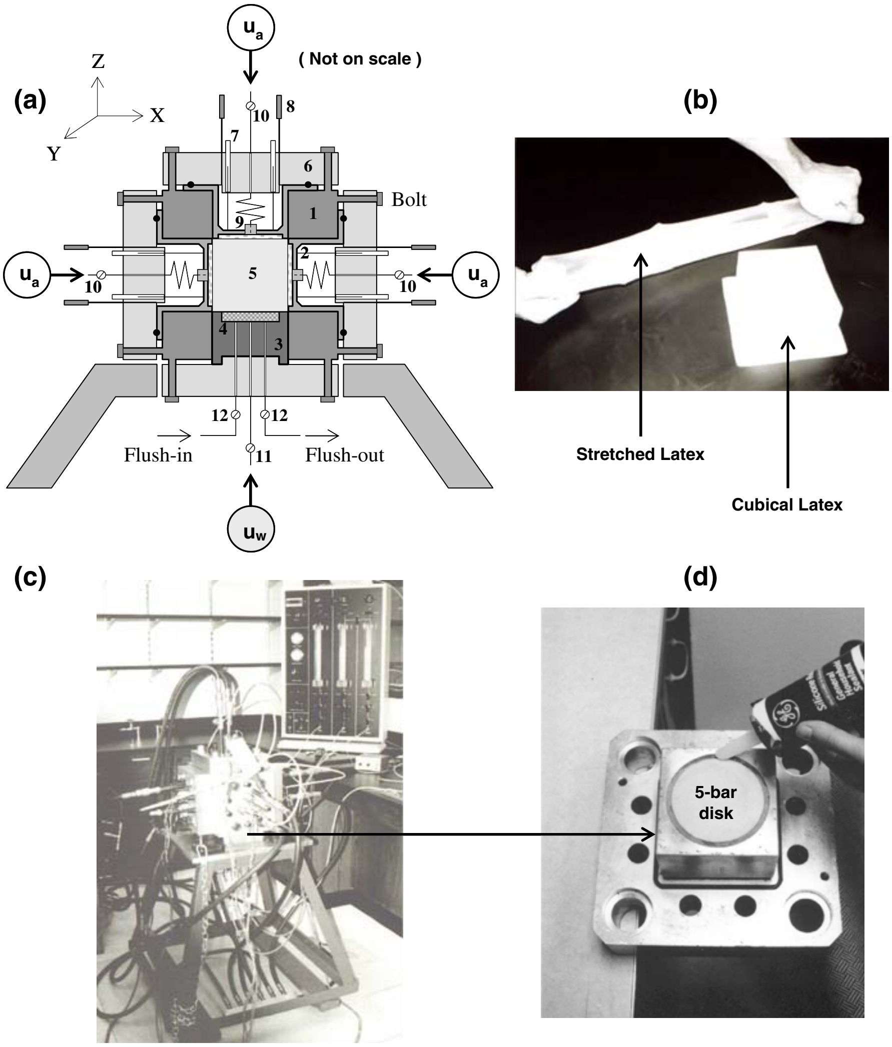

Fig. 13 True triaxial cell with flexible loading membranes: (**a**) layout; (**b**) latex; (**c**) general view; (**d**) bottom wall with HAE disk (Hoyos and Macari 2001)

0.11. Maximum pore size of the porex™ is about 130μ, considerably smaller than soil's D_{10}. Testing in the cell is stress-controlled, hence the adequate loading rate was empirically assessed. A 10 kPa/h loading rate (for isotropic loading and shearing), was found to be appropriate for adequate equalization. Response of silty sand in the net principal stress plane for 50, 100 and 200 kPa suctions is shown in Fig. 14.

4.4 Recent Refinements on True Triaxial Systems

The apparatus described above presented some serious limitations: (1) the steel frame is highly corrosive, which results in occasional clogging of the HAE disk, (2) the latex has low durability when exposed to hydraulic fluid (28–38°C) for an extended period of time, (3) pore-water temperature cannot be controlled, delaying equalization, (5) only stress-controlled testing is allowed, and (6) changes in pore-air and pore-water volumes cannot be measured.

Hoyos et al. (2005) have recently begun implementation of a novel true triaxial apparatus aimed at overcoming all of the above limitations, yielding a considerably enhanced performance. The working principle of the new cell is very similar to the one developed by Hoyos and Macari (2001). However, both u_a and u_w are applied simultaneously at the bottom face of a 3-in (7.6-cm) cubical soil specimen, while distilled de-aired water is used as pressurizing fluid against the latex (no porex™ involved).

Pore-air and pore-water pressure are applied at the bottom of the specimen via a full set of equally

Fig. 14 True triaxial results in net principal stress plane (Hoyos and Arduino 2005)

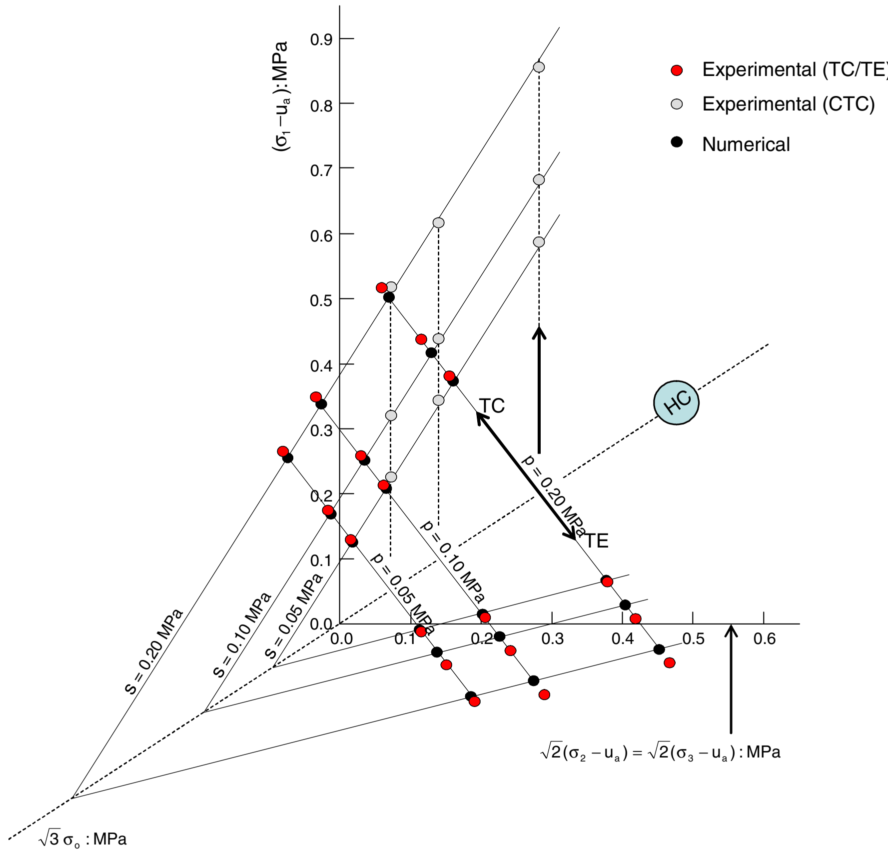

spaced, 0.75-in (1.9-cm) diameter, 5-bar disks and coarse porous stones (Fig. 15a). Air and water pressures are supplied via nylon tubing from a PCP-5000-UNSAT pressure control panel (from GCTS). Tests are entirely computer-driven.

The PCP-5000-UNSAT pressure control panel features pore-water volume (v_w) transducer with a 0.01-cc resolution. A photo of the setup is shown in Fig. 15b. Validation of the axis-translation technique was reported by Hoyos et al. (2005). On-going refinements include the incorporation of pore-fluids temperature control, tip tensiometers and bender elements.

5 Concluding Remarks

The present state-of-the-art report, which was intended to be neither comprehensive nor fully inclusive, concerns some of the recent advances in laboratory testing of unsaturated soils for stress–strain–strength–stiffness characterization under suction-controlled isotropic, axisymmetric, and true triaxial stress states. Main report sections were devoted to describing current methods and technologies using cylindrical triaxial systems, including advances in volume change measurements; resonant column/torsional shear systems; bender element-based systems; and suction-controlled testing under true triaxial stress states. The following concluding remarks can be drawn from the recent advances documented herein:

– Considerable improvements in applying axis translation technique via double-drainage systems have been reported, which involve simultaneous control of u_a and u_w at both ends of the specimen. Each end features a peripheral annular coarse stone and an internal HAE disk. This yields a significant reduction in equalization time;
– Several volume change measurement techniques have been considered for unsaturated soil specimens. In particular, improvements to the inner cylinder technique, as well as double-walled cells, have been highlighted. Other techniques are

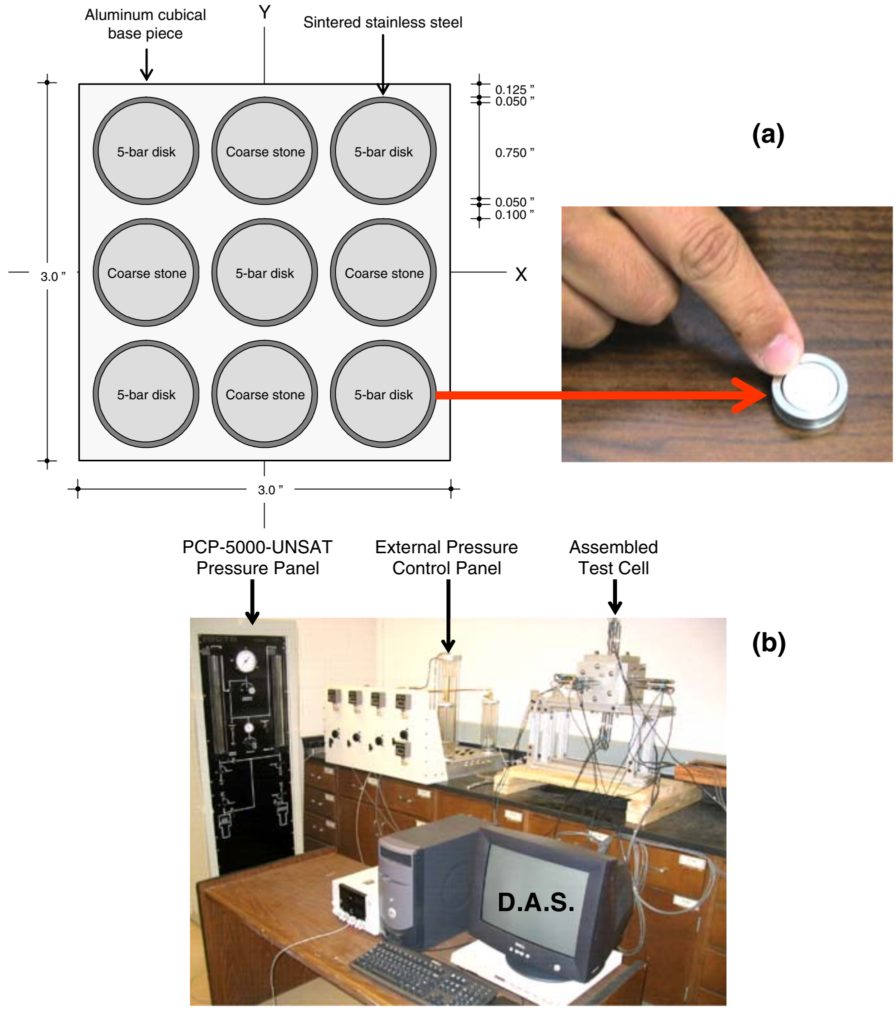

Fig. 15 A novel true triaxial system: (**a**) cubical pedestal with HAE disks; (**b**) general view (Hoyos et al. 2005)

currently being introduced, including local displacement sensors, laser based techniques and image processing;

– Experimental assessment of the evolution of dynamic shear modulus and material damping with respect to shear strain and suction levels is now possible using resonant column/torsional shear systems with suction control capabilities;
– Significant progress has been reported on suction-controlled testing using triaxial systems with self-contained bender elements. This technique allows determination of small-strain shear moduli G_o at different suction levels;
– Recent developments of true triaxial apparatuses, capable of testing specimens along multi-axial stress paths under controlled suction conditions, have facilitated the analysis of soil behaviour along a wide range of simple-to-complex stress–strain–suction paths not achievable in a conventional cylindrical cell.

Acknowledgements A novel TTX apparatus is currently being developed by the first author and his co-workers under a Major Research Instrumentation Award 0216545 sponsored by the U.S. National Science Foundation. This support is gratefully acknowledged. Contributions from the second author were supported by the Swiss NSF, grant 200021101917, and the Swiss State Secretariat for Education and Research SER, Grant OFES C03.0021. These supports are gratefully acknowledged. The third author would like to thank Prof. Claudio Mancuso for his invaluable assistance and advice during the design and setting up stages of the suction-controlled resonant column cell reported herein and the interpretation of results.

References

Adams BA, Wulfshon D, Fredlund D (1996) Air volume change measurement in unsaturated soil testing using a digital pressure–volume controller. Geotech Testing J 19(1):12–21

ASTM (2006) D4015-92 standard test methods for modulus and damping of soils by the resonant-column method. ASTM Book of Standards, Philadelphia, 04.08

Au WC, Chae YS (1980) Dynamic shear modulus of treated expansive soils. J Geotech Eng Div ASCE 106(GT3): 255–273

Aversa S, Nicotera MV (2002) A triaxial apparatus for testing unsaturated soils. Geotech Testing J 25(1):3–15

Barrera M (2002) Estudio experimental del comportamiento hidro-mecánico de suelos colapsables. Ph.D. Thesis, Universitat Politècnica de Catalunya, Barcelona, Spain

Bishop AW, Donald IB (1961) The experimental study of partly saturated soil in the triaxial apparatus. In: Proc. of the 5th international conference soil mechanics and foundation engineering, Paris, pp 13–21

Bishop AW, Henkel DJ (1962) The measurement of soil properties in the triaxial test. Edward Arnold, London

Cabarkapa Z, Cuccovillo T (2006) Automated triaxial apparatus for testing unsaturated soils. Geotech Testing J 29(1):21–29

Cabarkapa Z, Cuccovillo T, Gunn M (1998) A new triaxial apparatus for testing unsaturated soils. In: Proceedings of the 2nd international conference on unsaturated soils, UNSAT'98, Beijing, China, vol 2, pp 194–195

Chavez C, Romero E, Alonso EE (2005) Volume change measurement of partially saturated rockfill in triaxial tests. International symposium on advanced experimental unsaturated soil mechanics, EXPERUS 2005, Trento, vol 1, pp 93–98

Cho GC, Santamarina JC (2001) Unsaturated particulate materials—particle-level studies. J Geotech Geoenviron Eng ASCE 127(1):84–96

Clayton CRI, Khatrush SA (1986) A new device for measuring local axial strains on triaxial specimens. Géotechnique 36(4):593–597

Clayton CRI, Khatrush AS, Bica AVD, Siddique A (1989) The use of Hall effect semiconductors in geotechnical instrumentation. Geotech Testing J 12(1):69–76

Costa-Filho de LM (1982) Measurement of axial strains in triaxial tests on London Clay. Geotech Testing J 8(1):3–13

Cui YJ (1993) Etude du comportement d'un limon compacté non saturé et de sa modelisation dans un cadre élasto-plastique. Ph.D. Thesis, Ecole Nationale des Ponts et Chaussées, Paris, France

Cui YJ, Delage P (1996) Yielding and plastic behaviour of an unsaturated compacted silt. Géotechnique 46(2):291–311

Gachet P, Klubertanz G, Vulliet L, Laloui L (2003) Interfacial behaviour of unsaturated soil with small-scale models and use of image processing techniques. Geotech Testing J 26(1):12–21

Geiser F (1999) Comportement mécanique d'un limon non saturé: étude expérimentale et modélisation constitutive. Ph.D. Thesis, Ecole Polytechnique Fédérale de Lausanne, EPFL, Switzerland

Goto S, Tatsuoka F, Shibuya S, Kim YS, Sato T (1991) A simple gauge for local small strain measurements in the laboratory. Soils Found 31(1):169–180

Head KH (1986) Manual of soil laboratory testing, vol 3. Pentech Press, London

Hird CC, Hajj AR (1995) A simulation of tube sampling effects on the stiffness of clays. Geotech Testing J 18(1):3–14

Hoyos LR (1998) Experimental and computational modeling of unsaturated soil behavior under true triaxial stress states. Ph.D. Thesis, Georgia Institute of Technology, Atlanta, Georgia

Hoyos LR, Arduino P (2005) Modeling response of unsaturated silty sand in three-invariant stress space. In: Proc. of the 3rd MIT conference on computational fluid and solid mechanics, Boston, Massachusetts, pp 256–260

Hoyos LR, Macari EJ (2001) Development of a stress/suction-controlled true triaxial testing device for unsaturated soils. Geotech Testing J 24(1):5–13

Hoyos LR, Laikram A, Puppala AJ (2005) A novel true triaxial apparatus for testing unsaturated soils under suction-controlled multi-axial stress states. In: CD-Rom proc. of the 16th international conference on soil mechanics and geotechnical engineering, Osaka, Japan, pp 387–390

Isenhower WM (1979) Torsional simple shear/resonant column properties of San Francisco Bay Mud. M.S. Thesis, University of Texas at Austin, USA

Josa A, Alonso EE, Lloret A, Gens A (1987) Stress–strain behaviour of partially saturated soils. In: Proc. of the 9th European conference on soil mechanics and foundation engineering, Dublin, vol 2, 561–564

Klotz EU, Coop MR (2002) On the identification of critical state lines for sands. Geotech Testing J 25(3):288–301

Lade PV (1988) Automatic volume change and pressure measurement devices for triaxial testing of soils. Geotech Testing J 11(4):263–268

Laloui L, Péron H, Geiser F, Rifa'I A, Vulliet L (2006) Advances in volume measurement in unsaturated triaxial tests. Soils Found 46(3):341–349

Laudahn A, Sosna K, Bohac J (2005) A simple method for air volume change measurement in triaxial tests. Geotech Testing J 28(3):313–318

Leong EC, Agus SS, Rahardjo H (2004) Volume change measurement of soil specimen in triaxial test. Geotech Testing J 27(1):47–56

Maâtouk A (1993) Application des concepts d'état limite et d'état critique à un sol partiellement saturé effondrable. Ph.D. Thesis, Université de Laval, Montréal, Canada

Macari EJ, Parker JK, Costes NC (1997) Measurement of volume changes in triaxial tests using digital imaging techniques. Geotech Testing J 20(1):103–109

Mancuso C, Vassallo R, d'Onofrio A (2002) Small strain behavior of a silty sand in controlled-suction resonant column—torsional shear tests. Can Geotech J 39:22–31

Marinho EAM, Chandler RJ, Crilly MS (1995) Stiffness measurements on an high plasticity clay using bender elements. In: Proc. of the 1st international conference on unsaturated soils, UNSAT'95, Paris, France, vol 1, 535–539

Marinho FAM, Take WA, Tarantino A (2008) Measurement of matric suction using tensiometric and axis translation techniques. Geotech Geol Eng. doi:10.1007/s10706-008-9201-8

Matsuoka H, Sun DA, Kogane A, Fukuzawa N, Ichihara W (2002) Stress–strain behaviour of unsaturated soil in true triaxial tests. Can Geotech J 39:608–619

Ng CWW, Zhan LT, Cui YJ (2002) A new simple system for measuring volume changes in unsaturated soils. Can Geotech J 39:757–764

Picornell M, Nazarian S (1998) Effects of soil suction on the low-strain shear modulus of soils. In: Proc. of the 2nd international conference on unsaturated soils, UNSAT'98, Beijing, China, vol 2, pp 102–107

Quian X, Gray DH, Woods RD (1991) Resonant column tests on partially sarurated sands. Geotech Testing J ASCE 14(3):266–275

Rampino C (1997) Comportamento meccanico di una sabbia limosa ed argillosa costipata parzialmente satura. Ph.D. Thesis, University of Naples Federico II, Italy

Rampino C, Mancuso C, Vinale F (1999) Laboratory testing on an unsaturated soil: equipment, procedures, and first experimental results. Can Geotech J 36(1):1–12

Rifaï A, Laloui L, Vulliet L (2002) Volume measurement in unsaturated triaxial test using liquid variation and image processing. In: Proc. of the 3rd international conference on unsaturated soils, Recife, Brazil, vol 2, pp 441–445

Romero E (1999) Characterization and thermo-hydro-mechanical behaviour of unsaturated Boom clay: an experimental study. Ph.D. Thesis, Universitat Politècnica de Catalunya, Barcelona, Spain

Romero E (2001) Controlled-suction techniques. In: Gehling WYY, Schnaid F (eds) Proc. 4° Simposio Brasilerio de Solos Nao Saturadoes, ABMS, Porto Alege, pp 533–542

Romero E, Facio JA, Lloret A, Gens A, Alonso EE (1997) A new suction and temperature controlled triaxial apparatus. In: Proc. of the 14th international conference on soil mechanics and foundation engineering, Hambourg, pp 185–188

Sharma R.S. (1998) Mechanical behaviour of unsaturated highly expansive clays. Ph.D. Thesis, University of Oxford, UK

Sivakumar V (1993) A critical state framework for unsaturated soils. Ph.D. Thesis, University of Sheffield, UK

Tarantino A, Mongiovì L (2003) Calibration of tensiometer for direct measurement of matric suction. Géotechnique 53(1):137–141

Toyota H, Sakai N, Nishimura T (2001) Effects of stress history due to unsaturation and drainage conditions on shear properties of unsaturated cohesive soil. Soils Found 41(1):13–24

Vassallo R (2003) Comportamento di terreni costipati non saturi a piccole, medie e grandi deformazioni. Ph.D. Thesis, University of Naples Federico II, Italy

Vassallo R, Mancuso C, Vinale F (2007) Effects of net stress and suction history on the small strain stiffness of a compacted clayey silt. Can Geotech J 44(4):447–462

Vinale F, d'Onofrio A, Mancuso C, Santucci De Magistris F, Tatsuoka F (1999) The prefailure behaviour of soils as construction materials. In: Proc. of the 2nd int. conference on pre-failure behaviour of geomaterials, Torino, Italy, vol 2, pp 955–1007

Wheeler SJ (1988) The undrained shear strength of soils containing large gas bubbles. Géotechnique 38(3):399–413

Wu S, Gray DH, Richart FE (1985) Capillary effects on shear modulus at high strains. In: Proc. of the 11th international conference on soil mechanics and foundation engineering, San Francisco, vol 2, pp 1091–1094

Laboratory Hydraulic Testing in Unsaturated Soils

Farimah Masrouri · Kátia V. Bicalho · Katsuyuki Kawai

Originally published in the journal *Geotechnical and Geological Engineering*, Volume 26, No. 6, 691–704.
DOI: 10.1007/s10706-008-9202-7

Abstract This paper synthesizes the state-of-the art of the various laboratory testing techniques presently available for measuring the water hydraulic constitutive functions of unsaturated soils. Emphasis is on the laboratory testing techniques for measuring the soil–water retention curves and the water hydraulic conductivity functions of unsaturated soils. The significant recent advances in the investigation of the hydraulic behaviour of unsaturated swelling soils, are also presented. Comprehensive recent references on each measurement method are listed and discussed.

Keywords Unsaturated hydraulic conductivity · Unsaturated soils · Laboratory tests · Swelling soils · Soil suction

1 Introduction

Reliable measurements and predictions of soil water retention and unsaturated hydraulic conductivity functions are essential for solving unsaturated flow problems. The determination of the soil water retention curves is also important in modelling the stress-strain behaviour of unsaturated soils. Recent papers have shown the importance of hydro-mechanical coupling in unsaturated soil behaviour (Wheeler et al. 2003; Gallipoli et al. 2003).

Several laboratory testing techniques are now available to determine the water hydraulic constitutive functions of unsaturated rigid and deformable (shrinking-swelling) soils. The primary objective of this paper is to synthesize the present state-of-the art of these techniques into a form suitable for direct application by practicing engineers. At the same time the authors have attempted to identify sufficient references that interested readers will be able to locate more detailed information. Because of the substantial amount of literature published concerning hydraulic testing in unsaturated soils the review is restricted essentially to the literature on the laboratory testing techniques for measuring the soil–water retention and the water hydraulic conductivity functions of unsaturated soils. For simplicity, the word "water" corresponds to liquid water, unless stated otherwise.

In many practical engineering applications of unsaturated soils the external applied loads will result in changes of both soil fabric and soil suction. A change in soil suction causes a change in soil pore volume which may be important especially at low degrees of saturation, where the effect of soil suction on the average soil skeleton becomes comparable to

F. Masrouri (✉)
Laboratoire Environnement, Géomécanique & Ouvrages, Nancy-Université, Rue M. Roubault, 54501 Vandoeuvre-les-Nancy Cedex, France
e-mail: Farimah.Masrouri@ensg.inpl-nancy.fr

K. V. Bicalho
Federal University of Espirito Santo, Vitoria, Brazil

K. Kawai
Kobe University, Kobe, Japan

DOI: 10.1007/978-1-4020-8819-3_7

that of total stress, and the change in soil pore volume should therefore be included in the mass balance equation governing the problem of seepage (Richards' equation). In this paper the uncoupled hydraulic tests are considered and the effect of external loads on the soil are not taken into account.

2 Soil Water Retention Curves

The constitutive relationship between water content or degree of saturation and suction is called by many authors the soil–water "characteristic" curve. However, the term "characteristic" seems to imply that a unique relationship can characterise most of the hydraulic and mechanical behaviour of the unsaturated soil, regardless of the high dependency of this relationship on the initial state (void ratio and degree of saturation), fabric, hydraulic path (wetting or drying), state of stress, temperature, etc. Therefore, in this paper this relationship is called the soil water retention curve, SWRC. Figure 1 illustrates the primary boundary SWRC on drying and wetting conditions. There are infinite scanning curves between these boundary curves. The curve that might be obtained by starting at any particular saturation and either increasing or decreasing saturation is one of the scanning curves.

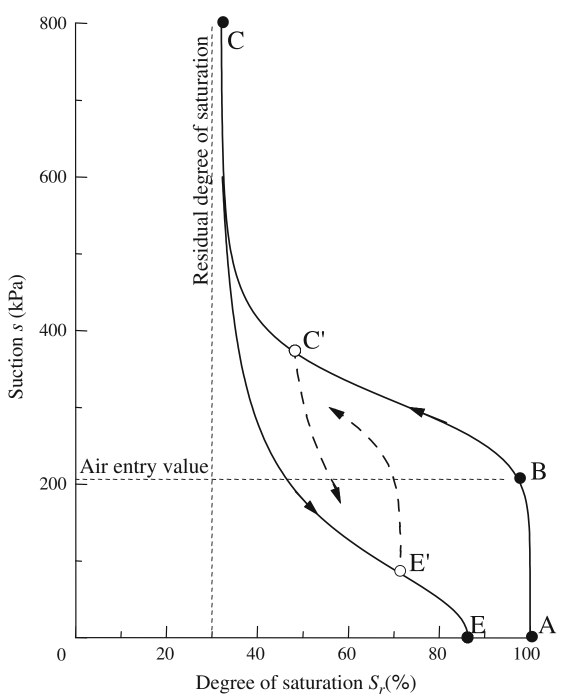

Fig. 1 A typical soil water retention curve. (A) initial saturated state, (B) approximate air-entry value, (C) approximate residual degree of saturation

The correct determination of the volumetric water content (or saturation) in the soil requires information on gravimetric water content and void ratio, but it is customary to assume that the void ratio is not changing along the presented SWRC. However, if there is deformation in the soil structure during the test, the volume changes should be measured. The image processing technique has been considered a viable method for volume change measurements for unsaturated soils (Gachet et al. 2003).

The total suction of a soil is made up of two components, the matric suction which includes the capillary suction and the osmotic suction (or solute suction). The SWRC relates matric and/or total suction to volumetric water content or the degree of saturation. A comprehensive description of the experimental techniques commonly used for measuring or controlling soil suction can be found in many references (Fredlund and Rahardjo 1993; Ridley and Wray 1996; Lu and Likos 2004; Marinho et al. 2008; Bulut and Leong 2008; Vanapalli et al. 2008; Blatz et al. 2008). The best technique to determine SWRC depends on the intended application, available human and financial resources, and the magnitude of the suctions that must be established. Table 1 briefly outlines the commonly applied working principles of these techniques and their ranges of applicability.

Techniques for measuring matric suction include tensiometers (Richards and Gardner 1938), electrical/thermal conductivity sensors and contact filter paper techniques. High-capacity tensiometers are used to directly measure negative pore water pressure up to 15 MPa (Ridley and Burland 1993; Tarantino and Mongiovi 2001, 2003). The electrical or thermal conductivity sensors, known as "gypsum block" sensors, for matric suction up to 4 MPa, are used to indirectly relate matric suction to the electrical or thermal conductivity of a porous medium embedded in a mass of unsaturated soil (Phene et al. 1971; Fredlund and Wong 1989). The contact filter paper techniques relies on measuring the equilibrium gravimetric water content of small filter papers in direct contact with unsaturated soil specimens (Gardner 1937; Chandler and Gutierrez 1986; Chandler et al. 1992, Houston et al. 1994; ASTM 1995). Marinho and Oliveira (2006) present a procedure for calibrating the filter paper method and the fundamental

Table 1 Summary of common laboratory techniques for measuring and controlling soil suction

Technique		Suction component	Measure suction from/control suction with	Suction range (MPa)	Available suction path
To measure suction	Tensiometer	Matric	Negative pore-water pressure	0–0.1 (1.5)	
	Electrical/thermal conductivity sensor	Matric	Thermal conductivity	0.01–4	
	Filter paper	Matric/ total	Water content of paper	0.1–3	
	Psycrometer chilled-mirror hygrometers, polymeter resist./capacit. sensors	Total	Humidity of vapour	0.1–100	
To control suction	Pressure plate	Matric	Air pressure	0.01–1.5	Drying/ wetting
	Soil column	Matric/ total	Negative water head	0–0.1	Drying
	Centrifuge	Matric	Centrifugal force	0.01–1.5	Drying
	Osmotic	Matric	Osmotic pressure	0–1	Drying/ wetting
	Vapour equilibrium	Total	Salt solution	3–100	Drying/ wetting

matters necessary for understanding the method. The centrifuge method measures centrifuge moisture equivalent reference to matric suction.

The techniques for measuring total suction include humidity measurement techniques, thermocoupe psychrometers (Spanner 1951), chilled-mirror hygrometers (Gee et al. 1992), and polymeter resistance/ capacitance sensors (Wiederhold 1997), and the non contact filter paper method (ASTM 1995).

The techniques used for controlling matric suction in a soil specimen include the pressure plate method, the soil column method, and the centrifuge method. The pressure plate method, for matric suction up to 15 MPa, uses porous ceramic stones that allow air and water pressure to be applied separately (Richards 1941; Hilf 1956; Bocking and Fredlund 1980). The soil column method is a traditional technique and the water table in soil column is changed to apply capillary force to soil. The osmotic technique to control the matric suction up to 10 MPa uses polyethylene glycol solutions (Delage et al. 1998; Cui 1993; Cuisinier and Masrouri 2005). The vapor equilibrium technique uses salt or acid solutions for controlling total suction ranging from 3 to 1000 MPa (Tessier 1984; Romero 1999; Villar 2000; Cuisinier 2002; Tang and Cui 2005).

Figure 2 presents a SWRC obtained on a kaolinite slurry using various methods by Fleureau et al. (1993). A good overall agreement is observed specially in the drying path. The osmotic suction can probably be neglected for this soil (i.e., matric and total suction are comparable).

An increased amount of water will be retained at the same suction in soils containing a larger clay fraction, and with high plasticity index. Araya and Paris (1981), Harverkamp and Parlange (1986), Fredlund (1998), Kamiya and Uno (2000) and Croney

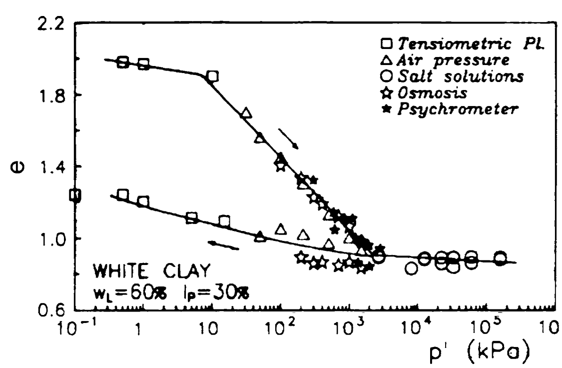

Fig. 2 Comparison between various suction controlled techniques (Fleureau et al. 1993)

and Coleman (1954) presented the differences on the SWRC between undisturbed and remoulded samples.

It is important that the geotechnical engineers be aware of the assumptions and limitations of the experimental techniques used for measuring the SWRC data. A number of papers have been published with SWRC data for various soils over a large range of suctions (Croney and Coleman 1954; Williams et al. 1983; Fleureau et al. 1993; Benson and Gribb 1997; Barbour 1998; Vanapalli et al. 1999; Bicalho 1999; Kawai et al. 2000; Romero and Vanuat 2000; Delage 2004; Fredlund 2004, Tang and Cui 2005). However, more research is still required for fully understanding the effects of the initial state (void ratio and degree of saturation), fabric, hydraulic path (wetting or drying), stress level, and temperature on the SWRC data.

3 Water Hydraulic Conductivity in Unsaturated Soils

The macroscopic approach based on the generalized form of Darcy's law states that the hydraulic flow rate is linearly proportional to the hydraulic gradient. The constant of proportionality, commonly termed the hydraulic conductivity in most disciplines (geotechnical engineers often use the term permeability coefficient), has units of length per time. In saturated and unsaturated soils, one must be constantly aware of the effect of many factors such as viscosity and density of the fluid (both functions of the temperature), the chemical composition of the soil and fluid and the geometry and topology of the porous space (connectivity, interface geometry) that affect the hydraulic conductivity test results. In unsaturated soils, it is also very important to take into account the degree of saturation and history of saturation that may affect the test results for measuring hydraulic conductivity.

The water hydraulic conductivity k_w of an unsaturated soil can be determined using either direct or indirect techniques. All methods assume the validity of Darcy's law, which may not be valid for low porosities or low hydraulic gradients (Hansbo 1960; Mitchell and Younger 1966; Matyas 1966). Richards (1931) and Childs and Collis-George (1950) have shown that Darcy's law also applies for the flow of water through unsaturated soils, but now hydraulic conductivity is a function of saturation (or pressure head, h_p) and void ratio of the soil. This function is not unique but depends on whether saturation has been reached by wetting or drying.

The k_w functions of unsaturated soils may be predicted by using empirical and macroscopic models (Kozeny 1927; Richards 1931; Averjanov 1950; Irmay 1954; Gardner 1958) and statistical models (Childs and Collis-George 1950; Burdine 1953; Kunze et al. 1968; Green and Corey 1971; Mualem 1976; Fredlund et al. 1994). Statistical models have been shown to be the most rigorous indirect method for estimating the k_w functions of unsaturated soil (Leong and Rahardjo 1997), but further investigation using more experimental data are recommended (Agus et al. 2003).

Numerous authors used the inverse problem solution to identify the soil hydraulic functions from outflow/inflow data and/or pressure/moisture local measurements obtained from evaporation or infiltration tests (Zachman et al. 1981, 1982; Dane and Hruska 1983; Kool et al. 1985; Abu-Hejleh et al. 1993; Wildenschild et al. 1997; Abdallah 1999; Bicalho 1999; Hwang 2002; Bicalho et al. 2003; Znidarcic et al. 2004). In this approach the experimental data is viewed as the solution to the initial value problem for which the governing equation and the initial and boundary conditions are known, but the material functions, the parameters in the governing equations are unknown. Yeh (1986) and McLaughlin and Townley (1996) provide excellent reviews of the available numerical methods which have been used for inverse problem solution. An adequate mathematical representation of the material functions and the availability of sufficient and precise experimental data are considered as key conditions for the parameter estimation approach. Since the solution to inverse problem leads often to a highly non linear optimization problem, Yeh (1986) suggested that its use should be done with much of caution. The solution of a well-posed inverse problem should simultaneously verify identifiability, uniqueness and stability conditions. Some attempts have been made in order to use this technique in cases for which alternative direct methods can not be used: swelling soils (Garnier et al. 1997; Rolland 2002), heterogeneous media (Zhang and Yeh 1997), presence of macropores (Abdallah 1999).

3.1 Direct Methods

Direct methods for measuring the k_w functions in the laboratory can be classified according to the flow mode as steady or unsteady state methods.

3.1.1 Steady State Methods

There are several variations of the steady state laboratory techniques for measuring unsaturated water hydraulic conductivity functions and detailed descriptions of these methods are provided in Klute (1972), Klute and Dirksen (1986), and Dirksen (1991).

In the steady state methods, a constant flow rate or hydraulic gradient is applied under specified average water pressure head (h_{pw}). Steady-state is supposed to occur as soon as the flow rate of the soil specimen is equal upstream and downstream and/or if a constant hydraulic gradient is observed through the tested soil specimen. The experiment can be repeated for different magnitudes of pressure or water content to yield a k_w–h_{pw} relationship.

Bjerrum and Huder (1957) describe a steady-state method for the measurement of k_w–S_w relationship wherein back pressure is used for soil specimen saturation. Their tests were performed in a triaxial cell. The k_w is determined for each increment of pore pressure. Boyle's and Henry's laws are used for determining the increase in saturation due to the increase in the back pressure. Corey (1957) proposed a steady state method of measuring k_w–S_w relationships. The technique is an extension of a system described by Richards (1931) where the pressure is controlled and the corresponding volumetric flow rate is measured. The technique is not adequate for very fine soils with high air-entry pressure values. The tests conducted in a triaxial cell have the advantage that the k_w functions may be examined under stress-controlled and simulated in-situ conditions.

A variety of constant flow methods using the flow pump technique have been developed for measuring the k_w functions of saturated and unsaturated soils (Olsen 1966; Olsen et al. 1985; Aiban and Znidarcic 1989; Znidarcic et al. 1991; Bicalho et al. 2000; Likos et al. 2005). The flow pump technique, beside being faster and having higher resolution than the conventional means of volume change measurement, provides a continuous steady state water flow in the withdrawal and infusion modes (Aiban and Znidarcic 1989). Bicalho et al. (2005) presented a testing technique for measurement of the relationship between the relative hydraulic conductivity, k_r, and degree of saturation, S_w, of a quasi-saturated compacted silt, by using a conventional triaxial cell connected to a flow pump. Data from the test results are used to validate an empirical k_r–S_w relationship for soils with discontinuous air phase. The function fits experimental data very well over the saturation range studied (occluded air bubbles). The experimental results suggest that k_r increases sharply when S_w increases from 0.9 to 1 and it has a very small value ($k_r \approx 0.1$) while $S_w \approx 0.8$, and that hysteretic effect on the k_w–S_w relationship can be neglected for soils with discontinuous air phase. The term quasi-saturated soil defines such a soil with entrapped air. "Unsaturated" here refers to the state in which soil air is connected to the atmosphere, and soil water is kept under negative pressure, while quasi-saturated conditions occur even when the pore water pressure is positive.

The steady state method may be costly, tedious and lengthy in low permeability materials. In order to minimize the long test time required on the traditional steady state methods, the steady state centrifuge method, CM, (uses centrifugal force as a fluid driving force) has been used to measure k_w on various porous media (Nimmo et al. 1987, 1992; Conca and Wright 1992; McCartney and Zorenberg 2005). One disadvantage of the CM is the higher initial cost for the equipment. The CM is only recommended for testing incompressible soil specimens with a pore structure insensitive to the state of stress, since a high net normal stress is applied to the soil specimen by centrifugation. Caputo and Nimmo (2005) proposed a new experimental approach called quasi-steady CM that uses a simple apparatus to establish a quasi-steady flow of water in unsaturated porous rock samples. The quasi-steady CM is adaptable to essentially any centrifuge suitable for hydrogeologic application over a wide range of sizes and operating speeds.

3.1.2 Unsteady State Methods

Klute (1972) and Benson and Gribb (1997) provided detailed descriptions of unsteady state methods of previous literature relating to the measurements of unsaturated k_w. The unsteady state methods are usually divided into two primary groups: outflow-inflow methods and instantaneous profile methods (Klute 1972).

The original outflow method for measuring k_w–S_w relationship by using a pressure plate apparatus was proposed by Gardner (1956). The method consists of subjecting a soil specimen to small incremental steps in matric suction and recording the rate of outflow and total outflow during each step. The method assumes that during the outflow process the k_w is constant, and the relation between the water content and matric suction is linear. The chosen steps must be small enough to meet the considered assumptions but large enough to provide a measurable volume of outflow. The SWRC is also obtained from this test by relating the applied matric suction to the equilibrium water content for each increment. This method was subsequently refined by Miller and Elrick (1958), Rijtema (1959), Kunze and Kirkham (1962) and others. The primary advantages of the method are good control on mass and simplicity of the equipment. However, there are few reliable and favourable comparisons with other methods (particularly for fine-grained soils).

There are some unsteady methods based on simplifying of Richards' equation to a diffusion equation using Boltzmann's transformation (Bruce and Klute 1956; Whisler et al. 1968; Vachaud 1968). The direct result of the out-inflow methods is a diffusivity function. If a k_w–S_w function is needed, the SWRC must be measured independently on other replicate soil specimens. Simplicity is the primary advance of these methods. However, there is significant scatter in the data and ambiguities in interpreting the data if the soil volume changes during drying or wetting conditions. In addition, the state of stress is difficult to control.

The instantaneous profile method, IPM, consists of inducing transient flow in a long cylindrical sample of soil and then measuring the resulting water content and/or pore water pressure profiles at various time intervals (Richards and Weeks 1953; Bruce and Klute 1956; Watson 1966; Wind 1968; Hamilton et al. 1981; Daniel 1983; Chiu and Shackelford 1998). Unsaturated k_w is computed by using transient profiles of water content and pore water pressure head in conjunction with Darcy's law. The laboratory method proposed by Wind (1968) is a direct evaporation technique that provides estimates of retention and conductivity curves in the tensiometric range and is quite easy to use and has been intensively studied in recent years (Tamari et al. 1993; Simunek et al. 1998). Hamilton et al. (1981) used a one-dimensional permeameter instrumented with thermocouple psychrometers for measuring the water hydraulic conductivity-suction relationship. They concluded that the IPM works reasonably well for clay with $30\% < S_w < 90\%$, and for sands with $S_w < 50\%$. Tensiometers should be used to measure suction under higher degrees of saturation. Daniel (1983) described a method of measuring unsaturated k_w of a silty fine sand and a very stiff silty clay using the IPM with a combination of tensiometers and psychrometers. The method requires about 3–4 weeks per test, not including calibration of psychrometers and/or tensiometers (Hamilton et al. 1981; Daniel 1983). Meerdink et al. (1996) described a testing procedure where both the pore water pressure profiles (tensiometers and/or thermocouple psychrometers) and the water content profiles (Time Domain Reflectometry, Topp et al. 1980) are measured. The cost and complexity of the tests increase when both pore water pressure profiles and water content profiles are measured. The water content profiles might also be directly measured by using external gamma-ray attenuation techniques, or resistive measurement systems. All variations of the IPM are based on the same theoretical principles, and primarily differ in the method used to remove or add water, and the technique of suction or moisture measurements. The soil should be continuously moistened/dried such that there is no hysteresis associated with alternately wetting and drying a soil. The advantages of the IPM are that the method is convenient, and that a broad range of the unsaturated water hydraulic conductivity and the soil water retention functions are obtained simultaneously provided profiles of pore water pressure and water content are measured. The IPM also has some disadvantages, such as the stress state which is very hard to be controlled during the tests and the pore air pressure is assumed to be equal to the atmospheric pressure but if air bubbles become occluded the assumption may be invalid. Daniel (1983) reported the possibility of errors when the saturation is approached (i.e., leakage, pressure may build up in occluded air bubbles, too low hydraulic gradients). He recommended an independent measurement of the saturated k_w for establishing the proper k_w at high degrees of saturation. Therefore, there is a need for experimental investigation of how the occluded air bubbles in water retention affect the water hydraulic conductivity.

Benson and Gribb (1997) recommend the thermal method for measuring k_w functions of drier superficial soils where the state of stress is not of great concern. The method consists of applying a temperature gradient across an insulated horizontal column of soil having uniform initial water content. The thermal method is fairly simple but requires instrumentation (e.g. thermal control system). The method can not be used for measuring k_w functions at high degrees of saturation.

Table 2 presents a summary of common laboratory direct techniques for measuring k_w for rigid soils.

Over the years a number of laboratory testing techniques have been suggested for direct determination of k_w functions of unsaturated soils but there are still limited literature and experimental data regarding the unsaturated hydraulic properties of low permeable fine-grained soils in a large degree of saturation domain. There are many questions still to be answered related to the subject of hydraulic testing of quasi-saturated soils (soils with entrapped air, in which soil air is not connected to the atmosphere, and soil water is kept under positive pressure). And, there is a lack of studies where the methods have been systematically compared. Most of the methods yield the k_w–S_w (or h_{pw}) relationship. There is, nevertheless, a great deal of experimental work yet to be done in studying the k_w functions in unsaturated soils which is undergoing a change in both structure and degree of saturation (hydromechanical coupling).

4 Measurement and Prediction of the Hydraulic Conductivity in Unsaturated Swelling–Shrinking Soils

In unsaturated swelling–shrinking soils, like clay soils, water content change results in significant volume change and drying is associated with high water content gradients and cracking. The water flow through these soils is a very complex process. The laboratory tests, even in the absence of cracks, need

Table 2 Summary of common laboratory direct techniques for measuring k_w for rigid soils

Test methods		Advantages	Disadvantages	Relative cost
Steady-state methods (SS)	Conventional constant head (CCH)	Simplicity, Can control stress state	Costly, tedious and lengthy in low permeability materials	Low
	Constant flow (flow pump technique)	Simplicity Can control stress state Faster and higher resolution than CCH Yields k_w and SWRC	Flow pump required	Moderate initial cost (equipment)
	Centrifuge	Short time for measuring low k_w	Centrifuge required Only for dense, stiff soil specimens High net normal stress Considerable operator attention	High initial cost (equipment)
Unsteady-state methods (USS)	Outflow-inflow	Quicker than SS Good control on mass Simplicity (equipment)	Few reliable and favourable comparisons with other methods (fine-grained soils)	Low
	Instantaneous profile	Simplicity Yields k_w and SWRC Good for clays ($30\% < S_w < 90\%$), and for sands ($S_w < 50\%$)	Poor mass control No control on stress state Possibility of errors when the S_w is approached	Moderate to high initial cost (equipment)
	Thermal method	Simplicity Good for low S_w	Lengthy No control on stress state Requires SWRC	Moderate (instrumentation)

in general heavy and expensive devices. Therefore, there is a very little data on the impact of soil swelling on water movement.

In rigid soils, two functions need to be evaluated, the SWRC and the k_w–h_{pw} relationship. In swelling soils, the so-called shrinkage curve relating the specific volume of a soil sample to its moisture content must also be defined. The possibility of hysteresis in these functions is recognized. Often, the shrinkage curve is determined in a separate experiment (Kim et al. 1993). Simultaneous measurements of the three functions may be obtained experimentally using the dual gamma-ray system (Angulo 1989).

In swelling soils, the porosity is coupled with the moisture content and the confining pressure. For different confining pressures, the porosity and the degree of saturation are different, therefore the k_w–S_w relationships are also different. The swelling curves of Tessier (1984), and Tariq and Durnford (1993) showed that the soil continues to swell well after saturation. This behaviour can be explained by the double layer theory. Kirby and Ringrose-Voase (2000) proposed that the two following conditions should be established at the same time to consider a swelling soil completely saturated (i.e., $S_w = 100\%$ and $h_{pw} = 0$).

4.1 Testing Methods

Techniques used for hydraulic testing of non deformable soils are not suitable for swelling soils, for at least two reasons. The first reason comes from the swelling pressure in constant volume tests. In some cases, this pressure can be dramatically high, for example, Imbert and Villar (2006) measured a swelling pressure of about 3.5 MPa for a compacted bentonite with a unit mass of 1.6 Mg/m^3 in infiltration tests. This pressure can deform and even damage the standard testing cells. In free volume change tests, the swelling rate of these soils changes very quickly the soil density and because of this property, certain measurement techniques of moisture appear also ineffective (e.g. mono gamma ray technique). The second reason is that the hydraulic conductivity and the diffusivity of these soils are in general much lower than for the other soils, this implies to have longer testing times. Therefore adapted devices, to impose high hydraulic gradients for example, are necessary to reduce these infiltration or saturation times.

4.1.1 Constant Volume

Very often, hydraulic measurements on swelling soils are carried out in a constant volume cell and equations proposed for non deformable media are applied to swelling soils. It is to be noted that from the rigid wall permeameters in the steady state regime, only the value of the saturated k_w state and possibly the swelling pressure can be obtained. Acar and D'Halosy (1987), Mitchell and Madsen (1987) and Kenney et al. (1992) used a consolidation cell to measure by falling-head method the k_w of swelling soils. Rhattas (1994) carried out a series of instantaneous profile wetting tests on constant volume cylindrical samples of different compacted clay soils. He used the Boltzmann's transformation to obtain the hydraulic diffusivity and calculated the k_w function using the diffusivity and the SWRC of the soil. This method based on the study of the water content mass at fixed times is also used by Fujita et al. (2001). As several identical samples are needed to carry out the tests, it is important to be able to prepare them by a precise compaction method.

4.1.2 Free or Controlled Swelling

For the tests where the soil swelling is completely free and monitored, some techniques exist but they still remain rather rare.

In steady state regime Boynton and Daniel (1985) and Tabani (1999) used a double cell flexible wall permeameter, with simultaneous pressure imposition in both cells to eliminate the volume variations of the internal cell. In this manner, the axial and volumetric swelling was correctly monitored. Kamon and Katsumi (2001) noted that the permeameter with flexible wall (triaxial cell) is the most suitable for swelling soils. The preferential flow paths along the walls are totally eliminated, the principal stresses are controlled and test durations are reduced.

In transient state regime, the k_w functions of swelling soils are generally studied by the IPM (i.e. Meerdink et al. 1996). During an imbibition or a desiccation test on a deformable porous medium, two parameters evolve simultaneously: the bulk density and the volumetric water content. Garnier et al. (1997) proposed a simple evaporation experiment to simultaneously determine all the three soil hydraulic properties using the inverse method solution (Fig. 3).

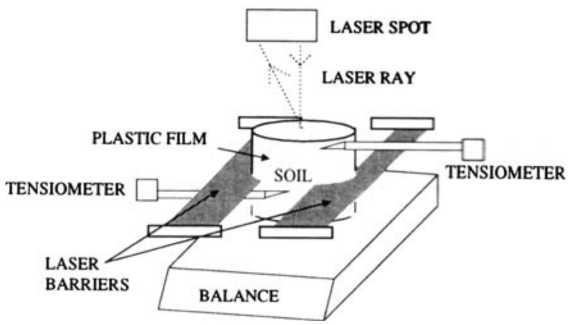

Fig. 3 Apparatus used to determine the hydraulic properties of a sample of swelling soil under evaporation (Garnier et al. 1997)

The non-intrusive dual-energy gamma-ray technique can also be used to measure the local variations of bulk density and humidity. This method needs complex installation and is very time consuming (Angulo 1989; Tabani et al. 2001; Rolland 2002). Figure 4 presents a schematic view of a dual-energy gamma-ray system (Rolland et al. 2005).

Rolland et al. (2005) used the dual gamma ray technique to study the effects of hydromechanical couplings during imbibition in a swelling compacted soil. They applied three different types of mechanical boundary conditions: free, oedometric and fixed volume.

Bulut et al. (2005) used the testing and analytical approach proposed by Mitchell (1979) to measure the diffusion coefficients of some clay soils. They performed one-dimensional water evaporation experiments to obtain unsaturated soil diffusivity coefficients. Their approach provides a very simple framework for experimental measurement of diffusion properties on an economical and routine basis. However, the most evident disadvantage of the diffusivity approach is in neglecting gravitational effects.

4.1.3 Lagrangian or Eulerian?

In general, a given water quantity in the swelling soils depends not only upon position but upon time as well. Askar and Jin (2000) specify that neglecting the soil swelling can lead to large mistakes in the hydraulic conductivity predictions. Angulo (1989) showed that, for deformable soils, errors can be made in the estimation of the hydraulic conductivity by the traditional equation of Richards' equation (1931).

The process of transient fluid flow in a swelling soil, can be described either by the field of velocity vector or by the paths (trajectories) of the particles of soil. The former is referred to as the Eulerian Description (ED) of motion (Prager 1953; Philip 1968), while the latter is referred to as the Lagrangian Description (LD) of motion (Smiles and Rosenthal 1968; Philip 1968). Kim et al. (1999) reported a detailed work on simulations using the Eulerian and Lagrangian descriptive hydraulic conductivities. The model proposed by Kim et al. (1999) leads to small differences between the two approaches, but the Lagrangian method seems to provide slightly better results (Fig. 5). Nakano et al. (1986) and Angulo (1989) showed that for swelling soils, finally the two approaches led to comparable results.

Fig. 4 Experimental set-up for monitoring a swelling soil during infiltration (Rolland et al. 2005)

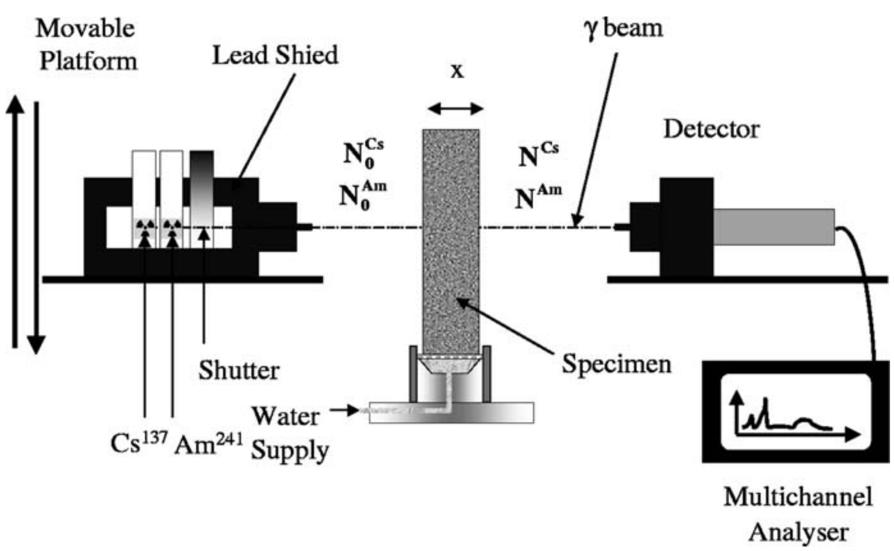

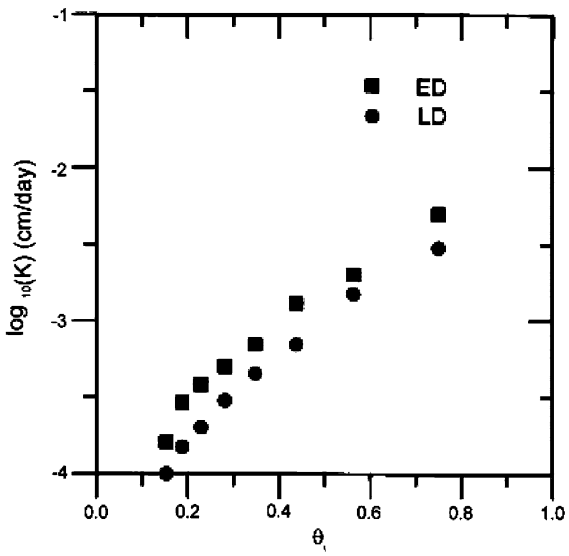

Fig. 5 Unsaturated hydraulic conductivities (log k_w (log K) – volumetric water content (θ): obtained using Lagrangian and Eulerian Descriptives (Kim et al. 1999)

4.1.4 Indirect Methods

Because of experimental difficulties for direct measurement of the hydraulic conductivity of the unsaturated deformable porous medium, it is often estimated using semi-empirical models based on the saturated hydraulic conductivity and SWRC parameters. Meerdink et al. (1996) compared measured laboratory and field hydraulic conductivity of compacted clays with three different models proposed by: van Genuchten (1980), Mualem (1978), Brooks-Corey (1964, 1966) and Fredlund et al. (1994). They concluded that these models underestimate the unsaturated hydraulic conductivity in such soils, because of their inability to capture the complexities of unsaturated flow in compacted clays.

Parent et al. (2004) proposed an indirect method to determine the hydraulic conductivity function of a highly compressible material based on relationships between saturated hydraulic conductivity and void ratio and between air-entry value and void ratio.

5 Conclusions

It is important that the geotechnical engineers be aware of the assumptions and limitations of the experimental techniques used for measuring the water hydraulic constitutive functions of unsaturated soils. More research is still required for fully understanding the effects of the initial state (void ratio and degree of saturation), fabric, hydraulic path (wetting or drying), stress level, and temperature on the SWRC data and the k_w functions of unsaturated soils.

The k_w functions of many soils do not follow the common functional forms and direct measurements of unsaturated k_w functions should always be preferred over the prediction using the idealized models. Over the years a number of testing techniques have been suggested for direct determination of k_w functions of unsaturated soils but there is still limited literature experimental data regarding the unsaturated hydraulic properties of low permeability fine-grained soils in a large degree of saturation domain. There is a lack of studies where the methods have been systematically compared. And, there are many questions still to be answered related to the subject of hydraulic testing of quasi-saturated soils (soils with entrapped air, in which soil air is not connected to the atmosphere, and soil water is kept under positive pressure).

Most of the laboratory methods for measurement of k_w functions yield the relationship between water hydraulic conductivity and corresponding saturation (or air and water pressure difference). There is, nevertheless, a great deal of experimental work yet to be done in studying the hydraulic conductivity functions in unsaturated soils which is undergoing a change in both structure and degree of saturation (hydromechanical coupling).

Dynamics of moisture movement is extremely complex in unsaturated swelling–shrinking soils, where a key conclusion is that we lack information, in particular in laboratory and also in case studies. A better knowledge of the soil fabric is necessary to better understand the hydro-mechanical behaviour of swelling soils. Therefore, it is difficult to currently either develop or verify models for water movement in swelling and cracking soils, and apply them to practical problems with any confidence. Given the complexity of theoretical and analytical methods, rigorous non-linear hysteretic analyses may not always be justified. The simplified methods in this domain should be developed.

Acknowledgements We appreciated helpful comments from Alessandro Tarantino and Adel Abdallah while preparing this report.

References

Abdallah A (1999) Modélisation de l'infiltration dans les sols fins compactés: intégration des écoulements préférentiels dans les macropores. Thèse de Doctorat, INPL, Nancy, France

Abu-Hejleh AN, Znidarcic D, Illangasekare TH (1993) Permeability determination for unsaturated soils. Unsaturated soils. Geotechnical Special Publication No. 39, pp 163–174

Acar YB, D'halosy E (1987) Assessment of pore fluid effects using flexible wall and consolidation permeameters. In: Woods RD (ed) Geotechnical practice for waste disposal' 87, specialty conference papers, Ann Arbor, Michigan. ASCE, Geotechnical Engineering Division. ASCE STP 13:231–245

Agus SS, Leong EC, Schanz T (2003) Assessment of statistical models for indirect determination of permeability functions from soil–water characteristics curves. Géotechnique 53(2):279–282

Aiban SA, Znidarcic D (1989) Evaluation of the flow pump and constant head techniques for permeability measurements. Géotechnique 39(4):655–666

Angulo R (1989) Caractérisation hydrodynamique des sols déformables partiellement saturés. Etude expérimentale à l'aide de la spectrométrie gamma double-source. Thèse de Doctorat. INPG, Grenoble

Araya LM, Paris JF (1981) A physicoempirical model to predict the soil moisture characteristic from particle-size distribution and bulk density data. Soil Sci Soc Am J 45:1023–1030

Askar A, Jin Y-C (2000) Macroporous drainage of unstaurated swelling soil. Water Resour Res 36(5):1189–1197

ASTM D5298–94 (1995) Standard test method for measurement of soil potential (suction) using filter paper. Annual book of American Society for Testing Materials Standards, Designation D3152–72, vol 4.08, Sep 1994, pp 1–6

Averjanov SF (1950) About permeability of subsurface soils in case of incomplete saturation. Engl Collect 7:19–21

Barbour SL (1998) The soil–water characteristic curve: a historical perspective. Can Geotech J 35:873–894

Benson CH, Gribb MM (1997) Measuring unsaturated hydraulic conductivity in the laboratory and field. unsaturated soil engineering practice. Geotechnical Special Publication No. 68, Logan, Utah, pp 113–168

Bicalho KV (1999) Modeling water flow in an unsaturated compacted soil. Ph.D. dissertation, University of Colorado, Boulder, Co, USA

Bicalho KV, Znidarcic D, Ko H-Y (2000) Air entrapment effects on hydraulic properties. Geotechnical Special Publication, ASCE 99:517–528

Bicalho KV, Znidarcic D, Ko H-Y (2003) Influence of air entrapment on the unsaturated hydraulic conductivity functions. 12 Panamerican Conf. on Soil Mech, Geotech. Engrg, vol 2. Culligan PJ, Einstein HH, Whittle AJ (eds) Cambridge, MA, USA, pp 1597–1602

Bicalho KV, Znidarcic D, Ko H-Y (2005) An experimental evaluation of unsaturated hydraulic conductivity functions for a quasi-saturated compacted soil. In: Proceedings of international symposium on advanced experimental unsaturated soil mechanics. Balkema, pp 325–329

Bjerrum L, Huder J (1957) Measurement of the permeability of compacted clays. Proceedings of fourth international conference on soil mechanics and foundation engineering. London, pp 6–8

Blatz J, Cui YJ, Oldecop LA (2008) Vapour equilibrium and osmotic technique for suction control. Geotech Geol Eng. doi:10.1007/s10706-008-9196-1

Bocking KA, Fredlund DG (1980) Limitations of the axis translation technique. IV Int Conf on Expansive Soils, Denver 1:117–135

Boynton SS, Daniel DE (1985) Hydraulic conductivity tests on compacted clay. J Geotech Eng 111(4):465–478

Brooks RH, Corey AT (1964) Hydraulic properties of porous media. Colorado State University Hydrology Papers No. 3, pp 1–27

Brooks RH, Corey AT (1966) Properties of porous media affecting fluid flow. J Irrig Drain Div ASCE 92(2):61–88

Bruce R, Klute A (1956) The measurement of soil moisture diffusivity. Soil Sci Soc Am Proc 20:458–462

Bulut R, Leong EC (2008) Indirect measurement of suction. Geotech Geol Eng. doi:10.1007/s10706-008-9197-0

Bulut R, Aubeny CP, Lytton RL (2005) Unsaturated soil diffusivity measurements. In: Proceedings of international symposium on advanced experimental unsaturated soil mechanics. Balkema, pp 281–286

Burdine NT (1953) Relative permeability calculation size distribution data. Trans Am Inst Min, Metal Petroleum Eng 198:71–78

Caputo MC, Nimmo JR (2005) Quasi-steady centrifuge method for unsaturated hydraulic characterization. Proceedings of international symposium on advanced experimental unsaturated soil mechanics. Balkema, pp 287–290

Chandler RJ, Gutierrez CI (1986) The filter paper method of suction measurement. Géotechnique 36, No. 2265–268

Chandler RJ, Crilley MS, Montgomery-Smith G (1992) A low-cost method of assessing clay desiccation for low-rise buildings. Proc Instn Civ Engrs Civ Engng 1992, May, pp 82–89

Childs EC, Collis-George N (1950) The permeability of porous materials. Proc Roy Soc 201A:392–405

Chiu T-F, Shackelford CD (1998) Unsaturated hydraulic conductivity of compacted sand-kaolin mixtures. J Geotech Geoenviron Eng 124(2):160–170

Conca JL, Wright JV (1992) The UFA method for rapid, direct measurements of unsaturated transport properties in soil, sediment, and rock. Aust J Soil Res 36:291–315

Corey AT (1957) Measurement of water and air permeability in unsaturated soil. Soil Sci Soc Am Proc 21(1):7–10

Croney D, Coleman JD (1954) Soil structure in relation to soil suction. Soil Sci 5:75–84

Cui YJ (1993) Étude du comportement d'un limon compacté non saturé et de sa modélisation dans un cadre élasto-plastique. Thèse de doctorat, Ecole Nationale des Ponts et Chaussées, 280 p.

Cuisinier O (2002) Comportement hydromécanique des sols gonflants compactés. Thèse de doctorat, Institut National Polytechnique de Lorraine, Nancy, France, 165 p

Cuisinier O, Masrouri F (2005) Hydromechanical behaviour of a compacted swelling soil over a wide suction range. Int J Eng Geol 81:204–212

Dane JH, Hruska S (1983) In-situ determination of soil hydraulic properties during drainage. Soil Sci Soc Am J 47:619–624

Daniel DE (1983) Permeability test for unsaturated soil. Geotech Test J 6(2):81–86

Delage P (2004) Experimental unsaturated soil mechanics. In: de Campos J, Marinho FAM (eds) Unsaturated soils, vol 3. Sweets and Zeitlinger, Lisse, pp 973–996

Delage P, Cui YJ, Yahia-Aïssa M, De Laure E (1998) On the unsaturated hydraulic conductivity of a dense compacted bentonite. In: Proceedings of the second international conference on unsaturated soils. Beijing, China, pp 27–30

Dirksen C (1991) Unsaturated hydraulic conductivity. In: Smith KA, Mullins CE (eds) Soil analysis. Physical methods. Marcel Dekker, New York, pp 209–270

Fleureau J-M, Kheirbek-Saoud S, Soemitro R, Taibi S (1993) Behavior of clayey soils on drying-wetting paths. Can Geotech J 30:287–296

Fredlund DG (1998) Bringing unsaturated soil mechanics int engineering practice. Proceedings of the 2nd international conference on unsaturated soils, pp 1–35

Fredlund DG (2004) Use of soil–water characteristic curves in the implementation of unsaturated soil mechanics. In: de Campos J, Marinho FAM (eds) Unsaturated soils, vol 3. Sweets and Zeitlinger, Lisse, pp 887–902

Fredlund DG, Rahardjo H (1993) Soil mechanics for unsaturated soils. Wiley, New York

Fredlund DG, Wong DKH (1989) Calibration of thermal conductivity sensors for measuring soil suction. Geotech Test J 12(3):188–194

Fredlund DG, Xing A, Huang S (1994) Predicting of the permeability function for unsaturated soil using the soil–water characteristic curve. Can Geotech J 31:533–546

Fujita T, Suzuki H, Sugita Y, Sugino H, Nakano M (2001) Hydraulic properties in compacted bentonite under unsaturated condition. In: Adachi K, Fukue M (eds) Clay science for engineering. Rotterdam, Balkema, pp 229–238

Gachet P, Klubertanz G, Vulliet L, Laloui L (2003) Interfacial behavior of unsaturated soil with small-scale models and use of image processing techniques. ASTM Geotech Test J, GTJ200310127_261, 26(1), p 10

Gallipoli D,Wheeler SJ, Karstunen M (2003) Modelling the variation of degree of saturation in a deformable unsaturated soil. Géotechnique 53(1):105–112

Gardner R (1937) A method of measuring the capillary tension of soil moisture over a wide moisture range. Soil Sci 43:227–283

Gardner W (1956) Mathematics of isothermal water conduction in unsaturated soils. Highway Research Board Special Report 40, International symposium on physico-chemical phenomenon in soils, pp 78–87

Gardner WR (1958) Some steady state solutions of the unsaturated moisture flow equation with application to evaporation from a water-table. Soil Sci 85:228–232

Garnier P, Rieu M, Boivin P, Baveye P (1997) Determinig the hydraulic Properties of a swelling soil from a transient evaporation experiment. Soil Sci Soc Am J 61:1555–1563

Gee G, Campbell M, Campbell G (1992) Rapid measurement of low soil potentials using a water activity meter. Soil Sci Soc Am J 56:1068–1070

Green RE, Corey JC (1971) Calculation of hydraulic conductivity: a further evaluation of some predictive methods. Proc Soil Sci Soc Am 35:3–8

Hamilton JM, Daniel DE, Olson RE (1981) Measurement of hydraulic conductivity of partially saturated soils. Permeability and groundwater contaminant transport. ASTM STP 746:182–196

Hansbo S (1960) Consolidation of clay, with special reference to influence of vertical sand drains. Swedish Geotech Inst Proc No 18, Stockholm 18:41–159

Harverkamp R, Parlange JY (1986) Predicting the water-retention curve from particle-size distribution: 1. Sandy soils without organic matter. Soil Science 142:325–339

Hilf JW (1956) An investigation of pore water pressure in compacted cohesive soils. Ph.D. dissertation, U.S. Dept. Interior Bur. Reclamation Tech. Memorandum 654, Denver, Co, USA

Houston SL, Houston W, Wagner AM (1994) Laboratory filter paper suction measurements. Geotech Test J 17:185–194

Hwang C (2002) Determination of material functions for unsaturated flow. Ph.D. dissertation, University of Colorado, Boulder, Co, USA

Imbert C, Villar MV (2006) Hydro-mechanical response of a bentonite pellets/powder mixture upon infiltration. Appl Clay Sci 32:197–209

Irmay S (1954) On the hydraulic conductivity of unsaturated soils. Trans Am Geophys Union 35:463–468

Kamiya K, Uno T (2000) Grain size and diameter distribution of sands. Proceedings of Asian conference on unsaturated soils, pp 399–404

Kamon M, Katsumi T (2001) Clay liners for waste landfill. In: Adachi K, Fukue M (eds) Clay science for engineering. Rotterdam, Balkema, pp 29–45

Kawai K, Kato S, Karube D (2000) The model of water retention curve considering effects of void ratio. Proceedings of Asian conference on unsaturated soils, pp 329–334

Kenney TC, van Veen WA, Swallow MA, Sungaila MA (1992) Hydraulic conductivity of compacted bentonite-sand mixtures. Can Geotech J 29:364–374

Kim DJ, Feyen J, Vereecken H (1993) Prediction of dynamic hydraulic properties in a ripening soil. Geoderma 57: 231–246

Kim DJ, Angulo-Jaramillo R, Vauclin M, Feyen J, Choi SI (1999) Modeling of soil deformation and water flow in a swelling soil. Geoderma (Amst.) 92(3–4):217–238

Kirby JM, Ringrose-Voase AJ (2000) Drying of some Philippine and Indonesian puddled rice soils following surface drainage: numerical analysis using a swelling soil flow model. Soil Tillage Res 57(1–2):13–30

Klute A (1972) The determination of the hydraulic conductivity and diffusivity of unsaturated soils. Soil Sci 113(4):264–276

Klute A, Dirksen C (1986) Hydraulic conductivity and diffusivity: laboratory methods. In: Klute A (ed) Methods of soil analysis. 1, Physical and mineralogical methods, Madison: American Society of Agronomy; Soil Science Society of America, 1982. 2nd edn., pp 687–734

Kool JB, Parker JC, van Genuchten MTh (1985) Determining soil hydraulic properties from one-step outflow experiments by parameter estimation; I. Theory and numerical studies. Soil Sci Soc Am J 49:1348–1354

Kozeny J (1927) Über Kapillare des Wassers im Boden. Zitzungsber Akad Wiss Wien 136:760–765

Kunze RJ, Kirkham D (1962) Simplified accounting for membrane impedance in capillary conductivity measurements. Soil Sci Soc Am Proc 26:421–426

Kunze RJ, Uehara G, Graham K (1968) Factors important in the calculation of hydraulic conductivity. Proc Soil Sci Soc Am 32:760–765

Leong EC, Rahardjo H (1997) Permeability functions for unsaturated soils. J Geotech Geoenviron Eng 123: 1118–1126

Likos WJ, Wayllace A, Lu N (2005) Numerical modeling of constant flow method for measuring unsaturated hydrologic properties. Proceedings of international symposium on advanced experimental unsaturated soil mechanics. Balkema, pp 291–297

Lu N, Likos WJ (2004) Unsaturated soil mechanics. Wiley, 556 p

Marinho FAM, Oliveira OM (2006) The filter paper method revised. ASTM Geotech Test J, USA 29(3):250–258

Marinho FAM, Take WA, Tarantino A (2008) Measurement of matric suction using tensiometric and axis translation techniques. Geotech Geol Eng. doi:10.1007/s10706-008-9201-8

McCartney JS, Zorenberg JG (2005) The centrifuge permeameter for unsaturated soils. Proceedings of international symposium on advanced experimental unsaturated soil mechanics. Balkema, pp 299–304

McLaughlin D, Townley LR (1996) A reassessment of the ground-water inverse problem. Water Resour Res 32(5):1133–1161

Matyas EL (1966) Air and water permeability of compacted soils. Permeability and capillary of soils. ASTM STP 417:160–175

Meerdink J, Benson C, Khire M (1996) Unsaturated hydraulic conductivity of two compacted barrier soils. J Geotechn Eng ASCE 122(7):565–576

Miller E, Elrick D (1958) Dynamic determination of capillary conductivity extended for non-negligible membrane impedance. Soil Sci Soc Am Proc 22:483–486

Mitchell PW (1979) The structural analysis of footings on expansive soils. Research Report No. 1, K.W.G. Smith and Assoc. Pty. Ltd., Newton, South Australia

Mitchell JK, Madsen FT (1987) Chemical effects on clay hydraulic conductivity. In: Proceedings of ASCE specialty conference, geotechnical practice for waste disposal. ASCE STP 13:87–116, Ann Arbor, Michigan

Mitchell JK, Younger JS (1966) Abnormalities in hydraulic flow through fine-grained soils. Permeability and Capillary of Soils. ASTM STP 417:106–141

Mualem Y (1976) A new model for predicting the hydraulic conductivity of unsaturated porous media. Water Resour Res 12(3):513–522

Mualem Y (1978) Hydraulic conductivity of unsaturated porous media: generalized macroscopic approach. Water Resour Res 14(2):325–334

Nakano M, Amemiya Y, et Fujii K (1986) Saturated and unsaturated hydraulic conductivity of swelling clays. Soil Sci 141(1):1–6

Nimmo JR, Rubin J, Hammermeister DP (1987) Unsaturated flow in a centrifugal field: measurement of hydraulic conductivity and testing of Darcy's law. Water Resour Res 23(1):124–134

Nimmo JR, Akstin KC, Mello KA (1992) Improved apparatus for measuring hydraulic conductivity at low water content. Soil Sci Soc Am J 56(6):1758–1761

Olsen HW (1966) Darcy's Law in saturated kaolinite. Wat Resour Res 2(6):287–295

Olsen HW, Nichols RW, Rice TL (1985) Low gradient permeability methods in a triaxial system. Géotechnique 35(2):145–157

Parent SE, Cabral A, Dell'Avanzi E, Zornberg JG (2004) Determination of the hydraulic conductivity function of a highly compressible material based on tests with saturated samples. Geotech Test J 27(6):1–5

Phene CJ, Hoffman GJ, Rawlins SL (1971) Measuring soil matric potential in-situ by sensing heat dissipation within a porous body – Part I and II, Soil Sci Soc Am Proc 53:27–33, 225–229

Philip JR (1968) Kinetics of sorption and volume change in clay-colloid pastes. Aust J Soil Res 6:249–267

Prager S (1953) Diffusion in binary systems. J Chem Phys 21:1344–1347

Rhattas, A., (1994) Transfert de masse dans les argiles à faible porosité. Analyse Théorique et résultats expérimentaux. Thèse Sciences. Université d'Orléans

Richards LA (1931) Capillary conduction of liquids through porous medium. J Phys 1:318–333

Richards LA (1941) A pressure—membrane extraction apparatus for soil solution. Soil Sci 51:377–386

Richards LA, Gardner W (1938) Tensiometers for measuring the capillary tension of soil water. J Am Soc Agron 28:352–358

Richards S, Weeks L (1953) Capillary conductivity values from moisture yield and tension measurements on soil columns. Proc Soil Sci Soc Am 17:206–209

Ridley AM, Burland JB (1993) A new instrument for the measurement of soil moisture suction. Géotechnique 43(2):321–324

Ridley AM, Wray WK (1996) Suction measurement—a review of current theory and practices. Proceedings of 1st international conference on unsaturated soils, pp 1293–1322

Rijtema P (1959) Calculation of capillary conductivity from pressure plate outflow data with non-negligible membrane impedance. Neth J Agric Sci 7:209–215

Rolland S (2002) Transfert hydrique dans des sols argileux gonflants: influence du confinement. Thèse de doctorat, INPL, Nancy, France

Rolland S, Stemmelen D, Moyne C, Masrouri F (2005) Experimental hydraulic measurements in an unsaturated swelling soil using the dual-energy gamma-ray technique. Proceedings of international symposium on advanced experimental unsaturated soil mechanics. Balkema, pp 305–310

Romero E (1999) Characterisation and thermo-hydro-mechanical behaviour of unsaturated boom clay: an experimental study. Thèse de l'Université Polytechnique de Catalogne, Barcelone, 405 pp

Romero E, Vaunat J (2000) Retention curves of deformable clays. Proceedings of international workshop on unsaturated soils, pp 91–106

Simunek J, Wendroth O, van Genuchten MTh (1998) Parameter estimation analysis of the evaporation method for determining soil hydraulic properties. Soil Sci Soc Am J 62:894–905

Smiles DE, Rosenthal MJ (1968) The movement of water in swelling materials. Aust J Soil Res 6:237–248

Spanner DC (1951) The Peltier effect and its use in the measurement of suction pressure. J Exp Bot 2:145–168

Tabani P (1999) Transfert hydrique dans des sols déformables. Thèse de Doctorat, INPL, Nancy, France

Tabani Ph, Masrouri F, Rolland S, Stemmelen D (2001) Hydromechanical Behaviour of a compacted bentonite-silt mixture. In: Adachi K, Fukue M (eds) Clay science for engineering. Rotterdam, Balkema, pp 245–250

Tamari S, Bruckler L, Halbertsmama J, Chadoeuf J (1993) A simple method for determining soil hydraulic properties in the laboratory. Soil Sci Soc Am J 57:642–651

Tang AM, Cui YJ (2005) Controlling suction by the vapour equilibrium technique at different temperatures and its application in determining the water retention properties of MX80 clay. Can Geotech J 42:1–10

Tarantino A, Mongiovi L (2001) Experimental procedures and cavitation mechanisms in tensiometer measurements. Geotech Geol Eng 19:189–210

Tarantino A, Mongiovi L (2003) Calibration of tensiometer for direct measurement of matric suction. Géotechnique 53(1):137–141

Tariq AUR, Durnford DS (1993) Analytical volume change model for swelling clay-soils. Soil Sci Soc Am J 155(57):1183–1187

Tessier D (1984) Étude expérimentale de l'organisation des matériaux argileux. Hydratation, gonflement et structuration au cours de la dessication et de la réhumectation. Thèse Sciences, Université de Paris VII

Topp GC, Davis JL, Annan AP (1980) Electromagnetic determination of soil water content: measurements in coaxial transmission lines. Water Resour Res 16(3): 574–582

Vachaud G (1968) Contribution à l'étude des problèmes d'écoulement en milieux poreux non saturés. Thèse de Doctorat. Faculté des Sciences de l'Université de Grenoble

Vanapalli SK, Fredlund DG, Pufahl DE (1999) The influence of soil structure and stress history on the soil–water characteristics of a compacted till. Geotechnique 49(2): 143–159

Vanapalli SK, Nicotera MV, Sharma RS (2008). Axis-translation and negative water column techniques for suction control. Geotech Geol Eng. doi:10.1007/s10706-008-9206-3

van Genuchten MTh (1980) A closed-form equation for predicting the hydraulic conductivity of unsaturated soils. Soil Sci Soc Am Proc 44:892–897

Villar MV (2000) Caracterización termo-hidro-mecánica de una bentonita de Cabo de Gata. Ph.D. thesis, Universidad Complutense de Madrid, Spain

Watson KK (1966) An instantaneous profile method determining the hydraulic conductivity of unsaturated porous materials. Water Resour Res 2:709–715

Wheeler SJ, Sharma RS, Buisson MSR (2003) Coupling of hydraulic hysteresis and stree-strain behaviorur in unsaturated soil. Géotechnique 53(1):41–54

Whisler FD, Klute A, Peters DB (1968) Soil water diffusivity from horizontal infiltration. Soil Sci Soc Am Proc 32:6–11

Wiederhold P (1997) Water vapor measurement methods and instrumentation. Marcel Dekker, New York

Wildenschild D, Jensen KH, Hollenbeck KJ, Illangasekare TH, Znidarcic D, Sonnenborg T, Butts MB (1997) A two-stage procedure for determining unsaturated hydraulic characteristics using a syringe pump and outflow observations. Soil Sci Soc Am J 61:347–359

Williams J, Prebble RE, Williams WT, Hignett CT (1983) The influence of texture, structure and clay mineralogy on the soil moisture characteristic. Aust J Soil Res 21:15–32

Wind GP (1968) Capillary conductivity data estimated by a simple method. Water in the unsaturated zone. In: Rijtema PE, Wassink H (eds) Proceedings of the Wageningen Symposium, vol 1, pp 181–191

Yeh WW-G (1986) Review of parameter identification procedures in ground-water hydrology: the inverse problem. Water Resour Res 22(2):95–108

Zachman DW, Duchateau PC, Klute A (1981) The calibration of the Richards flow equation for a draining column by parameter identification. Soil Sci Soc Am J 45:1012–1015

Zachman DW, Duchateau PC, Klute A (1982) Simultaneous approximations of water capacity and soil hydraulic conductivity by parameter identification. Soil Sci 134:157–163

Zhang J, Yeh T-CJ (1997) An iterative inverse method for steady flow in the vadoze zone. Water Resour Res 33(1):63–71

Znidarcic D, Illangasekare T, Manna M (1991) Laboratory testing and parameter estimation for two-phase flow problems. ASCE, Geotechnical Special Publication 27:1089–1099

Znidarcic D, Hwang C, Bicalho KV (2004) Experimental determination of hydraulic characteristics for unsaturated soils. In: de Campos J, Marinho FAM (eds) Unsaturated soils, vol 3. Sweets and Zeitlinger, Lisse, pp 1137–1141

Microstructure Investigation in Unsaturated Soils: A Review with Special Attention to Contribution of Mercury Intrusion Porosimetry and Environmental Scanning Electron Microscopy

Enrique Romero · Paul H. Simms

Originally published in the journal *Geotechnical and Geological Engineering*, Volume 26, No. 6, 705–727.
DOI: 10.1007/s10706-008-9204-5

Abstract With the advent of modern microstructural testing techniques and microstructure based constitutive models the microstructural characterisation of soils is gaining prominence. This paper reviews the history of microstructure investigation in unsaturated soils and discusses the engineering significance of this research to date. After a brief overview of the main microstructural techniques, the paper focuses on the evaluation of the current state of use and the development of two widely used techniques to study the microstructure of partially saturated soils, namely mercury intrusion porosimetry and the environmental scanning electron microscopy. The details of these techniques, their advantages and limitations, are first covered, followed by the presentation of selected test results. These results highlight the use of these techniques for understanding different hydro-mechanical behavioural features observed at macroscopic scale. Specifically, the paper shows the use of these techniques to explore the fundamental properties of water retention characteristics, water permeability, and micro and macrostructural interactions along different hydro-mechanical paths.

E. Romero (✉)
Department of Geotechnical Engineering and Geosciences, Universitat Politècnica de Catalunya, c/ Jordi Girona, 1-3, Campus Nord, módulo D2, 08034 Barcelona, Spain
e-mail: Enrique.romero-morales@upc.edu

P. H. Simms
Department of Civil and Environmental Engineering, Carleton University, Ottawa, Canada
e-mail: Paul_simms@carleton.ca

Keywords Microstructure · Mercury intrusion porosimetry · Pore size distribution · Environmental scanning electron microscopy · Unsaturated soil · Suction

1 Introduction

Micro and mesostructural studies are increasingly used to improve understanding of the macroscopic behaviour and physical properties of compacted and natural soils. Microstructural studies involve the use of techniques at particle/aggregation scale (<100 μm) to analyse the arrangement and distribution of particles, particle assemblies and pores—and their contacts and connectivity—in different soils (Collins and McGowan 1974; Delage and Lefebvre 1984; Delage et al. 1996, Al-Rawas and McGown 1999; Mitchell and Soga 2005). Mesostructural scanning techniques using time-domain reflectometry, near-infrared spectroscopic measurements, electric impedance tomography, neutron tomography, X-ray computed tomography, dual-energy gamma-ray technique, and so on, go a step forward in the analysed scale (Baker and Allmaras 1990; Fukue et al. 1999; Borsic et al. 2005; Desrues et al. 2006). However, much more powerful X-rays provided by synchrotron radiation and microfocus X-ray systems have recently allowed moving a step forward in the analysed domain and going to micrometric scale, narrowing the gap between meso and microstructural techniques (Bésuelle et al. 2006, Takahashi et al. 2006). Recent applications of these mesostructural techniques in unsaturated soils have been devoted to the monitoring of hydro-chemo-mechanical processes (Comina et al. 2008), to the detection of desiccation cracks (Gebrenegus et al. 2006; Mukunoki et al. 2006), to the visualisation of diffusion/hydration phenomena and to the study of fluid movements (Rolland et al. 2003; Rolland et al. 2005; Van Geet et al. 2005; Rodríguez-Rey et al. 2006; Carminati et al. 2006; Koliji et al. 2006a).

Since the pioneering works of Barden (1973), Barden et al. (1973), Collins et al. (1973), Tovey (1973), Tovey et al. (1973), Collins and McGown (1974), McGown and Collins (1975), Grabowska-Olszewska (1975) and Osipov and Sokolov (1978a, c) on the microstructure of natural collapsible and expansive soils, the increasing use of microstructural studies have led to improved techniques and their interpretations. In unsaturated soils, microscopic examination of the soil structure have traditionally concentrated on compacted soils, focusing on the aggregation or matrix structure of different states in the dynamic compaction curve, as well as on their relationship with main properties related to engineering behaviour, such as strength, compressibility and water permeability (Barden and Sides 1970; Ahmed et al. 1974; Osipov and Sokolov 1978b; Garcia-Bengochea et al. 1979; Prapaharan et al. 1985, 1991; Tessier et al. 1992; Delage et al. 1996; Delage and Graham 1996). These studies have illustrated that the microstructure of a given compacted soil is not unique, and strongly depends on the paths followed to reach a given point in the compaction plot. Attention have been also devoted to the microstructure of natural swelling clays (Tovey et al. 1973; Al-Rawas and McGown 1999), a topic that has recently gained increasing consideration within the context of clay-based engineering barriers for radioactive waste disposal (Wan et al. 1995; Al-Mukhtar et al. 1996; Saiyouri et al. 1998; Romero et al. 1999; Pusch et al. 1999; Saiyouri et al. 2000; Cui et al. 2002; Pusch and Yong 2003; Lloret et al. 2004; Saiyouri et al. 2004; Cuisinier and Masrouri 2005; Delage 2006, 2007; Delage and Cui 2007).

Understanding soil mechanics at the microscopic level is particularly pertinent to unsaturated soils—specifically clay-based materials, whose behaviour is complicated by the presence of both air and water in the pore-space. From a fundamental point of view, measurements and observations at the microstructural level involving clay units and their aggregations are very important, since they help in further understanding of higher structural levels, their interactions, the stability of the arrangements and their consequences for material properties and behaviour under various hydro-mechanical stress state conditions. In addition, these techniques can be used to monitor the changes undergone by unsaturated materials at aggregate and aggregate assembly scales, when subjected to complex hydro-mechanical paths. In this way, the methods are helpful in relating microstructure to macroscopic behaviour, for example in building up multi-structure constitutive models with coupling functions between the different structural levels (e.g., Alonso et al. 1999; Loret and Khalili 2000; Alonso et al. 2005; Sánchez et al. 2005).

The paper starts with a review of the literature that explores the relationship of soil microstructure to engineering properties, followed by sections describing techniques specifically aimed at characterising the microstructure of unsaturated soils. Among the various available techniques used to study unsaturated soil microstructure, mercury intrusion porosimetry (MIP) and environmental scanning electron microscopy (ESEM) are given special attention in the report: the former technique has been very frequently used while the latter is an emerging technique with great potential due to minimal sample preparation requirements. As well as detailed technical descriptions and discussion of advantages and limitations of each method, the body of research performed using each technique is reviewed and discussed. The paper concludes with a discussion of future research directions.

It is a difficult task to make a representative selection of the techniques, their use and interpretation, since it is an experimental subject of interest for geologists, soil scientists and geotechnical engineers. In fact, much of the previous work on the microstructure of fine-grained soils was initiated by soil scientists and developed by engineering geologists within the framework of highly sensitive post-glacial clays and soft soils (Gillott 1970, 1979; Pusch 1970; Delage and Lefebvre 1984; Bennet et al. 1991). The reader may observe that despite the representative selection of contributions there will be some tendency towards the works performed by the respective research groups of the authors. The authors hope that this scientific bias of the review will be compensated by a more in-depth knowledge of the main methods presented and their relation with macroscopic behavioural features.

2 Some Examples of the Relationship between Microstructure and Engineering Properties

Many macroscopic soil properties are often explained in terms of microstructural behaviour—distribution and connectivity of pores; particle size, shape and distribution, along with the arrangement of grains and grain contacts, in addition to volumetric and gravimetric state variables—void ratio, water content, degree of saturation—and the stress history—both mechanical and hydraulic—undergone by the material. A classic example is the variation in permeability of a soil at different compaction water contents; a soil compacted wet of optimum will exhibit lower permeability than the same soil compacted to the same porosity at dry of optimum. The difference was initially attributed to a change from a flocculated to a dispersed arrangement of clay particles (Lambe 1958), though more recent studies (Garcia-Bengochea et al. 1979; Delage et al. 1996) have explained the change in permeability in terms of the quantity of clay aggregates brought about by compaction at different levels of water content. Imaging of clay microstructure has also been used to explain the inapplicability of unique correlations between macroscopic parameters and hydraulic conductivity, compressibility, and shrinkage/swelling behaviour (Djeran-Maigre et al. 1998; Hetzel et al. 1994; Ben Rhaim et al. 1998; Pusch and Schomburg 1999). These studies illustrated the importance of the size, shape and arrangement of clay aggregations, as well as the distribution and connectivity of pores, on soil behaviour, and how such aggregations and pores can change during wetting/drying cycles, separating or combining depending on a number of factors, including type of clay mineral and the rate of drying or wetting. In general, the type and quantity of clay minerals in soils, as well as the interactions with the pore water in a soil have long been shown to strongly affect strength, permeability and compressibility (Marshall 1958).

A common technique to obtain a quantitative representation of the microstructure of materials with interconnected porosity is mercury intrusion porosimetry, from which it is possible to infer a pore-size distribution (PSD). The PSD is an essential fabric element that has been used in geotechnical engineering applications and correlated with macroscopic properties, such as its dependency on the type of compaction for clays (Ahmed et al. 1974; Kong et al. 2005); the differences between laboratory and field-compacted soils for equivalent dry density and moulding water content (Prapaharan et al. 1991; Jommi and Sciotti 2003); the saturated water permeability (Garcia-Bengochea et al. 1979; Juang and Holtz 1986a, b; Lapierre et al. 1990); frost-heave properties (Reed et al. 1979); and qualitatively with macroscopic volume changes—consolidation—(Delage and Lefebvre 1984; Griffiths and Joshi 1989; Coulon and Bruand 1989; Tessier et al. 1992; Qi et al. 1996). Regarding unsaturated soils, MIP results have been used to predict the water retention properties (Prapaharan et al. 1985; Romero et al. 1999; Aung et al. 2001; Simms and Yanful 2002, 2005); as well as macroscopic volume changes due to the effects of mechanical and hydraulic paths (Al-Mukhtar 1995; Al-Mukhtar et al. 1996; Qi et al. 1996, Cui et al. 2002; Simms and Yanful 2004; Cuisinier and Laloui 2004; Lloret et al. 2004; Romero et al. 2005; Koliji et al. 2006b; Hoffmann et al. 2007). Observed correlations between the water retention, volume change, and water permeability in unsaturated soils with the PSD as measured by MIP are presented in this report.

Understanding microstructural behaviour in unsaturated soils has particular relevance to geotechnical applications in which soils undergo water content and volume changes. For instance, in containment structures for domestic, mine, and nuclear waste, fine-grained soils are used as barriers to minimise the escape of contaminants by advection and diffusion. The performance of these barrier soils depends on maintaining a low hydraulic conductivity and a relatively high degree of saturation (to restrict gas transport). These barriers may undergo wetting/drying cycles due to environmental conditions or by heat generation in the waste facilities, which occur from both domestic and nuclear waste. The integrity of the barrier soils thus depends on its unsaturated properties (water and gas permeability), and its propensity for irreversible volume changes and associated cracking. Most of these properties are affected by microstructural changes.

These barrier soils are expected to perform in perpetuity or until some distant point in the future. Therefore it is important to understand their fundamental behaviour in order to make any sort of compelling assessment of their performance. Their resistance to wet/dry cycles is often evaluated using unsaturated flow models that solve the mass balance equations of water (liquid or evaporated in the gas phase) and air (dry air as gas or dissolved in the liquid phase), coupled with internal energy balance for the medium (Wilson et al. 1994; Olivella et al. 1994), which require the water retention curve and the unsaturated hydraulic conductivity function. As discussed below, these two parameters are dependent on the PSD, which as shown by Simms and Yanful (2002) in Fig. 1 and others, is affected by suction, and also by the number of weathering cycles. The PSD may also be affected by time-dependent processes such as creep and chemical reactions such as oxidation (Zhang et al. 2005) and precipitation or dissolution of solid phases. Biological processes may also affect the PSD through clogging.

As an example, consider the role of the hydraulic conductivity function in the performance of a barrier soil. This function is usually difficult to measure directly. It is commonly estimated from the drying branch of the water retention curve under unstressed conditions by the so-called statistical methods (Leong and Rahardjo 1997), most of which assume that the PSD is constant. This assumption can often lead to under-prediction of the hydraulic conductivity function for barrier soils, which may in turn lead to unconservative design (Simms 2004). The problem is that the unsaturated hydraulic conductivity of compacted soils is a function of a number of factors and state variables, and several of them (PSD, degree of saturation and void ratio) are affected by hydraulic paths (i.e., suction). To estimate the hydraulic conductivity on a pore by pore basis through microstructural models is a potential route, which requires the quantitative evaluation of soil microstructure.

3 Methods for Microstructural Characterisation of Unsaturated Soils

Several common methods used to study the microstructural features of unsaturated soils are listed in Table 1. A difference between saturated and unsaturated soils is that microstructural studies on the former soils have been mainly focused on the solid phase characterization—arrangement, distribution and contacts of particles and particle groups. Micromechanics theories and homogenisation techniques have been developed aimed at relating this solid phase microstructure to the macroscopic behaviour (Mitchell and Soga 2005). On the other hand, in unsaturated soils emphasis have been usually placed on the pore fluids—liquid and gas, which are mainly associated with the arrangement, distribution and connectivity of

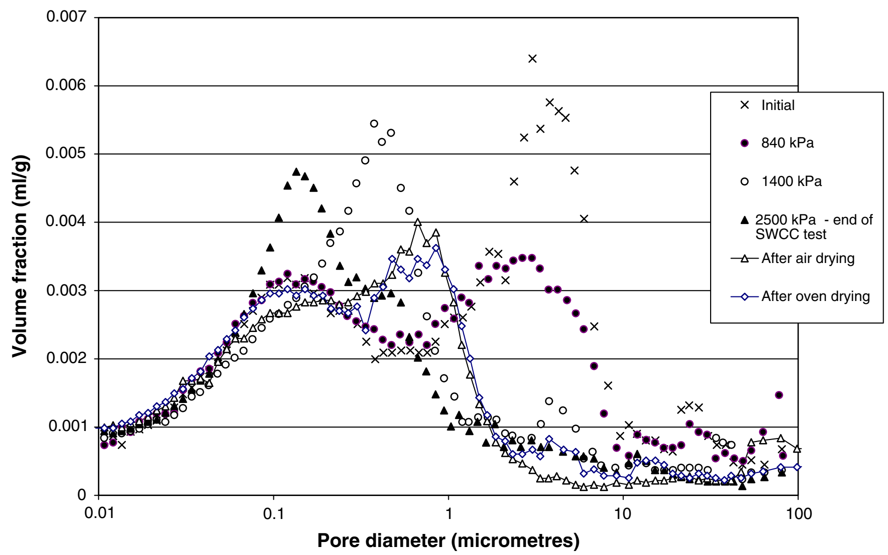

Fig. 1 Evolution of pore-size distribution during a water retention curve test and after air and oven drying for a glacial till, PI = 10% (Simms and Yanful 2002)

Table 1 Methods for microstructural studies in partially saturated soils

Microstructural method	Physical property at microstructural scale (scale of observation)	Macroscopic behaviour	Selected references
N_2 adsorption/desorption isotherms (N_2–BJH, N_2–BET) Methylene blue adsorption Keeling hygroscopicity	Quantitative technique Characterisation of voids Pore size distribution (0.3–300 nm) Characterisation of solid phase Specific surface (external/total)	Pore size distribution changes due to chemo-hydraulic paths Water retention properties in the high suction range	Webb and Orr (1997) Santamarina et al. (2002) Chiappone et al. (2004) Fernández and Rivas (2005)
Mercury intrusion porosimetry	Quantitative technique Characterisation of voids Pore size distribution (7 nm–400 µm) Characterisation of solid phase Specific surface (external)	Pore size distribution changes due to hydro-mechanical paths Water retention properties in the low suction range Unsaturated water permeability	Romero et al. (1999) Aung et al. (2001) Simms and Yanful (2001, 2002, 2004) Cuisinier and Laloui (2004) Romero et al. (2005) Kong et al. (2005) Delage (2006, 2007) Delage and Cui (2007)
Electron microscope Environmental ESEM Scanning SEM Field emission FESEM Transmission TEM Optical microscope Laser scanning microscope	Qualitative technique (quantitative with digital image analysis) Discern structural levels Liquid/solid interactions (ESEM)	Porosity changes due to hydro-mechanical paths Tests performed at different hydraulic conditions	Tovey and Krinsley (1975) Al-Rawas and McGown (1999) Pusch (1999) Romero (1999) Villar and Lloret (2001) Cui et al. (2002) Montes-H (2002) Montes-H et al. (2003a,b) Montes-H et al. (2004) Komine and Ogata (1996, 1999, 2004) Lloret et al. (2004) Suzuki et al. (2005) Viola et al. (2005) Zhang et al. (2005) Cuisinier and Masrouri (2005)

pores. Pores determine the liquid and gas permeability properties, as well as the water retention and chemical transport properties.

Based on the preceding discussion, the authors propose that the different methods for the microstructural characterisation of unsaturated soils should be adapted to the following requirements:

- The methods should help in the understanding of macroscopic behavioural features—for example, water retention, water/air permeability, volume change behaviour, by guiding in the setting out of hypotheses and building up constitutive models for micro and macrostructural interactions.
- The methods should help to qualitatively or quantitatively relate microstructural observations or measurements to macroscopic properties—for example, water retention, water/air permeability, volume change behaviour.
- The methods should help in the interpretation of experimental procedures, which involve tests at a non-measurable scale.
- The methods should help in the detection of non-uniformity patterns and monitoring of local

hydraulic, mechanical and chemical phenomena (tomography).

4 Mercury Intrusion Porosimetry (MIP)

4.1 Background, Advantages and Limitations. Sample Treatment

In the MIP technique an absolute pressure p is applied to a non-wetting liquid (mercury) in order to enter the empty pores. The following Washburn equation applies (Diamond 1970; Juang and Holtz 1986b; Webb and Orr 1997) for pores of cylindrical shape and parallel infinite plates (fissure-like microstructure)

$$p = -\frac{n\,\sigma_{Hg}\cos\theta_{nw}}{x} \qquad (1)$$

where σ_{Hg} is the surface tension of mercury ($\sigma_{Hg} = 0.484$ N/m at 25°C), θ_{nw} the contact angle between mercury and the pore wall, and x the entrance or throat pore diameter ($n = 4$) or the entrance width between parallel plates ($n = 2$). The value $n = 4$ is often used in MIP. The contact angle, which is very sensitive to surface roughness, is usually taken between 139° and 147° for clay minerals (Diamond 1970), although Penumadu and Dean (2000) have reported higher values with kaolin clay using the sessile drop technique (advancing angle of 162° and receding angle 158°).

MIP implicitly assumes a constant contact angle at equilibrium, whatever the penetration flow conditions are, and does not check the applicability of Equation (1), which is an equation for equilibrium state with null penetration velocity of mercury. In fact, the contact angle varies as a function of the flow dynamic conditions—penetration velocity—of the advancing interface, as shown experimentally by Hoffman (1975). Aït-Mokhtar et al. (2004) have studied the validity range of the constancy hypothesis of the contact angle of a non-wetting liquid during its penetration in a capillary. They showed, based on theoretical considerations using Poiseuille flow velocity, that for a given value of pressure, the contact angle between the mercury and the capillary wall starts to change significantly only from a 'critical' value of capillary radius. For this reason, sufficient time must be let in the pressure rising to allow for the quasi-static state condition to be reached.

The main limitations of MIP are: (a) isolated pores enclosed by surrounding solids are not measured—this enclosed porosity is not significant in soils; (b) pores that are accessible only through smaller ones (constricted porosity) are not detected until the smaller pores are penetrated; (c) the apparatus may not have the capacity to enter the smallest pores of the sample (non-intruded porosity); and (d) the minimum practical pressure of the apparatus limits the maximum pore size to be detected (non-detected porosity). In this way, when the clay sample is intruded by mercury, the intruded void ratio estimated under the maximum applied pressure does not coincide with the estimated void ratio of the sample. Differences mainly arise due to the non-intruded porosity with entrance pore sizes lower than 10 nm and the non-detectable porosity for pore sizes larger than 400 µm. In addition, an intrusion (pressure increase) and extrusion (pressure decrease) cycle does not close when the initial pressure is restored, indicating that some mercury has been permanently entrapped in the constricted porosity. A second intrusion will follow approximately the same extrusion path, thus defining the non-constricted or free porosity. Delage and Lefebvre (1984) assumed that the small intra-aggregate pores display a non-constricted or free porosity, while the inter-aggregate pore space corresponds to the entrapped porosity. Various theories concerning the cause of MIP hysteresis and entrapment—dead-end or ink-bottle shaped pores, throat chains, contact angle hysteresis, mercury snap-off, sample size phenomena—have been discussed and examined in detail by Matthews et al. (1995), Abell et al. (1999), and Moro and Böhni (2002). Another concern refers to the alteration in the pore geometry during pressure application. It has been reported that the soil structure is not affected during the high-pressure intrusion (Sills et al. 1973; Lawrence 1978; Reed et al. 1979), due to the fact that the pore system is mostly filled with incompressible mercury. However, this cannot be the case during low-pressure application and before the initial intrusion takes place in compressible materials. The occurrence of substantive initial volume change due to isotropic compression in clayey samples prior to intrusion was reported by Penumadu and Dean (2000), though for some initially compacted clays the volume change indicated by porosimetry is a good estimate of the macroscopic volume change

(Simms and Yanful 2004). Yet another consideration is the deformation of the sample container, which may cause an overestimate of the pore volume of the smaller pores—this deformation can be measured by running blank samples in the porosimeter (for a recent example on the degree of error that can result see Simms and Yanful 2004).

Mercury intrusion is used to find the pore-size distribution, relating the volume of intruded pores to the pressure required for intrusion. A typical graph of the MIP technique includes the log differential intrusion curve *vs.* entrance or throat pore size (pore size density function or frequency distribution, PSD), which aids the visual detection of the dominant pore modes. As previously discussed, such a PSD is not necessarily the true distribution of pores, due to various issues including pore accessibility and sample treatment, yet it gives a useful quantitative characterisation of microstructure.

Sample treatment for MIP requires the removal of water that occupies small pores and prevents the entry of mercury. Samples can be dehydrated using air-drying, oven-drying, freeze-drying or critical-point-drying techniques (Delage and Pellerin 1984 provided a good comparative discussion of these techniques). However, if the sample is heat and dry sensitive, then freeze drying is preferred, specially at high water contents (Ahmed et al. 1974). Freeze drying processes manipulate temperature and pressure conditions to eliminate the surface tension forces caused by air-water interfaces, and thus it is assumed that no shrinkage occurs on drying which could alter soil structure. Prior to freeze drying, soil samples must be cut into cubes less than 1 cm^3 in size to maximize heat transfer. Detailed accounts of freeze-drying techniques have been given by Ahmed et al. (1974), Delage et al. (1982), Delage and Pellerin (1984), Delage et al. (1996), Penumadu and Dean (2000), Mitchell and Soga (2005), and others.

4.2 Fractal Analysis of MIP Data

A further insight into the pore structure may be provided by the interpretation of MIP data in terms of the fractal character of the porous medium, admitting self-similarity or dilation invariance of the hierarchical void structure. Fractal dimension studies allow validating porosimetry results, since they are a powerful tool to detect anomalies of the pore network, such as the destruction of the natural structure due to sample preparation techniques. For the calculation of the surface fractal dimension D_s, the following expression, written as a function of the mercury pressure p, has been usually used (Korvin 1992; Meyer et al. 1994; Fadeev et al. 1996) (V is the intruded pore volume)

$$\log\left(\frac{\mathrm{d}V}{\mathrm{d}p}\right) \propto (D_s - 4)\log p \tag{2}$$

The intervals of self-similarity of the different pore types can be experimentally obtained from the linear sections of the log-log plot of $\mathrm{d}(V/V_{max})/\mathrm{d}p$ versus the intrusion pressure p, the slope of which yield the values of D_s, as shown in Fig. 2. In this figure, one pressure zone is identified in the high-density structure with a characteristic fractal dimension of $D_s = 3.09$, which reflects a more space-filling volumetric pore structure. On the other hand, two pressure regimes can be identified in the low-density structure: a low-pressure regime (1 MPa $< p <$ 5 MPa) for pore sizes between 300 nm and 1.5 μm exhibiting a fractal dimension of $D_s = 1.88$, which corresponds to a fissure-like structure, and a high-pressure regime ($p > 5$ MPa) for pore sizes less than 300 nm presenting a volumetric structure ($D_s = 3.04$). It is expected that with increasing aggregate angularity and roughness, the fractal surface becomes more space-filling tending to higher fractal dimensions (volumetric structure). Fractal concepts related to porosimetry studies have been used by Fadeev et al. (1996), De las Cuevas (1997), Giménez et al. (1997), Romero (1999), Jommi and Sciotti (2003) and Airò Farulla and Jommi (2005) as a complementary tool to detect microstructural changes and differences in pore geometry at various structural levels.

4.3 MIP—Water Retention Curve Relationships

MIP has been used to attempt quantitative derivation of the matric suction—saturation or water content relationships. The mercury intrusion process is similar to air-intrusion during the desorption path of the water retention curve. Thus, the injection of non-wetting mercury is equivalent to the ejection of water by the non-wetting front advance of air for the same diameter of pores being intruded. Therefore, the volume of pores not intruded by mercury—assuming a non-deformable soil—should be used to evaluate the water content or degree of saturation corresponding to the

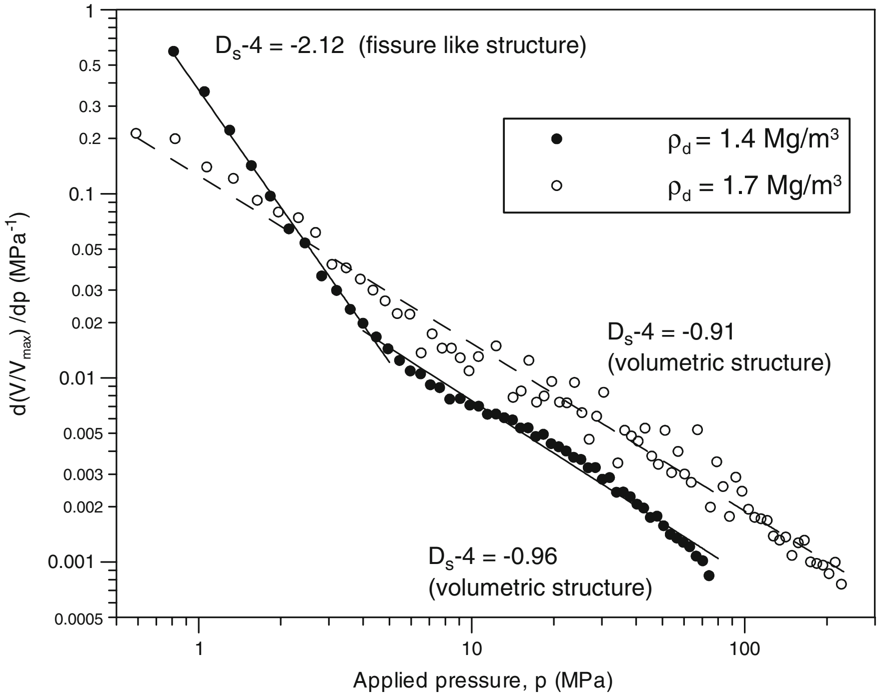

Fig. 2 Fractal description of the pore network for two dry densities of a kaolinitic-illitic clay (Romero 1999)

equivalent applied matric suction. However, a residual water content corresponding to the non-intruded porosity, which can be assumed saturated, should be taken into account before estimating the water content (Romero et al. 1999). In most soils, water is generally held due to capillarity at low suctions (usually <2 MPa), and by adsorption on particle surfaces and in clay inter-layers at higher suctions (Cases et al. 1992; Romero et al. 1999). The derivation of the matric suction—saturation relationship should be limited to the low-suction range, in which capillarity dominates the water retention properties.

Neither the cumulative PSD derived from the water retention curve or the PSD obtained by MIP is the true PSD, since it ignores the relative accessibility of pores to the intruding non-wetting phase, air or mercury. But one may assume that as both mercury and air are non-wetting fluids, there intrusion pathways would be the same, and therefore for an identical soil sample they should generate the same apparent PSD, and that therefore the cumulative PSD obtained from MIP would still give the water retention curve. However, predictions of the water retention curve from the PSD have not always been so straightforward. Prapaharan et al. (1985) significantly underestimated the measured water contents for suctions greater than 10 kPa. Romero et al. (1999) similarly compared predictions of the water retention curve with measurements on a moderately plastic clay, and found that the MIP predictions substantially underestimated water contents at suctions greater than 40 kPa.

The reasons for the discrepancies can be attributed to at least two important processes.

- In deformable soils the PSD changes during the hydraulic path.
- The accessibility of pores in a small MIP samples may be different than in a large sample on which the water retention curve is determined. Isolation of the wetting phase by the non-wetting phase may occur in water retention curve determinations.

Simms and Yanful (2001, 2002) measured the PSD at different suctions during water retention curve tests on clayey soils compacted dry and wet of optimum and subsequently saturated. They found that the PSD indeed changed significantly, not only in the total volume of pores but also in the distribution (Fig. 1). Therefore, any method to predict the water retention curve from the PSD for deformable soils must take into account the evolution of the PSD with suction. Simms and Yanful (2005) suggested one method, whereby volume change and desaturation are calculated on a pore by pore basis in a numerical pore-network model.

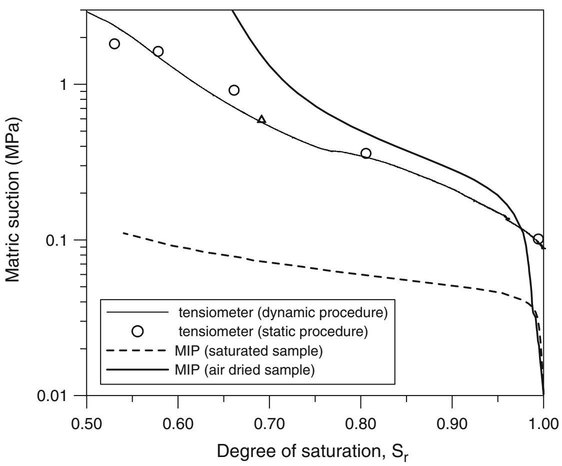

Fig. 3 Water retention results on drying of a clayey silt obtained from high-range tensiometer readings, which are compared to deduced data from MIP using freeze-dried samples (Boso and Romero, Personal communication)

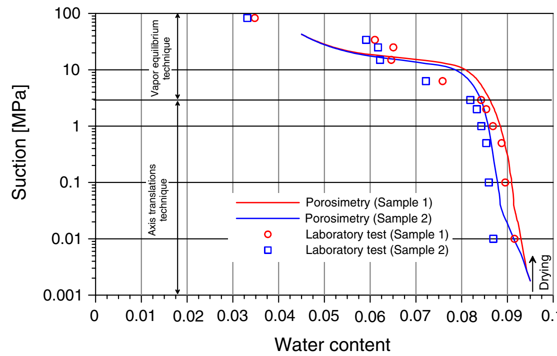

Fig. 4 Water retention results on drying obtained on Opalinus clay, a kaolinite-illite argillaceous rock: deduced data from MIP results compared to axis translation and vapour equilibrium readings (Muñoz 2007)

More simply, the air-entry value can be deduced from the PSD measured on a soil sample obtained at the end of the water retention curve test, after volume change has ceased. Figure 3 presents water retention results on drying of a clayey silt obtained from high-range tensiometer readings, which are compared to deduced data from MIP using freeze-dried samples. 'Dynamic' and 'static' procedures starting from saturated conditions and under unstressed conditions refer to the measurement of matric suction using tensiometers during a continuous drying process and under constant water content, respectively. This figure shows a good agreement in the determination of the air entry value using MIP, when the sample has been previously air-dried to a suction of 0.5 MPa (higher than the air entry value obtained with the continuous drying process). In this case, the denser state reached on pre-drying is associated with a higher air-entry value, which matches the tensiometer results with a distribution of pores that evolve with suction. On the contrary, deduced water retention results from MIP starting from saturated conditions, reflect a lower air entry value, which is in agreement with the higher porosity of the saturated state.

MIP results have been successfully used to determine water retention properties of soft rocks, which do not undergo important volume changes on drying. Figure 4 shows deduced data from MIP results compared to axis translation and vapour equilibrium readings performed on Opalinus clay, a kaolinite-illite argillaceous rock. A good agreement is observed between the different methods.

4.4 MIP—Water Permeability Relationships

Due to difficulty of measurement, the unsaturated water permeability function is often determined indirectly from the measured water retention curve. As described earlier, the so-called statistical methods posit certain assumptions about pore-geometry in their derivations. Most assume the pore-size distribution does not change during drying, which is not the case for fine-grained soils (Simms and Yanful 2002). Most methods also hypothesize that the water-retention curve can be simply related to the pore-size distribution, ignoring pore interconnectivity. They also assume certain simplifications of pore geometry to facilitate prediction of the unsaturated permeability. For example, the Marshall (1958) method represents pore geometry as two adjoining cross-sections filled with randomly distributed pores, and that the flow could be represented as perpendicular to the cross-section passing through linked pairs of pores. This derivation also forms the theoretical basis for the very commonly used Mualem-van Genutchen model (van Genutchen 1980). Leong and Rahardjo (1997) give a comprehensive review of the statistical methods.

Though the statistical methods work quite well for coarse-grained soils, they do not work as well for clayey soils. Permeability in clayey soils is a function of many parameters such as the size of the pores that change with the hydraulic history, the shape of the channels, the tortuosity, the clay mineralogy, physico-chemical interactions between clay particles and the pore water, and the direction of flow. As the methods calculate the unsaturated water permeability assuming an unchanging pore-size distribution, they are not appropriate for soils that undergo substantial volume changes. These functions will tend to underpredict the water permeability for deformable soils at a given suction. Predictive equations should allow for demonstration of the dependence of permeability on PSD and reflect the changes in soil microstructure caused by different stress and hydraulic histories.

Romero et al. (1999) determined the relative permeability for different measured pore sizes, which is shown in Fig. 5a (x_i is the maximum pore diameter that is considered). In this case, PSD data were obtained for a kaolinitic-illitic clay, which was compacted at two different dry densities (1.4 and 1.7 Mg/m^3). Cross-sections with identical PSD functions were considered to be connected in a correlated way. As observed in the figure, water permeability is mainly related to the distribution of the larger pore sizes (i.e. >1 μm). Pores of sizes less than this threshold diameter are considered negligible in the calculation of permeability. A conclusion that arises from the previous plot is that the permeability is very sensitive to the magnitude and frequency of the large pore mode, and that any factor that varies this part of the distribution, such as a compression or a hydraulic path, can be reflected in an appreciable change of the permeability. Figure 5b complements the information by showing relative permeability values for the two dry densities as a function of the effective degree of saturation, both evaluated from MIP data. As observed in the figure, inflow/outflow results using controlled-suction techniques and interpreted with a diffusion equation compare relatively well to relative permeability data calculated by integration over the contribution of correlated filled pores.

Simms and Yanful (2005) attempted to predict the unsaturated water permeability for a clayey soil with a significantly changing pore size distribution. They used a network model, where the nodes in the network purported to represent individual pores in a representative volume of soil. Water permeability in large networks has been shown to vary according to the following power law, for values of N_c near the percolation threshold (Berkowitz and Ewing 1998)

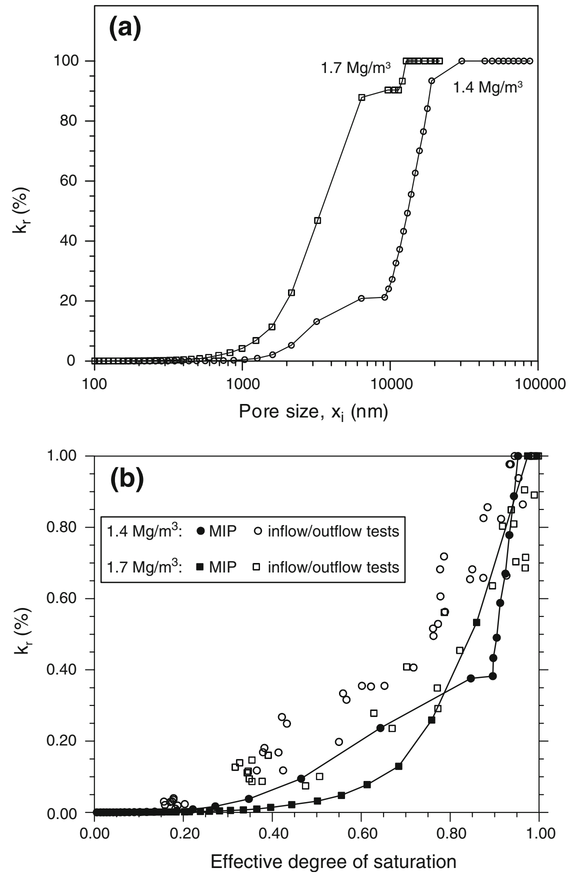

Fig. 5 Relative permeability evaluated from MIP data. Kaolinitic-illitic clay at different dry densities. (**a**) As a function of different pore sizes and (**b**) for different effective degrees of saturation (Romero et al. 1999)

$$k_w \propto \left(N_{pc} - N_p\right)^{\lambda} \tag{3}$$

in the case of unsaturated soils, N_p would represent the number of pores occupied by a the phase being modelled, either air or water, N_{pc} is the number of occupied pores at the percolation threshold, and λ is an exponent dependent on the structure of the lattice.

Water permeability across the network may be determined by applying analogies to Kirchoffs laws for electric circuits. For pores in series, the global hydraulic conductivity is the average of conductivities of pores still forming connected paths. For pores in parallel, k_w is the inverse of the sum of the inverted local conductivities. For a two dimensional network, the global connectivity for the whole network, k_{wg}, may be calculated

$$k_{wg} = \frac{1}{\sum_{1}^{n_c} \frac{1}{k_{wl}}} \tag{4}$$

in which k_{wl} is the average water permeability of a column in the grid, perpendicular to the direction of flow, and n_c is the number of columns. The relative water permeability, k_r, may then be calculated by dividing k_{wg} at the current suction by the k_{wg} at saturation (Berkowitz and Ewing 1998).

To integrate the effect of variation in the pore-size distribution, the volume change was computed on a pore-by pore basis, where the stiffness of each pore was assumed to increase linearly as the pores decreased in size (Simms and Yanful 2005) The model marches forward in small increments of suction; after each increment, pores are checked to see if they will drain, using the Young-Laplace equation. Subsequently, only those pores that remain saturated undergo volume changes due to increases in suction. The initial size of each pore is generated using the PSD measured at null suction as the pore frequency distribution. A prediction of the unsaturated hydraulic conductivity of a clayey soil is shown in Fig. 6. The general validity of network models can be evaluated by comparing the predicted hydraulic conductivity of a coarse grained soil (no volume change) with that predicted by the van Genuchten-Mualem method, using the same pore-size distribution in both analyses—this comparison is shown in Fig. 7.

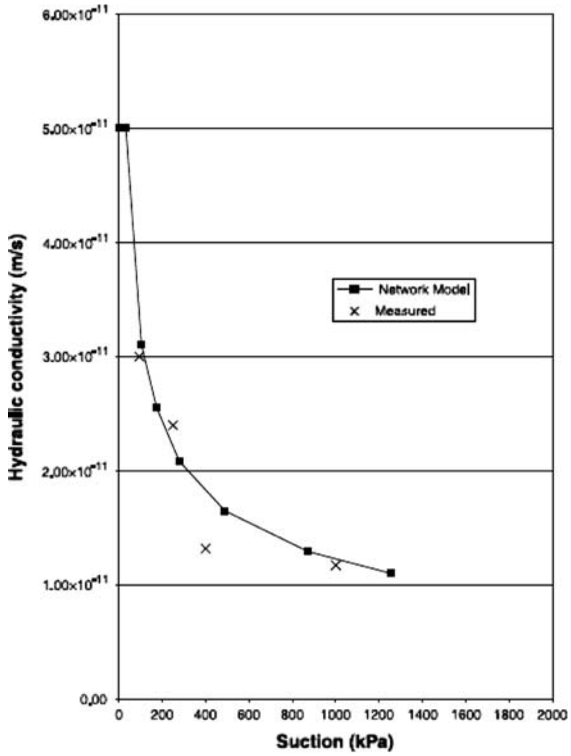

Fig. 6 Hydraulic conductivity predicted for a glacial till PI = 10% and air-entry value of 1000 kPa using a pore-network model (adapted from Simms and Yanful 2005)

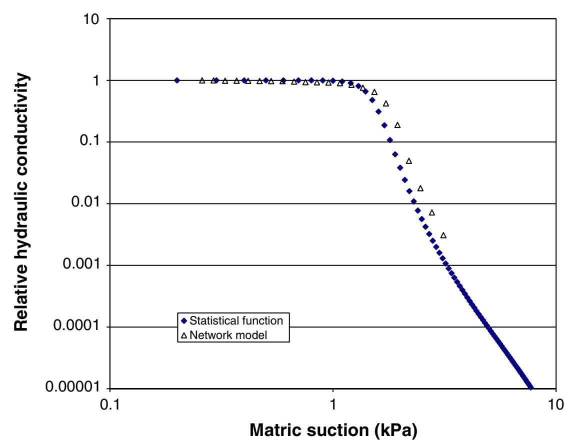

Fig. 7 Comparison of prediction of relative water permeability using a pore-network model and using Mualem's (1976) formula for a non-deformable soil, employing the same PSD

4.5 MIP for the Estimation of Macroscopic Volume Changes. Monitoring Changes along Hydro-Mechanical Paths

Different types of volume changes occur at different scales. For example, estimations of volume at the largest scale may be affected by the presence of cracks and other large scale features. Therefore, volume change measured on the microscopic scale is often only indirectly related to volume change at the macroscopic scale. However, there has been a strong correlation for some soils for a given range of suctions: Simms and Yanful (2004) found that for compacted clayey soils of low or moderate plasticity, the volume change on drying measured by calipers on 5 mm diameter and 5 mm thick samples, strongly correlated with the volume change in the pores in the range measurable by MIP (0.01–100 μm). For these soils, little or no cracking was observed at the macroscopic scale.

It has been suggested that the volume change measured by MIP may overestimate large scale volume change, if lacunar porosity develops. This type of porosity is formed by the shrinkage of finer grained particles away from a coarser-grained skeleton of particles (e.g., Fies and Bruand 1998; Viola et al. 2005). The volume contributing to lacunar porosity must come from inter-aggregate, inter-particle, or inter-layer void space, of which the first two are measured by MIP. Variations in inter-layer spacing only occur with significant variation in the relative humidity of soil pores, which occur for suctions greater than 3 MPa.

Despite these limitations, MIP measurements at the microstructural level are a helpful tool to understand material behaviour at macroscopic scale and to build up double-structure constitutive models with coupling functions relating micro and macro-structural behavioural features. In this way, MIP has been used to characterise the multiple-porosity network of different soils and to study their evolution along different mechanical and hydraulic stress paths. More recently, MIP has also been successfully used to detect PSD changes induced on low permeability soils when subjected to hydro-mechanical or heating pulse degradations. The evolution of PSDs on silty and clayey soils, as well as clayey rocks, during drying has been studied by Simms and Yanful (2002), Cuisinier and Laloui (2004), Kong et al. (2005),. (2006b), and Gasc-Barbier and Tessier (2007). Agus and Schanz (2005) also analysed the suction-induced changes in the PSD of heavily compacted bentonite-sand mixtures. Figure 1 shows the evolution during a drying path for a glacial till, in which suction increase leads to the destruction of a certain class of macropores. Figure 8 shows an equivalent plot when suction is increased from 0 to 400 kPa on a sandy loam. It is interesting to note that the reduction of certain class of macropores is accompanied by an increase in certain class of micropores, leading towards a bi-modal distribution. A model to account for this response on drying was proposed by Koliji et al. (2006b). Kong et al. (2005) also analysed the PSD evolution of a compacted clay at different stages of dehydration. These authors detected on drying some decrease of the pore volume contribution of the medium (0.1–10 μm) and small (0.05–0.1 μm) pore sizes, as well as some increase of the large pore volume (>10 μm), whereas no important changes

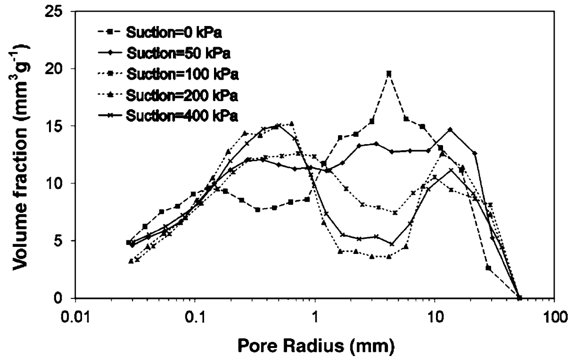

Fig. 8 Evolution of PSD functions when suction is increased from 0 to 400 kPa on a sandy loam (Cuisinier and Laloui 2004; Koliji et al. 2006b)

were observed in the micro pore volume contribution (<0.05 μm).

The influence of different mechanical (loading), hydraulic (wetting and drying) and chemical (pore water concentration changes) stress paths on the PSD of compacted FEBEX bentonite have been analysed by Musso et al. (2003), Romero et al. (2005), Hoffmann et al. (2007) and Lloret and Villar (2007). Figure 9 shows the evolution of the bi-modal PSD functions on loading under oedometer conditions and constant water content of 14% (maximum vertical stresses varied between 8 and 38 MPa to arrive to target dry densities 1.40–1.80 Mg/m^3). The smaller group of pores, which corresponds to the pores inside clay aggregations, remains essentially constant as the stress

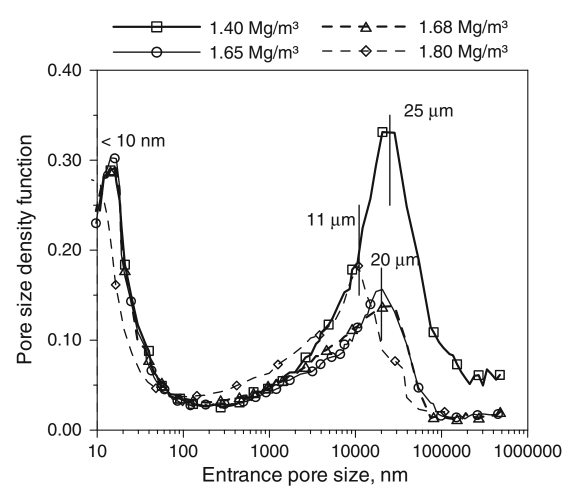

Fig. 9 Evolutionof PSD functions on loading. FEBEX bentonite at constant water content of 14% (Romero et al. 2005)

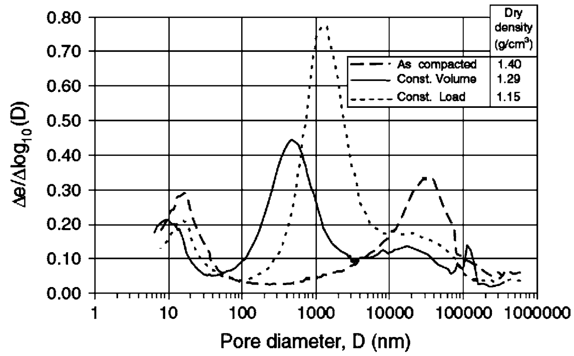

Fig. 10 Evolution of PSD functions on wetting at constant vertical stress and at constant volume. FEBEX bentonite at an initial dry density og 1.40 mg/m^3 (Lloret and Villar 2007)

increases. Changes in the void ratio result only in changes in the inter-aggregate porosity (macropores)—this has also been observed in compacted clayey soils by Delage et al. (1996). It is also evident in the figure that the size of inter-aggregate pores slightly decreases with increasing compaction effort. Figure 10 shows the evolution of the PSD functions when performing wetting paths on the same bentonite, along with the bi-modal PSD curve of the as-compacted state at an initial dry density of 1.40 mg/m^3. The series of hydraulic paths included single-stage wetting under constant volume and under a constant vertical stress of 2 MPa (the dry densities indicated in the figure are those just before the porosimetry determination). It can be observed that a new dominant mode emerges in the range between 350 and 1,100 nm, tending the microstructure to a one-mode distribution. This mode systematically reaches higher peaks on wetting under constant vertical stress, in which the swelling strains are higher than the small strains allowed under isochoric conditions. Simultaneously, and as a consequence of the constant volume condition and the high stresses applied during wetting, the inter-aggregate porosity is reduced, tending to its occlusion.

Figure 11a shows another PSD evolution plot when suction is decreased on a confined 70–30% Kunigel clay/Hostun sand mixture (Cui et al. 2002). This plot shows how the macroporosity is progressively filled by the expanding microstructure. Figure 11b complements the information of this process. Using a limit of pores of 0.2 μm, Cui et al. (2002) presented in the figure this progressive

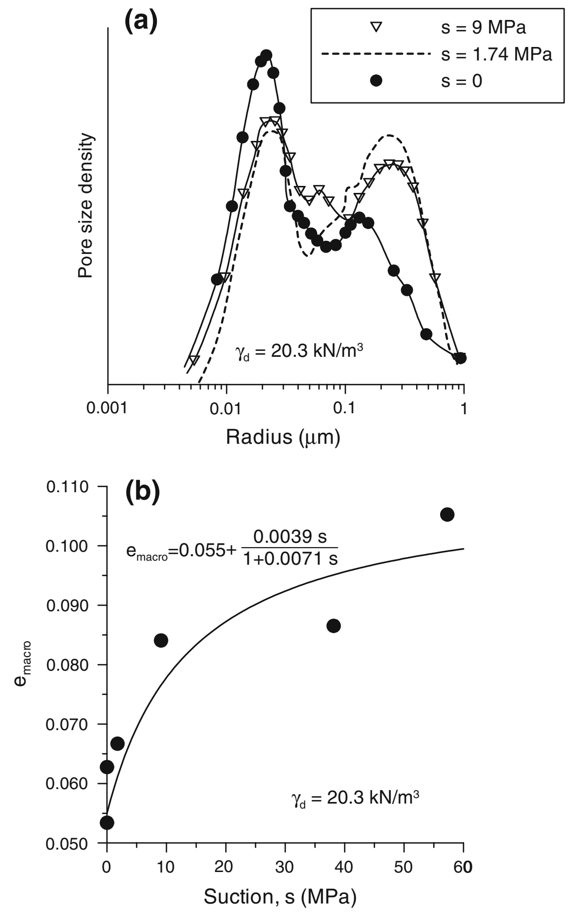

Fig. 11 (**a**) Evolution of PSD functions on wetting at constant volume. (**b**) Variation of the macroscopic void ratio as a function of suction. 70–30% Kunigel clay/Hostun sand (Cui et al. 2002)

clogging of the macroscopic void ratio e_{macro} as a function of suction. The decrease of e_{macro} with decreasing suction was not at the same rate for the different suction ranges analysed, and it was only in the low suction range (<10 MPa) where important microstructural changes were recorded. Recently, Thom et al. (2007) also followed the evolution of the PSD of unsaturated compacted kaolin on saturation, which resulted in aggregate expansion into the inter-aggregate void space.

The richness of the quantitative data now being obtained by researchers using MIP is such that microstructural models of hydro-mechanical coupling, such as those proposed by Koliji et al. (2006b) and Simms and Yanful (2005), now have a large data set for development and calibration.

5 Environmental Scanning Electron Microscopy (ESEM)

5.1 Background, Advantages and Limitations

One of the newer and most promising qualitative methods for studying and, where possible quantifying, the arrangements of aggregations/particles and voids in unsaturated soils is the environmental scanning electron microscopy (ESEM). ESEM is a special type of scanning electron microscope that works under controlled environmental conditions and requires no conductive coating on the specimen. This makes it possible to examine wet samples and to preserve their natural characteristics for further testing, which is an obvious advantage of ESEM compared to conventional SEM. A schematic cross section of the equipment is shown in Fig. 12. As observed in the figure, the sample chamber is at a higher pressure (absolute pressure up to 3 kPa) and separated from the increasing vacuum regions by the pressure-limiting apertures. It is expected that vacuum will not diffuse from one level to another through the small holes bored in the aperture discs, allowing maintaining a very good vacuum in the electron gun (10^{-5} Pa) as shown in the figure and a poor vacuum in the specimen chamber.

ESEMs are equipped with a gaseous secondary electron detector (GSED in Fig. 12) to produce surface images, which is based on the principle of gas ionisation and allows imaging of non-conductive

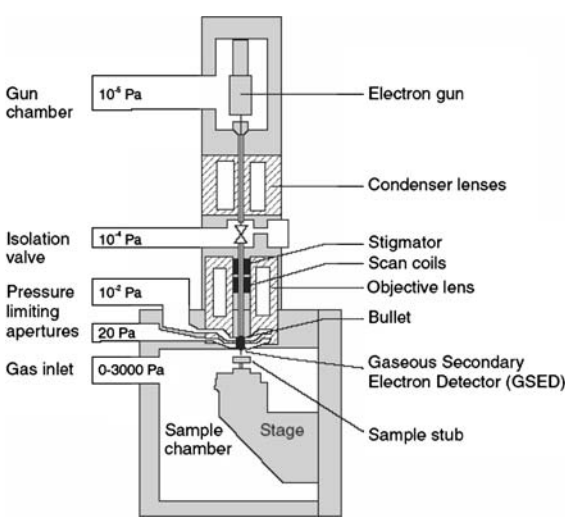

Fig. 12 Schematic cross section of an ESEM (Danilatos 1993)

samples. The energetic primary electron beam emitted from the electron gun penetrates the gas chamber with little apparent scatter and hits the specimen, scanning across the surface of the sample. This causes the specimen to emit secondary electrons, which are accelerated towards the positively charged GSED. As they travel through the gaseous environment, collisions occur between the secondary electrons and the gas particles that result in emission of additional secondary electrons that provide more signal and ionisation of the gas molecules (positive gaseous ions). The positively charged gas ions are attracted to the negatively charged sample—it has a negative charge from the primary electrons that have been bombarding it, suppressing the charging effects. This charge suppression allows imaging non-conductive samples without the need of conductive coating. The difference in signal intensity of secondary electrons emitted from different locations on the sample and collected at the positively charged GSED allows an image to be formed during a scan.

Water vapour is the most commonly used chamber gas, as it produces maximum signal amplification and a high charge neutralisation capacity. Vapour is introduced to the specimen chamber via a separate vacuum pump. A fully automatic electronic servo system is able to hold vapour pressure constant between 133 Pa and 2 kPa. The microscope is also equipped with a Peltier cooling/heating system installed underneath the sample stub (refer to Fig. 12) to control sample temperature. The Peltier heating/cooling stage allows working within 20°C above or below ambient temperature. This way, the examination of the sample can be continuously done under a H_2O environment at different vapour pressures and temperatures, and hence at different relative humidity and consequently different degrees of saturation, making it a suitable equipment to study the gradual effects of wetting and drying stages at microstructural scale. The equipment has also been used for the real-time characterisation of melting, corrosion, precipitation and crystallisation processes, as well as for carrying out mechanical tests. Further details of the equipment and applications can be found in Danilatos (1993), Thiel and Donald (1998), Jenkins and Donald (2000), Wei and Wang (2003), and Bogner et al. (2006).

A certain degree of resolution has been compromised when using this equipment, specially at elevated relative humidity of the sample chamber, and magnifications are usually maintained below $\times 5000$ to investigate specimens under controlled environmental conditions. This performance compares unfavourably with that from conventional scanning electron microscopes, in which much higher magnifications can be used without loosing resolution. When saturated samples are observed, the wet mode in ESEM only allows the observation of the surface, which is shown as if it were covered by a sheet, so that little information about the sample can be collected and makes image analysis difficult to carry out. In addition, freeze-dry fractured surfaces appear to give a clearer cut for image analysis compared to the plane obtained by breaking a humid sample. For these reasons, several authors still prefer to use optical microscope, laser scanning microscope and electron microscope observations, such as scanning SEM, transmission TEM and field emission SEM (FESEM), to analyse microstructural changes along different hydro-mechanical paths. For example, Al-Rawas and McGown (1999) and Katti and Shanmugasundaram (2001) used SEM micrographs to put forward methodologies to describe microfabric changes of expansive clays subjected to wetting. Katti and Shanmugasundaram (2001) observed an appreciable reduction in particle size on wetting—associated with the breakdown of clay agglomerates, which was detected by digital analysis of SEM images. Also using SEM, Cui et al. (2002) successfully detected microstructural changes –progressive expansion of aggregates clogging the macropores—undergone by 70–30% Kunigel clay/Hostun sand mixture on wetting under confined conditions. Cuisinier and Masrouri (2005) used thin sections of soil samples—prepared with special procedures to preserve their fabric—and an optical microscope to study fabric changes induced by the application of different suctions on a 40–60% silt/bentonite mixture. These authors observed how aggregates and macropores detected at high suctions disappeared at null suction, tending the clayey microstructure to an homogeneous fabric. Viola et al. (2005) used FESEM to observe at high magnification the microstructure of clay tactoids and their alignment at different hydration states. Suzuki et al. (2005) used a laser scanning microscope combined with digital image analysis to investigate the swelling at mesoscopic scale of bentonite aggregates exposed to various NaCl solutions.

5.2 ESEM Applications. Monitoring Microstructural Changes Along Hydraulic Paths

Early ESEM studies applied to geological materials were reported by Baker et al. (1995), Komine and Ogata (1996, 1999), Romero (1999), Watt et al. (2000), Buckman et al. (2000), Villar and Lloret (2001) and Montes-H (2002). Buckman et al. (2000) studied the wettability of fluids on soil minerals by condensing water droplets on samples surfaces that showed that the quartz surface was hydrophilic and the illite surface hydrophobic. Komine and Ogata (1999) and Villar and Lloret (2001) observed the swelling behavior of bentonite by ESEM. From their results, it was found that the macrovoids in the material were filled by swelling deformations of bentonite absorbing water. The hydration of clay aggregations under constant volume is shown in Fig. 13, in which the original space between aggregates (Fig. 13a) has been reduced due to the swelling of the bentonite particles. Figure 13b shows the final aspect of the same sample under nearly a relative humidity of 100%, in which a diminution of the size of some macrovoids can be observed despite the absence of confinement. These changes in the macropore network explain the large differences observed between the values of measured intrinsic permeability for dry and saturated states (Villar and Lloret 2001).

Montes-H (2002) and Montes-H et al. (2003a, b) used ESEM jointly with a digital image analysis program to estimate at aggregate scale the swelling–shrinkage behaviour of MX80 bentonite at different water potentials. More recently, Montes-H et al. (2004), Viola et al. (2005) and Agus and Schanz (2005) used the same technique to observe the changes and structural modifications undergone under different hydraulic conditions by an argillite, a clay-sand mixture and a 50/50 bentonite-sad mixture, respectively. Specifically, Fig. 14 shows the sequence of receding menisci and the evolution of inter-grain porosity during dehydration. Zhang et al. (2005) observed with ESEM the induced alteration to the microstructure of a dual porosity tropical soil induced on drying and wetting paths. The authors pointed out the difficulty in imaging due to the movement of particles induced by the drying path. However, after moisture equilibrium had been attained, the authors observed a well developed

Fig. 13 (**a**) ESEM image taken under relative humidity 50% and (**b**) nearly 100%. FEBEX bentonite compacted to dry density 1.70 mg/m^3 (Villar and Lloret 2001)

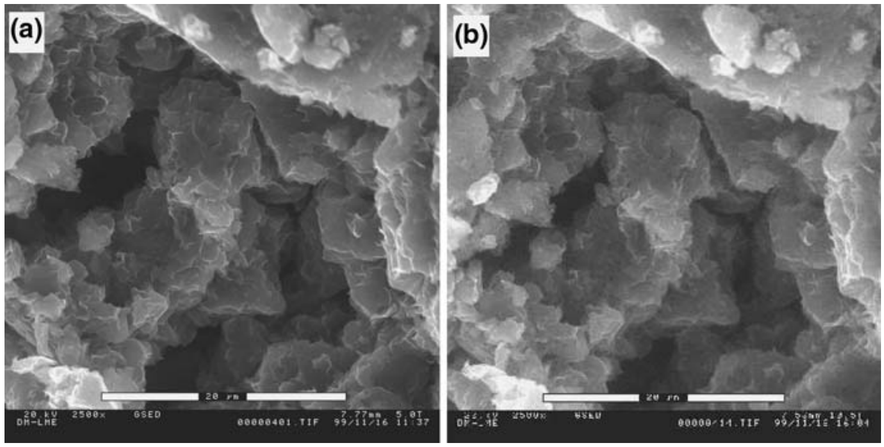

network of cracks and more densely packed clay aggregates and sand particles, resulting from significant suppression of inter-aggregate pores. Important expansion and crack healing was observed by the authors on subsequent clay hydration.

Figure 15 presents the paths followed on wetting and drying tests performed at micro and macrostructural scales on two different clayey materials (kaolinitic/illitic clay and bentonite). This study specifically investigates the reversibility or irreversibility features of the volume change behaviour of these clays at both structural scales on a wetting and drying episode. The volume change features at macroscopic scale are directly measured on soil cylindrical samples (38 mm in diameter and 40 mm high), which are subjected with vapour equilibrium technique to equivalent wetting and drying paths under unstressed conditions. Figure 15 shows the paths followed at macroscopic scale starting at point *A* at a relative humidity of 47% for the kaolinitic/illitic clay (left plot) and at 33% for the bentonite (right plot). After reaching point *B* (around 97%) along several intermediate equalisation stages, the different clays are progressively dried using the same equalisation steps to their initial and respective relative humidity. On the other hand, the swelling and shrinkage response at microstructural scale is observed directly by ESEM combined with digital image analysis using a commercial software along equivalent wetting and drying paths shown in Fig. 15. Compacted kaolinitic/illitic and bentonite powder on the dry side has been destructured to obtain an adequate size range of high-density aggregates. The microscopic scale observations are done with isolated aggregates, carefully stuck on the sample holder of the ESEM with a special adhesive tape. Images of the same aggregate are recorded at different equalisation stages, starting from point *A* at a relative humidity of 33% for both clays, as shown in Fig. 15. The relative humidity is defined as the ratio of the absolute chamber pressure to the saturation vapour pressure in the vapour-liquid phase boundary at the same temperature. Chamber pressure is isothermally lowered at 18°C to an absolute pressure of 0.66 kPa for the beginning of the wetting path (point *A*). A thermoelectric Peltier cooling stage to 10°C for the kaolinitic/illitic clay and to 12°C for the bentonite is applied at constant pressure to the sample holder to start the wetting phase. Several isothermal pressure increments are then applied to continue with the wetting episode up to a maximum absolute pressure of 1.33 kPa for the kaolinitic/illitic clay and 1.47 kPa for the bentonite (point *B* in Fig. 15). Afterwards, the aggregates are progressively dried along several intermediate equalisation stages to their initial relative humidity. Temperature and chamber pressure are maintained for approximately 15 min in each equalisation stage.

Figure 16 shows the evolution of the volume change response along the different wetting and drying stages. Regarding the microscale volume change determination, the images of the isolated aggregates are processed after tracing their contours, carrying out the binarisation and verifying the methodology. To quantify the volumetric deformation ε_v, the following expression was used

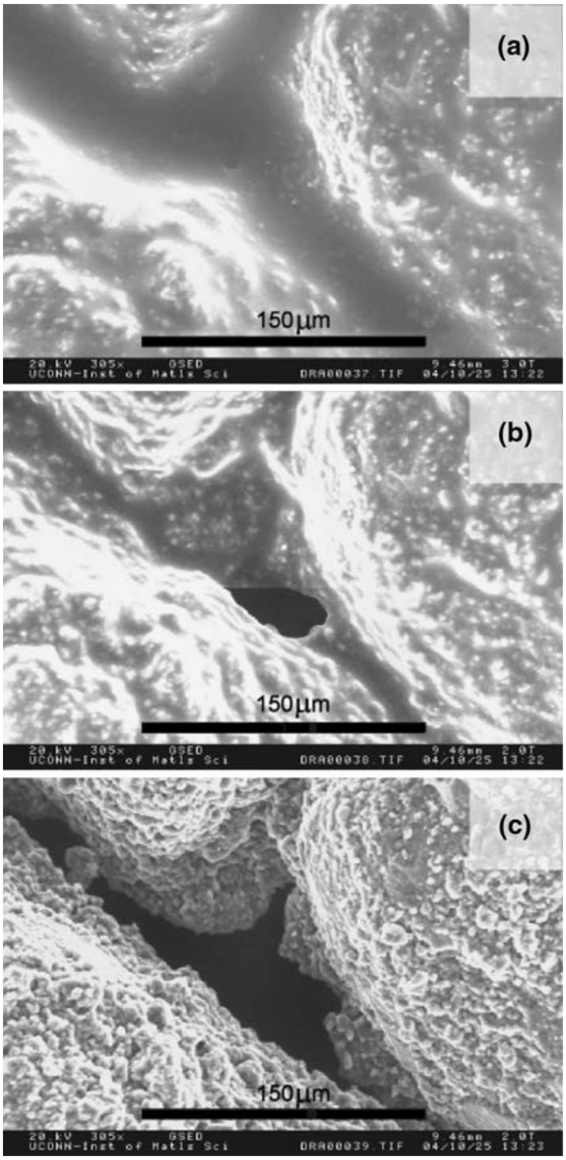

Fig. 14 ESEM micrographs showing the receding minisci and the evolution of the inter-grain porosity between sand grains during dehydration of a clay/sand mixture (Viola et al. 2005)

$$\varepsilon_v = \alpha\, \varepsilon_{2D} = 1.5\, \frac{(A - A_o)}{A_o} \tag{5}$$

where A and A_o are the area of an aggregate at the equilibrated and initial reference states, respectively. A value of $\alpha = 1.5$ has been considered to take into account isotropic straining perpendicular to the image. It is important to highlight that ESEM images are quite sensitive to working conditions (scan rate, chamber gas pressure and working distance). Particularly, when monitoring microstructural changes along drying and wetting paths with varying gas pressures, it is important to maintain a constant working distance.

Reversible and irreversible volume change features of both micro and macroscales are observed in Fig. 16 for the wetting and drying paths followed. Strains at microscopic scale are almost reversible, enclosing an hysteretic loop that is more evident in the bentonite aggregates. At macroscopic scale the irreversibility of the volume change response increases. These observation are consistent with the formulation for volumetric conditions of double-structure models as presented by Alonso et al. (1999, 2005). In their formulation, the behaviour at microscopic scale is considered to be appropriately described by an elastic model. In the case of the macrostructural level, an elastoplastic model is adopted. In addition, coupling between both scales is considered. That is, volumetric deformations at microstructural level can induce irrecoverable deformations at macrostructural scale. As a consequence, the results presented highlight the use of ESEM for understanding different hydro-mechanical behavioural features observed at macroscopic scale and for validating hypotheses used in the formulation of double-structure constitutive models.

Following an equivalent procedure—i.e., using ESEM combined with digital image analysis, Montes-H et al. (2003b) studied at microscopic scale the swelling-shrinkage behaviour of a Ca-saturated bentonite when subjected to a wetting/drying episode. The study was complemented at macroscopic scale by determining the water retention properties of the same bentonite following equivalent hydraulic paths and using vapour equilibrium technique. Figure 17 shows an adapted plot of their results, in which a clear reversible volume change response is detected at microscopic scale. As observed in the figure, the same reversible behaviour is also detected in the water retention behaviour at macroscopic scale. Again, these results emphasise the importance of using microstructural techniques to understand the behavioural features observed at macroscopic scale.

6 Summary and Concluding Remarks

The paper highlights the importance of microstructure investigation in unsaturated soils and presents its relevance to engineering properties. The paper

Fig. 15 Paths followed on wetting and drying tests performed at micro and macrostructural scales on two different clayey materials (kaolinitic/illitic clay and bentonite). Microstructural paths are performed on ESEM

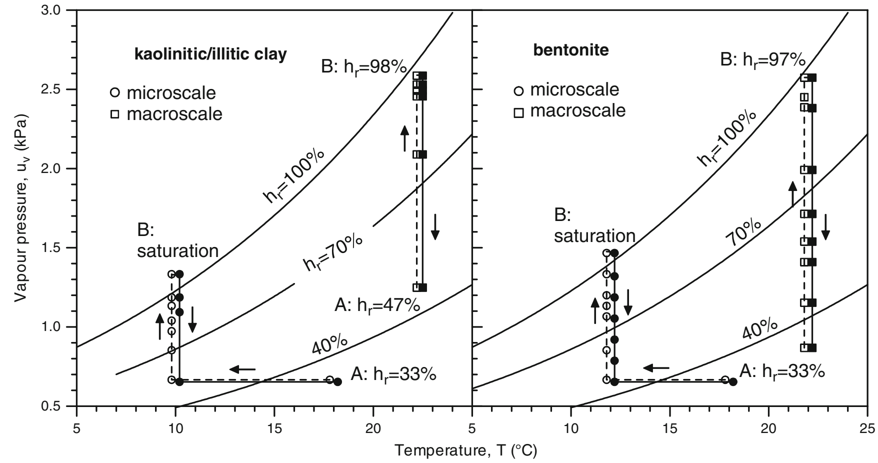

Fig. 16 Volume change response along different wetting and drying stages at micro and macroscales. Volume changes at microstructural scale are determined by digital image analysis of ESEM micrographs

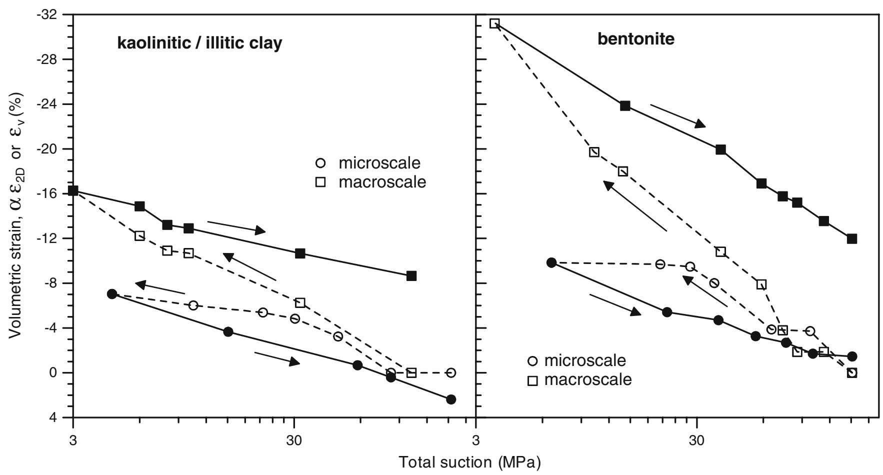

focuses on two microstructural techniques to characterise unsaturated soils, namely mercury intrusion porosimetry (MIP) and environmental scanning electron microscopy (ESEM). Both techniques have been used to make qualitative and quantitative inferences about unsaturated behaviour of soils (water retention and water permeability properties, evolution of pore size density functions along different hydro-mechanical paths, macroscopic volume change behaviour, micro and macroscale interactions, and so on). In addition, these complementary techniques may resolve some questions about the relationship between the dominant pore sizes observed directly with ESEM and the pore size distribution (PSD) measured by MIP, and whether soil preparation for MIP has some effect on soil microstructure.

It has been shown that the PSD obtained by MIP can be used to make predictions of volume changes, water retention and permeability properties, given that certain factors are taken into consideration, such as a recognition that the PSD changes with suction, the notion of pore accessibility and connectivity, and the proper preparation of the specimen prior to the MIP test.

ESEM visualisations combined with digital image analysis have been successfully used to monitor the volume change behaviour of soil aggregates at microscale along different hydraulic paths (wetting and drying cycle). Equivalent hydraulic paths have been carried out at macroscopic scale to study the interactions between the different scales.

Though many of the results discussed in this section are but initial forays at the problem, they have shown that quantitative analysis of microstructure coupled with macroscopic measurements is a realistic and powerful course for understanding the engineering

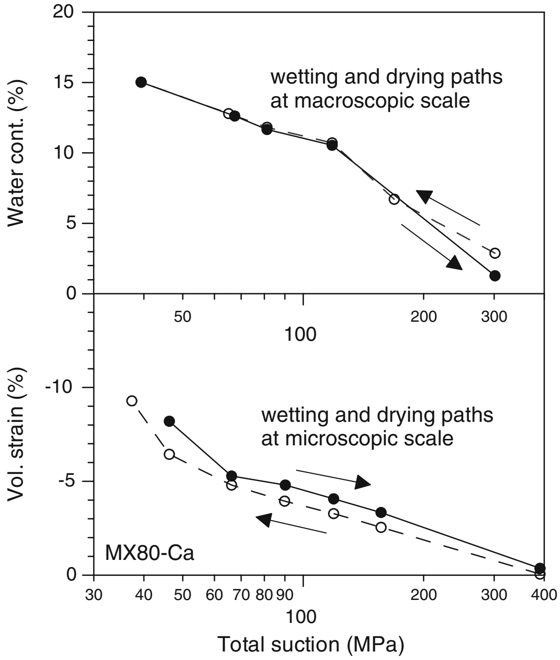

Fig. 17 Reversible swelling-shrinkage response of a Ca-saturated bentonite using ESEM and digital image analysis (lower plot). Reversible water retention properties obtained at macroscale on the same bentonite following equivalent hydraulic paths (upper plot) (adapted from Montes-H et al. 2003b)

behaviour of unsaturated soils, as well as in contributing to the generation of realistic hypotheses for homogenisation techniques and for formulating multi-scale constitutive models.

An important goal of microstructural investigation is the quantitative correlation between microstructural characteristics and macroscopic properties. Further advances in microstructure investigation should lead to soil models that follow the evolution of the PSD over stress and suction changes to facilitate improved predictions of soil behaviour. Already there are some attempts of general models with respect to unsaturated permeability. More rigorous integration between experimental micro-structural data and microstructure level models (discrete element models, pore-network models, and so on) will lead to further advances in this direction.

References

Abell AB, Willis KL, Lange DA (1999) Mercury intrusion porosimetry and image analysis of cement-based materials. J Colloid Interface Sci 211:39–44

Agus SS, Schanz T (2005) Effect of shrinking and swelling on microstructures and fabric of a compacted bentonite-sand mixture. In: H. Bilsel, Z. Nalbantoglu (eds) Proceedings of International Conference on Problematic Soils GEOPROB 2005, Famagusta, vol 2. Eastern Mediterranean University Press, Famagusta, pp 543–550, 25–27 May 2005

Ahmed S, Lovell CW, Diamond S (1974) Pore sizes and strength of compacted clay. J Geotech Eng Div ASCE 100(4):407–425

Airò Farulla C, Jommi C (2005) Suction controlled wetting-drying cycles on a compacted scaly clay. In: Bilsel H, Nalbantoglu Z (eds) Proceedings of International Conference on Problematic Soils GEOPROB 2005, Famagusta, vol 1. Famagusta, Eastern Mediterranean University Press, pp 229–237, 25–27 May 2005

Aït-Mokhtar A, Amiri O, Dumargue P, Bouguerra A (2004) On the applicability of Washburn law: study of mercury and water flow properties in cement-based materials. Mater Struct 37:107–113

Al-Mukhtar M (1995) Macroscopic behaviour and micro-structural properties of a kaolinite clay under controlled mechanical and hydraulic state. In: Alonso EE, Delage P (eds) Proceedings of 1st International Conference on Unsaturated Soils, Paris, vol 1. Balkema, Presses des Ponts et Chaussées, pp 3–9

Al-Mukhtar M Belanteur N Tessier D., Vanapalli SK (1996) The fabric of clay soil under controlled mechanical and hydraulic stresses. Appl Clay Sci 11(2–4):99–115

Alonso EE, Vaunat J, Gens A (1999) Modelling the mechanical behaviour of expansive clays. Eng Geol 54:173–183

Alonso EE, Romero E, Hoffmann C, García-Escudero E (2005) Expansive bentonite-sand mixtures in cyclic controlled-suction drying and wetting. Eng Geol 81(3):213–226

Al-Rawas AA, McGown A (1999) Microstructure of Omani expansive soils. Can Geotech J 36:272–290

Aung KK, Rahardjo H, Leong EC, Toll DG (2001) Relationship between porosimetry measurement and soil-water characteristic curve for an unsaturated residual soil. Geotech Geol Eng 19:401–416

Baker JM, Allmaras RR (1990) System for automating and multiplexing soil moisture measurement by time-domain reflectometry. Soil Sci Soc Am J 54(1):1–6

Baker JC, Grabowska-Olszewska B, Uwins PJR (1995) ESEM study of osmotic swelling of bentonite from Radzionkow (Poland). Appl Clay Sci 9:465–469

Barden L (1973) Macro and microstructure of soils. In: Pusch R. (ed). Proceedings of International Symposium on Soil Structure. Goteborg (Sweden),vol 1. Swedish Geotechnical Institute, Stockholm, pp 21–26

Barden L, Sides GR (1970) Engineering behavior and structure of compacted clay. J Soil Mech Found Div ASCE 96(4):1171–1200

Barden L, McGown A, Collins K (1973) The collapse mechanism in partly saturated soil. Eng Geol 7(1):49–60

Bennet RH, Bryant WR, Hulbert MH (eds). (1991) Microstructure of fine-grained sediments. From mud to shale. Springer-Verlag, New York

Ben Rhaim H, Tessier D, Pons CH, Amara BH (1998) Evolution of the microstructure of interstratified Ca-saturated clays during dehydration: SAXS and HRTEM analysis. Clay Miner 33:619–628

Berkowitz B, Ewing RP (1998) Percolation theory and network modeling applications in soil physics. Surveys in Geophysics 19:23–72

Bésuelle, P., Viggiani G, Lenoir N, Desrues J, Bornert M (2006) X-ray micro CT for studying strain localization in clay rocks under triaxial compression. In: Desrues J, Viggiani G, Bésuelle P (eds) Advances in X-ray tomography for geomaterials. ISTE Ltd, London, UK, 35–52

Bogner A, Jouneau P-H., Thollet G, Basset D, Gauthier C (2006) A history of scanning electron microscopy developments: towards "wet-STEM" imaging. Micron 38(4):390–401

Borsic A, Comina C, Foti S, Lancellotta R, Musso G (2005) Imaging heterogeneities with electrical impedance tomography: laboratory results. Géotechnique 55(7):539–547

Buckman JO, Todd AC, Hill PI (2000) Observations on reservoir rock wettability using an environmental scanning electron microscope. Microsc Anal 35–37

Carminati A, Kaestner A, Hassanein R, Koliji A (2006) Hydraulic properties of aggregate-aggregate contacts. In: Desrues J, Viggiani G, Bésuelle P (eds.) Advances in X-ray tomography for geomaterials. ISTE Ltd, London, UK, pp 325–331

Cases JM, Beraend I, Besson G, Francois M, Uriot JP, Thomas F, Poirer JE (1992) Mechanism of adsorption and desorption of water vapor by homoionic montmorillonite I. The sodium exchanged form. Langmuir 8:2730–2739

Chiappone A, Marello S, Scavia C, Setti M (2004) Clay mineral characterization through the methylene blue test: comparison with other experimental techniques and applications of the method. Can Geotech J 41:1168–1178

Collins K, McGown A, Barden L (1973) Microstructural features of some Israeli expansive soils. Proceedings of 3rd International Conference Expansive Soils, Haifa, Israel, pp 27–34

Collins K, McGown A (1974) The form and function of microfabric features in a variety of natural soils. Géotechnique 24(2):223–254

Comina C, Foti S, Musso G, Romero E (2008) EIT oedometer—an advanced cell to monitor spatial and time variability in soil. Geotech Test J (Accepted for publication)

Coulon E, Bruand A (1989) Effects of compaction on the pore space geometry in sandy soils. Soil Tillage Res 15:137–152

Cui YJ, Loiseau C, Delage P (2002) Microstructure changes of a confined swelling soil due to suction controlled hydration. Proceedings of 3rd International Conference on Unsaturated Soils, Recife, Brazil,. In: Jucá JFT, de Campos TMP, Marinho FAM (eds) Unsaturated Soils, vol 2. A.A. Balkema Publishers, Lisse, pp 593–598, 10–13 March 2002

Cuisinier O, Laloui L (2004) Fabric evolution during hydromechanical loading of a compacted silt. Int J Numer Anal Meth Geomech 28(6):483–499

Cuisinier O, Masrouri F (2005) Compressibility and fabric of an unsaturated compacted swelling soil. Proceedings of International Symposium on Advanced Experimental Unsaturated Soil Mechanics, Trento, Italy, 27–29 June 2005. In: Tarantino A, Romero E, Cui YJ (eds). Advanced Experimental Unsaturated Soil Mechanics. Taylor, Francis Group, London, pp 411–417

Danilatos GD (1993) Introduction to the ESEM instrument. Microsc Res Tech 25:354–361

Delage P (2006) Some microstructure effects on the behaviour of compacted swelling clays used for engineered barriers. Chin J Rock Mech Eng 25(4):721–732

Delage P (2007) Microstructure features in the behaviour of engineered barriers for nuclear waste disposal. In: Schanz T (ed) Experimental unsaturated soil mechanics. Springer Proceedings in Physics, vol 112. Springer, Berlin, pp 11–32

Delage P, Cui YJ (2007) Microstructure effects on the hydration and water transport in compacted bentonites used for radiactive waste disposal. In: Yin Z, Yuan J, Chiu ACF (eds) Proceedings of 3rd Asian Conference on Unsaturated Soils, Nanjing PR China, Science Press, Beijing, pp 85–96, April 2007

Delage P, Graham J (1996) Mechanical behaviour of unsaturated soils: understanding the behaviour of unsaturated soils requires reliable conceptual models. In: Alonso EE, Delage P (eds) Proceedings of 1st International Conference on Unsaturated Soils, Paris vol 3. Balkema, Presses des Ponts et Chaussées, pp 1223–1256

Delage P, Lefebvre G (1984) Study of the structure of a sensitive Champlain clay and of its evolution during consolidation. Can Geotech J 21:21–35

Delage P, Pellerin M (1984) Influence de la lyophilisation sur la structure d'une argile sensible du Quebec. Clay Miner 19:151–160

Delage P, Tessier D, Audiguier MM (1982) Use of the cryoscan apparatus for observation of freeze-fractured planes of a sensitive Quebec clay in scanning electron microscopy. Can Geotech J 19:111–114

Delage P, Audiguier M., Cui YJ, Howatt MD (1996) Microstructure of a compacted silt. Can Geotech J 33:150–158

De las Cuevas C (1997) Pore structure characterization in rock salt. Eng Geol 47:17–30

Desrues J, Viggiani G, Bésuelle P (eds) (2006) Advances in X-ray tomography for geomaterials. ISTE Ltd, London, UK

Diamond S (1970) Pore size distribution in clays. Clays Clay Miner 18:7–23

Djeran-Maigre I, Tessier D, Grundberger D, Velde B, Vasseur G (1998) Evolution of microstructure and of macroscopic properties of some clays during experimental compaction. Mar Petrol Geol 15:109–128

Fadeev AYu., Borisova OR, Lisichkin GV (1996) Fractality of porous silicas: a comparison of adsorption and porosimetry data. J Colloid Interface Sci 183:1–5

Fernández AM, Rivas P (2005) Analysis and distribution of waters in the compacted FEBEX bentonite: pore water chemistry and adsorbed water properties. Proceedings of International Symposium on Large Scale Field Tests in Granite, Sitges, Spain, 12–14th November 2003. In: Alonso EE, Ledesma A (eds) Advances in understanding engineered clay barriers. Taylor, Francis Group, London, pp 257–275

Fies JC, Bruand A (1998) Particle packing and organization of the textural porosity in clay-silt-sand mixtures. Eur J Soil Sci 49:557–567

Fukue M, Minato T, Horibe H, Taya N (1999) The microstructure of clay given by resistivity measurements. Eng Geol 54:43–53

Garcia-Bengochea I, Lovell W, Altshaeffl AG (1979) Pore distribution and permeability of silty clays. J Geotech Eng ASCE 105(7):839–856

Gasc-Barbier M, Tessier D (2007) Structural modifications of a hard deep clayey rock due to hygro-mechanical solicitations. Int J Geomech 7(3):227–235

Gebrenegus T, Tuller M-, Muhuthan B (2006) The application of X-ray computed tomography for characterisation of surface crack networks in bentonite-sand mixtures. In: Desrues J, Viggiani G, Bésuelle P (eds) Advances in X-ray tomography for geomaterials. ISTE Ltd, London, UK: 207–212

Giménez D., Perfect E, Rawls WJ, Pachepsky Ya (1997) Fractal models for predicting soil hydraulic properties: a review. Eng Geol 48: 161–183

Gillott JE (1970) Fabric of Leda clay investigated by optical, electron-optical, and x-ray diffraction methods. Eng Geol 4(2):133–153

Gillott JE (1979) Fabric, composition and properties of sensitive soils from Canada, Alaska and Norway. Eng Geol 14(2):149–172

Grabowska-Olszewska B (1975) SEM analysis of microstructures of loess deposits. Bull Eng Geol Environ 11(1):45–48

Griffiths FJ, Joshi RC (1989) Changes in pore size distribution due to consolidation of clays. Géotechnique 39(1):159–167

Hetzel F, Tessier D, Jaunet A-M., Doner H (1994) The microstructure of three Na+ Smectites: The importance of particle geometry on dehydration and rehydration. Clays Clay Miner 42(1):242–248

Hoffman R (1975) A study of the advancing interface. Interface shape in liquid–gas systems. J Colloid Interface Sci 50:228–241

Hoffmann C, Alonso EE, Romero E (2007) Hydro-mechanical behaviour of bentonite pellet mixtures. Phys Chem Earth 32:832–849

Jenkins LM, Donald AM (2000) Observing fibers swelling in water with an environmental scanning electron microscope. Textile Res J 70:269–276

Jommi C, Sciotti A (2003) A study of the microstructure to assess the reliability of laboratory compacted soils as reference material for earth constructions. In: Botempi F (ed) System-based vision for strategic and creative design, vol 3. A.A. Balkema, Lisse, pp 2409–2415

Juang CH, Holtz RD (1986a) Fabric, pore size distribution and permeability of sandy soils. J Geotech Eng ASCE 112(9): 855–868

Juang CH, Holtz RD (1986b) A probabilistic permeability model and the pore size density function. Int J Numer Anal Meth Geomech 10:543–553

Katti DR, Shanmugasundaram V (2001) Influence of swelling on the microstructure of expansive clays. Can Geotech J 38:175–182

Koliji A, Carminati A, Kaestner A, Vulliet L, Laloui L, Fluehler H, Vontobel P, Hassanein R (2006a) Experimental study of flow and deformation in aggregated soils using neutron tomography. In: Desrues J, Viggiani G, Bésuelle P (eds). Advances in X-ray tomography for geomaterials. ISTE Ltd, London, UK pp 341–348

Koliji A, Laloui L, Cuisinier O, Vulliet L (2006b) Suction induced effects on the fabric of a structured soil. Trans Porous Med 64:261–278

Komine H, Ogata N (1996) Observation of swelling behaviour of bentonite by new electron microscope. In: Proceedings of 2nd International Conference on Environmental Geotechnics (IS-Osaka '96), vol. 1, pp 563–568

Komine H, Ogata N (1999) Experimental study on swelling characteristics of sand–bentonite mixture for nuclear waste disposal. Soils Found 39(2):83–97

Komine H, Ogata N (2004) Predicting swelling characteristics of bentonites. J Geotech Geoenviron Eng ASCE 130(8):818–829

Kong LW, Guo AG, Zhao YW, Liu YY (2005) Influence of moisture content on porosity features of Red clay. Proceedings International Symposium on Advanced Experimental Unsaturated Soil Mechanics, Trento, Italy, 27–29 June 2005. In: Tarantino A, Romero E, Cui YJ (eds) Advanced experimental unsaturated soil mechanics. Taylor, Francis Group, London, pp 419–424

Korvin G (1992) Fractal models in the earth sciences. Elsevier, Amsterdam

Lambe TW (1958) The structure of compacted clays. J Soil Mech Found Div ASCE 84(2):1–34

Lapierre C Leroueil S, Locat J (1990) Mercury intrusion and permeability of Louisville clay. Can Geotech J 27:761–773

Lawrence GP (1978) Stability of soil pores during mercury intrusion porosimetry. J Soil Sci 29:299–304

Leong EC, Rahardjo H (1997) Permeability functions for unsaturated soils. J Geotech Eng ASCE 123(12):1118–1126

Loret B, Khalili N (2000) A three phase model for unsaturated soils. Int J Numer Anal Method Geomech 24(11):983–927

Lloret A, Romero E, Villar MV (2004) FEBEX II Project. Final report on thermo-hydro-mechanical laboratory tests. Ref. PT-10/04. ENRESA, Dirección de Ciencia y Tecnología, Madrid. Available on-line at: http://www.enresa.es/

Lloret A, Villar MV (2007) Advances on the knowledge of the thermo-hydro-mechanical behaviour of heavily compacted FEBEX bentonite. Phys Chem Earth 32:701–715

Marshall TJ (1958) A relation between hydraulic conductivity and size distribution of pores. J Soil Sci 9:1–8

Matthews GP, Ridgway CJ, Spearing MC (1995) Void space modelling of mercury intrusion hysteresis in sandstone, paper coating, and other porous media. J Colloid Interface Sci 171:8–27

McGown A, Collins K (1975) The microfabrics of some expansive and collapsing soils. Proceedins of 5th Panamerican Conference, vol 1 Soil Mechanics and Foundation Engineering, Buenos Aires, pp 323–332

Meyer K, Lorenz P, Böhl-Kuhn B, Klobes P (1994) Porous solids and their characterization. Methods of investigation and application. Cryst Res Technol 29(7):903–930

Mitchell JK, Soga K (2005) Fundamentals of soil behaviour, 3rd edn. John Wiley, Sons, Inc, New Jersey

Montes-H G (2002) Etude expérimentale de la sorption d'eau et du gonflement des argiles par microscopie électronique à balayage environnementale (ESEM) et analyse digitale d'images. PhD Thesis. Louis Pasteur University, Strasbourg I, France

Montes-H G, Duplay J, Martinez L, Mendoza C (2003a) Swelling-shrinkage kinetics of MX80 bentonite. Appl Clay Sci 22:279–293

Montes-H G, Duplay J, Martinez L, Geraud Y, Rousset-Tournier B (2003b) Influence of interlayer cations on the water sorption and swelling-shrinkage of MX80 bentonite. Appl Clay Sci 23:309–321

Montes-H G., Duplay J, Martinez L, Escoffier S, Rousset D (2004) Structural modifications of Callovo-Oxfordian argillite under hydration/dehydration conditions. Appl Clay Sci 25:187–194

Moro F, Böhni H (2002) Ink-bottle effect in mercury intrusion porosimetry of cement-based materials. J Colloid Interface Sci 246:135–149

Mualem Y (1976) A new model for predicting the hydraulic conductivity of unsaturated porous media. Water Resour Res 12:513–522

Mukunoki T, Otani J, Maekawa A, Camp S, Gourc JP (2006) Investigation of crack behaviour on cover soils at landfill using X-ray CT. In: Desrues J, Viggiani G, Bésuelle P (eds) Advances in X-ray tomography for geomaterials. ISTE Ltd, London, UK, pp 213–219

Muñoz JJ (2007) Thermo-hydro-mechanical analysis of soft rock. Application to a large scale heating test and large scale ventilation test. Ph. D. Thesis, Universitat Politècnica de Catalunya, Barcelona. http://www.tdcat.cesca.es/TDX-0511107–103122/

Musso G, Romero E, Gens A, Castellanos E (2003). The role of structure in the chemically induced deformations of Febex bentonite. Appl Clay Sci 23:229–237

Olivella S, Carrera J, Gens A, Alonso EE (1994). Nonisothermal multiphase flow of brine and gas through saline media. Trans Porous Med 15:271–293

Osipov VI, Sokolov VN (1978a) A study of the nature of the strength and deformation properties of clay soils with the help of the scanning electron microscope. Bull Eng Geol Environ 17(1):91–94

Osipov VI, Sokolov VN (1978b) Relation between the microfabric of clay soils and their origin and degree of compaction. Bull Eng Geol Environ 18(1):73–81

Osipov VI, Sokolov VN (1978c) Structure formation in clay sediments. Bull Eng Geol Environ 18(1):83–90

Penumadu D, Dean J (2000) Compressibility effect in evaluating the pore-size distribution of kaolin clay using mercury intrusion porosimetry. Can Geotech J 37:393–405

Prapaharan S, Altschaeffl AG, Dempsey BJ (1985) Moisture curve of a compacted clay: mercury intrusion method. J Geotech Eng ASCE 111(9):1139–1143

Prapaharan S, White DM, Altschaeffl AG (1991) Fabric of field- and laboratory-compacted clay. J Geotech Eng ASCE 117(12):1934–1940

Pusch R (1970) Microstructural changes in soft quick clay at failure. Can Geotech J 7:1–7

Pusch R (1999) Experience from preparation and investigation of clay microstructure. Eng Geol 54:187–194

Pusch R, Schomburg J (1999) Impact of microstructure on the hydraulic conductivity of undisturbed and artificially prepared smectite clay. Eng Geol 54:167–172

Pusch R, Yong RN, Grindrod P (eds) (1999) Special issue. Microstructural modelling with special emphasis on the use of clays for waste isolation. Eng Geol 54

Pusch R, Yong RN (eds) (2003) Special issue. Clay microstructure. Proceedings of Workshop Lund, Sweden. Applied Clay Science, vol 23, Issues 1–4, 15–17 October, 2002

Qi Y Al-Mukthar M, Alcover JF, Bergaya F (1996) Coupling analysis of macroscopic and microscopic behaviour in highly consolidated Na-laponite clays. Appl Clay Sci 11:185–197

Reed MA, Lovell CW, Altschaeffl AG, Wood LE (1979) Frost-heaving rate predicted from pore-size distribution. Can Geotech J 16:463–472

Rodríguez-Rey A, Ruiz de Argandoña VG, Calleja L, Suárez del Río LM, Velorio C (2006) Consolidants influence on sandstone capillarity. X-ray study. In: Desrues J, Viggiani G, Bésuelle P (eds) Advances in X-ray tomography for geomaterials. ISTE Ltd, London, UK pp 381–387

Rolland S, Stemmelen D, Moyne C, Masrouri F (2003) Transfert hydrique dans un sol argileux gonflant non saturé: influence du confinement. Rev Fr Géotech 104:21–35

Rolland S, Stemmelen D, Moyne C, Masrouri F (2005) Experimental hydraulic measurements in an unsaturated swelling soil using the dual-energy gamma-ray technique. Proceedings of International Symposium on Advanced Experimental Unsaturated Soil Mechanics, Trento, Italy. In: Tarantino A, Romero E, Cui YJ (eds) Advanced experimental unsaturated soil mechanics. Taylor, Francis Group, London, pp 305–310, 27–29 June 2005

Romero E (1999) Characterisation and thermo-hydro-mechanical behaviour of unsaturated Boom-clay: An experimental study. Ph. D. Thesis, Universitat Politècnica de Catalunya, Barcelona. http://www.tdcat.cesca.es/TDCat-0930102–092135/

Romero E, Gens A, Lloret A (1999) Water permeability, water retention and microstructure of unsaturated Boom clay. Eng Geol 54:117–127

Romero E, Hoffmann C, Castellanos E, Suriol J, Lloret A (2005) Microstructural changes of compacted bentonite induced by hydro-mechanical actions. Proceedings of International Symposium on Large Scale Field Tests in Granite, Sitges, Spain. In: Alonso EE, Ledesma A (eds) Advances in understanding engineered clay barriers. Taylor, Francis Group, London, pp 193–202, 12–14th November 2003

Saiyouri N, Hicher PY, Tessier D (1998) Microstructural analysis of highly compacted clay swelling. Proceedings of 2nd International Conference on Unsaturated Soils, Beijing, vol 1. International Academic Publishers, Beijing, pp 119–124

Saiyouri N, Hicher PY, Tessier D (2000) Microstructural approach and transfer water modelling in highly compacted unsaturated swelling clays. Mech Cohes Frict Mater 5(1):41–60

Saiyouri N, Tessier D, Hicher PY (2004) Experimental study of swelling in unsaturated compacted clays. Clay Miner 39(4):469–479

Sánchez M., Gens A, Guimarães L., Olivella S (2005) A double structure generalized plasticity model for expansive materials. Int J Numer Anal Method Geomech 29:751–787

Santamarina JC, Klein KA, Wang YH, Prencke E (2002) Specific surface: determination and relevance. Can Geotech J 39:233–241

Simms PH (2004) Appropriate use of the indirect methods to predict unsaturated hydraulic conductivity. Geotech News 22(2):34–36

Simms PH, Yanful EK (2001) Measurement and estimation of pore shrinkage and pore distribution in a clayey till during soil-water characteristic curve tests. Can Geotech J 38:741–754

Simms PH, Yanful EK (2002) Predicting soil-water characteristic curves of compacted plastic soils from measured pore-size distributions. Géotechnique 52(4):269–278

Simms PH, Yanful EK (2004) A discussion of the application of mercury intrusion porosimetry for the investigation of soils, including an evaluation of its use to estimate volume change in compacted clayey soils. Géotechnique 54(6):421–426

Simms PH, Yanful EK (2005) A pore-network model for hydromechanical coupling in unsaturated compacted clayey soils. Can Geotech J 42:499–514

Sills ID, Aylmore LAG., Quirk JP (1973) A comprison between mercury injection and nitrogen sorption as methods of determining pore size distribution. Proc Soil Sci Soc Am 37:535–537

Suzuki S, Prayongphan S, Ichikawa Y, Chae B-G (2005) In situ observations of the swelling of bentonite aggregates in NaCl solution. Appl Clay Sci 29:89–98

Takahashi M, Takemura T, Hirai H, Murakoshi A, Kato M (2006) Spatial and density resolution in microfocus X-ray CT applied to studies of microstructural changes in rocks with increasing hydrostatic pressure. In: Desrues J, Viggiani G, Bésuelle P (eds) Advances in X-ray tomography for geomaterials. ISTE Ltd, London, UK, pp 421–427

Tessier D, Lajudi A, Petit JC (1992) Relation between the macroscopic behaviour of clays and their microstructural properties. Appl Geochem 1(Suppl):151–161

Thiel BL, Donald AM (1998) In situ mechanical testing of fully hydrated carrots in the environmental SEM. Ann Bot 82:727–733

Thom R, Sivakumar R, Sivakumar V., Murray EJ, Mackinnon P (2007) Pore size distribution of unsaturated compacted kaolin: the initial states and final states following saturation. Géotechnique 57(5):469–474

Tovey NK (1973) Quantitative analysis of electron micrographs of soil structure. In: Pusch GR (ed) Proceedins of International Symposium on Soil Structure, vol 1. Swedish Geotechnical Institute, Stockholm, pp 50–57

Tovey NK, Krinsley DH (1975) A technique to enhance detail on scanning electron micrographs of geological materials. Géotechnique 25(1):146–151

Tovey NK, Frydman S, Wong KY (1973) A study of swelling clay in the scanning electron microscope. Proceedings of 3rd International Conference. Expansive Soils Haifa Israel, vol 2. pp 45–54

Van Geet M., Volckaert G., Roels S (2005) The use of microfocus X-ray computed tomography in characterising the hydration of a clay pellet/powder mixture. Appl Clay Sci 29:73–87

Van Genutchen MT (1980) A closed form solution for predicting the hydraulic conductivity of unsaturated soils. Soil Sci Soc of Am J 44:892–898

Villar MV, Lloret A (2001) Variation of the intrinsic permeability of expansive clays upon saturation. In: Adachi K, Fukue M (eds) Clay Science for Engineering. A.A. Balkema, Rotterdam, pp 259–266

Viola R, Tuller M, Or D, Drasdis J (2005) Microstructure of clay-sand mixtures at different hydration states. Proceedings of International Symposium on Advanced Experimental Unsaturated Soil Mechanics, Trento, Italy,. In: Tarantino A, Romero E, Cui YJ (eds) Advanced experimental unsaturated soil mechanics. Taylor, Francis Group, London, pp 437–442, 27–29 June 2005

Wan AWL, Gray MN, Graham J (1995) On the relations of suction, moisture content and soil structure in compacted clays. In: Alonso EE, Delage P (eds) Proceeedings of 1st International Conference on Unsaturated Soils, Paris, vol 1. Balkema, Presses des Ponts et Chaussées, pp 215–222

Watt GR, Griffin BJ, Kinny PD (2000) Charge contrast imaging of geological materials in the environmental scanning electron microscope. Am Miner 85:1784–1794

Webb PA, Orr C (1997) Analytical methods in fine particle technology. Micromeritics Instrument Corp, Norcross

Wei QF, Wang XQ (2003) Dynamic characterisation of industrial textiles using an environmental scanning electron microscope. J Indust Text 33(2):101–110

Wilson GW, Fredlund DG, Barbour SL (1994) Coupled soil-atmosphere modeling for soil evaporation. Can Geotech J 31:151–161

Zhang G, Germaine JT, Whittle AJ (2005) Drying induced alteration to the microstructure of a tropical soil. Proceedings of International Symposium on advanced experimental unsaturated soil mechanics, Trento, Italy. In: Tarantino A, Romero E, Cui YJ (eds) Advanced experimental unsaturated soil mechanics. Taylor & Francis Group, London, pp 443–449, 27–29 June 2005

Geoenvironmental Testing

Pierre Delage · Enrique Romero

Originally published in the journal *Geotechnical and Geological Engineering*, Volume 26, No. 6, 729–749.
DOI: 10.1007/s10706-008-9199-y

Abstract Geoenvironmental concerns involve unsaturated soils in problems like soil contamination, waste disposal and ground-atmosphere interactions. This paper deals with the two first points. To tackle geoenvironmental problems in unsaturated soils, it is necessary to identify experimentally the retention and transfer phenomena that govern the movements of fluids and chemical species in the unsaturated soil. Some of the experimental techniques used in unsaturated soils can be adapted to face these problems, but extensions accounting for the various physico-chemical processes involved in soil contamination and waste disposal are necessary, including temperature effects and the mechanical couplings resulting from the changes in temperature and chemical concentrations. After an introduction to the geoenvironmental problems that are related to unsaturated soils, the paper presents a series of experimental developments carried out in relation to retention and transfer properties of water (pure or with dissolved species), hydrocarbons and gas, also accounting for temperature effects and chemical effects. The techniques presented are applicable to soil contamination and waste disposal, with a special concern addressed to nuclear waste disposal, in which the effects of desaturation of the geological barrier together with the unsaturated nature of compacted engineered barriers appeared to be quite important.

P. Delage (✉)
Ecole Nationale des Ponts et Chaussées (CERMES, I. Navier), Paris, France
e-mail: pierre.delage@enpc.fr

E. Romero
Universitat Politècnica de Catalunya, Barcelona, Spain
e-mail: enrique.romero-morales@upc.edu

Keywords Geoenvironmental testing · Unsaturated soil · Contamination · Waste disposal · Retention · Transfer · Temperature · Chemical · NAPL · Nuclear waste · Engineered barrier · Vadose zone

1 Introduction

Unsaturated soils are involved in many geoenvironmental problems such as soil contamination, waste disposal and interactions between the ground and the atmosphere. Indeed, the safe and perennial confinement of gas or liquid pollutants is essential to preserve the environment. In these problems, the experimental techniques developed in unsaturated soils mechanics are certainly helpful to investigate and better understand various important issues linked to possible fluid transfers, either in the gas or in the liquid phase, heat and contaminant transport, temperature and chemical effects, and their possible interactions with the mechanical response of the materials. Also, investigation of the water exchanges occurring between the ground and the atmosphere are essential to identify the impact of climatic events on ground profiles. They have to be properly understood to better assess the efficiency and durability of waste disposal covers, as shown by Cui and Zornberg (Ibid.). Obviously, mass and heat transport processes and properties are essential, but possible mechanical effects through thermo-hydro-mechanical coupling should also be considered. In this regard, data on fluid transfer from papers by Benson and Gribb (1997) or Masrouri et al. (Ibid.) among others, are of interest.

As previously indicated, experimental techniques used in unsaturated soil mechanics are a starting point to study these processes and their interactions. However, the understanding of the constitutive behaviour of the material including multi-physics effects or multi-scale interactions demand the improvement of the conventional techniques to capture these complex phenomena and to include the different environmental variables (temperature; geochemical variables, such as solute concentration—i.e., osmotic suction - and nature and quantity of exchangeable cations; …).

In this paper, issues related to contamination and waste disposal will be considered in the light of recent developments conducted in the experimental techniques used in unsaturated soil mechanics. Selected changes and improvements carried out in these techniques will be introduced and discussed.

2 Geoenvironmental Problems Involving Unsaturated Soils

2.1 Soil Contamination

The different kinds of contamination that can affect soils and other geomaterials are described in Table 1, together with some physico-chemical phenomena involved. Soil contamination may be either accidental and localised or diffuse. Diffuse contamination concerns larger areas of ground, as for instance a consequence of an excessive use of fertilizers made in agriculture or/of atmospheric contamination originated from chimney plumes from industrial facilities. This paper will mainly concentrate on localised contamination.

Accidental contamination may occur below industrial facilities and may concern either immiscible hydrocarbon fluids (Non Aqueous Phase Liquid, NAPL, lighter or denser than water, LNAPL and DNAPL respectively), soluble chemical products and metals (trace elements). Contamination accidents can also occur anywhere during the transportation of the products. Accidental leaks in permanent industrial facilities can be a consequence of bad maintenance and of excessive ageing of the facilities. As compared to chemical products or metal pollution that concern both saturated and unsaturated soils, NAPLs only infiltrate into the ground when the soil is unsaturated (vadose zone) as shown in Fig. 1. Light NAPL progressively infiltrates down to the water table where the immiscible phase keeps floating above water. Since hydrocarbons are made up of a complex mixture of many different kinds of organic compounds, they generally contain a significant proportion of volatile and/or soluble components prone either to evaporate and migrate in the vadose zone or to dissolve in the water table and migrate according to local hydraulic gradients. To understand NAPL infiltration, unsaturated flow parameters such as the oil retention and the oil permeability properties have to be investigated. These parameters are also important to better assess the mechanisms involved in most of the remediation techniques used for the decontamination of NAPL polluted soils such as, for

Table 1 Phenomena involved in soil contamination

Nature of the contamination	Accidental, transportation	Below roads	Active and abandoned industrial facilities	Atmospheric
Pollutant	NAPL, chemical	Ions, heavy metals	Anything: hydro carbon (polar - non polar), chemical, heavy metals…	Heavy metals, chemical, ashes,…
Geomaterial	Vadose zone	Subgrade compacted layers	Vadose zone	Vegetal surface layer
Phenomena	Immiscible hydro carbon, Infiltration, evaporation, venting	Water infiltration, pollutant transfer, precipitation–dissolution	Water infiltration, pollutant transfer, precipitation–dissolution	Fixation, precipitation, infiltration, transfer

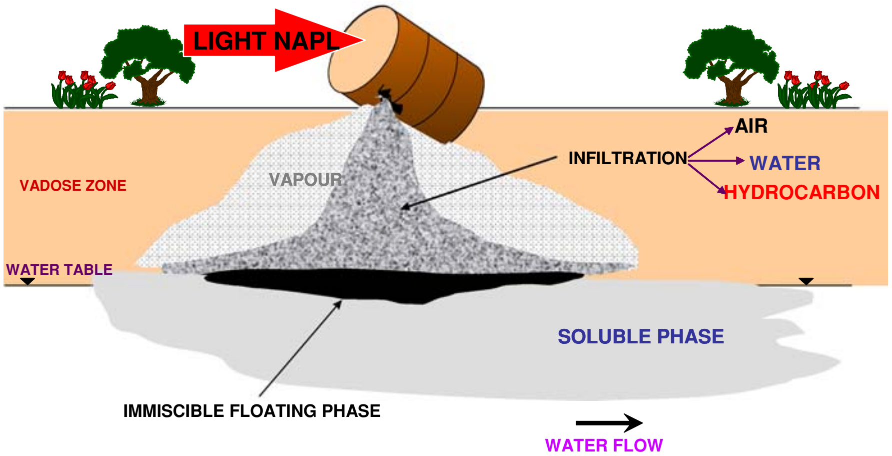

Fig. 1 Typical accidental light NAPL contamination

example, air stripping, soil venting and degradation enhancement by air and gas injection. Other contaminations come from the products generated by cars circulating on roads that are washed by rain and that go through the subgrades and infiltrate soils.

The retention and transfer phenomena that govern the behaviour of chemicals and metals in soils involve significantly strong physico-chemical interactions with the reactive compounds of the soils, i.e. clay, organic matter and oxides. They include adsorption, precipitation, dissolution, diffusion dispersion and hydrolysis. They depend on various chemical characteristics such as the soil acidity (pH) or the soil redox potential. These phenomena are now well documented in saturated soils where the status of each component is governed by a chemical potential. Studies on contamination in unsaturated soils are generally carried out in sand samples (with low suction levels) and most often account for the effects of capillarity (Bresler 1973; Gaudet et al. 1977; De Smet et al. 1986; Maciejewski 1993). The combined effect of capillarity and physico-chemical interactions in the reactive soil fraction in unsaturated soils is poorly documented.

2.2 Waste Disposal

Obviously, uncontrolled waste disposal is a serious source of soil contamination with possible consequences on ground water and rivers. In developed countries, the environment is protected from possible contamination from urban and industrial waste by a proper surface waste disposal policy. Considerable attention has also been paid to the disposal of nuclear waste, both in surface (low activity waste) and at great depth (high activity waste). In both cases, besides using geosynthetics, compacted soils are used to make confining layers with a sufficiently low permeability. Due to the diversity of the pollutants present in the waste, particularly in urban waste, a complete set of thermo-hydro-chemo-bio-mechanical couplings takes place in the waste, at the contact with the liner and inside the liner. A deeper understanding of the interactions between the waste and the confining layer has to be gained, as recently shown by Rowe (2005). Another important aspect is the behaviour of cover liners that are aimed at isolating the waste from the atmosphere (Bouazza et al. 2006). Exchanges between the ground and the atmosphere involve water phase changes from liquid to gas and possible desaturation of the cover. Here again, research conducted in unsaturated soil mechanics appear to be of interest in terms of parameter determination (e.g. Cui and Zornberg Ibid.).

Although temperature changes also occur in surface waste due to chemical and biological reactions and to atmospheric changes, more attention has been paid to temperature effects on the behaviour of soils in researches conducted on deep geological disposal of high level radioactive waste (HLRW), which is at present one of the preferred alternatives for the safe disposal of these wastes. Crystalline and clay-rich rocks have been usually considered as suitable host media in which repositories can be built by placing the canister that contain the radioactive waste in horizontal drifts or vertical boreholes excavated at great depths. A possible option is to backfill the space between the canisters and the excavation with engineered barriers made up of heavily compacted swelling clays that present specific properties as compared to common liners. These barriers placed at partially saturated states and at very high initial suctions (several tens of MPa) are designed to provide isolation by swelling with negligible volume change allowed. Thermal effects can be dominant as quite high temperatures are reached in these partially saturated barriers due to the heat generated by the radioactive waste decay (Gens et al. 1998; Cleall et al. 2006). The incorporation of new variables such as suction and temperature into current understanding of soil behaviour is required to account for these effects. For these reasons, specific attention has been devoted to thermal effects on engineered barriers and to the development of experimental techniques and testing cells, as described further on.

Table 2 shows the typical phenomena occurring in geomaterials involved in waste disposal that include compacted clay liners, attenuation liners and cover liners in the case of surface waste. Of course, liners are compacted in wet states located not far from the saturation curve in a compaction diagram. However, some air is still remaining in liners and some gas generation by chemical reaction can occur, confirming that such liners or covers should be considered in their unsaturated state. As previously described, unsaturated soil behaviour may also concern engineered barriers used in nuclear waste disposal schemes, as well as the host geological medium in which the deep underground facility is excavated, since it has been observed that significant desaturation could be induced by ventilation in the galleries (Fernández-García et al. 2005; Mayor et al. 2006).

The number of physico-bio-chemical phenomena occurring in geomaterials that are used or that are possibly affected in and around waste disposals is wide and involve full thermo-hydro-chemo-bio couplings, as shown by the Table. In most cases, relevant experimental techniques have been developed, starting generally in saturated state and then going to unsaturated states. This is typically the case for heat transfer properties, water retention properties and the propagation of soluble chemicals through advection and diffusion processes that are of utmost importance in the case of radionuclides. Phase changes also occur due to temperature gradients. They are better known for water but they should also concern other components, as for example hydrocarbon compounds in the case of methane generation.

Figure 2 shows a scheme of a surface waste disposal and provides an illustration of part of the phenomena described in Table 2. Temperature elevation in landfills is due to chemical reactions and affects the compacted bottom liner and the cover liner. The generation of methane and of other possible compounds as well as water evaporation involve temperature and phase changes. The properties of the liner are affected by the temperature increase in the landfill. Possible leaks and subsequent leachate infiltration in the vadose zone may lead to transfer, adsorption or precipitation of chemicals in the ground and in the aquifer. Finally, leaks of immiscible hydrocarbons (with either floating LNAPL or DNAPL penetrating in the aquifer) may

Table 2 Phenomena involved in waste disposal

Disposal	Surface waste disposal: urban, industrial, low activity nuclear waste	Deep waste disposal in rock: nuclear waste
Pollutant	Anything: polar-non polar hydrocarbons, chemical components, heavy metals, biological components, radionuclides	Radionuclides
Geomaterial	Compacted soil: clay liner, attenuation layer, cover liner (vegetation)	Compacted soil: engineered barrier Natural soil or rock: geological barrier
Phenomena	Leaks, leaching, leachate infiltration, ion diffusion, biological action, clogging, heat effects (heat transfer, water evaporation, vapour transfer, water condensation, liquid transfer), evaporation (cover liner), cracking, gas generation due to the decomposition of organic fractions	Water infiltration, confined swelling, microstructure changes, heat effects (heat transfer, water evaporation, vapour transfer, water condensation, liquid transfer), radionuclides diffusion, cracking, evaporation due to venting (galleries), gas generation due to anaerobic corrosion of metals

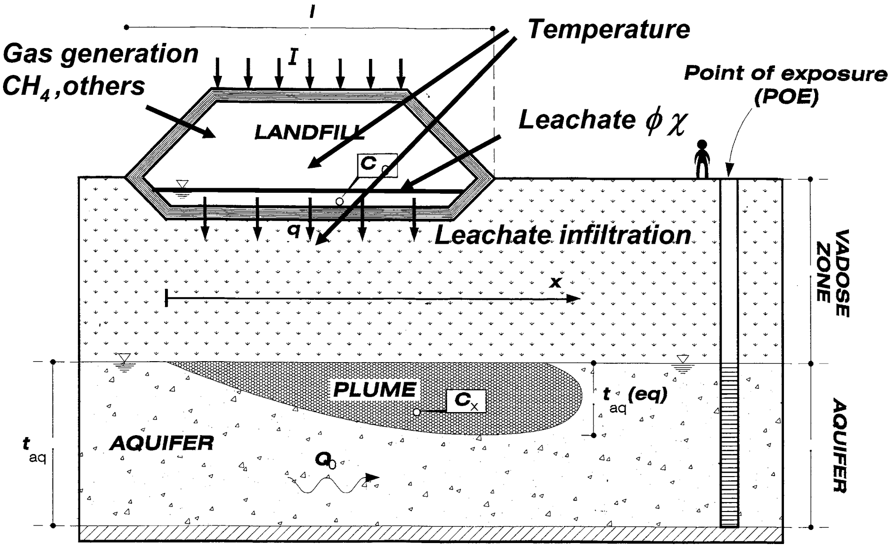

Fig. 2 Schematic scheme of a surface waste disposal (After Di Molfietta and Aglietto 1999)

occur. The cover is submitted either to drying paths due to evaporation or to wetting path due to raining period. One should also mention possible cracking in cover liners and sometimes in bottom liners due to specific reaction between the liners and some chemicals (Fernandez and Quigley 1991). Note that cracking of bottom liners can also appear due to temperature increase (Rowe 2006). Cracking obviously constitutes a serious concern since it can jeopardize the integrity of the liners.

As described in Table 1, gas generation and migration through clay-based barriers is an important design and research issue in waste isolation studies that has attracted increased attention in the last years. The generation of gases in surface waste disposal schemes is mainly associated with waste decomposition processes of the biodegradable organic matter. The decomposition sequence of the organic waste in the landfill is given in two clearly defined stages: one of fermentation and one of methane generation, as depicted in Fig. 2. The concepts of partially saturated soil mechanics allow the unification of the decomposition phenomena, the flow of gases, and the coupled mechanical response of the material. Following these concepts, Caicedo et al. (2002) modelled the gas flow coupled with a settlement analysis in a sanitary landfill. Gas generation is also an important issue in the case of HLW disposal schemes. Several possible mechanisms have been suggested (Ortiz et al. 2002): anaerobic corrosion of the iron contained in the canister with production of hydrogen, which is the largest gas generation source; degradation of organic matter with production of methane and carbon dioxide and radiolysis with production of hydrogen, oxygen, carbon dioxide, methane, etc. This gas generation at the inner boundary of the clay buffer may result in a gas pressure increase given the high degree of saturation and the relative impervious nature to gas flow of the clay barriers. Descriptions of the different gas transport mechanisms and selected testing techniques used to study these mechanisms will be presented in detail further on.

As mentioned in Table 2, many different pollutants can leak from waste disposals. As an example, Schleyer et al. (1988) give in Fig. 3 the 15 pollutants most frequently found below industrial waste sites in Germany and USA (US data taken from Plumb and Pitchford 1985). The importance of aliphatic chlorinated hydrocarbons (and particularly tetrachloroethene) is clear on both countries, with apparently much more frequent occurrence in the USA than in Germany. Note also the presence of aromatic hydrocarbons from the group of BTEX (benzene, toluene, ethylbenzene and xylene). For some reasons, all these compounds (that include many immiscible non polar fluids) have leaked through the liners and infiltrated in the vadose zone. The concern is to know, as shown in Fig. 2, if the aquifer or any point of exposition can be potentially reached.

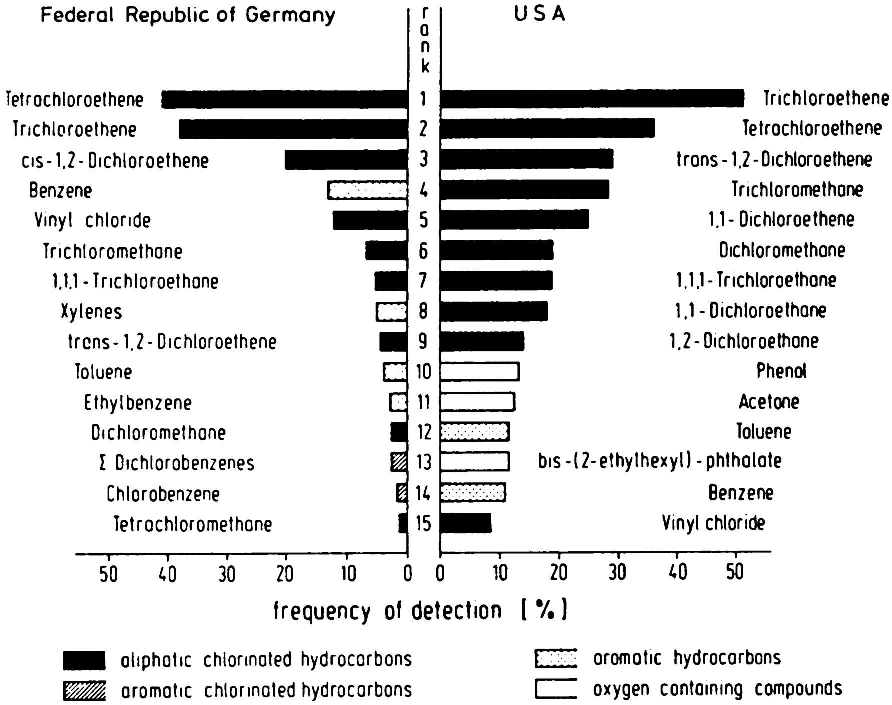

Fig. 3 The 15 most often pollutants detected below waste disposals in Germany and the USA (Schleyer et al. 1988)

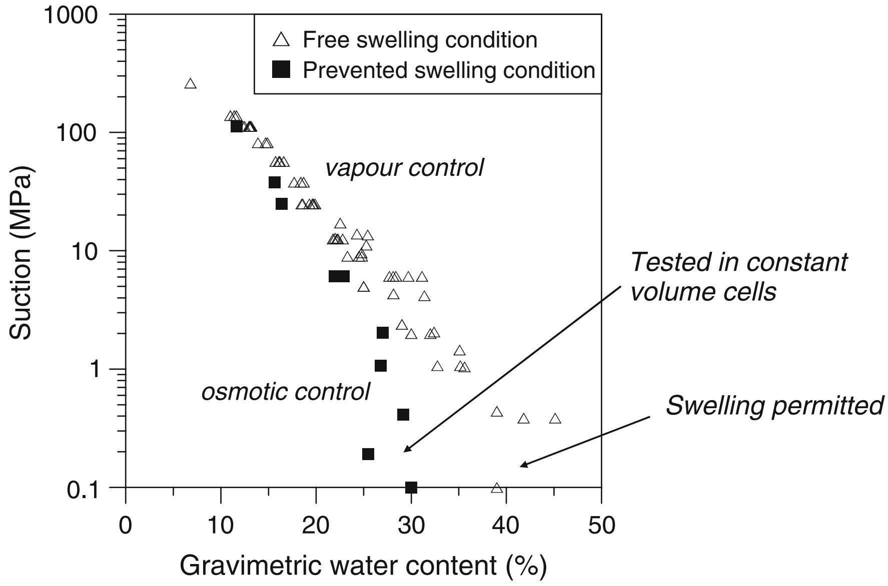

Fig. 4 Water retention properties of an engineered barrier of compacted bentonite (Yahia-Aissa et al. 2001)

3 Geoenvironmental Testing Methods

3.1 Water Retention and Transfer Properties

Compacted liners of surface waste disposal that are compacted wet of optimum are generally tested, in the laboratory or in-situ, by using standard saturated soil techniques that will not be commented here. Important research has been recently conducted to investigate the retention properties of engineered barriers that are made up of heavily compacted swelling clays. In the as-compacted state, these barriers have very high initial suctions (various tens of MPa) due to their high activity in terms of clay-water interactions. For this reason, many researchers adopted the technique of controlling suction by vapour control (see for instance Delage et al. 1998a). Following Esteban Moratilla (1990) and Oteo-Mazo et al. (1996), the technique has also been adapted on various geotechnical devices such as oedometer or isotropic compression equipments (Yahia-Aissa et al. 2000; Tang and Cui 2006; Hoffmann et al. 2005) or triaxial apparatuses (Blatz and Graham 2000).

Figure 4 (Delage et al. 1998a; Yahia-Aissa et al. 2000) shows the water retention curves of compacted FoCa7 clay determined by using both the vapour control technique and the osmotic technique. A remarkable reversibility in water content evidencing negligible hysteresis was observed under suction cycles in this clay. This trend was not observed on engineered barriers made up of other bentonites. In order to better simulate the in-situ conditions of engineered barriers, retention curves with swelling impeded were also investigated. To do so, special rigid cylindrical metal containers have been designed with vapour exchanges made possible on both sides through perforated metal plates (see Fig. 5). Compacted samples are 5 cm diameter and 1 cm high and each of the metal disk placed on both sides of the sample has been perforated with about 100 holes (diameter 0.5 mm). Figure 4 shows that retention in swelling clays with no volume change significantly affects the retention properties at suctions lower than 7 MPa. This difference is to be accounted for when trying to predict the water infiltration phase from the geological barrier into the engineered barrier.

Note that the effects of the changes in microstructure of a compacted bentonite with no swelling allowed

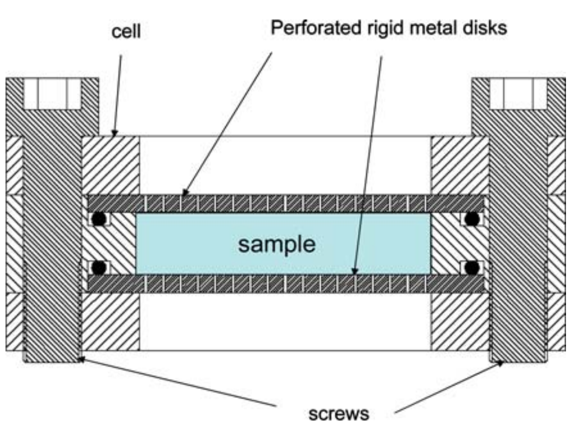

Fig. 5 Special cells designed for determining the water retention properties of swelling clay with no volume change (Yahia-Aissa 2000)

also have an effect on the water movements in the bentonite, as shown by Loiseau et al. (2002). By investigating the changes in permeability of a compacted bentonite during water infiltration by using the instantaneous profile method, these authors observed that the standard increase in relative water permeability during infiltration (as water content increases) was not observed. On the contrary, the relative water permeability was observed to decrease during infiltration, due to the progressive clogging of the inter-aggregate pores by the expanding hydrated aggregates. Also, this phenomenon is seldom accounted for in calculations, in which standard changes in partial permeability with water saturation are adopted.

3.2 NAPL Retention and Transfer Properties

NAPL infiltration in the vadose zone obeys to standard phenomena that control multiphase flow transfers in porous media. Note that, besides the infiltration of NAPLs in the vadose zone, the infiltration of DNAPL in a saturated soil also corresponds to a multiphase problem involving capillary interactions between water and DNAPL (Schwille 1988; Kueper et al. 1989; Bezuijen et al. 2000). Thus, standard experimental techniques developed in unsaturated soils can be adapted and used.

As for water flow in unsaturated soils, two constitutive parameters are necessary to predict NAPL transfers in unsaturated soils: the NAPL retention curve of the soil and the change in NAPL permeability with respect to the degree of saturation in NAPL. Infiltration in granular soils mainly involve capillarity whereas other physico-chemical effects also take place in fine grained soils in the clay fraction, in the organic fraction and along the oxides components (see for instance Lagaly 1984). As in unsaturated soils, techniques of controlling the “matrix” air-oil suction account for both capillary and physico-chemical soil-fluid interactions.

Early investigation carried out to investigate the retention properties of three phase fluid systems were aimed at confirming the Leverett (1941) proposal to extend the data from two phase retention curves to three phase fluid systems (under the hypothesis of negligible fluid-solid surface interactions). To do so, Lenhard and Parker (1988) developed a special cell with specially treated porous ceramics to control and monitor liquid movements and pressures (Fig. 6). In

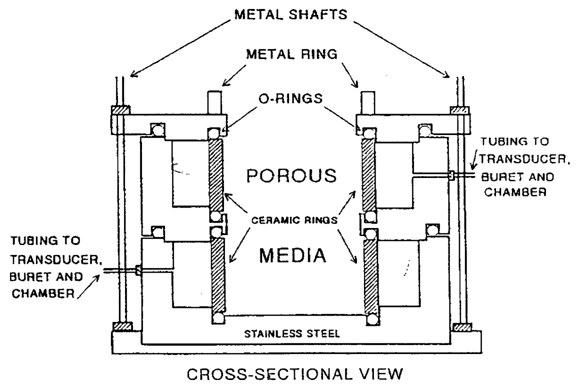

Fig. 6 Cross sectional view of the three phase retention cell developed by Lenhard and Parker (1988)

this system, a cylindrical sample of soil is placed in a cell composed of two ceramic high air entry value (HAEV) rings, respectively hydrophilic and hydrophobic (by using a Glassclad 18 solution). Negative fluid pressures were applied by applying vacuum, volume changes were monitored by using burettes and the negative fluids pressures were measured by using standard tensiometers (maximum suction 80 kPa). Steffy et al. (1997) used the cylindrical retention cell shown in Fig. 7 where two hydrophobic and hydrophilic porous plates were placed on both sides of the sample**.** Low negative fluid pressures were applied by the difference in fluid levels. In a carbonate sand sample containing water and decane, they observed a residual water saturation of 20% under a tension of 1 m of water (10 kPa).

In order to provide a relevant system for fine grained soils in which higher values of oil-air suction are expected, Cui et al. (2003) developed an axis translation cell with hydrophilic and hydrophobic ceramic porous stones placed on both faces of a cylindrical sample (30 mm high and 70 mm in diameter), shown in Fig. 8. In this device, the air pressure is imposed through the lateral connection and the oil volume exchanges are monitored with an inclined tube. The retention curves presented in Fig. 9 have been determined on a low plastic silt (I_p = 19) compacted at a dry density of 1.6 Mg/m^3 on the dry side of Proctor optimum (water content w = 15%, initial degree of saturation in water S_{rwi} = 60.7%) and the wet side of Proctor optimum (w = 21.5%, S_{rwi} = 82.6%). The samples were

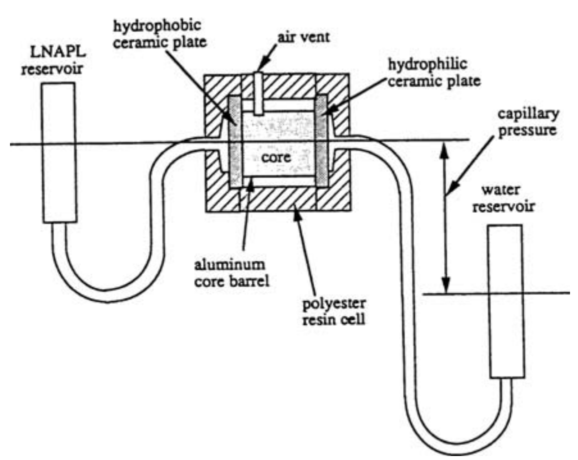

Fig. 7 Retention cell for LNAPL developed by Steffy et al. (1997)

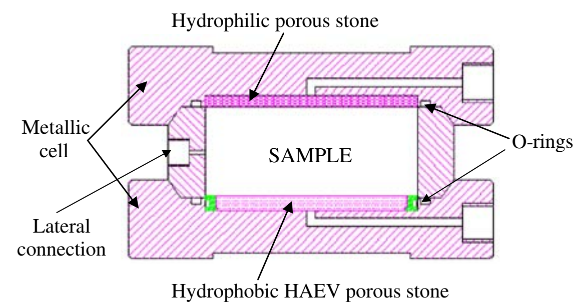

Fig. 8 Retention cell for NAPL developed by Cui et al. (2003)

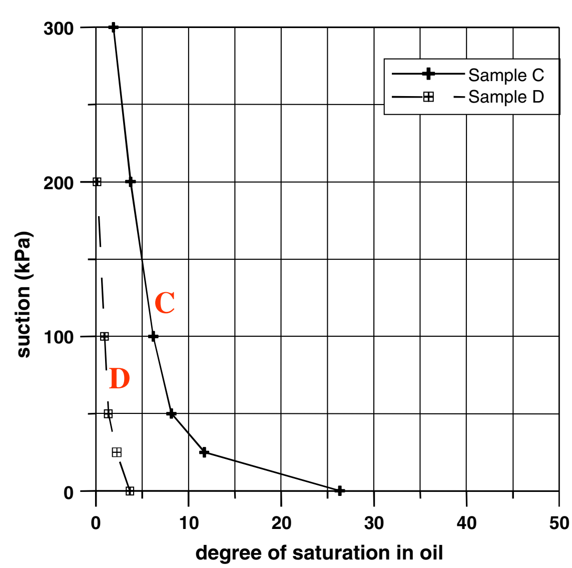

Fig. 9 NAPL retention curves of samples of a compacted silt (Cui et al. 2003). S_{ro}: degree of saturation in oil. Dry density ρ_d = 1.6 Mg/m^3. C: dry side of optimum with w = 15% (S_{rwi} = 60.7%). D: wet side of optimum with w = 21.5% (S_{rwi} = 82.6%)

initially soaked with Soltrol 170, a LNAPL with low volatility and low toxicity currently used in soil contamination investigations. The curves show that the Soltrol contained in the wetter sample is expelled at an air-oil suction of 200 kPa whereas a degree of saturation in oil of 2% is observed at a suction of 300 kPa in the drier sample. By using an axis-translation oedometer, Manassero et al. (2005) and Rabozzi et al. (2006) also investigated the retention curves and hydraulic properties of compacted soil samples contaminated with Soltrol.

Oil relative permeability is generally derived from oil retention properties and from pore size distribution models since few direct methods of determining the oil relative permeability have been published. In this regard, Cui et al. (2003) used the Gardner (1956) method of determining the unsaturated oil permeability of silt. This transient method consists in applying at $t = 0$ an increment of air pressure and to monitor the oil expulsion with time. An inverse analysis based on a simplified procedure to solve Richards's equation allows the determination of the relative oil permeability. Impedance effects due to the low permeability of the ceramic porous stone are accounted for using the Kunze and Kirkham (1962) approach.

As commented by Kechavarzi et al. (2005), few one-dimensional experiments have been developed to study the behaviour of NAPL in the unsaturated zone (Eckberg and Sunada 1984; Reible et al. 1990; Lenhard et al. 1993). More recently, an effort has been made in the developments of two-dimensional experiments in either homogeneous or heterogeneous sands (Pantazidou and Sitar 1993; Van Geel and Sykes 1994; Oostrom et al. 2003; Sharma and Mohamed 2003; Kechavarzi et al. 2005 among others). Various devices have been used in the laboratory to monitor the progression of the NAPL in the sand mass, as shown, as an example, in Fig. 10 (Sharma and Mohamed 2003). In this experiment where the oil infiltration is visually monitored through the direct observation of the change in shape and position of the interface through a glass wall, various sensors have been used. Time domain reflectometry (TDR) sensors have been used to monitor the change in water content whereas water and oil tensiometers have been placed at several locations to monitor the change in water or oil suction. To do so, the ceramic porous cups of the

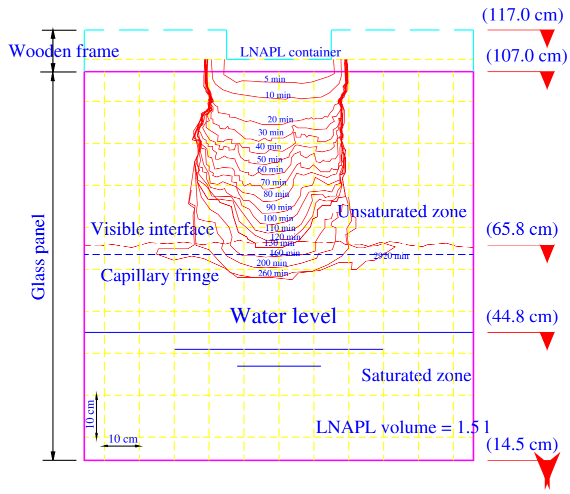

Fig. 10 A reduced scale model of LNAPL infiltration in a sand (Sharma and Mohamed 2003)

sensors have been saturated either with water or with oil after having previously treated the porous cup to render it hydrophobic (by immersing the cups in chlorotrimethylsilane for 2 h followed by thorough rinsing in toluene and methanol as suggested by Lenhard and Parker 1988). Being the sand non deformable, the changes in degree of saturation in water could be derived from TDR measurements, allowing for the simultaneous determination of the degree of saturation in oil. Simultaneous measurements of the suctions allowed the determination of the fluid retention properties of the sand, which appeared to present a residual degree of saturation in water of 12% at a suction of 34 cm of water. Similarly, Kechavarzi et al. (2005) used, in a two-dimensional laboratory test, water resistivity probes (Kechavarzi and Soga 2002) to monitor changes in water contents and tensiometers to measure suction in water and LNAPL. In this experiment, an image analysis technique developed by Kechavarzi et al. (2000) was used to determine LNAPL, water and air saturation distribution. Images where taken by using a digital near infra red camera and the saturation profiles were determined based on the measurement of the optical density defined for the reflected luminous intensity of the sample (a sand containing air, water and LNAPL).

As for other geoenvironmental problems, centrifuge testing has proven to be relevant for the investigation of transfer phenomena of NAPLs (Lord 1999) and it has been quite often used, mainly in

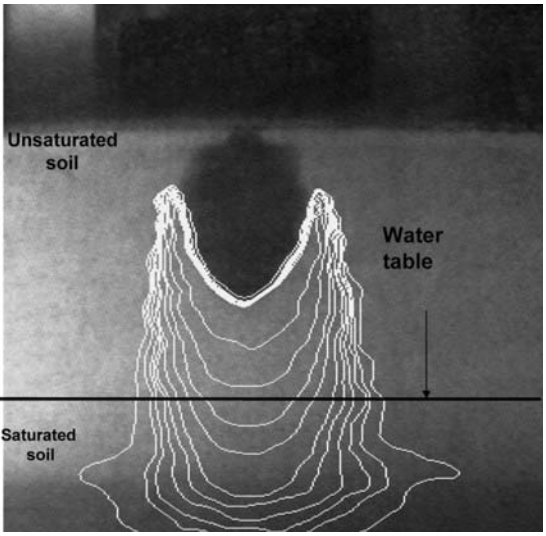

Fig. 11 Infiltration of a plume of DNAPL observed in the centrifuge (taken from NECER 2000)

granular media (sand or glass beads, Illangasekare et al. 1991; Knight and Mitchell 1996; Esposito et al. 1999; Pantazidou et al. 2000; NECER 2000, among others). Note however that Lo et al. (2004) compared the migration behaviour of BTEX (Benzene, Toluene, Ethylbenzene and O-Xylene) in a sand and in a clayey silt ($I_p = 11.8$) and found some significant differences in their migration patterns and retention behaviour. Various sensors have been used in centrifuge experiments, such as miniature resistivity probes and water tensiometers to measure water saturation and water pressures changes during centrifuge tests (Soga et al. 2000; Kechavarzi and Soga 2002; Chiu et al. 2005). Theses devices also allow the determination of the water retention curve of the soil used in the centrifuge test. Most often, the evolution of the NAPL plume during infiltration is monitored optically by analysing photographs taken at various times, as seen in Fig. 11 where the infiltration of DNAPL through the vadose zone and the water table is observed.

3.3 Temperature Effects

Temperature effects on saturated soils have been a subject with a long experimental research tradition that has recently attracted intense attention regarding soft argillaceous rocks and stiff clays, because they constitute the geological host media in deep disposal of nuclear waste (Hueckel and Peano 1996). Experimental studies on the effect of temperature on saturated clay-based materials have been recently reported by Burghignoli et al. (2000), Delage et al. (2000), Graham et al. (2001), Sultan et al. (2002), Cekerevac and Laloui (2004), and Cekerevac et al. (2005). Extension of these studies to unsaturated engineered barriers made up of compacted swelling clays has been conducted more recently, mainly regarding the determination of water retention curves (Romero et al. 2001a; Tang and Cui 2005; Duarte et al. 2005; Villar et al. 2005a) and the determination of thermal conductivity properties (Tang and Cui 2006; Duarte et al. 2006). In contrast, available information concerning temperature effects on the mechanical behaviour of unsaturated soils is more limited, in spite of its practical relevance; a situation caused, at least in part, by the experimental difficulties presented below. There is a need to examine more systematically the combined effects of suction and temperature on the mechanical behaviour of unsaturated soils under more controlled conditions. Basic questions concerning the sensitivity to temperature of swelling potential, soil collapsibility and soil shrinkage, or the effects of temperature on the stress path dependency of soil deformation and shear strength properties remain still unanswered in unsaturated soils. To achieve such an understanding it is necessary to perform tests under the simultaneous control of suction and temperature. A main challenge is the design of a reliable controlled-suction apparatus capable of working at elevated temperatures. Regarding thermo-mechanical aspects under partially saturated states, Saix and Jouanna (1990) and Saix (1991) reported the first experimental results in this area using low suction values. Recordon (1993) and Wiebe et al. (1998) studied the effects of thermal loading in partially saturated soils at constant water content, i.e. without suction control.

Standard experimental techniques used in unsaturated soils to control suction (axis translation, osmotic and vapour equilibrium techniques) have been adapted and used for hydro-mechanical testing at elevated temperatures. Axis translation and osmotic techniques are limited to low suctions (below 1.5 MPa when using axis translation with standard high air-entry value (HAEV) ceramic discs, and below 9 MPa (Delage et al. 1998a; Delage and Cui 2008) when using the osmotic technique), whereas vapour equilibrium covers with reasonable precision the upper suction range from 3 to 1000 MPa. Axis translation technique has demonstrated its applicability to study the combined effects of partial saturation and temperature on hydro-mechanical soil behaviour. However, a carefully controlled setup with auxiliary devices (vapour traps and diffused air flushing/measuring system) is required to use this technique at high temperatures (Fig. 12, Romero et al. 2003). The main problems refer to the control of the relative humidity in the air pressure system, to the thermally-enhanced accumulation of diffused air beneath the HAEV ceramic disc and to the progressive clogging of the ceramic disc due to cation exchange effects through water (Romero et al. 2001b). If relative humidity is not adequately controlled, then water phase changes—i.e., evaporative fluxes between the soil and the air pressure chamber—are not controlled and a progressive drying of the sample can occur. Vapour transfer between the soil upper surface and the air pressure chamber can be minimised with a vapour trap that maintains a high relative humidity in the chamber (Fig. 12).

Taïbi et al. (2005) presented a thermal triaxial cell specially adapted to use the osmotic technique to control suction (Fig. 13) based on the osmotic triaxial apparatus of Delage et al. (1987). Regarding the application of the osmotic technique at high temperatures, some problems that are currently under study are related to the changes of the physical properties of the dialysis membrane with temperature (microstructural and possible pore size changes) and to the thermal sensitivity of the polyethylene glycol solution (thermal dilation and activity, Taïbi et al. 2005). In spite of these limitations, the technique is very promising with regard to the extension of the range for matrix suction application and to the study of the thermo-hydro-mechanical response of nearly saturated soils.

Finally, the application of the vapour equilibrium technique at elevated temperatures has been recently used within different contexts, in order to extend the range of suction application. Romero et al. (2001a), Villar and Lloret (2004), Villar et al. (2005a) and Tang and Cui (2005) used this technique to study the water retention curves of high-active clays at different temperatures, in which soil samples were placed on a rigid grid above a saline solution inside a desiccator that was installed inside a thermostatically controlled chamber. Romero and Li (2005) and Villar and Lloret (2006) implemented the vapour equilibrium technique in oedometer cells to study the thermo-hydro-mechanical behaviour of active partially saturated clays at high temperature. The relative

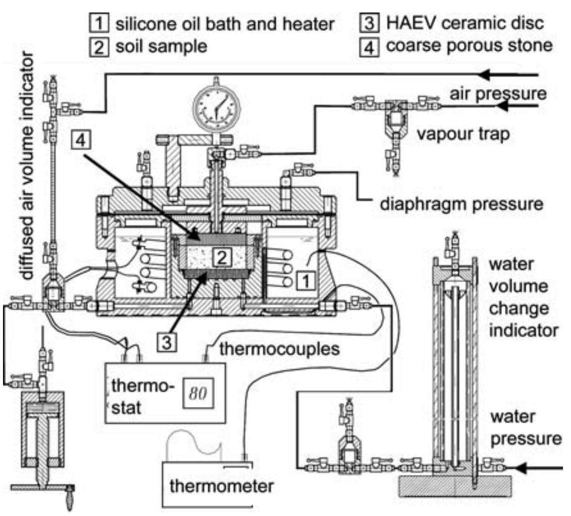

Fig. 12 Schematic layout of the experimental system and oedometer cell with simultaneous control of suction with axis translation and temperature (Romero et al. 2003)

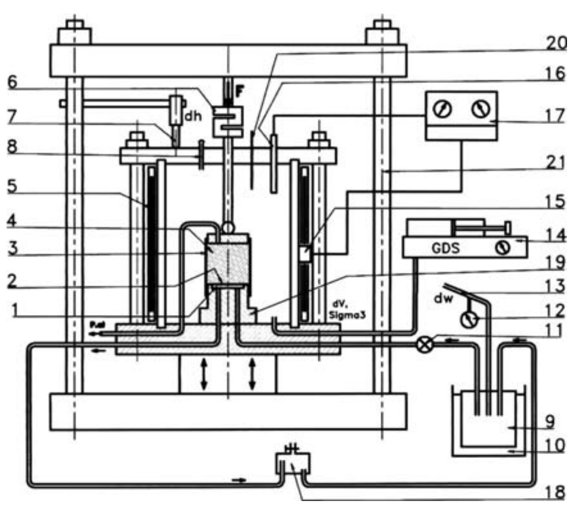

Fig. 13 Triaxial cell with controlled temperature and suction by osmotic technique (Taïbi et al. 2005). 1: Osmotic solution chamber. 2: Dialysis membrane. 3: Neoprene membrane. 4: Sample. 5: Collar heating. 6: Force sensor. 7: Displacement sensor. 8: Purge and thermostat. 9: PEG solution tank. 10: Thermostated bath. 11: Pump. 12: Pressure transducer. 13: Capillary tube. 14: GDS controller. 15: Electrical connector. 16: Pt100 temperature Probe. 17: Temperature regulator. 18: Air trap. 19: Osmotic pedestal. 20: Thermocouple. 21: Mechanical loading frame

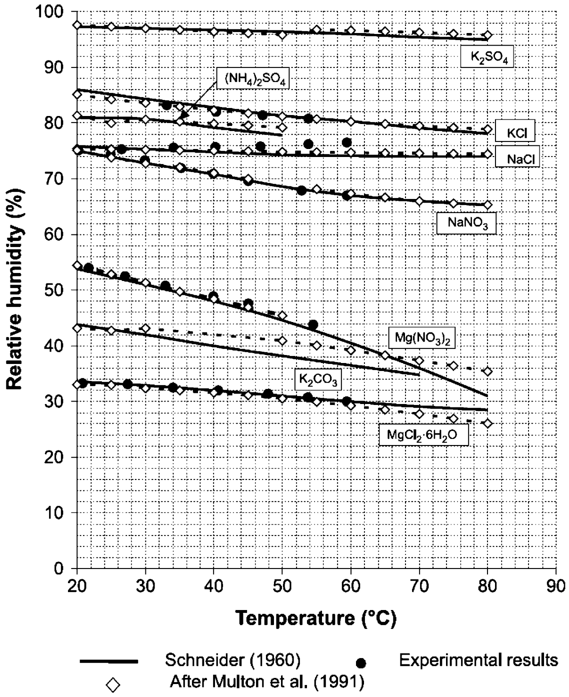

Fig. 14 Changes in relative humidity with temperature for different saturated salt solutions. Comparison of results presented by different authors. (Tang and Cui 2005)

humidity applied by saturated saline solutions varies with temperature, and this variation must be calibrated prior to testing, as shown in Fig. 14. This Figure presents careful calibration results compared to reported data by different authors. In this regard, Tang and Cui (2005) used an experimental setup (Fig. 15) in which a high sensitivity hygrometer and a dew point sensor placed in a constant-temperature water bath were used to measure the relative humidity at various temperatures. One of the main drawbacks of this technique refers to the long term required to reach equilibrium that can be reduced significantly using a forced convection system to transport humid air (Pintado 2002; Marcial 2003). In this last procedure, a pneumatic pump is used to transfer to the soil the humid air generated in a flask that contains a saturated saline solution to regulate the relative humidity. However, when using this last procedure at high relative humidity values and under a temperature field, small variations of temperature between the reference system and the soil can induce relative humidity changes due to temperature effects on the saturated vapour pressure and to the proximity to the dew point temperature.

3.4 Gas Permeability

As mentioned earlier, an important design and research issue in the long term behaviour of waste isolation is the gas generation and migration phenomena arising from metal container corrosion and biogenic gas generation from organic matter decomposition. Laboratory experiments have contributed, jointly with large scale experiments and theoretical/numerical developments, to provide sound knowledge of the mechanisms of gas transport through saturated or partially saturated compacted clay-based barriers and rock formations.

Gas transport through partially saturated soils is not only controlled by the intrinsic permeability and the degree of saturation of the material, but also by the stress state and the stress history (dilatancy-controlled permeability for example), by the microstructure, the temperature and the strength of the material. In this way, tests to study gas permeability must not only be focused on the mere passage of gas through the soil mass, but also on well-posed equipment that are able to apply stress paths by controlling suction and net stress.

The following gas migration mechanisms are usually assumed, which can be simultaneously present in a given material at variable degrees of importance and involving single phase (either liquid or gas) or two phase flow transport (Alonso et al.

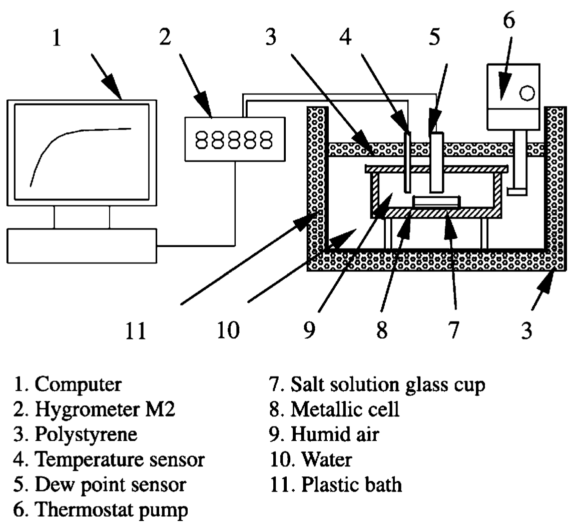

Fig. 15 Experimental setup to apply and calibrate relative humidity generated by a saturated salt solution at different temperatures (Tang and Cui 2005)

2002; Ortiz et al. 2002; Graham et al. 2002; Marshall et al. 2005):

- Gas migrates through the saturated clay transported in the pore water. In this advective-diffusive transport mechanism, gas dissolution in porewater and gas diffusion mechanisms play an important role in the gas transport and mass balance equations. Even at fully saturated state, the gas pressure is defined and assumed as the value it had at the time of saturation (Alonso et al. 2002). Test setups under saturated conditions are usually devoted to seek diffusion coefficients in water, tortuosity, air-filled and total accessible porosity effects, as well as the efficiency of the diffusion and consumption rate coefficients (Moldrup et al. 2000). Gas diffusion tests have been addressed within the context of oxygen-limiting covers for reactive mine tailings (Mbonimpa et al. 2003) and of the diffusion of hydrogen through highly compacted clay barriers for high-level radioactive waste disposal (Volckaert et al. 1995; Lassabatère et al. 2004). A testing setup for the measurement of the diffusion of oxygen through a soil is shown in Fig. 16. The setup includes measuring devices in the source and in the collecting reservoirs (Aubertin and Mbonimpa 2001).
- Gas flows through the clay mass, partially displacing the pore water. This capillary mechanism implies a two-phase advective flow. In this approach, once the gas entry pressure has been exceeded, the gas mobility is assumed to be controlled by the intrinsic permeability, the air/water relative permeability, and the water retention properties (Ortiz et al. 2002; Marshall et al. 2005). However, under the same accessible porosity to gas, gas permeability is also very sensitive to intrinsic permeability variations induced by the suction (hydraulic) history and its effect on the pore size distribution changes of the material (Villar and Lloret 2001; Romero et al. 2005), when testing high active clays under partially saturated conditions. In addition, soil non-homogeneity may also induce preferential paths of gas migration leading to an increase of the pore space and a change in the suction—saturation relationship. Different laboratory equipment, including oedometer, isotropic and triaxial cells have been used to determine the basic properties of the two-phase flow through compacted clayey soils, using constant gas pressure, gas pressure decay methods and constant gas volumetric rate as the gas inlet boundary conditions. Gas permeability test apparatuses under controlled-suction conditions have been described by Kamiya et al. (2005, 2006) using constant gas pressure conditions and by Delage et al. (1998b), Romero et al. (2005) and Villar et al. (2005b) using the gas pressure decay method from a constant volume vessel as initially proposed by Yoshimi and Osterberg (1963). In this last procedure, pressure decay in a tank is recorded and interpreted through an expression that assumes that the air in the tank undergoes isothermal expansion. Figure 17 presents a gas permeability setup under oedometer conditions with constant gas pressures for testing partially

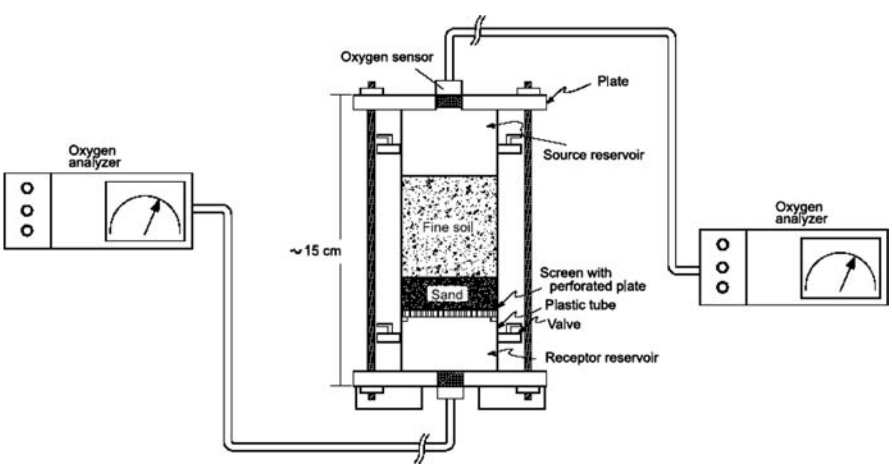

Fig. 16 Scheme of a cell to measure oxygen diffusion flow through a soil. Oxygen measuring devices in the source and in the collecting reservoirs (Aubertin and Mbonimpa 2001)

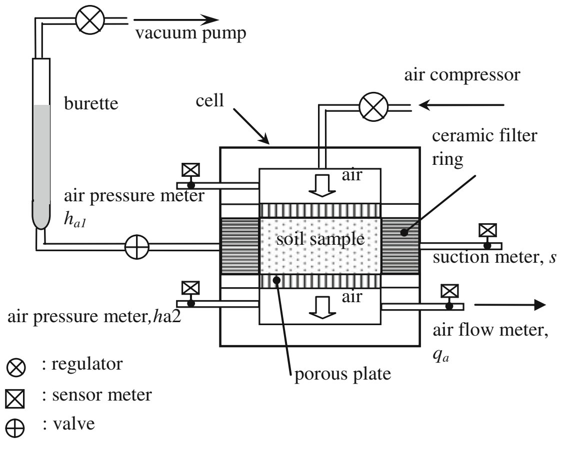

Fig. 17 Diagram of gas permeability test apparatus with constant gas pressure and vacuum pump to control suction (Kamiya et al. 2005)

saturated soils using a vacuum pump to apply suction (Kamiya et al. 2005). Figure 18 presents an alternative experimental layout for gas permeability determination under partially saturated conditions using gas pressure decay methodology, in which suction is applied by axis translation.

– Gas flows through cracks, fissures, compaction planes and interfaces, which are activated by the gas pressure. It is assumed that gas migrates through preferential pathways, the directions of which are expected to be perpendicular to the minor total principal stress component (Ortiz et al. 2002). Gas flow through these fractures can be seen as a dominant single-phase flow process in which no important desaturation of the material is expected—no water displacement is occurring inside the specimen (Horseman et al. 1999; Ortiz et al. 2002; Marshall et al. 2005). This mechanism of propagation is linked to the establishment of flow laws through discontinuities and to the development of fracture criteria to follow crack initiation and propagation. In this way, hydro-mechanical coupling is an important issue—the thickness of the induced air passage of higher transmissibility depends on the stress state and the stiffness of the soil around the passage (Alonso et al. 2002). Gas breakthrough experiments at laboratory scale have been mainly devoted to the study of the effects of volumetric gas injection rate, applied gas pressure, time to breakthrough, of the steady state situation that follows the first passage of gas (post-breakthrough gas migration), of peak pressures and peak discharge rates, outgoing pressure and outflow volumetric gas rates, confining stress, specimen density and degree of saturation. Gas breakthrough phenomena due to the aperture of high conductivity pathways are usually detected at the peak injection pressure or after a sudden increase in the gas outflow measured downstream of the sample. In addition, flow visualization of the gas pathways of higher conductivity is also an important issue, which has attracted recent attention. Different techniques, such as electric impedance tomography (Borsic et al. 2005) and the use of gas tracers have been proposed for the detection of gas flow paths. Experimental research on this topic, in which a constant gas injection rate has been used to increase the gas pressure to the point of breakthrough, has been reported by Horseman et al. (1999) on saturated soils using isotropic stress conditions, and by Gallé (2000), Hume (1999) and Graham et al. (2002) using constant volume oedometer cells. Figure 19 shows a scheme of the experimental gas migration testing system for gas breakthrough pressure determination with constant volumetric gas injection rate. Regarding unsaturated soils, Gallé (2000) and Graham et al. (2002) obtained gas breakthrough pressures for various degrees of saturation and dry densities. They observed that the breakthrough pressure increases as the degree of

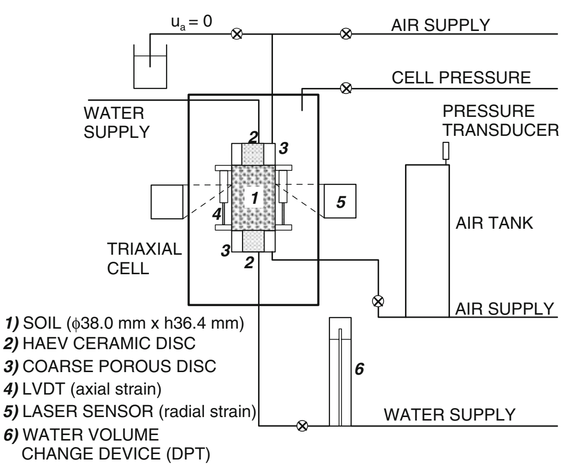

Fig. 18 Controlled-suction isotropic cell with axis translation technique and experimental layout for gas pressure decay method to determine gas permeability (Romero et al. 2005)

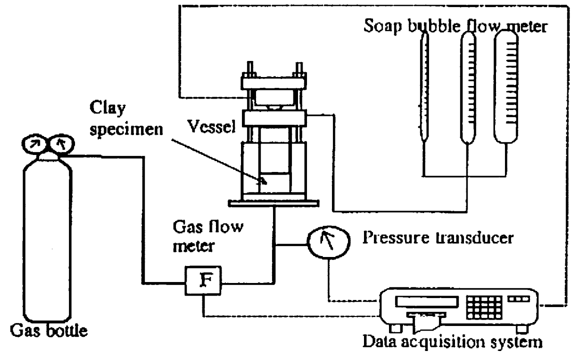

Fig. 19 Experimental setup of a gas migration system with controlled gas injection rate and a constant volume oedometer cell (Tanai et al. 1997; Gallé 2000)

saturation increases, the increase being more sudden—the resistance to gas migration increases sharply—at degrees of saturation higher than 95% as shown in Fig. 20 for a wide range of bentonite dry densities varying from 0.95 to 1.45 Mg/m^3.

3.5 Chemical Aspects

In saturated soils, the interaction between a chemical compound and a soil is investigated by determining the adsorption isotherms that give the amount of adsorbed chemical compound as a function of its concentration in a solution that also contains some quantity of remoulded soil. This technique does not account for any microstructure effect since it is carried out in batch configurations.

Adsorption in unsaturated soils is most often investigated in sands by using instrumented columns of unsaturated sand in which a solution containing either one or various pollutants are infiltrated (Rowe and Badv 1996). In these experiments, the evolution of various profiles with time is monitored: TDR probes are frequently used in recent works for water content profiles and tensiometers are used for measuring low suctions (<80 kPa). The profile of chemical concentration is followed by using electrical conductivity probes previously calibrated in the soil used. The elution curves (also called breakthrough curves) that give the changes in concentration with time in the water outflow are determined by standard concentration measurements made on the water flowing out at the bottom of the column. Figure 21 (Nützmann et al. 2002) shows a column infiltration test (internal diameter 206 mm, height 1.5 m) in which a chloride solution was infiltrated from the top at a controlled rate. The figure shows the disposition of the TDR probes (T_i in the Figure) and platinum probes ($C_{i,i}$) used for the electrical conductivity measurements. This work was carried out to investigate the influence of the effect of partial saturation on the transfer of pollutants. Due to a higher variability of flow directions and microscopic velocities, an increased dispersion was observed in unsaturated sands with a linear relationship between the coefficient of hydrodynamic dispersion and the velocity. As compared with the previous techniques, Inoue et al. (2005) proposed an original approach based on the image analysis of an infiltration column in which dye tracers are infiltrated in an unsaturated porous medium made up of glass beads. These authors derived the dispersion coefficient and dispersivity of the medium.

As commented by Delolme et al. (2004), the interactions between heavy metals and soil components have been described by many authors (e.g. Bourg 1988; Evans 1989; Yong et al. 1992). Interest about the retention and transfer properties of heavy metals into unsaturated soils has been driven by the development of infiltration basins to evacuate urban stormwater as an alternative to directing it towards urban drainage systems. Infiltration occurs through the bottom of the basins that is often composed of coarse sand and it is necessary to investigate the metal transfer properties in the sand. In this case also, infiltration column tests with controlled infiltration rates are carried out. However, due to the difficulty of

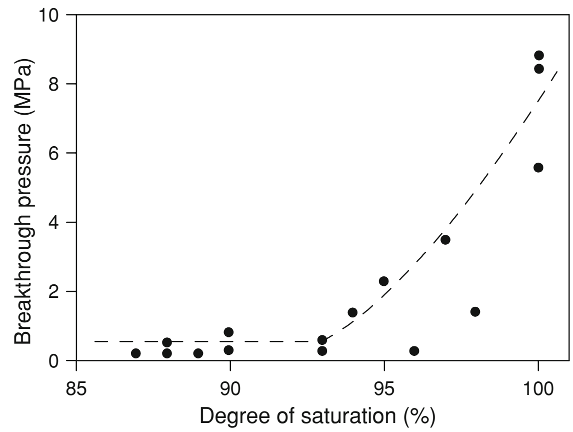

Fig. 20 Breakthrough pressures on bentonite (clay dry densities varying between 0.95 and 1.45 Mg/m^3) as a function of degree of saturation (Graham et al. 2002)

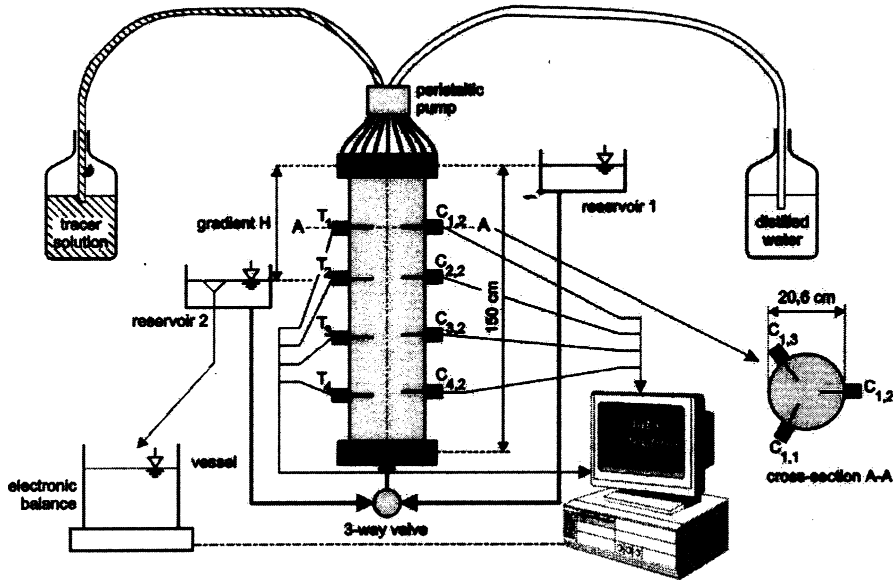

Fig. 21 Infiltration column in which a chloride solution has been infiltrated in an unsaturated sand (Nützmann et al. 2002) (T: TDR probe, C platinum probe)

directly monitoring the changes in metal content inside the sample, retention phenomena are considered through a comparison between the entering and eluted concentrations that are interpreted using back analysis. The adsorption of metal on some reactive site on the silica surface of the sand grains (previously washed with acids) has been identified.

Figure 22 (Alimi-Ichola and Gaidi 2005) presents the results of a column test carried out by infiltrating a leachate through compacted clay. Contrary to the tests on sand columns, this test also accounts for possible adsorption of chemical compounds on clay minerals. TDR and electrical conductivity probes have been used to determine water contents and impedance profiles, with previous calibration of the electrical conductivity of the soil and the leachate. In this figure, the comparison between the profiles gives some interesting information on possible retardation factors and on the combined effects of convection and diffusion on the movement of the solute in an unsaturated compacted soil.

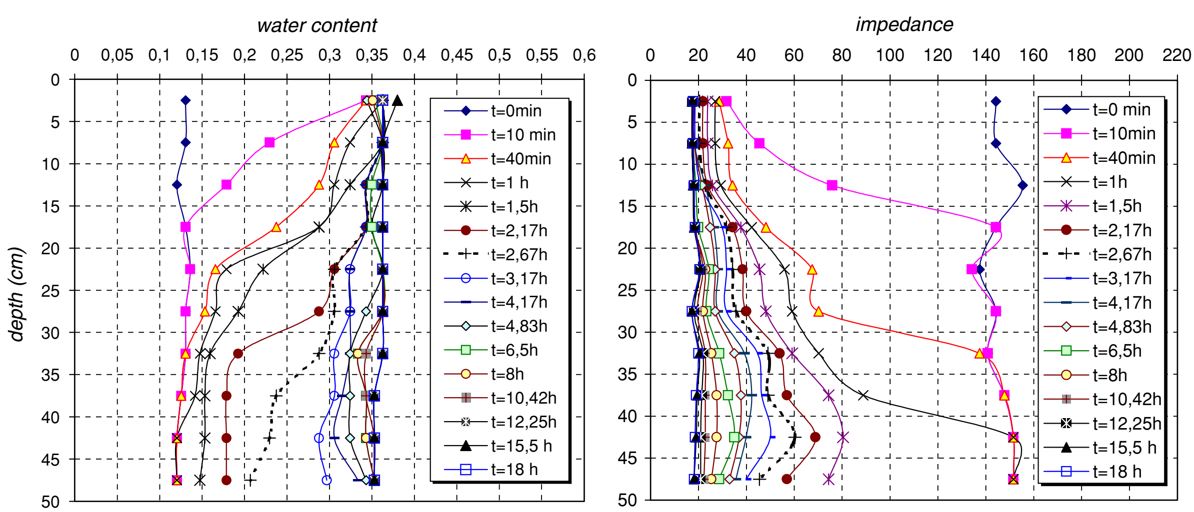

Fig. 22 Simultaneous profiles of water content and impedance, compacted clay infiltrated by a leachate (Alimi-Ichola and Gaidi 2005)

Chemical effects on the behaviour of engineered barriers used in nuclear waste disposal have also been investigated since it is well known that the hydro-mechanical behaviour of smectites is sensitive to the changes in concentration of the pore water and to the valence of the dissolved ions (Di Maio 1996; Marcial et al. 2002; Musso et al. 2003). In this regard, Mata et al. (2002) examined the effect of pore water salinity on the retention properties of a sand/bentonite mixture by using transistor psychrometers (Woodburn and Lucas 1995) to measure total suction. The effect of water salinity on compacted bentonite was also examined by Castellanos et al. (2006) and Villar (2006) who infiltrated compacted specimens with water at various salt concentrations, confirming the reduction of swelling and showing an increase in permeability with increased concentration.

4 Concluding Remarks

Unsaturated soils are involved in geoenvironmental problems such as soil contamination or waste disposal. Experimental unsaturated soil mechanics, that commonly faces the difficulty of investigating hydromechanical couplings and water retention and transfer properties, appears to be a sound basis to extend experimental investigations to the complex problems that are typical of geoenvironmental engineering. Conversely, some techniques used in saturated soils in disciplines also concerned with geoenvironmental problems (hydrology, soil science) appear to be adaptable to unsaturated soils. As shown in this paper, significant extension has been conducted to investigate the retention and transfer properties of non miscible liquids (NAPL) and chemical species in unsaturated soils, also accounting for temperature effects and gas formation and migration. In this regard, recent investigations carried out in the particular field of high activity nuclear waste disposal certainly provided significant advances. Many techniques are now available and their use to improve the practice of soil decontamination and perennial waste disposal will probably appear to be quite fruitful in the future.

Acknowledgements The authors wish to acknowledge the support given by the European Community through the Marie-Curie Research and Training Network MUSE - Mechanics of Unsaturated Soils for Engineering - (MRTN-CT-2004-506861).

References

Alimi-Ichola I, Gaidi L (2005) Etude de la migration du soluté d'un lixiviat dans un sol non saturé par la méthode TDR. Rev Fr Géotechnique 111:45–58

Alonso EE, Olivella S, Delahaye C (2002) Gas migration in clays. In: Vulliet L, Laloui L, Schrefler B (eds) Proceedings of the environmental engineering. Presses Polytechniques et Universitaires Romandes, EPFL, Lausanne, pp 83–94

Aubertin M, Mbonimpa M (2001) Diffusion of oxygen through a pulp and paper residue barrier: discussion. Can Geotech J 38:658–660

Benson CH, Gribb MM (1997) Measuring hydraulic conductivity in the laboratory and in the field. Unsaturated soil in engineering practice, ASCE Geotechnical Special Publication N°68, pp 113–168

Bezuijen A, Oung O, Westrate F (2000) Centrifuge research on the entry pressure and flow of a DNAPL in water-saturated sand. In: Garnier J, Thorel L, Haza E (eds) Proceedings of international symposium on physical modelling and testing in environmental geotechnics. LCPC Paris, pp 335–342

Blatz J, Graham J (2000) A system for controlled suction in triaxial tests. Géotechnique 50(4):465–469

Borsic A, Comina C, Foti S, Lancellotta R, Musso G (2005) Imaging heterogeneities with electrical impedance tomography: laboratory results. Géotechnique 55(7):539–547

Bouazza A, Vangpaisal T, Jefferis S (2006) Effect of wet–dry cycles and cation exchange on gas permeability of geosynthetic clay liners. J Geotech Geoenviron Eng 132(8):1011–1018

Bourg ACM (1988) Metals in aquatic and terrestrial systems: sorption, speciation and mobilization. In: Chemistry and biology of solid waste, Springer-Verlag, Berlin, pp 3–30

Bresler E (1973) Simultaneous transport of solutes and water under transient unsaturated flow conditions. Water Resour Res 9:975–986

Burghignoli A, Desideri A, Miliziano S (2000) A laboratory study on the thermomechanical behaviour of clayey soils. Can Geotech J 37:764–780

Caicedo B, Giraldo E, Behrentz E (2002) Modeling leachate and gas flor in sanitary landfills. In: Jucá JFT, de Campos TMP, Marinho FAM (eds) Proceedings of the 3rd international conference on unsaturated soils, March 10–13, 2002, vol 1. A.A. Balkema Publishers, Lisse, Recife, Brazil, pp 107–112

Castellanos E, Gens A, Lloret A, Romero E (2006) Influence of water chemistry en the swelling capacity of a high density bentonite. Proceedings of the 4rd international conference on unsaturated soils (1), pp 962–972

Cekerevac C, Laloui L (2004) Experimental study of thermal effects on the mechanical behaviour of a clay. Int J Numer Anal Meth Geomech 28:209–228

Cekerevac C, Laloui L, Vulliet L (2005) A novel triaxial apparatus for thermo-mechanical testing of soils. Geotech Test J 28(2):1–10

Chiu CF, Cui YJ, Delage P, De Laure E, Haza E (2005) Lessons learnt from suction monitoring during centrifuge modelling. Proceedings of the international symposium on advanced experimental unsaturated soils mechanics EXPERUS, Trento, Balkema, pp 3–8

Cleall PJ, Melhuish TA, Thomas HR (2006) Modelling the three-dimensional behaviour of a prototype nuclear waste repository. Eng Geol 85:212–220

Cui YJ, Zornberg JG (Ibid.) Water balance and evapotranspiration monitoring in geotechnical and geoenvironmental engineering. Geotech Geol Eng. doi:10.1007/s10706-008-9198-z

Cui YJ, Delage P, Alzoghbi P (2003) Retention and transport of a hydrocarbon in a silt. Géotechnique 53(1), 83–91

Delage P, Suraj De Silva GPR, De Laure E (1987) Un nouvel appareil triaxial pour les sols non saturés. Proceedings of the IX^{e} European conference on soil mechanical and foundation engineering, Dublin, pp 25–28

Delage P, Howat M, Cui YJ (1998a) The relationship between suction and swelling properties in a heavily compacted unsaturated clay. Eng Geol 50(1–2): 31–48

Delage P, Cui YJ, De Laure E (1998b) Air flow through an unsaturated compacted silt. Proceedings of the 2nd international conference on unsaturated soils UNSAT'98, vol. 1, Beijing, 563–568

Delage P, Sultan N, Cui YJ (2000) On the thermal consolidation of Boom clay. Can Geotech J 37:343–354

Delage P, Cui YJ (2008) An evaluation of the osmotic technique of controlling suction. Geomech Geoengin Int J 3(1):1–11

Delolme C, Hébrard-Labit C, Spadini L, Gaudet JP (2004) Experimental study and modelling of the transfer of zinc in a low reactive sand column in the presence of acetate. J Contam Hydrol 70:205–224

De Smet F, Wauters F, Sevilla J (1986) Study of tracer movement through unsaturated sand. J Hydrol 85: 169–181

Di Maio C (1996) Exposure of bentonite to salt solution: osmotic and mechanical effects. Géotechnique 46(4):695–707

Di Molfietta A, Aglietto I (1999) Valutazione dei siti inquinanti mediante analisi dir rischio. Proceedings of the XVII Conference of Geotechnics of Torino

Duarte APL, de Campos TMP, Rocha Filho P, Araruna JT Jr (2005) Temperature effects on the water content-suction relation of two soils. In: Tarantino, Romero, Cui (eds) Proceedings of the international symposium on advanced experimental unsaturated soil mechanics, June 27–29, 2005, Trento, Italy. Taylor & Francis Group, London, pp 453–458

Duarte APL, de Campos TMP, Araruna JT Jr, Rocha Filho P (2006) Thermal properties for unsaturated soils. In: Miller GA, Zapata CE, Houston SL, Fredlund DC (eds) Proceedings of the 4th international conference on unsaturated soils. April 2–6, 2006, Carefree, Arizona. Geotechnical Special Publication No. 147, vol. 2. ASCE, Virginia, pp 1707–1718

Eckberg DK, Sunada DK (1984) Non steady three-phase immiscible fluid distribution in porous media. Water Resour Res 33:569–576

Esposito G, Allersma HGB, Selvadurai APS (1999) Centrifuge modeling of LNAPL transport in partially saturated sand. J Geotech Geoenviron Eng 125(12):1066–1071

Esteban Moratilla F (1990) Caracterizacion experimental de la expansividad de una roca evaporitica. Identificacion de los mecanismos de hinchamiento. PhD thesis, Universidad de Cantabria, Santander, 352 pp

Evans LJ (1989) Chemistry of metal retention by soils. Environ Soil Technol 23:1046–1056

Fernandez F, Quigley RM (1991) Controlling the destructive effects of clay-organic liquid interactions by application of effective stresses. Can Geotech J 28(3):388–398

Fernández-García D, Gómez-Hernández JJ, Mayor JC (2005) Modeling a ventilation experiment: Combined effect of desaturation and EDZ. Geophysical Research Abstracts, vol. 7, 02057, European Geosciences Union

Gallé C (2000) Gas breakthrough pressure in compacted Fo-Ca clay and interfacial gas overpressure in waste disposal context. Appl Clay Sci 17:85–97

Gardner R (1956) Calculation of capillary conductivity from pressure plate outflow data. Proc Soil Sci Soc Am 20: 317–320

Gaudet JP, Jegat H, Vachaud G, Wierenga PJ (1977) Solute transfer with exchange between mobile and stagnant water through unsaturated sand. Soil Sci Soc Am J 41:665–670

Gens A, García-Molina AJ, Olivella S, Alonso EE, Huertas F (1998) Analysis of a full scale in situ test simulating repository conditions. Int J Numer Anal Meth Geomech 22:515–548

Graham J, Tanaka N, Crilly T, Alfaro M (2001) Modified cam-clay modelling of temperature effects in clays. Can Geotech J 38:608–621

Graham J, Halyko KG, Hume H, Kirkham T, Gray M, Oscarson D (2002) A capillarity-advective model for gas break-trough in clays. Eng Geol 64: 273–286

Hoffmann C, Romero E, Alonso EE (2005) Combining different controlled-suction techniques to study expansive clays. Proceedings of the international symposium on advanced experimental unsaturated soils mechanics EXPERUS, Trento, Balkema, pp 61–67

Horseman ST, Harrington JF, Sellin P (1999) Gas migration in clay barriers. Eng Geol 54:139–149

Hueckel, T, Peano, A (eds) (1996) Special issue on thermomechanics of clays and clay barriers. 3rd International workshop of clay barriers, Ismes, Bergamo, Italy, October 2003. Engineering Geology 41

Hume HB (1999) Gas break-through in compacted Avonlea bentonites. MSc Thesis, University of Manitoba, Winnipeg, 169 pp

Illangasekare TH, Znidarcic D, Al Sheridda M, Reible DD (1991) Multiphase flow in porous media. In: Ko HY, McLean FG (eds) Centrifuge '91. Balkema, Rotterdam, pp 517–523

Inoue K, Tanaka T, Inoue K, Kobayashi A (2005) Image analysis to determine the dispersion coefficient and dispersivity in capillary and saturated zone. Proceedings of the international symposium on advanced experimental unsaturated soils mechanics EXPERUS, Trento, Balkema, pp 467–473

Kamiya K, Bakrie RT, Honjo Y (2005) Evaluation of air permeability of unsaturated sandy soils. In: Tarantino A, Romero E, Cui YJ (eds) Proceedings of the international symposium on advanced experimental unsaturated soil mechanics. June 27–29, 2005, Trento, Italy. Taylor & Francis Group, London, pp 369–375

Kamiya K, Bakrie RT, Honjo Y (2006) A new method for the measurement of air permeability coefficient of unsaturated soil. In: Miller, Zapata, Houston, Fredlund (eds) Proceedings of the 4th international conference on unsaturated soils, Carefree, Arizona, vol. 2, Geotechnical Special Publication No. 147, ASCE, Virginia, pp 1741–1752

Kechavarzi C, Soga K, Wiart P (2000) Multispectral image analysis method to determine dynamic fluid saturation distribution in two-dimensional three-fluid phase flow laboratory experiments. J Contam Hydrol 46:265–293

Kechavarzi C, Soga K (2002) Determination of water saturation using miniature resistivity probes during intermediate scale and centrifuge multiphase flow laboratory experiments. J Geotech Test 25(1):95–103

Kechavarzi C, Soga K, Illangasekare TH (2005) Two-dimensional laboratory simulation of LNAPL infiltration and redistribution in the vadose zone. J Contam Hydrol 76:211–233

Knight MA, Mitchell RJ (1996) Modelling of light nonaqueous phase liquid (LNAPL) releases into unsaturated sand. Can Geotech J 33:913–925

Kueper BH, Abbott W, Farquhar G (1989) Experimental observations of multiphase flow in heterogeneous porous media. J Contam Hydrol 5:83–95

Kunze RJ, Kirkham D (1962) Simplified accounting for membrane penetration in capillary conductivity determination. Proc Soil Sci Soc Am.26:421–426

Lagaly G (1984) Clay-organic interactions. Phil Trans Royal Soc Lond A 311:315–332

Lassabatère T, Dridi W, Servant G (2004) Gas transfer and mechanical incidence on storage barriers. Appl Clay Sci 26: 511–520

Lenhard RJ, Parker JC (1988) Experimental validation of the theory of extending two phase saturation-pressure relations to three fluid phase system for monotonic drainage paths. Water Resour 24(3):373–380

Lenhard RJ, Johnson TG, Parker JC (1993) Experimental observation of non aqueous phase liquid subsurface movement. J Contam Hydrol 12:79–101

Leverett MC (1941) Capillary behaviour in porous solids. Trans Am Inst Metall Eng (142):152–169

Lo IMC, Hu LM, Meegoda JN (2004) Centrifuge modeling of light nonaqueous phase liquids transport in unsaturated soils. J Geotech Geoenviron Eng 130(5):535–539

Loiseau C, Cui YJ, Delage P (2002) The gradient effect on the water flow through a compacted swelling soil. Proceedings of the 3nd international conference on unsaturated soils, UNSAT'2002 (1), Recife, Brazil, Balkema, pp 395–400

Lord AE (1999) Capillary flow in the geotechnical centrifuge. Geotech Test J 22(4):292–300

Maciejewski S (1993) Numerical and experimental study of solute transport in unsaturated soils. J Contam Hydrol 14:193–2065

Manassero M, Musso G, Rabozzi C, Ribotta L (2005) Retention curves for a polluted soil. Proceedings of the international symposium on advanced experimental unsaturated soil mechanics, Trento, Balkema, pp 459–465

Marcial D (2003) Comportement hydromécanique et microstructural des matériaux de barrière ouvragée. PhD Thesis, École nationale des ponts et chaussées, Paris, France. In French

Marcial D, Delage P, Cui YJ (2002) On the high stress compression of bentonites. Can Geotech J 39(4):812–820

Marshall P, Horseman S, Gimmi T (2005) Characterisation of gas transport properties of the Opalinus Clay, a potential host rock formation for radioactive waste disposal. Oil Gas Sci Technol–Rev IFP 60(1):121–139

Masrouri F, Bicalho KV, Kawai K (2008) Hydraulic testing in unsaturated soils. Geotech Geol Eng. doi:10.1007/s10706-008-9202-7

Mata C, Romero E, Ledesma A (2002) Hydro-chemical effects on water retention in bentonite-sand mixture. In: Recife, Brazil. Jucá, de Campos, Marinho (eds) Proceedings of the 3rd international conference on unsaturated soils, vol 1. A.A. Balkema Publishers, Lisse, pp 107–112

Mayor JC, García-Sineriz JL, Velasco M (2006) Desaturation effects in Opalinus clay. Geophysical research abstracts, vol. 8, 02294, European Geosciences Union

Mbonimpa M, Aubertin M, Aachib M, Bussière B (2003) Diffusion and consumption of oxygen in unsaturated cover materials. Can Geotech J 40(5):916–932

Moldrup P, Olesen T, Schjønning P,Yamaguchi T, Rolston DE (2000) Predicting the gas diffusion coefficient in undisturbed soil from soil water characteristics. Soil Sci Soc Am J 64:94–100

Musso G, Romero-Morales E, Gens A, Castellanos E (2003) The role of structure in the chemically induced deformation of FEBEX bentonite. Appl Clay Sci (23):229–237

NECER (2000) In: Garnier J, Thorel L, Haza E (eds) Proceedings of the international symposium on physical modelling and testing in environmental geotechnics. La Baule, LCPC Paris

Nützmann G, Maciejewski S, Joswig K (2002) Estimation of water saturation dependence of dispersion in unsaturated porous media: experiments and modelling analysis. Adv Water Resour 25:565–576

Oostrom M, Hofstee C, Lenhard RJ, Wietsma TW (2003) Flow behaviour and residual saturation formation of liquid carbon tetrachloride in unsaturated heterogeneous porous media. J Contam Hydrol 64:93–112

Ortiz L, Volckaert G, Mallants D (2002) Gas generation and migration in Boom clay, a potential host rock formation for nuclear waste storage. Eng Geol 64:287–296

Oteo Mazo C, Saez Aunon J, Esteban F (1996) Laboratory tests and equipment with suction control. In: Alonso EE, Delage P (eds), Proceedings of the 1st international conference on unsaturated soils UNSAT'95 3, Paris, Balkema, Rotterdam, pp 1509–1515

Pantazidou M, Sitar N (1993) Emplacement of nonaqueous liquids in the vadose zone. Water Resour Res 29:705–722

Pantazidou M, Abu-Hassanein ZS, Riemer M (2000) Centrifuge study of DNAPL transport in granular media. J Geotech Geoenv Eng 126(2):105–115

Pintado X (2002) Caracterización del comportamiento termo-hidro-mecánico de arcillas expansivas. PhD Thesis, Universitat Politècnica de Catalunya, Barcelona, Spain. In Spanish

Plumb RH, Pitchford AM (1985) Volatil organic scans: implications for groundwater monitoring. Proceeedings of the natural water well association/American petroleum institution conference on petroleum hydrocarbons and organic chemicals in groundwater, Houston, Texas, pp 1–15

Rabozzi C, Ribotta L, Gremigni G (2006) Retention curves and hydraulic properties of a soil contaminated by NAPL. Proceedings of the 5th international conference on environmental geotechnics, vol 2, pp 1232–1239

Recordon E (1993) Déformabilité des sols non saturés à diverses températures. Revue Française de Géotechnique 69:37–56

Reible DD, Illangasekare TH, Doshi DV, Malheit ME (1990) Infiltration of immiscible contaminant in the unsaturated zone. Groundwater 28:685–692

Romero E, Li XL (2005) Thermo-hydro-mechanical tests using vapour and liquid transfer on a clay-based mixture. In: Tarantino A, Romero E, Cui YJ (eds) Proceedings of the international symposium on advanced experimental unsaturated soil mechanics. June 27–29, 2005, Trento, Italy. Taylor & Francis Group, London, pp 483–488

Romero E, Gens A, Lloret A (2001a) Temperature effects on the hydraulic behaviour of an unsaturated clay. Geotech Geol Eng 19: 311–332

Romero E, Gens A, Lloret A (2001b) Laboratory testing of unsaturated soils under simultaneous suction and temperature control. Proceedings of the 15th international conference on soil mechanical and geotechnical and engineering, Istambul. A.A. Balkema/Swets & Zeitlinger B.V., Lisse, vol. 1, pp 19–622

Romero E, Gens A, Lloret A (2003) Suction effects on a compacted clay under non-isothermal conditions. Géotechnique 53(1): 65–81

Romero E, García I, Knobelsdorf J (2005) Gas permeability evolution of a sand/bentonite during controlled-suction paths. In: Tarantino, Romero, Cui (eds) Proceedings of the international symposium on advanced experimental unsaturated soil mechanics. June 27–29, 2005, Trento, Italy. Taylor & Francis Group, London, pp 385–390

Rowe RK (2005) Long-term performance of contaminant barrier systems. Géotechnique 55(9):631–678

Rowe RK (2006) Some factors affecting geosynthetics used for geoenvironmental applications. Proceedings of the 5th international conference on environmental geotechnics, pp 43–69

Rowe RK, Badv K (1996) Advective diffusive contaminant migration in unsaturated sand and gravel. ASCE J Geotech Eng 122(12):965–975

Saix C (1991) Consolidation thermique par chaleur d'un sol non saturé. Can Geotech J 28:42–50

Saix C, Jouanna P (1990) Appareil triaxial pour l'étude du comportement thermique d'un sol non saturé. Can Geotech J 27:119–128

Schwille F (1988) Dense chlorinated solvents in porous and fractured media model experiments. Lewis Publishers, Boca Raton, Florida, 146 pp

Sharma RS, Mohamed MHA (2003) Patterns and mechanisms of migration of light non-aqueous phase liquid in an unsaturated sand. Géotechnique 53(2):225–239

Schleyer R, Arneth JD, Kerndorff H, Milde G (1988) Main contaminants and priority pollutants from waste sites: criteria for selection with the aim of assessment on the groundwater path. Contaminated soil '88 2, Kluwer, pp 247–251

Soga K, Kechavarzi C, Coumoulos H., Shu S., Kawabata J., Esposito G, Allersma HGB (2000) Centrifuge modelling of water drainage and LNAPL infiltration in unsaturated soil deposits. In: Garnier J, Thorel L, Haza E (eds) Proceedings of the international symposium on physical modelling and testing in environmental geotechnics, LCPC Paris, pp 293–300

Steffy DA, Barry DA, Johnston CD (1997) Influence of antecedent moisture content on residual NAPL saturation. J Soil Contam 6(2):113–147

Sultan N, Delage P, Cui YJ (2002) Temperature effects on the volume change behaviour of Boom clay. Eng Geol 64:135–145

Taïbi S, Ghembaza MS, Fleureau (2005) On the suction control techniques in studying the THM behaviour of unsaturated soils. In: Tarantino A, Romero E, Cui YJ (eds) Proceedings of the international symposium on advanced experimental unsaturated soil mechanics, Trento, Italy. Taylor & Francis Group, London, pp 69–75

Tanai K, Kanno T, Gallé C (1997) Experimental study of gas permeabilities and breackthrough pressures in clays. Proceedings of the fall meeting of the material research society, Boston, USA, vol. 465, pp 995–1002

Tang AM, Cui YJ (2005) Controlling suction by the vapour equilibrium technique at different temperatures and its application in determining the water retention properties of MX80 clay. Can Geotech J 42:287–296

Tang AM, Cui YJ (2006) Determining the thermal conductivity of compacted MX80 clay. In: Miller, Zapata, Houston, Fredlund (eds) Proceedings 4th international conference on unsaturated soils, Carefree, Arizona. Geotechnical Special Publication No. 147, vol. 2, ASCE, Virginia, pp 1695–1706

Van Geel PJ, Sykes JF (1994) Laboratory and model simulations of a LNAPL spill in variably-saturated sand: 1. Laboratory experiment and image analysis techniques. J Contam Hydrol 17:1–25

Villar MV (2006) Infiltration tests on a granite/bentonite mixture: influence of water salinity. Appl Clay Sci (31):96–109

Villar MV, Lloret A (2001) Variation of the intrinsic permeability of expansive clays upon saturation. In: Adachi K, Fukue M (ed) Clay science for engineering. Balkema, Rotterdam, pp 259–266

Villar MV, Lloret A (2004) Influence of temperature on the hydromechanical behaviour of a compacted bentonite. Appl Clay Sci 26:337–350

Villar MV, Martín PL, Lloret A (2005a) Determination of water retention curves of two bentonites at high temperature. In: Tarantino A, Romero E, Cui YJ (eds) Proceedings of the international symposium on advanced experimental unsaturated soil mechanics. June 27–29, 2005, Trento, Italy. Taylor & Francis Group, London, pp 77–82

Villar MV, Romero E, Lloret A (2005b) Thermo-mechanical and geochemical effects on the permeability of high-density clays. Proceedings of the international symposium on large scale field tests in granite. Advances in understanding engineered clay barriers. In: Alonso EE, Ledesma A (eds) A.A. Balkema Publishers, Leiden, pp 177–191

Villar MV, Lloret A (2006) Experimental investigation on the mechanical behaviour of unsaturated bentonite at high temperature. In: Miller, Zapata, Houston, Fredlund (eds) Geotechnical Special Publication No. 147, vol. 2. ASCE, Virginia, pp 1719–1730

Volckaert G, Ortiz L, De Cannière P, Put M., Horseman ST, Harrington JF, Fioravante V, Impey MD (1995) MEGAS: Modelling and experiments on gas migration in repository host rocks. Final report-Phase 1. CEC Nuclear Science & Technology Series, Luxembourg, European Commission Report EUR 16235 EN

Wiebe B, Graham J, Tang G X, Dixon D (1998) Influence of pressure, saturation and temperature on the behaviour of unsaturated sand-bentonite. Can Geotech J 35:194–205

Woodburn JA, Lucas B (1995) New approaches to the laboratory and field measurements of soil suction. In: Alonso EE, Delage P (eds) Proceedings of the 1st international conference on unsaturated soils, vol 2. Balkema/Presses des Ponts et Chaussées, Paris, pp 667–691

Yahia-Aissa M (2000) Comportement hydromécanique d'une argile gonflante fortement compactée. PhD thesis, Ecole Nationale des Ponts et Chaussées, Paris

Yahia-Aissa M, Delage P, Cui YJ (2000) Volume change behaviour of a dense compacted swelling clay under stress and suction changes. Experimental Evidence and Theoretical Approaches in Unsaturated Soils, Trento, Balkema, pp 65–74

Yahia-Aissa M, Delage P, Cui YJ (2001) Suction-water relationship in swelling clays. In: Adachi K, Fukue M (eds) Clay science for engineering, IS-Shizuoka International symposium on suction, swelling, permeability and structure of clays, Balkema, pp 65–68

Yong RN, Mohammed AMO, Warkentin BP (1992) Principles of contaminant transport in soils. Elsevier, Amsterdam, 327 pp

Yoshimi Y, Osterberg JO (1963) Compression of partially saturated cohesive soils. J Soil Mech Found Div. ASCE SM4:1–24

Field Measurement of Suction, Water Content, and Water Permeability

Alessandro Tarantino · Andrew M. Ridley · David G. Toll

Originally published in the journal *Geotechnical and Geological Engineering*, Volume 26, No. 6, 751–782.
DOI: 10.1007/s10706-008-9205-4

Abstract This paper presents a review of techniques for field measurement of suction, water content, and water hydraulic conductivity (permeability). Main problems in the use of field tensiometers are addressed and hints on how to improve tensiometer performance are given. Advantages and limitations of instruments for indirect measurement of suction including electrical conductivity sensors, thermal conductivity sensors, dielectric permittivity sensors, filter paper, and psychrometer are discussed. Techniques for water content measurement based on dielectric methods are then presented. These include time and amplitude domain reflectometry and capacitance. Finally, a brief overview of methods for measurement of water permeability in the field is presented.

Keywords Field monitoring · Partially saturated soil · Suction · Water content · Tensiometer · Porous block sensors · Psychrometer · Filter paper · TDR sensor · ADR sensor · Capacitance sensor

A. Tarantino (✉)
Dipartimento di Ingegneria Meccanica e Strutturale, Università degli Studi di Trento, Via Mesiano, 77, 38050 Trento, Italy
e-mail: tarantin@ing.unitn.it

A. M. Ridley
Geotechnical Observations Limited, London, UK

D. G. Toll
School of Engineering, University of Durham, Durham, UK

1 Introduction

The state of knowledge in experimental and theoretical unsaturated soil mechanics is ripe for transferring unsaturated soil concepts into engineering practice. In recent years, significant progress has been made in laboratory and field testing (Ridley and Burland 1993; Ridley and Wray 1996; Romero 1999; Delage 2004), constitutive modelling (Alonso et al. 1990; Vaunat et al. 2000; Gallipoli et al. 2003) and numerical modelling (Olivella et al. 1996; Gatmiri and Delage 1997; Gatmiri et al. 1997; Alonso et al. 1998). In addition, commercial software for modelling the hydro-mechanical coupled behaviour of unsaturated soils has become available. However, the implementation of unsaturated soil mechanics into engineering practice is hampered by lack of field data, needed to assess the capability of models and approaches.

Variables controlling the hydro-mechanical behaviour of unsaturated soils include soil variables such as suction, water content, and temperature and also boundary variables such as precipitation, air temperature, air relative humidity, wind speed, total and net solar radiation. This report will focus on the soil variables whereas boundary variables are examined in another report in this issue (Cui and Zornberg, this issue).

DOI: 10.1007/978-1-4020-8819-3_10

Reviews of techniques for direct and indirect suction measurement have been presented by Marinho et al. (this issue) and Bulut and Leong (this issue) respectively. Although these methods have been discussed with reference to laboratory measurement, basic working principles, capabilities, and limitations of these techniques generally apply also to field measurement. This report will then focus on problems specific to field applications.

On the other hand, measurement of water content based on dielectric methods is exclusively discussed in this report and much room will be given to these methods. Numerous reviews have been published in the literature on dielectric methods (O'Connor and Dowding 1999; Gardner et al. 2001; Noborio 2001; Dane and Topp 2002; Jones et al. 2002; Robinson et al. 2003a). Here, an attempt is made to provide the essential elements of the dielectric methods and to help new users to systematize the large information available in the literature in several hundreds of technical papers. The overview will be limited to conventional practice as advanced use of these techniques requires knowledge which is generally outside the geotechnical engineer's background.

Measurement techniques based on neutron method will not be discussed herein. Radiation hazard precludes semipermanent installation and hence automation, and acquisition, use, transport, storage and eventual disposal of neutron probe is subject to strict regulation because of the potential hazard to human health and the environment. Nowadays, the neutron method tends to be replaced by dielectric methods. The reader may refer to the literature for further details (Gardner et al. 2001; Hignett and Evett 2002).

Finally, a brief overview for methods to determine the hydraulic conductivity in the field is presented. Again, methods for investigating the hydraulic conductivity in the laboratory have been discussed in a separate report (Masrouri et al., this issue) and only applications to field measurement will be discussed.

2 Direct Measurement of Suction

The instruments used for measuring pore water pressures are called piezometers. Where piezometers have been specifically designed for measuring water stress states that are below the prevailing atmospheric pressure condition the devices have been given the specific name of tensiometers.

The essential components of both piezometers and tensiometers are the same, namely: a porous filter; a reservoir of liquid (usually water) and a means of measuring stress. Piezometers and tensiometers work by allowing water to move between the water reservoir of the instrument and the soil until the water stress state in both is equal. If the porous filter is located below the prevailing ground water table, water will flow from the ground into the instrument causing a positive pressure to develop in the reservoir of liquid. If the porous filter is located above the prevailing ground water table, water can be drawn out of the instrument and into the soil, causing tension to develop in the reservoir of liquid.

To function correctly in the field, tensiometers require a forth component: a means of removing air (if it forms) from the reservoir of liquid. In addition, to maximise the range of measurements in the field it is necessary to establish a system in which the pressure sensor and the porous filter are located at the same elevation. These two aspects of field tensiometers have not always been appreciated and continue to give the most problems for the measurement of suctions in the field.

2.1 Historical Development of Tensiometers

2.1.1 Pre 1950 Tensiometers

The first tensiometers were developed in the early 1900's (Livingston 1908; Lynde and Dupre 1913). They were developed to investigate the capillary tensions generated in soil by small plants as they grew. In 1928, Richards (1928) developed a tensiometer, which for the first time took the classic features and shape that have been commonly adopted since (see Fig. 1). It consisted of a porous filter formed out of ceramic material and a reservoir of water connected to a mercury manometer. Air could be removed from Richards' tensiometer by removing a rubber bung at the top of the porous filter and refilling the system with de-aired water. Through the 1930s and 1940s Richards reported many improvements to tensiometers and covered many of the essential aspects of their design (Richards et al. 1937; Richards 1942, 1949).

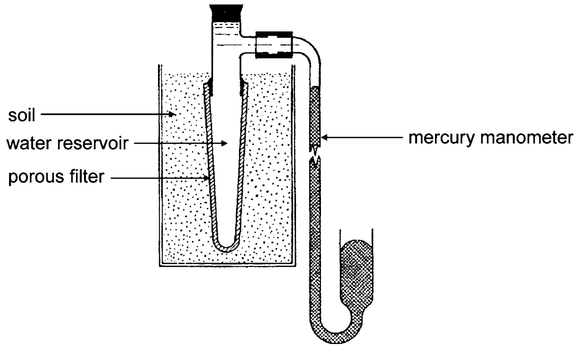

Fig. 1 An early tensiometer (after Richards 1928)

2.1.2 Tensiometers in the 1950's and 1960's

In the 1950's the significance of pore water tensions began to be appreciated by engineers and workers at the Road Research Laboratory started to investigate the movement of water in soil beneath paved areas. Black et al. (1958) published a hugely underestimated piece of work on this subject. Their report presented a tensiometer (Fig. 2) with all the classic features, which was capable of continuous measurements of pore water tensions as high as 90 kPa. However, the most significant aspect of their publication was an acknowledgement of tensile measurements as high as 60 ft of water (about 200 kPa). The ability to record tensions hitherto unrecognised in the field of soil mechanics was attributed to the use of very fine porous filters, although the means of filling the tensiometers with water was almost certainly a contributory factor. Previously de-aired water was introduced into the tensiometers by drawing it through the very fine porous filters using a vacuum, thus avoiding the possibility of trapping air within the tensiometer. Without any trapped air in the tensiometer and with a fine grained porous filter, which was capable of inhibiting air from entering into the reservoir of de-aired water, the water could sustain tensions greater than those normally associated with nucleation. Unfortunately, the possibility that water could sustain tensions greater than 1 atmosphere (approximately 100 kPa) was, at the time, not properly understood and it would be another four decades before this property of water could be properly exploited for the measurement of soil suctions.

Bishop et al. (1964) introduced a piezometer for use in the compacted fills of earth dams with a flushing system for removing air from the piezometer (Fig. 3). They noted that the hydraulic tensions in their piezometers would gradually reduce as air diffused through the porous filters, thereby replacing the liquid in the piezometers. By removing the air they were able to record tensions close to those that had been measured before the air had formed (Fig. 4). The magnitude of the hydraulic tension that could be measured by the Bishop "twin-tube" piezometer was reduced by increases in the elevation separating the porous filter and the pressure sensor (in this case a Bourdon gauge) and was limited by the porosity of the porous filter. To maximise the range of the measurements Bishop placed the gauge at the same level as the porous filter and ran the tubes, used for circulating the water and removing the air, horizontally through the fill. Problems were introduced however when settlements caused variations in elevation along the tubes. In extreme circumstances the strains introduced would break the tubes but more seriously the variation in elevation made it difficult to remove air from the piezometers.

2.1.3 Tensiometers in the 1970's and 1980's

During the 1970s and 1980s various instruments evolved from the Bishop apparatus, which used small bore tubing to connect a porous filter to a Bourdon gauge (e.g. Fig. 5). Sweeney (1982) used this method to successfully make discrete measurements inside a deep shaft, thereby overcoming the range limitation caused by elevation differences and simplifying the de-airing procedure. Chipp et al. (1982) linked a series of porous filters to a single electrical pressure sensor using a rotating valve (known as a scanivalve), which connected the small bore tubing of each measuring filter in turn to the pressure sensor and isolated the remaining tubes (Fig. 6). Air was removed manually from the space behind the porous filter through a bleed tube. Measurements up to 60 kPa were recorded, but problems were encountered because of leakage as the scanivalve was rotated. Moreover, deep measurements were only possible by installing tensiometers at discrete depths inside an exploratory shaft.

At the same time technology drifted back towards the measurement of soil suction for agricultural purposes. A range of tensiometers was developed for the measurement of suctions in the range 0 to

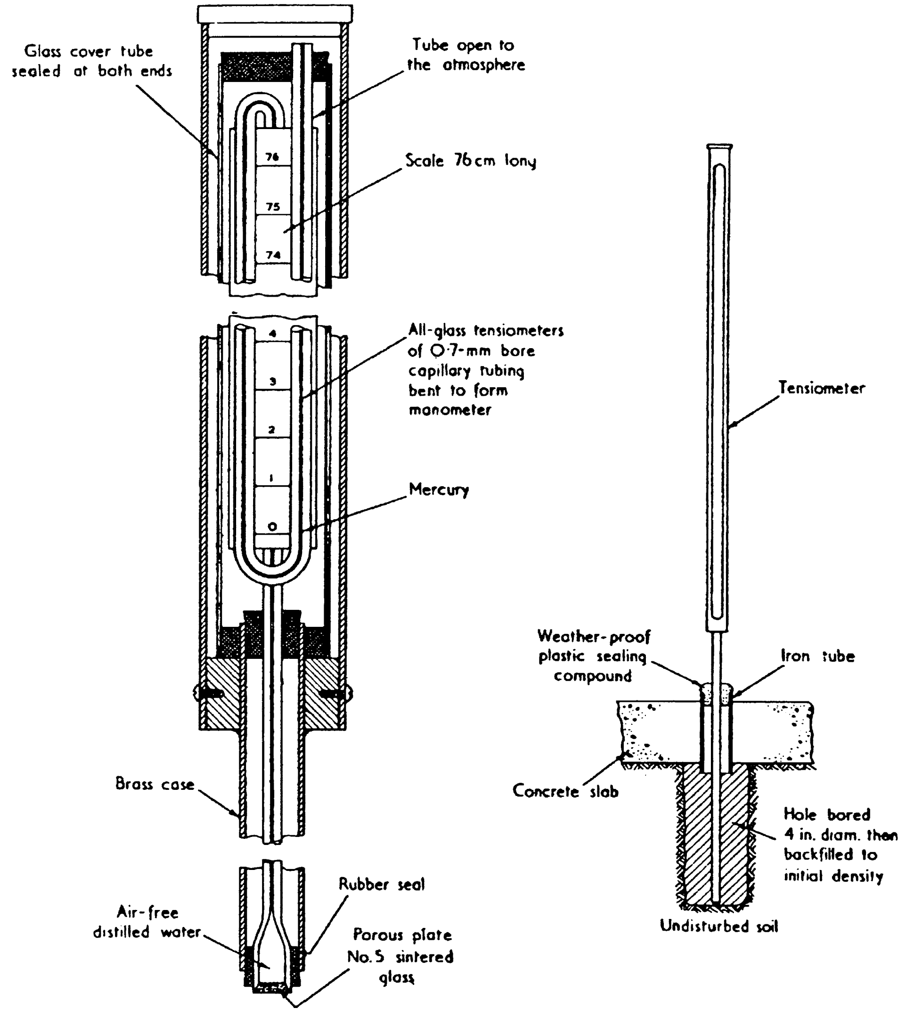

Fig. 2 Tensiometer developed by the Road Research Laboratory (after Black et al. 1958)

40 kPa. This is the range over which crops grow best. At suctions greater than 40 kPa cereals struggle to remove moisture from soil, whereas if the suction becomes zero the soil becomes waterlogged and the crops die. Therefore the requirement for limiting the elevation separating the porous filter and the pressure sensor became less important and elevation differences of up to 3 m became acceptable without reducing the range below that for which the instrument had been designed. The so called "jet-fill" tensiometer (Fig. 7) is named because of the supplementary reservoir located at the top of the instrument, which is used to allow air to escape and the reservoir of water to be re-filled. Ridley et al. (1998) showed that the useful range of these tensiometers was really only 0 to 50 kPa for an instrument that was 1.5 m in length, because at suctions greater than 50 kPa the formation of air in the instrument becomes uncontrollable and too rapid to be removed manually. Scotto di Santolo et al. (2005) reported similar results. Moreover if the formation of air is not arrested, the tensiometer eventually becomes completely dry and the gauge indicates a tension of zero. This can easily be confused with a real measurement of zero, which would be indicative of "wet" conditions and obviously grossly incorrect.

2.2 Recent Developments in Tensiometers

In the 1990s the range of measurements was maximised by once again placing the pressure sensor at the same depth as the porous filter. Öberg (1995) used BAT piezometers to measure suctions at depths of 20 m. In the BAT piezometer the pressure sensor is

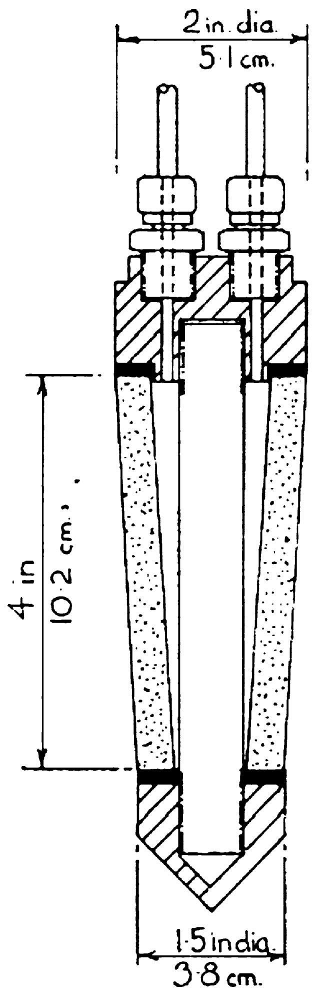

Fig. 3 A twin-tube flushable piezometer (after Bishop et al. 1964)

linked to the reservoir of water through a hyperdermic needle (Fig. 8). The process used to remove air from these piezometers involves the application of a vacuum in situ, which draws air from the reservoir of water. Ridley and Burland (1993) introduced the concept of measuring suctions greater than 100 kPa. Ridley and Burland (1995) presented a new tensiometer, which could measure suctions up to 1,500 kPa (Fig. 9). The new tensiometers use a combination of fine porous filters (capable of remaining saturated to 1,500 kPa) and a technique of preconditioning the instrument (previously used by physicists to apply and measure tension in water) by pressurising the water in the instrument to very high pressures (e.g. 4,000 kPa). The hydraulic tension can then be maintained in the tensiometers whilst they remain

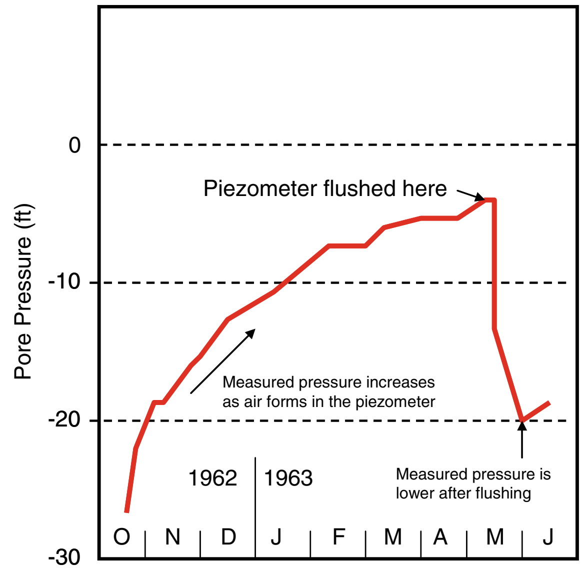

Fig. 4 Pore pressures measured with "twin-tube" piezometer (after Bishop et al. 1964)

saturated. If air forms in the reservoir of the tensiometer the tension will reduce instantly to −1 Atmosphere and the water in the tensiometer must be re-pressurised. A technique was developed (Ridley and Burland 1996) for placing the new tensiometers at depths up to 5 m. However, to remove air from the tensiometers using the pressurisation technique, it is necessary to remove them from the ground. Recent developments by Cui et al. (2008) and Mendes et al. (2008) show that tensiometers can be left insitu for long-term measurements.

Ridley et al. (2003) introduced a refinement of the Bishop "twin-tube" piezometer (Fig. 10) in which the pressure sensor is located adjacent to the porous filter and in which the tubes used to remove air from the piezometer and introduce fresh de-aired water can be isolated by a valve close to the filter and the sensor, thereby maximising the range of measurements irrespective of the depth to which the filter and the sensor are installed. These piezometers are installed in boreholes, which are subsequently filled with a cement-bentonite grout. Therefore they can be installed throughout a site without the need for expensive shafts. The grout acts as a secondary filter for transmitting the negative pore water pressures from the soil to the piezometer. If it is designed correctly the grout will not desaturate until the suction is equal to or greater than 100 kPa and therefore it

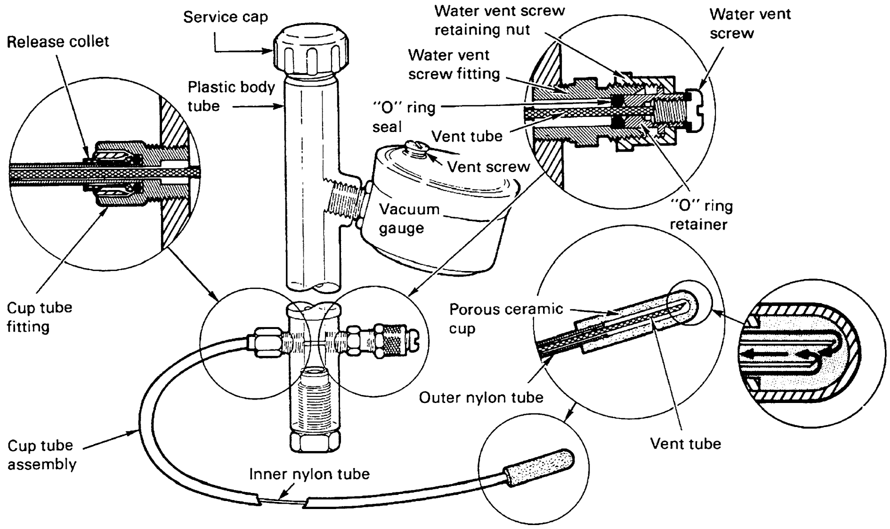

Fig. 5 Small tip tensiometer with flexible tubing (from Soilmoisture Equipment Corporation)

will not restrict the range of suctions that can be measured by the tensiometers. Moreover, if the piezometer has a small volume of water it is easy to show that, for a wide range of soils, the permeability of the grout will not influence the response of the piezometer to changes of pore water pressure. Table 1 shows the air entry values and permeabilities of three grout mixes together with the typical properties of a porous ceramic filter. Figure 11 shows a measurement of −80 kPa at a depth of 6 m in clay fill, which demonstrates that the new piezometers can be used to measure suctions up to 100 kPa at any depth. The new piezometers also respond rapidly to changes of pore water pressure (see Fig. 12). This can be particularly important in environments where the ground has a relatively high permeability and intensive rain storm events occur. Such events can cause temporary rises of pore water pressure, which are capable of inducing conditions that can bring about instability in slopes. The new piezometer is better suited to these situations than conventional tensiometers, which may not respond rapidly enough to detect such rapid rises of pore water pressure (Evans and Lam 2003).

2.3 Recommendations

To summarise the principal problems when making suction measurements in the field are (i) inhibiting air forming in the tensiometers as the suctions are measured, (ii) removing the air if it does form and (iii) maximising the range of suction measurements. Air can be inhibited from forming by (a) using a high air entry ceramic filter, (b) minimising the volume of water in the tensiometer and (c) pre-pressurising the water in the tensiometer. Unfortunately minimising the volume of water would make removing air from the tensiometer difficult and pre-pressurising the water is difficult to do without removing the tensiometer from the ground. Therefore, until recently, continuous field measurements of suction using tensiometers were restricted to the low suction range (i.e. less than 90 kPa). There are a wide variety of suitable instruments for doing this, but many of them require a shaft to be constructed in order to maximise the range of measurements that can be made. Ideally the three essential components (the pressure sensor, the reservoir of water and the porous filter) should be located as close as possible to each other and the volume of water in the piezometer should be as small as possible whilst allowing the incorporation of a system for removing air from the tensiometer. A new piezometer has been introduced (Ridley et al. 2003) that has all of these attributes, can measure negative pore water pressures to −95 kPa and positive pressures up to 65 kPa. Finally, it is essential that there is continuity between the soil water and the water in the piezometer at all times. Cement-bentonite grout has been shown to work well in this respect, remaining saturated to suctions in excess of 100 kPa.

3 Indirect Measurement of Suction

This section aims at updating the state-of-the-art report by Ridley and Wray (1996) who have

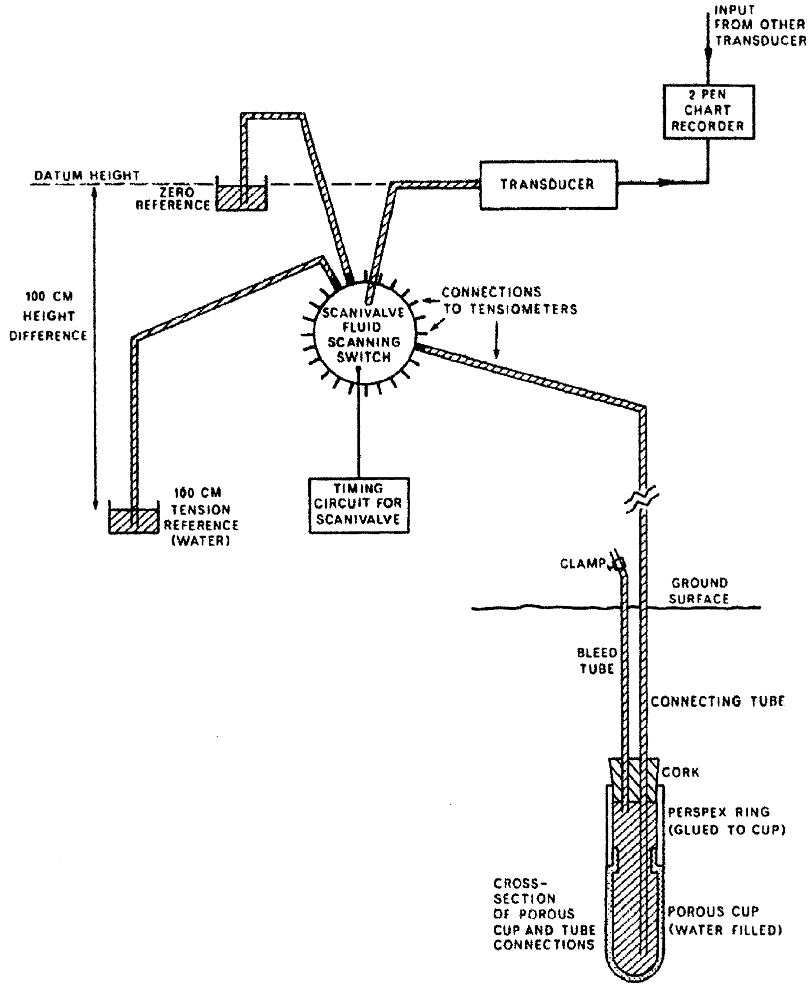

Fig. 6 Scanivalve system for reading and de-airing multiple tensiometers (after Chipp et al. 1982)

previously reported on techniques for indirect measurement of suction. Reference should also be made to the report by Bulut and Leong (this issue) who describe the devices and their operating principles. This section focuses on field applications using three main types of device for indirect measurement of suction: porous block sensors which include electrical conductivity, thermal conductivity and dielectric permittivity (equitensiometer) sensors, filter paper methods and psychrometers.

3.1 Electrical Conductivity Sensor

Electrical conductivity sensors rely on the measurement of the electrical conductivity of the porous block which is related to the water content of the block. The porous element is either of gypsum or a granular matrix of silt size (Watermark™ sensors). Such devices are generally inexpensive, but are more suitable for trend measurement rather than accurate determinate of suction.

Electrical conductivity is affected by soil salinity (Aitchison et al. 1951), so calibrations for these devices are needed to take account of saline soils. Gypsum blocks have the advantage that they tend to buffer the soil salinity thereby decreasing this effect. They do this by dissolution of the gypsum, which means that gypsum block sensors have a limited life. Skinner et al. (1997) suggest a life of 5 years in alkaline or neutral soils but they usually need to be replaced every 2–3 years in acid soils. Johnston (2000) reports that suctions recorded with gypsum blocks at two field sites compared favourably with filter paper estimates for suction, provided the blocks were individually calibrated (range −20 to −2,100 kPa).

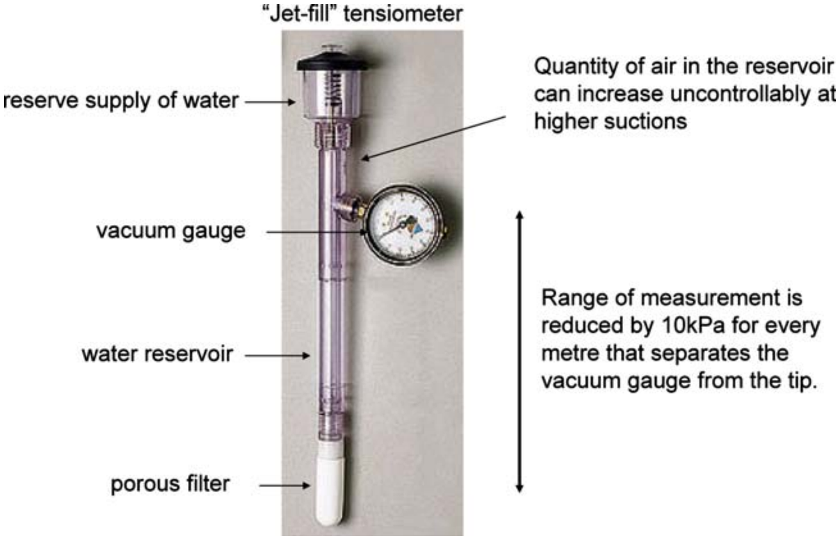

Fig. 7 A "jet-fill" vacuum gauge tensiometer (Soilmoisture Equipment Corp., Santa Barbara, CA)

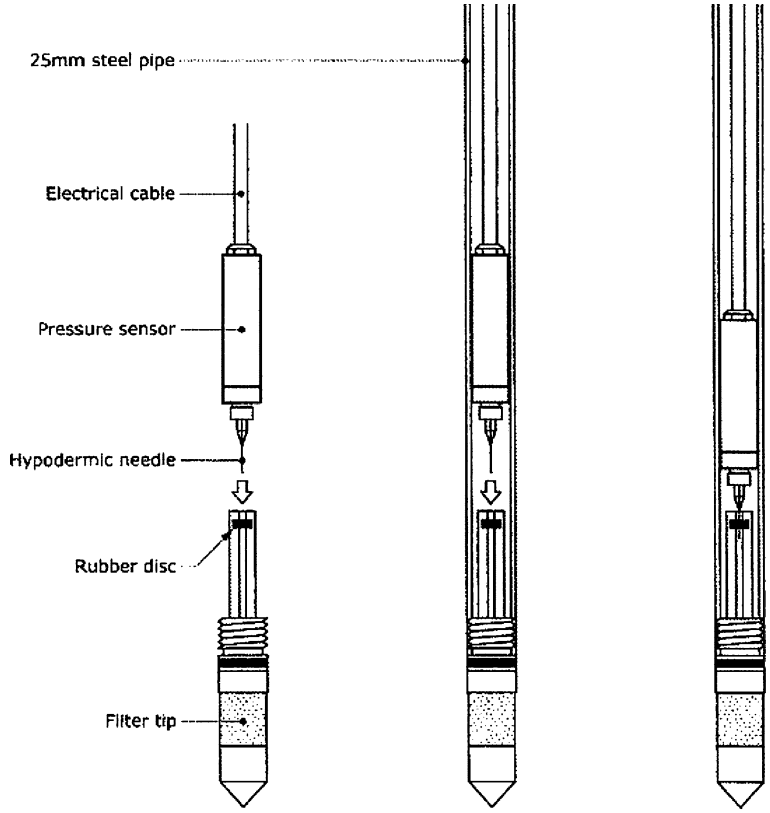

Fig. 8 A BAT piezometer (BAT Geosystems AB, Vallentuna, Sweden)

Since porous block sensors have to reach a suction equilibrium with the surrounding soil there can be a lag time (2–3 weeks) in establishing a suction reading. This makes them unsuitable for use in a rapidly changing moisture environment (Aitchison and Richards 1965). Similarly Bertolino et al. (2002) showed that the response of Watermark sensors is slow compared to tensiometers (lags by about 2 days). However, the results obtained from the two types of device were similar.

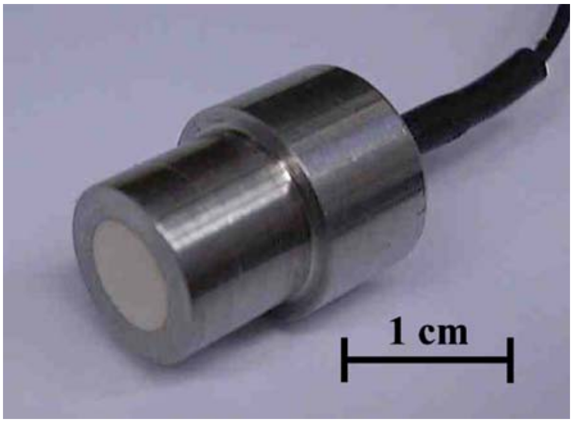

Fig. 9 A high range tensiometer (suction probe) (Ridley and Burland 1996)

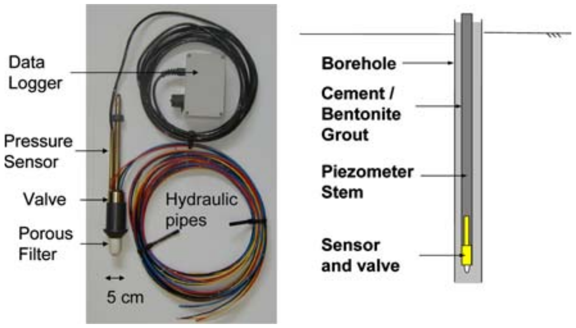

Fig. 10 A flushable piezometer with extended range (after Ridley et al. 2003)

Table 1 Properties of cement grouts and a typical porous ceramic filter

Water:Cement ratio*	Air entry value (kPa)	Hydraulic conductivity (m/s)
4:3	70	2.0×10^{-8}
1:1	172	4.5×10^{-10}
2:3	650	3.1×10^{-11}
1 bar porous ceramic	170	8.6×10^{-8}

* 4–7% bentonite added to prevent bleed

3.2 Thermal Conductivity Sensor

Thermal conductivity sensors rely on the measurement of the water content of the block by measurement of the temperature rise induced by a heater embedded in the centre of the porous block. Early use of these devices by Oloo and Fredlund (1995) showed a high failure rate of sensors for field trials in Kenya (50% failed within 1 year). However, there have been successful field studies. O'Kane et al. (1998) report suctions measured in excess of 400 kPa which showed sensible responses to rainfall. Ng et al. (2003) show general agreement between thermal conductivity sensors and tensiometers (suction around 20 kPa) although one sensor showed a significantly higher value (250 kPa).

As with other porous block sensors, equalisation between the block and the surrounding soil can be a slow process. Shuai and Fredlund (2000) show that full equalisation time can be about 2 weeks although a dry sensor may only take 4 days. Ng et al. (2003) show that thermal conductivity sensors showed a slower response (2 days lag) compared to tensiometers. In addition, these devices need corrections for temperature changes and hysteresis (Flint et al. 2002; Feng and Fredlund 2003). Nichol et al. (2003) also identified problems with drifting of readings which they attributed to be due either to "relaxation" when operated at low matric suctions or alteration of the ceramic over time.

3.3 Dielectric Permittivity Sensors (Equitensiometer)

The Equitensiometer is a new device that uses a "specially formulated porous matric material" (Delta-T 2005) which is intended to eliminate hysteretic behaviour between drying and wetting. A ThetaProbe sensor is used to measure the water content of the porous block. The manufacturers suggest that pressure equalisation takes place at 6 kPa/h but that it is unsuitable for use in saline soils. Mahler et al. (2004) report that the equitensiometer shows agreement with a high-suction tensiometer to −300 kPa. However, Ireson et al. (2005) shows that the Equitensiometer cannot be used for low suctions (less than −10 kPa). Comparisons with tensiometer data between −10 kPa and −80 kPa correspond reasonably well, but they suggest there may be some hysteresis in the sensor.

3.4 Filter Paper Measurements

While filter paper techniques have been widely adopted for laboratory testing, there are severe difficulties in using the method in the field. Greacen et al. (1987) first described equipment for field

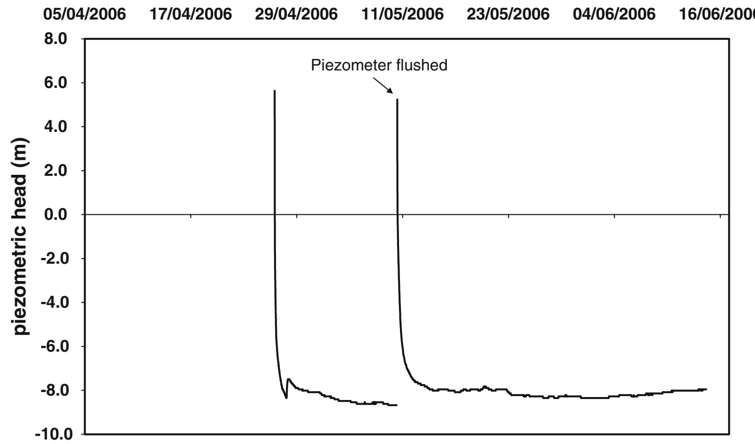

Fig. 11 Measurements of approximately -80kPa at 6 m made using a flushable piezometer

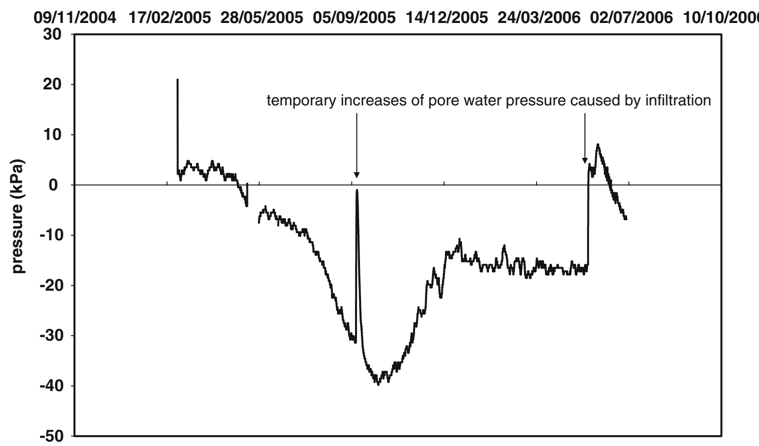

Fig. 12 Field measurements of suction using new piezometer in a rapidly changing environment

measurement using filter paper but Campbell and Gee (1986) identified a number of sources of error (equilibration time, temperature differences between soil and filter paper). Nevertheless, a field probe for filter paper measurements was developed by Crilley et al. (1991). This was based on non-contact (total suction) measurement and was used in studies in the UK and in Kenya (Waweru 1990; Gourley and Schreiner 1995). Wang and Lao (2002) have also developed a contact field method which can be used for matric suction measurement. The device involves an expanding rubber tube that presses the filter paper against the side of a borehole.

3.5 Psychrometer

Psychrometers use either thermocouples or transistors to measure the temperature difference between a wet and dry contact, thus giving a measure of relative humidity. Generally psychrometers are used in a sample chamber to measure total suctions on specimens that have been taken from the field (e.g. Cameron 2001). This is because psychrometers are not good for direct use in the field because of temperature variation. The manufacturers suggests that to maintain temperature equilibrium, the psychrometer must be buried at least 150 mm under the soil surface (Wescor 2005). However, for a temperature variation of ±5°C, suctions can vary as much as ±0.5 MPa in a dry soil.

4 Water Content Measurement Using Dielectric Methods

Dielectric methods are based on the measurement of the soil dielectric permittivity which in turn depends on soil water content. Techniques for measurement of soil dielectric permittivity include Time Domain Reflectometry (TDR), Amplitude Domain Reflectometry

(ADR), and Capacitance. Limitations of TDR, which is broadband high-frequency method, and ADR and Capacitance, which are single low-frequency methods, can be better appreciated if the interaction between electromagnetic waves and soil components is explored. This requires a more fundamental understanding of soil dielectric properties and transmission line theory.

4.1 Soil Dielectric Permittivity

Relative permittivity of air is 1, ranges from 3 to 5 in most soil mineral grains, and is approximately 80 for water (at 20°C). As a result, the permittivity of the unsaturated soil is strongly influenced by the permittivity of water. The origin of the high permittivity of water is the asymmetry of charge in the water molecule that produces a permanent dipole.

4.1.1 Dielectric Permittivity of Free Water in Static and Alternating Electric Field

Let us consider the capacitor shown in Fig. 13, where the static electric field generated by the surface charge σ causes water molecules (permanent dipoles) to line up. At the surface, there are unbalanced charges that produce an additional *surface polarization charge* σ_P that partly neutralises the original charge. The electric field E resulting from this additional polarisation charge is lower than the static electric field in vacuum E_0 by a factor ε_r, which is referred to as *relative permittivity* ($E = E_0/\varepsilon_r$). The higher the polarisation, the higher the dielectric permittivity.

When a time-harmonic field propagates as a wave through the material, the dipoles align with the field, oscillating, and in turn establishing a polarization wave that propagates through the material superposing to the driving field. This alignment manifests itself as the real (in-phase) part of the relative permittivity (ε'_r). As the frequency is increased, the molecules being aligned by the alternating field can no longer keep up with the speed of field alternation (*dipole relaxation*). This reduces the intensity of polarisation and gives rise to a time lag between the applied field and the polarisation wave. This phase shift manifests itself as the imaginary (out-of-phase) part of the relative permittivity (ε''_r) and causes dissipation of energy in the form of heat (as in microwave ovens).

The real and imaginary part of dielectric permittivity of water, ε'_r and ε''_r respectively, are plotted in Fig. 14 at two different temperatures. As temperature increases, random collisions between dipoles increase and this statistically reduces the number of dipoles that align with the electric field. As a result, polarisation decreases and so does the low-frequency (static) dielectric permittivity. At the same time, the dipoles are less difficult to push back and forth (thermal effects can be thought as viscous forces slowing down dipole rotation) and this increases the frequency at which relaxation occurs (Fig. 14). The figure also reports the upper bound of TDR bandwidth ($\sim$1.5 GHz) showing that the TDR frequencies are well below the relaxation frequency of free water and are therefore associated with negligible dielectric losses.

4.1.2 Dielectric Permittivity of Aqueous Solution

Water in soils is rarely pure and usually contains charge carriers such as ions. Ionic conductivity causes a loss of energy (*conductive loss*) in addition to loss due to dipole relaxation (*relaxation loss*). This is conveniently expressed by an equivalent permittivity given by:

$$\varepsilon_r^* = \varepsilon'_r(N,T) - j\varepsilon''_r(N,T) - j\frac{\sigma_{dc}(N,T)}{2\pi f \varepsilon_0} \tag{1}$$

where ε_0 is the permittivity in free space, σ_{dc} the direct current electric conductivity, and f is the

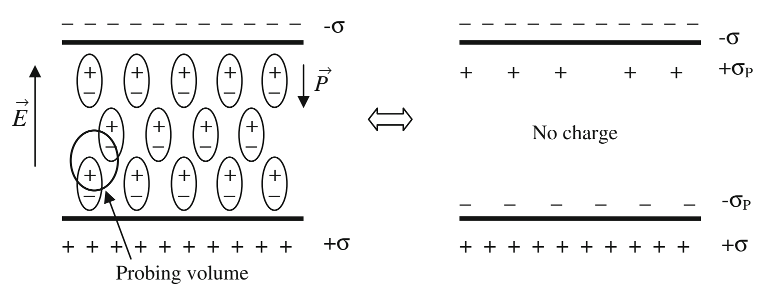

Fig. 13 Capacitor filled with dielectric material

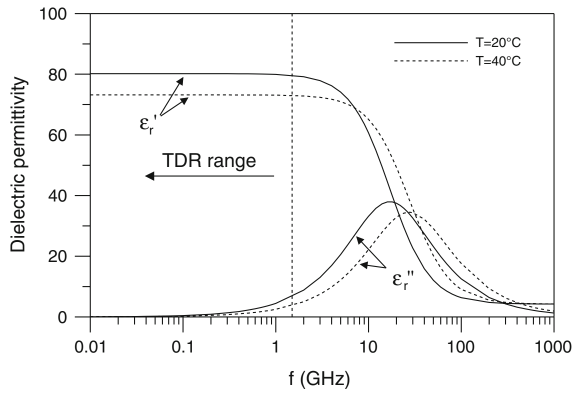

Fig. 14 Real and imaginary part of water relative permittivity for two different temperatures (Debye 1929 parameters fitted on experimental data from Hasted 1973)

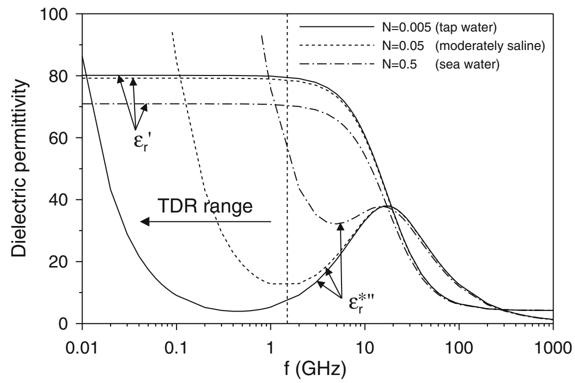

Fig. 15 Real and imaginary part of relative permittivity of aqueous solution at different normalities according to Stogryn (1971)

frequency. According to Stogryn (1971), ε_r', ε_r'', and σ_{dc} depend on temperature T and normality N of the aqueous solution. Figure 15 shows the real and imaginary part of relative permittivity of aqueous solutions at different normalities. The static permittivity ε_{rs} decreases with increasing concentration of dissolved ions. The ions orient the water molecules around them, thereby reducing their ability to orient in the applied fields, and so reducing the static dielectric permittivity. The effect of ionic loss on the imaginary part of dielectric permittivity is inversely proportional to frequency and tends to become negligible at high frequencies.

4.1.3 Dielectric Permittivity of Bound Water

Water molecules that are 'bound' to solid surfaces are subject to surface forces that hinder their reorientation in response to an imposed electromagnetic field. This results in both a lower relaxation frequency and lower dielectric permittivity relative to free liquid water. Experimental studies and theoretical predictions suggest that most of the bound water extends to two to three molecular layers, although this may increase depending on mineralogy (Bockris et al. 1966; Sposito and Prost 1982; Sposito 1984).

The dielectric properties of bound water may be assumed to lie somewhere between those of ice and liquid water. Logsdon and Laird (2002) for hydrated Ca-smectite and Ishida and Makino (1999) for montmorillonite suspensions report relaxation frequencies of bound water in the range 2–25 MHz. A relaxation frequency of 2 MHz can be inferred from a molar activation enthalpy of approximately 42 kJ/mol^{-1} for water adsorbed on kaolinite (Hasted 1973) according to Hilhorst et al. (2001). Soil dielectric spectroscopy carried out by Hoekstra and Delaney (1974) also seems to support values of bound water relaxation frequency less than 10 MHz (Hilhorst et al. 2001).

A range of 1–20 MHz is likely to be a realistic assumption for bound water relaxation frequency. These frequencies are considerably lower than frequencies in the TDR bandwidth and this would suggest the permittivity of bound water in TDR measurement to be close to the high-frequency permittivity, $\varepsilon_{r\infty}$. According to Friedman (1998), the high-frequency permittivity of water molecules bound to the surface of soil minerals can be assumed equal to the high-frequency permittivity of free water, which is in the range $\varepsilon_{r\infty}$ = 4–5 (Hasted 1973).

4.1.4 Dielectric Permittivity of Solids and Air

Dielectric permittivity of air can be assumed equal to dielectric permittivity in free space (ε_{air} = 1) whereas the dielectric permittivity of solids is real and frequency-independent (Saarenketo 1998) lying in the range 4.5 to 10 (Keller 1989; Robinson and Friedman 2003).

4.1.5 Dielectric Permittivity of Soil (Mixing Models)

The composite dielectric permittivity of a heterogeneous medium depends on dielectric permittivity and volume fraction of the individual constituents and their geometrical shape and arrangement. A common approach for estimating the permittivity of a mixture, ε_m^*, is based on the Litchteneker (1926) formula (α-model) which can be written for a four-phase soil as follows (Heimovaara et al. 1994):

$$\left[\varepsilon_m^*(f)\right]^\alpha = V_s\varepsilon_s^{*\alpha} + V_{fw}\left[\varepsilon_{fw}^*(f)\right]^\alpha + V_{bw}\left[\varepsilon_{bw}^*(f)\right]^\alpha + V_a\varepsilon_a^{*\alpha} \tag{2}$$

where f is the frequency, V and ε_m^* are the volume fraction and equivalent complex permittivity of each component, respectively, the subscripts *s*, *fw*, *bw*, and *a* refer to soil solids, free water, bound water, and air, respectively, and α is a fitting parameter that accounts for soil structure. Theoretical evidence for this formula is provided by Zakri et al. (1998). It is worth noticing that soil bulk dielectric permittivity ε_m^* is complex and frequency-dependent (Hoekstra and Delaney 1974; Dobson et al. 1985) as is the dielectric permittivity of bound and free water. As a result, mixing models should not be written in terms of a single apparent permittivity (the concept of apparent permittivity is developed later on in this paper). Another common approach is the Maxwell-De Loor model (De Loor 1968), which is based on polarisation analyses of dielectric mixtures and considers the soil to be made up of isotropically mixed plate-like particles. This model has been extended to a four-phase soil by Dobson et al. (1985).

The Litchteneker and De Loor's formulas are difficult to validate for the case of a four-component mixture because somewhat arbitrary assumptions have to be made about the volume fraction of bound water and its dielectric properties (Dobson et al. 1985; Heimovaara et al. 1994). In addition, assumptions have to be made about the electrical conductivity of soil free water, which may significantly differ from the measured conductivity of extracts from saturated soil pastes in presence of solids with high specific surface (Dobson et al. 1985).

For the case where the amount of bound water is negligible (low clay content and/or low specific surface) three-phase Litchteneker and De Loor's models are often used to characterise the bulk dielectric permittivity. These models can be validated in terms of apparent permittivity using TDR measurement provided the apparent permittivity remains fairly constant in the range of TDR effective frequency (0.7–1 GHz according to Robinson et al. 2005). As shown later on, this occurs for low bulk soil electrical conductivity and Robinson et al. (1999) suggest a value of $\sigma < 0.05$ S/m. The Litchteneker model with $\alpha = 0.5$ has been found to satisfactorily capture experimental data (Roth et al. 1990; Robinson et al. 1999). Other physically based three-phase mixture equations for soils have been presented by Friedman (1997, 1998) and Hilhorst et al. (2000).

4.2 Transmission Lines

4.2.1 Transmission Line Equations

Electromagnetic wave propagation inside a transmission line is described by the line current I and the voltage V between the conductors. If V and I are time-harmonic cosine functions with angular frequency ω and the symbolic representation of sinusoidal signal is adopted, the following transmission line equations can be obtained (Kraus and Fleisch 1999):

$$\begin{cases} \vec{V}(t,z) = \vec{V}_0^{+} e^{-\gamma z + j\omega t} + \vec{V}_0^{-} e^{\gamma z + j\omega t} \\ \vec{I}(t,z) = \dfrac{\vec{V}_0^{+}}{\vec{Z}_c} e^{-\gamma z + j\omega t} - \dfrac{\vec{V}_0^{-}}{\vec{Z}_c} e^{\gamma z + j\omega t} \end{cases} \tag{3}$$

where the two terms in each equation denotes travelling waves in positive and negative direction respectively.

The *propagation constant* γ and the *characteristic cable impedance* $\vec{Z}_c$ are the two parameters governing the propagation of electromagnetic waves along the transmission line and can be expressed for the case of non-ferromagnetic materials as follows:

$$\gamma = \frac{j\omega}{c}\sqrt{\varepsilon_r^*} = \alpha + j\beta \tag{4}$$

$$\vec{Z}_c = \frac{Z_p}{\sqrt{\varepsilon_r^*}} \tag{5}$$

where c is the speed of an electromagnetic wave in free space ($c = 3 \cdot 10^8$ m/s), ε_r^* is the equivalent permittivity and Z_p the characteristic impedance in vacuum, which is only a function of the cross-sectional geometry of the transmission line and can be assumed, as a first approximation, to be equal to the characteristic impedance in air.

The real part, α, of the propagation constant is called the attenuation constant as it accounts for signal attenuation along the line given by $\exp(-\alpha z)$.

The imaginary part, β, is called the phase constant of the line and accounts for the propagation velocity of the wave through the transmission line.

4.2.2 Propagation Velocity and Apparent Permittivity

The propagation velocity V_p through the transmission line can be obtained from Eqs. 3 and 4:

$$V_p = \frac{\omega}{\mathrm{Im}[\gamma]} = \frac{c}{\sqrt{\frac{\varepsilon_r'}{2}\left[\sqrt{1+\left(\frac{\varepsilon_r''+\sigma/2\pi f\varepsilon_0}{\varepsilon_r'}\right)^2}+1\right]^{\frac{1}{2}}}} \tag{6}$$

where f is the frequency ($f = \omega/2\pi$). If the frequency is sufficiently lower than relaxation frequency f_{rel}, so that the imaginary part of dielectric permittivity ε'' is small, and is sufficiently higher than electrical conductivity so that the term $\sigma/2\pi f\varepsilon_0$ is also small, the velocity of propagation reduces to:

$$V_p \approx \frac{c}{\sqrt{\varepsilon_r'}} \tag{7}$$

If this is not the case, the velocity of propagation may be expressed in terms of apparent permittivity, K_a

$$V_p = \frac{c}{\sqrt{K_a}} \tag{8}$$

with K_a given by

$$K_a = \frac{\varepsilon_r'}{2}\left[\sqrt{1+\left(\frac{\varepsilon_r''+\sigma/2\pi f\varepsilon_0}{\varepsilon_r'}\right)^2}+1\right] \tag{9}$$

In general, the apparent permittivity is a function of frequency f and temperature since ε' and ε'' depends themselves on frequency and temperature. As an example, Fig. 16 shows the apparent permittivity of tap water ($\sigma \sim 0.05$ S/m) and moderately saline water ($\sigma \sim 0.5$ S/m) at different temperatures obtained using expressions from Stogryn (1971). It can be noticed that the apparent permittivity in high frequency range of TDR bandwidth is fairly constant and equal to the static permittivity of pure water. Besides, the apparent permittivity decreases with temperature in this range.

Figure 17 shows the apparent permittivity for saline water having electrical conductivity of about 5 S/m (sea water) at different temperatures. In this case, the apparent permittivity in the high frequency range of TDR bandwidth is significantly higher than static permittivity of pure water due to the contribution of the term the $\sigma/2\pi f\varepsilon_0$. In addition, the apparent permittivity increases with temperature in contrast to the moderately saline water. In this case, the increase in electrical conductivity associated with temperature prevails over the decrease in static permittivity.

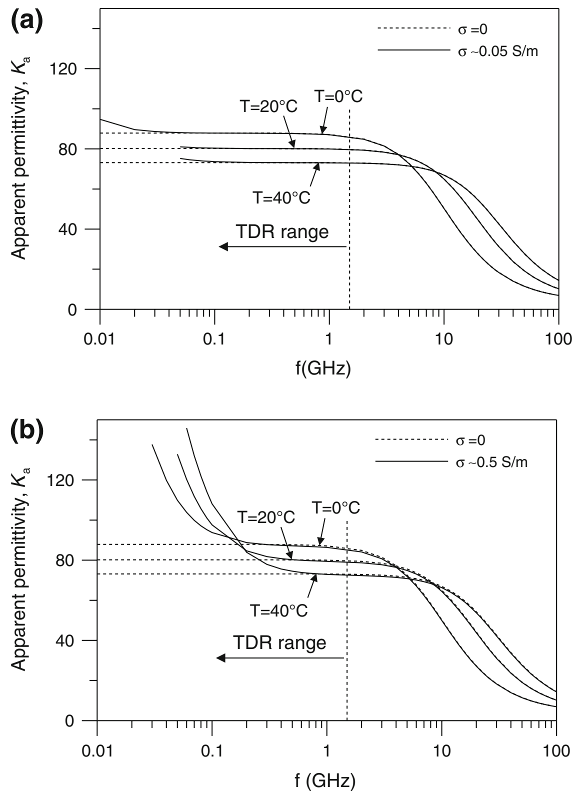

Fig. 16 Apparent permittivity K_a of (**a**) tap water and (**b**) moderately saline water (data from Stogryn 1971)

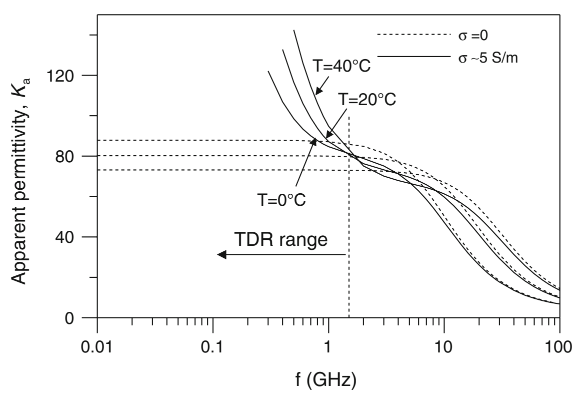

Fig. 17 Apparent permittivity K_a of aqueous solution water having $\sigma \sim 5$ S/m (data from Stogryn 1971)

4.2.3 Terminations and Reflection

An equivalent circuit for a uniform transmission line is shown in Fig. 18. The line is terminated at $z = 0$ with an independent voltage source V_s and a source impedance Z_s and at $z = l$ with a load impedance Z_L ($=\vec{V}_L/\vec{I}_L$). It can be shown that the *voltage reflection coefficient* ρ, defined as the amplitude of the reflected voltage wave normalised to the amplitude of the incident voltage wave at $z = l$ is given by (Kraus and Fleisch 1999):

$$\rho = \frac{\vec{V}_0^{-} e^{\gamma z + j\omega t}}{\vec{V}_0^{+} e^{-\gamma z + j\omega t}} = \frac{Z_L - Z_c}{Z_L + Z_c} = \frac{1 - Z_c/Z_L}{1 + Z_c/Z_L} \tag{10}$$

If the relative permittivity is real ($\varepsilon_r'' \sim 0$ and $\sigma/2\pi f \varepsilon_0 \sim 0$) and the load impedance Z_L is a resistance, the impedances Z_c and Z_L are both real and so is the reflection coefficient ρ. The reflection coefficient will range from -1 (shorted ended circuit) to 1 (open ended circuit). When $Z_c = Z_L$ (matched line) there is no reflection.

4.3 TDR Applied to Volumetric Water Content Measurement

A TDR system consists of a step pulse generator, an oscilloscope, a coaxial cable and a rod probe (Fig. 19). The step pulse generator launches a fast-rise time voltage step associated with a bandwidth up to 1.5 GHz and the reflection waveform is recorded by an equivalent time sampling oscilloscope. The highest frequencies are sufficiently lower than relaxation frequency of water (Fig. 16) and fall in the range where the effect of electrical conductivity is often negligible (Fig. 16).

TDR working principle may be illustrated following Nissen and Moldrup (1994). Let us assume that impedance of segment AB, Z_C, is greater than that of segment BC, Z_P. This is the case of a probe inserted in water or wet soil. At time $t = 0$, the step pulse generator starts to launch electromagnetic waves to produce a voltage step, V_0. At time $t = t_A$, the front of the voltage step reaches the oscilloscope that records an instantaneous rise in voltage, V_0 (stage 1). At point B, some of the voltage step is reflected back towards the sampler, $U_{r,1}$, and some is transmitted further on, $U_{t,1}$. Since $Z_C > Z_P$, $\rho < 0$ (see Eq. 10) and a negative reflected step is observed (the reflected wave travels in counterphase with the wave transmitted by the pulse generator). The superposition of these two waves causes a drop in voltage amplitude with respect to the original wave (stage 2). At time $t = t_B$, the front of the reflected step has reached the oscilloscope, which detects a drop in voltage. On the other side, the transmitted voltage step $U_{t,1}$ is totally reflected in phase at the end of the transmission line (open ended circuit) because $Z_L \rightarrow \infty$ and $\rho = 1$ (stage 3). The reflection of the transmitted voltage step $U_{t,1}$ reaches back to point B. Here it is partly reflected in phase ($\rho > 0$) towards point C, $U_{r,2}$, and partly transmitted in phase toward the sampler, $U_{t,2}$ (stage 4). The transmitted voltage step $U_{t,2}$ reaches the sampler at $t = t_C$. Because it is in phase with the waves transmitted by the pulse generator, the sampler measures a rise in voltage (stage 5). Multiple reflection will then take place in the system until a stable level is reached.

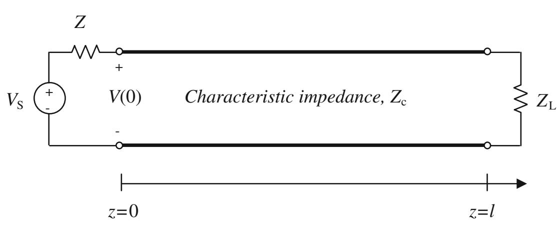

Fig. 18 Equivalent circuit of a uniform transmission line

The apparent permittivity K_a of the medium in which the probe is inserted can be obtained from the propagation velocity of the pulse in the probe according to Eq. 8:

$$K_a = \left(\frac{c}{V_p}\right)^2 = \left(c\frac{t_C - t_B}{2L_{BC}}\right)^2 \tag{11}$$

In their early work, Topp et al. (1980) assumed that the apparent dielectric permittivity could directly be related to volumetric water content θ through a polynomial calibration curve (*Topp's equation*):

$$\theta = -5.3 \cdot 10^{-2} + 2.92 \cdot 10^{-2} K_a - 5.5 \cdot 10^{-4} K_a^2 + 4.3 \cdot 10^{-6} K_a^3 \tag{12}$$

They suggested that such a calibration curve was almost independent of soil density, texture, temperature, and salt content. This equation was derived for volumetric water contents between 0.02 to 0.55 and dry densities between 1 to 1.5 g/cm^3 and was found

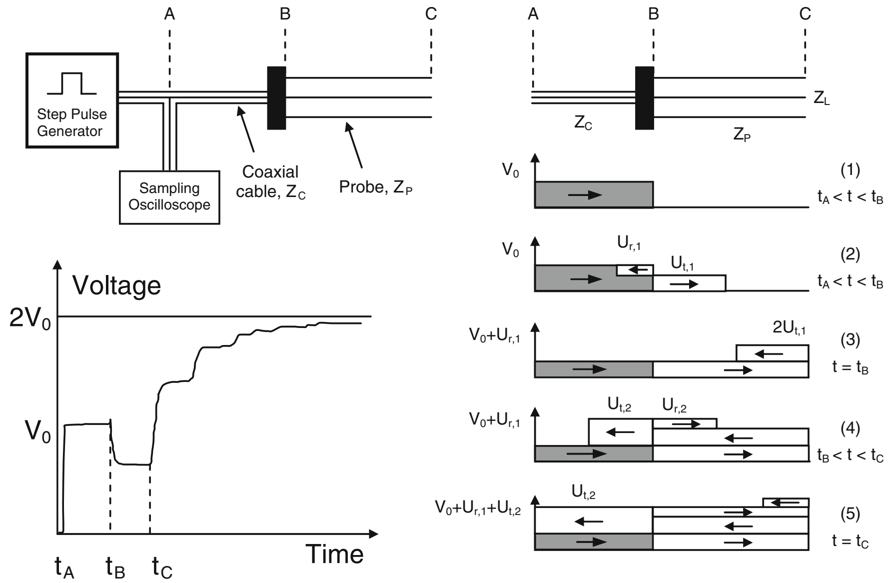

Fig. 19 Voltage step reflections in an open ended transmission line having an impedance discontinuity (after Nissen and Moldrup 1994)

to have standard error of estimate of $\Delta\theta = \pm 0.013$ over the complete range of water contents.

To appreciate the assumptions implicitly made by Eq. 12, it may be useful to consider Eq. 2 by assuming $\alpha = 0.5$ and rewriting the volume fractions:

$$\theta = \frac{\sqrt{K_a} - 1 - \frac{\rho_d}{\rho_s}\left(\sqrt{\varepsilon_s} - 1\right) - \delta\rho_d A_s\left(\sqrt{\varepsilon^*_{bw}} - \sqrt{\varepsilon^*_{fw}}\right)}{\sqrt{\varepsilon^*_{fw}} - 1} \tag{13}$$

where ρ_d is the bulk dry density of the soil, ρ_s is the average density of the solid phase, and the product $\delta\rho_d A_s$ represents the volumetric bound water content, with A_s and δ being the specific surface of the soil and thickness of the bound water layer respectively. Equation 13 suggests that θ only depends on K_a if the soil density does not change significantly ($\rho_d/\rho_s \sim$ constant), the amount of bound water is negligible ($A_s \sim 0$), and ε^*_{fw} is constant in the high frequency range of the TDR bandwidth. As shown in Figs. 16 and 17, this latter condition occurs when changes in temperature are small and pore water electrical conductivity is also relatively small.

In fact, Topp's equation has been proven successful in soils that do not contain substantial amount of bound water, do not have pores filled with saline water, and do not have high porosity (Patterson and Smith 1981; Topp et al. 1982, 1984; Smith and Patterson 1984; Topp and Davis 1985a; Drungil et al. 1989). Dirksen and Dasberg (1993) investigated eleven different soils and concluded that Topp's equation may be valid for soils with dry densities between 1.35 and 1.50 g/cm^3 and specific surfaces between 0 and 100 m^2/g (low clay content). As a first approximation, specific surface can be estimated from hygroscopic water content according to Banin and Amiel (1970) and Dirksen and Dasberg (1993).

In contrast, Eq. 12 has shown poor response in fine-textured soils (Dasberg and Hopmans 1992; Dirksen and Dasberg 1993) and organic soils (Topp et al. 1980; Herkelrath et al. 1991; Pépin et al. 1992; Paquet et al. 1993). In fine-textured soils, the apparent permittivity at low water contents decreases due to the presence of tightly bound water near particle surfaces having lower dielectric permittivity than free water. As a result, Topp's equation underestimates the volumetric water content in the lower water content range (Dasberg and Hopmans 1992; Dirksen and Dasberg 1993; Robinson et al. 2002). At higher water contents, the apparent permittivity may increase due to dispersion associated with Maxwell-Wagner effects, electrical conductivity of free and bound water. Topp's equation may then overestimate volumetric water content in the high water content range (Dirksen and Dasberg 1993). On the other hand, deviations from Topp's equation observed in organic soils can partly be attributed to the low dry density typically exhibited by these soils (Malicki et al. 1996).

Since 1980, other researchers have shown that the relationship between θ and $\sqrt{K_a}$ is practically linear

(Ledieu et al. 1986; Yu et al. 1997; Topp and Reynolds 1998) and any of these two-parameter equations is preferable to the four-parameter Topp's equation for isotropic distribution of soil and water content (Yu et al. 1997). A comparison between Topp's equation and 'linear' equations is presented in Fig. 20 and shows that all equations are essentially coincident up to $\theta = 0.40$–0.45. Outside this range, Topp's equation significantly underestimates water content (Roth et al. 1990) and its use should be avoided.

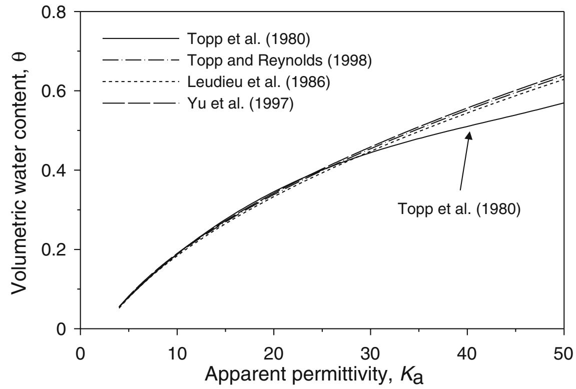

Fig. 20 Comparison between different calibration curves presented in the literature

4.4 Interpreting Reflection Waveform for Travel Time

Conventional interpretation of the reflection waveform involves determining the apparent permittivity K_a using Eq. 11. However, the use of this equation is not straightforward. The electrical length L may slightly differ from the physical length because of the fringing field at the end of the probe. The time t_{probe} (t_B in Fig. 19) at which the step pulse leaves the head and enters the probe electrodes and the time t_{end} (t_C in Fig. 19) corresponding to the reflection at the end of the rods may be difficult to identify.

Figure 21 shows the measurement in air and demineralised water using a 150 mm three-rod probe. The waveform is reported in terms of reflection coefficient ρ which is given by:

$$\rho = \frac{V - V_0}{V_0} \tag{14}$$

where V is the voltage recorded by the sampling oscilloscope and V_0 is the step voltage launched into the transmission line.

The impedance of the probe filled with air is greater than the cable impedance and this results in the ascent of the reflected waveform as the step voltage leaves the head and enters the rods (see Eq. 10). This response is typical of dry soils. In contrast, the lower impedance of the probe filled with water causes the descent of the reflected waveform (as in wet soils). The waveform in water is characterised by an initial dip followed by a bump. This broadly marks the reflections at the beginning of the head and the beginning of rods but the exact location of the time t_{probe} is not clear. The bump is absent in the waveform in air making the determination of the time t_{probe} even more difficult.

4.4.1 Time at Which the Step Pulse Enters the Head

The time at which the wave enters the head of the probe, t_{head}, can be obtained by the intersection between the line tangent to the first rising limb at the inflection point and the base line before the first inflection. This construction is not shown in the figure and the reader may refer to Heimovaara and Bouten (1990) and Robinson et al. (2003b) for further details.

However, probes commercially available today incorporates an electrical marker causing a dip in the reflected waveform. This dip can be used to easily locate the time t_{head} as shown in Fig. 21b. This is very useful in field applications where long cables and high temperature fluctuations can make the time t_{head} difficult to identify (Robinson et al. 2003b).

4.4.2 Time at Which the Step Pulse Enters the Soil

The time at which the wave leaves the head and enter the probe electrodes, t_{probe}, is sometimes determined by considering the apex bump (Or et al. 2002; Feng et al. 1999) or sometimes by considering the intersection between the tangent to the first descending limb at the inflection point and the horizontal line through the bump apex (Baker and Allmaras 1990; Herkelrath et al. 1991) (Fig. 21b). These approaches have several limitations. In dry soils and soils with low bulk density, the first descending limb is almost absent making the bump difficult to detect. Another phenomenon sometimes found in low dry density soils is a double peak in the waveform. This may due to the compression of a thin layer of soil next to the handle during installation.

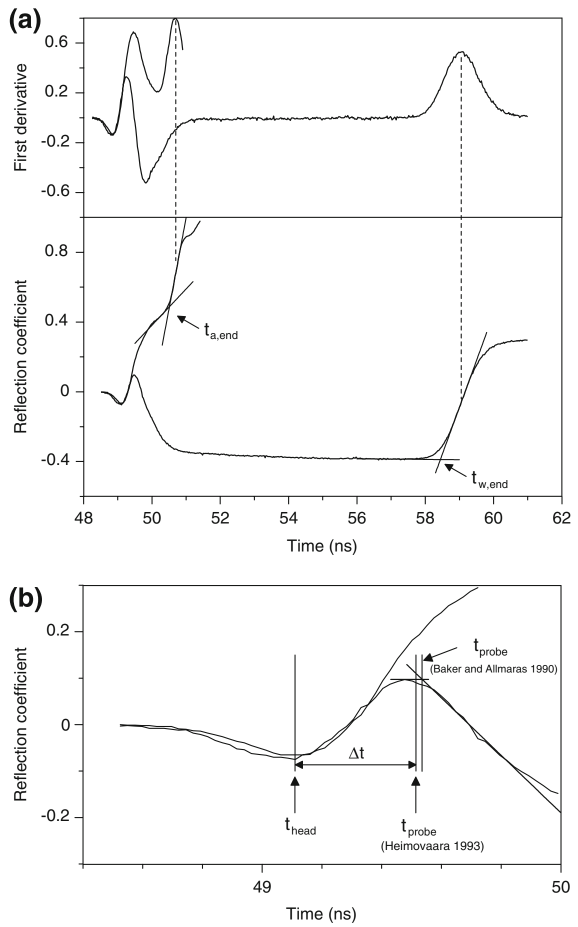

Fig. 21 (**a**) Waveform in air and water with a 15-cm three-rod probe (**b**) time at which the wave enters the probe

This high dry density soil layer exhibits lower impedance due to lower porosity thus causing a second dip in the waveform after the head (Evett 2000). At a more fundamental level, the use of the bump apex to locate the time at which the pulse enter the rods may result in significant errors in moderately dry soil and layering of dry soil over wet soil, as often occurs in surface installation (Robinson et al. 2003b).

The time t_{probe} can effectively be determined by calibrating the probe in air and water (Robinson et al. 2003b) according to the procedure suggested by Heimovaara (1993). By referring to Eq. 15, we can write the following equation:

$$2L\frac{\sqrt{K_a}}{c} = t_{end} - t_{probe} = t_{end} - (t_{head} + \Delta t) \qquad (15)$$

where Δt is the difference between t_{probe} and t_{head} (Fig. 21b), L is the electrical length of the probe, and t_{end} is the time corresponding to the reflection at the end of the probes as discussed in the next paragraph. If Eq. 15 is written for air and water ($K_{a,air}$ = 1 and $K_{a,water}$ = 80.2 at 20°C) the two unknowns Δt and L can be determined. The time t_{probe} can therefore be obtained by adding the time Δt to the time t_{head}.

For example, the probe shown in Fig. 21 is characterised by $L = 0.1495$ m and $\Delta t = 0.405$ ns. In this case, the electrical length is very close to the physical length. From Fig. 21, it can also be observed that the time t_{probe} determined using Heimovaara's approach slightly differs from the value obtained by referring to the bump apex. As observed by Robinson et al. (2003b), this difference may be sometimes significant and lead to considerable errors in relatively dry soils where lower travel times are measured.

Probe calibration using Eq. 15 can also be performed using liquids of known dielectric properties other than demineralised water. However, this procedure should be followed with care. If the relaxation frequency of the calibration liquid is lower than the TDR frequency range, relaxation will take place and the apparent dielectric permittivity will be much lower than the 'reference' static permittivity of the calibration solution put in Eq. 15 (Heimovaara 1994). As a result, L can be significantly underestimated. Demineralised water is a suitable calibration liquid due to its very high relaxation frequency compared to the TDR bandwidth as shown in Fig. 16.

4.4.3 Time at Which the Step Pulse is Reflected at the Rod Ends

The time t_{end} corresponding to the reflection at the end of the probes can be determined by considering the intersection between the line tangent to the second rising limb at the inflection point and the line fitting the base section of the reflection according to Heimovaara and Bouten (1990) (Fig. 21a). The inflection point is marked by the peak in the first derivative.

An alternative method consists in determining the intersection between the line tangent to the second rising limb at the inflection point and the horizontal line tangent to the minimum of the reflection waveform (Baker and Allmaras 1990). However, this second method is not applicable in dry soils (see Fig. 21a) and is not recommended because it is more susceptible to temperature induced errors (Wraith and Or 1999).

These two methods may not be applicable in high bulk conductivity soils (saline soils and clays with high cation exchange capacity). In these soils, the electrical conductivity σ_{DC} attains high values at high water contents. As a result, the frequency-dependent imaginary part of the complex permittivity is no longer negligible. The different frequencies will therefore feel different apparent permittivity (Figs. 16, 17) and hence will move through the transmission lines at different velocities. This tends to reduce the slope of the descending and ascending limb of the waveform as shown in Fig. 22a for an active clay (high CEC). Because the waveform 'softens', the time t_{end} of the reflection at the end of the probe rods may become difficult to detect as the peak in the first derivative tends to disappear (Fig. 22a). In this case, Evett (2000) suggests to determine the time t_{end} by adding a user-defined time to the time corresponding to the minimum in the reflected waveform. It is worth noticing that softening and attenuation is generally not observed in non-active clay (Fig. 22b) where the travel time of the step pulse can be clearly distinguished.

4.5 Interpreting Reflection Waveform for Bulk Electrical Conductivity (BEC)

One of the great strength of TDR is that it can be used to measure bulk electrical conductivity (BEC) in addition to dielectric permittivity (Dalton et al. 1984; Topp et al. 1988; Nadler et al. 1991).

The most reliable estimates of bulk electrical conductivity are based on the Giese and Tiemann (1975) thin-section approach which uses the amplitude of the TDR signal at long times. The Giese and Tiemann equation as presented by Topp et al. (1988) may be written in terms of voltage or reflection coefficient:

$$\sigma = \frac{1}{Z_c}\frac{\varepsilon_0 c Z_0}{L}\left[\frac{1-\rho_\infty}{1+\rho_\infty}\right] \equiv \frac{1}{Z_c}\frac{\varepsilon_0 c Z_0}{L}\left[\frac{2V_0}{V_F}-1\right] \quad (16)$$

where ε_0 is the permittivity of free space ($8.854 \cdot 10^{-12}$ F m^{-1}), c is the speed of light in a vacuum ($3 \cdot 10^8$ m s^{-1}), L is the probe length (m), ρ_∞ the reflection coefficient at infinite time, V_0 is the voltage entering the head of the probe, V_F the final voltage recorded by the oscilloscope after all multiple reflections had taken place, Z_c is the characteristic impedance of the cable tester, and Z_0 is characteristic impedance of the probe. The Giese and Tiemann approach agrees well with other low frequency measurements of electrical conductivity (Topp et al. 1988; Zegelin et al. 1989; Heimovaara 1992, Baker and Spaans 1993; Topp et al. 2000).

The probe characteristic impedance Z_0 appearing in Eq. 16 can be determined by measurement in deionised water using Eqs. 10 and 14 according to Baker and Spaans (1993) or, alternatively, the term $\varepsilon_0 c Z_0/L$ can be lumped into a geometric probe constant, K_p, which can be determined by immersion of the probe in one or more solutions of known electrical conductivity (Zegelin et al. 1989).

Although Eq. 16 was first derived for thin samples, Castiglione and Shouse (2003) and Lin et al. (2007) showed that this equation is rigorous at very low frequencies regardless of the samples size. Castiglione and Shouse (2003) also pointed out that Eq. 16 is exact when no signal dissipation occurs other than in the sample. When losses occur in the cable, connectors, multiplexers, and other discontinuities, they suggested to scale the reflection coefficient at infinite time according to the reflection coefficient for an

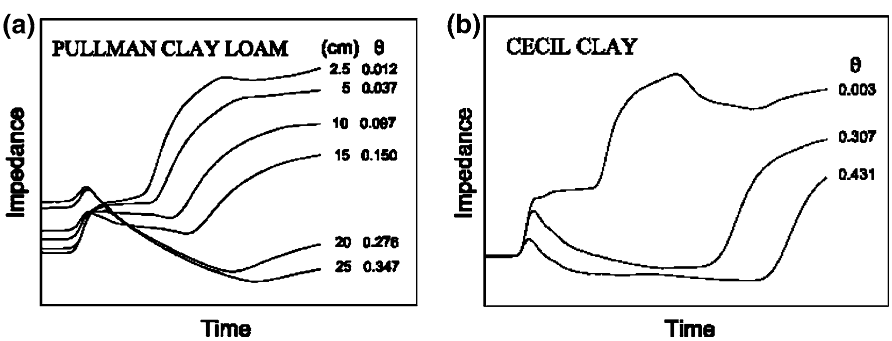

Fig. 22 Typical TDR waveforms in clay. (**a**) active clay; (**b**) non active (kaolinitic) clay. (Evett 2000)

open circuit in air and for a shorted circuit, and to use the scaled reflection coefficient in Eq. 16. Castiglione and Shouse (2003) also concluded that the common approach consisting in modelling the cable and sample as resistors in series leads to incorrect measurement for low conductivity samples.

This conclusion has recently been refuted by Lin et al. (2007). They demonstrated that the series resistor model is indeed theoretically sound according to the well-established circuit theory and verified by full waveform analysis. Discrepancies reported in the literature for the case of long cables between measured and TDR electrical conductivity predicted using the series resistor model can be explained by time effects. It takes much longer time than conventionally thought to reach the steady state when long cables are used, in particular at very high electrical conductivity. On the other hand, it is the linear scaling proposed by Castiglione and Shouse (2003) that is incorrect since the effect of cable resistance on steady-state reflection coefficient is nonlinear. The error introduced by the Castiglione-Shouse method can be compensated by fitting the probe constant K_p to known electrical conductivity values, even though the probe constant becomes a function of cable length (resistance) which is theoretically incorrect.

Another error in TDR electrical conductivity measurement may arise from imperfect amplitude calibration when transforming the voltage signal into the reflection coefficient signal. A calibration (correction) method for the measured reflection coefficient to account for both the instrument error and effect of cable resistance was proposed by Lin et al. (2008).

4.6 Waveforms Modelling

First attempts to model the reflection waveform go back to Yanuka et al. (1988) who analysed a single transmission line without considering the frequency-dependency of the soil dielectric permittivity and the multi-section characteristics of the TDR transmission line and by ignoring the second and high-order reflections. Heimovaara (1994) used the S_{11} scatter function to model the TDR waveform but his method considered only a uniform transmission line (matched system). Feng et al. (1999) combined the work of Yanuka et al. (1988) and Heimovaara (1994) and formulated a model for multi-section transmission line that uses a linear-time-invariant feedback system to model each section and links each section in a bottom-up fashion. Lin (2003a, b) presented a different approach to formulating multiple reflections in a non uniform and dispersive TDR measurement system using spectral analysis and the concept of input impedance. This formulation is based on Eq. 3 with appropriate boundary conditions and is simpler and more systematic than the approach described by Feng et al. (1999).

To model TDR waveform, the parameters describing the soil dielectric permittivity (i.e. the permittivity, electrical conductivity and layer thickness of bound water, the electrical conductivity of free water, and the α parameter in the Litchteneker's model) need to be determined by fitting to the discrete measured waveform (inverse analysis). This fitting may take place in the time domain or, after Fourier transform, in the frequency domain (Lin 2003b; Huisman et al. 2006). Other problems in the inverse modelling are associated with the choice of the input function and optimisation algorithm (Huisman et al. 2006) and in the proper modelling of cable resistance (Lin and Tang 2007).

The capability of reproducing the measured waveform is shown in Fig. 23. Models can be therefore used to analyse the TDR signal in the frequency domain and then extract the ε_r' spectrum that can be associated with volumetric water content. On the other side, the model can be successfully used to investigate the effect of TDR bandwidth, probe length, probe impedance, soil density, dielectric relaxation, and electrical conductivity on the apparent dielectric permittivity (Lin 2003b). Another interesting application of frequency domain models is the possibility to measure dielectric

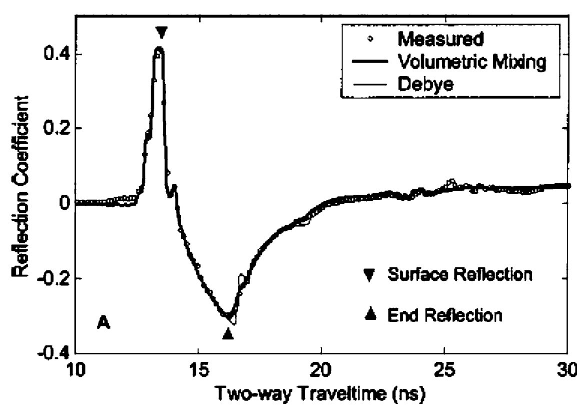

Fig. 23 Measured and predicted wafeform (Lin 2003)

permittivity in a shorter probe, where the travel time cannot be detected (Jones and Or 2001).

4.7 Factors Affecting Apparent Dielectric Permittivity K_a

4.7.1 Effect of Dry (bulk) Density

In geotechnical engineering, soil density may widely vary, especially if compacted soils are considered. Soil dry density affects the apparent permittivity of the soil as shown by Eq. 13 and as observed experimentally (Ledieu et al. 1986; Whalley 1993). Figure 24 shows the effect of soil bulk dry density on the relationship between water content and apparent permittivity as suggested by Eq. 13 assuming $A_s = 0$ (mineral soil) and average values for ρ_s and ε_s. The increase in volumetric water content associated with a decrease of bulk density $\Delta\rho_d = -0.5$ g/cm^3 is equal to $\Delta\theta = 0.023$ and this value is essentially in agreement with the values of $\Delta\theta = 0.017$ and $\Delta\theta = 0.018$ reported by Leudieu et al. (1986) and Jacobsen and Schjønning (1993).

A different empirical formula to include the effect of soil density was suggested by Malicki et al. (1996) who tested mineral and organic soils, the latter characterised by very low bulk density:

$$\theta = \frac{\sqrt{K_a} - 0.819 - 0.168\rho_d - 0.159\rho_d^2}{7.17 + 1.18\rho_d} \tag{17}$$

where ρ_d is the dry bulk density (g/cm^3). Malicki's equation is shown in Fig. 25 and the increase in water

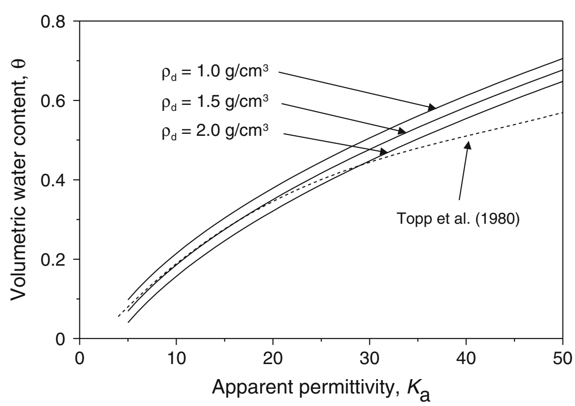

Fig. 24 Effect of soil bulk dry density ρ_d on the relationship between water content and apparent permittivity for mineral soils as suggested by Eq. 13 ($A_s = 0$, $\rho_s = 2.7$ g/cm3, $\varepsilon_{fw} = 80.2$, $\varepsilon_s = 5$)

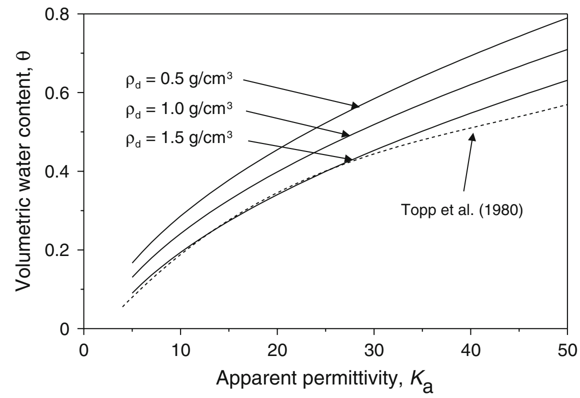

Fig. 25 Effect of soil bulk dry density ρ_d on the relationship between water content and apparent permittivity as suggested by Malicki et al. (1996) for mineral and organic soils

content associated with a decrease in bulk density $\Delta\rho_d = -0.5$ g/cm^3 is significantly greater ($\Delta\theta =$ 0.033–0.07). In this case, however, a decrease in bulk density is also associated with the presence of organic matter and, hence, bound water, which causes a further decrease in apparent permittivity at given water content due to the lower permittivity of bound water with respect to that of free water. It may be inferred that the effect of soil density in Malicki's equation implicitly accounts for the effect of bound water in low-density organic soils and, as a result, this equation should be extrapolated to high-density mineral soils with care.

4.7.2 Effect of Bulk Water Conductivity (BEC)

In high saline soils (BEC approximately greater than 0.6–0.7 S/m, waveform reflections necessary for dielectric permittivity measurements can be totally attenuated (Jones et al. 2002). This problem is more significant in longer probes and cables (Topp et al. 2000).

Conventional TDR applications are therefore limited to soils with low to moderate salinity, unless measures are taken to preserve the waveform reflection occurring at the end of the waveguides. Rod coatings have been successfully used to reduce signal attenuation and to preserve information needed to evaluate the dielectric constant in high saline soils (Knight et al. 1997; Mojid et al. 1998; Nichol et al. 2002). Since these coatings significantly influence the resulting apparent permittivity, specific $\theta - K_a$

calibration is required. Another approach to measure water content in high saline soils has been presented by Jones and Or (2001) which consists in using shorter probes (2–3 cm) and analysing the signal in the frequency domain after time-to-frequency domain transformation using appropriate algorithms (Nicolson 1973).

Although reflection at the end of the probes can be detected in soils with low to moderate salinity, the time t_{end} at which the waveform is reflected at the end of the probe may be difficult to identify (see previous section). In addition, BEC increases the apparent permittivity K_a at given water content (see Eq. 9 and Figs. 16, 17), which can make the conventional $\theta - K_a$ calibration highly inaccurate. Noborio et al. (1994) found that Topp's equation overestimated θ in soils moistened with saline water.

Topp et al. (2000) found that TDR signal electric loss is a function of the bulk electrical conductivity σ, regardless of whether this conductivity arises from soil water solution conductivity or from clay type and content. This suggests that the effects of soil water conductivity and clay content can be lumped together and taken into account by including the bulk electrical conductivity σ in the TDR calibration.

Wyseure et al. (1997) suggest to include the bulk electrical conductivity in addition to travel time into the TDR calibration curve. Evett et al. (2005) extended the model by Wyseure et al. (1997) by including effective frequency:

$$\theta = a + b\sqrt{K_a} + c\sqrt{\frac{\sigma}{2\pi f^* \varepsilon_0}} \tag{18}$$

where a, b, c are empirical coefficients, K_a is the apparent permittivity given by Eq. 11, σ is the bulk electrical conductivity determined using Eq. 16 possibly corrected to account for cable resistance effects and instrument errors (Lin et al. 2007, 2008), ε_0 is the dielectric permittivity in free space, and f^* is the effective frequency determined from the second rising limb of the reflection waveform according to the method suggested by the authors. A detailed discussion on the different ways to define the effective frequency is provided by Robinson et al. (2003a). An important advantage of Eq. 18 is that the effects of temperature on BEC and effective frequency are implicitly taken into account (temperature is still needed because it affects the static dielectric permittivity of water and, hence, K_a). In addition, Eq. 18 can also take into account the low-pass filtering effect of longer cables.

4.7.3 *Effect of Temperature*

Understanding the effect of temperature on TDR measurements is of great importance in field measurements due to the daily temperature fluctuations which can be as high as 20°–30° degrees in surface installations (Or and Wraith 1999). The value of K_a may increase or decrease with temperature depending on soil texture (Campbell 1990; Persson and Berndtsson 1998; Wraith and Or 1999; Pepin et al. 1995).

In soils having low pore water electrical conductivity and negligible amount of bound water, the soil bulk apparent permittivity is essentially controlled by the static permittivity of free water, which decreases with temperature as shown in Fig. 16a. The effect of temperature on the relationship $\theta - K_a$ can adequately be described by including the temperature-dependent apparent permittivity of free water in Eq. 13 (Pepin et al. 1995). This is illustrated in Fig. 26 showing that the effect of temperature may be significant at high water contents.

Soils having significant amount of bound water exhibit a complex response to temperature changes. K_a decreases with increasing temperature at higher water contents, as in mineral soils, whereas it increases with temperature at lower water contents (Wraith and Or 1999). This latter response has been

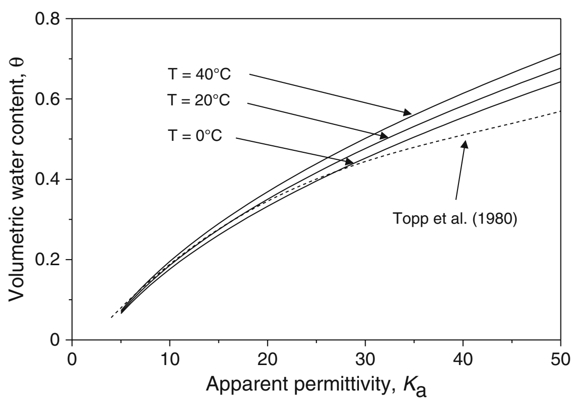

Fig. 26 Effect of temperature on the relationship between water content and apparent permittivity for mineral soils as suggested by Eq. 13 ($A_s = 0$, $\rho_s = 2.7$ g/cm^3, $\rho_d = 1.5$ g/cm^3 = 80.2, $\varepsilon_{fs} = 5$)

assumed to be associated with bound water, whose relative proportion is significant at lower water contents. Or and Wraith (1999) assume that the change of apparent permittivity with temperature results from two competing responses, the reduction of free water static permittivity with increased temperature, and the release of bound water with increased temperature. This latter process causes an overall increase in soil permittivity because water moving from the bound to the free state increases its permittivity from $\sim$4 to $\sim$80. According to this mechanism, Or and Wraith (1999) suggest a correction to account for these two competing temperature effects on soil bulk permittivity.

The increase in bulk soil permittivity with temperature observed in soils with significant amount of bound water may be explained in an alternative fashion. Fig. 16 shows that the apparent permittivity increases with temperature for the case of high electrical conductivity, and this is typically the case of soils having significant proportion of bound water.

4.7.4 Effect of Cable Length

As the pulse moves down the cable to the probe, its higher frequency components are selectively attenuated because the cable acts as a low pass filter (Lin and Tang 2007). This means that a longer cable causes a slower rise time of the pulse probe, and less steep descending and rising limbs of the inflections caused by probe handle and end of rods respectively (Herkelrath et al. 1991; Hook et al. 1992; Hook and Livingston 1995). If the probe is short enough, the descending limb (soil reflection) will intersect the rising limb (end-of-rod reflection), causing the travel time to be incorrect. This problem can be solved with a longer probe, unless measurement is carried out in a high bulk electrical conductivity soil. If this is the case, a longer probe may cause the rising limbs of the inflections caused by the end of rods to disappear. A probe length adequate for longer cable and high bulk electrical conductivity soils may be difficult to find (Evett 2000).

Another problem of long cable is that loss of high frequency components of the TDR pulse will decrease the effective frequency. Bulk electrical conductivity may then affect the apparent permittivity as the quantity $\sigma/2\pi f$ in Eq. 9 becomes larger as f becomes smaller (Robinson et al. 2005).

4.8 TDR Probes

4.8.1 Probe Design

Early types of TDR probe consisted of two stainless steel rods with the proximal ends connected to the splits ends of a bifilar antenna cable. Connections were made using alligator clips or made by clamping the wire to the rod with a screw. Connections were exposed to the surrounding medium (air in surface installation and wet or dry soil in deep installation) and their geometry could vary depending on installation. This made the connection impedance difficult to predict making it difficult to locate the point at which the wave entered the waveguides (Evett 2000). For these reasons, TDR probes commercially available today are made with the split in the cable and the cable connections to the rods embedded in a material of consistent and constant permittivity.

The two-rod probes also required a balun to convert the unbalanced signal in the coaxial cable to a balanced signal in the two rods thus lowering signal distortion (Spaans and Baker 1993). Three-rod probe commercially available today responds to this concern by providing a waveguide that is geometrically similar to a coaxial waveguide. Measurement by Zegelin et al. (1989) showed only minor differences in waveform shape between trifilar and coaxial waveguides.

4.8.2 Sampling Volume

Topp and Davis (1985b) suggests that the volume measured by a two-rod TDR probe is approximately a cylinder having diameter 1.4 times the spacing between the rods. Ledieu et al. (1986) indicates that 94% of the energy of the electromagnetic waves propagating along a two-rod probe is restricted to a diameter about two times the spacing between the rods.

The addition of a central rod as in three-rod probes drastically reduces the sample area (Ferre et al. 1998; Zegelin et al. 1989). For a three-rod probes, the sampling volume, i.e. the volume contributing to the probe response, is essentially a cylinder having diameter approximately equal to the spacing between the outer rods (Ferre et al. 1998). A detailed discussion on sampling volume of probes having different design can be found in Ferre et al. (1998) and Robinson et al. (2003a).

4.9 Water Content Measurement Using Capacitance

Due to installation difficulties, TDR systems are not always adapted for determination of water content at relatively large depths. Depth capacitance probes have then been designed to sense the soil from within an access tube (Fig. 27). Due to the emergence of high quality, low-cost high frequency oscillators, these probes are relatively inexpensive and easy to operate, and are becoming a popular choice for routine monitoring purposes. Surface capacitance insertion probes (SCIP) have also been developed and may be an interesting alternative to TDR when measurements at few locations in the field have to be made.

The depth capacitance installation probe consists of an electrode pair separated by a plastic dielectric. The upper and lower electrodes and the plastic separator are in the shape of a cylinder that fits closely inside the plastic access tube. A resonant *LC* circuit ($L =$ inductance, $C =$ capacitance) in the probe includes the ensemble of the soil outside the access tube, the access tube itself, plus the air space between the probe and the access tube, as one of the capacitive element. The LC circuit is included in the tuned circuit of an oscillator to measure the resonant frequency F_{res} of the LC circuit. The resonant frequency depends on the capacity of the soil-access tube system C as follows (Dean et al. 1987):

$$F_{res} = \frac{1}{2\pi\sqrt{L}}\left(\frac{1}{C} + \frac{1}{C_b} + \frac{1}{C_c}\right)^{0.5} \tag{19}$$

where L is the inductance of the coil in the *LC* circuit, C_b and C_c are the base capacitance and collector

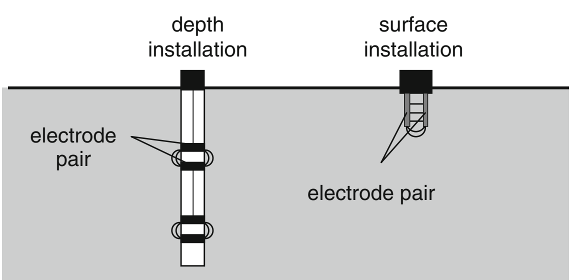

Fig. 27 Surface and depth installation capacitance probes and relative electric fields

capacitance respectively. The capacitance C is in turn linked to the soil apparent permittivity by the following linear relationship:

$$C = gK_a \tag{20}$$

where g is a geometrical factor that is difficult to calculate except for simple electrode geometries. The surface capacitance installation probe consists of two rod-shaped electrodes that are inserted into the soil and shares the same working principle as the depth probe. The relationship that links the resonant frequency to the capacity C can be written according to Dean (1994) and is similar in nature to Eq. 19.

Water content measurements can be performed by directly relating the resonant frequency F_{res} to the water content (Paltineanu and Starr 1997; Sentek 2001) or by calibrating the parameters in Eqs. 19 and 20 (or similar equations) to derive the apparent permittivity K_a which can be in turn related to water content using the empirical TDR relationships (Robinson et al. 1998; Kelleners et al. 2004). The major disadvantage of the single step calibration is that one cannot separate errors due to the instrument from errors due to the calibration between capacitance and soil water content (Robinson 2001).

It should be noted that the operating frequency of the capacitance probe is in the range 70–150 MHz (Robinson et al. 1998). In this frequency range, the apparent permittivity is more sensitive to electrical conductivity with respect to TDR. As an example, consider the aqueous solution shown in Fig. 16b having $\sigma \sim 0.5$ S/m. In the high-frequency range of TDR bandwidth, the apparent permittivity is equal to the static permittivity in contrast with the capacitance probe range ($\sim$70–150 MHz) where the apparent permittivity is significantly affected by electrical conductivity. If this aqueous solution would have resided in the soil, the bulk apparent permittivity would have essentially depended on water content in TDR measurement whereas it would have been significantly affected by electrical conductivity when using the capacitance probe (Baumhardt et al. 2000). In addition, in the low-frequency range, apparent permittivity is significantly affected by the Maxwell-Wagner effect (Chen and Or 2006a, b).

In other words, 'universal' calibration curves for capacitance probes relating resonant frequency to volumetric water content can be valid only for soils with low electrical conductivity (0.05–0.1 S/m according to Robinson et al. 1998) and relatively low water content ($\theta < \sim 0.30$ according to Kelleners et al. 2004). For soils having relatively high bulk electrical conductivity (saline water or high cation exchange capacity), either a soil-specific calibration curve needs to be obtained or the electrical conductivity needs to be measured independently and used to correct apparent permittivity (Robinson et al. 1998; Kelleners et al. 2004). Capacitance probes allowing the simultaneous measurement of resonant frequency and the bulk soil electrical conductivity are commercially available.

Because of the greater sensitivity of capacitance sensors to soil bulk electrical conductivity, empirical single-step calibration curves for capacitance probes tend to be scattered. As an example, Fig. 28 reports different single-step calibration curves for the Sentek multicapacitance probe reported in the literature.

Concerning radial and axial sensitivity of depth installation capacitance probes, Paltineanu and Starr (1997), using brass rings electrodes 50.5 mm diameter and 25 mm high, separated by a 12 mm plastic ring, observed that axial sensitivity is about 100 mm and radial sensitivity is about 130 mm (i.e the sampling volume is approximately a cylinder 260 mm diameter and 100 mm high).

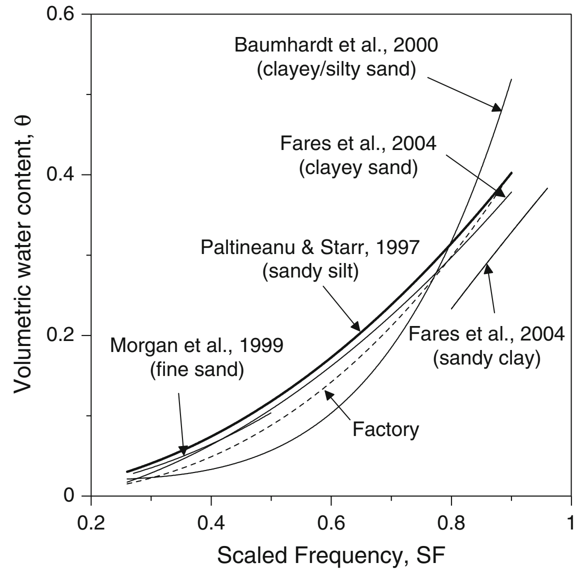

Fig. 28 Single-step calibration curves for the Sentek multicapacitance probe reported in the literature

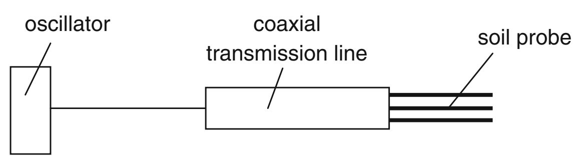

Fig. 29 Amplitude Domain Reflectometry probe

4.10 Water Content Measurement Using Amplitude Domain Reflectometry (ADR)

This probe consists of a sinusoidal oscillator (typically 100 MHz), a fixed impedance section of a coaxial line, and a stainless steel wire sensing probe which behaves as an additional section of the transmission line with an impedance dependent on the dielectric permittivity of the soil surrounding the probe wires (Fig. 29). If this impedance differs from that of the internal coaxial transmission line, then a proportion of the signal is reflected back from the junction between the probe rods and the coaxial transmission line according to Eq. 10.

The difference between the peak voltage at its start and the peak voltage at the junction can be related to the impedance Z_L of the soil surrounding the probe wires through Eq. 10, and this impedance can be in turn related to soil permittivity through Eq. 5 (Gaskin and Miller 1996; Miller and Gaskin 1999).

The main limitation of this type of probe is, similarly to the capacitance probes, the low operating frequency (100 MHz). As shown in Fig. 16, the apparent permittivity of water is equal to static permittivity only if the pore water bulk conductivity is relatively small (0.05 S/m as in tap water). Universal or manufacturer calibrations are therefore applicable as long the soil does not contain saline water and/or or clays having high cation exchange capacity. If it is not the case, the apparent permittivity measured by the impedance probe at given water contents tends to be higher than that measured using TDR (Cosh et al. 2005) and a soil specific calibration is highly recommended.

5 Field Measurement of Water Permeability

Direct measurement of unsaturated permeability to water (hydraulic conductivity) in the field is a very difficult task. Normally the permeability function relating unsaturated permeability to suction is estimated from the saturated permeability, k_{sat}, and the water retention curve. However, it is important to have methods for field determination of flow under a suction gradient. As Benson et al. (1997) point out, there is little value in using small specimens in the laboratory to assess field hydraulic conductivity. This report will consider four methods: Infiltrometers, the Disc Permeameter, the Guelph Permeameter and the Cone Permeameter. A more complete discussion of some of the equipment is given by Stephens (1995).

5.1 Infiltrometer

Infiltrometers are simple and widely used to estimate infiltration into a soil. They are usually used to estimate the permeability under field saturated conditions by continuing flow until a steady state is observed. Double ring infiltrometers are used to ensure one-dimensional vertical flow from the inner ring where measurements are made. Tensiometers can be used to observe the movement of the wetting front and to calculate hydraulic gradient (which otherwise have to be assumed). A sealed double ring infiltrometer may be used to prevent evaporation for long term tests (Neupane et al. 2005).

5.2 Disc Permeameter

A Tension Disc Permeameter (Perroux and White 1988) can be used to determine near saturated permeability, but is limited to suctions of 3–5 kPa. A bubbling tower is used to create negative pressure. Reynolds and Elrick (1991) describe the analysis to obtain the near saturated permeability. Nishimura et al. (2003) report good agreement between field measurements and laboratory measurements on cores of the same soil.

5.3 Guelph Permeameter

The Guelph Permeameter (Reynolds and Elrick 1985) can be fitted with a tension adapter that allows measurement under suction. Coutinho et al. (2000) used the Guelph permeameter in a residual soil and showed that the ratio of the unsaturated/saturated permeability (k/k_{sat}) drops to 10^{-5}–10^{-12} at a suction of 20 kPa, indicating very low values of unsaturated permeability at quite low suctions. Morii et al. (2003) used TDR for moisture content measurement near the Guelph ring and used an unsaturated flow finite element code to back-analyse unsaturated permeability. They show that k/k_{sat} dropped to very low values for a suction of only 3–4 kPa in a gravelly sand.

5.4 Cone Permeameter

The Cone Permeameter (Kodešová et al. 1998) has a porous filter close to the tip of a cone penetrometer with two tensiometer rings fitted 50 and 90 mm above the filter. A constant head is applied to the filter for 5–10 min and tensiometer readings are observed during water redistribution. Inverse analysis is used to determine α_w, α_d, n (van Genuchten's parameters, with the subscripts α_w and α_d indicating different values for wetting and drying) k_{sat} and k^A (ratio of horizontal/vertical permeability) (Šimůnek et al. 1998).

Gribb et al. (2004) show that for a silty sand k/k_{sat} drops to virtually zero by suctions of 10–20 kPa.

6 Conclusions

This paper has presented a review of techniques for field measurement of suction and water content. The main problems in the use of field tensiometers have been addressed and hints on how to improve tensiometer performance have been given. These include locating the three essential components (the pressure sensor, the reservoir of water and the porous filter) as close as possible to each other and keeping the volume of water in the piezometer as small as possible whilst allowing the incorporation of a system for removing air from the tensiometer. In addition, it is essential that there is continuity between the soil water and the water in the piezometer at all times. Cement-bentonite grout has been shown to work well in this respect. To date, tensiometers that can measure suction continuously over a relatively long period time have a suction range limited to $\sim$80 kPa.

Advantages and limitations of instruments for indirect measurement of suction have also been discussed. Electrical conductivity, thermal conductivity, and dielectric permittivity sensors all share an unsaturated porous element that comes to equilibrium with the surrounding soils. This inevitably introduces a time-lag in the response of these instruments which can be of the order of days and that make them unsuitable for use in a rapidly changing moisture environment. The same problem affects the psychrometer as equalization occurs through the water vapour phase. The main advantage of these sensors is that they do not require maintenance and can be left unattended for long periods of time.

Water content measurement is less problematic than suction measurement, the sensor response is much faster and soils can be continuously monitored also when suction is outside the range of 0–80 kPa. In this paper, the dielectric properties of the soil and its constituents and also the interaction between electromagnetic waves and the soil components have been examined first. It has then been shown that interpretation of dielectric measurement is relatively straightforward as long as the measurement frequency falls in a range where ionic losses are negligible. In practice, this occurs when the pore water has low electrical conductivity and the amount of bound water is negligible (soils having low cation exchange capacity). When this is not the case, interpretation may be problematic. In this respect, TDR is preferable to capacitance and ADR methods as it is less sensitive to bulk electrical conductivity.

Methods for measurement of field hydraulic conductivity have been only briefly reviewed to show how suction and water content field measurement can be used to determine field hydraulic conductivity. A more detailed review is out of the scope of the paper and the reader may refer to other reports found in the literature.

Acknowledgements The authors wish to acknowledge the support given by the European Community through the Marie-Curie Research and Training Network MUSE—Mechanics of Unsaturated Soils for Engineering—(MRTN-CT-2004-506861).

References

Aitchison GD, Richards BG (1965) A broad-scale study of moisture conditions in pavement subgrades throughout Australia. In: Proceedings of conference on moisture equilibrium and moisture changes in soils beneath covered areas. Sydney, Butterworths, pp 198–204

Aitchison GD, Butler PF, Gurr CG (1951) Techniques associated with the use of gypsum block soil moisture meters. Aust J Appl Sci 2:57–75

Alonso EE, Gens A, Josa A (1990) A constitutive model for partially saturated soils. Géotechnique 40(3):405–430

Alonso EE, Lloret A, Delahaye CH, Vaunat J, Gens A, Volckaert G (1998) Coupled analysis of a backfill hydration test. Int J Numer Anal Methods Geomech 22:1–27

Baker JM, Allmaras RR (1990) System for automating and-multiplexing soil moisture measurement by time-domain reflectometry. Soil Sci Soc Am J 54(1):1–6

Baker JM, Spaans EJA (1993) Comments on ''Time domain reflectometry measurements of water content and electrical conductivity of layered soil columns.''. Soil Sci Soc Am J 57:1395–1396

Banin A, Amiel A (1970) A correlative study of the chemical and physical properties of a group of natural soils in Israel. Geoderma 3:185–198

Baumhardt RL, Lascano RJ, Evett SR (2000) Soil material, temperature, and salinity effects on calibration of multisensor capacitance probes. Soil Sci Soc Am J 64:1940–1941

Benson CH, Gunter JA, Boutwell GP, Trautwein SJ, Berzanskis PH (1997) Comparison of four methods to assess hydraulic conductivity. J Geotech Geoenviron Eng 123(10):929–937

Bertolino AVFA, Souza AP, Fernandes NF, Rangel AM, de Campos TMP, Shock CC (2002) Monitoring the field soil matrix potential using mercury tensiometer and granular matrix sensors. In: Jucá JFT, de Campos TMP, Marinho FAM (eds) Unsaturated soils, Proceedings of 3rd international conference on unsaturated soils, vol 1. Balkema, Recife, Lisse, pp 335–338

Bishop AW, Kennard MF, Vaughan PR (1964) Developments in the measurement and interpretation of pore water pressure in earth dams. Trans. 8th Int. Cong. On Large Dams, Edinburgh, vol. 1, pp 47–71

Black WPM, Croney D, Jacobs JC (1958) Field studies of the movement of soil moisture. Road Research Technical Paper No. 41. HMSO. London

Bockris JO, Gileadi E, Muller K (1966) Dielectric relaxation in the electric double layer. J Chem Phys 44:1445–1456

Bulut R, Leong EC (2008) Indirect measurement of suction. Geotech Geol Eng. doi:10.1007/s10706-008-9197-0

Cameron DA (2001) The extent of soil desiccation near trees in a semi-arid environment. In: Toll DG (ed) Unsaturated soil concepts and their application in geotechnical practice. Dordrecht: Kluwer Academic, pp 357–370

Campbell JE (1990) Dielectric properties and influence of conductivity in soils at one to fifty megahertz. Soil Sci Soc Am J 54:332–341

Campbell GS, Gee GW (1986) Water potential: miscellaneous methods. In: Klute A (ed) Methods of soil analysis, Part 1, 2nd ed. Agron. Monogr. 9, Madison, WI: ASA, CSSA and SSSA, pp 619

Castiglione P, Shouse PJ (2003) The effect of ohmic cable losses on time-domain reflectometry measurements of electrical conductivity. Soil Sci Soc Am J 67:414–424

Chen Y, Or D (2006a) Geometrical factors and interfacial processes affecting complex dielectric permittivity of partially saturated porous media. Water Resour Res 42:W06423

Chen Y, Or D (2006b) Effects of Maxwell-Wagner polarization on soil complex dielectric permittivity under variable temperature and electrical conductivity. Water Resour Res 42:W06424

Chipp PN, Clare DG, Henkel DJ, Pope RG (1982) Field measurement of suction in colluvium covered slopes in Hong Kong. In: Proceedings of 7th Southeast Asian Geotechnical conference, vol 1, pp 49–62

Cosh MH, Jackson TJ, Bindlish R, Famiglietti JS, Ryu D (2005) Calibration of an impedance probe for estimation of surface soil water content over large regions. J Hydrol 311:49–58

Coutinho RQ, Souza Neto JB, Costa FQ (2000) Design strength parameters of a slope on unsaturated gneissic residual soil. In: Shackleford CD, Houston SL, Chang NY (ed) Advances in unsaturated geotechnics. Geotechnical Special Publication No. 99, Reston: American Society of Civil Engineers, pp 247–261

Crilley MS, Schreiner HD, Gourley C (1991) A simple field suction measurement probe. In: Proceedings of 10th African regional conference on soil mechanics and foundation engineering, Lesoto, pp 291–298

Cui YJ, Zornberg JG (2008) Water balance and evapotranspiration monitoring in geotechnical and geoenvironmental engineering. Geotech Geol Eng. doi:10.1007/s10706-008-9198-z

Cui YJ, Tang AM, Mantho AT, De Laure E (2008) Monitoring field soil suction using a miniature tensiometer. Geotech Testing J 31(1):95100

Dalton FN, Herkelrath WN, Rawlins DS, Rhoades JD (1984) Time domain reflectometry: simultaneous measurements of soil water content and electrical conductivity with a single probe. Science 224:989–990

Dane JH, Topp GC (eds) (2002) Methods of soil analysis. Part 4-physical methods. SSSA Books Ser. 5. SSSA, Madison, WI, USA

Dasberg S, Hopmans JW (1992) Time domain reflectometry calibration for uniformly and non-uniformly wetted sandy and clayey loam soils. Soil Sci Soc Am J 56:1341–1345

De Loor GP (1968) Dielectric properties of heterogeneous mixtures containing water. J Microwave Power 3:67–73

Dean TJ (1994) The IH capacitance probe for measurement of soil water content. IH Report No. 125. Institute of Hydrology, Wallingford, Oxon

Dean TJ, Bell JP, Baty ABJ (1987) Soil moisture measurement by an improved capacitance technique. Part I. Sensor design and performance. J Hydrol 93:67–78

Debye P (1929) Polar molecules. Chemical Catalog Company, New York

Delage P (2004) State of the art report—Experimental unsaturated soil mechanics. In: Proceedings of 3rd international conference on unsaturated soils, Recife, Brasil 3:973–998

Delta-T (2005) Delta T Devices—Soil moisture sensors. http://www.delta-t.co.uk

Dirksen C, Dasberg S (1993) Improved calibration of time domain reflectometry soil water content measurements. Soil Sci Soc Am J 57:660–667

Dobson MC, Ulaby FT, Hallikainen MT, El-Rayes MA (1985) Microwave dielectric behavior of wet soil-Part II: dielectric mixing models. IEEE Trans Geosci Remote Sens Ge-23(1):35–46

Drungil CEC, Abt K, Gish TJ (1989) Soil moisture determination in gravely soils with time domain reflectometry. Trans ASAE 32:177–180

Evans NC, Lam JS (2003) Soil moisture conditions in vegetated cut slopes and possible implications for stability. GEO published report no. 140. Geotechnical Engineering Office, Hong Kong Special Administrative Region, 48 pp

Evett SR (2000) The TACQ computer program from automatic time domain reflectyometry measurement: II. Waveform interpretation methods. Trans ASAE 43(6):1947–1956

Evett SR, Tolk JA, Howell TA (2005) Time domain reflectometry laboratory calibration in travel time, bulk electrical conductivity, and effective frequency. Vadose Zone J 4:1020–1029

Feng M, Fredlund DG (2003) Calibration of thermal conductivity sensors for measuring soil suction. Can Geotech J 40(5):1048–1055

Feng W, Lin C-P, Deschamps RJ, Drnevich VP (1999) Theoretical model of a multisection time domain reflectometry measurement system. Water Resour Res 35(8):2321–2331

Ferre PA, Knight JH, Rudolph DL, Kachanoswki RG (1998) The sample areas of conventional and alternative time domain reflectometry probes. Water Resources Res 36:2461–2468

Flint AL, Campbell GS, Ellett KM, Calissendorff C (2002) Calibration and temperature correction of heat dissipation matric potential sensors. Soil Sci Soc Am J 66(5):1439–1445

Fredlund DG, Rahardjo H (1993) Soil mechanics for unsaturated soils. Wiley

Friedman SP (1997) Statistical mixing model for the apparent dielecflectometry tric constant of unsaturated porous media. Soil Sci Soc Am J 61:742–745

Friedman SP (1998) A saturation degree-dependent composite spheres model for describing the effectivve dielectric constant of unsaturated porous media. Water Resources Res 34(11):2949–2961

Gallipoli D, Gens A, Sharma R, Vaunat J (2003) An elasto-plastic model for unsaturated soil incorporating the effects of suction and degree of saturation on mechanical behaviour. Géotechnique 53(1):123–136

Gardner CMK, Robinson DA, Blyth K, Cooper JD (2001) Soil water content measurement. In: Smith K, Mullins C (eds) Soil and environmental analysis: physical methods, 2nd edn. Marcell Dekker, Inc., 270 Madison Ave, New York, pp 1–64

Gaskin GJ, Miller JD (1996) Measurement of soil water content using a simplified impedance measuring technique. J Agric Res 63:153–160

Gatmiri B, Delage P (1997) A formulation of fully coupled thermal-hydraulic-mechanical behaviour of saturated porous media: numerical approach. Int J Anal Numer Methods Geomech 21:199–225

Gatmiri B, Delage P, Cerrolaza M (1997) U-Dam: a powerful finite element software for the analysis of unsaturated porous media. Int J Adv Eng Software 29(1):29–43

Giese K, Tiemann R (1975) Determination of the complex permittivity from thin-sample time domain reflectometry improved analysis of the step response waveform. Adv Mol Relax Processes 7:45–59

Gourley C, Schreiner HD (1995) Field measurement of soil suction. In: Alonso EE, Delage P (eds) Unsaturated soils. Proceedings of 1st international conference on unsaturated soils, vol 2. Balkema, Paris, Rotterdam, pp 601–607

Greacen EL, Walker GR, Cook PG (1987) Evaluation of the Filter Paper Method for Measuring Soil Water Suction, Int. Conf. on Measurement of Soil and Plant Water Status, pp 137–143

Gribb MM, Kodešová R, Ordway SE (2004) Comparison of soil hydraulic property measurement methods. J Geotech Geoenviron Eng 130(10):1084–1095
Hasted JB (1973) Aqueous dielectrics. Chapman and Hall, London
Heimovaara TJ (1992) Comments on ''Time domain reflectometry measurements of water content and electrical conductivity of layered soil columns''. Soil Sci Soc Am J 56:1657–1658
Heimovaara TJ (1993) Design of triple-wire time domain reflectometry probes in practice and theory. Soil Sci Soc Am J 57:1410–1417
Heimovaara TJ (1994) Frequency domain analysis of TDR waveforms 1. Measurement of the complex dielectric permittivity of soils. Water Resour Res 30(2):189–199
Heimovaara TJ, Bouten W (1990) A computer-controlled 36 channel time domain reflectometry system for monitoring soil water contents. Water Resour Res 26:2311–2316
Heimovaara TJ, Bouten W, Verstraten JM (1994) Frequency domain analysis of time domain reflectometry waveform. 2. A four-component complex dielectric mixing model for soils. Water Resour Res 30(2):201–209
Herkelrath WN, Hamburg SP, Murphy F (1991) Automatic, real-time monitoring of soil moisture in a remote field area with TDR. Water Resour Res 27(5):857–864
Hignett C, Evett SR (2002) Neutron thermalisation. In: Dane JH, Topp GC (eds) Methods of soil analysis. Part 4. SSSA Book Ser. 5. SSSA, Madison, WI
Hilhorst MA, Dirksen C, Kampers FWH, Feddes RA (2000) New dielectric mixture equation for porous materials based on depolarization factors. Soil Sci Soc Am J 64:1581–1587
Hilhorst MA, Dirksen C, Kampers FWH, Feddes RA (2001) Dielectric relaxation of bound water versus soil matric pressure. Soil Sci Soc Am J 65:311–314
Hoekstra P, Delaney A (1974) Dielectric properties of soils at UHF and microwave frequencies. J Geophys Res 79(11):1699–1708
Hook WR, Livingston NJ (1995) Propagation velocity errors in time domain reflectometry measurements of soil water. Soil Sci Soc Am J 59:92–96
Hook WR, Livingston NJ, Sun ZJ, Hook PB (1992) Remote diode shorting improves measurememt of soil water by time domain reflectometry. Soil Sci Soc Am J 56:1384–1391
Huisman JA, Lambot S, Vereecken H (2006) Determining soil water content variation along the TDR probe with inverse modelling: theory, practice and challenges. In: Proceedings of TDR 2006, Purdue University, West Lafayette, USA, Sept. 2006, Paper ID 28, 10 p, http://engineering.purdue.edu/TDR/Papers
Ireson AM, Wheater HS, Butler AP, Finch J, Cooper JD, Wyatt RG, Hewitt EJ (2005) Field monitoring of matric potential and soil water content in the chalk unsaturated zone. In: Proceedings of international symposium on advanced experimental unsaturated soil mechanics, Trento, Italy, pp 511–518
Ishida T, Makino T (1999) Effects of pH on dielectric relaxation of montmorillonite, allophane, and imogolite suspensions. J Colloid Interf Sci 212:152–161
Jacobsen OH, Schjønning P (1993) A laboratory calibration of time domain reflectometry probes for soil water measurement including effects of bulk density and texture. J Hydrol 151:147–158
Johnston WH (2000) Calibration of gypsum blocks and data loggers and their evaluation for monitoring soil water status. Aust J Exp Agric 40(8):1131–1136
Jones SB, Or D (2001) Frequency-domain methods for extending TDr measurement range in saline soils. Symposium and Workshop on TDR for innovative geotechnical applications. Available at http://www.iti.northwestern, 2001
Jones SB, Wraith JM, Or D (2002) Time domain reflectometry measurement principles and applications. Hydrol Process 16:141–153
Kelleners TJ, Soppe RWO, Ayars JE, Skaggs TH (2004) Calibration of capacitance probe sensors in a saline silty slay. Soil Sci Soc Am J 68:770–778
Keller GV (1989) Electrical properties. Section V. In: Carmichael RS (ed) CRC practical handbook of physical properties of rocks and minerals. CRC Press, Boca Raton, FL
Knight JH, Ferre PA, Rudolph DL, Kachanoski RG (1997) A numerical analysis of the effects of coatings and gaps upon relative dielectric permittivity measurement with tome domain reflectometry. Water Resour Res 33:1455–1460
Kodešová R, Gribb MM, Šimůnek J (1998) A new CPT method for estimating soil hydraulic properties. In: Robertson PK, Mayne PW (eds) Proceedings of 1st international conference on site characterization, vol 2. Balkema, Rotterdam 1998, pp 1421–1425
Kraus JD, Fleisch DA (1999) Electromagnetics with applications. McGraw-Hill
Ledieu J, De Ridder P, De Clerck P, Dautrebande S (1986) A method of measuring soil moisture by time domain reflectometry. J Hydrol 88:319–328
Lichtenecker K (1926) Die dielektrizitatskonstante naturlicher und kunstlicher mischkorper. Physikalische Zeitschrift 27:115–158
Lin CP (2003a) Analysis of nonuniform and dispersive time domain reflectometry measurement systems with application to the dielectric spectroscopy of soils. Water Resour Res 39 doi:10.1029/2002 WR001418
Lin CP (2003b) Frequency domain versus travel time analyses of TDR waveforms for soil moisture measurement. Soil Sci Soc Am J 67:720–729
Lin C-P, Tang SH (2007) Comprehensive wave propagation model to improve TDR imtepretation for geotechnical applications. Geotech Testing J 30(2):90–97
Lin C-P, Chung C-C, Tang S-H (2007) Accurate time domain reflectometry measurement of electrical conductivity accounting for cable resistance and recording time. Soil Sci Soc Am J 71:1278–1287
Lin C-P, Chung C-C, Huisman JA, Tang S-H (2008) Clarification and calibration of reflection coefficient for TDR electrical conductivity measurement. Soil Sci Soc Am J, accepted for publication
Livingston BE (1908) A method of controlling plant moisture. Plant World 11:39–40
Logsdon SD, Laird DA (2002) Dielectric spectra of bound water in hydrated Ca-smectite. J Non-Cryst Solids 305:243–246
Lynde CJ, Dupre HA (1913) On a new method of measuring the capillary lift of soils. J Am Soc Agron 5:107–116

Mahler CF, Gonçalves H, Pacheco AC (2004) Development of an automatic tensiometer in laboratory using a mini-lysimeter. In: Jucá JFT, de Campos TMP, Marinho FAM (eds) Unsaturated soils. Proceedings of 3rd international conference on unsaturated soils, vol 3. Balkema, Recife, Lisse, 2004, pp 1021–1027

Malicki MA, Plagge R, Roth CH (1996) Improving the calibration of dielectric TDR soil moisture determination taking into account the soild soil. Eur J Soil Sci 47:357–366

Marinho FAM, Take, WA, Tarantino A (2008) Measurement of matric suction using tensiometric and axis translation techniques. Geotech Geol Eng. doi:10.1007/s10706-008-9201-8

Masrouri F, Bicalho KV, Kawai K (2008) Hydraulic testing in unsaturated soils. Geotech Geol Eng. doi:10.1007/s10706-008-9202-7

Mendes J, Toll DG, Augarde CE, Gallipoli D (2008) A system for field measurement of suction using high capacity tensiometers. Proceedings of 1st European conference on unsaturated soils, Durham, UK, July 2008

Miller JD, Gaskin GJ (1999) ThetaProbe ML2x. Principles of operation and applications. MLURI Technical Note (2nd edn)

Mojid MA, Wyseure GCL, Rose DA (1998) The use of insulated time-domain reflectrometry sensors to measure water content in highly saline soils. Irrig Sci 18:55–61

Morii T, Takeshita Y, Inoue, M (2003) In-situ measurement and evaluation of soil permeability in sand sediment. In: Karube D, Iizuka A, Kato S, Kawai K, Tateyama K (eds) Proceedings of 2nd Asian conference on unsaturated soils, Kobe, UNSAT-ASIA 2003, pp 107–112

Nadler A, Dasberg S, Lapid I (1991) Time domain reflectometry measurements of water content and electrical conductivity of layered soil columns. Soil Sci Soc Am J 55:938–943

Neupane D, Bowders JJ, Loehr JE, Bouazza A, Trautwein SJ (2005) Sealed double-ring infiltrometers for estimating very low hydraulic conductivities. Geotech Testing J 28(3):247–252

Ng CWW, Zhan LT, Bao CG, Fredlund DG, Gong BW (2003) Performance of an unsaturated expansive soil slope subjected to artificial rainfall infiltration. Geotechnique 53(2):143–157

Nichol C, Beckie R, Smith L (2002) Evaluation of uncoated and coated time domain reflectometry probes for high electrical conductivity systems. Soil Sci Soc Am J 66:1454–1465

Nichol C, Smith L, Beckie R (2003) Long-term measurement of matric suction using thermal conductivity sensors. Can Geotech J 40:587–597

Nicolson AM (1973) Forming the fast fourier transform of a step response in time-domain metrology. Electronics Lett 9:317–318

Nishimura T, Irshad U, Kato M, Inoue M (2003) Measurement of near saturated hydraulic conductivity in situ. In: Karube D, Iizuka A, Kato S, Kawai K, Tateyama K (eds) Proceedings of 2nd Asian conference on unsaturated soils, Kobe, UNSAT-ASIA 2003, pp 375–378

Nissen HH, Moldrup P (1994) Theoretical background for the TDR methodology. In: Proceedings of the symposium: time domain reflectometry applications in soil science, 16 September 1994, Tjele, Denmark. SP report no. 11, June 1995,vol 3, pp 9–23

Noborio K (2001) Measurement of soil water content and electrical conductivity by TDR: a review. Comput Electron Agric 31:213–237

Noborio K, McInnes KJ, Heilman JL (1994) Field measurements of soil electrical conductivity and water content by time-domain reflectometry. Comput Electron Agric 11:131–142

O'Connor KM, Dowding CH (1999) Geomeasurements by pulsing TDR cables and probes. CRC Press

O'Kane M, Wilson GW, Barbour SL (1998) Instrumentation and monitoring of an engineering soil cover system for mine waste rock. Can Geotech J 35:828–846

Öberg AL (1995) Negative pore pressures—seasonal variation and importance in slope stability analysis. In: Unsaturated soils—Proceedings of 1st international conference on unsaturated soils, Paris, 1995

Olivella S, Gens A, Carrera J, Alonso EE (1996) Numerical formulation for a simulator (CODE_BRIGHT) for the coupled analysis of saline media. Eng Comput 13:87–112

Oloo SY, Fredlund DG (1995) Matric suction monitoring in an expansive soil subgrade in Kenya. In: Alonso EE, Delage P (eds) Unsaturated soils, Proceedings of 1st international conference on unsaturated soils, vol 2. Balkema, Paris, Rotterdam, pp 631–635

Or D, Wraith JM (1999) Temperature effects on soil bulk dielectric permittivity measured by time domain reflectometry: a physical model. Water Resour Res 35:371–383

Or D, VanShaar T, Fisher JR, Hubscher RA, Wraith JM (2002) WinTDR99-Users guide. Utah State University—Plants, Soils, Metereology, Logan, UT. [online]—Available at http://soilphysics.usu.edu/wintdr/Documents/Manuals/2002Spr/WinTDRManual_Spr2002.pdf Accessed 08 May 2007

Paltineanu IC, Starr JL (1997) Real-time soil water dynamics using multisensor capacitance probes: laboratory calibration. Soil Sci Soc Am J 61:1576–1585

Paquet JM, Caron J, Banton O (1993) In situ determination of the water desorption characteristics of peat substrates. Can J Soil Sci 73:329–339

Patterson DE, Smith MW (1981) The measurement of frozen water content by time domain reflectometry: results from laboratory tests. Can Geotech J 18:131–144

Pepin S, Livingston NJ, Hook WR (1995) Temperature-dependent measurement erros in time domain reflectometry determinations of soil water. Soil Sci Soc Am J 59:38–43

Pépin S, Plamondon AP, Stein J (1992) Peat water content measurement using the time domain reflectometry. Can J For Res 115:564–540

Perroux KM, White I (1988) Designs for disc permeameters. Soil Sci Soc Am J 52:1205–1215

Persson M, Berndtsson R (1998) Texture and electrical conductivity effects on temperature dependency in time domain reflectometry. Soil Sci Soc Am J 62:887–893

Reynolds WD, Elrick DE (1985) In situ measurement of field-saturated hydraulic conductivity, sorptivity and the α-parameter using the Guelph Permeameter. Soil Sci 140:292–302

Reynolds WD, Elrick DE (1991) Determination of hydraulic conductivity using a tension infiltrometer. Soil Sci Soc Am J 55(3):633–639

Richards LA (1928) The usefulness of capillary potential to soil moisture and plant investigators. J Agric Res (Cambridge) 37:719–742

Richards LA (1942) Soil moisture tensiometer materials and construction. Soil Sci 53:241–248

Richards LA (1949) Methods of measuring soil moisture tension. Soil Sci 68:95–112

Richards LA, Russell MS, Neal OR (1937) Further developments on apparatus for field moisture studies. Proc Soil Sci Soc Am 2:55–63

Ridley AM, Burland JB (1993) A new instrument for the measurement of soil moisture suction. Géotechnique 43(2):321–324

Ridley AM, Burland JB (1995) Measurement of suction in materials which swell. Appl Mech Rev 48(9):727–732

Ridley AM, Burland JB (1996) A pore pressure probe for the in situ measurement of a wide range of soil suction. Advances in site investigation practice. Thomas Telford London, pp 510–520

Ridley AM, Wray WK (1996) State of the art report—Suction measurement: a review of current theory and practices. In: Alonso EE, Delage P (eds) Proceedings of 1st international conference on unsaturated soils, unsaturated soils, vol 3. Paris, pp 1293–1322

Ridley AM, Patel AR, Marsland F (1998) Tensiometers: their design and use for civil engineering purposes. Geotechnical Site Characterisation. Balkema Rotterdam, pp 851–856

Ridley AM, Dineen K, Burland JB, Vaughan PR (2003) Soil matrix suction: some examples of its measurement and application in geotechnical engineering. Géotechnique 53(2):241–253

Robinson DA (2001) Discussion on: 'Field calibration of a capacitance water content probe in fine sand soils' by Morgan et al. 1999. Soil Sci Soc Am J 65:1570–1571

Robinson DA, Friedman SP (2003) A method for measuring the solid particle permittivity or electrical conductivity of rocks, sediments, and granular materials. J Geophys Res B 108, B2 5:1–9

Robinson DA, Gardner CMK, Evans J, Cooper JD, Hodnett MJ, Bell JP (1998) The dielectric calibration of capacitance probes for soil hydrology using an oscillation frequency response model. Hydrol Earth Syst Sci 2(1):111–120

Robinson DA, Gardner CMK, Cooper JD (1999) Measurement of relative permittivity in sandy soils using TDR, capacitance and theta probes: comparison, including the effects of bulk soil electrical conductivity. J Hydrol 223:198–211

Robinson DA, Cooper JD, Gardner CMK (2002) Modelling the relative permittivity of soil using soil hygroscopic water content. J Hydrol 255:39–49

Robinson DA, Jones SB, Wraith JM, Or D, Friedman SP (2003a) A review of advances in dielectric and electrical conductivity measurement in soils using TDR. Vadose Zone J 2:444–475

Robinson DA, Schaap M, Jones SB, Friedman SP, Gardner CMK (2003b) Considerations for improving the accuracy of permittivity measurement using time domain reflectometry: air-water calibration, effects of cable length. Soil Sci Soc Am J 67:62–70

Robinson DA, Schaap MG, Or D, Jones SB (2005) On the effective measurement frequency of time domain reflectometry in dispersive and nonconductive dielectric materials. Water Resour Res 41:W02007

Romero E (1999) Characterisation and thermo-hydromechanical behaviour of unsaturated Boom Clay: an experimental study. PhD Thesis, Universitad Politecnica de Cataluna

Roth K, Schulin R, Flühler H, Attinger W (1990) Calibration of TDR for water content measurement using a composite dielectric approach . Water Resour Res 26(10):2267–2273

Saarenketo T (1998) Electrical properties of water in clay and silty soils. J Appl Geophys 40:73–88

Scotto di Santolo A, Nicotera MV, Evangelista A (2005) Monitoring matric suction profiles in partially saturated pyroclastic topsoil slopes. In: Tarantino A, Romero E, Cui YJ (eds) Advanced experimental unsaturated soil mechanics. Taylor and Francis Group, London. pp 533–539

Sentek (2001) Calibration of the Sentek Pty Ltd soil moisture sensors. Sentek Pty Ltd, Kent Town, South Australia

Shuai F, Fredlund DG (2000) Use of a new thermal conductivity sensor to measure soil suction. In: Shackleford CD, Houston SL, Chang NY (eds) Advances in unsaturated geotechnics. Geotechnical Special Publication No. 99, Reston, American Society of Civil Engineers, pp 1–12

Šimůnek J, Gribb MM, Hopmans JW, van Genuchten MT (1998) Estimating soil hydraulic properties from field data via inverse modeling. In: Proceedings of 2nd international conference on unsaturated soils, vol 1. International Academic Publishers, Beijing, 1998, pp 515–520

Skinner A, Hignett C, Dearden J (1997) Resurrecting the gypsum block for soil moisture measurement, Australian Viticulture, October/November 1997, http://www.sowacs.com/feature/mea/mea.html

Smith MW, Patterson DE (1984) Determining the unfrozen water content in soils by time-domain reflectometry. Atmosphere-Ocean 22 261–263

Spaans EJA, Baker JM (1993) Simple baluns in parallel probes for time domain reflectometry. Soil Sci Soc Am J 57:668–673

Sposito G (1984) The surface chemistry of soils. Oxford University Press, New York

Sposito G, Prost R (1982) Structure of water adsorbed on smectites. Chem Rev 82:553–572

Stephens DB (1995) Vadose zone hydrology. CRC Press, Boca Raton, 347 pp

Stogryn A (1971) Equations for calculating the dielectric constant of saline water. IEEE Trans Microwave Theory Tech 19:733–736

Sweeney DJ (1982) Some insitu soil suction measurements in Hong Kong's residual soil slopes. Proc 7th Southeast Asian Geotechnical Conf 1:91–106

Topp GC, Davis JL (1985a) Measurement of soil water content using time-domain reflectometry (TDR): a field evaluation. Soil Sci Soc Am J 49:19–24

Topp GC, Davis JL (1985b) Time domain refelctometry and its application to irrigation scheduling. Advances in irrigation, vol 3, Academic Press, pp 107–127

Topp GC, Reynolds WD (1998) Time domain reflectometry: a seminal technique for measuring mass and energy in soils. Soil Tillage Res 47:125–132

Topp GC, Davis JL, Annan AP (1980) Electromagnetic determination of soil water content: measurements in coaxial transmission lines. Water Resour Res 16:574–582

Topp GC, Davis JL, Annan AP (1982) Electromagnetic determination of soil water content using TDR: II. Evaluation of installation and configuration of parallel transmission lines. Soil Sci Soc Am J 46:678–684

Topp GC, Davis JL, Bailey WG, Zebchuk WD (1984) The measurement of soil water content using a portable TDR hand probe. Can J Soil Sci 64:313–321

Topp GC, Yanuka M, Zebchuk WD, Zegelin S (1988) Determination of electrical conductivity using TDR: soil and water esperiments in coaxial lines. Water Resour Res 24(7):945–952

Topp GC, Zegelin S, White I (2000) Impacts of the real and Imaginary components of relative permittivity on TDR measurements in soils. Soil Sci Soc Am J 64:1244–1252

Vaunat J, Romero E, Jommi C (2000) An elastoplastic hydromechanical model for unsaturated soils. In: Proceedings of international workshop on unsaturated soils: experimental evidence and theoretical approaches, Trento, Italy, pp 121–138

Wang Z, Lao YD (2002) Measurement of matric suction of Loess in Shanxi Province. In: Jucá, JFT, de Campos, TMP, Marinho FAM (eds) Unsaturated soils. Proceedings of 3rd internaitonal conference on unsaturated soils, vol 1. Recife, Lisse, Balkema, pp 347–350

Waweru K (1990) Measurement of soil suction under road pavements in tropical soils, MSc Dissertation, School of Engineering, University of Durham

Wescor (2005) Wescor Inc.—Enviromental Products Division, http://www.wescor.com/environmental/

Whalley WR (1993) Considerations on the use of time-domain reflectometry for measuring soil water content. J Soil Sci 44:1–9

Wraith JM, Or D (1999) Temperature effects on soil bulk dielectric permittivity measured by time domain reflectometry: experimental evidence and hypothesis development. Water Resour Res 35:361–369

Wyseure GCL, Mojid MA, Malik MA (1997) Measurement of volumetric water content by TDR in saline soils.European. J Soil Sci 48:347–354

Yanuka M, Topp GC, Zegelin S, Zebchuk WD (1988) Multiple reflection and attenuation of time domain reflectometry pulse: theoretical considerations for application to soil and water. Water Resour Res 24:939–944

Yu C, Warrick AW, Conklin MH, Young MH, Zreda M (1997) Two- and three-parameter calibrations of time domain reflectometry for soil moisture measurement. Water Resour Res 33:2417–2421

Zakri T, Laurent J-P, Vauclin M (1998) Theoretical evidence for 'Lichtenecker's mixture formulae' based on the effective medium theory. J Phys D: Appl Phys 31:1589–1594

Zegelin SJ, White I, Russel GF (1989) Improved field probes for soil water content and electrical conductivity measurement using time domain reflectometry. Water Resour Res 25(11):2367–2376

Water Balance and Evapotranspiration Monitoring in Geotechnical and Geoenvironmental Engineering

Yu-Jun Cui · Jorge G. Zornberg

Originally published in the journal *Geotechnical and Geological Engineering*, Volume 26, No. 6, 783–798.
DOI: 10.1007/s10706-008-9198-z

Abstract Among the various components of the water balance, measurement of evapotranspiration has probably been the most difficult component to quantify and measure experimentally. Some attempts for direct measurement of evapotranspiration have included the use of weighing lysimeters. However, quantification of evapotranspiration has been typically conducted using energy balance approaches or indirect water balance methods that rely on quantification of other water balance components. This paper initially presents the fundamental aspects of evapotranspiration as well as of its evaporation and transpiration components. Typical methods used for prediction of evapotranspiration based on meteorological information are also discussed. The current trend of using evapotranspirative cover systems for closure of waste containment facilities located in arid climates has brought renewed needs for quantification of evapotranspiration. Finally, case histories where direct or indirect measurements of evapotranspiration have been conducted are described and analyzed.

Y.-J. Cui (✉)
ENPC, 6 et 8 av. Blaise Pascal,
Cité Descartes, Champs-sur-Marne,
77455 Marne La Vallee cedex 2, France
e-mail: cui@cermes.enpc.fr

J. G. Zornberg
The University of Texas, Austin, TX, USA

Keywords Evapotranspiration · Water balance · Cover system · Unsaturated soils · Measurement

1 Introduction

The interaction between ground surface and the atmosphere has not been frequently addressed in geotechnical practice. Perhaps the applications where such evaluations have been considered the most are in the evaluation of landslides induced by loss of suction due to precipitations (e.g., Alonso et al. 1995; Shimada et al. 1995; Cai and Ugai 1998; Fourie et al. 1998; Rahardjo et al. 1998). Yet, the quantification and measurement of evapotranspiration has recently received renewed interest. This is the case, for example, due to the design of evapotranspirative cover systems for waste containment and mining sites. In cases like this, quantification of the flow boundary condition at the earth-atmosphere interface becomes an integral aspect of the analysis and design of the geotechnical system.

Paradoxically, examination of the atmospheric water balance in different regions through the world has shown that evapotranspiration often exceeds precipitation (Blight 1997). This is the case of arid or semi-arid regions over most of the year as well as of most regions with temperate climate over long portion of the year. Recent assessment on hazards caused by droughts showed that the evapotranspiration is an important phenomenon that should be accounted for in natural hazards analysis. In France, the extensive drought from 1989 to 1990 affected shallowly founded buildings of 216 communes in 17 departments (Vandangeon 1992). In the decree of November 1, 2005 (French Official Journal 1.2), more than 870 communes were considered affected by the 2003 drought. In other countries, a number of case studies involving the effect of prolonged periods of evapotranspiration were performed (Driscoll 1983; Biddle 1983; Williams and Pidgeon 1983; Ravina 1983; Holtz 1983; Gao 1995; Allman et al. 1998). It is now recognized that hazards related to droughts have an important economical impact, and deserve additional research.

In addition to the geotechnical engineering problems associated with the changes in mechanical properties of soil induced by infiltration and evapotranspiration, current advances in geoenvironmental engineering have often focused on the effect of infiltration and evapotranspiration on the hydraulic properties of soils. Quantification of evapotranspiration has been particularly relevant for the design of cover systems, which is one of the key engineered components of municipal and hazardous waste landfills as well as mine disposal sites. The cover system should be designed to minimize percolation of rainwater into the waste and prevent leachate generation that may lead to environmental contamination of soil and groundwater. A conventional “resistive barrier” type cover system involves a liner (e.g., a compacted clay layer) constructed with a low saturated hydraulic conductivity (typically 10^{-9} m/s or less) to reduce percolation. Figure 1a illustrates the water balance components in this comparatively simple system, in which percolation control is achieved by maximizing overland flow. However, designing a truly *impermeable* barrier (i.e., one leading to zero percolation) should not be within any engineer’s expectations. Instead, the engineer should be able to design a system that *minimizes* percolation to environmentally safe values. Quantification of this minimized, though finite, percolation of liquid into the waste poses significant challenges.

Figure 1b illustrates schematically the water balance components in an evapotranspirative cover system. Evapotranspiration and moisture storage, two components that are not accounted for in the design of resistive barriers, are significant elements in the performance of this system. The uniqueness of this approach is the mechanism by which percolation control is achieved: an evapotranspirative cover acts not as a barrier, but as a sponge or a reservoir that stores moisture during precipitation events, and then releases it back to the atmosphere by evapotranspiration. The adequacy of alternative cover systems for arid locations has been acknowledged by field experimental assessments (e.g., Anderson et al. 1993; Dwyer 1998; Nyhan et al. 1997), and procedures for quantitative evaluation of the variables governing the performance of this system have been compiled in a systematic manner for final cover design (e.g., Zornberg and Caldwell 1998; Zornberg et al. 2003).

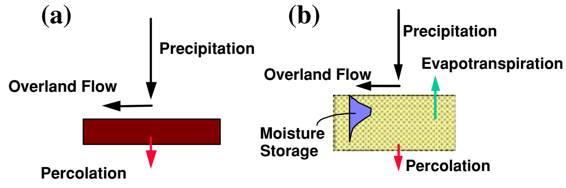

Fig. 1 Water balance components: (**a**) in a resistive barrier; (**b**) in an evapotranspirative cover system

Recent developments in unsaturated soil mechanics enable preliminary predictions of evapotranspiration and infiltration of surface water. Water flux on the ground surface is often calculated as a function of the recorded precipitation. On the other hand, evapotranspiration through the upper boundary has been often defined based on the soil suction and temperature at the ground surface. However, evapotranspiration can also be determined based on the energy balance between solar radiation, sensitive heat of air, soil heat flux and heat latent for the need of evaporation. The main advantage of this energy balance approach is that it avoids direct suction measurement. Yet, evapotranspiration has been probably the most difficult water balance component to quantify and measure experimentally. Accordingly, the most common approach has involved quantifying evapotranspiration indirectly by monitoring other components of the water balance. Methods for direct measurement of evapotranspiration, energy balance methods, and water balance methods are discussed in this paper.

2 Solar Radiation

Evapotranspiration is governed by part of the energy coming from the sun. It is well known (see for instance Pidwirny 2006) that the emission rate of the sun is estimated as 63 million W/m^2. However, as this radiation travels away from the sun, the amount that strikes another object depends on its distance from the sun. The portion that reaches the earth's atmosphere is called the solar constant (approximately 1380 W/m^2). Once solar radiation reaches the top of the atmosphere, it is absorbed, scattered, or transmitted through the atmosphere. Since 30% is scattered back to space (earth's albedo), the earth's atmosphere only receives 70% of the incoming (incident) radiation.

Of the 70% radiation that is transmitted through the atmosphere, 19% get absorbed by gases, primarily molecular oxygen and ozone. The remaining 51% is transmitted to the earth's surface. The solar constant can be used to calculate the possible limit to daily evapotranspiration. Specifically, assuming that (i) 51% energy flux (i.e. 704 W/m^2) is used for evaporation of pure water (it is of course not the case as discussed subsequently), (ii) the solar power is parabolically distributed during the day, and (iii) from zero at dawn to zero at sunset, the albeto is 15% (the value can be vary variable according to the soil surface nature, from 5% to 50% in most cases), the maximum solar energy needed to produce evaporation is 17.2 MJ/m^2 for a 12 h day (i.e. $2/3 \times 704 \times 0.85 \times 12 \times 3600 = 17233917$ J/m^2). The latent heat of evaporation of water is about 2.47 MJ/kg and hence the maximum possible evapotranspiration 6.9 mm of water (i.e. $17.234/2.47 = 6.9$ kg water/m^2).

The balance at the earth's surface between incoming and outgoing components of radiant energy is characterized by the net radiation R_n (W/m^2):

$$R_n = (S + D)(1 - a) + \left(L_{\text{down}} - L_{\text{up}}\right) \tag{1}$$

where S (W/m^2) is the direct shortwave radiation corresponding to the shortwave radiation penetrating directly to the surface without being affected by the atmosphere constituents; D (W/m^2) is the diffuse shortwave radiation corresponding to the shortwave radiation scattered or diffused by atmosphere constituents (clouds, dust etc.); a is the albedo corresponding to the proportion of radiation reflected from the ground surface, governed primarily by surface color and incitation angle of the sun; L_{up} (W/m^2) is the terrestrial radiation corresponding to the longwave radiation emitted by the earth's surface; L_{down} (W/m^2) is the atmospheric counter radiation corresponding to the longwave radiation emitted by the atmosphere directed towards the surface. The magnitudes of L_{up} and L_{down} depend on the temperature of the emitting body.

3 Soil Water Balance

The soil water balance can be represented as follows:

$$P - (I_{\text{nt}} + R_{\text{off}}) = ET + R_{\text{wt}} + \Delta S \tag{2}$$

where P (mm/day) is precipitation; I_{nt} (mm/day) is interception; R_{off} (mm/day) is the runoff on ground surface; ET (mm/day) is evapotranspiration; R_{wt} (mm/day) is the water recharged to the water table; ΔS is the change in soil water storage.

Interception corresponds to the storage of water above the ground surface, mostly in vegetation. It is usually negligible but can reduce precipitation intensity in case of dense forest canopy. The term (R_{wt} + S) represents the water infiltration I, therefore:

$$I = (R_{\text{wt}} + S) = P - (I_{\text{nt}} + ET + R_{\text{off}}) \tag{3}$$

In soil water balance, the evapotranspiration term ET is governed by the energy and mass exchanges between soil and atmosphere. It is discussed in more detail in Sect. 4.

4 Evapotranspiration

Evapotranspiration is composed of the direct evaporation, which takes place from the soil surface, and of the transpiration from vegetation. The roots of vegetation capture soil water, part of which evaporates through the stomata (micropores) of the leaves, while the rest is used for photosynthesis. Evapotranspiration depends on two elements: the heat supplied by solar radiation and the water available in the soil. While the quantity of solar energy reaching the ground surface is approximately constant, evapotranspiration is very sensitive to the climate variations and plant characteristics.

4.1 Evaporation

Evaporation involves the change in water state from liquid to water vapor due to an increase of water kinetic energy. During evaporation, hydrogen bonds are broken and water vapor is diffused from regions of higher to lower vapor pressure, i.e., from the ground surface to the surrounding air. Water vapor consists entirely of free water molecules, while liquid water consists of both free and bonded molecules.

Evaporation from soils is an important phenomenon that should be quantified in order to define the surface flux boundary condition in an unsaturated flow analysis. Evaluation methods based on either soil water balance or experimental characterization have been proposed by Philip (1957), Gardner and Hillel (1962), Gardner (1973), Brutsaert (1982), Boast (1986), Evett et al. (1994), Wilson et al. (1994, 1999) and Raghuywanshi and Wallender (1998). Evaporative processes are typically modeled isothermally. This is a simplified analysis because thermally induced flow of water through unsaturated soil may also occur by vapor diffusion. A more realistic evaporation analysis requires consideration of thermal effects. The phenomenon of thermally induced water flow was investigated by Milly (1996) and Kampf and Von der Hude (1995). Heat flux phenomena in soils that lead to thermally induced flow was also investigated by Qualls and Brutsaert (1996a, b). Fischer et al. (1996) modeled soil vapor extraction, and compared experimental data to calculation results. Additional discussion on surface flux boundary conditions was provided by Wilson (1997, 2000).

Evaporation rate is governed by several factors, as follows (see Dingman 1994):

(1) General factors, including: (i) latent heat for evaporation, the major source of which is the solar energy so that the distribution of radiation and evaporation is strongly correlated (maximum evaporation in the tropics and during the warmest part of the day); (ii) sensitive heat of air; (iii) air temperature, which is a measure of heat energy and of the capacity of air to hold water vapor (i.e. the saturation vapor pressure increases with increasing air temperature); (iv) air humidity, an increase of which causes a decrease in the rate of evaporation; (v) wind, which causes eddy (turbulent diffusion) and thereby maintains the vapor pressure gradient between air and the evaporation surface (evaporation increases dramatically with increasing turbulence, which is function of wind speed and surface roughness).

(2) Additional factors controlling the rate of evaporation from water bodies, such as water salinity.

(3) Additional factors controlling the rate of evaporation from soil, including: (i) soil water potential, as the rate of evaporation decreases significantly as soil dries out; (ii) depth of water table, as evaporation rate decreases significantly with increasing depth to the water table to a critical depth below which groundwater does no longer affect the evaporation rate, this critical depth depending on the nature of the soils involved; (iii) soil color, with greater absorption of heat and thus evaporation for dark soils (small albedo); (iv) vegetation, which reduces evaporation by shading soil, reducing wind at the ground surface and increasing vapor pressure by transpiring water pressure.

4.2 Transpiration

Transpiration is the evaporation from the vascular system of plants. Water absorbed by the roots raises by capillary action to stomata cavities in the leaves, from where it evaporates. The vapor pressure gradient between the leaf tissue (and bark, to a lesser extent) and the surrounding air draws water from soil into the roots and up the plant through the xylem. As water evaporates within the leaves tissue, salt can precipitate and further attract water by osmotic effect. However, if the soil is saline, the salt concentration gradient is reversed and water may be even drawn out of plants.

Water uptake by plants and rooting depth of the plant cover are another issue of relevance in the analysis of evapotranspirative covers. Transpiration is also used as boundary conditions in unsaturated flow analyses. Ritchie (1972), Ritchie and Burnett (1971), and Tratch et al. (1995) provide a summary of plant transpiration in terms that engineers are familiar with. The combination of evaporation and transpiration into evapotranspiration has been discussed by Hargreaves (1994) and Pereira et al. (1999), and has been modeled by Chudhury et al. (1986), Levitt et al. (1996), Xu and Qiu (1997), etc. The ecology of plant systems used for transpiration has also been a topic of significant relevance, studied by Anderson et al. (1987) and Anderson (1997). These studies concluded that a diverse group of plant species of different heights and rooting depths are required for a stable plant population.

Transpiration from different plants has been evaluated by Anderson et al. (1987, 1993), and Waugh et al. (1991). Wu and Oster (1997) provide details on several instruments used by agricultural scientists for management of plants and soil water. Because of the difficulty in measuring evaporation and transpiration in the field, a common approach has been to conduct water balance back calculation using lysimeters. Nonetheless, Evett (1994) has used time domain reflectrometry (TDR) to investigate thermal properties in soil, which is related to the amount of potential evaporation. Evett (1993) used TDR and neutron scattering to measure evapotranspiration.

5 Prediction of Evapotranspiration

Numerous predictive methods have been developed to estimate evapotranspiration, including Penman's method, Penman–Monteith's method, and Turc's method (see Guyot 1997 for a comprehensive review). These methods are based on the concept of Potential Evapotranspiration (PET). According to Penman (1948), PET corresponds to the evapotranspiration rate from a large area completely and uniformly covered with growing vegetation which has unlimited supply of water without advection (wind) and heat—storage effects. Since evapotranspiration depends on the type of vegetation, short grass was adopted. Penman (1948) proposed the following equation for *PET* (kg water/m^2/day, i.e. mm/day) calculation:

$$PET = \frac{1000\Delta R_n/(\rho_w L_v) + \gamma E_a}{\Delta + \gamma} \quad (4)$$

where $\Delta = \frac{4099P_{vs}}{(T+237.3)^2}$ (Pa/°C) is the slope of the curve of saturated vapor pressure (Pa) versus temperature (°C) at the prevailing temperature; $E_a = 0.165$ $(P_{vs} - P_v)$ $(0.8 + u_2/100)$ (mm/day) where R_n is the net radiation flux (J/(m^{2}day)); ρ_w is water density (kg/m^3); L_v is the latent heat of vaporization of water (J/kg); γ is the psychrometric constant (Pa/°C); P_{vs} is the saturated vapor pressure (mbar); P_v is the actual vapor pressure in air (mbar); u_2 is the wind speed at 2 m elevation (km/day). When wind speed is measured at elevations other than 2 m, the speed at 2 m can be estimated as:

$$u_2 = u_z\left(\frac{4.87}{\ln(67.8z - 5.42)}\right) \quad (5)$$

where u_z is the wind speed at elevation z above the ground surface. Note that in Penman's equation, no vegetation parameters are used even though short grass is referred to.

6 Measurement of Evapotranspiration

6.1 Direct Measurement

For evapotranspirative covers, lysimetry involves the use of buried containers used to collect percolating soil water. Unlike apparatus involving monitoring of suction profiles and indirect determination of flux, lysimetry provides measurement of percolation rate from an soil cover. Among the various types of lysimeters, weighing lysimeters (Fig. 2) allow direct measurement of evapotranspiration as they measure the total weight of soil and stored water (Fayer and Gee 1997; Benson et al. 2001). Changes of soil water storage in a lysimeter can be determined by integrating profiles of water content measured using nests of probes. Consequently, the remaining changes in mass can be attributed to losses by evapotranspiration.

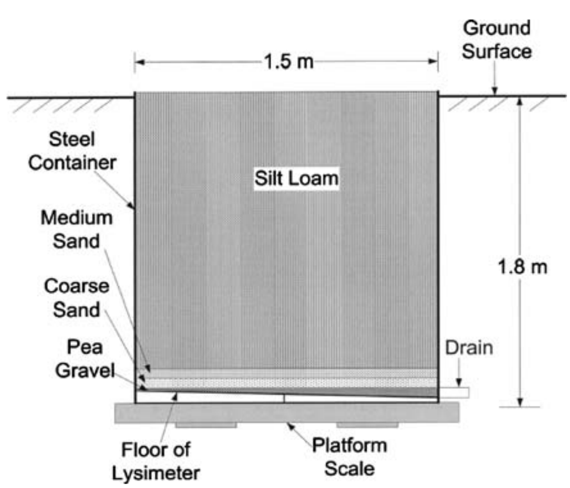

Fig. 2 Weighing lysimeter used in final cover studies at the Hanford reservation in Washington, USA. (from Benson et al. 2001)

Weighing lysimeters are typically limited to small test sections (1–2 m^2) because of the limited capacity of scales (Waugh et al. 1991).

6.2 Energy Balance Approach

This approach involves quantification of exchanges between soil and atmosphere. Specifically, these exchanges involve energy (heat) and mass exchanges, mostly by convection. The energy balance in the earth-atmospheric system can be presented as:

$$R_n = L_e + H + G \tag{6}$$

where L_e is the latent energy transfer (positive for evaporation and negative for condensation); H is the sensitive heat transfer (positive when energy is used to warm the air and negative when the air loses energy due to cooling); G is the ground heat transfer (positive when energy is transferred to the subsurface and negative when energy is transferred to the atmosphere).

There are several methods for evapotranspiration measurement: eddy correlation, flux profiles, residual method and Bowen ratio method Kolle (1996). Consistent with the Bowen ratio method, the sensitive heat flux within a few meters of the surface, H, can be expressed as:

$$H = \rho_a C_p k_H \frac{\partial T}{\partial z} \tag{7}$$

where ρ_a (kg/m^3) = 1.2929 (273.13/T (K)) [(P (mm) − 0.3783 P_v (mm))/760] is air density which depends on vapor pressure; the value of dry air is generally considered: ρ_a (kg/m^3) = 1.2929 (273.13/T (K)); C_p is specific heat of air (also the value for dry air, 1.01 kJ/(kg K), can be generally assumed); T is temperature (K); z is elevation (m); k_H, eddy diffusivity for air. The latent heat flux L_e can be expressed as follows

$$L_e = \frac{L_v \rho \varepsilon k_v}{P} \frac{\partial P_v}{\partial z} \tag{8}$$

where L_v (kJ/kg) = 2501 − 2.361T (°C) is latent heat of vaporization; ε is the ratio of molecular weight of water to molecular weight of air ($\varepsilon = 0.622$); k_v (m^2/s), is eddy diffusivity for vapor; P_v (kPa) is vapor pressure; P (kPa) is atmospheric pressure which depends on elevation, as follows (Wallace and Hobbs 1977):

$$P = 101.325\left(1 - \frac{z}{44307.69231}\right)^{5.25328} \tag{9}$$

In general, k_v and k_H are not known but are assumed to be equal (Blight 1997). The ratio of H to L_e is then used to partition the available energy at the surface into sensitive and latent heat flux. This ratio was first defined by Bowen (1926), and is known as the Bowen ratio β:

$$\beta = \frac{H}{L_e} = \frac{PCp}{L_v \varepsilon} \frac{\partial T}{\partial P_v} = \gamma \frac{\partial T}{\partial P_v} \tag{10}$$

where $\gamma = PCp/(L_v\varepsilon)$ is the psychrometric constant.

Knowing the net radiation flux R_n, the total soil heat flux G and the Bowen ratio β, the latent heat flux can be obtained as:

$$L_e = \frac{R_n - G}{1 + \beta} \tag{11}$$

Bowen ratio can be determined by measuring the temperature T and the vapor pressure P_v at two elevations: water vapor pressure is often measured with a single cooled mirror dew point hygrometer (e.g., Campbell Scientific BR023 1998). Air temperature can be measured using different thermocouples. For example, Campbell Scientific uses two chrome—constantan thermocouples. Soil heat flux can be measured using heat flux plates buried in the soil at a fixed depth. The plates are typically buried at a depth of 8 cm (Campbell Scientific 1998). The average temperature of the soil layer above the plate is measured using 2–4 thermocouples. The heat flux at the surface can be calculated by adding the heat flux measured by the plates to the energy stored in the soil layer. The storage term is calculated by multiplying the soil heat capacity C_s by the change in soil temperature ΔT over the averaging period t:

$$S = \frac{\Delta T C_s d}{t} \tag{12}$$

where d is the plate depth. The soil heat capacity can be calculated by adding the specific heat of the dry soil C_d to that of the soil water C_w:

$$C_s = \rho_d(C_d + wC_w) = \rho_d C_d + \theta \rho_w C_w \tag{13}$$

where ρ_d and ρ_w are soil dry density (kg/m^3) and water density (kg/m^3) respectively; w and θ are gravimetric and volumetric water content respectively. Figure 3 illustrates a soil heat flux system (Campbell Scientific 1998).

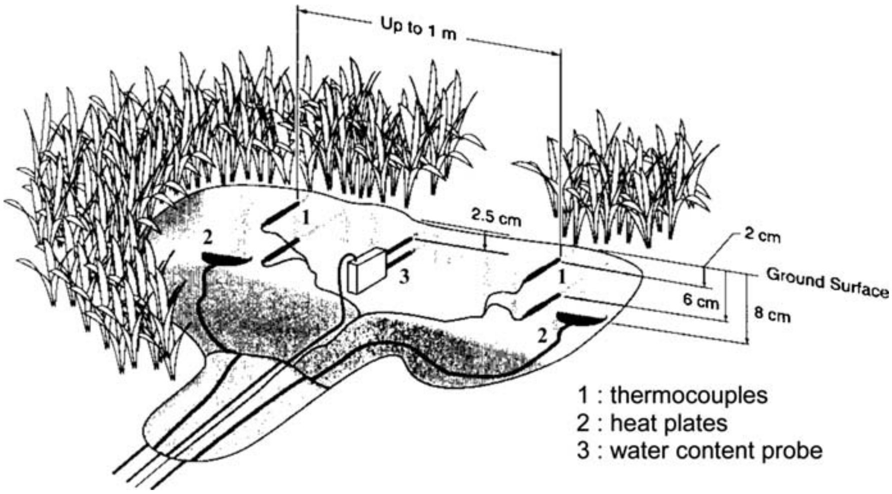

Fig. 3 Soil heat flux measurement (Campbell Scientific system 1998)

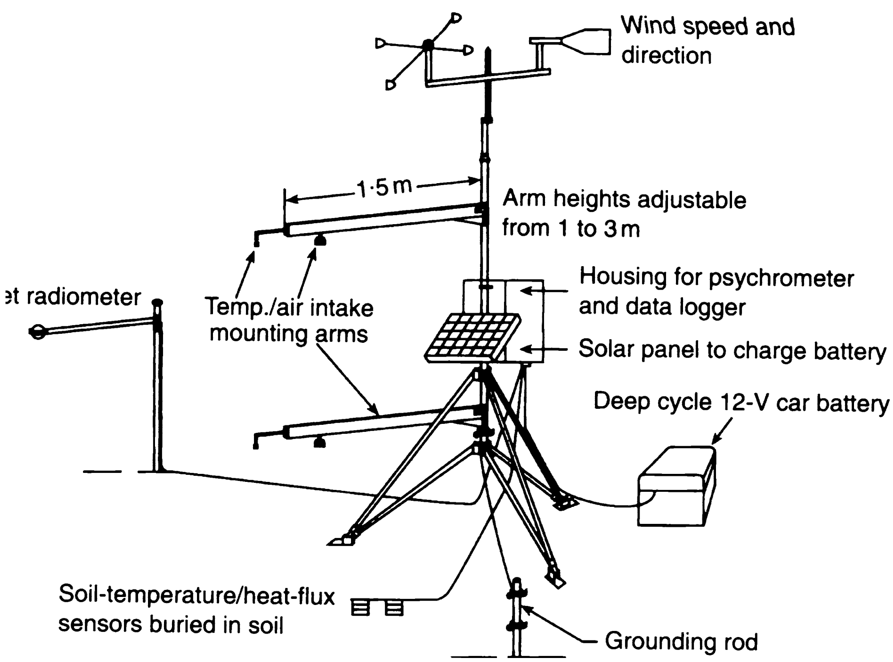

Fig. 4 System of Bowen ratio measurement (Blight 1997)

The measurement of R_n is carried out using a net radiometer. Figure 4 illustrates a Bowen ratio system (Blight 1997), which includes two arms at different elevations where temperature and vapor pressure are monitored. A net radiometer is also installed for R_n measurement.

6.3 Water Balance Approach

Evapotranspiration can also be measured indirectly by quantifying other components in the water balance. Specifically, precipitation, surface water runoff, changes in moisture storage, and basal percolation. As mentioned, lysimeters have been used to monitor basal percolation (e.g., Fig. 5). Note that in a natural soil profile, monitoring of basal percolation is usually not possible because of difficulties associated with the installation of a draining layer. In addition, the possible recharge of the soil from the water table may affect water content measurements. This limits the use of lysimeters in natural soil profiles.

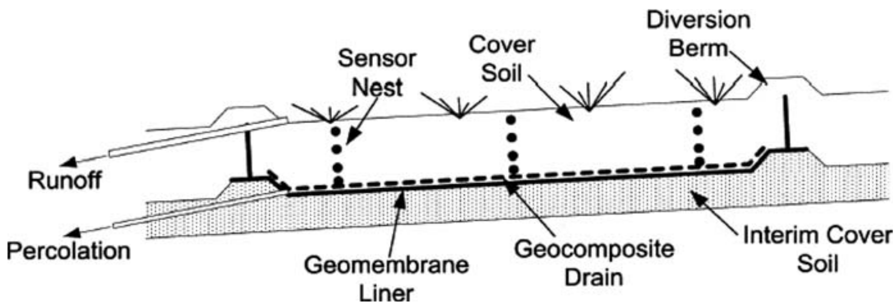

Fig. 5 Schematic of lysimeter used in final cover studies (Khire et al. 1997)

Basal percolation, precipitation, changes in soil moisture storage, and surface water runoff are typically monitored on a daily basis. In addition, solar radiation, wind speed and direction, and percentage cloud cover are also measured. Figure 6 shows typical monitoring layout used in sites where evapotranspiration is defined indirectly using a water balance approach.

Considering the conservation of mass of water into and out of the cover, the evapotranspiration may be obtained as follows:

$$ET = P - G - \Delta S - R_{off} \quad (14)$$

where ET = evapotranspiration; P = precipitation; G = basal percolation; ΔS = change in moisture storage; R_{off} = surface water runoff. Rain and snow can be measured using an all season gauge. Percolation is channeled from the lysimeter by gravity and measured in a sump using a tipping-bucket rain gauge. The moisture content profile is typically measured in the center of the lysimeter using an array of time domain reflectometer sensors, wave content reflectometer (WCR) sensors, or moisture probes spaced evenly with depth. Surface water runoff is typically collected in geomembrane swales around the cover perimeter.

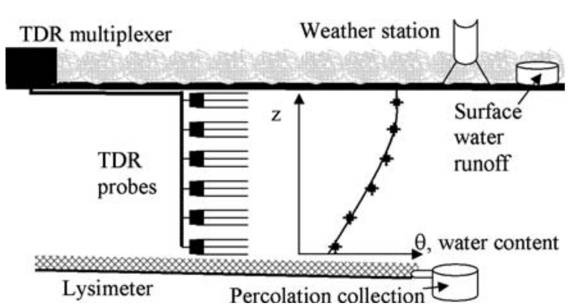

Fig. 6 Monitoring system layout

TDR, nuclear moisture probes and other techniques have been used to measure suction-saturation curves and other unsaturated flow phenomena. Benson et al. (1994) describes the monitoring system for a typical landfill cover. Several field studies were discussed by Gee et al. (1991), Phillips et al. (1991), and Allison et al. (1994). Gee and Hillel (1988) reviewed several methods for estimating percolation through soil covers. Campbell et al. (1991) describes the use of lysimeters to conduct water balances. Additional water balance studies were reported by Nyhan et al. (1990, 1997), Warren et al. (1994, 1996), Hakonson et al. (1994), Khire et al. (1997a, b), Waugh et al. (1991), and Anderson et al. (1998). Water balance approaches have often been used in the US as part of the selection and performance evaluation of alternative cover systems suitable for arid or semi-arid climates, as discussed by Anderson et al. (1998), Stormont (1995), Benson and Khire (1995), Wing and Gee (1989, 1994), Gee and Ward (1997), and Dwyer (1998, 2001).

7 Case Histories Involving Monitoring of Evapotranspiration

This section presents some cases studies aiming at illustrating each of the three methods for quantification of evapotranspiration.

7.1 Direct Measurement: Monticello (US)

The U.S. Department of Energy (DOE) conducted a series of field lysimeter experiments to help design and then monitor the performance of an engineered cover for a uranium mill tailings disposal cell at a Superfund Site in Monticello, Utah (Waugh 2002). The lysimeter test facility evolved as a sequence of

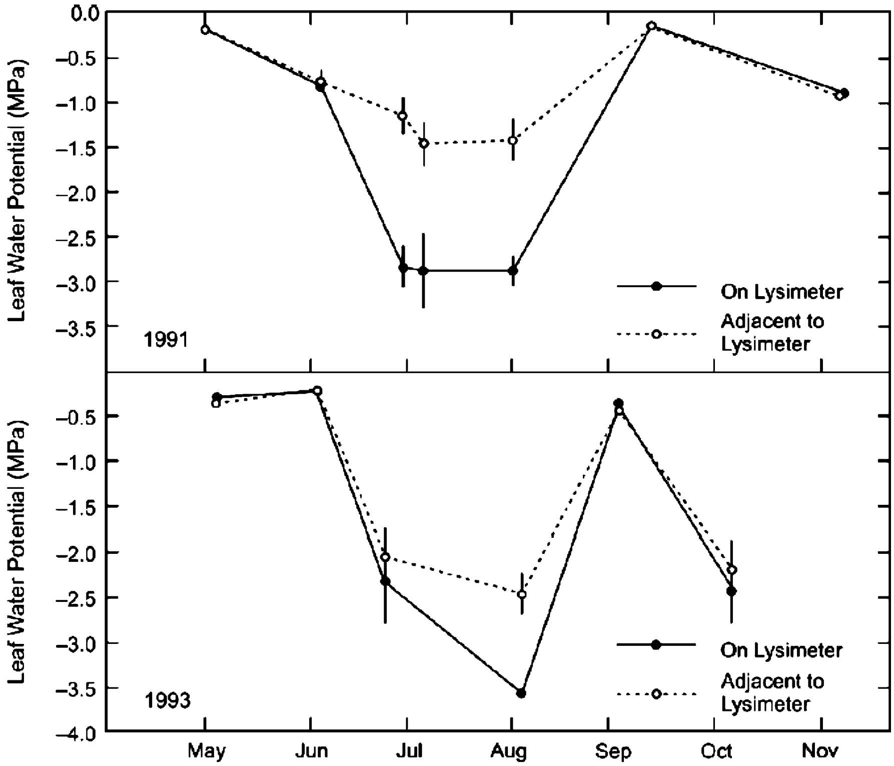

Fig. 7 Predawn leaf water potential values for *P. smithii* growing on and adjacent to the small monolith lysimeters between May and November 1991 and between May and October 1993 (Waugh 2002)

installations, first to test the concept of using an evapotranspirative cover at Monticello, next to evaluate the soil–water balance of the final engineered design, and finally to monitor the hydrologic performance of a large facet of the completed disposal cell cover. Small weighing lysimeters were installing containing intact, 100-cm-deep profiles of undisturbed silt loam soil (monoliths) overlying a pea-gravel capillary barrier and supporting mature native grasses. Leaf water potential and leaf transpiration of plants on and adjacent to the lysimeters were compared to evaluate the effect of the small weighing lysimeter design on plant behavior. Because of favorable monolith lysimeter results, 15 additional small weighing lysimeters were installed to test the effects of varying soil types and soil layer thickness on soil-water balance and water-storage capacity. This study evolved into the construction of large caisson lysimeters to evaluate the water balance of the final cover design for the Monticello disposal cell. The cover layer constructed inside the caissons matched as-built engineering parameters for the actual cover.

Plants growing on and adjacent to the lysimeters (*P. smithii*) were sampled to evaluate the effects of isolating a soil monolith on plant water status. Predawn leaf water potential values were measured monthly during the growing season using a pressure chamber technique (Scholander et al. 1965). Predawn potential values for *P. smithii* growing on and adjacent to the lysimeters were similar early in the growing season, diverged significantly during the mid-summer moisture depletion period, and then reconverged following the late-summer monsoons (Fig. 7).

Some divergence of predawn potential values for *P. smithii* on and adjacent to the lysimeters was observed, indicating that plants were seasonally more stressed inside the lysimeters than in the adjacent plant community. This suggests that small lysimeters moderately underestimates ET. However, for screening tests consisting of multiple treatments and replications, it was concluded that the small lysimeters provided reasonable comparisons of the hydrologic performance of evapotranspirative cover designs.

Overall, the use of weighing lysimeters allowed direct quantification of the ET; on the other hand, the use of small devices may have compromised quantification of flow through macro-fractures as cracks.

The use of large lysimeters (without weighing capabilities) is discussed in the case history presented in Sect. 7.3.

7.2 Energy Balance Approach: Boissy-le-Châtel (France)

In a common meteorology station only data at 2 m elevation are available and thus the Bowen ratio is generally not measured. In this case, it is necessary to use numerical methods to determine L_e indirectly. From a point of view of geotechnical engineering, knowing L_e is essential to subsequently analyze the soil settlement and slope stability problem due to evapotranspiration, because it is possible to determine the variations of soil temperature and water content using an appropriate method. Cui et al. (2005) used the two coupled equations (Eq. 15 and Eq. 16) proposed by Wilson et al. (1994) to calculate β and determine the temperature and water content profiles in the soil:

$$\frac{\partial h_W}{\partial t} = C_W^1 \frac{\partial}{\partial y}\left(k_W \frac{\partial h_W}{\partial y}\right) + C_W^2 \frac{\partial}{\partial y}\left(D_V \frac{\partial P_V}{\partial y}\right) \qquad (15)$$

with $C_W^1 = \frac{1}{\rho_W g m_2^W}$ and $C_W^2 = \frac{P+P_V}{P(\rho_W)^2 g m_2^W}$ where $h_w =$ water head; $k_w =$ water permeability depending on the suction; $D_v, =$ vapour diffusivity; $P_v =$ vapour partial pressure; $P =$ atmospheric pressure; $m_2^W =$ slope of the water retention curve expressed in terms of volumetric water content versus suction; y = elevation.

$$C_h = \frac{\partial T}{\partial t} = \frac{\partial}{\partial y}\left(\lambda \frac{\partial T}{\partial y}\right) - L_V \frac{P+P_V}{P}\frac{\partial}{\partial y}\left(D_V \frac{\partial P_V}{\partial y}\right) \qquad (16)$$

where $Ch =$ soil heat capacity; $T =$ temperature, $t =$ time; $\lambda =$ soil thermal conductivity. Note that because of the lack of information, a constant value of G/H ratio was adopted in the calculation, suggesting that the heat fluxes through soil and air remain proportional. An initial β value of 0.01 was considered, enabling the calculation of H and L_e from the energy balance equation (Eq. 6), and thus the determination of initial upper boundary condition at the ground surface. The numerical resolution of the two-coupled equations (Eqs. 15 and 16) provided a profile of temperature T and of partial vapour pressure P_v that allowed the calculation of vapour flux or evaporation at the ground surface. This evaporation was compared with the target value calculated from field data using Penman–Monteith equation and the difference was compared to a maximum acceptable value taken equal to 0.01. In case of a larger difference, the iterative process was renewed based on a different value of β, until the required convergence was reached. The profiles of temperature, volumetric water content were then determined.

Data from the site of Boissy-le-Châtel (France) were evaluated using this method. The site is located about 50 km East of Paris in the South of the Orgeval basin. Main meteorology data of 2003 (air temperature, air relative humidity and solar radiation) are presented in Figs. 8–10, respectively. It is observed that the air temperature is generally above 0°C, with August the hottest month (maximum temperature reaches 40°C). Comparison between Figs. 8 and 10 show that the air temperature changes correlate well with solar radiation. The relative humidity varies between 30 and 100% (Fig. 10), but it does not necessary follow the precipitation pattern. This confirms that relative humidity depends not only on precipitation, but also on air temperature and wind speed.

The potential evapotranspiration PET calculated using Penman–Monteith equation is presented in Fig. 11. Summer is the season where evaporation is most pronounced (July and August). Intense evaporation is also observed by the middle of April (6 mm/day), which corresponds to the particularly low relative humidity observed during that period (30%, Fig. 10).

Figure 12 presents the soil temperature variation obtained from TDR probes. The data shows that

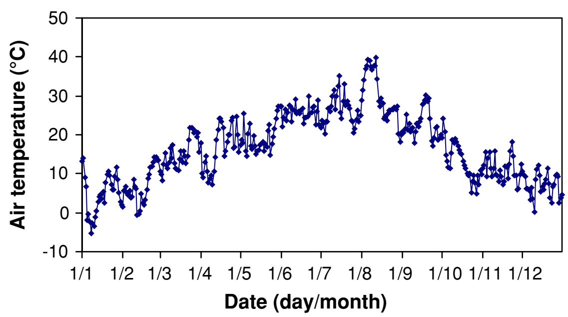

Fig. 8 Air temperature variation during the year 2003 in Boissy-le-Châtel

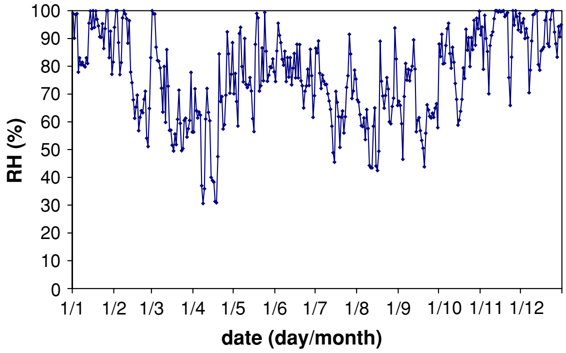

Fig. 9 Air relative humidity variation during the year 2003 in Boissy-le-Châtel

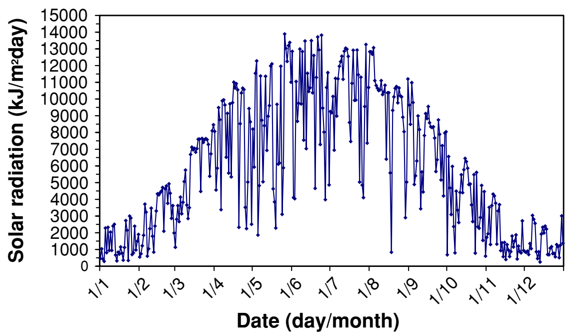

Fig. 10 Solar radiation during the year 2003 in Boissy-le-Châtel

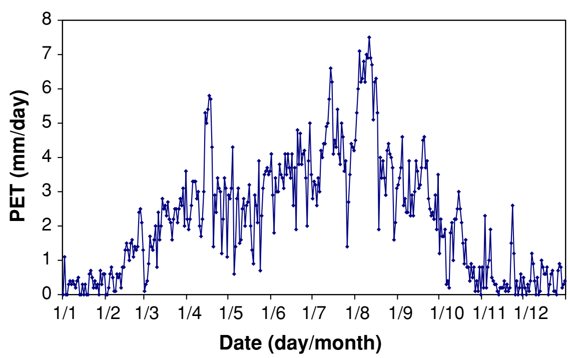

Fig. 11 PET during the year 2003 in Boissy-le-Châtel

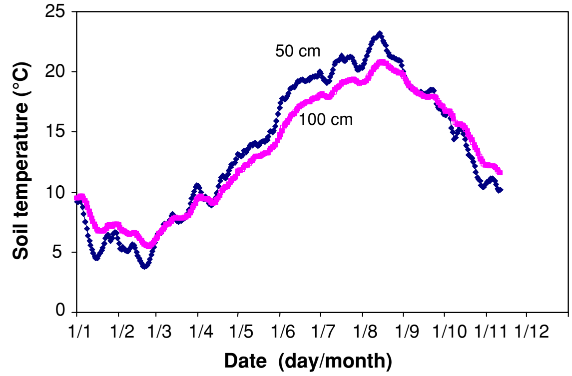

Fig. 12 Soil temperature variation during the year 2003 in Boissy-le-Châtel

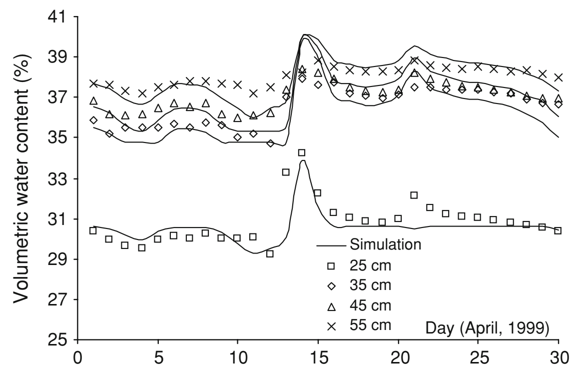

Fig. 13 Comparison between measured and calculated water content at different depth, (Boissy-le-Châtel, Cui et al. 2005)

temperature is higher at deeper soil layer in cold seasons (January–March, October–December), but this trend inverses in the other seasons. Examination of Fig. 11 shows that evaporation is negligible in the cold seasons. Figure 13 shows the comparison between the measured and predicted volumetric water content at four different depths (25, 35, 45 55 cm) for the period of April 1999 (Cui et al. 2005). The good agreement clearly shows the validity of the adopted method. Figure 14 presents the comparison between measured and calculated temperature at 0.5 m depth, with equally satisfactory results.

7.3 Water Balance Approach: Rocky Mountain Arsenal (US)

A series of instrumented test plots were constructed at the Rocky Mountain Arsenal, located near Denver, Colorado, USA, in Summer 1998 (Kiel et al. 2002; Zornberg and McCartney 2003). The climate in Denver is semiarid, with an average annual precipitation of 396 mm and an average pan evaporation of 1,394 mm (quantified from 1948 to 1998). The wettest months of the year (April–October) are also the months with the highest pan evaporation; which are optimal conditions for an evapotranspirative

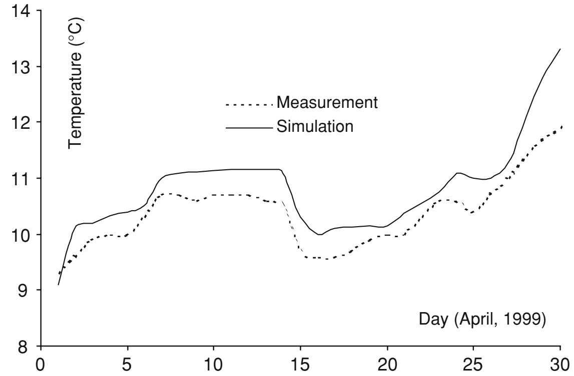

Fig. 14 Comparison between measured and calculated soil temperature at 0.5 m depth, (Boissy-le-Châtel, Cui et al. 2005)

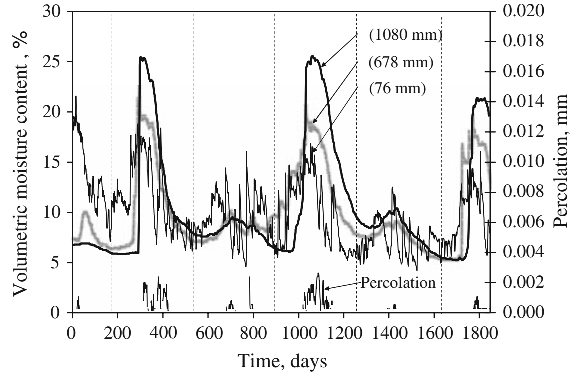

Fig. 15 Percolation and volumetric moisture content at three depths (76 mm, 678 mm, and 1080 mm)

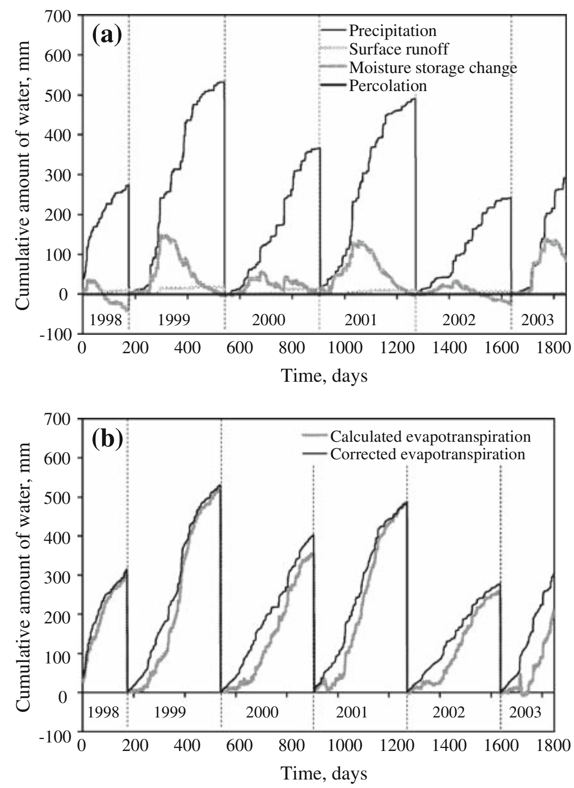

Fig. 16 Water balance variables: (**a**) Measured values; (**b**) Calculated values

cover. The test cover analyzed in this study was constructed by placing a 1,168 mm layer of low plasticity clay soil atop a large pan lysimeter (9.1 m by 15.2 m). The soil was placed at 70% relative compaction with respect to standard proctor maximum dry density (1,960 kg/m^3). The lysimeter consists of a geocomposite for water collection (consisting of a geonet for in-plane drainage sandwiched between two geotextiles) underlain by a geomembrane. The lysimeter was placed on a 3% grade, which allows gravity drainage through the geocomposite. The soil used was a low plasticity clay (CL), with an average fines content of 43%, and an average plasticity index (PI) of 15.4. The cover and surrounding buffer zone were vegetated with local grasses and shrubs, such as Cheatgrass.

Measurements obtained for water balance components in the evapotranspirative cover at the Rocky Mountain Arsenal were used to define the evapotranspiration component. The indirectly measured evapotranspiration was subsequently compared against predictions obtained using energy balance methods and numerical simulations. Monitoring commenced on July 10, 1998 (day 1), and continued until July 31, 2003. Figure 15 shows the variation in moisture content with time at three depths in the test cover along with the percolation collected from the lysimeter. The vertical dashed lines in the figures denote January 1st of each monitoring year.

This figure indicates that the time periods when percolation was collected in the lysimeter correspond with the periods of increased moisture within the cover. The surface moisture content fluctuates on a daily basis, while the basal moisture content changes in response to significant wetting events. The moisture content was integrated over the cover depth to calculate the cover moisture storage. Figure 16a shows the cumulative values for the measured water balance. Above average amounts of precipitation occurred in 1999 and 2001, which corresponds to the periods of increased moisture content observed in

Fig. 15. The cover moisture storage increases in the early portion of each year in response to higher precipitation in the spring, while it decreases in response to high evapotranspiration in the summer and fall. Runoff was minimal, but it was observed to follow the pattern of precipitation and was greatest in the spring during heavy storms. Little runoff was collected from melting snow. The percolation was a comparatively small component of the water balance, typically less than 0.02% of the precipitation.

Figure 16b shows the cumulative ET calculated on a daily basis using Eq. 14. The program REF-ET was used to calculate the potential evapotranspiration (PET) for the years 1999 to 2002 (Allen 2001). This program solves for the PET using the Penman–Monteith equation. The potential evapotranspiration from REF-ET must be partitioned into the potential transpiration T_p and the potential evapotranspiration PET. This was achieved by using the Ritchie model (Ritchie and Burnett 1971) to correlate the variation in the leaf area index *LAI* with the partitioned evapotranspiration PET. LAI corresponds to the ratio of the leaves area of plants to the area occupied by the plants. Transpiration by root uptake is modeled using a sink term in the Richards' equation at each node (Simunek et al. 1998). The Feddes model was used to calculate the actual root uptake based on the available moisture at each node and the capacity of the plants (Feddes et al. 1978). The model requires a distribution of root length density with depth, and an estimation of the range of water contents at which plants will transpire.

Figure 17a shows the calculated change in moisture content at three depths. The results shown in this figure indicate that the numerical results obtained by solving Richards' equation yield similar results to those observed in Fig. 15. However, the wetting front does not reach the base of the cover (1,080 mm) until 2003. This may be due to preferential flow in the field, or to difficulties in modeling the boundary condition representative of a lysimeter. Figure 17b shows a comparison between the simulated surface evaporation and transpiration values. This figure indicates that the surface evaporation contributes approximately 1.5 times more to the removal of water from the cover than plant uptake. The depth of influence of evaporation depends on the moisture content of the near ground surface soil. Roots remove moisture from the full cover profile, but the amount of removal depends on water availability and the season of year. Evaporation occurs throughout the year, while transpiration occurs mostly during the vegetation growing season.

Figure 17c shows a comparison between the simulated and the measured evapotranspiration. The two quantities compare quite well. The measured ET typically is slightly greater than the calculated ET. Over the four-year monitoring period, ET removed 96% of the precipitation (1,565 mm out of 1,626 mm). Negligible runoff was collected. Although Fig. 15

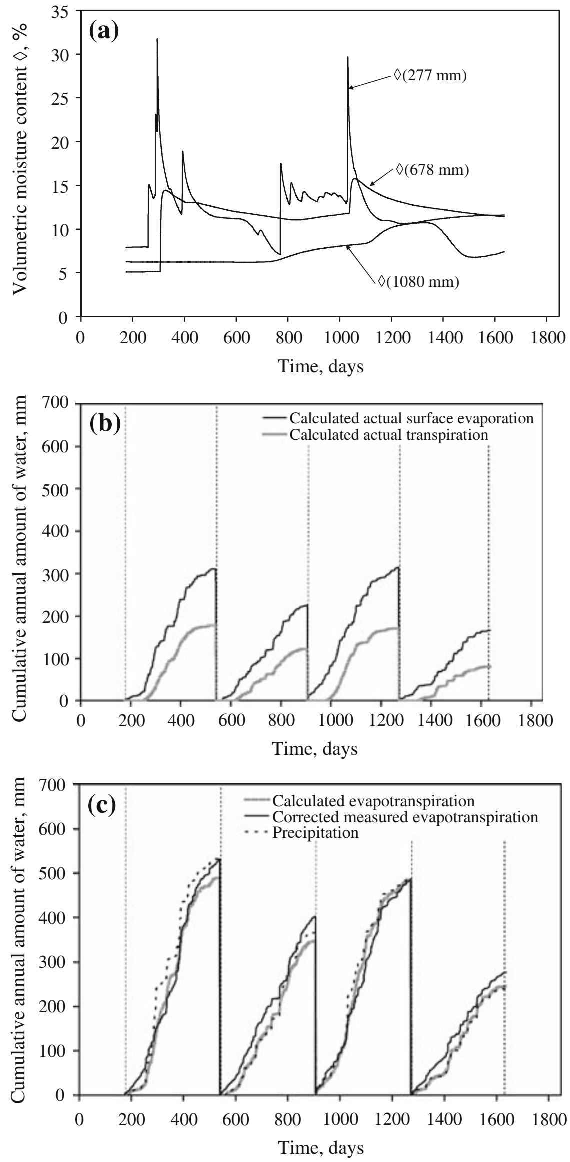

Fig. 17 Hydrus-1D results: (**a**) Moisture content at three depths (277 mm, 678 mm and 1,080 mm); (**b**) Surface evaporation and root flux (transpiration); (**c**) Comparison between calculated and measured evapotranspiration

indicates an increase in moisture content on several occasions, ET led to relatively low moisture contents throughout the soil profile at the end of the simulation. Also, the percolation throughout the four-year simulation period was less than 0.1 mm (0.02% of the precipitation), indicating that the ET adequate enough to lead to satisfactory cover performance.

8 Final Remarks

Among the various components of the water balance, the evapotranspiration component has probably been the most difficult component to quantify and measure experimentally. Some attempts for direct measurement of evapotranspiration have included the use of weighing lysimeters. However, quantification of evapotranspiration has been typically conducted using energy balance approaches or indirect water balance methods that rely on quantification of all other water balance components. This report initially presented the fundamental aspects of evapotranspiration as well as of its evaporation and transpiration components. Typical methods used for prediction of evapotranspiration based on meteorological information were also discussed. The current trend of using evapotranspirative cover systems for closure of waste containment facilities located in arid climates has brought renewed needs for quantification of evapotranspiration. Accordingly, a brief overview of evapotranspirative cover systems was presented in this paper. Finally, case histories in which direct or indirect measurements of evapotranspiration have been conducted are described and analyzed.

Overall, significant improvements have been recently made regarding monitoring of evapotranspiration using direct methods (weighing lysimeter), energy balance methods, and water balance approaches. However, significant additional advances should be made towards integrating the unsaturated soil mechanics concepts with other areas such as meteorology, agronomy, and biology in order to further advance our ability to predict evapotranspiration.

References

Allen RG (2001) REF-ET: reference evapotranspiration calculation software for FAO and ASCE standardized equations. Version 2. The University of Idaho

Allison GB, Gee GW, Tyler SW (1994) Vadose-zone techniques for estimating groundwater recharge in arid and semiarid regions. Soil Sci Soc Am J 58:6–14

Allman MA, Delaney MD, Smith DW (1998) A field study of seasonal ground movement in expansive soils. In: Proceedings of the second international conference on unsaturated soils UNSAT'98, Beijing, pp 309–314

Alonso E, Gens A, Lloret A, Delahaye C (1995) Effect of rain infiltration on the stability of slopes. In: Proceedings of the first international conference on unsaturated soils UNSAT'95, vol. 1. Paris, pp 241–256

Anderson JE (1997) Soil-plant cover systems for final closure of solid waste landfills in arid regions. Landfill capping in the semi-arid west: problems. Perspectives and Solutions, Idaho Falls, pp 27–38

Anderson JE, Shumar ML, Toft NL (1987) Control of soil water balance by sagebrush and three perennial grasses in a cold-desert environment. Arid Soil Res Rehabil 1:229–244

Anderson JE, Nowak RS, Ratzlaff TD, Markham OD (1993) Managing soil moisture on waste burial sites in arid regions. J Environ Qual 22:62–69

Anderson JE, Ratzlaff TD, Duffin E, Morris A (1998) Comparisons of four protective cap designs for burial of hazardous waste at the idaho national engineering and environmental laboratory. In: Reynolds TD, Warren RW (eds) Environmental science and research foundation annual technical report for 1997. ESRF, Idaho Falls, ID

Benson CH, Khire MV (1995) Earthen covers for semi-arid and arid climates. In: Proceedings ASCE convention, landfill closures—environmental protection and land recovery. San Diego, CA, pp 201–217

Benson CH, Bosscher PJ, Land DT, Pliska RJ (1994) Monitoring system for hydrologic evaluation of landfill final covers. ASTM Geotech Test J 17(2):138–149

Benson CH, Abichou T, Albright WH, Gee G, Roesler AC (2001) Field evaluation of alternative earthen final covers. Int J Phytoremediation 3(1):105–127

Biddle PG (1983) Patterns of soil drying and moisture deficit in the vicinity of trees on clay soils. Géotechnique 33(2):107–126

Blight GE (1997) Interaction between the atmosphere and the earth. Géotechnique (47):715–767

Boast CW (1986) Evaporation from Bare Soil Measured with High Spatial Resolution. In: Dinauer RC (ed) Methods of soil analysis, part I: physical and mineralogical methods. SSSA, pp 889–899

Bowen IS (1926) The ratio of heat losses by conduction and by evaporation from any water surface. Phys Rev 27:779–787

Brutsaert W (1982) Evaporation into the atmosphere: theory, history, and applications. Kluwer Academic Publishers

Cai F, Ugai K (1998) Finite element analysis of rainfall effects on slope stability. In: Proceedings of the second international conference on unsaturated soils UNSAT'98, vol 1. Beijing, pp 200–205

Campbell Scientific Inc (1998) BR023 Bowen ratio system instrumentation manual. http://weather.austincollege.edu/ACWX.manuals/bowen.pdf

Campbell MD, Gee GW, Kirkham RR, Phillips SJ, Wing NR (1991) Water balance lysimetry at a nuclear waste site.

Lysimeters for Evapotranspiration and Environmental Measurements, Honolulu, HI, pp 125–132

Choudhury BJ, Reginato RJ, Idso SB (1986) An analysis of infrared temperature observations over wheat and calculation of latent heat flux. Agric Forest Meteorol 37:75–88

Cui YJ, Lu YF, Delage P, Riffard M (2005) Field simulation of in-situ water content andtemperature changes due to ground—atmospheric interactions. Géotechnique 55(7): 557–567

Dingman SL (1994) Physical hydrology. Prentice Hall, p 575

Driscoll R (1983) The influence of vegetation on the swelling and shrinking of clay soils in Britain. Géotechnique 33(2):93–105

Dwyer SF (1998) Alternative landfill covers pass the test. Civil Eng, ASCE 68(9):50–52

Dwyer SF (2001) Finding a better cover. Civil Eng, ASCE 71(1):59–63

Evett SR (1993) Evapotranspiration by soil water balance using tdr and neutron scattering. In: Management of irrigation and drainage systems conference, Park City Utah

Evett SR (1994) TDR-temperature arrays for analysis of field soil thermal properties. In: Symposium on time domain reflectrometry in environmental, infrastructure and mining applications. Northwestern University, Evanston, IL

Fayer M, Gee G (1997) Hydrologic model tests for landfill covers using field data. In: Proceedings landfill capping in the semi-arid west: problems, perspectives, and solutions. Environmental Science and Research Foundation, Idaho Falls, ID, pp 53–68

Feddes RA, Kowalik PJ, Zaradny H (1978) Simulation of field water use and crop yield. Wiley, Inc

Fischer V, Schulin R, Keller M (1996) Experimental and numerical investigation of soil vapor extraction. Water Resour Res 32:3413–3427

Fourie AB, Bhana Y, Blight GE (1998) The contribution of matric suction to the stability of an ash dump. In: Proceedings of the second international conference on unsaturated soils UNSAT'98, vol. 1. Beijing pp 225–230

Gao DZ (1995) The cause of a large number of houses damage. In: Proceedings of the first international conference on unsaturated soils UNSAT'95. Paris, pp 863–867

Gardner HR (1973) Prediction of evaporation from homogenous soil based on the flow equation. Soil Sci Soc Am J 37:513–516

Gardner HR, Hillel DI (1962) The relation of external evaporative conditions to the drying of soils. J Geophys Res 67(11):4319–4325

Gee GW, Hillel DI (1988) Groundwater recharge in arid regions: review and critique of estimation methods. Hydrol Processes 2:255–266

Gee GW, Ward AL (1997) Still in quest of the perfect cap. In: Landfill capping in the semi-arid West: problems, perspectives and solutions, Idaho Falls, pp. 145–164

Gee GW, Campbell MD, Link SO (1991) Arid site water balance using monolith lysimeters. In: Lysimeters for evapotranspiration and environmental measurements, Honolulu, HI, pp 219–227

Guyot G (1997) Climatologie de l'environnement. De la plante aux écosystèmes. In: Masson (ed) Elsevier, Paris, 505 p, ISBN 2-225-85514-5

Hakonson TE, Bostick KV, Trujillo G, Manies K, Warren RW, Lane L, Kent J, Wilson W (1994) Hydrologic evaluation of four landfill cover designs at hill air force base. LA-ur-93-4469, Sandia National Laboratory, DOE Mixed Waste Landfill Integrated Demonstration, Albuquerque

Hargreaves GH (1994) Defining and using reference evapotranspiration. J Irrig Drain Eng, ASCE 120(6):1132–1139

Holtz WG (1983) The influence of vegetation on the swelling and shrinking of clays in the United States of America. Géotechnique 33(2):159–163

Kampf M, Von der Hude N (1995) Transport phenomena in capillary barriers: influence of temperature on flow processes. In: Proceedings Sardinia 95, fifth international landfill symposium, II, pp 565–576

Khire M, Benson C, Bosscher P (1997) Water balance modeling of earthen final covers. J Geotech Eng, ASCE 123(8):744–754

Khire MV, Benson CH, Bosscher PJ (1997) Water balance of two earthen landfill caps in a semi-arid climate. ICTCE, pp 1–9

Kiel RE, Chadwick DG, Lowrey J, Mackey CV, Greer LM (2002) Design of evapotranspirative (ET) covers at the Rocky Mountain Arsenal. In: Proceedings: SWANA 6th annual landfill symposium

Kolle O (1996) Long-term comparison of energy flux calculation methods over an agriculture field. Phys Chem Earth 21:111–117

Levitt DG, Sully MJ, Lohrstorfer CF (1996) Modeling evapotranspiration from arid environments: literature review and preliminary model results. Bechtel Nevada

Milly PCD (1996) Effects of thermal vapor diffusion on seasonal dynamics of water in the unsaturated zone. Water Resour Res 32:509–518

Nyhan JW, Hakonson TE, Drennon BJ (1990) A water balance study of two landfill cover designs for semi-arid regions. J Environ Qual 19:281–288

Nyhan JW, Schofield TG, Starmer RH (1997) A water balance study of four landfill cover designs varying in slope for semi-arid regions. J Environ Qual 16:1385–1392

Penman HL (1948) Natural evaporation from open water, bare soil and grass. Proc R Soc London, Ser A 193:120–146

Pereira LS, Perrier A, Allen RG, Alves I (1999) Evapotranspiration: concepts and future trends. J Irrig Drain Eng, ASCE 125(2):45–51

Philip JR (1957) Evaporation and moisture and heat flow in the soil. Meteorol J 14:354–366

Phillips SJ, Relyea JF, Kemp CJ, Wing NR, Campbell MD, Gee GW, Graham MJ, Kirkham RR, Ruben MS (1991) Development of Hanford site lysimeter facilities. In: Lysimeters for evapotranspiration and environmental measurements, Honolulu, HI, pp 19–27

Pidwirny M (2006) Fundamentals of physical geography, 2nd edn. http://www.physicalgeography.net/fundamentals/contents.html

Qualls RJ, Brutsaert W (1996a) Effect of vegetation density on the parameterization of scalar roughness to estimate spatially distributed sensitive heat fluxes. Water Resour Res 32(3):645–652

Qualls RJ, Brutsaert W (1996b) Evaluation of spatially distributed ground-based and remotely sensed data to estimate spatially distributed sensitive heat fluxes. Water Resour Res 32(8):2489–2495

Raghuywanshi NS, Wallender WW (1998) Converting from pan evaporation to evapotranspiration. J Irrig Drain Eng, ASCE 124(5):275–277

Rahardjo H, Leong EC, Gasmo JM, Tang SK (1998) Assessment of rainfall effects on stability of residual soil slopes. In: Proceedings of the second international conference on unsaturated soils UNSAT'98, vol. 1. Beijing, pp 78–83

Ravina I (1983) The influence of vegetation on moisture and volume changes. Géotechnique 33(2):151–163

Ritchie JT (1972) Model for predicting evaporation from a row crop with incomplete cover. Water Res Res 8(5):1204–1213

Ritchie JT, Burnett E (1971) Dry-land evaporative flux in a sub-humid climate, 2, plant influences. Agron J 63:56–62

Scholander PF, Hammel HT, Bradstreet ED, Hemmingsen EA (1965) Sap pressure in vascular plants. Science 148:339–346

Shimada K, Fujii H, Nishimura S, Morii T (1995) Stability analysis of unsaturated slopes considering changes of matric suction. In: Proceedings of the first international conference on unsaturated soils UNSAT'95, vol. 1, Paris, pp 293–299

Simunek J, Sejna M, van Genuchten M (1998) HYDRUS-1D: code for simulating the one-dimensional of water, heat, and multiple solutes in variably saturated porous media. Version 2.02. International Groundwater Modeling Center. Colorado School of Mines. Golden, CO

Stormont JC (1995) Alternative barrier layers for surface covers in dry climates. asce special geotechnical publication no.7: geo-environmental issues facing the Americas, ASCE, pp 150–155

Tratch DJ, Wilson GW, Fredlund G (1995) An introduction to analytical modeling of plant transpiration for geotechnical engineers. In: 48th Annual Canadian Geotechnical Conference, Vancouver BC, pp 771–780

Vandangeon P (1992) Exemple de sinistres en région parisienne. Revue Française de Géotechnique, n°58, pp 7–14

Wallance JM, Hobbes PV (1977) Atmospheric science : a introductory survey. Academic Press, 350 p

Warren RW, Hakonson TE, Trujillo G (1994) Water balance relationships in four alternative cover designs for radioactive and mixed waste landfills. Los Alamos National Laboratories, DOE, Los Alamos

Warren RW, Hakonson TE, Bostick KV (1996) The hydrologic evaluation of four cover designs for hazardous waste landfills at Hill Air Force Base. Federal Facilities Environ J, Winter, 91–110

Waugh WJ (2002) Monticello field lysimetry: Design and monitoring of an alternative cover. In: Proceedings of the waste management '02 conference, Tucson, AZ

Waugh WJ, Thiede ME, Cadwell LL, Gee GW, Freeman HD, Sackschewsky MR, Relyea JF (1991) Small lysimeters for documenting arid site water balance. Lysimeters for evapotranspiration and environmental measurements. Honolulu, HI, pp 151–159

Williams AAB, Pidgeon JT (1983) Evapo-transpiration and heaving clays in South Africa. Géotechnique 33(2): 141–150

Wilson GW (1997) Surface flux boundary modeling for unsaturated soils. Unsaturated Soil Eng Pract 38–65

Wilson GW (2000) The role of climate and soil properties in the evaluation of flux boundary conditions for application to unsaturated soil mechanics. XI PANAM, Brasil, pp. 209–218

Wilson GW, Fredlund G, Barbour SL (1994) Coupled soil atmosphere modeling for soil evaporation. Can Geotech J 31:151–161

Wilson GV, Albright WH, Gee GW, Fayer MJ, Ogan B (1999) Alternative cover assessment project, phase I report. August 1999, prepared for the U.S. Environmental Protection Agency

Wing NR, Gee GW (1989) Protective barrier development: overview. In: 28th Hanford symposium, environmental monitoring, restoration, and assessment: what have we learned? (DOE), Richland, WA, pp 1–8

Wing NR, Gee GW (1994) Quest for the perfect cap. Civil Eng, ASCE, pp 38–41

Wu L, Oster J (1997) Instruments for water and plant management. University of California, Riverside

Xu Q, Qiu CJ (1997) A variational method for computing surface heat fluxes from ARM surface energy and radiation balance systems. J Appl Meteorol 36(1):3–11

Zornberg JG, Caldwell JA (1998) Design of monocovers for landfills in arid locations.In: Seco e Pinto PS, Balkema AA (eds) Proceedings of the third international conference on environmental geotechnics, , vol. 1. Lisbon, Portugal, September 1998, pp 169–174

Zornberg JG, McCartney JS (2003) Analysis of monitoring data from the evapotranspirative test covers at the Rocky Mountain Arsenal. Geotechnical research report, US Environmental Protection Agency, Region 8, December 2003, 227 p

Zornberg JG, LaFountain L, Caldwell JC (2003) Analysis and design of evapotranspirative cover for hazardous waste landfill. J Geotech Geoenviron Eng, ASCE 129(5):427–438

Monitoring the Performance of Unsaturated Soil Slopes

Charles W. W. Ng · Sarah M. Springman · Eduardo E. Alonso

Originally published in the journal *Geotechnical and Geological Engineering*, Volume 26, No. 6, 799–816.
DOI: 10.1007/s10706-008-9203-6

Abstract Field monitoring is necessary for the geotechnical engineer to verify design assumptions. More importantly, the field data may also be assembled into a comprehensive case record that is available for use when checking validity of any analytical and numerical models. The ongoing process of back-analysis in unsaturated soil engineering can help to refine and improve our understanding, providing guidance for future designs, where the effects of soil suction and hydraulic hysteresis are still being explored. A range of recent field studies of the mechanisms of rainfall infiltration into slopes is presented. In addition, some physical simulations of unsaturated soil slopes subjected to rainfall, rising ground water table and changes of moisture in centrifuge model tests are reported.

Keywords Field monitoring · Unsaturated · Slope · Centrifuge

C. W. W. Ng (✉)
Department of Civil Engineering, Hong Kong University of Science and Technology, Clear Water Bay, Kowloon, Hong Kong
e-mail: charles.ng@ust.hk

S. M. Springman
Swiss Federal Institute of Technology (ETHZ), Zurich, Switzerland

E. E. Alonso
Universitat Politècnica de Catalunya, Barcelona, Spain

1 Introduction

Risk and unexpected ground response is inherent in geotechnical engineering when dealing with natural materials such as soil and rock. Field monitoring is therefore essential and the data obtained may assist with checking the validity of any analytical and numerical models (Ng 1992). Back-analysis of data from case histories is essential to assess how conservative future design of soil-structures and soil slopes will be, especially in unsaturated soil engineering, where the influence of soil suction and hydraulic hysteresis are now being considered in practice.

Recent field studies of the mechanisms of rainfall infiltration into initially unsaturated weathered and expansive soil slopes are reported. The importance of monitoring both the suction and net stress state variables and their effects on ground deformations and earth pressure changes in an unsaturated expansive soil slope are highlighted. Further examples from slopes in well-graded alpine moraines, in more uniformly graded fluvial sandy deposits and in alpine permafrost are presented and the reliability of instrumentation discussed. Geophysical measurement techniques are proposed as an alternative to long-term field monitoring procedures. In addition, some physical simulations of unsaturated soil slopes subjected to rainfall, rising groundwater table and changes of moisture are reported. Experience of measuring soil suctions in centrifuge model tests is discussed.

2 Field Monitoring of Unsaturated Soil Slopes

Most on-shore soil slopes are initially unsaturated prior to any rainfall. In addition to triggering by earthquakes, extreme rainfall has caused many landslides, worldwide (Fukuoka 1980; Brand 1984; Premchitt et al. 1986; Wolle and Hachich 1989; Fourie 1996; Lim et al. 1996; Sun et al. 2000; Chan and Ho 2001; Ng 2005; Ng and Zhan 2007; Ng and Menzies 2007), and this may be expected to become even more critical due to climate change effects in terms of increased intensity of rainfall events and shorter return periods (e.g. Schaer et al. 1998; Proclim 2000). Additional challenges to slope stability may arise through potential for melting of ice from alpine permafrost (e.g. Dramis et al. 1995; Haeberli et al. 1997; Arenson et al. 2002; Arenson 2003; Arnold et al. 2005).

Many rainfall-induced landslides occur above the groundwater table, especially in tropical and subtropical weathered soils (Brand 1984). With advances in field instrumentation, numerous case histories (Sweeney 1982; Lim et al. 1996; Deutscher et al. 2000; Adib 2000; Wang et al. 2000; Yagi et al. 2000; Springman et al. 2003) have been reported in the literature to investigate the mechanisms of rainfall infiltration and their influence on slope stability in various ground conditions worldwide. However, most of the reported case histories appear to measure the effects of one single stress state variable—suction or water content and the second stress state variable—net stress is generally ignored.

2.1 Field Monitoring in Weathered Geomaterials in the Far East

Mechanisms and effects of rainfall infiltration into weathered slopes have been monitored and studied extensively in the Far East, particularly in Singapore and Hong Kong (Sweeney 1982; Premchitt et al. 1992; Lim et al. 1996; Deutscher et al. 2000; Rahardjo et al. 2005). The geology in the Far East is influenced heavily by tropical and sub-tropical weathering (Guan et al. 2001; Ng et al. 2001a), with superficial deposits of fill, alluvium and marine deposits in Hong Kong overlying weathered rock of varied depth or colluvium on hillsides, above fresh rock. The weathering profiles may include corestones and may be somewhat erratic but can also vary gradually from soil to rock. Table 1 sets out the classification of rock decomposition grades used in Hong Kong (GCO 1988). Saprolites are used to describe "rock" of decomposition grades IV and V, usually described as "soil". The term "rock" refers only to material of decomposition grades I–III, with I representing fresh rock. The occurrence of weathering grade VI, referred to as "residual soil", is more common in Singapore than in Hong Kong, due to different degrees of weathering under local climatic conditions.

Conventional tensiometers (i.e., those measuring less than 100 kPa suction) and piezometers have been used to measure negative and positive pore water pressures (PWPs), respectively, in the field (see Fig. 1). In addition to measuring PWPs, a rain gauge has often been used to record rainfall intensity (Lim et al. 1996; Rahardjo et al. 2005); and in situ double-ring infiltrometer tests have been carried out to measure mass permeability in the field (Deutscher et al. 2000). To control rainfall duration, pattern and intensity in the field and to differentiate the relative percentages of rainfall infiltration and surface runoff, artificial rainfall simulator and catchment areas have been created (Premchitt et al. 1992; Springman et al. 2003; Rahardjo et al. 2005). Based on these reported field studies, valuable data revealing the characteristics and mechanisms of rainfall infiltration in weathered materials were collected and used to investigate rainfall-induced failure mechanisms in the Far East (Rahardjo et al. 1998; Sun et al. 2000; Ng et al. 2001b).

Despite the significant progress being made to improve the understanding of the mechanisms of rainfall infiltration in weathered geomaterials by correlating relationships between the measured rainfall infiltration (and moisture contents) and soil suction, no information about soil movements/deformations and reliable earth pressures are available for engineers to design their slopes/retaining walls for the serviceability limit state and for academics to calibrate their constitutive models fully, in terms of two stress state variables (i.e., suction and net stress). Usually, only a suction-water content relationship has been considered, and the relationship between net stress/earth pressure-displacement has been ignored in most field monitoring programmes.

Table 1 Classification of rock material decomposition grades (from GCO 1988)

Descriptive term (1)	Grade symbol (2)	General characteristics for granitic and volcanic rocks (3)
Residual soil	VI	Original rock texture completely destroyed
		Can be crumbled by hand and finger pressure into constituent grains
Completely decomposed	V	Original rock texture preserved
		Can be crumbled by hand and finger pressure into constituent grains
		Easily indented by point of geological pick
		Slakes when immersed in water
		Completely discoloured compared with fresh rock
Highly decomposed	IV	Can be broken by hand into smaller pieces
		Makes a dull sound when struck by geological hammer
		Not easily indented by point of geological pick
		Does not slake when immersed in water
		Completely discoloured compared with fresh rock
Moderately decomposed	III	Cannot usually be broken by hand; easily broken by geological hammer
		Makes a dull or slight ringing sound when struck by geological hammer
		Completely stained throughout
Slightly decomposed	II	Not broken easily by geological hammer
		Makes a ringing sound when struck by geological hammer
		Fresh rock colours generally retained but stained near joint surfaces
Fresh	I	Not broken easily by geological hammer
		Makes a ringing sound when struck by geological hammer
		No visible signs of decomposition (i.e., no discolouration)

2.2 Application of Field Monitoring in Unsaturated Expansive Clays in China

2.2.1 The Study Site and Ground Conditions

Expansive soils can be found almost on all continents. A major infrastructure project in China, the 1,200-km long South-to-North Water Transfer Project (SNWTP), carries potable water from the Yangtze River region in the south to many arid and semi-arid areas in the northern regions of China, including Beijing. During the preliminary design, an 11-m high cut slope (see Fig. 2) in a typical medium-plastic expansive clay in Zaoyang, close to the "Middle-route" of the SNWTP in Hubei, was selected for a comprehensive instrumented field study of rainfall infiltration, since at least 180 km passes through areas of unsaturated expansive soils.

One of the major geotechnical problems is the potential instability of the unsaturated expansive soil slopes during rainfall (Bao and Ng 2000; Ng et al. 2003). To improve the fundamental understanding of the mechanisms of rain-induced retrogressive landslides observed in the unsaturated expansive soils in the area, a comprehensive field study was carried out (Ng et al. 2003). The instrumentation included tensiometers, thermal conductivity suction sensors, moisture probes, earth pressure cells (EPCs), inclinometers, settlement markers, a tipping bucket rain gauge, a vee-notch flow meter and an evaporimeter. The instrumentation was intended to investigate the influence of the two independent stress state variables

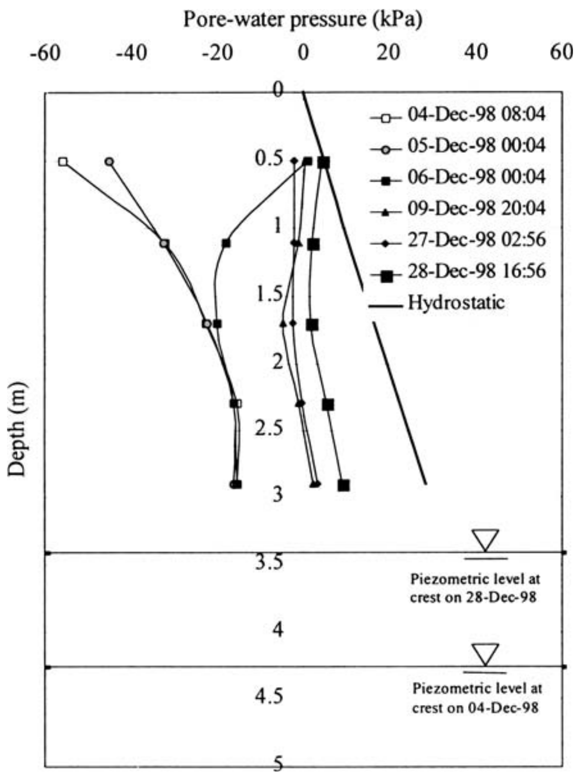

Fig. 1 Typical measured PWP distributions at shallow depths in weathered soils in Singapore (Deutscher et al. 2000)

(i.e., soil suction and net stress) on the performance of the slope.

As shown in Figs. 2 and 3, the study site area had a uniform slope angle of 22° and there was a 1-m wide berm at the mid-height of the slope. An area, 16-m wide by 31-m long, with a cleared surface and a significant depth of typical unsaturated expansive soil, was selected for instrumentation and artificial rainfall simulation tests. The ground level at the toe of the slope is approximately +96-m Ordinary Datum. The predominant stratum in the slope was a brown and yellow stiff over consolidated fissured clay, which was sometimes inter-layered with thin layers of grey clay or iron concretions. The brown–yellow clay contained about 15% hard and coarse calcareous concretions (particle size generally from 30 to 50 mm). X-ray diffraction analyses indicated that the predominant clay minerals are illite (31–35%) and montmorillonite (16–22%), with some kaolinite (8%) (Liu 1997). The natural water content was generally slightly greater than the plastic limit ($w_P = 19.5\%$, $I_p = 30\%$), although this was much lower within the top 1 m. The dry density profile down to 2 m indicated a relatively dense soil layer was present at a depth of about 1.5 m. Figure 3 shows the locations and layout of some instruments (e.g. Ng et al. 2003).

2.2.2 Key Results Obtained from Monitoring

Rainfall was produced artificially at the test site using a sprinkler system, comprising a pump, a main water-supply pipe, five branches and 35 sprinkler heads (Zhan 2003; Zhan et al. 2006). The system could produce three levels of rainfall intensity (i.e., 3, 6 and 9 mm/h). The site was fairly dry from November 2000 to April 2001, with a total rainfall of only

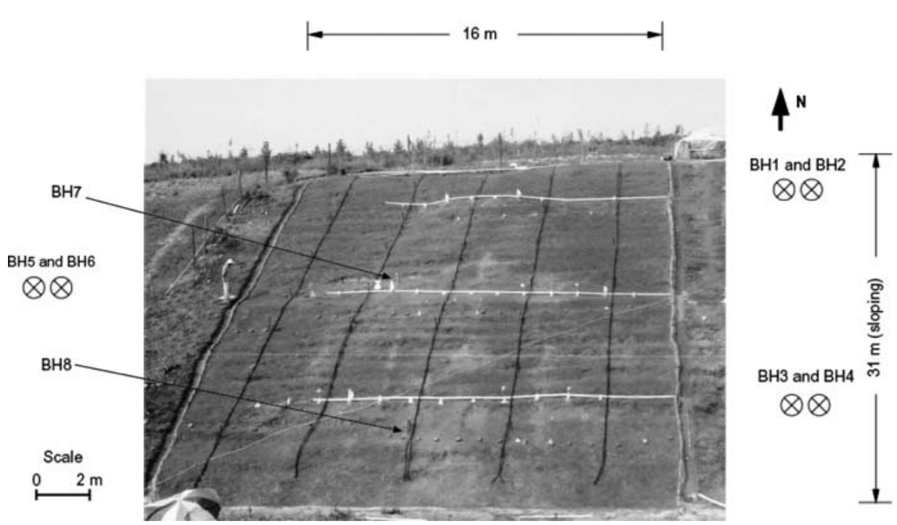

Fig. 2 Instrumented 16 m by 31 m (sloping distance) slope in expansive soils in China (Ng et al. 2003)

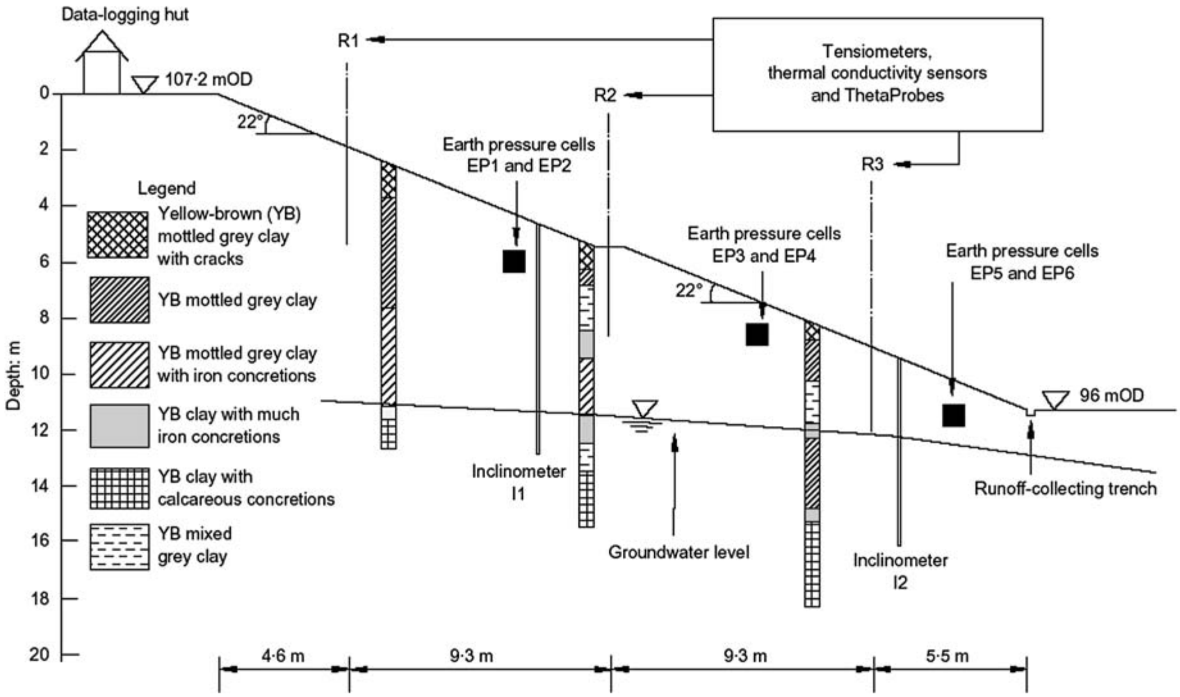

Fig. 3 Cross-section of the instrumented slope (Ng et al. 2003)

60 mm. Only about 40 mm of rainfall fell in May, when the wet season generally begins. From June to 18 August, the monitored area was protected against rainfall infiltration with a plastic membrane so that the subsequent rainfall simulation tests started from relatively dry soil conditions. Two artificial rainfall events were simulated during the one-month monitoring period, from 13th August to 12th September, 2001. The first lasted for 7 days, from the mornings of 18th–25th August, with an average daily rainfall of 62 mm. The second lasted from the morning of 8th September to the afternoon of the 10th. The artificial rainfall was stopped for two or 3 h during both rainfall periods, in the morning of each day, to allow measurement of horizontal displacements and soil swelling, as well as to auger disturbed specimens for the determination of gravimetric water content (GWC) profiles. Apart from this, the artificial rainfall intensity was maintained at 3 mm/h.

2.2.2.1 Responses of Soil Suction to Rainfall Typical data are recorded by four tensiometers and four thermal conductivity sensors at the middle section (R2) (Fig. 4). Immediately prior to the first artificial rainfall on 18th August, negative PWPs ranged from 18 to 62 kPa (Fig. 4a). As expected, the higher the elevation of the tensiometer, the larger the negative PWP. With the exception of the thermal conductivity sensor (R2-TC-0.6) showing a very high soil suction of about 250 kPa at 0.6 m below ground level (Fig. 4b), soil suctions deduced from the remaining three sensors were generally consistent with the measurements obtained from the tensiometers.

After the first artificial rainfall event was started, the negative PWP and soil suction measured by most sensors only began to decrease after about 2 days of rainfall (about 90 mm of rain). There was a clear delay in PWP response to rainfall infiltration, even at a depth of 0.6 m (Fig. 4a). Extending to a depth of 1.5 m, the duration of delay appeared to decrease as depth increased. Based on field reconnaissance and observations in trial pits, it was found that many cracks and fissures occurred near the ground surface and a layer of relatively impermeable material was identified at about 1.5 m below the ground surface. It is postulated that since the intact expansive clay has relatively low water permeability, water can only ingress the clay through cracks and fissures so the tensiometers did not register any significant changes of soil suction around their tips, leading to the initial delay in response. Subsequently,

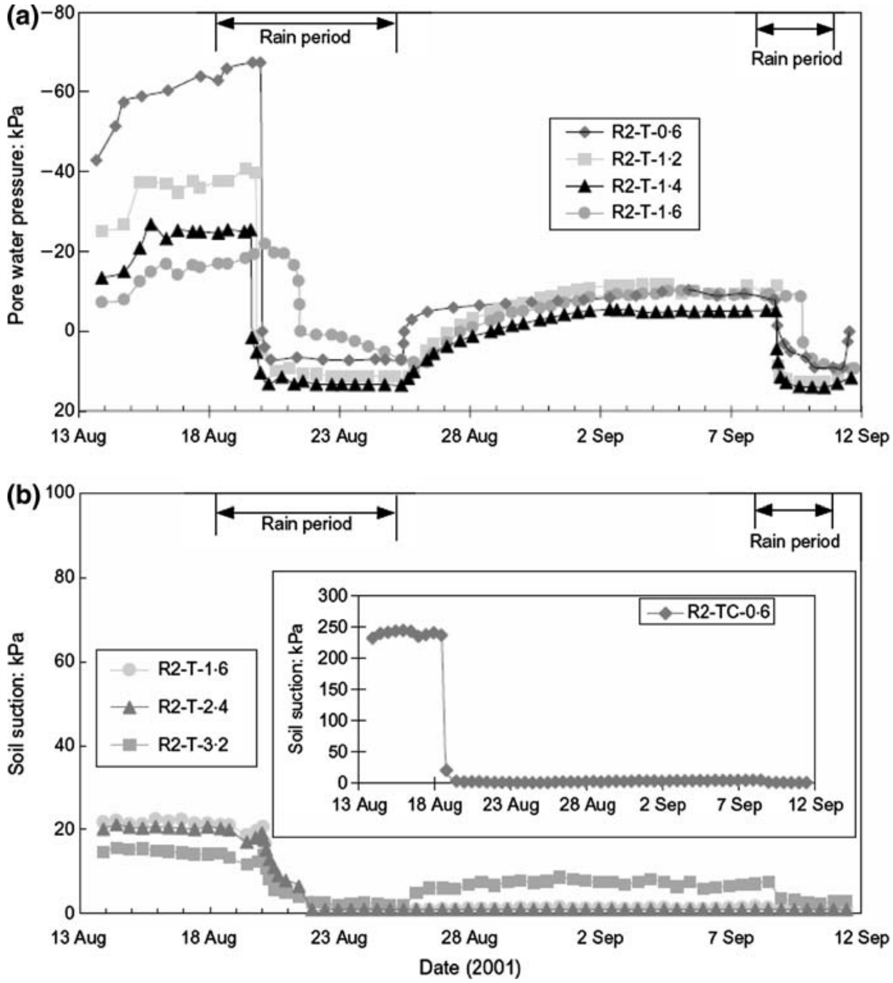

Fig. 4 Response from suction sensors located at R2: (**a**) PWPs measured by tensiometers; (**b**) soil suctions measured by thermal conductivity sensors (Ng et al. 2003)

when the infiltrated rain water started to rise from the bottom of the cracks or from a perched water table formed due to the presence of the impeding layer and seep in all directions, the lower the tensiometer, the quicker the response (i.e., the shorter the delay). Obviously, a rapid response was shown by a sharp reduction in negative PWP when water reached the locations of the tensiometers above the impeding layer. The tensiometer located below the impeding layer showed the slowest and the most gradual rate of response to rainfall and the lowest magnitude of reduction of negative PWP.

After the first rainfall event, the lower three tensiometers showed a gradual increase (or recovery) in negative PWP, reaching an apparent steady state condition after 2nd September, recording negative PWP from 3 to 10 kPa. The rate of recovery was very similar for the lower three tensiometers, although the top one showed a much more rapid recovery initially. However, the final magnitudes of recovered negative PWP fell within a narrow range and did not appear to be strongly governed by the depths of the tensiometers.

During the second artificial rainfall event, the lower three tensiometers showed almost no delay in response to the rainfall. There was a change in PWP from negative to positive, although the magnitude of the change (about 10 kPa) was not very significant. The top tensiometer showed a 1-day delay in response. However, the “final equilibrium” PWPs recorded during the second rainfall event were similar to those measured during the first one.

The general responses of indirect soil suction measurements by thermal conductivity sensors to the two artificial rainfall events (see Fig. 4b) were similar to those recorded by the tensiometers, except that the former showed a slower rate of response than the latter.

The magnitude of PWPs measured by the two different types of sensor was generally consistent, particularly at the depth of 1.6 m below ground. However, the inconsistency shown between the two sensors located at the depth of 0.6 m before the first rainfall may be due to the inherent limitation of tensiometers caused by cavitation at suctions greater than circa 80 kPa.

Measurements of volumetric and GWCs are not discussed in this paper (see Ng et al. 2003; Zhan 2003).

2.2.2.2 Changes of Horizontal Total Stresses Figure 5 shows the total stress ratio (σ_h/σ_v) measured with time from six vibrating-wire EPCs. All EPCs were installed at a depth of 1.2 m, giving rise to an estimated total vertical stress (σ_v) of about 23.4 kPa, which corresponded to an average dry density of 1.56 Mg/m^3. Pressure cells EP1, EP3 and EP5 (refer to Fig. 3 for locations) measured the stress changes acting in the East–West (EW) direction (i.e., perpendicular to the inclination of the slope), whereas EP2, EP4 and EP6 recorded pressures acting in the north–south (NS) direction (i.e., parallel to the inclination of the slope).

Prior to the first rainfall event on 18th August, an initial equilibrium total stress ratio appeared to have been established for each cell and values recorded by all of the cells were lower than 0.3. Two out of six cells registered a small tensile stress, probably induced as a result of soil drying (note: vibrating-wire cells are able to record tensile stress). During installation, the clearance between the wall of the EPC and the soil was backfilled with an epoxy resin. The thin layer of epoxy resin glued the cell securely to the soil and it allowed transmission of tensile force between the cell and the soil (Ng et al. 2003; Zhan 2003; Zhan et al. 2006).

After the start of the first rainfall event, a significant change of stress was registered after about one and a half days. The delayed response of the pressure cells was consistent with the PWP measurements shown in Fig. 4 and measured volumetric water contents (Ng et al. 2003). Once the EPCs started to respond, the ratios (σ_h/σ_v) increased rapidly within 1 day, and then approached a steady value for the subsequent duration of the first rainfall event. It appeared that the magnitude of increase in total horizontal stress was strongly related to the elevation of the EPCs and the initial negative PWP. The higher the EPC's elevation, the larger the initial negative PWP present in the ground, and hence the greater the increase in σ_h/σ_v. This performance appeared to be consistent with the relationship between swelling potential of expansive soils and initial soil suction, i.e., the swelling potential of an expansive soil generally increases with an increase in the initial negative PWP or suction of the soil (Fredlund and Rahardjo 1993; Alonso 1998). For a given pair of pressure cells located at the same elevation, the measured stress ratio in the EW direction was always larger than that in the NS direction. This is probably related to a higher constraint imposed as a result of sloping ground in the EW direction as opposed to that in the NS direction (Ng et al. 2003; Zhan 2003).

During the 2-week no-rain period (from 25th August to 7th September), a further increase in σ_h/σ_v was observed at EP1 and EP2, whereas the EP3 and

Fig. 5 Changes of in situ total stress ratio measured by EPCs (Ng et al. 2003)

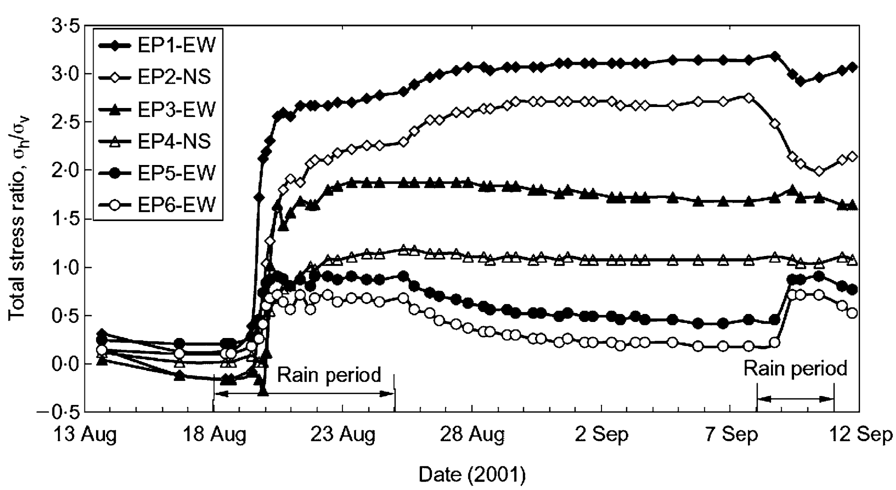

EP4 pressure cells showed a slight decrease in stress ratio, and EP5 and EP6 recorded a larger reduction in stress ratio than EP3 and EP4. The reduction in σ_h/σ_v appeared to be primarily due to a decrease in the positive PWP at a depth of 1.2 m during the no-rain period (see Fig. 4). However, the continuous and gradual increase in σ_h/σ_v at EP1 and EP2 (but at a reduced rate) may be due to an ongoing "soaking" of the soil near the location of the EPCs at R2, even after the first rainfall event.

After the start of the second rainfall event, the responses at the three pairs of EPCs were distinctly different. At EP1 and EP2, the observed σ_h/σ_v decreased rather than increased. This may be attributed to the softening of the soil after prolonged swelling during the no-rain period. For the pressure cells (EP5 and EP6) near the toe of the slope, an increase in σ_h/σ_v was recorded due to regaining positive PWP. The performance of EP3 and EP4 fell between the former two cases.

2.2.2.3 Responses of Horizontal and Vertical Ground Deformations Horizontal Displacements Due to Changes of Soil Suction Figure 6 presents the monitored horizontal displacements from inclinometer I2 (near the toe of the slope, as shown in Fig. 3) in the down-slope and the WE directions. For convenience, the measured displacements from the NS direction (i.e., up-slope direction) and from the west–east direction are taken as positive. The measured results indicate that the ground moves towards the down-slope direction and towards the east direction during rainfall. The magnitudes of displacement and deformed shapes observed were consistent in both directions but the magnitudes were significantly larger and the depth of influence was substantially deeper (deep-seated) than those observed at the mid-slope (i.e., at I1). The larger displacements at the toe are attributed to the lower initial negative PWP (or soil suction) present at I2 relative to those at I1 (Ng et al. 2003), resulting in a lower soil stiffness near the toe. The greater influence depth near the toe of the slope was consistent with the deeper influence of the simulated rainfall events on the GWC measured at section R3, as opposed to section R2 (Zhan 2003).

2.3 Field Monitoring of Granular Slopes in Alpine and Pre-alpine Regions

2.3.1 Well-graded Moraine

A field monitoring exercise with combined artificial and natural rainfall was carried out for periods during two consecutive summer seasons (1999 and 2000) on a 100 m^2 plan area for a 31° slope in a moraine bastion at ca. 2,800 m above sea level (ASL) just beneath the Gruben glacier in the Valais, Switzerland. A smaller and steeper area was also instrumented (55 m^2, 42°) in 2000 (Teysseire et al. 2000; Springman and Teysseire 2001; Springman et al. 2003). Earlier geophysical

Fig. 6 Observed horizontal displacement in response to rainfall from I2 (NS-downslope and EW-lateral) (Ng et al. 2003)

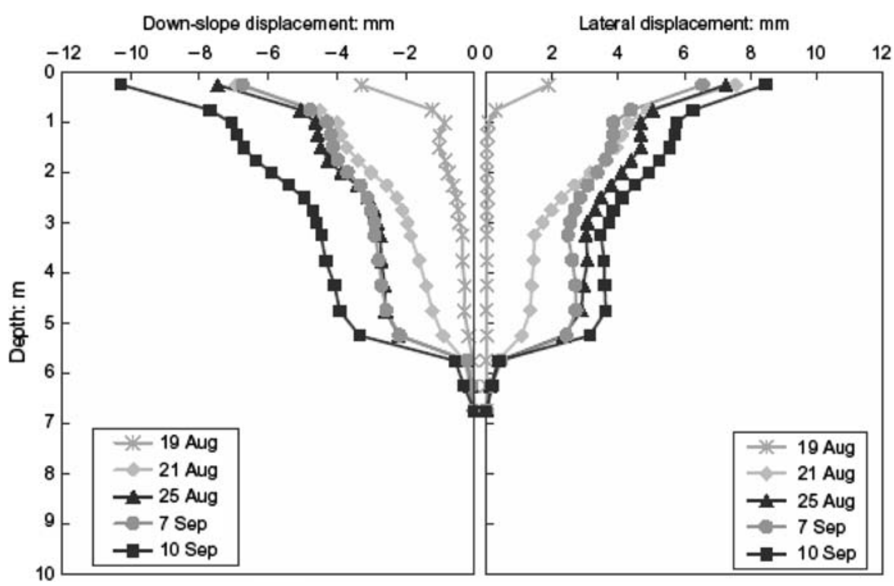

investigations (Vonder Mühll et al. 1996) had revealed an extremely heterogeneous deposit, which increased in density with depth, although the challenges of obtaining meaningful geophysical data in such a geomaterial were also emphasised. Instrumentation was newly installed each year due to the extreme temperature conditions in the ground during the winter season.

Although eight Time Domain Reflectometers (TDRs) and four Moisture Point (MP) devices were installed for determination of volumetric water content, ten jet-fill tensiometers for measurement of suction, together with a sprinkler system, rain gauges, a temperature and humidity sensor and several fibre optic extensometers of different lengths (Fig. 7), there was considerable attrition in the sensors buried in the ground. Only a few eventually delivered usable data. Many of the problems arose due to the range of particle sizes encountered during installation, with up to 10% silt size particles and boulders over 1 m in diameter. The challenge was to obtain good contact between the TDR prongs, MP rod, the ceramic cups of the tensiometers and the soil, if the pipe rammed into the moraine as preparation for the insertion of the device happened to expose a coarser zone with larger particles.

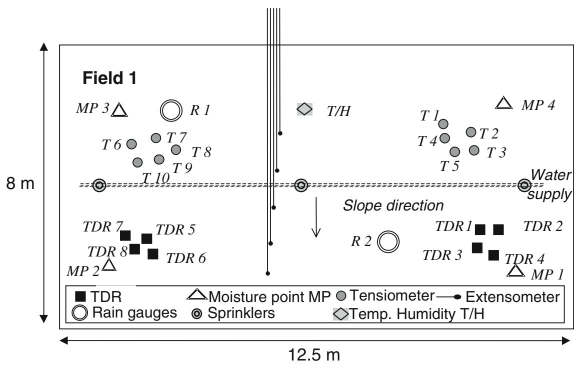

Fig. 7 Plan on the Field 1/1999 test-site with distribution of instrumentation (Springman et al. 2003)

In 1999, effective installation was only achieved for one complete MP (five sensors from 0 to 1.2 m in depth) and roughly half of the TDRs, all of which produced quite consistent data, confirming trends from other investigations (Teysseire et al. 2000). Saturation degree only reached over 90% in the top 0.15 m depth, with a further significant drop off below 0.3 m, despite artificial rainfall more extreme than a 1:500 year storm (Springman et al. 2003; Fig. 8). None of the tensiometers delivered good quality data and the surface erosion caused by this rainfall event with a base rate of 10 mm/h for a week and peaks of up to 30–40 mm/h (with ca. 80–85% run off) on such a steep slope, undermined the fibre optic extensometers and washed out their anchoring locations. Some parts of the instruments that extended above ground surface were also damaged by rolling stones that were destabilised by the surface flow. Clearly, the particle size range meant that suctions were unable to act uniformly to retain the stability of the slope locally and this is an important factor when dealing with well-graded granular materials on steep

Fig. 8 Data of rainfall (mm/h) and degree of saturation between depths of 0–0.15, 0.15–0.3, 0.3–0.6, 0.6–0.9, 0.9–1.2 m from MP readings, Gruben test site, 1999 (Teysseire et al. 2000)

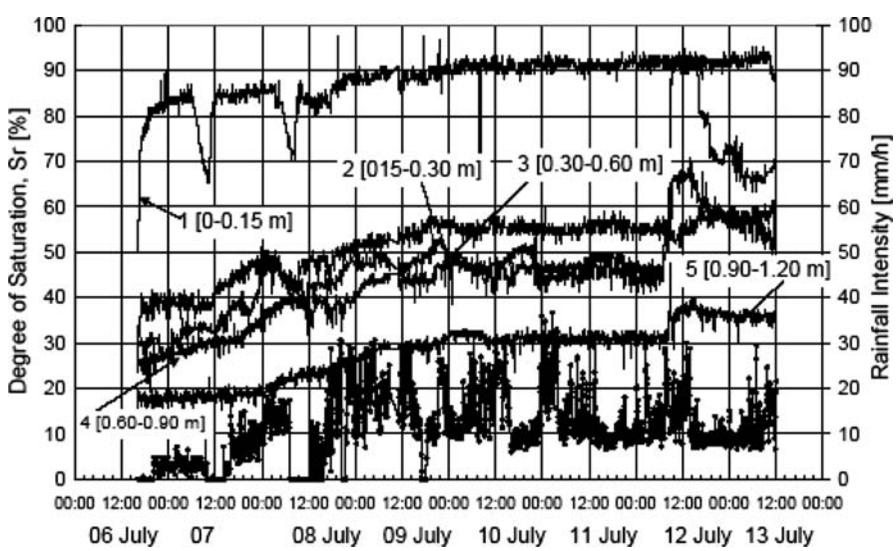

slopes inclined at angles approaching their internal angle of friction.

This experience was helpful for the preparation of the two instrumented field sites in 2000 (Springman and Teysseire 2001). Since the top 0.5 m of soil was of the greatest interest, the deeper tensiometers (−0.8 m, −1.2 m) were omitted. More care was exerted by pre-boring with a smaller diameter than the respective rod to ensure that contact between probe and soil was better (for tensiometers and MPs). The tensiometers were also installed 3–4 weeks before the artificial rain test began so that action could be taken in advance for those that did not appear to be responding. The sealing at the surface between tensiometer standpipe and soil surface was also improved to be able to limit the local erosion.

Data was obtained from both TDR devices and tensiometers at comparable depths, for a 2-day storm (ca. 16 and then 12 mm/h per day) that eventually led to rupture on the steeper 42° slope. Comparisons between data from 1999 and 2000 confirmed the general trends in the uppermost 0.5 m for the 31° slope (Fig. 9a, b; Springman et al. 2003). Attempts were also made to install tensiometers in the 42° slope, but it was not possible to obtain data, where the only information was delivered from TDRs, showing good agreement with previous data (Fig. 9a).

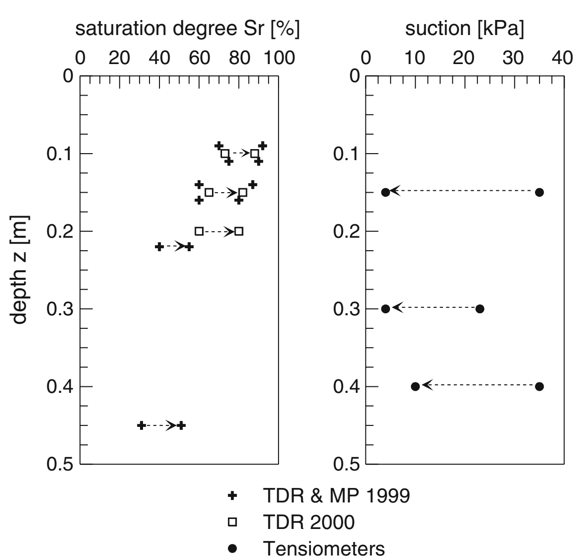

Fig. 9 Immediate pre- and post-rainfall event data. (**a**) Saturation degree determined from TDR and MP probes: Fields 1/1999 & 1/2000 (31° slope), Gruben. (**b**) Suctions determined from tensiometers: Field 1/2000 (31° slope), Gruben (Springman et al. 2003)

Considerable attrition of sensors was still in evidence and it is suggested that allowance should be made for a 50% loss and hence the number of sensors in areas of most interest should be doubled.

A final observation for consideration in the design of such field monitoring sites is the effect of wind and rain droplet size. Some protection was provided against prevailing mountain top winds for up to 1 m above ground level, but the supply of artificial rainfall through sprinklers may not necessarily produce a uniform precipitation (usually attributed to the average value obtained from the two rain gauges) over the entire test area. It is also known that artificial rainfall delivers droplets. Care must be taken in the transfer of knowledge obtained from artificial rainfall events to natural cases.

2.3.2 Uniformly Graded Silty Sand

A longer term field monitoring exercise is currently underway at Tössegg, on a 27° slope on the banks of the river Rhine in Switzerland, with first results reported by Thielen and Springman (2005). Extensive soil profiling to bedrock has been conducted over a larger area than the eventual 15 m by 15 m test site, using geophysical electrical resistivity tomography and ground penetrating radar in addition to more traditional geotechnical site investigation techniques. A coherent model of the ground has been obtained together with basic classification and indexing parameters (Thielen et al. 2005; Thielen and Springman 2005; Friedel et al. 2006). Additional laboratory testing is underway to obtain more advanced characterisation in terms of saturated and unsaturated soil properties for the overlying uniformly graded clayey, silty sand and the underlying sandier layers. Bedrock is located between ca. 1 and 2 m below ground level for the eventual test field area.

A similar range of instruments (TDRs, MPs, jet-fill Tensiometers, rain gauge, Fig. 10) have been installed at various depths and locations, together with piezometers sealed into standpipes above the test slope at depths just above the rock base to observe any flow of water above bedrock. The run off has also been measured by means of an eaves gutter to collect the water and a Vee-notch weir to measure outflow.

In general, the instrumentation has been more reliable than at Gruben. Installation into more

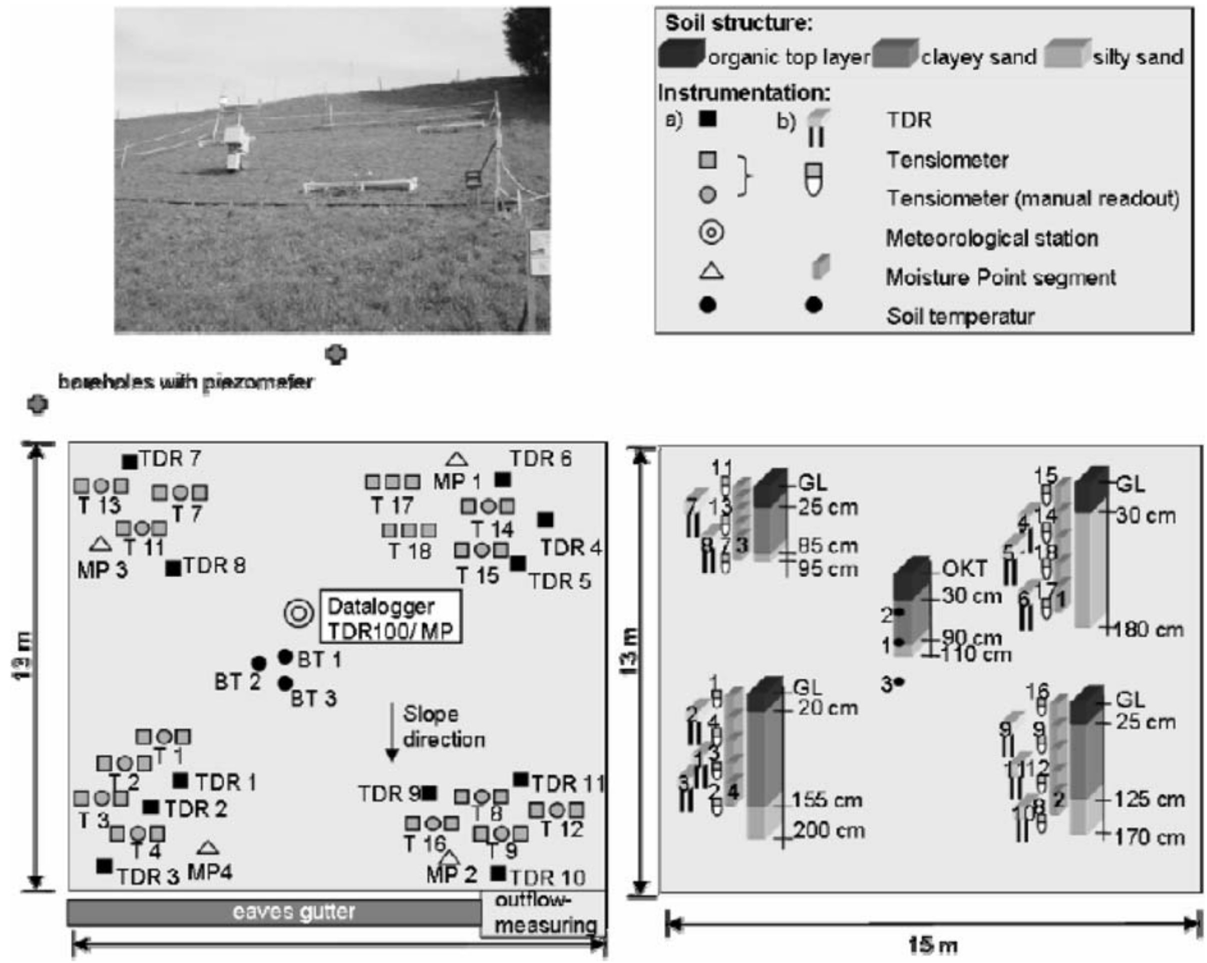

Fig. 10 Toessegg field test site: layout of instrumentation (Thielen and Springman 2005)

uniformly graded soil has been straightforward and all instruments are functioning, after over 2 years of activity. Some of the problems that have arisen are due to animal influences, requiring protection of the test field from cows and rodents, who attempted to expose and eat cables or were drowned in the Vee-notch reservoir. Minor levels of vandalisation have also been dealt with.

Problems of a more technical nature include the cut-off at suctions greater than 80 kPa by the tensiometers. This was reached quite regularly last autumn after installation and is not of major concern in terms of the instability of the slope unless sudden rainstorms of the order of the local 2002 event (Fischer et al. 2003) occur. Clearly this soil is very susceptible to saturation and sudden loss of suction-induced strength and this is likely to be exacerbated by any existing high suctions, as also observed in S.E. Asia, e.g. by Yagi et al. (2000) and Mofiz et al. (2005).

Subsequently, protection against frost was essential over the winter period when the soil was almost completely saturated at all depths. Water was replaced in the reservoirs of the jet-fill tensiometers with an antifreeze-water mixture with a relative density of 0.95. This seemed to function well and all instruments are still delivering plausible data. The performance of the sensors that deliver regular sets of electronic data has been validated by additional manually read instruments at regular intervals. This was also noted by Ireson et al. (2005) in respect of manual spot-checks and electronically recorded data.

One promising additional opportunity to monitor the development of saturation degree lies with electrical resistivity tomography (Friedel et al.

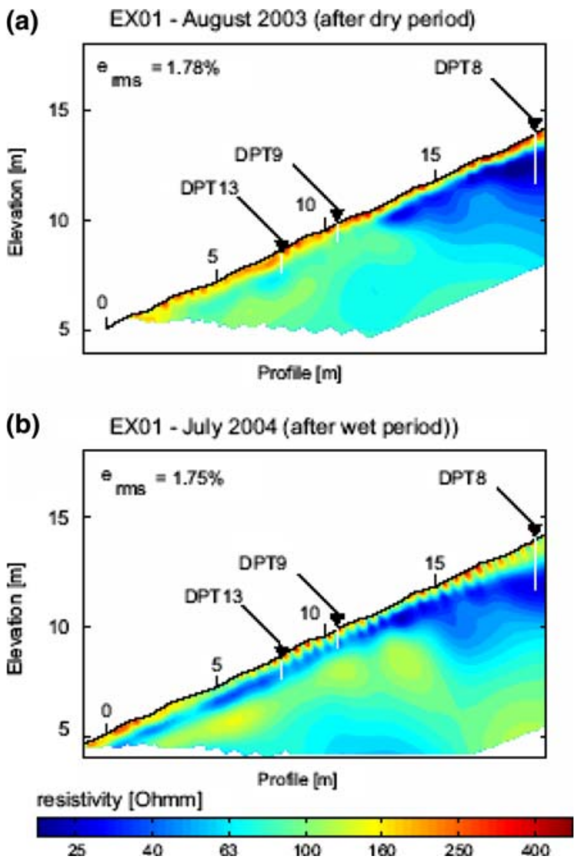

Fig. 11 Resistivity tomograms along an identical profile (EX01) at the Toessegg field site (**a**) during the dry summer of 2003 and (**b**) after a wet period in summer 2004 (Friedel et al. 2006)

2006). Two sets of data obtained during a relatively dry (Fig. 11a) and a wet period (Fig. 11b) show very clearly how the resistivity differs and how this supports the contention that it is possible to detect and quantify these changes in resistivity as a function of saturation degree. Future work on calibrating actual field data of saturation degree to the resistivity tomogram could lead to this being adopted more widely as a very useful non-intrusive form of monitoring for relatively simple slope and soil layer geometries. Homogeneous uniformly graded soils are also advantageous. Ground penetration radar (GPR) profiling was attempted, but was neither successful as a field tool for identifying spatial distribution of layers nor for ongoing determination of the saturation degree with the slope. Machado et al. (2005) were successful in determining water content in reconstituted and homogenous models in the laboratory, but there remains significant doubt about GPR as an effective monitoring tool in the field. Extensive laboratory calibration will be required and the influence of fabric and uneven pore space (e.g. due to root holes or uneven compaction) in real soils will further complicate the field data. Seismic profiling was not adopted by Friedel et al. (2006) because of the proximity of the bedrock to the ground surface.

2.3.3 Alpine Permafrost

Whereas year round instrumentation of partially saturated slopes may be complicated at 1,000 m ASL, at ca. 2,500 m ASL it becomes severely limited. The active layer overlying the alpine permafrost, formed as a rock glacier (Barsch 1996), melts in summer and freezes in winter to depths of several metres in the Alps, and is potentially unstable during the thawing process (Haeberli et al. 1997; Arenson et al. 2002; Arnold et al. 2005). The surface is mantled with large blocks since any fine material has been washed through the large voids and flushed out along the permafrost table. Furthermore, the entire area is blanketed in snow for several months of the year and is often unreachable due to fear of avalanches, so that extensive on site data storage is essential or a transmission mast must be erected and protected from wind, snow and avalanches until the spring thaw begins.

The partially frozen geomaterial has four phases, with solid particles surrounded by an unfrozen water layer with interstitial ice and air, the relative degrees of these four phases being dependent on a number of factors including temperature below zero and particle size and shape (e.g. Andersland and Ladanyi 2004). The presence of both interstitial air and specific drainage channels in degrading ice-rich permafrost (Vonder Mühll et al. 2003) becomes important when trying to evaluate the stability of this slope. Furthermore, the presence of unfrozen water around the particles associated with significant suctions is also a positive benefit until drainage channels form throughout the degrading permafrost body.

Monitoring tends to include installation of devices in boreholes, such as inclinometers (although all of these are sheared off in the rock glaciers investigated, Arenson et al. 2002), thermistor chains and TDR cables, as well as surface measurements of deformation and temperature. The normal range of field instrumentation is excluded in regions of alpine permafrost because of the challenges of the winter freeze on the ceramic tips of these sensors.

Geophysics has been used to characterise one rock glacier (Musil et al. 2002; Maurer et al. 2003) in conjunction with information obtained from boreholes and laboratory testing (Arenson 2003; Arenson et al. 2003, 2004; Hauck et al. 2003; Arenson and Springman 2005). However, the extreme conditions in such remote locations, as well as the relatively large surface areas under threat and the blocky nature of the ground, which complicates the application of the shock/electromagnetic waves, meaning that regular monitoring using geophysics (Hauck and Vonder Mühll 2003; Hauck et al. 2005) may not be able to be sufficiently constrained to deliver an accurate enough indication of the unsaturated state of the ground. Nonetheless, work is ongoing to endeavour to link degree of saturation in frozen soils in terms of air, ice and water to various parameters obtained from geophysical testing methods and this geotechnical-geophysical monitoring axis will certainly be an area of interest in the future.

3 Centrifuge Modelling of Unsaturated Soil Slopes with Suction Measurements

Various attempts have been made recently to measure soil suctions during centrifuge tests of initially unsaturated slopes subjected to rainfall, rising groundwater levels or due to change of moisture content inside a model container (Ng et al. 2002; Zhou and Ng 2004; Take et al. 2004; Chiu et al. 2005; Zhou et al. 2006). Challenges include the miniaturisation and corresponding robustness of sensors in the enhanced g environment. Modifications have been made to commercially available miniature pore pressure transducers (PPTs) to measure suctions in centrifuge model tests (Take and Bolton 2003). Soil displacements have been measured by various methods in a centrifuge.

3.1 Centrifuge Modelling of Unsaturated Dense and Loose Fill Slopes

Figures 12 and 13 show a dense and loose fill model slope tested at the Geotechnical Centrifuge Facility of the Hong Kong University of Science and Technology (Ng et al. 2001c) and the Schofield Centre in the University of Cambridge (Take et al. 2004), respectively. The effects of transient seepage on the stability of densely filled soil slopes subjected to rising groundwater table were investigated as well as the possibility of static liquefaction in a loose fill slope due to heavy rainfall (Fig. 14a) in a centrifuge. The soil used in both series of experiments was sieved completely decomposed granite from Beacon Hill in Hong Kong. A large number of miniature PPTs were installed. Take et al. (2004) used a network of new miniature (7 mm in diameter) pore pressure and tension transducers (PPTT) buried within the model fill at each of locations indicated by open circles in Fig. 13. After a saturation programme, these devices were capable of measuring negative water pressures as low as −140 kPa reliably, when fitted with a nominal 1 bar ceramic filter (Take and Bolton 2003). The deformations of the model fill slopes were measured by a new image-based system of deformation measurement that combines the technologies of digital imaging, the image processing technique of particle

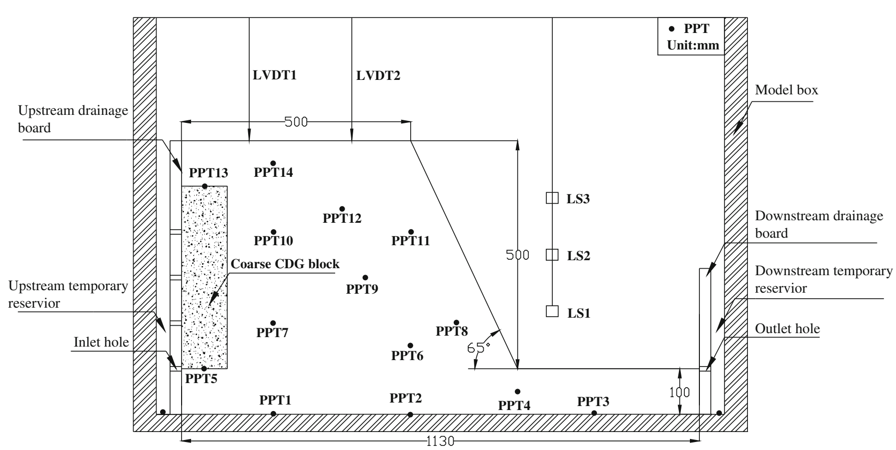

Fig. 12 A densely filled centrifuge model slope (dimensions are in millimetres) (Zhou and Ng 2004)

Fig. 13 The state liquefaction model test geometry (Take et al. 2004)

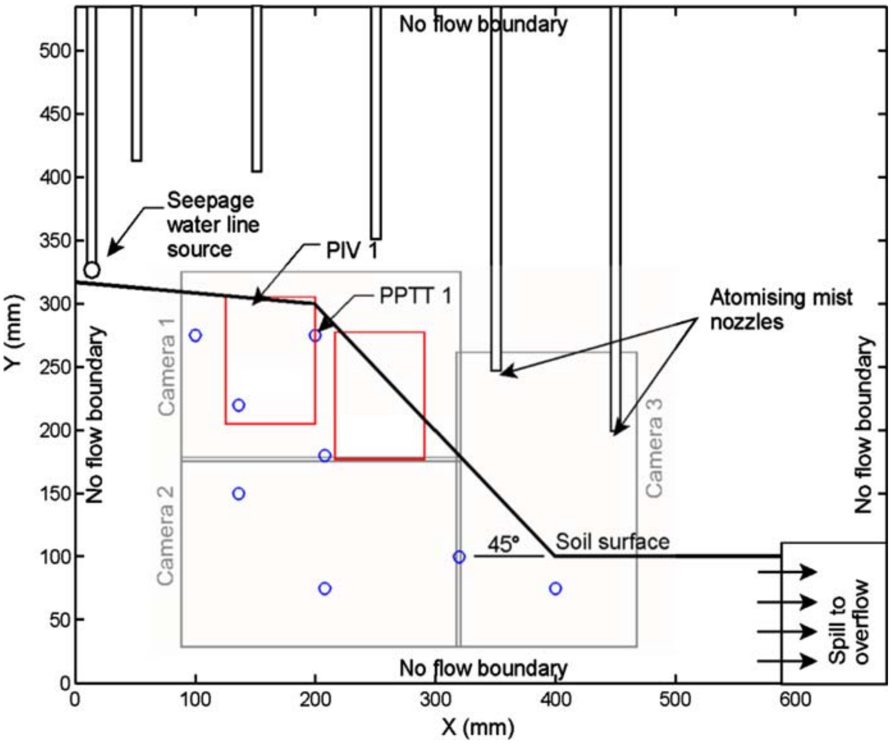

image velocimetry (PIV), and close-range photogrammetry (White et al. 2003). Digital images are captured through the transparent window of the atmospheric chamber and compared through time, allowing the determination of displacements at potentially thousands of points in each camera view of the model by tracking the soil texture (the unique way the grains are orientated at every location in the model) without resorting to embedded target markers.

The response of the very loose fill slope to the stepwise increase in stress is summarised in terms of observed pore pressure and displacements of the crest region (tensiometer PPTT1 and 32 × 32 pixel patch PIV1) in Fig. 14b, c, respectively. As the loose fill material becomes incrementally heavier, a cumulatively larger percentage of the loose fill can no longer support this increase in total stress and the void ratio rapidly decreases. The reason for this very compressible behaviour becomes abundantly clear when the initial fabric of the soil is inspected visually.

At each increment of effective stress, the rapid reduction in void ratio is observed to cause a small increase in PWP of the order of 1–2 kPa (Fig. 14b), despite experiencing large volumetric strains: void spaces are very compressible due to the low degree of saturation of the fill. As increments of "gravity" are progressively turned on, the height of the fill above the phreatic surface effectively becomes higher, requiring progressively higher capillary forces to be developed if the soil moisture is to be retained. As a result, the biggest pores shed their pore water vertically downwards into the fill, creating an initial suction distribution that increases with elevation from a value of approximately zero at the toe to −25 kPa at the crest (PPTT1 in Fig. 14b).

3.1.1 Response to Rainfall Infiltration

After the initial self-weight consolidation phase of the model test, the fill slope was subjected to the equivalent of six weekly periods of rainfall infiltration (Fig. 14a). Figure 14b shows that the arrival of rainfall on the slope surface at time A destroys a significant portion of the soil suction very rapidly at the shallow location of PPTT1. The resulting settlement of the bench above the fill slope is purely vertically downwards. Similarly, the loss of suction in the region of static shear stress (i.e., beneath the sloping portion of the embankment) also causes macro-voids to collapse, now with a significant down-slope displacement (Take et al. 2004).

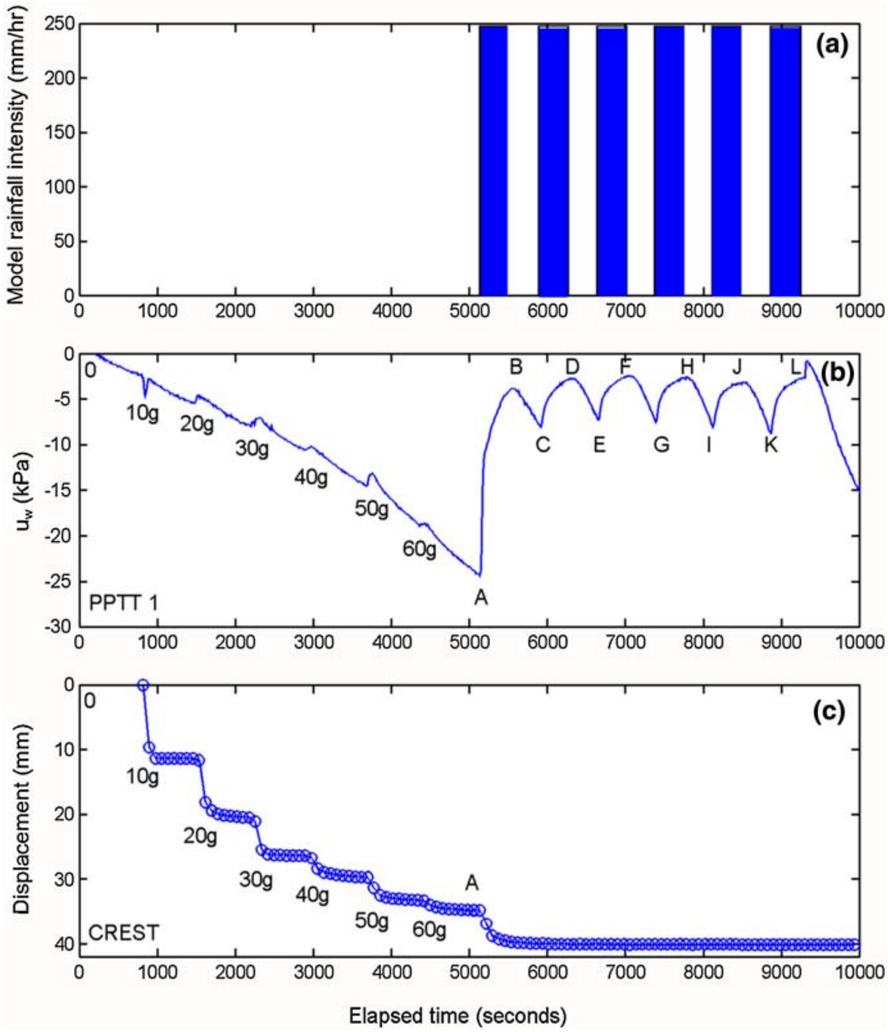

Fig. 14 Observed model responses during the centrifuge test on a loose CDG fill slope (**a**) model rainfall intensity (**b**) pore pressure data (**c**) vertical displacements (Take et al. 2004)

As rainfall infiltration continues, the rate of suction loss decreases, as does the rate of settlement (Take et al. 2004). Further rainfall infiltration results in the development of a water table at the toe of the slope—the prescribed elevation of the overflow control. Above this elevation, the slope is experiencing vertical percolation at roughly zero PWP. By the time the model was subjected to rainfall for an equivalent duration of 1 week (Time B in Fig. 14b), the rate of PWP increase has diminished almost to zero, becoming asymptotic to a small negative value. At this point, the mist nozzles were turned off and the fill slope was allowed to experience gravity drainage for an equivalent period of 1 week.

Despite being subjected to an additional five infiltration events of identical severity, the model slope was observed neither to achieve positive PWPs nor to experience any significant additional deformation.

3.2 Reliable Suction Measurements in Centrifuge

To ensure reliable suction measurements, it is vital to conduct an initial saturation process correctly (Take and Bolton 2003). For high degrees of saturation, filters must first be oven-dried and placed quickly in a vessel containing dry air, and then subjected to very low absolute pressures (i.e., less than 1 kPa). Water under vacuum can then be introduced from a second chamber prior to the vacuum being released. This procedure alone has been shown to be sufficient to saturate a 1-bar air-entry porous stone to achieve reliable suction measurements (Take and Bolton 2003). A finer 3-bar air-entry filter is more difficult to saturate and an additional single over-pressure cycle is required to achieve an ideal response. Poor saturation not only limits the measurable suction but also introduces pressure hysteresis, which can create errors even in positive PWP measurement, and give poor response times (Take and Bolton 2003).

Similarly, Chiu et al. (2005) reported a miniature tensiometer developed to measure suctions smaller than 500 kPa for centrifuge tests. The tensiometer was first saturated by an initial vacuum and subsequently by cycles of pre-pressurisation and cavitation. During the pre-pressurisation, a maximum pressure of 700 kPa was used to avoid damaging the low-pressure range tensiometer. Long-term suction measurement in a compacted unsaturated silt was carried out in the laboratory. It took about 4 h for the tensiometers to reach the target suction (about 110 kPa) and the suction measurements could be maintained for at least 24 h. Six tensiometers were installed at different depths in an unsaturated silt specimen to monitor the suction profile during a centrifuge test. The results showed that the responses of the tensiometers were consistent before cavitation occurred. However, at elevated g conditions, the tensiometer cavitated over a shorter duration and maintained a lower maximum sustainable suction than those observed in the laboratory. Further research is needed to develop devices to measure high suctions beyond 200 kPa reliably and economically (Zhou et al. 2006).

4 Concluding Remarks

In unsaturated soil slope engineering, relationships of rainfall infiltration/water content and soil suction have been monitored and studied extensively in various ground conditions over the last 20 years. Significant progress has been made in understanding of the rainfall infiltration mechanisms governed by the suction stress-state variable. These measured data are extremely useful for numerical modellers to calibrate their hydraulic models in the water content-suction space. However, very limited data are available for engineers and numerical modellers to understand the role played by the second stress-state variable (i.e., net stress) in unsaturated soil slopes during rainfall and to calibrate their predictions in the mechanical space, i.e., displacement-earth pressure space. More field monitoring programmes are encouraged to measure the changes of the two stress-state variables and their influence on the hydraulic as well as mechanical responses during rainfall infiltrations.

The role of site conditions and soil types on the likelihood of obtaining quality data from monitoring experiments has been discussed. Extreme care during the installation phase is essential but challenges still exist in well graded soils, coarser than the key scaling length of the sensors, on steep slopes approaching the critical state angle of friction and at high altitudes where a fourth phase (ice) will form in winter.

Various degrees of success have been achieved in simulating unsaturated soil slopes subjected to rainfall, rising groundwater table and changes of moisture conditions in the geotechnical centrifuge. Miniature devices have been developed to measure negative PWPs down to about −200 kPa, but further research is needed to develop devices to measure suctions greater than 200 kPa, reliably and economically.

References

Adib ME (2000) Slope failure in weathered claystone and siltstone. J Geotech Geoenviron Eng ASCE 126(9):787–797

Alonso EE (1998) Modeling expansive soil behaviour. In: Proceedings of the 2nd international conference on unsaturated soils, vol 2. International Academic Publishers, Beijing, China, pp 37–70

Andersland OB, Ladanyi B (2004) An introduction to frozen ground engineering. Wiley, Hoboken, NJ

Arenson L, Hoelzle M, Springman SM (2002) Borehole deformation measurements and internal structure of some rock glaciers in Switzerland. Permafrost Periglac Process 13(2):117–135

Arenson LU (2003) Unstable Alpine permafrost: a potentially important natural hazard—variations of geotechnical behaviour with time and temperature. Dissertation, ETHZ No. 14801, Switzerland

Arenson LU, Hawkins PG, Springman SM (2003) Pressuremeter tests within an active rock glacier in the Swiss Alps. In: Phillips M, Springman SM, Arenson LU (eds) Proceedings 8th international conference on permafrost, Zürich, Balkema, Lisse, The Netherlands, vol 1, pp 33–38

Arenson LU, Johansen MM, Springman SM (2004) Effects of volumetric ice content and strain rate on shear strength under triaxial conditions for frozen soil samples. Permafrost Periglac Process 15(3):261–271

Arenson LU, Springman SM (2005) Triaxial constant stress and constant strain rate tests on ice-rich permafrost samples. Can Geotech J 42(2):412–430

Arnold A, Thielen A, Springman SM (2005) On the stability of active layers in alpine permafrost. In: Proceedings 11th international conference and field trip on landslides (ICFL), Trondheim, Norway, pp 19–25

Bao CG, Ng CWW (2000) Keynote lecture: some thoughts and studies on the prediction of slope stability in expansive soils. In: Proceedings of 1st Asian conference on unsaturated soils, Singapore, pp 15–31

Barsch D (1996) Rockglaciers: indicators for the present and former geoecology in high mountain environments. Springer, New York

Brand EW (1984) Landslides in south Asia: a state-of-art report. In: Proceedings of 4th international symposium on landslides, Toronto, vol 1, pp 17–59

Chan RKS, Ho KKS (2001) Enhancing slope safety through lessons learnt from landslides. In: Proceedings of 14th Southeast Asian geotechnical conference, Hong Kong, vol 1, pp 709–714

Chiu CF, Cui YJ, Delage P, De Laure E, Haza E (2005) Lessons learnt from suction monitoring during centrifuge modeling. In: Tarantino A, Romero E, Cui YJ (eds) International symposium on advanced experimental unsaturated soil mechanics, Trento, pp 3–8

Deutscher MS, Gasmo JM, Rahardjo H, Leong EC, Tang SK (2000) Field measurements of pore-water pressure profiles in residual soil slopes of the Bukit Timah Granite Formation, Singapore. In: Proceedings of Asian conference on unsaturated soils, Singapore, pp 777–782

Dramis F, Govi M, Guglielmin M, Mortara G (1995) Mountain permafrost and slope instability in the Italian Alps. The Val Pola landslide. Permafrost Periglac Process 6:73–81

Fischer C, López J, Springman SM (2003) Remediation of an eroded steep slope in weathered sandstone after a major rainstorm. In: International conference on landslides, Hong Kong, pp 878–883

Fourie AB (1996) Predicting rainfall-induced slope instability. Proc Inst Civil Eng Geotech Eng 119:211–218

Fredlund DG, Rahardjo H (1993) Soil mechanics for unsaturated soils. Wiley, New York

Friedel S, Thielen A, Springman SM (2006) Investigation of a slope endangered by rainfall-induced landslides using 3D resistivity tomography and geotechnical testing. J Appl Geophys 60(2):100–114

Fukuoka M (1980) Landslides associated with rainfall. Geotech Eng J Southeast Asia Soc Soil Eng 11:1–29

GCO (1988) Guide to rock and soil descriptions. Geoguide 3, 1994 edition. Geotechnical Control Office, Hong Kong

Guan P, Ng CWW, Sun M, Tang WH (2001) Weathering indices for rhyolitic tuff and granite in Hong Kong. Eng Geol 59(1–2):147–159

Haeberli W, Wegmann M, Vonder Mühll D (1997) Slope stability problems related to glacier shrinkage and permafrost degradation in the Alps. Eclo Geol Helv 90: 407–414

Hauck C, Vonder Mühll D (2003) Permafrost monitoring using DC resistivity tomography. In: Phillips M, Springman SM, Arenson LU (eds) Proceedings 8th international conference on permafrost, Zürich, Balkema, Lisse, The Netherlands, vol 1, pp 361–366

Hauck C, Vonder Mühll D, Hoelzle M (2005) Permafrost monitoring in high mountain areas using a coupled geophysical and meteorological approach. In: de Jong C, Ranzi R (eds) Hydrological and meteorological coupling in mountain areas: experiments and modelling. Wiley

Hauck C, Vonder Mühll D, Maurer H (2003) Using DC resistivity tomography to detect and characterise mountain permafrost. Geophys Prospect 51:273–284

Ireson A, Wheater H, Butler A, Finch J, Cooper JD, Wyatt RG, Hewitt EJ (2005) Field monitoring of matric potential and soil water content in the Chalk unsaturated zone. In: Tarantino A, Romero E, Cui YJ (eds) Advanced experimental unsaturated soil mechanics, Trento, pp 511–517

Lim TT, Rahardjo H, Chang MF, Fredlund DG (1996) Effect of rainfall on matrix suctions in residual soil slope. Can Geotech J 33:618–628

Liu TH (1997) Problems of expansive soils in engineering construction. Architecture and Building Press of China (In Chinese)

Machado SL, Botelho MAB, Amparo NS, Dourado TC (2005) The use of the ground penetrating radar, GPR as a non intrusive method to measure soil water content. In: Tarantino A, Romero E, Cui YJ (eds) International symposium, advanced experimental unsaturated soil mechanics, Trento, pp 519–525

Maurer HR, Springman SM, Arenson LU, Musil M, Vonder Mühll D (2003) Characterisation of potentially unstable mountain permafrost—a multidisciplinary approach. In: Phillips M, Springman SM, Arenson LU (eds) Proceedings 8th international conference on permafrost, Zürich, Balkema, Lisse, The Netherlands, vol 2, pp 741–746

Mofiz SA, Sarkar DC, Sobhan MA., Rahman MM, Awall MR, Taha MR, Hossain MK (2005) Instrumentation and matric soil suction measurement in a decomposed granite soil slope. In: Tarantino A, Romero E, Cui YJ (eds) International symposium, advanced experimental unsaturated soil mechanics, Trento, pp 527–532

Musil M, Maurer H, Green AG, Horstmeyer H, Nitsche FO, Vonder Mühll D, Springman SM (2002) Case history: shallow seismic surveying of an Alpine rock glacier. Geophysics 67(6):1701–1710

Ng CWW (1992) An evaluation of soil-structure interaction associated with a multi-propped deep excavation. PhD thesis, University of Bristol, UK

Ng CWW (2005) Invited country report: “Failure mechanisms and stabilisation of loose fill slopes in Hong Kong”. In: Proceedings of international seminar on slope disasters in geomorphological/geotechnical engineering, Osaka, 10 September, pp 71–84

Ng CWW, Guan P, Shang YJ (2001a) Weathering mechanisms and indices of igneous rocks of Hong Kong. Q J Eng Geol Hydrol 34(2):133–151

Ng CWW, Wang B, Tung YK (2001b) 3D numerical investigations of groundwater responses in an unsaturated slope subjected to various rainfall patterns. Can Geotech J 38(5):1049–1062

Ng CWW, Van Laak P, Tang WH, Li XS, Zhang LM (2001c) The Hong Kong geotechnical centrifuge. In: Proceedings of the 3rd international conference soft soil engineering, Hong Kong, pp 225–230

Ng CWW, Menzies B (2007) Advanced unsaturated soil mechanics and engineering. Taylor & Francis, 687 p, ISBN: 978-0-415-43679-3

Ng CWW, Zhan LT (2007) Comparative study of rainfall infiltration into a bare and a grassed unsaturated expansive soil slope. Soil Found 47(2):207–217

Ng CWW, Zhang M, Shi XG (2002) An investigation into the use of soil nails in loose fill slopes. Invited keynote paper (In Chinese). In: Proceedings of the first Chinese symposium on geoenvironment and geosynthetics, Hangzhou, Zhejiang, China, pp 61–80

Ng CWW, Zhan LT, Bao CG, Fredlund DG, Gong BW (2003) Performance of an unsaturated expansive soil slope subjected to artificial rainfall infiltration. Géotechnique 53(2):143–157

Premchitt J, Brand EW, Phillipson HB (1986) Landslides caused by rapid groundwater changes. Groundwater in Engineering Geology, in Proceedings of 21st Annual conference engineering group of geological society, London, pp 87–94

Premchitt J, Lam TSK, Shen JM, Lam HF (1992) Rainstorm runoff on slopes. GEO Report No. 12, Civil Engineering Department, Hong Kong

Proclim (2000) Climate Press Nr. 8, May. www.proclim.ch

Rahardjo H, Lee TT, Leong EC, Rezaur RB (2005) Response of a residual soil slope to rainfall. Can Geotech J 42: 340–351

Rahardjo H, Leong EC, Gasmo JM, Deutscher MS (1998) Rainfall-induced slope failures in Singapore: investigation and repairs. In: Proceedings of 13th Southeast Asian conference, vol 1, pp 147–152

Schaer C, Davies T, Frei C, Wanner H, Widmann M, Wild M, Davies HC (1998) Current Alpine climate. In: Cebon P, Dahinden U, Davies HC, Imboden D, Jaeger C (eds) A view from the Alps: regional perspectives on climate change, chapter 2. MIT, Boston

Springman SM, Jommi C, Teysseire P (2003) Instabilities on moraine slopes induced by loss of suction: a case history. Géotechnique 53(1):3–10

Springman SM, Teysseire P (2001) Artificially induced rainfall instabilities on moraine slopes. In: Kühne M et al (eds) Proceedings of the international conference on landslides, Davos, VGE, Essen, pp 209–223

Sun HW, Law WHY, Ng CWW, Tung YK, Liu JK (2000) The 2nd July 1997 Lai Ping Road Landslide, Hong Kong—hydrogeological characterisation. In: Proceedings of the 8th international symposium on landslides, Cardiff, vol. 3, pp 1431–1436

Sweeney DJ (1982) Some in situ soil suction measurements in Hong Kong residual soil slopes. In: Proceedings of the 7th Southeast Asian Geot. conference, Hong Kong, pp 91–106

Take WA, Bolton MD (2003) Tensiometer saturation and the reliable measurement of soil suction. Géotechnique 53(2):159–172

Take WA, Bolton MD, Wong PCP, Yeung FJ (2004) Evaluation of landslide triggering mechanisms in model fill slopes. Landslides 1:173–184

Teysseire P, Cortona L, Springman SM (2000) Water retention in a steep moraine slope during periods of heavy rain. In: Rahardjo H, Toll D, Leong C (eds) Proceedings of unsaturated soils for Asia, Singapore, Balkema, Rotterdam, pp 831–836

Thielen A, Friedel S, Plötze M, Springman SM (2005) Combined approach for site investigation in terms of the analysis of rainfall induced landslides. In: 16th International conference on soil mechanics and geotechnical engineering, Osaka, Japan, pp 2591–2594

Thielen A, Springman SM (2005) First results of a monitoring experiment for the analysis of rainfall induced landslides. In: Tarantino A, Romero E, Cui YJ (eds) International symposium on advanced experimental unsaturated soil mechanics—EXPERUS 2005, Trento, pp 549–554

Vonder Mühll DS, Arenson LU, Springman SM (2003) Temperature conditions in two Alpine rock glaciers. In: Phillips M, Springman SM, Arenson LU (eds) Proceedings 8th international conference on permafrost, Zürich, Balkema, Lisse, The Netherlands, vol 2, pp 1195–1200

Vonder Mühll D, Haeberli W, Klingele E (1996) Geophysikalische Untersuchungen zur Struktur und Stabilität eines Moränendammes am Grubengletscher (Wallis). Interpraevent 123–132

Wang Z, Gong BW, Bao CG (2000) The measurement of matric suction in slopes of unsaturated soil. In: Rahardjo H, Toll D,Leong C (eds) Proceedings of the Asian conference on unsaturated soils, Singapore, Balkema, Rotterdam, pp 843–846

White DJ, Take WW, Bolton MD (2003) Soil deformation measurement using particle image velocimetry (PIV) and photogrammetry. Géotechnique 53:619–631

Wolle CM, Hachich W (1989) Rain-induced landslides in south-eastern Brazil. In: Proceedings of 12th international conference soil mechanics and foundation engineering, Rio de Janeiro, vol 3, pp 1639–1644

Yagi N, Yatabe R, Yokota K, Bhandary NP (2000) Suction measurement for prediction of slope failure due to rainfall. In: Rahardjo H, Toll D, Leong C (eds) Proceedings of the Asian conference on unsaturated soils, Singapore, Balkema, Rotterdam, pp 847–851

Zhan LT (2003) Field and laboratory study of an unsaturated expansive soil associated with rain-induced slope instability. PhD Thesis, The Hong Kong University of Science and Technology, Hong Kong. China

Zhan LT, Ng CWW, Fredlund DG (2006). Instrumentation of an unsaturated expansive soil slope. Geotech Test J 30(2):1–11

Zhou ZB, Ng CWW (2004) Centrifuge modelling of a densely recompacted unreinforced CDG fill slope. Interim Factual Testing Report VIII-CG65_30, Hong Kong University of Science and Technology

Zhou RZB, Take A, Ng CWW (2006) A case study in tensiometer interpretation: centrifuge modelling of unsaturated slope behaviour. In: Proceedings of 4th international conference on unsaturated soils, April, Arizona, vol 2, pp 2300–2311

Monitoring Large-Scale Tests for Nuclear Waste Disposal

Eduardo E. Alonso · Sarah M. Springman · Charles W. W. Ng

Originally published in the journal *Geotechnical and Geological Engineering*, Volume 26, No. 6, 817–826.
DOI: 10.1007/s10706-008-9195-2

Abstract Two large-scale "in situ" demonstration experiments and their instrumentation are described. The first test (FEBEX Experiment) involves the hydration of a compacted bentonite barrier under the combined effect of an inner source of heat and an outer water flow from the confining saturated granite rock. In the second case, the progressive de-saturation of Opalinus clay induced by maintained ventilation of an unlined tunnel is analyzed. The paper shows the performance of different sensors (capacitive cells, psychrometers, TDR's) and a comparison of fill behaviour with modelling results. The long term performance of some instruments could also be evaluated specially in the case of FEBEX test. Capacitive sensors provide relative humidity data during long transient periods characterised by very large variations of suction within the bentonite.

E. E. Alonso (✉)
Department of Geotechnical Engineering and Geosciences, Universitat Politècnica de Catalunya, c/ Gran Capitán s/n, Módulo D-2, Barcelona 08034, Spain
e-mail: eduardo.alonso@upc.edu

S. M. Springman
Institute for Geotechnical Engineering, Swiss Federal Institute of Technology (ETHZ), Zurich, Switzerland

C. W. W. Ng
Hong Kong University of Science and Technology, Clear Water Bay, Kowloon, Hong Kong

Keywords Field record · Case history · Bentonite · Suction · Relative humidity · Capacitive sensor · TDR sensor · Psychrometer · Modelling · Reliability

1 Introduction

Theoretical and experimental research in recent years has contributed to an improved understanding of unsaturated soil behaviour. However, few comprehensive field records have been published. Ideally, a good case history requires a complete description of field conditions, a proper programme of laboratory (and field) tests combined with interpretation of the results, an analysis using acceptable tools for representation of unsaturated soil performance, measurement of field performance in terms of two stress state variables (i.e., suction and net stress) and a comparison of estimated and actual field data. This paper is focused on the measurement of field performance for two case histories associated with the behaviour of impervious barriers for nuclear waste disposal applications. Despite the specific nature of the tests, they may be useful for a wider range of circumstances because monitoring has been carried out with standard sensors that may find applicability in other environments dealing with unsaturated soils.

A distinctive feature of an unsaturated soil, if compared with a saturated soil, is the energy state of the water in voids. Different "measures" of this state are available, from a relatively simple determination of water content to the more complex determinations of negative pore water pressures and suction or Relative Humidity.

Two recent large-scale and highly instrumented demonstration experiments of nuclear waste isolation are presented. In these applications, long term performance and reliability of instruments are of specific concern. Data is offered in this regard, as well as a discussion of the value of different instruments, to provide consistent information for advanced modelling.

The paper provides the instrument layout, time records of some relevant variables (mainly those associated with soil suction) and an interpretation of the recorded field behaviour, assisted by appropriate modelling of each of the cases presented.

Successful field monitoring requires effective calibration and subsequent installation of the sensors as well as robustness in terms of all elements from the instrument itself through the acquisition and storage of data. Some challenges presented in this regard by a range of environmental conditions will be discussed.

2 Hydration of Compacted Bentonite Barriers

2.1 Background

A widely accepted design concept for nuclear waste disposal in a geological formation is to isolate the nuclear canister inside a ring of highly impervious plastic clay. This barrier reduces the likelihood of migration of radio nuclides to the geological or "distant field" environment. A few large-scale demonstration tests have been designed and built in the past two decades in underground laboratories excavated in granite and clay rock formations. Relevant large-scale tests related to high level nuclear waste disposal include the Prototype Repository, Backfill and Plug and Temperature Buffer Experiments (Sandén et al. 2005), performed in the Äspö rock underground laboratory in Sweden (granite), the "Febex" test at the Grimsel test site (GTS) in the Swiss Alps (granite) (Huertas et al. 2000; Alonso et al. 2005), and the "Engineered Barrier" (EB) test in the Mont-Terri underground laboratory in the Jura, Switzerland (clay shale). Some designs for the disposal of low to medium level waste also include engineered clay-based barriers and a recent large-scale demonstration test includes the "Gas Migration Test" (GMT), that has just been dismantled at the GTS.

An additional purpose of all the tests mentioned is to gain information about the barrier performance during the transient hydration phase, by monitoring a number of variables (water content, relative humidity, stresses and displacements, temperature, etc.) linked to the physical phenomena taking place during barrier saturation. Hundreds of sensors have been installed in different locations and they are monitored during extended periods of time (typically more than 1 or 2 years). Recorded data offer an excellent opportunity to verify current models for the prediction of barrier performance within detailed modelling exercises (Ledesma and Chen 2005; Thomas et al. 2005; Fälth et al. 2005; Alonso et al. 2005). They, in turn, contribute to the declared objective of understanding the physical phenomena taking place in the barrier.

The final stage of the large-scale demonstration tests is a dismantling operation. Samples from the barrier are recovered and tested in the laboratory. Furthermore, sensors may be recovered and recalibrated, in order to gain experience about their long-term performance and reliability.

These expensive tests offer a unique opportunity to examine the behaviour of a large variety of devices and, in particular, monitoring devices for soil suction or related variables (water content, relative humidity). In fact, the clay barrier is initially unsaturated, since it is made of highly compacted bentonite blocks (or pellets in one of the experiments mentioned).

Bentonite blocks reach, in practice, dry unit weights of 1.65−1.71 kN/m^3 and initial degrees of saturation close to $S_{\mathrm{ro}} = 0.5-0.6$. When saturated, they may develop swelling pressures in excess of 5 MPa. The swelling pressure helps to maintain the tightness of fit and continuity of the barrier. Once placed around the simulated canister (a cylindrical heater), the barrier (Fig. 1) is subjected to a heat inflow through its inner boundary in contact with the dummy canister and to a water inflow coming from the host rock, usually saturated. It is therefore expected that the outer periphery of the barrier will experience a saturation process, whereas the inner boundary will be dried. The barrier evolution depends critically on the inner and outer boundary conditions. Given the decay of heat supplied by the real canisters

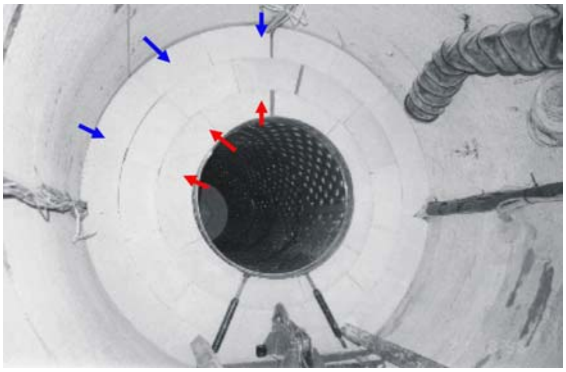

Fig. 1 Scheme showing the compacted clay barrier and the heat (arrows pointing outwards) and water flows, that take place during the initial transient period

and the constant water pressure imposed by the host rock, it is expected that full barrier saturation will eventually be achieved. However, in none of the demonstration tests mentioned, was the barrier fully saturated at the end of the testing period. Therefore, most of the experiments provided useful data on the transient initial period, where the heat and water fluxes compete to de-saturate and saturate the barrier in a relatively complex manner.

One of the tests mentioned (Febex) has been selected in order to discuss a number of relevant issues related to the performance of the test and the behaviour of sensors. Data is also available from the dismantling and subsequent testing, and this provides added value from this particular test. Additional data on sensor reliability for several large-scale tests performed in the Swedish Äspö Laboratory is provided by Sandén et al. (2005).

2.2 The Febex Large-Scale Test: Instrument Layout and Long-Term Behaviour

The Febex test is a near to full-scale simulation of a high-level waste disposal facility. The testing area was located at the end of a 2.28 m Ø tunnel, excavated in granite using a Tunnel Boring Machine. Two electrical heaters, whose dimensions and weight are equivalent to a nuclear canister, were centrally placed in the drift; the space left between the rock surface and the heaters being filled with blocks of compacted bentonite (Fig. 2). A concrete plug isolated the 17.2 m long testing area from the access tunnel.

Statically compacted blocks (w = 14.4%; γ_d = 16.9 kN/m^3) of crushed bentonite rock were arranged in annular rings, as shown in Fig. 1. Six hundred and thirty two sensors of different types were installed and arranged in cross sections, shown also in Fig. 2.

In Section C, not directly affected by the heaters, sensors measuring relative humidity (capacitive "WC" sensors), total suction (psychrometer probes: "WP"), volumetric water content (TDR sensors: "WT") and pore pressure sensors ("Q") were placed as shown in Fig. 3. In sections directly affected by heaters (such as F1 or F2, see Fig. 2), relative humidity sensors were located at three radial distances: near the heater (r = 0.52 m), at a mid position (r = 0.82 m) inside the bentonite barrier and close to the granite boundary (r = 1.07 m).

Heating started on February 27th, 1997, which is day "0" of the time-scale of the history plots given here. Power was increased until a maximum temperature of 100°C was reached at the hottest point of the heater-bentonite interface. Data for 5 years of operation is available.

The experiment has been extensively modelled with the help of the finite element computer code CODE_BRIGHT (DIT-UPC 2002; Olivella et al. 1994, 1996). An extensive experimental data base on the properties of the compacted bentonite (Villar et al. 2005; Lloret et al. 2003) helped to define model parameters. The calculations shown in the comparison plots given here integrate all the experimental information available at the beginning of year 2004.

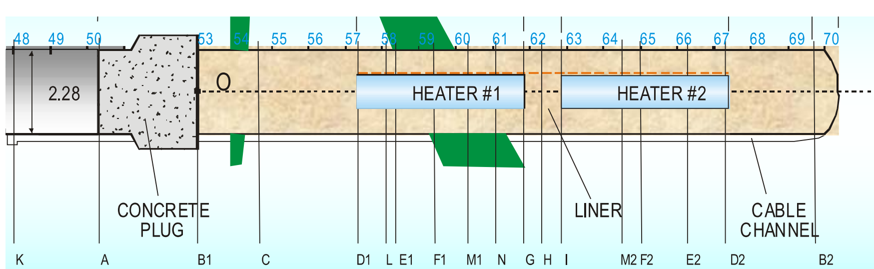

Fig. 2 Position of instrumented sections of the Febex experiment, dimensions in metres

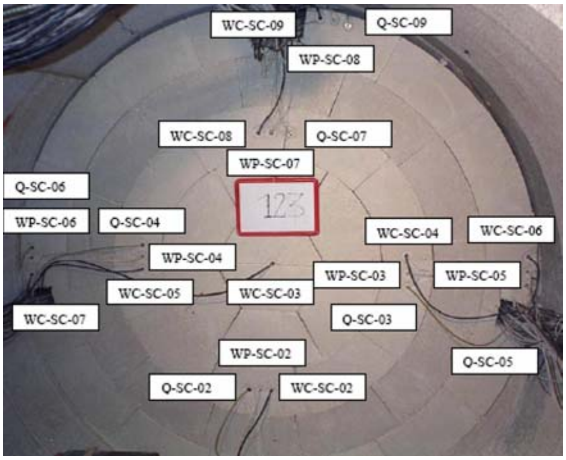

Fig. 3 Location and type of sensors for water content monitoring in section C of the Febex in situ test (García-Siñeriz et al. 2004)

Figure 4 shows a comparison between the calculated evolution of relative humidity and the values registered by a number of capacitive sensors, located in different radial directions in the central cross section of the experiment (Section H; see Fig. 2). The outer sensors (r = 1.07 m) start at a high relative humidity and they reach full saturation soon. Capacitive sensors lose their accuracy when they become saturated, however. Capacitive measurements in

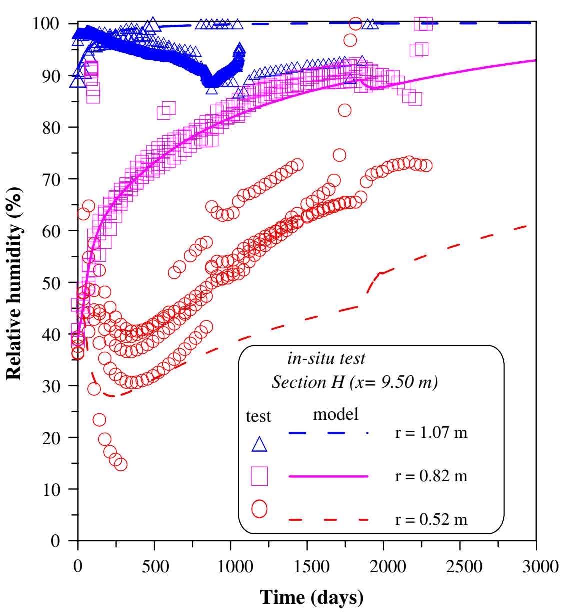

Fig. 4 Measured and calculated relative humidity in section H of the clay barrier

points at a mid position (r = 0.82 m) within the barrier are remarkably well-reproduced by the model. This mid zone experiences continuous wetting. When the heaters are switched on, points close to the heater (r = 0.52 m) experience a wetting-drying cycle first. The first wetting event is due to the condensation of a migrating flow of hot vapour from a bentonite ring, adjacent to the heater. As the drying conditions expand, sensors record a drop in relative humidity and, at later dates, a slow increase in water content as the humidity coming from the granite boundary is entering the inner most part of the bentonite barrier. It appears that the wetting process of these inner points is faster than model predictions. A comprehensive evaluation of Febex barrier performance and the ability of a number of thermo-hydro-mechanical computer models to reproduce the observed behaviour may be found in Sánchez (2004) and Alonso et al. (2005).

2.3 Instrument Performance

A high density compacted bentonite barrier is a very aggressive environment for sensors. In fact, the medium has a high saline content due to the high Cation Exchange Capacity of the clay, swelling stresses are high (5–7 MPa), and there are the added effects of temperature and suction changes during the lifetime of the experiment. Of particular interest for unsaturated soil applications are the sensors for relative humidity and water content changes. Their performance in the Febex test will be reviewed here.

Half of the Febex test (the part of the buffer associated with the heater closer to the concrete plug) was dismantled during the summer of 2002, after a cooling period. The concrete plug was demolished and the rings of bentonite blocks were carefully removed. Specimens were taken for laboratory testing, and this allowed the bentonite state variables to be checked directly (mainly dry density and water content), as well as the hydro-mechanical and chemical properties. Sensors were also recovered and some of them could be calibrated. As a result, some variables recorded by the sensors could be compared with the actual values, determined from the recovered specimens. The calibration of sensors was also used to correct some of the available 5-year records of buffer properties. Most of the sensors had been in operation for a time well beyond the nominal operational lifetime, as defined by manufacturers. The total number of sensors placed in the buffer and the failure rate, determined after dismantling is shown in Table 1.

Pressure effects, corrosion and bentonite invasion of some cables was generally observed. The ceramic filters of psychrometers were often found to be broken or separated from the sensor. Cable cuts were found often at the junction between the sensor and the cable.

The capacitive sensors behaved better than expected, especially since their expected operative lifetime is 1 year. Full saturation (which was achieved in the outer ring of the buffer) was a likely cause of the malfunctioning of some of the capacitive sensors. The failure rate was also high for sensors located in the vicinity of the heater. The calibration of some of the retrieved sensors (Fig. 5) shows that the response is systematically below the expected relative humidity value. However, in most cases, the error is small. It should be added that capacitive sensors provided the most consistent and useful set of data during the evolution of the bentonite barrier from an 'as-constructed' to a later stage after a few years of operation. This is due to the wide range of suctions being measured. In fact, the initial saturation state of the barrier (50% relative humidity) was low and full saturation was expected in the outer part of the barrier. In addition, the relative humidity decreased strongly in a ring around the heater, during a transient stage immediately after the beginning of heating. These processes were captured accurately by the capacitive sensors.

In contrast, psychrometers were only operative for a narrow range of relative humidity close to saturation (>95% relative humidity). Their value in monitoring the performance of the barrier was, therefore, quite limited. They proved also to be quite fragile in the demanding environment created by the swelling barrier. It was estimated that half of the sensors failed because of mechanical effects of the measuring head, and the other half, as a result of full saturation. Only four sensors could be calibrated (against solutions at prescribed relative humidities), and none of them behaved satisfactorily. It is believed that better mechanical protection of the psychrometer's head could improve their reliability substantially.

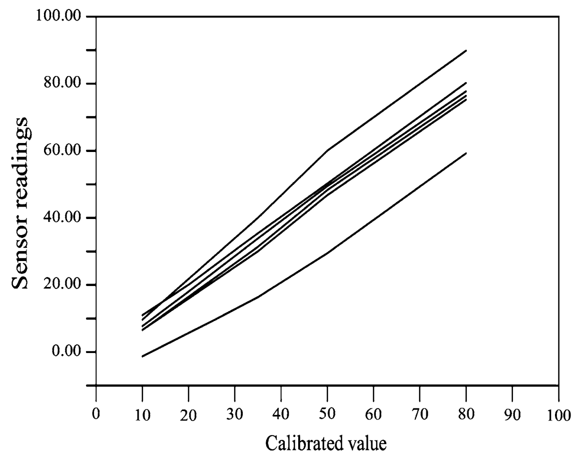

Fig. 5 Calibration of humidity sensors once retrieved after 5 years of operation

TDRs exhibited the highest failure rate. They were affected by mechanical deformations (both, the sensor and the connecting cables). Some systematic errors of the water content measured during the test operation were detected. A correction was made after calibrating some of the surviving probes.

There was an interest also in comparing sensor data with the direct determination of bentonite properties on samples recovered during the dismantling operations. The number of samples retrieved provided an accurate description of water content and dry density distributions, at the end of the 5 years of simultaneous heating and wetting. An example is given in Fig. 6, which provides the radial change in

Table 1 Capacitive sensors, psychrometers and TDR sensors in Febex bentonite buffer. (Data from García-Siñeriz et al. 2004)

Type of sensor	Manufacturer	Model	Total number	Sensors out of order before dismantling	Failure rate after 5 years of operation (%)
Capacitive (relative humidity)	Vaisala	HMP233	27	16	60
Psychrometers (total suction)	Wescor	PCT-55	24	17	70
TDR (volumetric water content)	Edi Meier + Partner AG	–	10	8	80

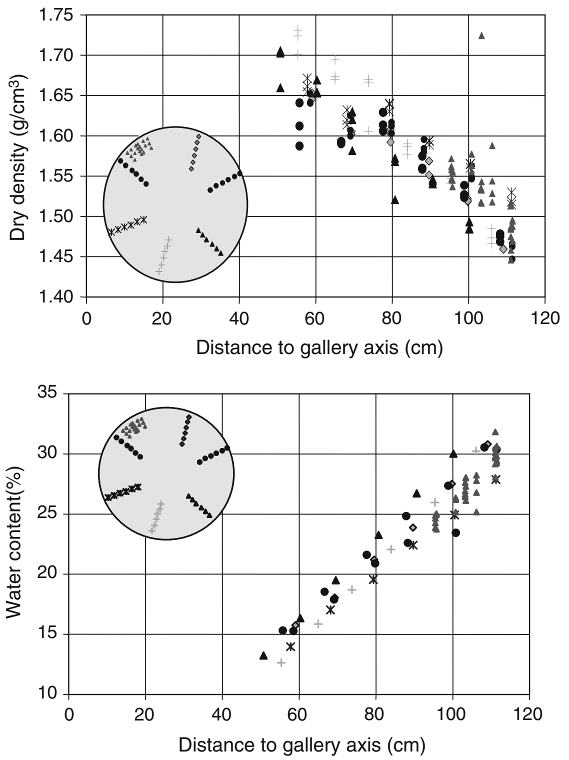

Fig. 6 Water content and dry density distribution determined in specimens recovered from a section (Sect. 22) directly affected by Heater n° 1. (Villar et al. 2005)

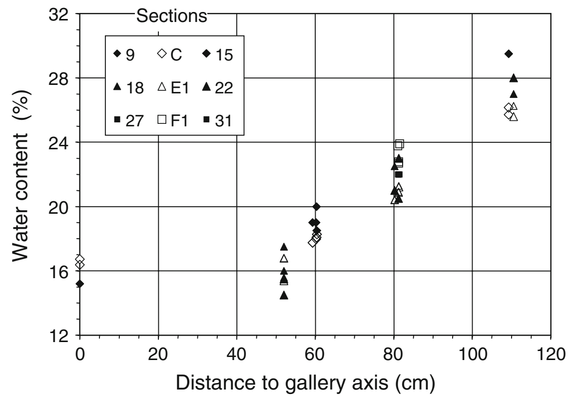

Fig. 7 Water content measured in samples retrieved (9, 15, 18, 22, 27 and 31) and values derived from capacitive sensor data (marked as C, E1 and F1). (Villar et al. 2005)

water content and dry density in a cross section, directly affected by Heater n° 1 (Villar et al. 2005). Strong gradients in water content and dry density are observed across a relatively thin bentonite barrier. It is clear that the barrier became a heterogeneous material after a few years of heating and outer wetting.

In order to compare capacitive sensor data with laboratory determinations of water content, the measured relative humidity was first converted into suction through Kelvin's law. Then, the water retention curve of the bentonite was determined for samples compacted at different dry densities and for different temperatures.

A comparison of the water contents, derived from capacitive sensor data through the water retention curve and direct determinations, is given in Fig. 7. The sensor data corresponds to the final reading before dismantling the sensors. The agreement is good, in general terms, and this result provides confidence to the sensor data (capacitive instruments in this case).

2.4 Some Conclusions

The Febex "in situ" test is a heavily instrumented test (more than 600 sensors have monitored the bentonite clay buffer and the immediate rock). Of particular interest for the purpose of this paper are the sensors for relative humidity or water content changes, located in the buffer. Three types of instruments have been used: capacitive sensors, psychrometers and TDR's. Among them, the capacitive sensors proved to be esspecially useful and reliable. Their extended measuring range, which covers, in practice, all the range of expected relative humidities, provided the best data for modelling purposes. Most of the sensors have been in operation for extended periods of time (several years), a time interval well beyond the expected lifetime of these instruments. The re-calibration of some of the capacitive sensors, recovered after dismantling part of the experiment, generally showed an accurate response. A comparison of water contents derived from relative humidity measurements and a direct determination of water content in specimens taken from the partially hydrated bentonite buffer was satisfactory.

The set of psychrometers and TDRs had a more limited value. Both had a higher failure rate than the capacitive sensors. The psychrometers used had the fundamental limitation of not providing readings for relative humidity values lower than 95%. They also experienced breakage problems, attributed to deformations of the bentonite. TDRs provide data on volumetric water content. However, they were found to deliver unreliable data in this experiment.

3 Tunnelling in Argillaceous Rock

3.1 A Ventilation Experiment (VE) in Opalinus Clay

"Opalinus clay" is a marine Jurassic clay shale with a high proportion (40–80%) of clay minerals. Other constituents are quartz (sand and silt particles), calcite and pyrite, among others. The "in situ" water content is low (4–8%). From a geotechnical perspective, it may be described as anisotropic stiff overconsolidated low plasticity clay. Clay structure is dominated by the bedding planes, which dip 45° in the Mont Terri Laboratory area. As for many other soft clayey rocks, Opalinus clay loses its strength rapidly as the water content increases (Martin and Lanyon 2003).

Opalinus clay is a highly impervious material ($k = 2 \times 10^{-13}$ m/s for undeformed rock). The pore water is of marine origin (dissolved solids amount to 20 g/l). When subjected to cycles of desiccation and wetting, it experiences significant shrinkage and swelling. Figure 8 shows the vertical stress recorded as a swelling pressure in a confined specimen of Opalinus clay during the application of a wetting–drying–wetting cycle (w = 7%–9%–2%–9%) in a suction controlled oedometer cell. The clay develops swelling pressures close to 1.8 MPa when suction is reduced to low values. Note also the elastic character of the response and the parallel change in water content during suction changes.

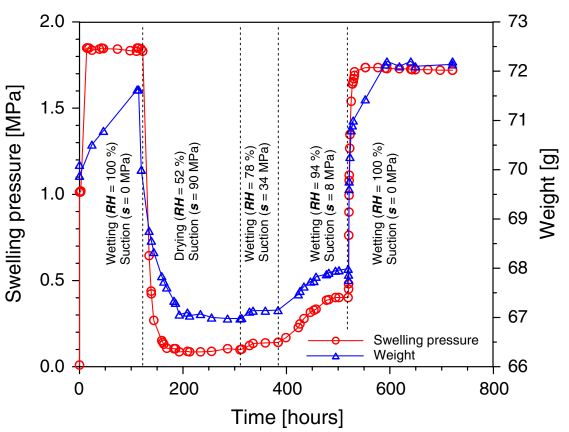

Fig. 8 Recorded vertical stresses and weight of a specimen of Opalinus clay subjected to a cycle of wetting-drying-wetting in a confined suction controlled oedometer cell

Two effects contribute to the degradation of the Opalinus clay, when tunnels are excavated: the stress release and the new environment applied to the exposed surface of the claystone. The second effect is of importance in soft clayey rock (Olivier 1979).

A novel experiment was built in Mont Terri (The Ventilation Experiment, "VE"; Mayor et al. 2005) to investigate the changes in suction of the Mont-Terri clay, when an excavated tunnel was subjected to changes in the ambient relative humidity. The experiment was performed in a 1.3 m diameter unlined horizontal tunnel. A 10 m long section of the tunnel was isolated by two double doors. Then, prolonged ventilation (8 months) induced a de-saturation, followed by a 3 month period of re-saturation. The estimated relative humidity in the test section, prior to the beginning of the experiment, was 90–95%. The relative humidity was decreased in steps, during the ventilation period, and it was maintained at 15% for 5 months. During re-saturation, an atmosphere of relative humidity of 95% was kept constant for 3 months. Flow rates and hygrometers installed at the inflow and outflow pipes provided data to perform global balance calculations.

3.2 Field Instrumentation and Results

Humidity sensors were located at different radial positions and varying depths inside the rock formation. Figure 9 provides profiles of de-saturation. De-saturation was performed during phases 4, 5 and 6 of the experiment. At the beginning of phase 4, the rock was almost fully saturated. At the end of the de-saturation period (end of phase 6), a 30 cm thick annular ring reached a relative humidity below 95%

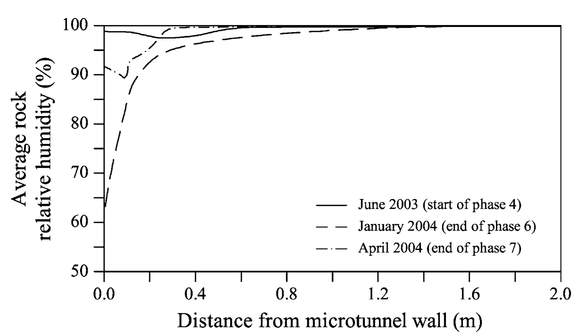

Fig. 9 Evolution of relative humidity of the clay rock around the ventilation tunnel during the ventilation and re-saturation phases (Velasco and Pedraza 2004)

(Velasco and Pedraza 2004). In the close vicinity of the tunnel wall, a minimum value of relative humidity of 62% was recorded. At the end of the re- saturation period (end of phase 7), the 30 cm thick ring around the wall had recovered relative humidity values in excess of 90%. A sensor located very close to the surface (2 cm inside the rock) registered the evolution of relative humidity shown in Fig. 10.

It is interesting to realise that the relative humidity in the rock, very close to the tunnel atmosphere is very high, compared with the imposed value (relative humidity: 15%), for a long time during the ventilation stage. The relative humidity recovery rate (Fig. 10) during re-saturation is faster than the drying rate.

Moderate positive pore water pressures were recorded at a distance of 2 m inside the rock at the beginning of the de-saturation period. They decreased steadily during the ventilation stage and reached a minimum average value of 0.1 MPa (absolute value).

The VE experiment has been simulated using the finite element program CODE_BRIGHT. The main emphasis in the modelling performed was an accurate description of the relative humidity changes in the rock, as well as the global balance of humidity interchange at the scale of the tunnel. Details of this work may be found in Velasco and Pedraza (2004). The model meets some difficulties in capturing the decaying flow rates (Fig. 11) during the constant relative humidity phases, although the global experiment is well represented, especially the recovery during the re-saturation phase.

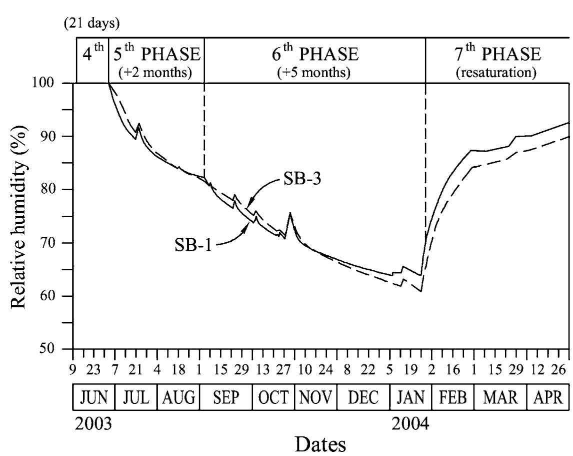

Fig. 10 Drying and wetting cycle applied to the surface of the ventilation experiment (Velasco and Pedraza 2004)

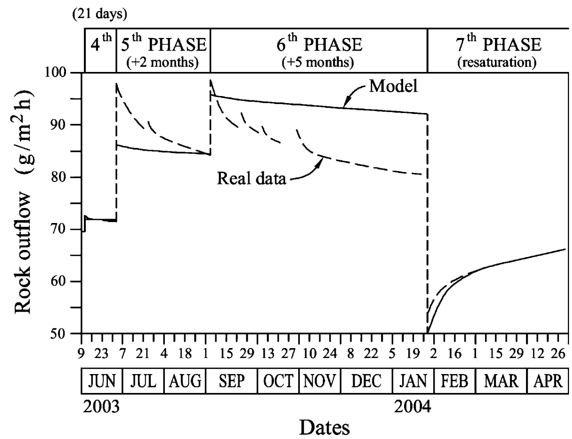

Fig. 11 Calculated and measured inflow and outflow rates in the tunnel, during the ventilation experiment (Velasco and Pedraza 2004)

3.3 Some Conclusions

The VE experiment has provided precise information of the expected de-saturation phenomena associated with tunnel construction and operation (in the absence of any lining). Capacitive sensors provided good data on the rock behaviour in a relatively thin annulus (~2 m) around the tunnel. Piezometers located in deeper positions also helped to establish the limit of the de-saturation effect in this case. The estimation of the overall humidity interchanges (always in the vapour phase) at the tunnel scale was also necessary to derive estimations of the "turbulent coefficient" parameter, which is always difficult to approximate.

It was found that a relatively large period of de-saturation (5 months) led to a limited de-saturation of the impervious Opalinus clay formation. Strong suction gradients developed near the tunnel wall, but the minimum relative humidity recorded (61%) in a shallow sensor (2 cm in depth) was still much higher than the imposed relative humidity in the tunnel atmosphere (16% during 5 months). It was also found that permeability determinations at the scale of small specimens were only slightly lower than the permeability derived from back analysis of the test.

4 Concluding Remarks

Compacted bentonite buffers, proposed for deep underground nuclear waste isolation schemes, have, at the time of installation, a low degree of saturation (around 50%). They become progressively saturated during a long transient period in which major changes take place in the barrier because of the high swelling pressures developed by the bentonite. Sensors capable of recording this process should have an extended range for reliable suction (or relative humidity) measurement. In addition, monitoring should be carried out for relatively long periods (years) to get a reliable view of the transient wetting process. The compacted bentonite environment is also demanding for the sensors because of the high pressures developed in the highly confined buffer and the high salinity of the interstitial water. The performance of several sensors (TDR's, capacitive sensors and psychrometers) has been evaluated in a real scale experiment simulating repository conditions. It was found that capacitive sensors performed very satisfactorily under these circumstances and that the re-calibration of some surviving instruments after 5 years of operation was similar to the original relationship. Direct determinations of the barrier water content, after dismantling, were also compared with indirect calculations based on the recorded Relative Humidity and the water retention relationship determined in laboratory for wetting paths. The comparison was satisfactory and it provides an added reliability to the RH "in situ" measurements. Psychrometers and TDR's did not perform as well, although Sandén et al. (2005) report a more positive experience in a similar case.

A second case presented involved the monitoring of the progressive de-saturation of the walls of a tunnel excavated in a highly impervious rock, induced by forced ventilation. Capacitive sensors also provided an accurate description of the depth of the unsaturated annulus of rock around the tunnel wall here. Piezometers helped to establish the unsaturated-saturated boundary. It was found that a large finite jump in RH seemed to exist at the air-rock interphase. A hydro-mechanical numerical model of this case helped to derive the rock hydraulic and interphase (evaporation) parameters, which are always difficult to establish.

References

Alonso EE, Alcoverro J, Coste F, Malinsky L, Merrien-Soukatchoff V, Kadiri I, Nowak T, Shao H, Nguyen TS, Selvadurai APS, Armand G, Sobolik SR, Itamura M, Stone CM, Webb SW, Rejeb A, Tijani M, Maouche Z, Kobayashi A, Kurikami H, Ito A, Sugita Y, Chijimatsu M, Borgesson L, Hernelind J, Rutqvist J, Tsang C-F, Jussila P (2005) The FEBEX benchmark test: case definition and comparison of modelling approaches. Int J Rock Mech Min Sci 42:611–638

DIT-UPC (2002) CODE_BRIGHT. A 3-D program for thermo-hydro-mechanical analysis in geological media. USER'S GUIDE. Centro Internacional de Métodos Numéricos en Ingeniería (CIMNE), Barcelona

Fälth B, Börgesson L, Hökmark H, Hernelind J (2005) THM predictive modelling of the Temperature Buffer Test- clay technology's contribution. In: Alonso EE, Ledesma A (eds) Advances in understanding engineered clay barriers. Balkema, Rotterdam, pp 461–482

García-Siñeriz JL, Bárcena I, Fernández PA, Sanz FJ (2004) Instrument analysis report. Project deliverable D14, Aitemin internal report, Madrid. Project NO.70-AIT-L-6-9, 79 pp.

Huertas F, Fuentes-Cantillana JL, Jullien F, Rivas P, Linares J, Fariña P, Ghoreychi M, Jockwer N, Kickmaier W, Martinet MA, Samper J, Alonso EE, Elorza FS (2000) Full scale engineered barriers experiment for a high-level radioactive waste in crystalline host rock (FEBEX Project). Final Report, European Commission, Report n° EUR 19147 EN

Ledesma A, Chen GJ (2005) T-H-M modelling of the prototype repository experiment: comparison with current measurements. In: Alonso EE, Ledesma A (eds) Advances in understanding engineered clay barriers. Balkema, Rotterdam, pp 337–346

Lloret A, Villar MV, Sánchez M, Gens A, Pintado X, Alonso EE (2003) Mechanical behavior of heavily compacted bentonite under high suction changes. Géotechnique 53(1):27–40

Martin CD, Lanyon GW (2003) Measurement of in-situ stress in weak rocks at Mont Terri Rock Laboratory, Switzerland. Int J Rock Mech Min Sci 40:1077–1088

Mayor JC, García-Siñeriz JL, Velasco M, Gómez-Hernández J, Lloret A, Matray JM, Coste F, Giraud A, Rothfuchs T, Marschall P, Rösli U, Mayer G (2005) Ventilation experiment in Opalinus clay for the management of radioactive waste. Technical Publication 07/2005. Enresa, Madrid

Olivella S, Carrera J, Gens A, Alonso EE (1994) Nonisothermal multiphase flow of brine and gas through saline media. Transp Porous Media 15:271–293

Olivella S, Gens A, Carrera J, Alonso EE (1996) Numerical formulation for simulator (CODE_BRIGHT) for coupled analysis of saline media. Eng Comput 13(7):87–112

Olivier HJ (1979) Some aspects of the influence of mineralogy and moisture redistribution on the weathering behaviour of mudrock. In: Proceedings of the 4th international conference on rock mechanics. Montreux, Switzerland, vol 3. pp 467–474

Sánchez M (2004) Thermo-hydro-mechanical coupled analysis in low permeability media. PhD Thesis, UPC, Spain

Sandén T, Goudarzi R, Börgesson L (2005) Transducers and cable connections for measuring THM-processes in engineering barriers—design and experiences. In: Alonso EE, Ledesma A (eds) Advances in understanding engineered clay barriers. Balkema, Rotterdam, pp 21–34

Thomas HR, Cleall PJ, Melhuish TA (2005) Simulation of the prototype repository. In: Alonso EE, Ledesma A (eds) Advances in understanding engineered clay barriers. Balkema, Rotterdam, pp 347–352

Velasco M, Pedraza L (2004) Ventilation experiment in Opalinus clay "VE" experiment. Hydromechanical interpretation and modelling (Task T71). Project Deliverable 19a, EC Contract FIKW-CT 2001-00126, Enresa, Madrid

Villar MV, García-Siñeriz JL, Bárcena I, Lloret A (2005) State of the bentonite barrier after five years of operation of an in situ test simulating a high level radioactive waste repository. Eng Geol 80:175–198